2. SITES 552–553[1]

Shipboard Scientific Party[2]

HOLE 552

Date occupied: 31 July 1981

Date departed: 3 August 1981

Time on hole: 69 hr., 10 min.

Position (latitude; longitude): 56°02.56′N; 23°13.88′W

Water depth (sea level; corrected m, echo-sounding): 2301

Water depth (rig floor; corrected m, echo-sounding): 2311

Bottom felt (m, drill pipe): 2315

Penetration (m): 314

Number of cores: 25

Total length of cored section (m): 237.5

Total core recovered (m): 79.19

Core recovery (%): 36

Oldest sediment cored:
  Depth sub-bottom (m): 282.7
  Nature: Ferruginous diatomaceous claystone
  Age: early Eocene
  Measured velocity (km/s): 1.72

Basement:
  Depth sub-bottom (m): 282.7
  Nature: Basalt
  Velocity range (km/s): 3.1–3.5

Principal results: See Chapter 1, Introduction and Explanatory Notes.

HOLE 552A

Date occupied: 4 August 1981

Date departed: 7 August 1981

Time on hole: 72 hr., 3 min.

Position (latitude; longitude): 56°02.56′N; 23°13.88′W

Water depth (sea level; corrected m, echo-sounding): 2301

Water depth (rig floor; corrected m, echo-sounding): 2311

Bottom felt (m, drill pipe): 2311

Penetration (m): 183.5

Number of cores: 38

Total length of cored section (m): 183.5

Total core recovered (m): 182.98

Core recovery (%): 99.7

Oldest sediment cored:
  Depth sub-bottom (m): 183.5
  Nature: Glauconitic nannofossil chalk, biosiliceous marlstone
  Age: middle Eocene
  Measured velocity (km/s): 1.55

Principal results: See Chapter 1, Introduction and Explanatory Notes.

HOLE 553

Date occupied: 7 August 1981

Date departed: 8 August 1981

Time on hole: 10 hr., 56 min.

Position (latitude; longitude): 56°05.32′N; 23°20.61′W

Water depth (sea level; corrected m, echo-sounding): 2329

Water depth (rig floor; corrected m, echo-sounding): 2339

Bottom felt (m, drill pipe): 2339

Penetration (m): 9

Number of cores: 1

Total length of cored section (m): 9

Total core recovered (m): 8.33

Core recovery (%): 90

Oldest sediment cored:
  Depth sub-bottom (m): 9
  Nature: Nannofossil-foraminifer ooze and marl
  Age: late Pleistocene
  Measured velocity (km/s): 1.72

Principal results: See Chapter 1, Introduction and Explanatory Notes.

HOLE 553A

Date occupied: 10 August 1981

Date departed: 25 August 1981

Time on hole: 191.47 hr.

Position (latitude; longitude): 56°05.32′N; 23°20.61′W

Water depth (sea level; corrected m, echo-sounding): 2329

Water depth (rig floor; corrected m, echo-sounding): 2339

Bottom felt (m, drill pipe): 2339

Penetration (m): 682.5

Number of cores: 59

Total length of cored section (m): 531.5

Total core recovered (m): 288.97

Core recovery (%): 54.4

---

[1] Roberts, D. G., Schnitker, D., et al., *Init. Repts. DSDP*, 81: Washington (U.S. Govt. Printing Office).

[2] David G. Roberts (Co-Chief Scientist), Institute of Oceanographic Sciences, Wormley, Godalming, Surrey, United Kingdom (present address: British Petroleum Co. Ltd., Britannic House, Moor Lane, London, United Kingdom); Detmar Schnitker (Co-Chief Scientist), Department of Oceanography, University of Maine, Walpole, Maine; Jan Backman, Geologiska Institutionen, Stockholms Universitet, Kungstensgaten 45, S-113 86 Stockholm, Sweden; Jack G. Baldauf, Paleontology and Stratigraphy Bureau, U.S. Geological Survey, Menlo Park, California; Alain Desprairies, Laboratoire de Géochimie des Roches Sédimentaires, Université de Paris XI, 91405 Orsay, France; Reiner Homrighausen, Laboratorium fur Erdolgewinnung, Deutsche Texaco AG, 3101 Wietze, Federal Republic of Germany; Paul Huddlestun, Georgia Geological Survey, Atlanta, Georgia; Alfred J. Kaltenback, Denver Research Center, Marathon Oil Company, Littleton, Colorado; John B. Keene, Deep Sea Drilling Project, Scripps Institution of Oceanography, La Jolla, California (present address: Department of Geology, University of Sydney, NSW, Australia); Klaus A. O. Krumsiek, Geologisches Institut, Bonn, Nussallee 8, D 53 Bonn 1, Federal Republic of Germany; Andrew C. Morton, British Geological Survey, Keyworth, United Kingdom; John W. Murray, Department of Geology, University of Exeter, Exeter, Devon, United Kingdom; Jean Westberg-Smith, Geological Research Division, Scripps Institution of Oceanography, La Jolla, California; Herman B. Zimmerman, Department of Civil Engineering, Union College, Schenectady, New York.

Oldest sediment cored:
Depth sub-bottom (m): 499.35
Nature: Tuffaceous mudstone
Age: late Paleocene/early Eocene
Measured velocity (km/s): 1.7

Basement:
Depth sub-bottom (m): 499.35
Nature: Basalt
Velocity range (km/s): 3.5–6.0

HOLE 553B

Date occupied: 26 August 1981

Date departed: 26 August 1981

Time on hole: 14.23 hr.

Position (latitude; longitude): 56°05.32′N; 23°20.61′W

Water depth (sea level; corrected m, echo-sounding): 2328

Water depth (rig floor; corrected m, echo-sounding): 2338

Bottom felt (m, drill pipe): 2338

Penetration (m): 33.5

Number of cores: 4

Total length of cored section (m): 33.5

Total core recovered (m): 33.23

Core recovery (%): 99.2

Oldest sediment cored:
Depth sub-bottom (m): 285
Nature: Nanno-foram ooze
Age: Pleistocene
Measured velocity (km/s): 1.7

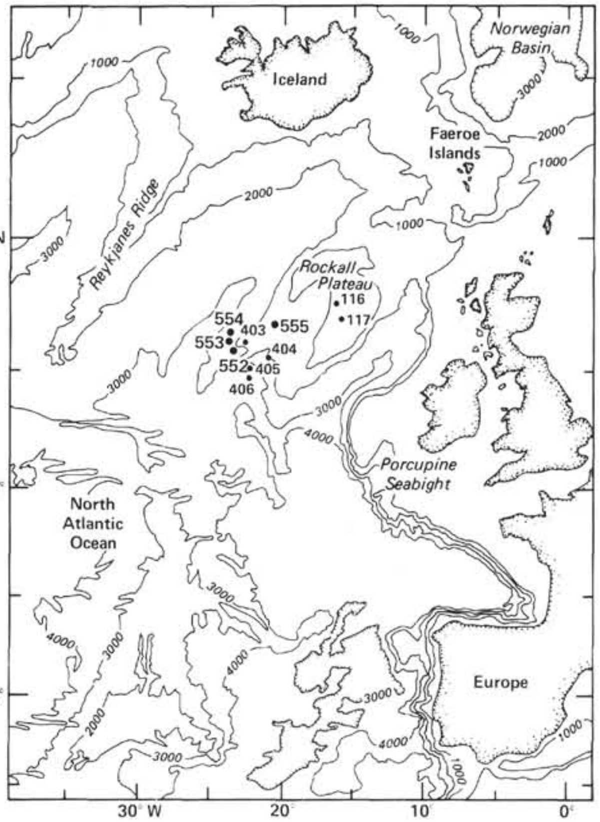

Figure 1. Northeast Atlantic bathymetry showing site locations.

BACKGROUND AND OBJECTIVES

The Rockall Plateau is the only major microcontinent (Figs. 1, 2, and 3) in the North Atlantic Ocean. It is a topographically isolated and shallow area whose principal relief consists of a series of shallow banks partly surrounding the Hatton–Rockall Basin. The shallowest banks are the Rockall Bank, Hatton Bank, and Edoras Bank. To the east, west, and southwest, the Plateau is bounded by steep margins, but to the north the margins are ill-defined and merge with the eastern part of the Iceland–Faeroes Ridge.

Regional Geology

Many geological and geophysical studies relevant to the structure and evolution of the Rockall Plateau have been done since Bullard et al. (1965) postulated a continental composition. Deep seismic refraction profiles have given continental seismic velocities and mantle depths of 33 and 22 km beneath the Rockall Bank and Hatton-Rockall Basin (Scrutton, 1970, 1972; Scrutton and Roberts, 1971). Based on these data, gravity modeling has confirmed earlier suggestions that the whole plateau is a microcontinent (Bullard et al., 1965; Roberts, 1970, 1971). More recent geophysical and geochemical evidence of continental crust beneath the thick Tertiary lavas of the Faeroes may indicate a more northward extension of the Rockall Plateau (Bott et al., 1971; Casten 1973; Bott et al., 1974; Bott, pers. comm., 1981; Bott, Saxov, et al., 1983). Laxfordian and Grenvillian granulites dredged and drilled on the Rockall Bank have proved the presence of continental rocks previously inferred from geochemical evidence (Moorbath and Welke, 1969; Roberts, et al., 1972, 1973; Miller et al., 1973). Studies of the planated intrusive complex around Rockall Island suggest phases of igneous activity at 52 ± 9 and 81 ± 3 m.y. ago (Roberts, et al., 1973). Dredge hauls on the northern flank of Hatton Bank have yielded lower Tertiary arkosic conglomerates (Watts, et al., 1975).

West of the Rockall Plateau, the oldest oceanic crust adjoining the margin is, from the identification of magnetic Anomaly -24B (Fig. 3), 52 m.y in age (Vogt et al., 1969; Ruddiman, 1972; Laughton, 1971; Vogt and Avery, 1974; Roberts, 1975; Roberts et al., 1979). The age of the oceanic basement abutting the southwest margin (Fig. 3) is 73 m.y., by the position there of Anomaly -32. (Vogt et al., 1971; Vogt and Avery, 1974; Roberts, 1975; Jones and Roberts, 1975; Roberts et al., 1979). Early–Late Cretaceous oceanic crust probably underlies the Rockall Trough (Roberts, 1975; Jones and Roberts, 1975; Kristoffersen, 1978; Roberts et al., 1981).

Syntheses of the plate tectonic evolution of the North Atlantic based on these data have demonstrated that three distinct phases of rifting and spreading have structurally isolated the Rockall Plateau (Vogt et al., 1969; Le Pichon et al., 1972; Laughton, Berggren et al., 1972; Olivet et al., 1974; Roberts, 1975; Kristoffersen, 1978; Kristoffersen and Talwani, 1978; Srivastava, 1978). The first phase in post-Albian–Late Cretaceous time(?) opened the Rockall Trough following Late Jurassic–Early Cretaceous rifting (Roberts, 1975; Roberts et al., 1982; Roberts et al., 1983). By Anomaly 31–32 time (Anomaly -33

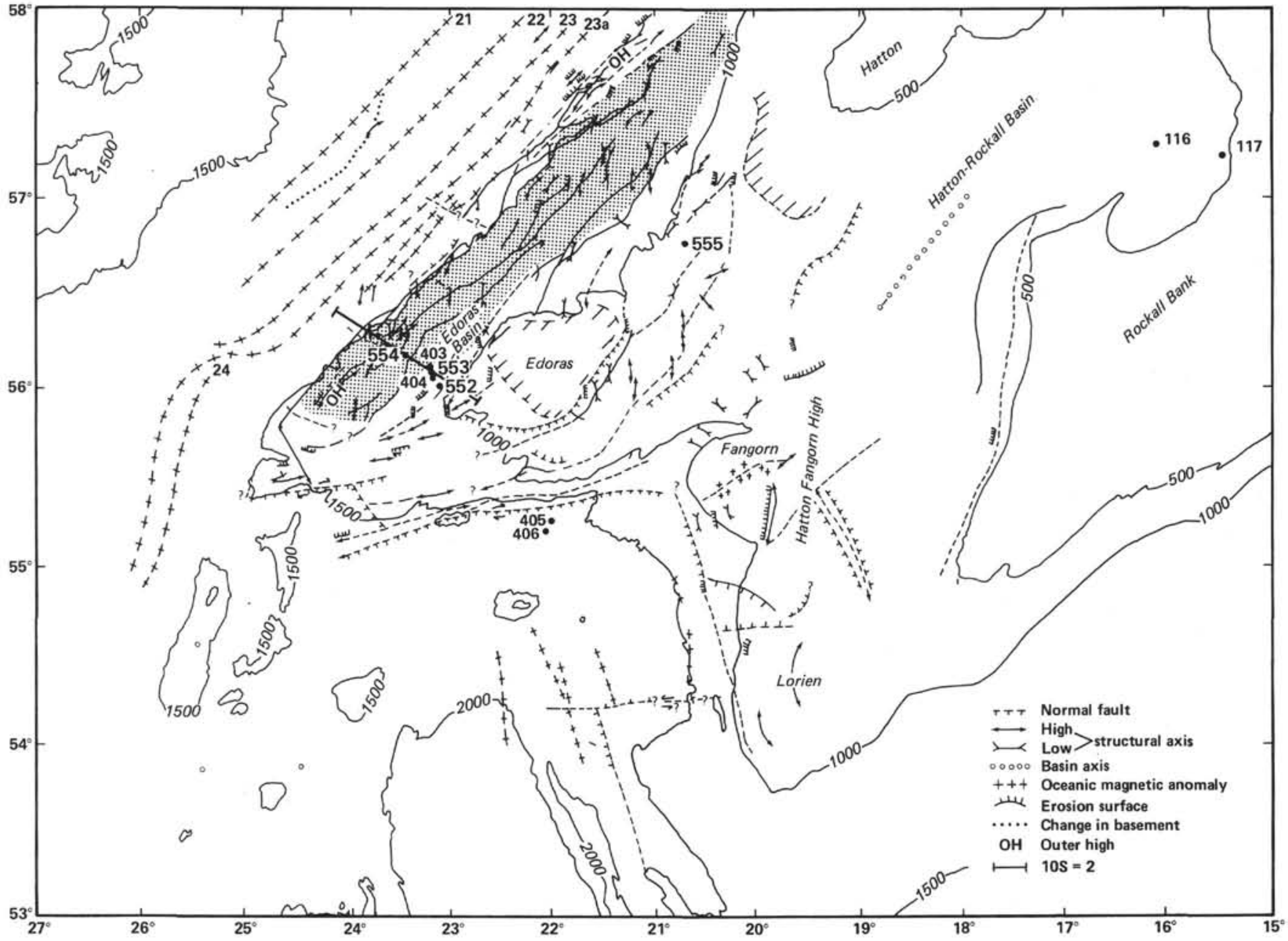

Figure 2. Main structural elements of the Rockall Plateau and Trough (from Roberts, 1975).

according to Kristoffersen, 1978), spreading had ceased in the Rockall Trough, and the spreading axis had shifted westward to open the Labrador Sea, thereby spreading the Greenland-Rockall Plate away from North America. Spreading may have begun earlier in the southern Labrador Sea than in the north (Srivastava, 1978). This rifting and spreading phase was responsible for the creation of the Gibbs Fracture Zone and the east–west transform fault now marked by the prominent scarp along the southwest margin of Rockall Plateau (Le Pichon et al., 1972; Olivet et al., 1974; Vogt and Avery, 1974; Roberts, 1975; Roberts et al., 1979). In this area the adjacent oceanic magnetic anomalies are truncated at the base of the scarp and young westward from Anomaly -32, close to Rockall Plateau to Anomaly -24 at 25°30′W (Roberts, 1975; Jones and Roberts, 1975) (Figs. 2 and 3).

The formation of this right-angled segment of the margin clearly predates the adjacent northeast–southwest trending part of the margin to the north, drilled during Legs 48 and 81, where the identification of Anomaly -24B indicates spreading began 52 m.y. ago. (Roberts, 1975; Roberts et al., 1979). Spreading in the Labrador Sea was arguably contemporaneous with the rifting between Greenland and Rockall Plateau that initially structured the northeast–southwest trending part of the margin. The rifting was accompanied by voluminous eruption of basic lava flows now exposed in east Greenland and the Faeroes (Noe-Nygaard, 1976; Brooks, 1973; Rasmussen, and Noe-Nygaard, 1969). Discrepancies in the fit between Greenland and the Rockall Plateau as well as some weak evidence of linear anomalies predating Anomaly 24B have been cited as evidence for the accretion of about 60 km of oceanic crust prior to Anomaly 24B (Laughton, 1971). Nonetheless, active seafloor spreading between Greenland and Rockall Plateau had certainly begun out along the line of Reykjanes Ridge by 52 m.y. ago, representing the third phase that completed the isolation of the Rockall Plateau. Spreading continued in the Labrador Sea until about 40 m.y. ago. On the Reykjanes Ridge, spreading decelerated from 1 cm/yr. between 52 and 38 m.y. ago to 0.7 cm/yr. between 38 and 10 m.y. ago, accelerating to the present rate of 1.1 cm/yr. at 10 m.y. ago (Vogt et al., 1969; Vogt and Avery, 1974).

During most of the last 52 m.y., sedimentation processes on the flanks of the Reykjanes Ridge, in the Iceland Basin, and on the Rockall Plateau have been dominantly influenced by bottom currents associated with the outflow and subsequent mixing of Norwegian Sea Water across the various sills in the Iceland–Faeroes Ridge (Jones

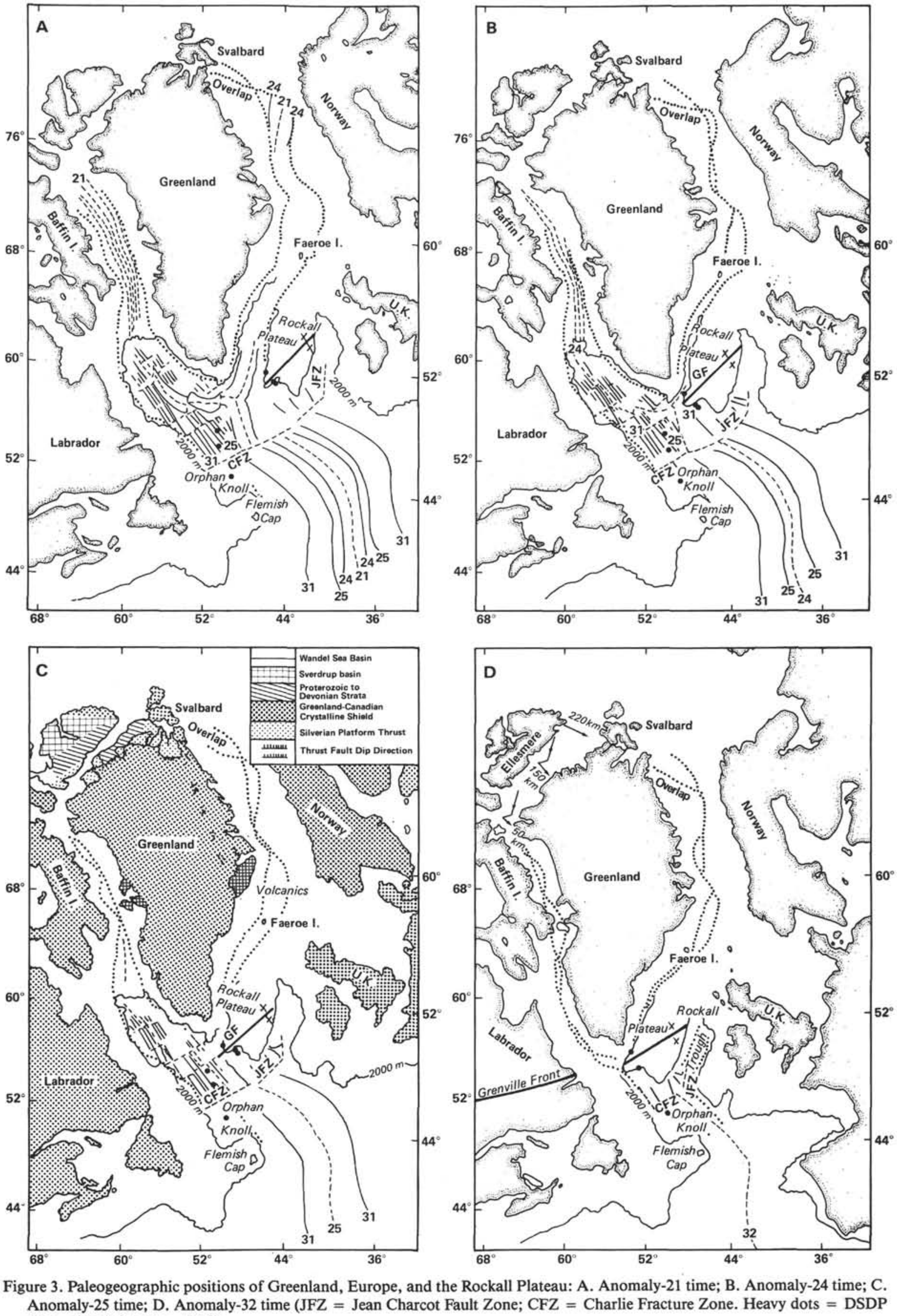

Figure 3. Paleogeographic positions of Greenland, Europe, and the Rockall Plateau: A. Anomaly-21 time; B. Anomaly-24 time; C. Anomaly-25 time; D. Anomaly-32 time (JFZ = Jean Charcot Fault Zone; CFZ = Charlie Fracture Zone. Heavy dots = DSDP sites, after Srivastava, 1978).

et al., 1970; Ruddiman, 1972; Roberts, 1975). The onset of the influence of bottom currents in the region is marked by the prominent reflector R4 of Eocene–Oligocene age (Roberts, 1975). The post-Eocene sediments have been fashioned into a series of prominent sediment drifts in the Gardar Drift along the west margin of the Iceland Basin and the Hatton Drift on the west margin of the Rockall Plateau (Ruddiman, 1972; Roberts, 1975) that are related to the outflow of Norwegian Sea Water across the Iceland–Faeroes Ridge into the North Atlantic. Although the main body of the ridge may not have subsided below sea level until mid-Miocene time (Vogt, 1972; Talwani, Udintsev et al., 1976; Thiede, 1980; Detrick et al., 1977; van Hinte, 1979), there is a possibility that some of the deeper sills such as the Denmark Strait and Faeroe Bank Channel may have subsided earlier (Roberts et al., 1983; Bott et al., in press). However, global sea level changes coupled to the opening of connections to the Arctic Ocean via the Greenland Sea may have been contributory factors.

In the context of this regional geological history, the Leg 81 drilling on the west margin of Rockall Plateau was intended to specifically examine the transition from rifting to spreading as well as the paleoceanographic history of the region.

Geological Setting and Problems of Sites 552 and 553

The west margin of the Rockall Plateau (Figs. 2 and 4) consists of the shallow Hatton and Edoras Banks flanked westward by a gentle slope broken in part by a discontinuous linear northeast–southwest trending ridge (Roberts, 1975). Regional studies (Roberts, et al., 1979) show that the west margin is characterized by a series of northeasterly trending troughs that generally trend subparallel to the adjacent Anomaly -24B. The most prominent of these, the Edoras Basin, lies at the foot of the west slope of Hatton and Edoras banks and can be traced along much of the length of the west margin. Oceanward, the Edoras Basin is separated from the oldest ocean crust by a linear ridge or outer high that varies in relief and prominence.

During Leg 48, Sites 403 and 404 were drilled in the Edoras Basin (Figs. 1 and 5) but penetrated only the sedimentary section above the main unconformity recognized on the seismic profiles. Above this unconformity, two seismic sequences are present (Fig. 5) and comprise a relatively transparent sequence separated by a prominent reflector from a well-bedded sequence below. In brief summary the transparent sequence above corresponds to the early Miocene–Recent foraminifer–nannofossil ooze and marls of the Hatton Drift, the underlying reflector to a tuff slightly older than Anomaly 24B age, and the well-bedded interval below the tuff to a westward thickening sequence of volcaniclastics that predate Anomaly 24B and thus the onset of spreading (Montadert, Roberts et al., 1979; Roberts et al., 1979).

Present below the main seismic unconformity defining the base of the volcaniclastic sequence is an unusual sequence of strong oceanward dipping reflectors, some 1 to 3 s in thickness. On some seismic profiles across the margin, these reflectors apparently flatten with depth (Figs. 5 and 6) but on others they diverge. In both cases, the reflectors seem to terminate against the outer high. Based on interval velocity data, the sequence is estimated to be between 2.5 and 7 km thick.

The margin thus does not show the classical tilted fault block topography documented on the margins of Biscay and Galicia (De Charpal et al., 1978), and a different mechanism is required to explain the origin of the dipping reflectors.

Establishing the origin of these reflectors has become especially important in view of their hitherto unrecognized widespread occurrence on many passive margins. On the conjugate margin of East Greenland, a mirror image of the dipping reflectors of west Rockall Plateau is present (Featherstone, et al., 1976; Roberts, unpub.). Farther north, similar sets of reflectors occur northwest of the Faeroes and, in the Norwegian Sea, on the Lofoten Margin, the Vøring Plateau, and in the Møre Basin (Talwani, Udintsev et al., 1974; Hinz, 1981; Talwani et al., 1981; Mutter et al., 1982). Elsewhere similar sets of reflectors have been observed off eastern North America (Grow, et al., 1980), southwest Africa (Gerard, et al., 1981), Antarctica (Hinz, 1981); India (Hinz, 1981), and off southern Australia (Keene, pers. comm.).

Despite the widespread occurrence and obvious importance of the dipping reflectors, information on their age and origin is scant. Drilling off southwest Africa and the Vøring Plateau has penetrated basalt ostensibly at the top of the sequence (Gerard et al., 1981; Talwani, Udintsev et al., 1974) but in south Australia, where the sequence is exposed in the Otway Basin and can be mapped seismically offshore, they are known to consist of sediments and volcaniclastics (Gleadow and Duddy, 1980; Duddy, in press). At Site 404, the conglomerate cored at total depth may represent the top of the sequence and Watts, et al. (1975) have dredged arkosic sandstones from an outcrop of the reflectors north of Hatton Bank.

Despite their obvious global importance, there has been no firm agreement as to their origin, composition, or age. One hypothesis considers that they comprise a sequence of lavas and pyroclastics intercalated with sediments derived by rapid erosion of nearby volcanic and metamorphic terrains; voluminous extrusion and deposition took place subaerially or in shallow marine conditions on rifting continental crust (Roberts et al., 1979). Another hypothesis considers that the reflectors comprise a sequence of subaerial lava flows formed by subaerial seafloor spreading in a manner akin to the thick oceanic crust of Iceland (Palmason, 1979; Talwani et al., 1981). In terms of this hypothesis, the crust between Anomaly -24B and the Hatton-Edoras Bank would be entirely oceanic in origin. These hypotheses have obvious implications for the position of the continent/ocean boundary and in turn for the early structural evolution of not only this but also other ocean basins. It should be noted that oceanward dipping intrabasement reflectors can also be seen in the undisputed oceanic crust west of the outer high. However, these reflectors are

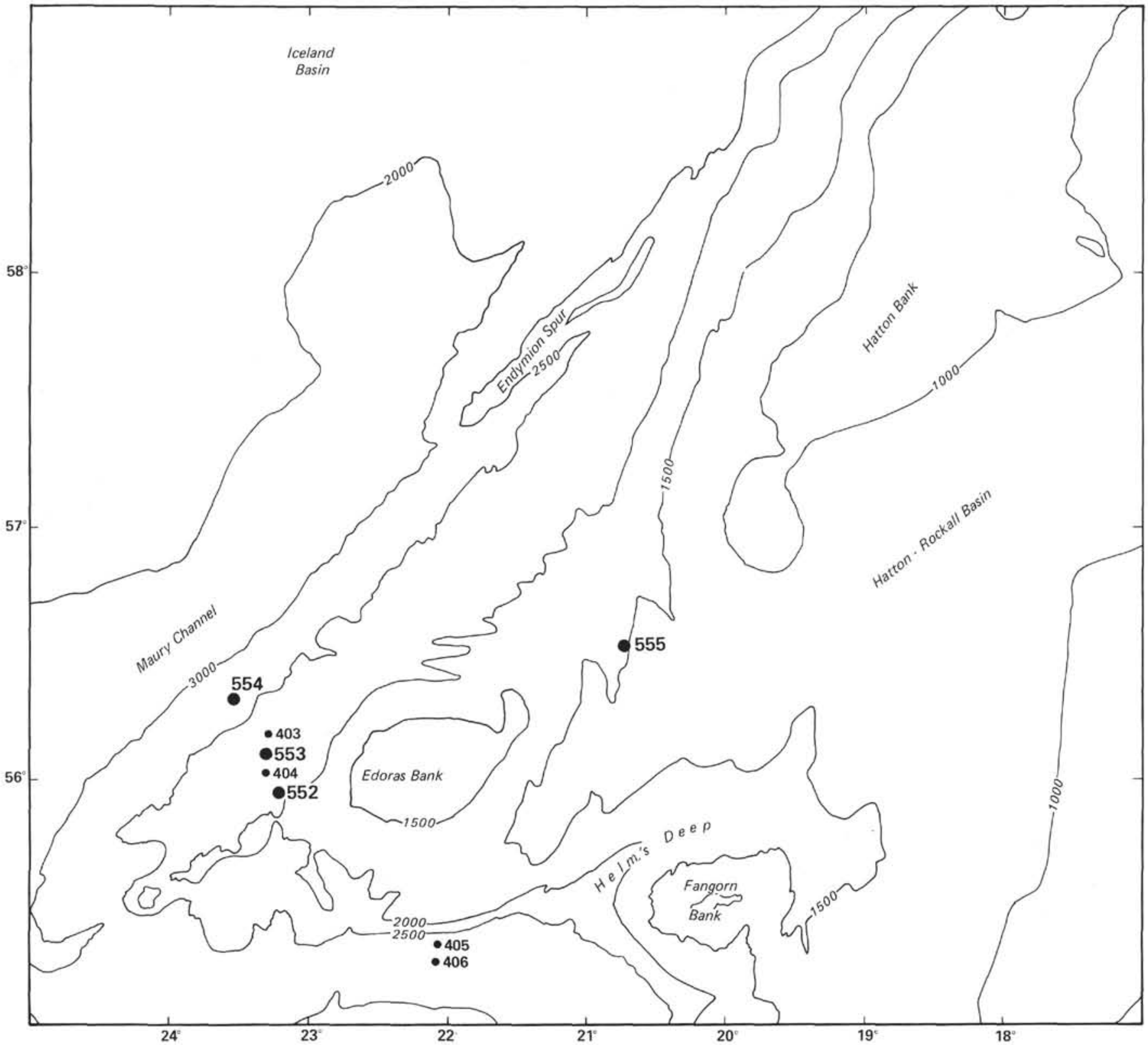

Figure 4. Bathymetry of Sites 552, 553, 554, and 555, Rockall Plateau (Sites 403, 404, 405, and 406 are also shown).

more impersistent in character. Testing the origin of the dipping reflectors was thus the prime objective of Sites 552 ands 553.

The position of Sites 552 and 553 on the Hatton Drift that trends along the west margin of Rockall Plateau also allowed examination of the influence of changing ocean circulation and climate on deposition. The drift is thought to have been deposited under the influence of bottom currents flowing northeastward against the slope. Bottom water at the sites lies above the southward-flowing North Atlantic Deep Water that fills the deeper part of the Iceland Basin and mantles the Reykjanes Ridge, but on the Hatton Drift it may represent Labrador Sea Water mixed with Norwegian Sea Water that has traveled down the Rockall Trough (Ruddiman, 1972; Roberts, 1975). Use of the hydraulic piston corer to give complete sedimentary section and in turn a complete oxygen isotope, biostratigraphic, and lithologic record for the Miocene–Recent sequence would provide important new high resolution data at a high latitude site in the North Atlantic. Specifically, the data would help document the transition from the nonglacial to the glacial state and the evolution of North Atlantic circulation in response to global circulation changes and the history of water exchange between the Norwegian Sea and the North Atlantic Ocean. In view of evidence of erosion and nondeposition at Sites 403 and 404, recovery of a complete Eocene–Oligocene sequence was less assured but, if present, would provide a valuable record of climatic changes across this important boundary.

Location of Sites 552 and 553

The choice of Sites 552 and 553 was made from regional multichannel seismic surveys made by the Insti-

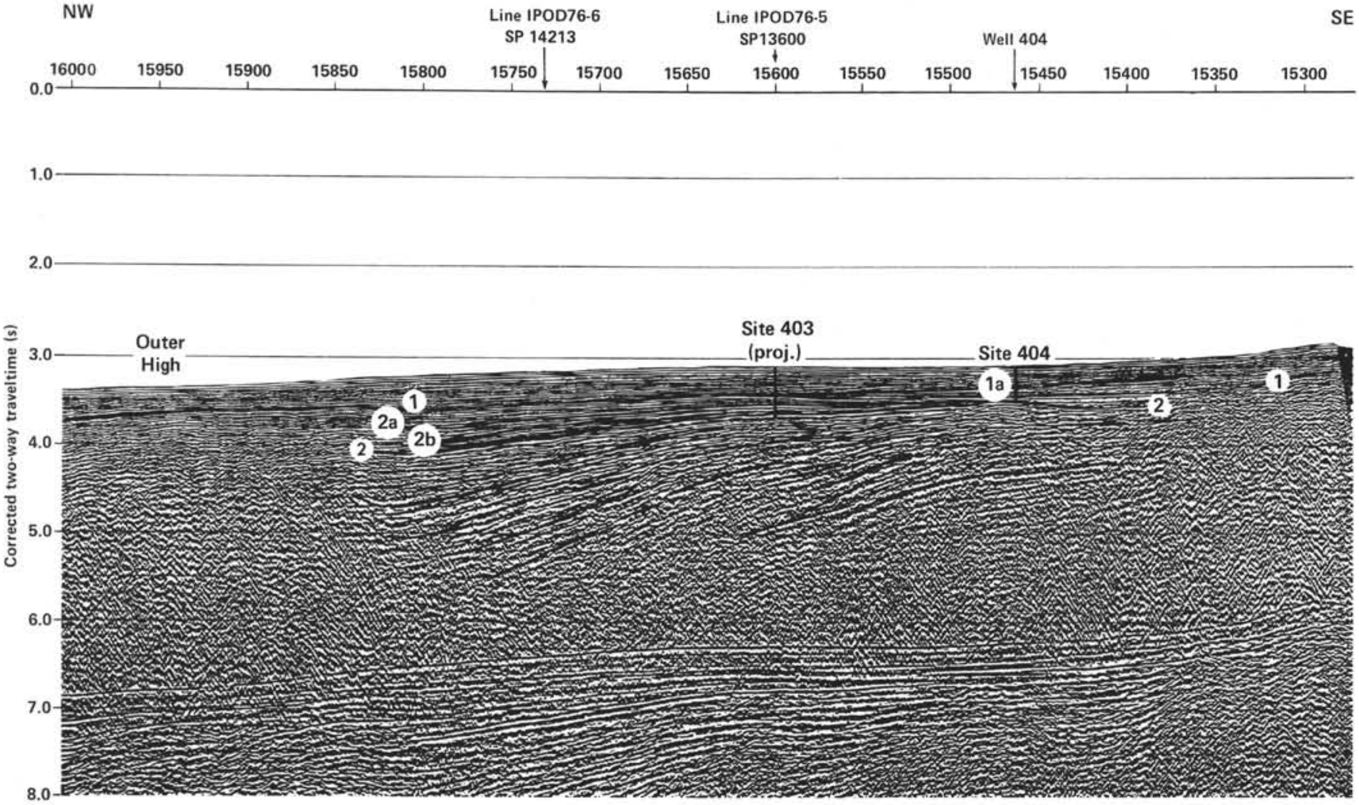

Figure 5. Multichannel line through Sites 552 and 553.

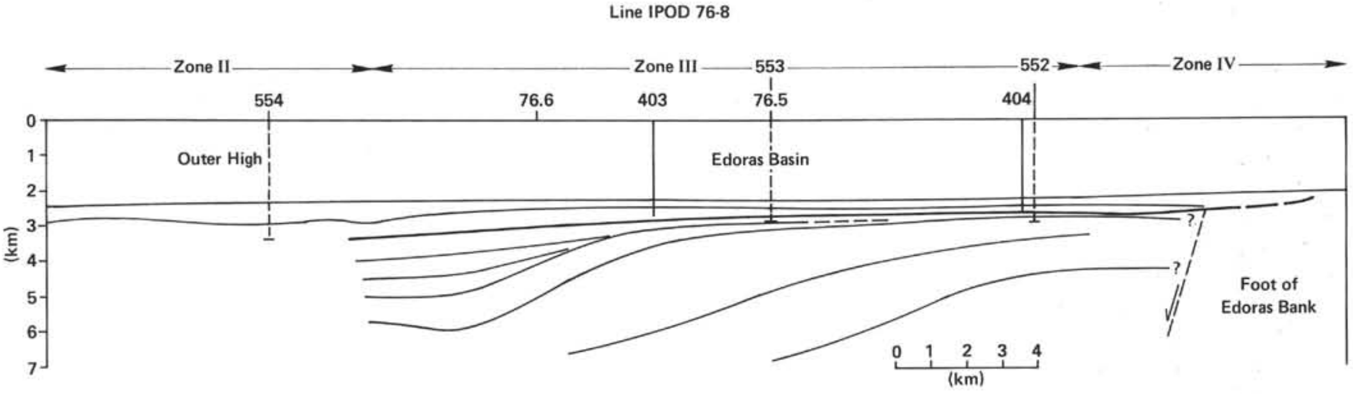

Figure 6. True-scale section across the Edoras Basin.

tute of Oceanographic Sciences (U.K.) and the Institut Français du Pétrole supplemented by single-channel seismic profiles made by Lamont-Doherty Geological Observatory. Site 552 was located near Site 404 where an apparent offlap might allow penetration of an older part of the dipping reflector sequence. Since only shallow single-bit penetration was needed to reach the top of the sequence, results at Site 552 would help determine whether a re-entry cone would be required at Site 553 to achieve deep penetration of the dipping reflector sequence.

In summary, the objectives of Sites 552 and 553 were as follows:

1. To determine the age, composition, and origin of the dipping reflectors: Shoreside geochemical studies (viz., strontium isotope ratios) would contribute to establishing the presence of oceanic crust or stretched continental crust beneath the sequence.

2. Subsidence of the margin during rifting and early spreading: Definition of the subsidence history of the sites using quantitative paleobathymetric data would contribute to the problem of crustal attenuation and origin posed by the models of McKenzie (1978) and Royden et al. (1980). Heat-flow measurements were planned at all sites.

3. Paleoceanography: The sites were to examine the evolution of Quaternary and Tertiary climate and ocean circulation. In particular the consequences of subsidence of the Iceland–Faeroes Ridge as well as the transition

from the nonglacial to the glacial state were of interest.

4. Diagenesis: The study was intended to examine the diagenetic history of the volcaniclastic section and the maturation of organic matter in relation to rapidly changing thermal conditions on the young margin.

5. Paleomagnetism: Correlation of the Tertiary and Quaternary magnetic reversal history with biostratigraphic data in continuously cored sections was a prime objective. The magnetostratigraphy may provide the only chronological guide in the comparatively barren Eocene–Paleocene sequences.

6. Logging: Correlation of the electric logs with seismic reflection data and lithological logs. Construction of synthetic seismograms to understand the origin of the dipping reflectors was to be an integral part of the study.

SITE APPROACH AND DRILLING OPERATIONS

Site 552

Glomar Challenger departed Southampton at 1230 BST, 27 July, in calm weather. No geophysical gear was streamed while in transit from Southampton to the shelf edge. The shelf edge south of Ireland was crossed at 1327Z, 29 July, when the seismic gear and magnetometer were streamed. Course was then set 307° for Site 552.

Site 552 was neared at 1515Z, 31 July, on course 307°. At 1642Z, 31 July, course was set to 317° and speed reduced to 150 rpm to run along the control multichannel profile IPOD 76-8 crossing through the site. The site was passed at about 1816Z but course was maintained to obtain a good crossing. At 1831Z, course was set to 316° and speed reduced to 140 rpm to return across the site. Course was adjusted to 133° at 1845Z and 162° at 1858Z to converge with the site (Fig. 7). The beacon was dropped at 1908Z and geophysical gear recovered at 1917Z when *Glomar Challenger* began positioning and maneuvering to the beacon. The final position of the site (Fig. 7) lay about 0.9 n. mi. southeast of old Site 404 and within about 0.35 n. mi. east of SP 15450 on line IPOD 76-8. The uncorrected depth was 2307 m which corrected to 2285 or 2245 m according to the Matthews (1939) and H.O. (1980) tables. Depths corrected to rig floor were 2301 and 2311 m, respectively.

At 2018Z, the bottom-hole assembly was made up and pipe started to run in hole. Preparations to spud began at 0307–0330Z. The first core was a water core, but the second at 0438Z cut a 3.5 m core of mud. The mudline was taken at 2315 m. Drilling commenced by washing down to 51.0 m subsea where drill barrel and ship motion measurements were made. A heat flow measurement was taken after cutting Core 2. The interval from 60.5 to 117.5 m was washed and a second heat flow measurement taken after cutting core 3. Continuous coring then began with variable recovery (see Table 1). A third heat flow measurement was taken after Core 6. Continuous coring continued. A fourth heat flow measurement was planned after Core 8 but was precluded by the recovery of chert in stiff Eocene marls in Core 8. Continuous coring then continued with generally poor recovery in calcareous tuffs. Slow drilling at Core 21 suggested a plugged bit, and a 5 m core was cut prior to an attempt to clear the bit. Inspection of the core showed however that basalt, cored in the last section and core catcher, was the likely cause of the slow drilling. Core 22 also cut 1.80 m of basalt. Cores 23 to 24 were cut with poor recovery. Throughout the day, weather conditions had deteriorated steadily, and helm assistance was required to maintain position. By 0600Z, winds gusting to 50 mph were observed with occasional rolls of 9°. Because of the unfavorable weather and difficulty in maintaining position, pipe was pulled out of the hole at 0648Z and the mudline cleared at 0839Z; Hole 552 was then abandoned.

Poor weather conditions continued overnight but by 0736Z, 4 August, had moderated sufficiently to allow positioning in automatic mode. The bottom-hole assembly was made up for HPC, and pipe was run in hole at 2297.0 m between 0848Z and 1533Z, 4 August. The HPC was picked up between 1750Z and 1839Z preparatory to taking the first 9.5 m HPC core. The first attempt using the old Matthew's tables to determine the depth below seafloor failed to cut a core. Between 1920 and 1940Z, the vessel drifted off position by 120 ft. Between 1940 and 2020Z repeated attempts were made to seat the HPC tool, but it proved impossible to achieve full pressurization. At 2020Z, the tool was pulled to check the cause of the problem. Apparently the pins had sheared before the tool seated. The pins were replaced and at 2112Z, the pressure again failed to build up again, apparently as a result of shearing of the pins on the way down. At 2126Z, the tool was returned to the drill floor, and it was found that the pins were not sheared. On running in the tool, no pressure build-up was observed, but the shear pin on the overshot was apparently sheared and no core was cut. Some difficulty was found in retrieving the tool and, at 2309Z, 4 August, the 9.5 m core barrel was found to be broken at both the outer body link and the piston rod. At 2325Z, a collet was run in to latch into the collet head sub to offer a seat for the barrel. At 2356Z, it was found that the collet had not released. During these operations, it was found that a collet-head sub had been inadvertently used instead of the HPC seal sub, thus explaining the difficulty in seating the HPC core barrel. At 2356Z, attempts to core were abandoned, and the pipe was pulled to replace the collet head subs with the HPC seal sub. The drill floor was reached at 0445Z and after changing to the HPC seal sub, pipe was run in hole at 0530Z, 5 August. Because of the damage sustained to the 9.5 m core barrel a 4.5 m barrel had to be used, thus doubling the time required to HPC the Neogene and Recent section. No core was cut at the mudline depth predicted from the old Matthew's tables, but the second core was cut at 2311.0 m (in exact agreement with the value predicted from the new tables) and gave a 4.0 m core of yellow brown clayey ooze at 1345Z, 5 August. Continuous HPC coring began, using the orientation device throughout. Although there were several failures, about 80% of the cores were oriented successfully. Recovery was excellent, averaging 99%, and only two or three cores exhibited significant disturbance.

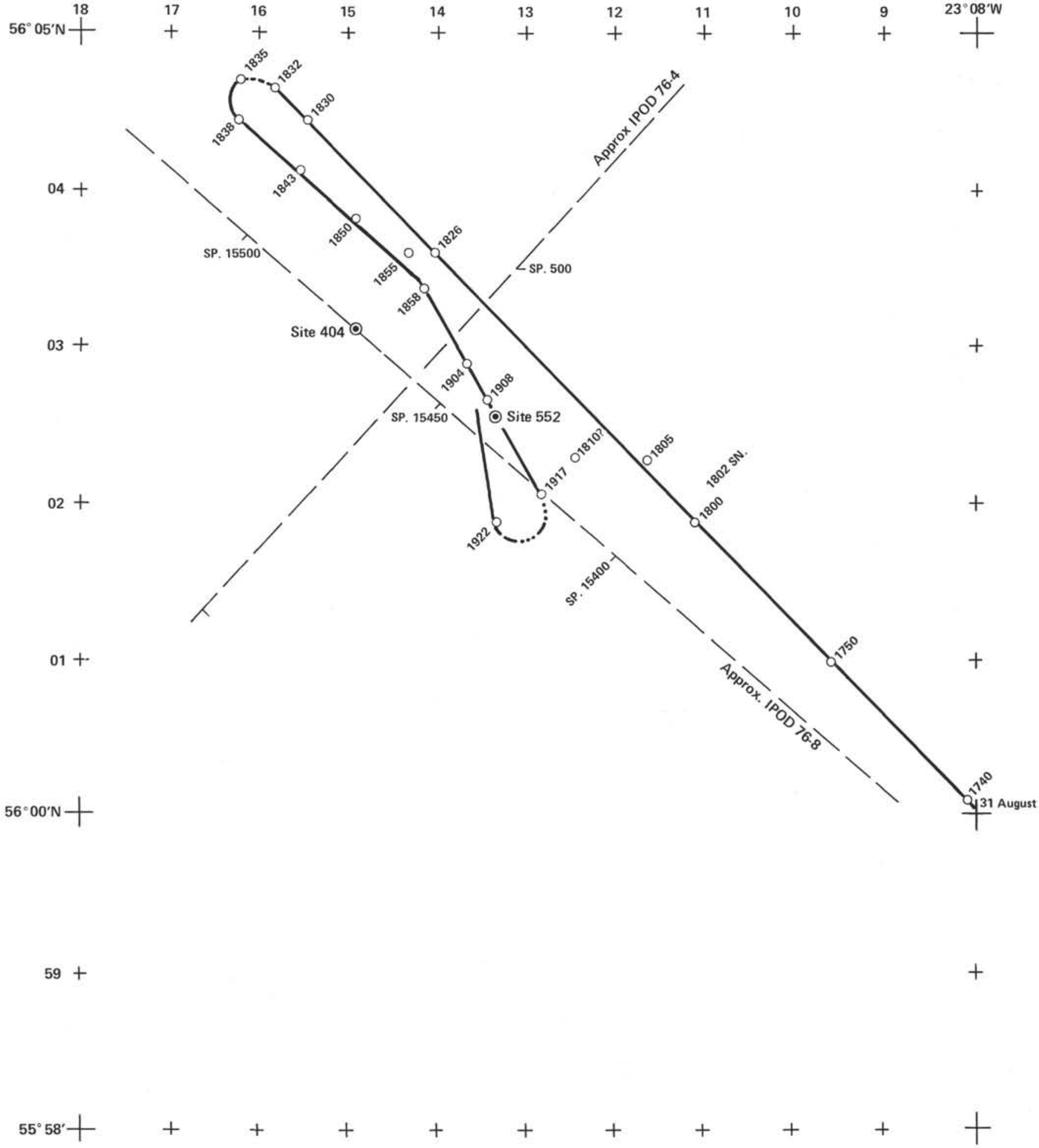

Figure 7. Approach of *Glomar Challenger* to Sites 552 and 553 showing location of seismic reflection profiles.

Table 1. Coring summary, Sites 552, 553.

Core	Date (August 1981)	Time (Z)	Depth from drill floor (m) Top Bottom	Depth below seafloor (m) Top Bottom	Length cored (m)	Length recovered (m)	Percent recovered
Hole 552							
1	1	0513	2315.0–2318.5	0.0–3.5	3.50	3.45	98
H1	1	0818	2318.5–2366.0	3.5–51.0	Wash	0.02	
2	1	0912	2366.0–2375.5	51.0–60.5	9.5	1.13	12
H2	1	1200	2375.5–2423.0	60.5–108.0	Wash	0.13	
3	1	1307	2423.0–2432.5	108.0–117.5	9.5	9.05	95
4	1	1516	2432.5–2442.0	117.5–127.0	9.5	6.05	64
5	1	1613	2442.0–2451.5	127.0–136.5	9.5	6.61	69
6	1	1715	2451.5–2461.0	136.5–146.0	9.5	5.63	59
7	1	1937	2461.0–2470.5	146.0–155.5	9.5	5.41	57
8	1	2043	2470.5–2480.0	155.5–165.0	9.5	5.51	58
9	1	2151	2480.0–2489.5	165.0–174.5	9.5	7.28	77
10	1	2308	2489.5–2499.0	174.5–184.0	9.5	0.2	0.1
11	2	0016	2499.0–2508.5	184.0–193.5	9.5	0.0	0
12	2	0224	2508.5–2518.0	193.5–203.0	9.5	9.72	100
13	2	0351	2518.0–2527.5	203.0–212.5	9.5	1.47	17
14	2	0415	2527.5–2537.0	212.5–222.0	9.5	4.92	52
15	2	0615	2537.0–2546.5	222.0–231.5	9.5	1.34	14
16	2	0815	2546.5–2556.0	231.5–241.0	9.5	1.01	10.6
17	2	1002	2556.0–2565.5	241.0–250.5	9.5	0.44	0.5
18	2	1136	2565.5–2575.0	250.5–260.0	9.5	2.31	24
19	2	1239	2575.0–2584.5	260.0–269.5	9.5	0.05	1
20	2	1353	2584.5–2594.0	269.5–279.0	9.5	0.0	0
21	2	1547	2594.0–2599.0	279.0–284.0	5.0	4.01	80
22	2	1921	2599.0–2603.5	284.0–288.5	4.5	1.80	49
23	3	0057	2603.5–2613.0	288.5–298.0	9.5	1.80	19
24	3	0340	2613.0–2622.0	298.0–307.0	9.0	0.0	0
25	3	0925	2622.0–2629.0	307.0–314.0	7.0	0.0	0
					219.0	79.19	36.2
Hole 552A							
X	5	1300	2313.0–2318.0	0.0–5.0			
1	5	1354	2311.0–2315.0	0.0–4.0	4.0	4.08	102
2	5	1545	2315.0–2320.0	4.0–9.0	5.0	5.14	103
3	5	1640	2320.0–2325.0	9.0–14.0	5.0	5.10	102
4	5	1739	2325.0–2330.0	14.0–19.0	5.0	5.03	100
5	5	1840	2330.0–2335.0	19.0–24.0	5.0	5.17	103
6	5	1935	2335.0–2340.0	24.0–29.0	5.0	4.79	95
7	5	2023	2340.0–2345.0	29.0–34.0	5.0	4.80	96
8	5	2124	2345.0–2350.0	34.0–39.0	5.0	5.20	104
9	5	2215	2350.0–2355.0	39.0–44.0	5.0	4.95	99
10	5	2314	2355.0–2360.0	44.0–49.0	5.0	5.17	103
11	6	0007	2360.0–2365.0	49.0–54.0	5.0	5.12	102
12	6	0110	2365.0–2370.0	54.0–59.0	5.0	4.94	99
13	6	0203	2370.0–2373.0	59.0–62.0	3.0	2.87	96
14	6	0255	2373.0–2378.0	62.0–67.0	5.0	4.90	98
15	6	0346	2378.0–2383.0	67.0–72.0	5.0	4.93	99
16	6	0440	2383.0–2388.0	72.0–77.0	5.0	5.16	103
17	6	0538	2388.0–2393.0	77.0–82.0	5.0	5.15	103
18	6	0632	2393.0–2398.0	82.0–87.0	5.0	5.03	101
19	6	0758	2398.0–2403.0	87.0–92.0	5.0	4.77	95
20	6	0951	2403.0–2406.0	92.0–95.0	3.0	3.48	110
21	6	1044	2406.0–2410.0	95.0–99.0	4.0	3.95	99
22	6	1138	2410.0–2415.0	99.0–104.0	5.0	4.27	85
23	6	1237	2415.0–2419.5	104.0–108.5	4.5	4.46	99
24	6	1337	2419.5–2424.5	108.5–113.5	5.0	4.72	94
25	6	1553	2424.5–2429.5	113.5–118.5	5.0	4.73	94
26	6	1642	2429.5–2434.5	118.5–123.5	5.0	4.95	99
27	6	1734	2434.5–2439.5	123.5–128.5	5.0	4.89	98
28	6	1858	2439.5–2444.5	128.5–133.5	5.0	5.10	102
29	6	2010	2444.5–2449.5	133.5–138.5	5.0	5.07	101
30	6	2045	2449.5–2454.5	138.5–143.5	5.0	5.12	102
31	6	2144	2454.5–2459.5	143.5–148.5	5.0	4.86	97
32	6	2235	2459.5–2464.5	148.5–153.5	5.0	5.13	103
33	6	2340	2464.5–2469.5	153.5–158.5	5.0	4.96	99
34	7	0044	2469.5–2474.5	158.5–163.5	5.0	5.07	101
35	7	0135	2474.5–2479.5	163.5–168.5	5.0	5.18	104
36	7	0226	2479.5–2484.5	168.5–173.5	5.0	5.11	102
37	7	0317	2484.5–2489.5	173.5–178.5	5.0	4.70	95
38	7	0409	2489.5–2494.5	178.5–183.5	5.0	4.92	99
					183.5	182.79	99.7

Table 1. (Continued).

Core	Date (August 1981)	Time (Z)	Depth from drill floor (m) Top Bottom	Depth below seafloor (m) Top Bottom	Length cored (m)	Length recovered (m)	Percent recovered
Hole 553							
1	7	2351	2339–2348	0–9.5	9.0	8.33	92.5
Hole 553A							
1	11	0058	2404.5–2414.0	65.5–75.0	9.5	5.88	62
2	11	0414	2442.5–2452.0	103.5–113.0	9.5	9.64	101
3	11	0810	2490.0–2499.5	151.0–160.5	9.5	9.73	102
4	11	1129	2518.5–2528.0	179.5–189.0	9.5	9.49	99
5	11	1283	2528.0–2537.5	189.0–198.5	9.5	9.10	96
6	11	1454	2537.5–2547.0	198.5–208.0	9.5	8.04	85
7	11	1603	2547.0–2556.5	208.0–217.5	9.5	8.19	86
8	11	1708	2556.5–2566.0	217.5–227.0	9.5	4.96	52
9	11	1803	2566.0–2575.5	227.0–236.5	9.5	8.40	88
10	11	1900	2575.5–2585.0	236.5–246.0	9.5	9.73	102
11	11	1959	2585.0–2594.5	246.0–255.5	9.5	8.40	88
12	11	2110	2594.5–2604.0	255.5–265.0	9.5	6.43	68
13	11	2226	2664.0–2613.5	265.0–274.5	9.5	3.50	37
14	11	2333	2613.5–2623.0	274.5–284.0	9.5	9.53	100
15	12	0110	2623.0–2632.5	284.0–293.5	9.5	5.84	61
16	12	0215	2632.5–2642.0	293.5–303.0	9.5	0.61	06
17	12	0351	2642.0–2651.5	303.0–312.5	9.5	0.70	07
18	12	0502	2651.5–2661.0	312.5–322.0	9.5	2.99	29
19	12	0611	2661.0–2670.5	322.0–331.5	9.5	6.23	66
20	12	0710	2670.5–2680.0	331.5–341.0	9.5	9.03	95
21	12	0810	2680.0–2689.5	341.0–350.5	9.5	6.50	68
22	12	0912	2689.5–2699.0	350.5–360.0	9.5	9.18	97
23	12	1015	2699.0–2708.5	360.0–369.5	9.5	6.53	69
24	12	1117	2708.5–2718.0	369.5–379.0	9.5	3.05	32
25	12	1238	2718.0–2727.5	379.0–388.5	9.5	3.00	31.5
26	12	1341	2727.5–2737.0	388.5–398.0	9.5	2.47	26
27	12	1444	2737.0–2746.5	398.0–407.5	9.5	8.40	88
28	12	1554	2746.5–2756.0	407.5–417.0	9.5	0.14	1
29	12	1656	2756.0–2765.5	417.0–426.5	9.5	0.08	0.5
30	12	1754	2765.5–2775.0	426.5–436.0	9.5	0.00	0
31	12	1909	2775.0–2784.5	436.0–445.5	9.5	0.05	5
32	12	2020	2784.5–2794.0	445.5–455.0	9.5	0.10	0.1
33	12	2159	2794.0–2803.5	455.0–464.5	9.5	0.00	0
34	12	2354	2803.5–2813.0	464.5–474.0	9.5	0.85	9
35	13	0129	2813.0–2822.5	474.0–483.5	9.5	1.24	13
36	13	0236	2822.5–2832.0	483.5–493.0	9.5	4.30	45
37	13	0403	2832.0–2841.5	493.0–502.5	9.5	6.64	70
38	13	0622	2841.5–2851.0	502.5–512.0	9.5	2.40	25
39	13	0822	2851.0–2860.5	512.0–521.5	9.5	1.38	14
40	13	1154	2860.5–2870.0	521.5–531.0	9.5	5.24	55
41	13	1356	2870.0–2879.5	531.0–540.5	9.5	2.90	24
42	13	1545	2879.5–2889.0	540.5–550.0	9.5	3.55	37
43	13	1911	2889.0–2898.5	550.0–559.5	9.5	6.25	66
44	14	1919	2898.5–2901.0	559.5–562.0	2.5	3.43	136
45	14	2342	2901.0–2910.5	562.0–571.5	9.5	7.02	74
46	15	0333	2910.5–2919.5	571.5–580.5	9.0	7.37	77
47	22	0017	2919.5–2926.5	580.5–587.5	7.0	5.36	56
48	22	0427	2926.5–2935.5	587.5–296.5	9.0	8.20	86
49	22	0916	2935.5–2944.5	596.5–605.5	9.0	7.99	84
50	22	1205	2944.5–2953.5	605.5–614.5	9.0	3.60	38
51	22	1440	2953.5–2957.0	614.5–618.0	3.5	3.08	88
52	22	1737	2957.0–2962.5	618.0–623.5	5.5	4.28	78
53	22	2037	2962.5–2971.5	623.5–632.5	9.0	4.47	49
54	23	0010	2971.5–2980.5	632.5–641.5	9.0	5.90	65
55	23	0402	2980.5–2989.5	641.5–650.5	9.0	6.86	72
56	23	0646	2989.5–2998.5	650.5–659.5	9.0	2.83	31
57	23	0902	2998.5–3007.5	659.5–668.5	9.0	1.06	11
58	23	1613	3007.5–3012.0	668.5–673.0	4.5	2.68	59
59	23	3012	3012.0–3021.5	673.0–682.5	9.5	4.4	46
					531.5	288.97	54
Hole 553B							
1	26	1120	2338.0–2342.5	0.0–4.5	4.5	4.62	100
2	26	1240	2337.5–2347.0	0.0–9.5	9.5	9.42	99
3	26	1400	2347.0–2356.5	9.5–19.0	9.5	9.71	102
4	26	1500	2356.5–2366.0	19.0–28.5	9.5	9.48	99
					33.5	33.23	99.2

Coring was continued to sample the Miocene–Eocene contact near 170 m. This was successfully cut in Core 37, and a final Core 38 was cut at 0409Z, 7 August, before we began to pull out of the hole at 0515Z, 7 August. The mudline was cleared at 0533Z and at 1051Z, 7 August, the vessel was secured for departure to Site 553.

Error in Core Depths, Site 552

Shipboard and subsequent shoreside correlation of the results of Holes 552 and 552A show a discrepancy of between 8.5 and 12.5 m in the depth of a prominent marker horizon observed in cores from both holes. The cause of the discrepancy is probably a miscount in drill barrel lengths while washing Site 552. No correction has been made to the core depths listed in Table 1. However, all users are asked to add 12.5 m to depths at Site 552 to ensure precise correlation.

Site 553

Although Site 552 was prematurely abandoned because of bad weather, basalt was encountered at total depth. Shipboard correlation of seismic reflectors with the lithologic log using interval velocities and physical properties data suggested that the basalt probably caused the topmost flat-lying reflector above the dipping reflector sequence. This reflector could be followed with some confidence to Site 553, although it is thought to be displaced by a small fault. This interpretation indicated the possibility that the basalt causing the flat-lying reflector would be found again at Site 553. Analysis of the seismic data suggested that at least 100 m of basalt might be present at this site, thus precluding the possibility of penetration of the dipping reflectors below in a single-bit hole. In view of this and the prevailing poor weather conditions, it was decided to set the re-entry cone at Site 553 to ensure penetration of the dipping reflectors and achievement of the main objective of the leg. In view of the complete recovery of a Pliocene–Pleistocene section at Hole 552A and its great importance for high latitude paleoenvironment studies, it was decided to again HPC the uppermost 110 m of the section encompassing the Pliocene–Pleistocene.

Site 553 was located at SP 15460 on IOS Line IPOD 76-8 close to the intersection of IOS Line 76-5 and approximately 4 n.mi. northwest of Site 552.

After completing Site 552 at 1051Z, 7 August, *Glomar Challenger* departed for Site 553. No geophysical gear was streamed for the brief transit, and navigation was done entirely by LORAN-C at a speed of 5 knots. Careful intercomparison of LORAN-C and satellite fixes while on position at Site 552 had confirmed the excellent repeatability of the LORAN-C fixes, which differed systematically from the satellite fixes by only 0.1 to 0.05 n. mi.

On crossing the site at 1205Z, 7 August, a long life beacon was dropped, and *Glomar Challenger* began positioning and maneuvering to the beacon. At 1245Z, it was found that the beacon signal was too weak and a second beacon was deployed at 1316Z. *Glomar Challenger* began positioning in automatic mode at 1348Z and preparing to run pipe. Predicted water depths for the site were 2329 m (BRF)-(Matthew's tables) and 2339 m (H.D., 1980). At 1945Z, pipe was run in to 2319.5 m. The bumper subs were picked up between 1945Z and 2030Z preparatory to spudding. Between 2030Z and 2050Z, operations were suspended because 40 mph winds and heavy seas resulted in excursions of as much as 200 ft. Site 553 was finally spudded at 2315Z. The first core at 2341.5 m was water, but the second attempt cut a core at 2348.0 m although the liner was shattered. A second mudline core was cut between 2315 and 2400Z, 8 August. Drill pipe motion measurements were made between 0000 and 0118Z, 9 August, and then the hole was washed to 59.5 m subsea in 18 min. to determine the casing depth for the re-entry cone. Tripping the drill string began at 0240Z and the mudline was cleared at 0312Z; the bit reached the drill floor at 1007Z, terminating the pilot Hole 553.

Assembly of the re-entry cone began at 1130Z, 9 August, and was completed at 1800Z. Preparations for keelhauling were completed by 2100Z. However, in view of deteriorating weather conditions and a poor forecast, this operation was deferred pending an improvement. By 0600Z, 10 August, weather had moderated sufficiently for keelhauling to begin. Unfortunately, when the pick up line was released, a crossbar holding one of the hang off cables broke so that the re-entry cone was left hanging, off axis, beneath the ship. Attempts to recover the cone began at 0720Z, and it was successfully brought on board at 1045Z thanks to the efforts of the drilling crew and seamen. The ship had been allowed to drift off station during this difficult operation. During the period 1045–1400Z, the cone was re-rigged and the ship returned to the site. At 1400Z, operations were suspended pending passage of another storm. The weather had moderated by 0630Z, 11 August, when the cone was keelhauled again. This operation was completed by 0718Z and 54.6 m of casing were made up between 0820 and 1220Z. The bottom-hole assembly was made up between 1200 and 1230Z, and the cone plus casing was run in hole at 1522Z in moderately calm conditions.

Hole 553A was spudded at 0058Z, 12 August. Casing was washed to 54.62 m before spot coring to 179.5 m. Heat flow measurements were taken with cores at 75.0, 143.0, and 160.5 m. Continuous coring began at 179.5 m with a further heat flow measurement being made at 198.5 m. The unconformity between the Miocene and the Eocene was cut in Core 12 at 255.5 m. Drilling and coring through the Eocene tuffs, tuffaceous sandstones, and mudstones yielded particularly poor recovery in Cores 28 to 35, possibly as a result of interbeds of lithified sandstones and softer sediment. Drill pipe motion measurements were made while cutting Core 34. However, recovery improved in the last cores (36 and 37) and above the basalt cut in Core 37 at 500 m. Cores 38 to 43 were in basalt.

After cutting Core 43, the pipe became stuck; several wiper runs were required to clear the hole. As the core diameter had decreased to 5.6 cm, it was decided to change bits and, after circulating 40 barrels of 80 vis 9.4 gel mud and 20 barrels of GUAR, pipe was pulled out of the hole at 2100Z. The mudline was cleared at 2203Z, 13 August, and the rig floor reached at 0126Z, 14 August. A new bottom-hole assembly was made up and pipe run in hole to 2329.0 m by 0630Z when preparations began to run in the re-entry tool. The tool malfunctioned because of a broken cable that required reheading. This was completed by 1000Z. The tool located the cone at 1115Z and after several attempts, Hole 553A was successfully re-entered at 1245Z, 14 August. Pipe was run at 1405Z and coring began again at 1710Z.

During the evening, the operations manager was notified that his wife had been hospitalized. Attempts were made through the AMVER system and shore radio to locate ships that might convey him to the United Kingdom but to no avail. The situation was also discussed via ham patch with DSDP. It was decided to leave Hole 553A immediately to steam to Limerick, Ireland, in order to transfer the operations manager ashore and to pick up his replacement. After cutting Core 46, pipe was pulled out of the hole at 0505Z and *Glomar Challenger* secured for departure to Limerick at 0930Z, 15 August. Loophead, off Limerick, was reached at 1525Z, on 17 August.

Glomar Challenger set course to return to Hole 553A at 1530Z, 17 August. The return passage to the site was delayed for more than 24 hr. by 40 knot headwinds and 16 ft. seas encountered throughout 19 August. Signals from the beacon at Hole 553A were picked up at 2020Z, 20 August, and *Glomar Challenger* began positioning and maneuvering to the beacon at 2025Z. Pipe was run in hole with a new F94CK bit at 2155Z. The re-entry tool was run in at 0442Z. The first re-entry attempt was made at 0647Z, 21 August, and was unsuccessful although it appeared from the rig floor tachometer that the pipe might have hit the cone. In subsequent re-entry attempts, only two reflectors could be clearly seen, and it is possible that the third reflector may have been damaged at that time. A second re-entry attempt between 0825Z and 1157Z was unsuccessful.

The third attempt successfully stabbed the cone at 1438Z, 21 August. After pulling out the re-entry hole, pipe was run in the hole with some sticking above the basalt. The first core, 47, was cut between 2200Z, 21 August and 0017Z, 22 August, in basalt. Continuous coring proceeded throughout 24 August and the morning of 25 August with drilling rates varying between 2.86 and 5.87 m hr^{-1}. At 0902Z, 25 August, the ten joints of knobby drill pipe were set back for replacement by 5 in. pipe prior to a DBMI and IDSS run. A 4.5 m core (Core 58) was cut to balance the new connections, but at 1110Z the pipe was found to be plugged; it was cleared at 1145Z. Fifty-two barrels of gel and twenty barrels of GUAR were spotted to clean the hole. After cutting Core 59, pump pressures indicated that the bit had been released accidentally—the cause may have been activation of the hydraulic release mechanism by the high pump pressures needed to unplug the bit. After discussing the feasibility of fishing for the bit, we agreed to carry out the logging program to assess whether the desired scientific objective had been met and to follow with the HPC program. During this time it was also intended to consider carefully the feasibility of fishing for the bit.

Between 2115Z and 2230Z, 23 August, the hole was flushed with 50 barrels of gel and 40 barrels of GUAR and a further 75 barrels of gel were displaced in the hole. Pipe was pulled back to 2822 m between 2230 and 2400Z. In logging the hole, it was agreed to keep the whole bottom-hole assembly in the hole. Relevant depths were: casing shoe: 57.0 m; drill pipe: 127.0 m; BHA length: 114.27 m.

Logging preparations continued from 0000–0355Z, 24 August, when the combined sonic-gamma-caliper tool was run in hole. Bottom was found at 3012.5 m, indicating little sloughing of sediment downhole. However, excessive noise was recorded on the sonic log, possibly a result of the bare calipers dragging on the basalt. The sonic combination tool was withdrawn from the hole and rerun (1000–1430Z) without centralizers in combination with the dual induction and gamma logs. Good logs were recorded from the latter, but the noise problem remained on the sonic. The density-neutron gamma combination was made up between 1430 and 1545Z, but the density tool was found to be unserviceable. The density tool was rechecked, and the cable head changed between 1600Z and 1845Z without effect. Meanwhile, new pads had been mounted on the sonic centralizers and the sonic-gamma-caliper tool was run successfully between 1845 and 2245Z. The "noise" encountered previously may have been the natural rapid and great variation in velocity within and between the basalt flows. As the density log was still inoperable, the temperature log was run between 2245 and 2400Z, 25 August, pending attempts to repair the density tool by the electronic technicians. The temperature log run was successful, and the recorded total depth of 2991.6 m indicated little infill of the hole. Since the density log was still inoperable, a gamma-neutron combination run was made at 0245Z, 25 August, and completed successfully by 0715Z. Successful repairs in the density tool had been made in the interim thanks to the diligent efforts of the technicians, and the gamma-density-neutron logging run was successfully made between 0905 and 1230Z, 25 August, thus completing the logging program in Hole 553A. Logging equipment was set down between 1230 and 1310Z and pipe pulled back to the mudline, thus completing Hole 553A.

Hole 553B

After clearing the mudline and picking up the Bowen sub, the collet was run-in prior to starting to HPC. Hole 553B was offset some 100 ft. north of Hole 553A. Between 1500 and 1700Z the 9.5 m VLPHC was made up and first shot at 1700Z. The barrel pulled hard out of the collet, and the seals were apparently leaking. Inspection of the HPC on deck indicated that it did not scope. Between 1700 and 1815Z, the HPC was run in hole again. This time the tool did not pressure up and line pulls in excess of 11,000 lbs. failed to unseat the tool. Eventually the sandline parted 250 ft. from the rope socket, resulting in the loss of about 3500 ft. of sand line and requiring a complete trip. The rig floor was reached at 0000Z, 26 August. Considerable force was required to dislodge the collet head sub from the HPC barrel. On inspection, it was found that two deep gouges in the collet space had kept the collet from seating the final 2 in. A new HPC seal sub was made up and pipe run in hole again by 0630Z. The first barrel was shot at 0700Z but came out of the hole with the bottom part of the tool missing. A second 9.5 m barrel was rigged and a first core cut at 0915Z, 26 August. As this core failed to establish the mudline, a second core was cut after pulling back one joint but it yielded only water. A third attempt to cut a mudline core at 1120Z was finally successful, yielding a 4.62 m core. To adjust lengths, the drill pipe was pulled back and Core 2 was cut between 2337.5 and 2347.0 m, yielding a third core also at or just below the mudline. After these diversions, continuous HPC began in earnest. However, as Core 5 was being cut at 1536Z, 26 August, the barrel could not be unseated. Attempts to unseat the barrel by pulling on the sand line failed, and the overshot pin sheared at 1630Z. In an attempt to free the barrel, jars and sinkers were rigged on the sand line and two attempts were made to loosen and retrieve the barrel. Both failed and at 1900Z, 26 August, pipe was pulled clear of the mudline, thus completing Hole 553B. Subsequent investigation showed that the core barrel had jammed in the bit disconnect but the cause remains unknown. The rig floor was reached at 2335Z and secured by 0134Z, 27 August, when *Glomar Challenger* departed for Site 554.

During these unfortunate events, full consideration had been given to fishing for the bit. In view of the lack of suitable tools on board and the impact of a prolonged fishing operation on an already delayed program, it was decided to abandon the operation. In the case of the HPC program, the same time consideration did not justify a further attempt that would require at least 24 hr. It was therefore decided to proceed to Site 554 to continue with the drilling program.

SEDIMENT LITHOLOGY

Site 552

The section drilled to 282.7 m at Site 552 can be divided into four principal sedimentary units, distinguished from each other on the basis of composition, texture, and sedimentary structures. Units II and IV are further subdivided into two and four subunits, respectively. The lithologic divisions are summarized in Table 2 and Figure 8. The sub-bottom depths for Units I, II, III, and the top of IVa are taken from Hole 552A data rather than from the Hole 552 depths, which are approximately 12.5 m too shallow as a result of operational errors (see Operations section). Hole 552 was washed to 108.0 m, whereas Hole 552A was hydraulically piston cored to 183.5 m. *The two holes have been treated together.* Smear slide data are given in Appendix A to this chapter.

Unit I: Cores 552-1 and 552A-1 to 552A-9 (0 to 44 m sub-bottom, 44 m thick). Age: Quaternary to late Pliocene.

This uppermost unit is characterized by alternating beds of foraminiferal–nannofossil ooze and calcareous marls and mud and extends from the seafloor to a depth of 44 m. The base of this unit is defined by the lowermost marl, which is also the base of high magnetic intensity in the sediments. This unit was continuously cored using the HPC, resulting in almost 100% recovery. Most of the cores were undisturbed, thus excellently preserving the detailed sedimentology of the unit. Preliminary analysis of the sediments recovered at this hole suggest that the section represents the most complete Pliocene–Pleistocene record recovered to date at a high latitude North Atlantic location.

One of the most striking characteristics of these sediments is their cyclicity of color and carbonate content (Fig. 9). The color cycles are clearly coupled with carbonate content (on board $CaCO_3$ bomb analyses), the lighter shade correlating with high carbonate values. The calcareous oozes in general have a sharp base and then grade up into the overlying marl and calcareous mud. The marl and calcareous mud layers are various shades of olive gray and brown (5Y 4/2 and 10YR 5/3) and represent glacial periods, whereas the calcareous oozes are shades of white and light gray (N9 and 5Y 7/1) and represent the interglacials (Zimmerman et al., this volume). The only exception to this repetitious sequence is a 3 cm thick vitric ash layer at 23 m (Section 5-3) consisting of dark glass with minor feldspar crystals and light glass. This layer possibly arises from a large eruption on Iceland and can be correlated with the ash found at Site 404 at 28 m. In several cycles the boundary between the layers is gradational with bioturbation causing a mottled zone averaging 10 cm in thickness. Burrowing also occurs within the layers but is less distinct because of their homogenous initial composition. Laminated sediment is rare in this subunit; however, thin beds (1 to 5 cm) of foraminiferal ooze, nannofossil ooze, foraminiferal mud, and silty mud occur in both parts of the cycles. This variation in lithology reflects the differing ratios of foraminifers: nannofossils: terrigenous clay-silt and may be the result of winnowing by bottom currents.

The bulk of the noncarbonate component is either clay minerals or coarser terrigenous particles. The detailed composition is listed in Appendix A and in the results of X-ray diffraction analyses. The XRD data from bulk samples clearly distinguish the cycles on the basis of clay mineralogy. The clay that is present in the calcareous oozes is predominately smectite whereas in the marls and muds the clay minerals illite, kaolinite, and chlorite dominate with a smaller proportion of smectite. Detrital quartz and feldspar are also present throughout the unit, although they are more abundant in the marls and muds than in the calcareous oozes. Cobbles, pebbles, granules, and sand-size terrigenous particles are common throughout, and their abundance distinguishes these sediments from the underlying unit. The larger particles are rock fragments of a wide range of lithologies (igneous, metamorphic, and sedimentary) whereas the sand particles are either quartz, feldspar, heavy minerals, or mica. The pebbles and the few cobbles sampled are dropstones and many are well faceted, indicating abrasion during ice transport.

Minor particles in the coarse fraction (greater than 62 μm) include rare radiolarians, diatoms, opaline sponge spicules, benthic foraminifers, ostracods, echinoid spines, and fish debris. The echinoid spines are of the irregular variety belonging to sediment-burrowing species; these

Table 2. Lithologic units, Site 552.

Unit	Lithology	Sub-bottom depth (m) 552	552A	Thickness (m)	Sedimentation rate (m/m.y.)	Age	Core-Section Hole 552	Hole 552A
I	Foram-nanno ooze interbedded with foram-nanno marl and calcareous mud. Terrigenous dropstones common; volcanic ash layer present.	0–?	0–44.00	44.00	14	Quaternary to late Pliocene	1-1 to 1,CC	1-1 to 9,CC
IIa	Foram-nanno ooze and nanno ooze with minor biosiliceous nanno ooze and nanno-foram ooze; becomes chalk below 142 m in Hole 552A.	?–155.50	44.0–168.50	126.50	25 to 6	late Pliocene to mid Miocene	2-1 to 7,CC	9,CC to 35,CC
IIb	Glauconitic nanno-foram chalk.	155.50–160.40	168.50–172.90	4.40	6	middle Miocene	8-1 to 8-4, 45 cm	36-1, to 36-3, 140 cm
III	Foram-nanno chalk with Mn nodules at base and clasts from underlying unit.	Absent	172.90–174.20	1.30	<1	early Oligocene		36-3, 140 cm to 37-1, 75 cm
IVa	Nanno chalk, zeolitic mudstone, biosiliceous mudstone, minor volcanic tuff, spiculiferous foram-nanno chalk. Calcareous porcellanite and chert at base.	160.40–193.50	174.20–183.50	33.10	48	middle Eocene	8-4, 45 cm to 11,CC	37-1, 75 cm to 38
IVb	Calcareous biosiliceous tuff and vitric tuff. Minor glauconitic spiculite, tuffaceous biosiliceous chalk, biosiliceous tuff and mudstone.	193.50–241.00		47.50	48	early Eocene	12-1, to 16,CC	
IVc	Glauconitic nanno chalk, biosiliceous marlstone and siliceous mudstone. Minor calcareous biosiliceous claystone, calcareous diatomite, calcareous porcellanite and volcanic tuff.	241.00–282.30		41.30	48	early Eocene	17-1 to 21-3, 30 cm	
IVd	Ferruginous diatomaceous claystone.	282.30–282.70		0.40	48	early Eocene	21-3, 30 cm to 21-3, 70 cm	
V	Basalt	282.70–314.00		31.30+		probably early Eocene	21-3, 70 cm to 25	

are probably responsible for at least part of the bioturbation in this unit.

The sediment in this unit is unlithified, although some diagenesis has occurred. In particular some darker olive-colored layers contain authigenic pyrite concentrations, minor amounts of glauconite, and rhombs of authigenic dolomite.

The cyclical nature of these sediments is clearly reflected in the carbonate content. The carbonate ($CaCO_3$) content fluctuates between the extreme values of 4 to 8% for the mud and 80 to 92% for most of the calcareous oozes. The variation in carbonate represents a local combination of factors: productivity of calcareous organisms and dilution by noncalcareous sediment. Dissolution after deposition is probably not significant here.

One of the most fascinating features of these sediments is the abruptness with which the cycles begin at about 2.5 m.y. ago. Preliminary examination of carbonate curves from the Caribbean (HPC Site 502) indicate that climatic cycles extend back through the early late Miocene. Although the curve for the North Atlantic suggests cyclic phenomenon prior to 2.5 m.y. ago, the signal is weak; carbonate content fluctuates in a very narrow range around 90%.

From the point of initiation of the cyclical sedimentation to about 1.4 m.y. ago, the Hole 552A data show a high amplitude glacial signal of short duration with long intervening periods of high rates of carbonate deposition. During this time, therefore, Northern Hemisphere glaciation may have been intense but of short duration.

For the time period of the Brunhes to the present, the North Atlantic carbonate and equatorial Pacific oxygen isotope curves (core V28-239, Shackleton and Opdyke, 1976) may be directly correlated with the Hole 552A curve (Zimmerman et al., this volume), indicating that

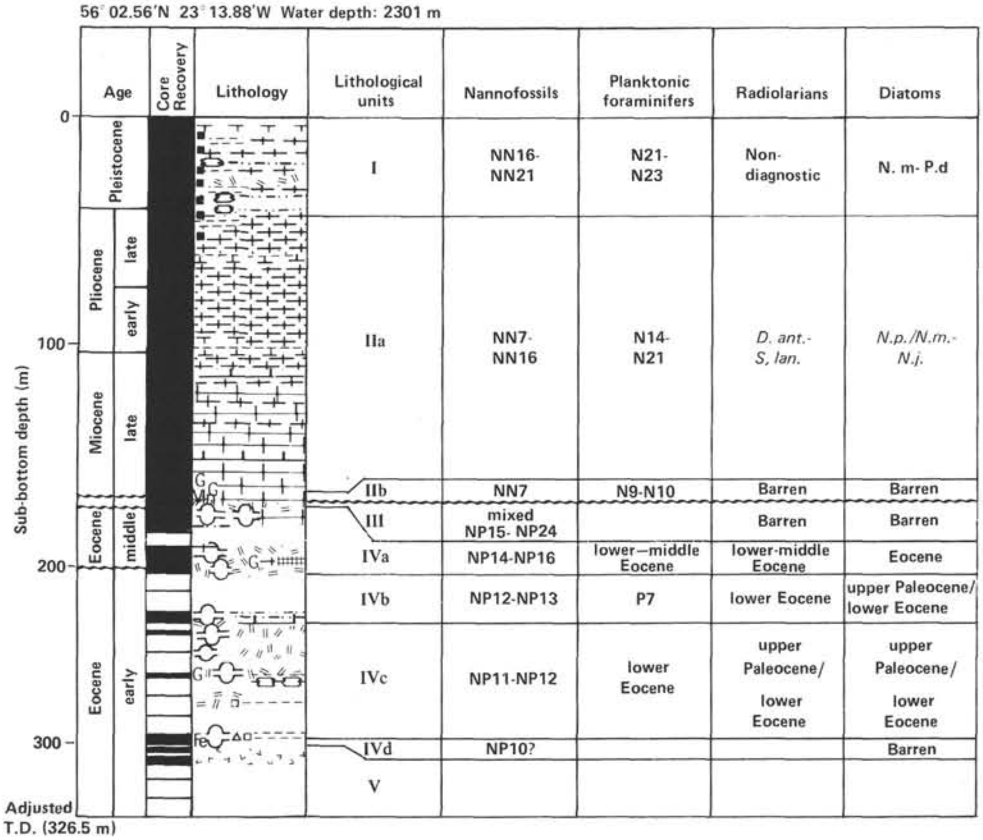

Lithological units	Nannofossils	Planktonic foraminifers	Radiolarians	Diatoms
I	NN16-NN21	N21-N23	Non-diagnostic	N. m- P.d
IIa	NN7-NN16	N14-N21	*D. ant.- S, lan.*	*N.p./N.m.- N.j.*
IIb	NN7	N9-N10	Barren	Barren
III	mixed NP15- NP24		Barren	Barren
IVa	NP14-NP16	lower—middle Eocene	lower-middle Eocene	Eocene
IVb	NP12-NP13	P7	lower Eocene	upper Paleocene/ lower Eocene
IVc	NP11-NP12	lower Eocene	upper Paleocene/ lower Eocene	upper Paleocene/ lower Eocene
IVd	NP10?			Barren
V				

Figure 8. Lithologic and biostratigraphic summary of Holes 552 and 552A. Depths in Hole 552 have been adjusted downward by 12.5 m to correlate with Hole 552A (see Operations summary for details).

the climatic behavior of the world ocean and that of the North Atlantic are linked. The relatively small offsets in peaks are probably effects of varying rates of deposition (more likely in the North Atlantic) and disturbance between sections of the HPC.

Climatic events appear to be the predominant forcing function for both carbonate and isotope fluctuations in oceanic sediment of the Quaternary (Cline and Hays, 1976). In HPC cores from Hole 552A we have for the first time, a high resolution record of the history of these fluctuations in the North Atlantic Ocean.

Unit II: Core 552-2 to Sample 552-8-4, 45 cm; Samples 552A-9,CC to 552A-36-3, 140 cm (44 to 172.9 m sub-bottom, 128.9 m thick). Age: late Pliocene–middle Miocene.

Subunit IIa: Section 552-2-1 to Sample 552-7,CC; Samples 552A-9,CC to 552A-35,CC (44 to 168.5 m sub-bottom). Age: late Pliocene–middle Miocene.

This subunit consists of relatively uniform foraminiferal–nannofossil ooze (chalk) and nannofossil ooze (chalk) over its entire interval (44 to 168.5 m sub-bottom). The subunit has a minor (about 10%) but persistent component of biogenic silica from sponges, radiolarians, and diatoms. The dominant color is bluish white (5B 9/1) and white (5Y 8/1). There are faint color cycles at th top of this subunit in Cores 552A-10 and 11 (44 to 55 m), but there is no variation in detrital input or magnetic intensity, and the carbonate content remains at more than 90% throughout the subunit. This is in contrast to the fluctuating carbonate content in the overlying sequence. The base of this subunit is gradational with an increase in abundance of foraminifers and gradually increasing occurrences of glauconite. The base lies within the middle Miocene (NN9) Zone in Hole 552A but coincides with a hiatus between the late (NN10) Miocene and middle (NN6) Miocene in Hole 552.

Laminations are abundant in Cores 552A-11 to 29 but are rare or absent in the base of the subunit (Cores 552A-30 to 36). The laminations are recognized by color (light bluish gray, 5B 7/1, and light greenish gray, 5G 8/1) and only rarely were compositional or textural variations observed (Fig. 10). Some of the laminae (Cores 552A-14 and 18) are sandy (foraminifer-rich) and may represent current winnowing of the sediment. Bioturbation is minor to moderate throughout but is insufficient to destroy the laminations. In Core 552A-26 large burrows with a diameter of 1 cm are present which are infilled with sediment from a layer 1 m above.

Besides planktonic foraminifers the coarse fraction contains rare benthic foraminifers, ostracods, echinoid spines, fish debris, and trace amounts of volcanic glass. A few dropstones were present in Cores 552A-10 and 11. Bulk X-ray diffraction (XRD) analyses show, besides biogenic calcite, minor amounts of detrital quartz and smectite.

The most important diagenetic alteration in this subunit is the transition from calcareous ooze to chalk. The first appearance of chalk laminae (less than 1 cm thick)

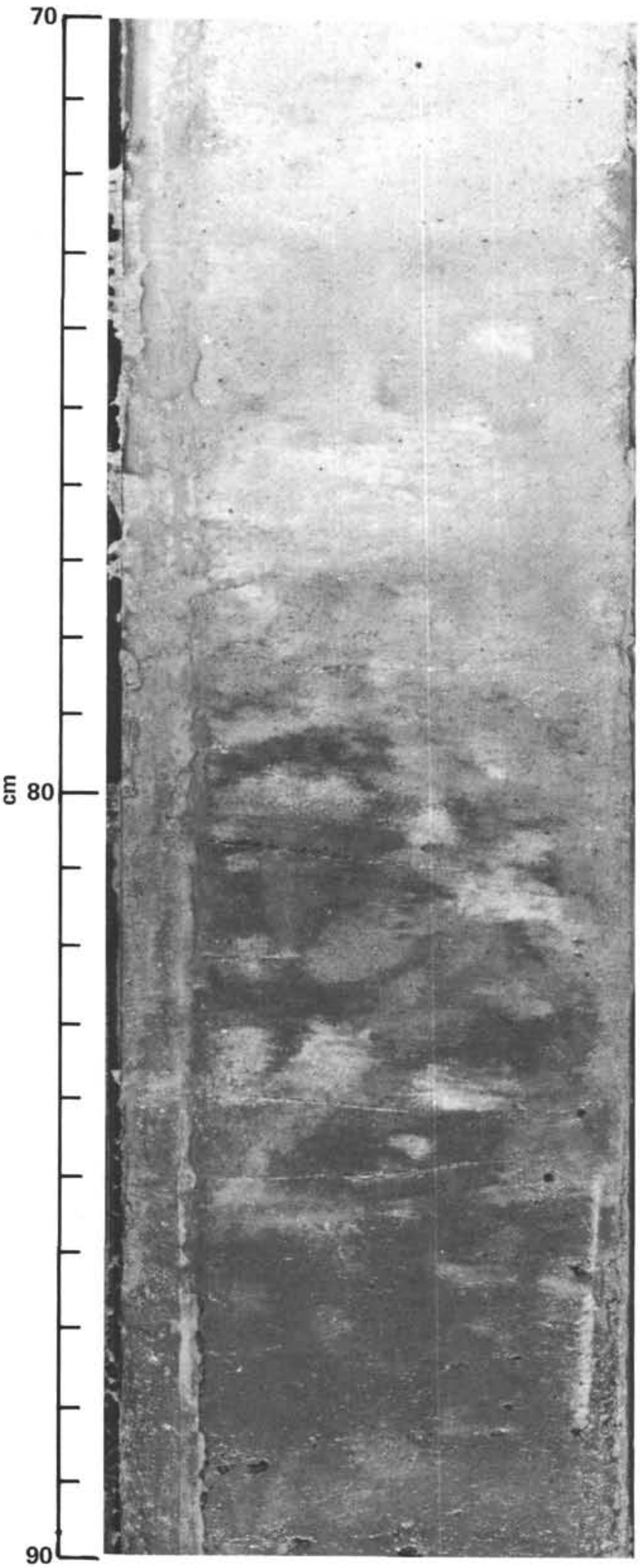

Figure 9. Sharp transition from calcareous mud to foram-nanno ooze (Sample 552A-7-2, 70–90 cm). Similar contacts characterize the glacial–interglacial transitions throughout the Pliocene–Pleistocene section.

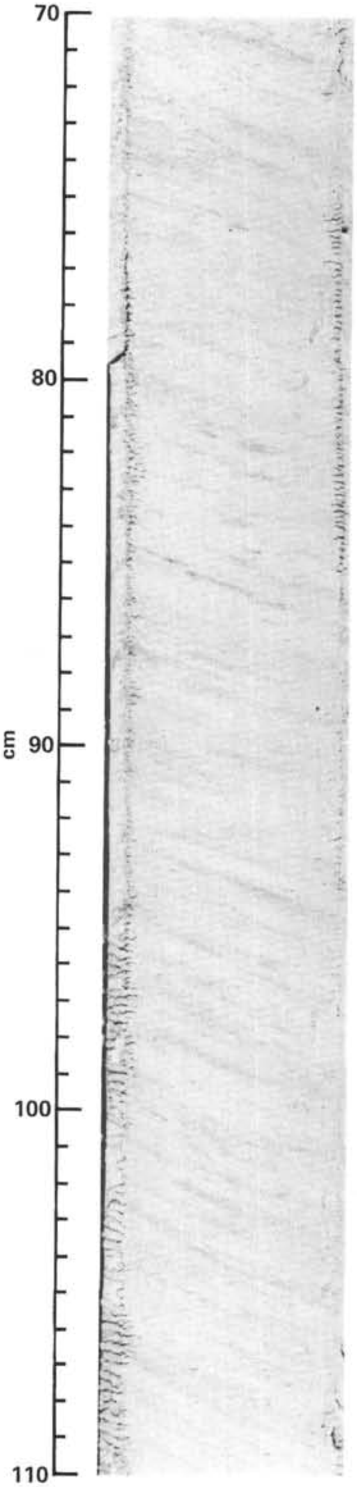

Figure 10. Light bluish-gray to light greenish-gray laminae characteristic of Subunit IIa (Sample 552A-23-2, 70–110 cm).

occurs in Section 552A-25-1 at a depth of 114 m and below this depth chalk becomes more common. Below 142 m (Section 552A-30-3) most of the sediment could be considered lithified enough to be termed chalk. The chalk is formed by compaction and the precipitation of calcite both as a cement and as overgrowths on nannofossils.

Another diagenetic effect in this subunit is the common occurrence of authigenic pyrite generally associated with burrows. The pyrite forms black or greenish halos around the larger burrows and has infilled other burrows.

Subunit IIb: Section 552-8-1 to Sample 552-8-4, 45 cm; Section 552A-36-1 to Sample 552A-36-3, 140 cm (168.5 to 172.9 m sub-bottom). Age: middle Miocene.

When compared with the overlying sequence this basal subunit is richer in foraminifers, lacks laminations, and contains abundant glauconite. The subunit is only 4.4 m thick but represents a distinct subfacies in this pelagic unit. The top of this subunit is 3 m below a brief hiatus in Hole 552A, but coincides with the hiatus in Hole 552. The base is also defined by a significant unconformity (Fig. 11). The lithology grades from a nannofossil–foraminiferal chalk down into a glauconitic foraminiferal chalk with minor biosiliceous chalk. The color is white (10YR 8/1), becoming yellowish gray (5Y 8/1) and dark olive gray (5Y 3/2) as the glauconite content increases. The subunit is well burrowed throughout, giving the sediments a mottled appearance.

The carbonate content decreases from 94% at the top to 53% at the base, reflecting the increase in glauconite and biogenic silica (predominately sponge spicules with some radiolarians). There are minor amounts of feldspar, light-colored volcanic glass, benthic foraminifers, ostracods, echinoid spines, and fish debris.

There are three possible origins for the Miocene glauconites at this site and at Site 553, as discussed by Morton et al. (this volume):

1. Derivation by reworking of Eocene glauconite.
2. Glauconite formation taking place during the Miocene, but in relatively shallow water, with subsequent transportation to the present site of deposition.
3. Glauconite formation taking place during the Miocene in deep water, without significant input from elsewhere.

The dating of the glauconite as middle Miocene (15.8 ± 0.8 m.y. ago at Site 552 and 16.2 ± 0.9 m.y. ago at Site 553) and the difference in chemistry between the Eocene and Miocene glauconites (Morton et al., this volume) argues strongly against the first alternative. The absence of shallow water benthic foraminifers in the subunit (Murray, this volume) argues against the second. It is therefore considered that the Miocene glauconites at Sites 552 and 553 are of deep water origin, developed in response to periods of slow or nondeposition during the early and middle Miocene related to strong bottom-water currents.

Unit III: Samples 552A-36-3, 140 cm to 552A-37-1, 75 cm; absent in Hole 552 (172.9 to 174.2 m sub-bottom, 1.3 m thick). Age: early Oligocene.

This unit is bounded by hiatuses and represents a condensed section of Oligocene–late Eocene sediments. The absence of this unit in Hole 552 may reflect mechanical removal by the drilling, since it is a relatively soft chalk with more lithified strata above and below. Alternatively the Oligocene may be laterally discontinuous on an irregular Eocene surface. In the HPC Hole 552A the entire unit was sampled.

The unit consists of a foraminiferal–nannofossil chalk grading down into a chalk containing intact, and broken, manganese nodules (Fig. 12) together with angular clasts (up to 5 mm) of the underlying unit. The chalk is colored pale yellow (5Y 7/3) to very pale brown (10YR 8/3) with burrow mottling in its lower part.

The upper contact is sharp but uneven, with glauconitic sediment burrowed in from the overlying unit. The burrows are up to 3 cm in diameter. The exact position of the underlying contact is less distinct as a result of intense burrowing and abundance of eroded mud clasts (Fig. 13).

The manganese nodules contain nuclei of lithified Eocene volcanogenic sediment (Despraires et al., this volume) and probably represent a period of relatively slow deposition, but the occurrence of NP22 both above and below the nodule suggests it formed in a relatively short time.

The carbonate content of the upper part of this unit is 88% but is less in the lower part where manganese nodules and lithoclasts are more common. Also in the coarse fraction are minor amounts of sponge spicules, and fish teeth. Benthic foraminifers are more abundant than in the overlying units.

Unit IV: Samples 552-8-4, 45 cm to 552-21-3, 70 cm; Section 552A-37-1 to Core 38 (160.4 to 282.7 m sub-bottom, 122.3 m thick [Hole 552 depths]). Age: middle to early Eocene.

This unit is characterized by the accumulation of biogenic silica and volcaniclastic sediment in a relatively shallow-water marine environment and overlies basalt. There is a noticeable scarcity of terrigenous detritus throughout. It can be subdivided into four subunits based on the relative abundances of biogenic silica and volcaniclastic particles as well as sediment texture. Because of relatively poor recovery the boundaries between the subunits are only approximately located.

Subunit IVa: Samples 552-8-4, 45 cm to 552-11,CC; Sample 552A-37-1, 75 cm to total depth (160.4–193.5 m sub-bottom). Age: middle Eocene.

This subunit is approximately 15 m thick and consists of zeolitic mudstone, biosiliceous mudstone, spiculite, porcellanite, and chert. There is a minor amount of chalk and volcanic tuff. The upper 9 m of this subunit was completely recovered by HPC, and sedimentary structures are beautifully preserved. The lower part of the section, however, was poorly sampled by rotary drilling because of the presence of chert. The base of the subunit is defined by the lowermost occurrence of chert. The principal color of the subunit is various shades of brown and olive (2.5Y 8/4, 2.5Y 7/4, 2.5Y 6/4, 2.5Y 3/2, and 10YR 5/4).

The carbonate content varies from zero in the zeolite mudstone to 25% in the biosiliceous layers and over 60% in the chalks. The most abundant particles are nannofossils and sponge spicules with a large variety of minor particles: radiolarians, diatoms, foraminifers, mollusk fragments, fecal pellets, basaltic glass, feldspar, heavy minerals (augite, iddingsite), and clay minerals. XRD analyses have enabled a distinction to be made between one clay mineral suite at the top of the subunit and an-

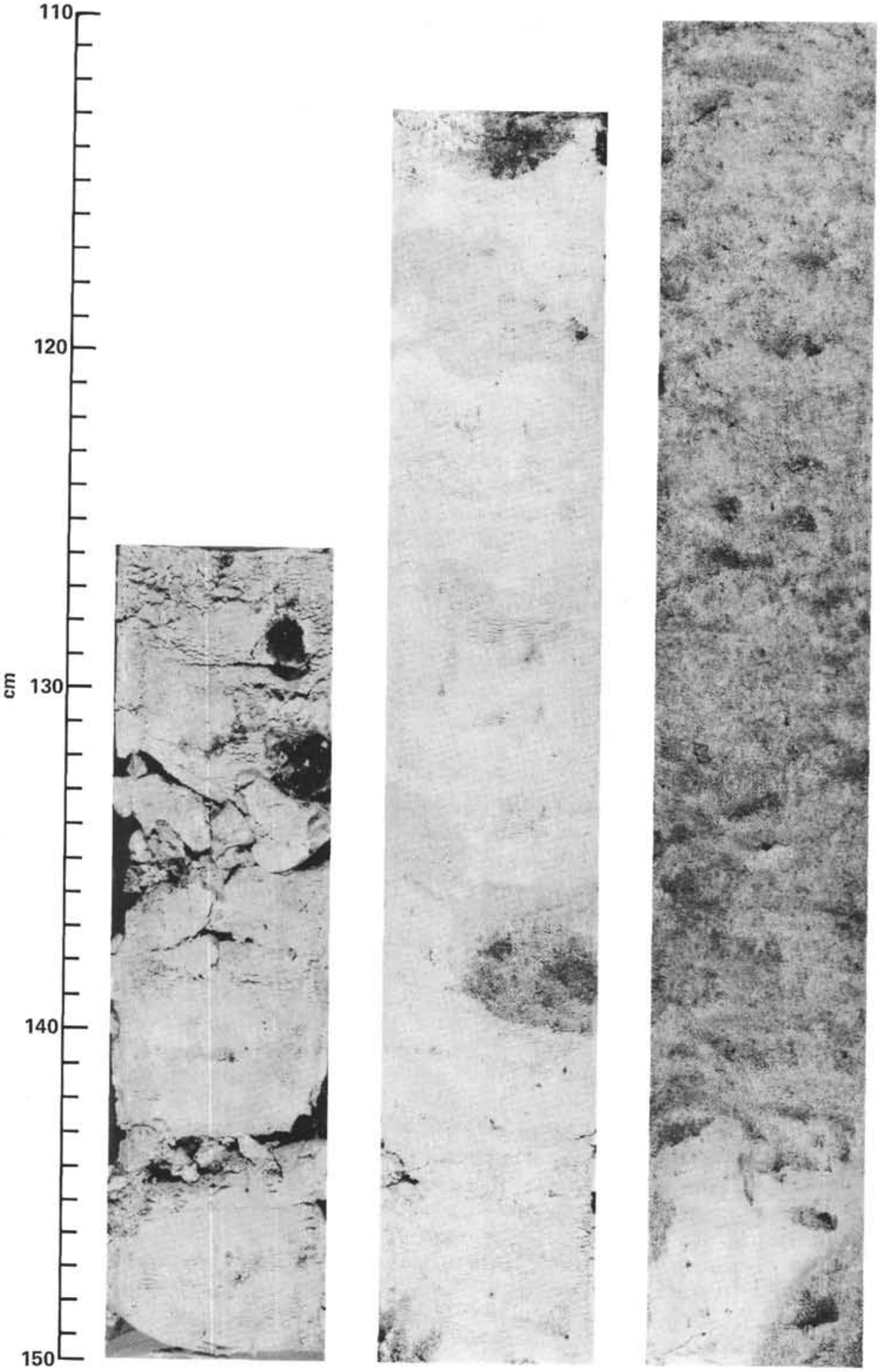

Figure 11. Contact between glauconitic chalk of Subunit IIb (mid Miocene) and foraminifer–nannofossil chalk of Unit III (Oligocene) (Sample 552A-36-3, 4 cm).

other below. The upper suite, just below the unconformity, contains a concentration of smectite with illite and kaolinite, which may represent terrigenous detritus. Below is a suite consisting of smectite and illite (perhaps glauconite) which may be authigenic. The smectite could be from the devitrification of the volcanic glass. The following authigenic phases are also present: zeolite (clinoptilolite), calcite, opal-CT, quartz and minor pyrite, and dolomite.

The sedimentary structures include vertical and horizontal burrows (*Zoophycus, Chondrites*, and others), fine-scale laminae, lenticular bedding, and ripple-drift cross-lamination. There is also a fairly high proportion of mud intraclasts. Some thin (1 cm) beds of almost

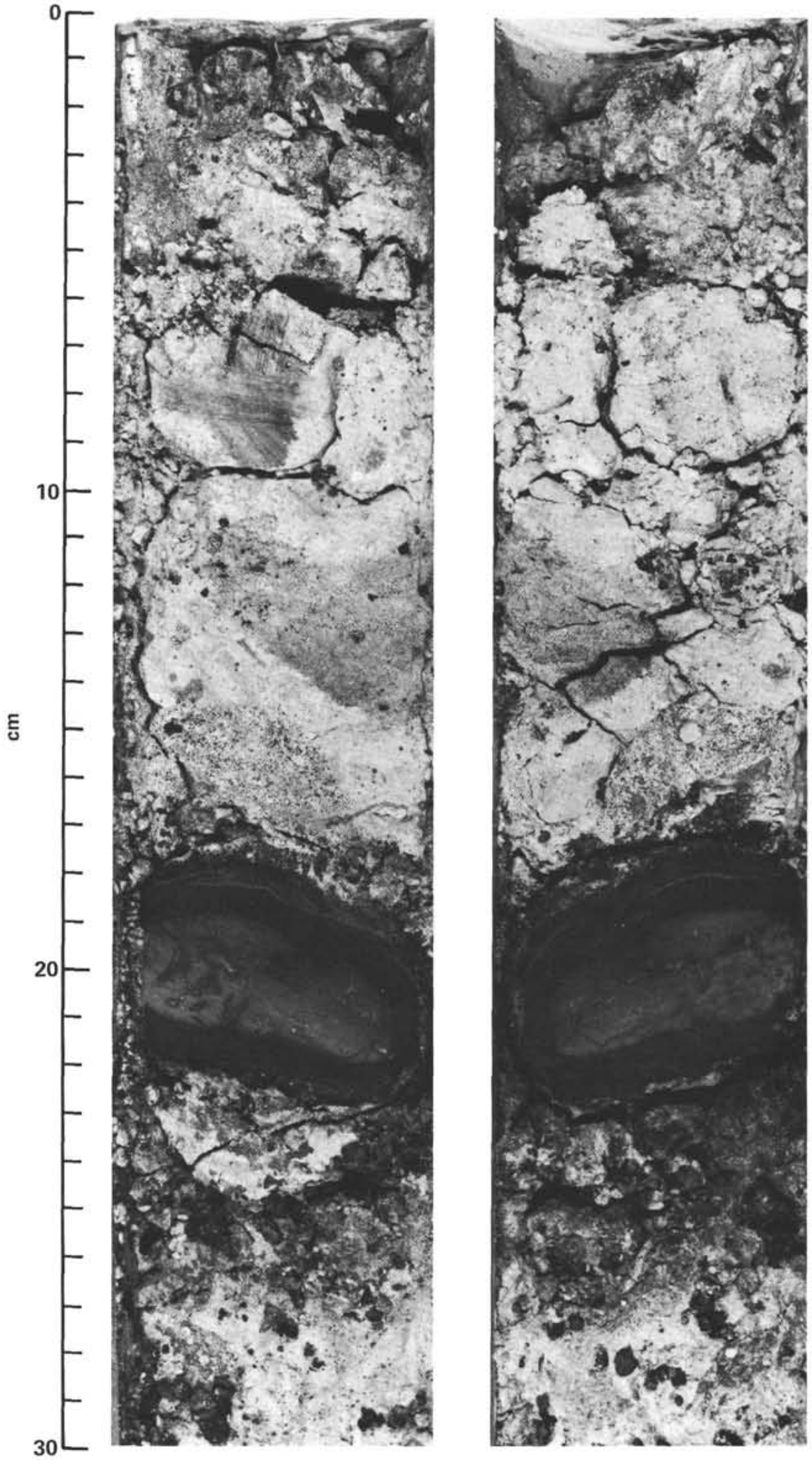

Figure 12. Manganese nodule and clasts in condensed sequence of Unit III (Sample 552A-37-1, 0–30 cm).

pure sponge spicules may be the result of winnowing by bottom currents.

The diagenesis of this subunit is quite complex. The upper part has two unusual diagenetic features which may be associated with the unconformity. The first is the development of features which resemble stylolites in the mudstone and between the mudstone and chalk layers. These may, in fact, be fractures and bedding planes along which manganese oxide has precipitated. The second is the formation of euhedral quartz crystals and authigenic carbonate as fracture fillings in the mudstone. Both these features require further study. Diagenesis is

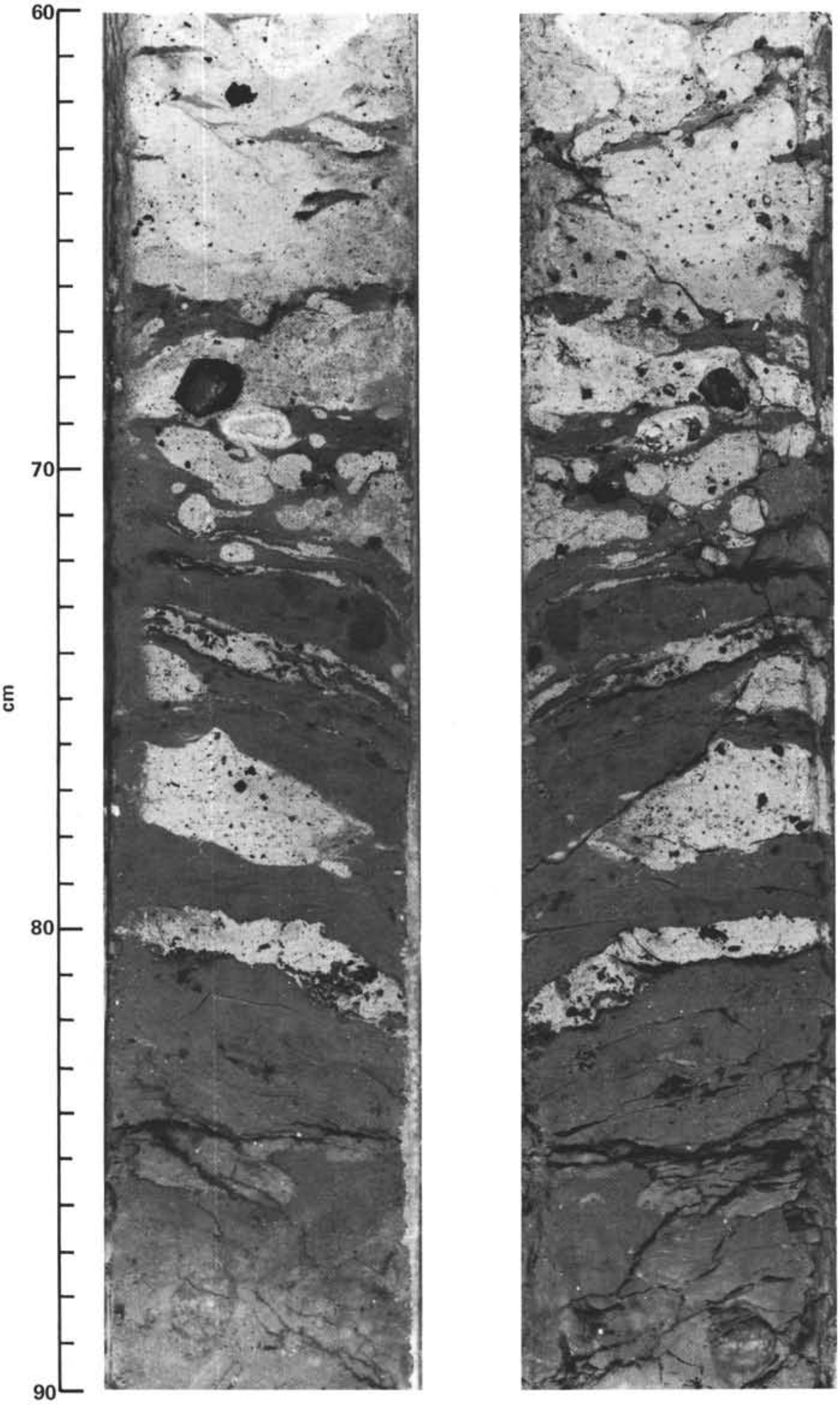

Figure 13. Contact between Units III and IV showing burrowing, clasts, and soft-sediment deformation (Sample 552A-37-1, 60–90 cm).

also evident in the volcanic ash near the unconformity. It has lithified to form a tuff and the glass has devitrified with the formation of zeolites and possibly opal.

The porcellanite and chert occurs in Cores 552-9 and 10 near the base of the unit. The chert is bedded and probably represents silicified sponge spicule layers and tuffaceous interbeds.

Subunit IVb: Section 552-12-1 to Sample 552-16,CC (193.5 to 241.0 m sub-bottom). Age: early Eocene.

This subunit is 47.5 m thick and consists primarily of volcanogenic sediments with some biogenic calcareous and siliceous input. It is distinguished from the units above and below by the abundance of volcanic ash and lapilli, the well-preserved biogenic silica, and the lack of chert. The color of this unit is a distinct olive black (5Y 2/1) to brownish black (5YR 2/1), becoming more olive gray (5Y 3/2, 5Y 4/1) towards the base.

The principal lithologies are vitric volcanic ash, calcareous and biosiliceous volcanic ash, glauconitic spiculite, tuffaceous biosiliceous chalk, and biosiliceous tuffaceous mudstone. Truly pyroclastic layers of ash are rare since most of the ash is mixed with biogenic material. The carbonate content of these lithologies is generally less than 15% but is variable depending on the nannofossil and foraminiferal input. Sponge spicules are again the most abundant form of biogenic silica. The volcanic glass is of basaltic composition and is frequently unaltered; lapilli up to 10 mm in size are common. Detrital quartz is very rare in these sediments but augite, iddingsite, and feldspar occur commonly and are less abundant in the ash layers than in the surrounding sediment.

The sediments are generally well bedded with sharp contacts; laminated sediment is common. Ripple-drift cross-laminae are present in a few silty layers. The amount of bioturbation varies through the unit from intense to minor with distinct reaction rims present around some burrows. The presence of intraclasts, small microfaults, and some contorted bedding suggests some syndepositional instability on the seafloor.

Below Core 552-14 (213 m) the sediments become more lithified as a result of silicification and calcification.

Subunit IVc: Section 552-17-1 to Sample 552-21-3, 30 cm (241 to 282.3 m sub-bottom). Age: early Eocene.

Between Cores 552-17 and 18 there is a gradual change to a less volcaniclastic group of lithologies. Calcareous and biosiliceous mudstones and claystones become dominant with a relatively minor tuffaceous component. The colors vary from dark gray (10YR 4/1) to shades of greenish gray (5GY 6/1). Minor lithologies are glauconitic nannofossil chalk, biosiliceous marlstone, calcareous diatomite and porcellanite. The base of this subunit is defined by the top of the reddish ferruginous layer above the basalt.

Sedimentary structures are similar to the previous subunit and include burrows, slump folds, microfaults, laminations and intraclasts.

In the coarse fraction, benthic foraminifers are relatively abundant together with ostracods, echinoid spines, and bryozoan and gastropod fragments. The dominant biogenic particles are still sponge spicules and nannofossils with lesser amounts of planktonic foraminifers, radiolarians, and diatoms. Heavy minerals are less abundant than in Subunit IVb. Clay is relatively abundant in this subunit and XRD analyses show it to be a well-crystallized smectite, probably derived from diagenetic alteration of volcanic ash. The XRD analyses also show that some of the claystones are silicified by opal-CT (disordered cristobalite).

Subunit IVd: Samples 552-21-3, 30 cm to 552-21-3, 70 cm (282.3 to 282.7 m sub-bottom). Age: early Eocene.

This subunit consists of 45 cm of ferruginous diatomaceous claystone overlying the basalt at this site. It is dark reddish brown (10YR 4/2) in color and consists of calcite, opal-CT, well-crystallized smectite (saponite), and iron oxide with rare volcanic glass, zeolite and pyrite. It contains nannofossils, diatoms and sponge spicules. The biogenic opal has been recrystallized to opal-CT. This layer is well lithified by silica and carbonate cements and contains no obvious sedimentary structures.

The presence of marine organisms directly above the basalt suggests that the flow was submarine as does a small pebble exhibiting chilling which may be a small pillow (Fig. 14). This subunit is an oxidized layer that is probably related to the alteration of the basalt. Whether this alteration and cementation occurred at high or low temperatures is unknown. Heat from the cooling flow may have aided the recrystallization of the biogenic opal in this layer. In the immediately overlying layers, the biogenic opal is still X-ray amorphous and isotropic.

Site 553

The sequence drilled at Site 553 has been divided into five lithological units; I to IV are composed of sediments and V consists of igneous rocks. Units II and IV are further subdivided into two and six sub-units respectively (Table 3; Fig. 15). The units and subunits recognized on a lithological basis can also be recognized on the sonic-gamma logs (Fig. 16), although some boundaries show slight depth discrepancies (up to 5 m). The core depths and lithological descriptions of the units are summarized in Table 3 and the smear slide data in Appendix B.

Unit I: Core 553-1; Section 553B-1-1 to Sample 553B-4,CC (0–60 m sub-bottom). Age: Quaternary to late Pliocene.

Unit I is characterized by cyclic sedimentation, with alternations of foraminiferal or nannofossil–foraminiferal oozes with mud or calcareous mud. The calcareous oozes have sharp lower contacts (although bioturbation locally obliterates the contact) and grade upwards through marl into the calcareous muds or muds. The cored interval is unfortunately intensely disturbed by drilling, which caused difficulty in recognition of individual cycles.

Nevertheless, the site yielded additional information on the character of the cycles and, in particular, the relationships of dropstone occurrence to sediment type. In Hole 552 dropstones appeared to be equally common in the calcareous (interglacial) sediments as in the terrigenous (glacial) sediments, but at Hole 553B this was not the case: dropstones were conspicuous only in the terrigenous part of the cycle. The definition of the cycles was also better at Hole 553B (although drilling disturbance has obliterated several contacts); burrowing at the base of cycles in Hole 552A regularly caused mottling and partial homogenization over a 10 cm zone. This has occurred to a lesser extent in Hole 553B, possibly because of the higher sedimentation rate.

The cycles are not only defined on a compositional basis, but also on color and texture. The calcareous sediments are pale, ranging from white (2.5Y 8/2, 5Y 8/1), through bluish white (5B 9/1), to light gray (2.5Y 7/2, 5Y 7/1, N8), whereas the muds are in shades of brown, olive or dark gray: light olive brown (2.5Y 5/4) and ol-

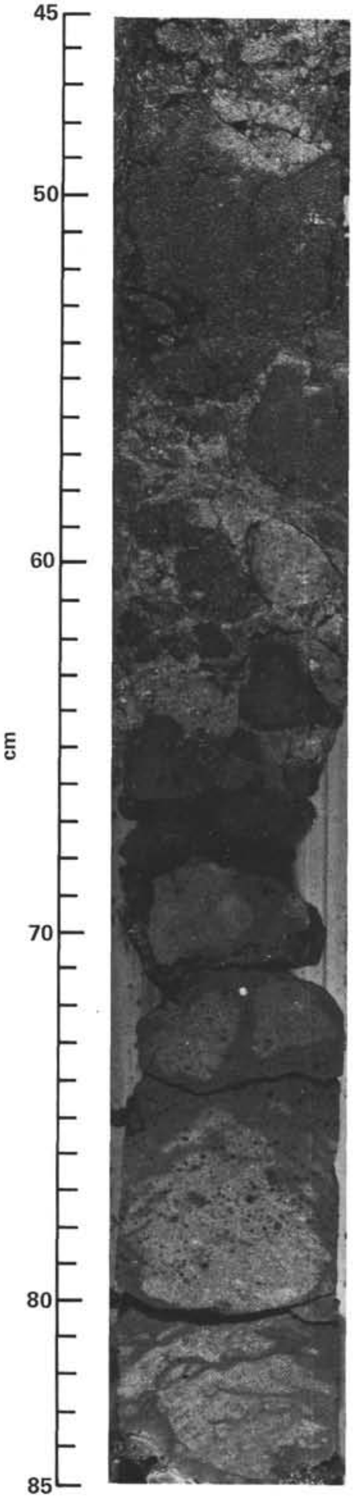

Figure 14. Contact between Subunit IVd and underlying basalt (Sample 552-21-3, 45–85 cm).

ive gray (5Y 5/2) predominate. Texturally the calcareous sediments are sands or sandy muds as a result of their high foraminifer content; the muds are dominantly clay-grade but contain common coarse granule, gravel, or cobble-sized clasts. These dropstones are variable in composition, faceted quartzites, amphibolites, and slate being the most common. One clast of marl proved to contain nannofossils indicative of a Maestrichtian age, and in one mud unit in Cores 1 and 2 abundant clasts of pumice were found. Sand (quartz, feldspar, heavy minerals, and mica) is common throughout, but is again more abundant in the mud and calcareous mud horizons.

Carbonate content fluctuates widely throughout the unit, with low values (5–20%) for the terrigenous layers, high values (70–85%) for the oozes, and intermediate values for the transitional sediment types (e.g., marls). The carbonate variations reflect both changes in productivity and terrigenous input; dissolution effects are probably minor.

Minor components of the sediments include diatoms, radiolarians, and sponge spicules, according to smear slide data. Diagenesis has played only a minor role in these sediments; no lithification was discernible, but authigenic pyrite is sometimes associated with burrows, causing the development of bluish gray mottling.

Unit II: Section 553A-1-1 to Sample 553A-8-3, 13 cm (60–221.8 m sub-bottom). Age: late Pliocene to middle Miocene.

Subunit IIa: Core 553A-1 to Sample 553A-7,CC (60–217.50 m sub-bottom). Age: late Pliocene to middle Miocene.

Subunit IIa is dominated by pelagic biogenic calcareous sediments, largely nannofossil and foraminiferal nannofossil oozes and chalks, locally becoming more foraminifer-rich. Sponge spicules, diatoms, and radiolarians are minor but conspicuous constituents; echinoid spines, ostracods, and fish bones and teeth occur rarely. Carbonate content is consistently about 90%.

The base of the subunit is marked by the appearance of glauconite, and the top by the presence of more terrigenous sand and clay interbeds. Unfortunately, the exact position of this boundary is unknown because of the absence of cores over the pertinent interval: Hole 553B reached total depth at 28.50 m sub-bottom, still well within Unit I, and the first core in Hole 553A was taken at 65.50 m, within Unit II. No logs could be run over the interval. However, the late Pliocene (NN16) age for Core 553A-1 suggests that the top of this core may not lie far below the boundary: extrapolation from the sedimentation-rate curve indicates a position close to 60 m subsea.

The sediment color varies from white (N9, 5Y 8/1) to bluish white (5B9/1), and very light gray (N8), and the texture ranges through mud and sandy mud to muddy sand, depending on foraminifer content. Laminae are fairly common throughout and are picked out by light gray (5Y 7/1), white (10YR 8/1, 5Y 8/1, 5Y 8/2), and light greenish gray (5GY 8/1) colors, but are apparently unrelated to textural or mineralogical variations. Bioturbation occurs throughout, although rarely intensely enough to destroy laminae. Burrows are often picked out by a light gray (N7) color, related to the presence of pyrite.

The only major diagenetic process to have operated is the burial-depth controlled transformation of ooze to chalk. Chalk interbeds first appear in Core 553A-4 (188 m) although ooze still persists to the base of Core 6 (208.0 m).

Table 3. Lithologic units, Site 553.

Unit	Lithology	Sub-bottom depth (m)	Thickness (m)	Sedimentation rate (m/m.y.)	Age	Core-Section Hole 553A	Core-Section Hole 553B
I	Alternations of nanno-foram ooze, nanno-foram marl, calcareous mud, and mud. Dropstones common in mud and calcareous mud.		c. 60	30	Quaternary to late Pliocene		1-1 to 4,CC
IIa	Nanno ooze and foram-nanno ooze grading to chalk towards base	c. 60–217.50	c. 155	6	late Pliocene to mid-Miocene	1-1 to 7,CC	
IIb	Glauconitic foram chalk	217.50–221.80	4.30		middle to early Miocene	8-1 to 8-3, 130 cm	
III	Nanno-foram chalk with iron smectite nodule at base	221.80–234.80	13.00	<1	early Miocene to late Oligocene	8-3, 130 cm to 9-6, 30 cm	
IVa	Biosiliceous nanno-foram chalk	234.80–240.32	5.52	8	middle Eocene	9-6, 30 cm to 10-3, 82 cm	
IVb	Volcanic tuff interbedded with zeolitic/biosiliceous nanno-foram chalk; highly glauconitic mudstone at base.	240.32–261.50	21.18	15	middle to early Eocene	10-3, 82 cm to 12-4	
IVc	Volcanic tuff interbedded with mudstone and marly mudstone	261.50–388.70	127.20	55	early Eocene	12-5 to 26-1, 20 cm	
IVd	Micaceous sandstone with calcite cement	388.70–464.65	75.95	55	late Paleocene	26-1, 20 cm to 34-1, 15 cm	
IVe	Lapilli tuff	464.65–479.50	14.85	55	early Eocene late Paleocene	34-1, 15 cm to 35,CC	
IVf	Tuffaceous mudstone with minor tuff interbeds	479.50–499.35	19.85	55	early Eocene late Paleocene	36-1 to 37-5, 35 cm	
V	Basalt	499.35–682.50	183+		early Eocene late Paleocene	37-5, 35 cm to 59	

This increase in lithification is shown on the sonic log, with a steady decrease in traveltime beginning at 161 m sub-bottom, immediately below Core 3.

Subunit IIb: Section 553A-8-1 through Sample 553A-8-3, 130 cm (217.5–221.8 m sub-bottom). Age: middle Miocene.

This subunit is primarily distinguished from the overlying sediments by the appearance of glauconite grains; foraminifers are also more abundant. The base of the unit is marked by a sharp, burrowed contact with the underlying nannofossil–foraminiferal chalk. The lower surface is marked by an unconformity, with NN2–4 missing (see Biostratigraphy section).

The principal characteristic of the subunit is the downward gradual increase in glauconite content, from 1 to 2% at the top to around 15 to 20% at the base. Subsequently, the lithology grades downward from foraminiferal chalk and nannofossil–foraminiferal chalk to glauconitic–foraminiferal chalk, in association with a gradual color change from bluish white (5B 9/1) through light greenish gray (5GY 8/1) to greenish gray (5G 8/1). Biogenic silica, mainly sponge spicules, is also more conspicuous toward the base. The increase in glauconite and biogenic silica corresponds with a decline in carbonate content, which decreases to 51% at the base of the unit. The subunit is lithologically identical to Subunit IIb at Site 552 and the comments made on the genesis of the glauconite at that site hold here also.

Unit III: Section 553A-8-3, 130 cm through Sample 553A-9-6, 30 cm (221.8–234.8 m sub-bottom). Age: early Miocene–late Oligocene.

This unit consists essentially of nannofossil foraminiferal chalk with a downward increase in abundance of palagonitized ash. The top of the unit is picked at the sharp, burrowed contact with the highly glauconitic middle Miocene; the base is picked at the first downhole disappearance of iron–smectite nodules. Both upper and lower surfaces are marked unconformities, with NN2–4 missing above and NP17–24 missing below.

The dominant lithology of the unit is nannofossil foraminiferal chalk, but palagonitized ash becomes more common downwards, largely as disseminated particles. The absence of direct ash fall units and the gradual downward increase in palagonite abundance suggests that the grains may be reworked from the underlying Eocene. In the basal 45 cm, iron–smectite nodules up to 5 cm in diameter occur, as well as dendritic manganese staining of the sediment. Biogenic silica (mainly sponge spicules), fish remains, and micronodules also occur in this section, probably suggesting a period of slow deposition. Carbonate content is consistently around 80% for the unit.

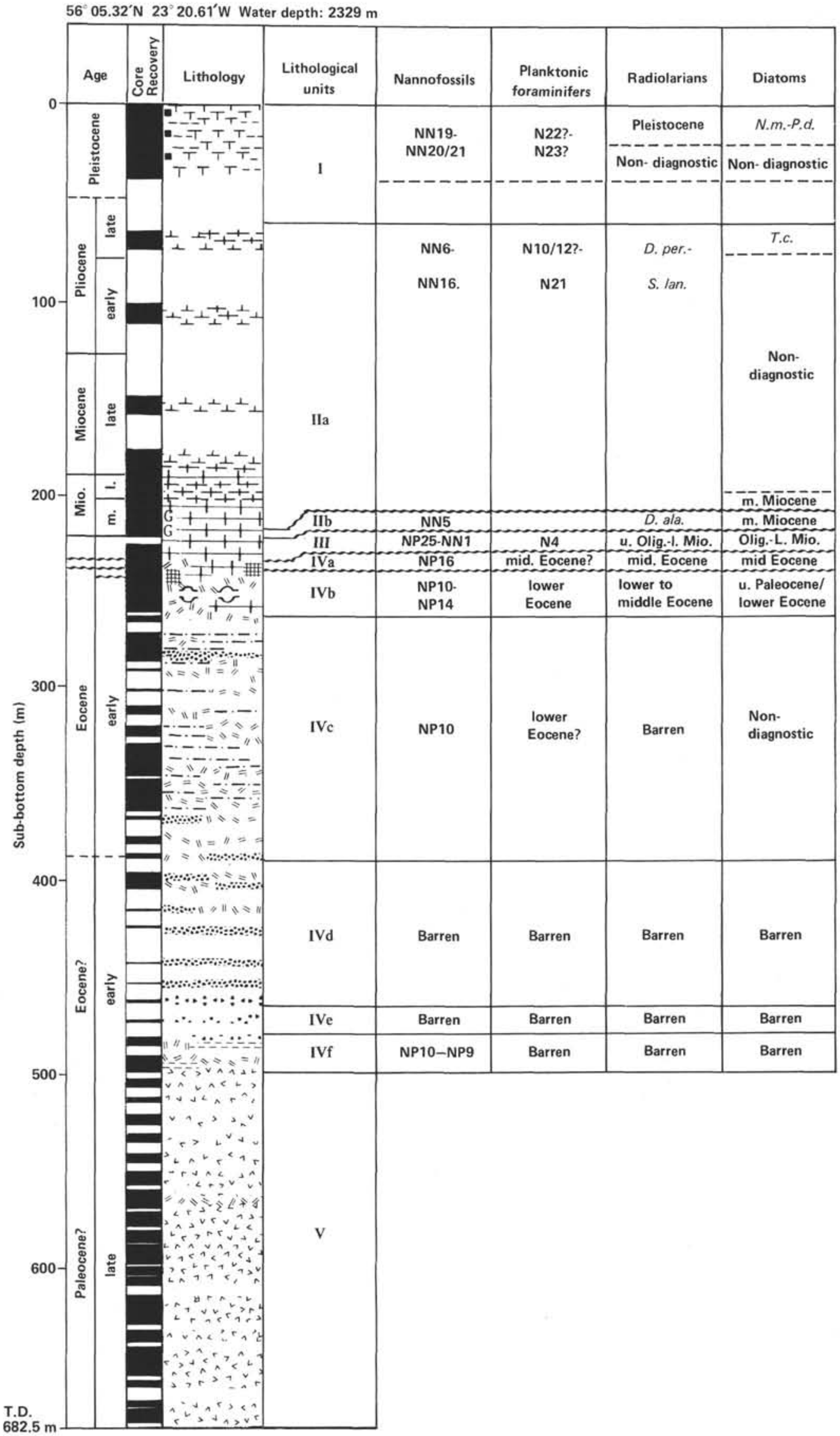

Figure 15. Lithologic and biostratigraphic summary, Holes 553, 553A, and 553B.

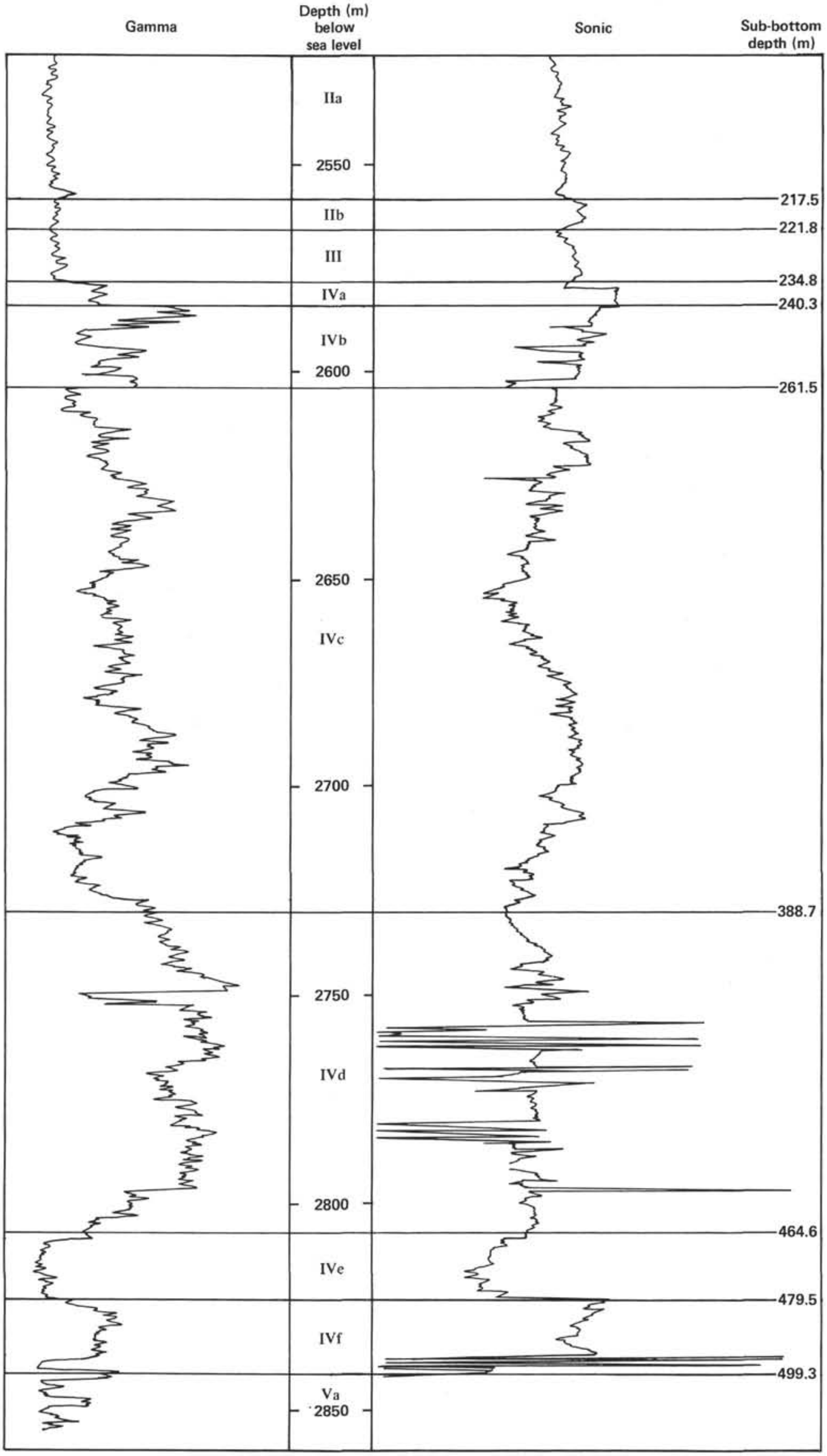

Figure 16. Gamma-sonic log response of principal lithologic units, Hole 553A.

The sediment color varies from light greenish gray (5GY 8/1) to white (5Y 8/2). Laminations of greenish gray (5G 8/1) occur in the upper part of the unit, and the lower part is extensively burrowed. The burrows are mainly horizontal (*Zoophycus, Chondrites*, etc.), and the fills are lighter in color than the surrounding sediment, generally in shades of white (5Y 8/1, 2.5Y 8/2).

Unit IV: Samples 553A-9-6, 30 cm to 553A-37-5, 35 cm (234.80–499.35 m sub-bottom). Age: early to middle Eocene.

This unit is dominated by the presence of volcanic tuff and lapilli, although the background sediment type varies widely, from biosiliceous nannofossil–foraminiferal chalk and zeolitic nannofossil–foraminiferal chalk to mudstone, sandy mudstone, and sandstone. The background sediment type defines the six subunits into which the unit can be divided.

The upper limit of the unit is marked by the downward disappearance of iron-smectite nodules and the increase in the ratio of biogenic silica to calcium carbonate. The base is defined by the top of the basaltic flow sequence.

Subunit IVa: Samples 553A-9-6, 30 cm to 10-3, 82 cm (234.80–240.32 m sub-bottom). Age: middle Eocene.

Subunit IVa essentially consists of biosiliceous nannofossil–foraminiferal chalk. Both upper and lower limits are unconformities, the boundaries being marked by burrowing. NP17–24 is missing above, and the underlying hiatus comprises at least all of NP15. The sediments range from pale brown (10Y 8/4) to pale yellow (2.5Y 8/4 and 2.5Y 7/4), with pale olive mottles (10Y 6/2) locally. This mottling results from the presence of palagonitized ash in minor amounts.

The dominant components of the sediment are foraminifers and nannofossils, with common sponge spicules and minor radiolarians and diatoms. Volcanic glass, partly palagonitized, is a minor constituent. Detrital grains and zeolites are absent; the clay mineral suite is confined to smectite. Carbonate content is close to 70%.

The only visible sedimentary structures are burrows, which are abundant throughout; they are mainly horizontal (*Zoophycus, Chondrites*) and are generally paler than the surrounding sediment, being mainly white (2.5Y 8/2 and 10Y 8/2). The absence of soft sediment deformation structures, scours, and crossbedding and the absence of macrofossils suggests that this subunit was probably deposited in quieter and deeper waters than the underlying sediments and probably in outer shelf depths.

Subunit IVb; Sample 553A 10-3, 82 cm to Section 553A 12-4 (240.32 m to 261.50 m sub-bottom). Age: early–middle Eocene.

This subunit is dominated by volcanic tuff beds, which occur throughout the subunit, reworked into and interbedded with zeolitic nannofossil foraminiferal chalk. A thinly bedded sequence of slightly silicified tuffs appears at the very top of the subunit, at the contact with the unconformity below middle Eocene biosiliceous nannofossil–foraminiferal chalk (Fig. 17).

In the lower part of the subunit there are tuffaceous, highly glauconitic mudstones, the latter defining the base of the subunit. This level is close to the level above which

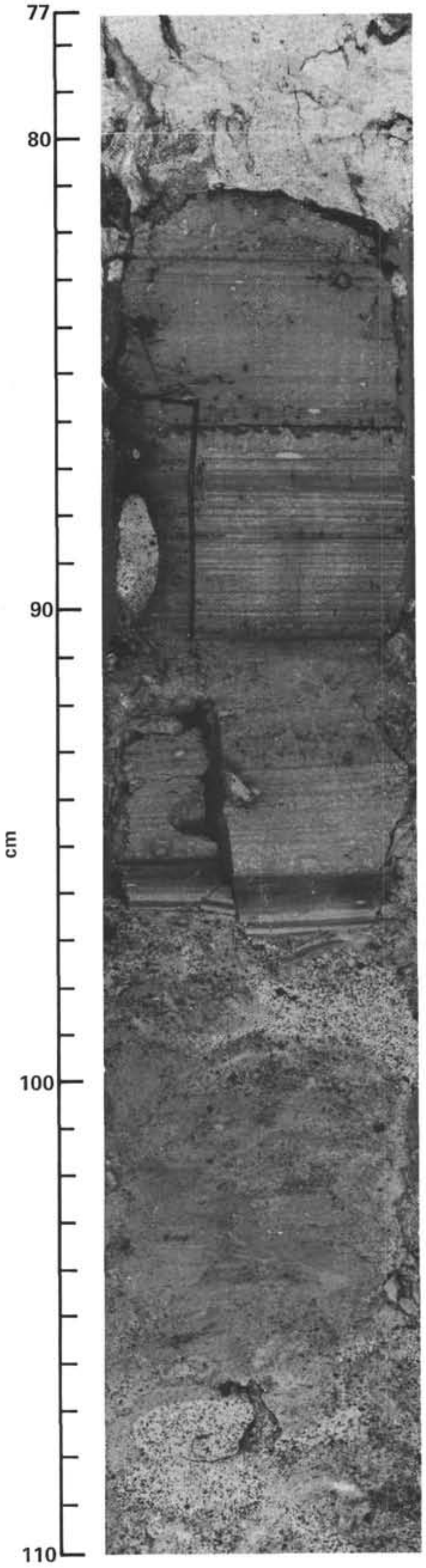

Figure 17. Unconformable contact between middle Eocene biosiliceous nannofossil–foraminiferal chalk and thinly bedded slightly silicified tuffs (Sample 553A-10-3, 77–110 cm).

epidote and amphibole disappear from the heavy mineral assemblage.

The volcanic tuffs are generally fine-grained, although scattered lapilli-size clasts occur in several units. The tuffs are essentially vitric and of basaltic composition. Alteration of the tuffs is relatively minor. Several tuff units show grading, but intense bioturbation has caused partial homogenization, destroying many original sedimentary structures. The tuffs are generally greenish black (5GY 2/1, 5G 2/1), dark olive gray (5Y 3/2), or dark greenish gray (5G 4/1), but the tuffs present higher in the sequences are higher in color (light olive brown, 2.5Y 7/4). Lapilli are generally light olive (10Y 5/4) palagonitized glass.

The background sediments are nannofossil-foraminiferal chalks, often with a high zeolite (clinoptilolite) and biogenic silica (largely spicules) content, but the intense burrowing and mixing with the volcanogenic sediments have produced many transitional sediment types. The nannofossil-foraminiferal chalks range from pale yellow (5Y 7/4) through light olive brown (2.5Y 6/4) to olive (5Y 5/3).

As already mentioned, burrows are extremely common, mainly horizontal (*Zoophycus, Chondrites*); some excellent examples of echinoid feeding burrows are present. Macrofossils are rare in the upper part of the subunit but become more abundant in Core 13, where serpulid worms, gastropods, bryozoans, and *in situ* bivalves occur.

The occurrence of scours, cross-laminations, and soft sediment deformation (slumps, microfaults, and sedimentary dykes) suggests a higher energy environment and higher sedimentation rates than the overlying unit.

The heavy minerals in this unit are confined to augite and iddingsite, indicating derivation from a basaltic landmass and suggesting a correlation of this subunit (and the overlying one) with the entire Unit IV section at Site 552. The clay mineral suite is confined to smectite: carbonate content varies from 47% in the chalks to less than 1% in the tuffs.

Subunit IVc: Section 12-5 to Sample 26-1, 20 cm (261.50–388.70 m sub-bottom). Age: early Eocene.

This subunit is characterized by a greater amount of volcanogenic material than the overlying sediments, and by a difference in the background sediment: nannofossil-foraminiferal chalk disappears and is replaced by sandy mudstone, with the first appearance of common detrital quartz. A change in the heavy mineral suite, to an epidote-hornblende association, also takes place close to this level. The lower boundary is marked by the vertical disappearance of volcanogenic sediment and change to sandstone.

The tuffs are generally fine- to medium-grained, although scattered lapilli occur throughout and in several cases are sufficiently abundant for the units to be termed lapilli tuffs. Tuffs are generally greenish black (5GY 2/1, 5G 2/1) grading to olive gray (5Y 4/1), and many display fining-upward tendencies, although burrowing often obscures this trend. Volcanic glasses are of basic and intermediate compositions. The lapilli show a wide range of lithology, from palagonitized glass (greenish black, 5G 2/1), to basalt (black N9 to dark olive gray 5Y 3/2), reddened basalt (dusky red 2.5YR 3/2) and, most common, vesicular pumice (olive gray 5Y 4/1). The frequency of tuff-lapilli beds is variable, with two maxima: one in Cores 12 to 16 (characterized by thick tuff-lapilli units) and another near the base (Cores 21 to 26) marked by abundant relatively thin tuffs with occasional thick lapilli units. Zeolites are often associated with these tuff units: clinoptilolite, chabazite, analcite, and phillipsite have been recognized in smears and by XRD.

The background sediment is also highly tuffaceous, probably through reworking of tuff units and bioturbation. Nevertheless, they are essentially terrigenous mudstones and sandy mudstones, with a gradual downward increase in sand content.

Heavy minerals are abundant, particularly hornblende and epidote; first-cycle derivation from the metamorphic basement of South Greenland seems likely. Clay minerals group as 100% smectite in tuff beds and as illite-smectite-kaolinite in the terrigenous sediments, the former representing alteration products of volcanic glass and the latter the detrital suite. Disseminated carbonaceous material occurs throughout, often concentrated in laminae. The carbonate content is low, invariably less than 4%, except in concretionary horizons.

Foraminifers, calcareous nannofossils, diatoms, and spicules are rare, but the macrofauna is often abundant, particularly bivalves, gastropods, and serpulids. Bivalves are generally thin-shelled, but in Core 19 thick-shelled oysters are present, suggesting higher energy conditions and/or closer proximity to shore.

Burrowing is often extensive, horizontal burrows (*Zoophycus, Chondrites*) still the most common, and echinoid feeding burrows were noted. Burrows are often pyritized or calcite-cemented, and calcite concretions also occur frequently at the bases of graded volcanic units.

Scouring, cross-laminae, and intraclasts provide evidence for fairly strong current activity, and the common occurrence of slumps testifies to the rapid sedimentation rate. The sediments probably accumulated in an inner-shelf environment, possibly becoming brackish at times.

Subunit IVd: Sample 553A-26-1, 20 cm to 553A-34-1, 15 cm (388.70–464.65 m sub-bottom). Age: early Eocene/late Paleocene.

Subunit IVd consists largely of feldspathic, micaceous, slightly tuffaceous sandstones, which in the lower part of the subunit are commonly calcite-cemented. These concretionary horizons caused the poor core recovery from Cores 27 to 33. The top of the unit is marked by the sudden decrease in abundance of tuff beds, and the base by the reappearance of volcanogenic material. The sandstones are highly micaceous (up to 15%) and highly feldspathic (quartz:feldspar being approximately 60:40); they possess identical heavy mineral and clay mineral assemblages compared to those of the overlying subunit. The nontuffaceous sandstones are light gray (N6); those with some tuffaceous content are greenish black (5GY 2/1). Little evidence of sedimentary structures can be found in the meager pieces of core recovered, but some show extensive burrowing. In view of the coarse-grained nature of the sediment, the subunit is perhaps best regarded as the culmination of the coarsening downward trend observed in Subunit IVc, and was probably deposited in a similar environment.

Subunit IVe: Samples 553A-34-1, 15 cm to 553A-35,CC (464.65–479.50 m sub-bottom). Age: early Eocene/late Paleocene.

This subunit wholly consists of lapilli tuffs, the upper contact being marked by the change from calcite-cemented sandstone and the lower by the appearance of tuffaceous mudstone. The lapilli tuffs are not graded, possibly because of bioturbation, although burrows are not conspicuous. They are olive black in color (5Y 2/1), although some horizons are calcite-cemented, and are largely composed of basaltic lapilli up to 2 cm diameter, some showing alteration haloes. The groundmass consists largely of glass, partially altered to trioctahedral smectites (saponite) and zeolites (analcite).

Subunit IVf: Sections 553A-36-1 to 553A-37-5, 35 cm (479.50–499.35 m sub-bottom). Age: early Eocene/late Paleocene.

This subunit is dominated by tuffaceous mudstone with volcanic tuff and lapilli interbeds: its upper limit is defined by the downhole appearance of tuffaceous mudstone, and its base by the top of the basalt flow sequences.

Tuffaceous mudstone is the most common lithology, varying from very dark grayish brown (10YR 3/2) to dark grayish brown (10YR 4/2) and brown (10YR 5/3). Little quartz or feldspar is present, and the clay mineral assemblage is limited to dioctahedral smectites. Disseminated carbonaceous matter, pyrite framboids, and biogenic material, including diatoms, foraminifers, and calcareous nannofossils, are present.

Examination of smear slides reveals that the mudstone is practically wholly formed of altered volcanic material, but it is so distinct from the interbedded tuffs and lapilli that it is here termed tuffaceous mudstone. Direct ash-fall volcanogenic sediments are a fairly minor constituent of the subunit, and rarely show grading, possibly because of bioturbation. They are greenish black in color (5GY 2/1, 5G 2/1) and are commonly of coarse tuff or lapilli size. Basaltic glass is the most common lapilli type. Zeolites (clinoptilolite, chabazite, and analcite) are commonly associated with the tuffs.

The subunit is extensively burrowed throughout, with several burrow margins showing alteration to palagonite and pyrite. Burrows are generally horizontal. There is little evidence of current activity: where the sediments have not been thoroughly bioturbated, fine laminations occur, indicating a quiet, possibly lagoonal, depositional environment. The macrofauna consists of thin-shelled bivalves, gastropods, and serpulids. Carbonate content is again low (around 1%) except in calcite-cemented horizons which frequently occur in the tuff units.

At the base of the subunit, however, a very strongly cross-bedded (up to 15°) coarser-grained sandy tuff unit is developed, containing slump structures and a clast of mudstone similar to those above (Fig. 18). This unit may be a basal transgressive deposit overlying the basalt. The contact with the underlying basalt is sharp, and no reddening of the sediment has taken place, un-

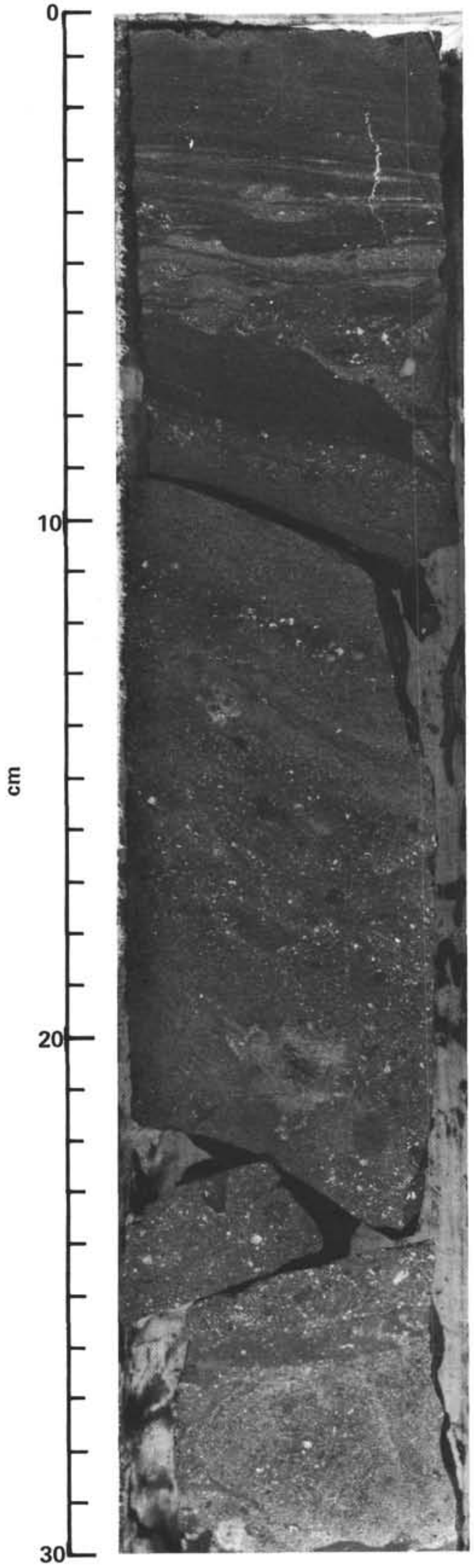

Figure 18. Strongly cross-bedded coarse sandy tuffs rest disconformably on subaerial basalt (Section 553A-37-5).

like Site 552, suggesting either a different mode of emplacement (subaerial rather than submarine) or the presence of a hiatus between basalt eruption and the deposition of the overlying sediment.

BASALT LITHOLOGY

Site 552

Hole 552 encountered iron-rich tholeiites below Eocene sediments from 282.7 m below the seafloor (Section 552-21-3) to 290.60 m (Core 552-23-2) and probably to total depth at 314 m. A single basalt flow was present in the sampled section, which may be divided into two subunits on a lithological basis.

Subunit Va: Section 552-21-3 to Sample 552-21,CC (282.70 to 284.00 m sub-bottom).

This consists of relatively fine-grained, dark gray to grayish black phyric vesicular basalt. One small pillow was observed. Several plagioclase laths (up to 3 mm) are visible in hand specimens. Vesicles up to 5 mm in diameter are common (although less so than in Subunit Vb), forming about 10% of the whole rock. They are largely unfilled and have plagioclase laths fluxioned around them.

Thin sections show that the basalt consists of common labradorite and rare augite phenocrysts set in an extremely altered groundmass composed of small plagioclase laths and clay with abundant fine-grained opaques scattered throughout. The plagioclase forms two distinct grain-size populations. XRD indicates that the clay is smectite (saponite) and the opaques are pyrite. Well-crystallized saponite also occurs as a lining to the vesicles but rarely wholly infills them.

Subunit Vb: Sections 552-22-1 to 23-2 (284.00 to 290.60 m sub-bottom).

This subunit is distinguished in hand specimen from the overlying unit by its coarser grain and the presence of infilled vesicles. The vesicles range up to 8 mm in diameter and are abundant throughout the section, forming up to 15% of the whole rock. Although large (up to 3 mm) plagioclase laths are visible in hand specimens, thin sections show that the plagioclase does not form two distinct grain-size populations as it did in the overlying subunit. The plagioclase is labradorite (An_{60}), and the laths are frequently fluxioned around the vesicles. Augite is again uncommon and only occurs in significant amounts in the thin section from Sample 22-2, 2 cm where it forms 5% of the whole rock. However, in all sections, from this and the overlying unit, there is abundant evidence of replacement of augite by clays, indicating its original presence as a major phase. Opaques are common, and up to 50% occur in crystals up to 0.5 mm in size which show the distinctive skeletal form commonly displayed by ilmenite. However, in reflected light the opaques show a brassy yellow color indicating that they are composed of pyrite; it seems likely that these are pseudomorphs after pyrite, possibly via an intermediate leucoxene stage. The groundmass is again largely smectite which also infills vesicles. Fibrous calcite occurs rarely as fracture fills.

This variation in lithology essentially results from the more rapid cooling at the top of the basalt flow. Subunit Va thus represents the fine-grained cooled margin and Subunit Vb the main body of the flow. Alteration appears to become less intense lower in the flow and therefore is related to downward fluid migration.

Shallow-water extrusion of the basalt is suggested by the marine origin of the overlying sediments and by the presence of the small pillow.

Site 553

In Hole 553A, basalt was encountered at 499.35 m. Below this depth a sequence of basaltic lava flows were drilled and cored to total depth at 682.5 m (thickness 183.0 m), with an average recovery of 53.23%. The description of the lava flows given here is based primarily on megascopic, thin section, and XRD studies made by the shipboard scientists using additional data from the downhole logs, paleomagnetic studies, and a preliminary petrographic description by Harrison and Merriman (pers. comm.). This account should be regarded as very preliminary, and the reader is also referred to the reports in this volume of full petrological and geochemical studies made ashore.

Basalt Lithostratigraphy

The sequence of basalts drilled and cored in Hole 553A has been divided into three subunits (Fig. 19A) from the physical and magnetic properties data and the downhole logs. No major petrographic differences are apparent between the units. The principal differences seem to relate to the presence or absence of sediments between flows or the degree of development of weathered scoriaceous tops to the flows, flow thickness, their cooling history (revealed by differences in their magnetic properties; see Krumsiek and Roberts, this volume), and the degree of fracturing. In addition, ferri-celadonite and the abundance of vesicle clasts varies downsection but not apparently in relation to subunit boundaries.

Subunit Va: Cores 553A-37 to 44, thickness 61.0 m (499.35 to 562.0 m sub-bottom).

The unit (Fig. 19A) consists primarily of a sequence of tholeiitic basaltic lava flows characterized by scoriaceous or agglomeratic tops. Although nine flow units were identified in the cored section, the resistivity log suggests that as many as 12 flow units may be present. Increased gamma response at the top of the flow units may indicate tuffs, weathering, or possibly sediments.

An average lava flow is sketched in Figure 19A and B. The upper part of the flow consists of a reddened or purple gray scoriaceous vesicular basalt or basaltic agglomerate that passes downward with a decrease in the red color into a medium gray (N5) vesicular phyric basalt in which vesicles are commonly lined with light green (5G 5/2) celadonite or smectite. The scoriaceous or agglomerate top consists of lithic angular to subangular fragments of vesicular basalt commonly showing fracturing, penetration, and corrosion by the deeply reddened groundmass, which consists of small angular lithic fragments; open vesicles lined with celadonite are common in the groundmass. The reddening decreases downward, and the contact with the underlying basalt is transitional. The underlying basalt surface is penetrated by

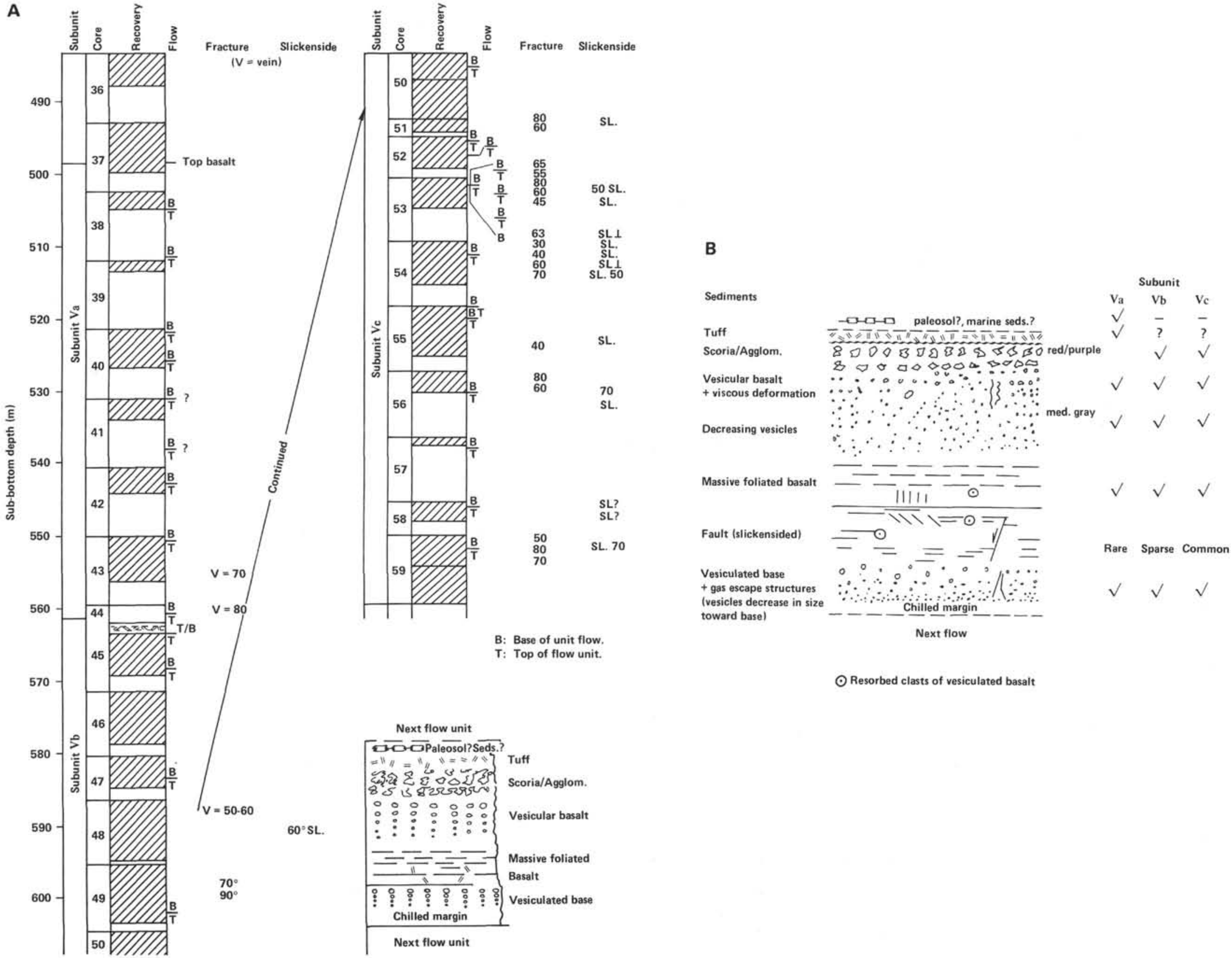

Figure 19. A. Basalt lithostratigraphic subunits and cored flow units, Hole 553A. B. Insert shows generalized flow unit structure of basalt Subunits Va, Vb, Vc.

the overlying groundmass of the agglomerate into which fragments of the basalt have been incorporated. The basalt is characterized by abundant open and infilled vesicles but becomes massive and much less vesicular downward. Abundant clasts of vesicular basalt, commonly showing resorption rims, are present in both the overlying vesicular and the underlying less-vesicular basalt. The more massive parts of the flow show a well-developed cooling fabric that tends to be associated with a decrease in vesicularity. The fabric is most commonly horizontal to subhorizontal but is sometimes vertical or inclined at a high angle. The latter sets are sometimes sharply cut off by the horizontal fabric. Where best developed, the fabric is typically spaced at about 0.3 to 0.5 cm and commonly braided. In general, the fabric sharply decreases as does groundmass grain size toward the base of the unit, where the basalt again becomes more vesicular. Shrinkage cracks occur sparsely in the massive basalt. The basal part of the flow is characterized by the appearance of sparse large vesicles marking the start of a downward increase in vesicle abundance and decrease in size that merges with the basal aphanitic vesicular chilled margin of the flow. In several flow units, the proportion of phenocrysts increase toward the drilled margin. Trachytic textures are common.

Vuggy and open vesicles occur throughout each lava flow, varying in abundance as described above. Filled vesicles typically have a black lining of smectite (Mg-saponite) around a dusky green core of ferri-celadonite. Vugs are also lined with smectite, which is intergrown with the calcite and quartz crystals forming the center of the vug. Sparse veins lined with smectite intergrown with quartz and calcite are also present (Section 553A-42-3) but show no evidence of displacement.

Two small pebbles of grayish green (5G 5/2) chert containing ferri-celadonite in quartz and low cristobalite were found in Section 553A-40-1. This silica also contained minor amounts of native copper and may represent precipitation from cooling hydrothermal solutions. Native copper is also present in vesicle fillings in Sample 553A-46-4, 58 cm.

Downhole logs through this interval are characterized by seven prominent peaks in the gamma log. These lie directly below the basal part of individual flows shown by the SFLU log (Fig. 20). These high gamma zones also correlate with low sonic velocities. Although recovery was poor in these zones, correlation of the cored section with the logs suggests that the high-gamma, low-sonic zone possibly corresponds to the scoriaceous weathered tops of the flow tuffs or unrecovered sediments above. Typically, the flows, as in the other subunits, show a decrease in porosity down-flow with a sharp increase in the vesicular zone above the base that is matched by an increase in density and then a decrease towards the base of the flow (Fig. 20). The resistivity log also shows divergence of the ILD and ILR logs which may indicate fracturing of the thicker flows. This is particularly so in the case of Core 43 and reflects the obvious veining in Sections 4 and 5.

Subunit Vb: Cores 553A-45 to 50, thickness 52.5 m (562.0–614.5 m sub-bottom).

The subunit (Fig. 19) is defined on the basis of the lower gamma response and the absence of prominent peaks in the gamma curve. Magnetic measurements indicate low susceptibilities and high intensities. Five lava flows have been identified in the unit from the resistivity log and four were recovered in the cores. Rarity of increasing gamma response at the top of flows suggests that sediments, tuffs, or weathered zones are sparse. Flows within the unit are all tholeiitic. Glomerophyric and trachytic textures are common throughout.

The top of the subunit is defined by the deeply reddened vitric tuff found in Section 553A-45-1. In its upper part, the tuff is predominantly composed of glass with small lithic fragments. Vertical structures within the tuff may be gas escape structures. Dark reddish gray (10R 3/1) and dark reddish brown (5BG 3/2) laminae at a millimeter scale are common. Grading is present

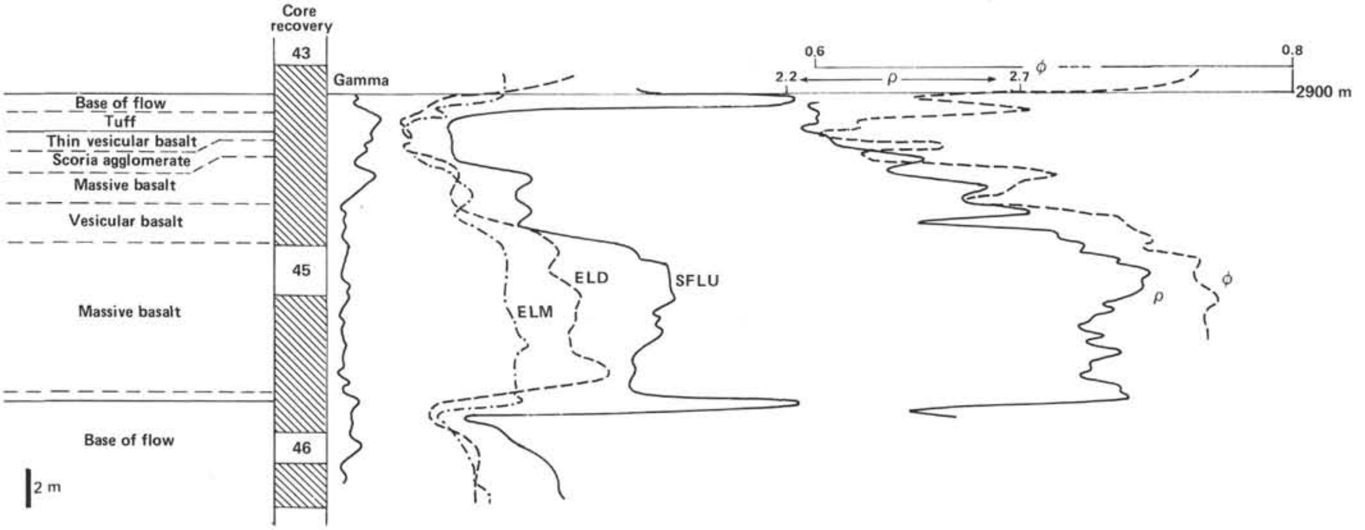

Figure 20. Correlation between logs and lithology in a single flow unit, Hole 553A.

(Fig. 21) in the upper part of the tuff. Angular and convoluted contacts are also present. The red color decreases downward to become very dark (N3) with sparse red patches. The contact with the underlying basalt flow is sharp, and the basalts is chilled, suggesting that the tuff may be subaqueous. The underlying basalt is variegated in color from weak red (2.5YR 4/2) to dark greenish gray (5GY 4/1). The latter occurs in irregular patches or infilling vesicles and may be smectite or ferriceladonite. The groundmass is also deeply altered and reddened. Below this thin (50 cm) basalt is the grayish red purple (5RP 4/2) to medium gray (N4) scoriaceous agglomeratic top of the underlying lava flow. The vesicular agglomerate consists of angular to subangular reddened fragments of vesicular basalt that are fractured as well as penetrated and corroded by the reddened groundmass that consists of small angular to subrounded fragments of vesicular basalt. The reddening decreases downward and the contact with the underlying basalt is transitional, consisting of a fractured surface penetrated by the groundmass of the overlying agglomerate.

Individual flows within Subunit Vb show comparable lithologies to those of Subunit Vc. Below the scoriaceous agglomerate tops, vesicular (open and filled) medium gray phyric basalts pass downward to sparsely vesicular basalts. Within the uppermost part of the vesicular basalt are present spectacular flow structures that are emphasized by flattening of the vesicles (Sample 553A-45-3, 100–120 cm). Evidence of late stage viscous deformation is shown by a small recumbent fold in Sample 553A-45-4, 95–105 cm. Vertical gas escape structures (Fig. 22) are present in Core 4, Section 4. These structures consist of a zone of phyric medium gray basalt with sparse vesicles in contact with highly vesicular basalt. The phyric basalt decreases in grain size toward the contact with the vesicular basalt, which is commonly marked by a resorption rim.

Below the highly vesicular upper part of the flow, vesicles become typically filled and less abundant. Small vugs (up to 1 cm) infilled with chalcedony and calcite and lined with black smectite are present. In that zone horizontal and vertical foliation become abundant, commonly displaying sharply cross-cutting contacts (Fig. 23). Toward the base of the flow, large open vuggy vesicles become more abundant, and in the last 20–30 cm, vesicles increase rapidly in abundance while rapidly decreasing in size; gas escape structures are present (Fig. 24). In this interval, vesicles show a strong vertical orientation, and the lowermost part of the flow is commonly aphyric and appears to be chilled. Large rounded fragments of vesicular basalt (1 to 5 cm), often showing reaction (resorption?) rims, occur commonly through each flow. A reddened zone 10 cm thick (in Sample 553A-48-2, 15–25 cm) contains red mineral grains that may be iddingsite or goethite-hematite. The lava flow in Cores 45 and 46 is nearly complete and is shown together with the resistivity, sonic, and density-porosity logs in Figure 20.

It should be noted that a significant gamma response is only rarely observed at the top of each flow in Unit Vb compared to Va. One explanation is that a weathered (i.e., clay-rich) zone is not always present at the top of

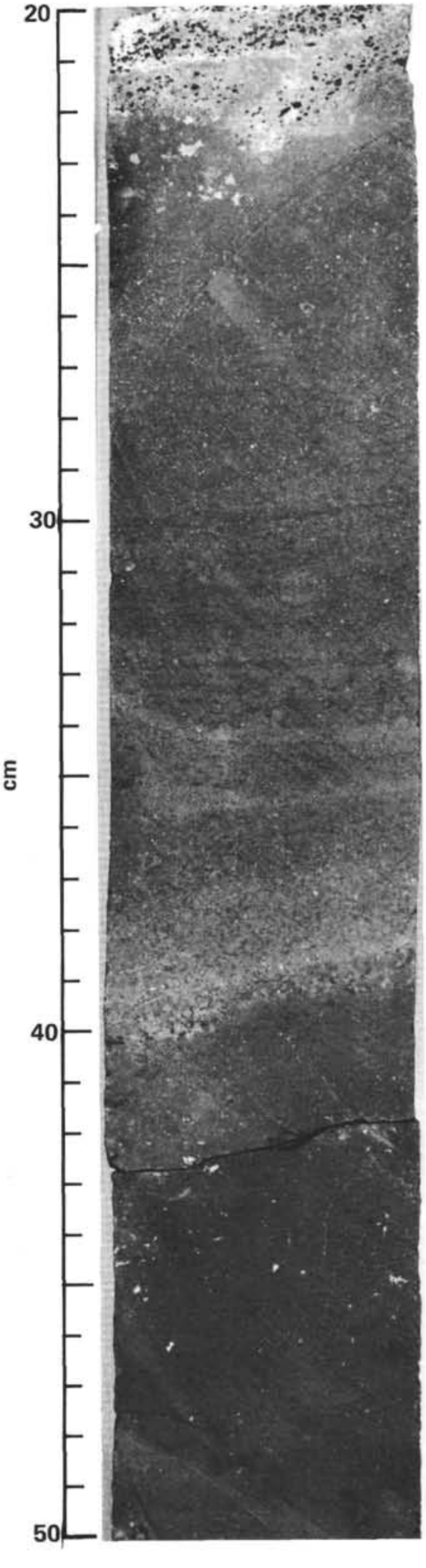

Figure 21. Hyaloclastite bed in Subunit Vb (Sample 553A-45-1, 20–50 cm). Glass and small lithic fragments comprise hyaloclastite and are in sharp contact with the underlying basalt.

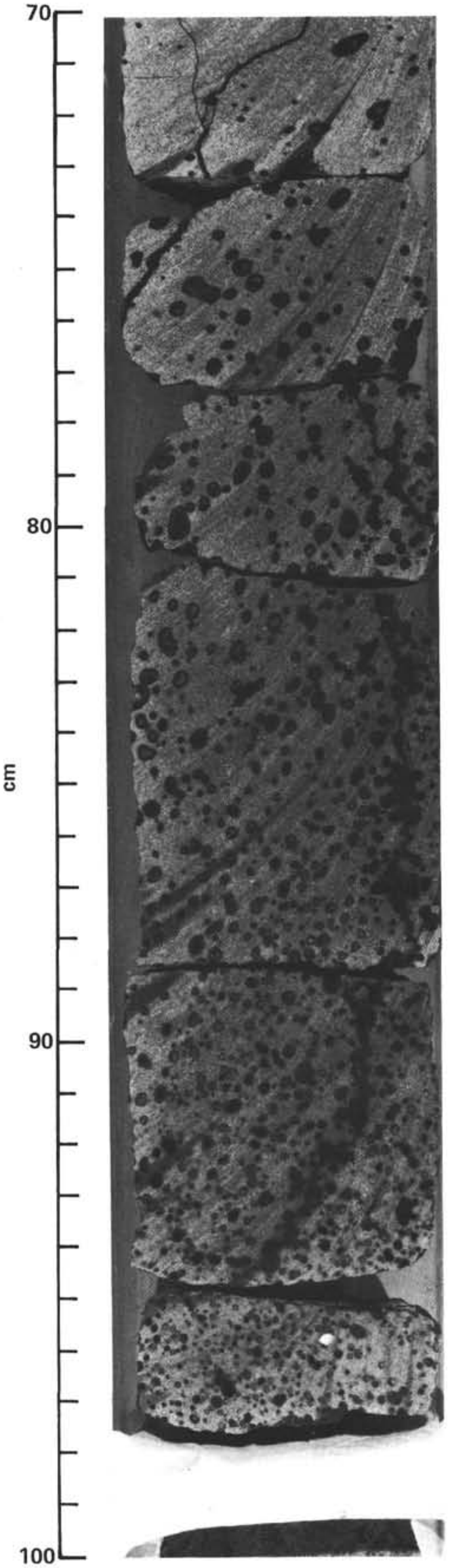

Figure 22. Strongly vesiculated basalt exhibiting vertical gas escape structures (Sample 553A-46-4, 70–100 cm).

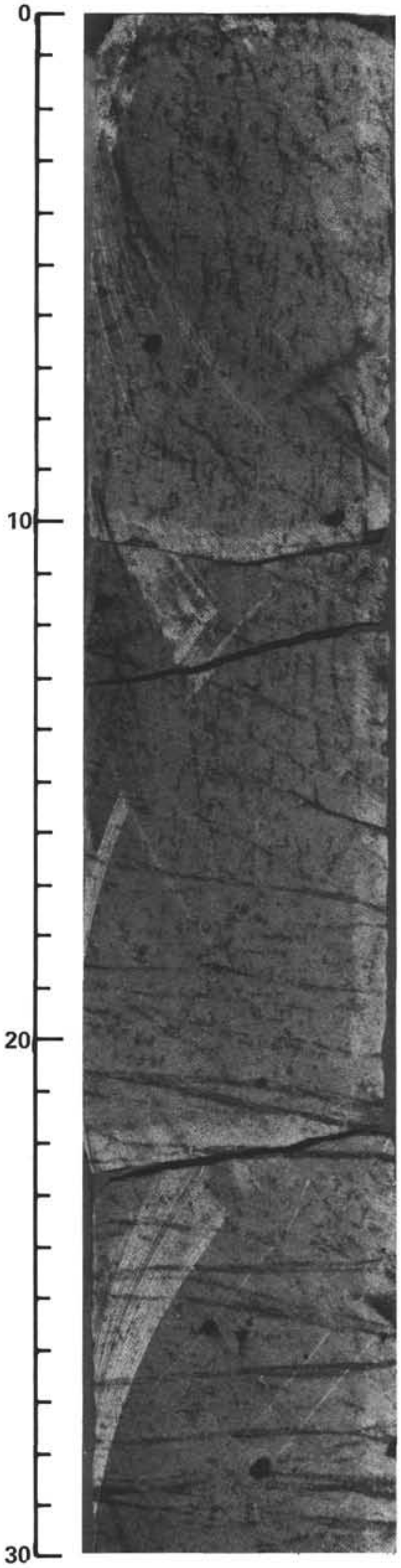

Figure 23. Horizontal and vertical cooling fabric exhibiting sharp cross cutting contacts. Small vugs lined with smectite and unfilled by chalcedony and calcite are present (Sample 553A-46-2, 0–30 cm).

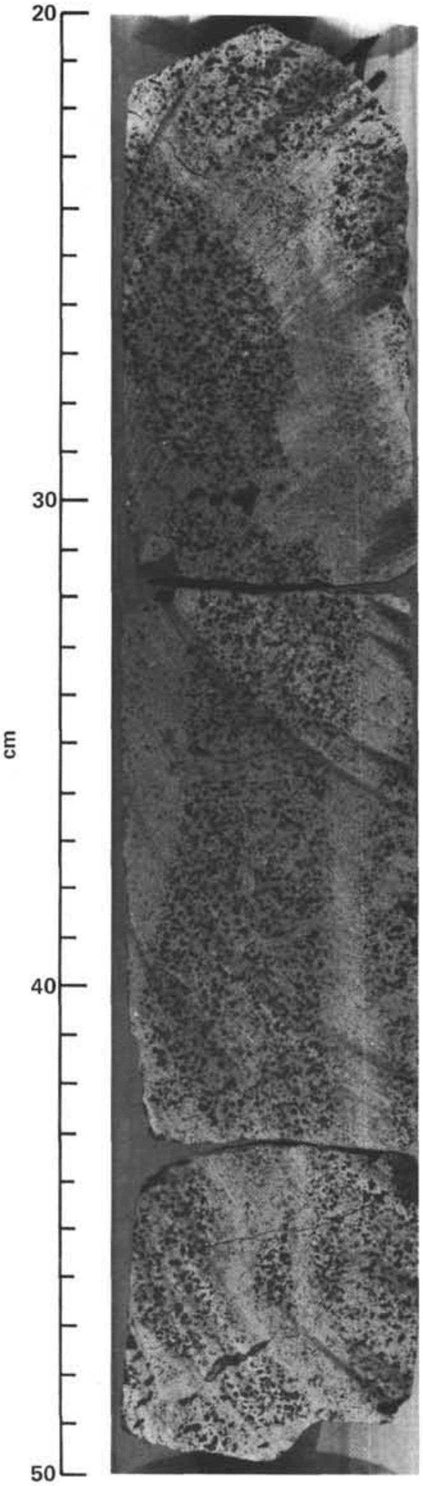

Figure 24. Large near vertical gas escape structures developed toward base of lava flow (Sample 553A-46-6, 20–50 cm).

each flow. Divergence between the ILD and ILM logs indicates fracturing in the flow units. Minor horizontal and inclined (50–80°) fractures, the latter sometimes showing evidence of displacement (e.g., Sections 553A-46-3 and 47-3), occur in several of the units. One 1-cm-wide fault in Core 553A-49-6 (Fig. 25), which is infilled by

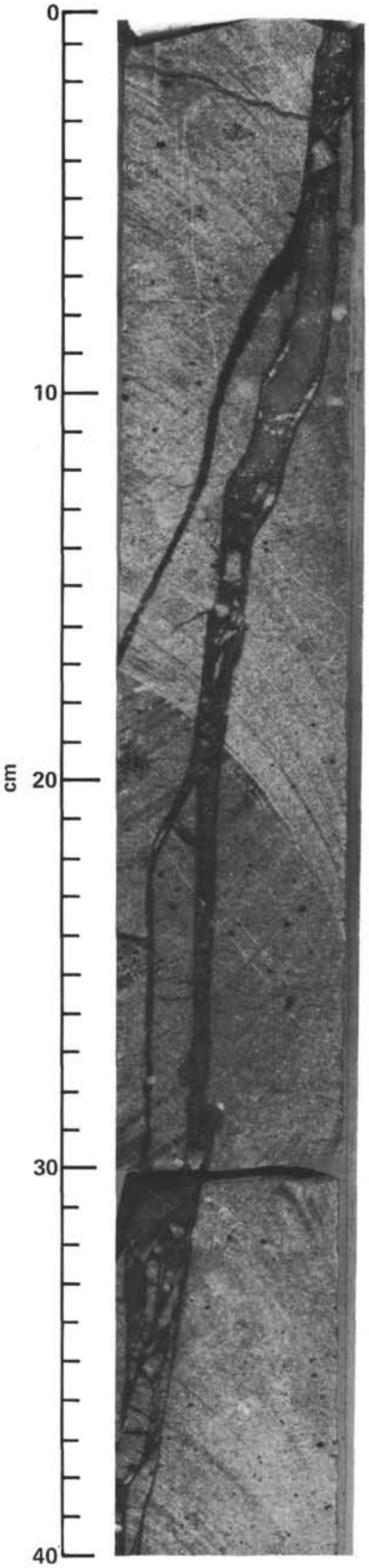

Figure 25. Well-developed fracture vein unfilled with smectite and brecciated basalt; induration of vein is approximately 80° (Sample 553A-49-6, 0–40 cm).

smectite around brecciated basalt clasts and affects the scoriaceous top of the underlying flow, can be clearly seen at 2941.0 m on the resistivity log.

Subunit Vc: Cores 553A-51 to 59, 68.0 m thickness. (614.5 to 682.5 m total depth sub-bottom).

Subunit Vc is characterized by its stronger gamma response and an increase in susceptibility and intensity of magnetization with depth. Interpretation of the resistivity log suggests that 13 or 14 flows are present, and 14 were identified in the recovered core. In contrast to Subunit Vb, individual flows are thinner (1–6 m) and are characterized by more slickensided fracturing than Subunit Vb. The top of the unit may correspond to the top of the suite of dipping reflectors below the topmost reflector of the sequence. The flows are composed of tholeiitic basalts.

Individual flows typically consist of an upper grayish red (5RY 4/2) to blackish red (5R 3/2) vesicular, scoriaceous agglomeratic basalt; vesicles are typically lined with dark dusky green (5BG 3/2) or dark greenish gray (5GY 4/1). In the thicker more massive flows, vesicularity decreases as a typically strong foliation is developed. Horizontal foliations are commonly spaced at 0.5 cm and show streaking of pyroxenes. Vertical and steeply inclined foliation cross-cutting the horizontal set is common. In the thinner flow units, vesicles occur throughout, increasing in abundance toward the base of the flow. The basalt is commonly labradorite–augite glomerophyric. Fracturing associated with well-developed slickensides is common throughout. The fractures are typically inclined at between 30 and 80°. Slickensides, often associated with fibrous pale olive (10Y 5/4) calcite, are inclined both parallel to and obliquely to the fault surfaces. Veins along the fractures are infilled with smectite and calcite and occasionally brecciated basalt (e.g., Section 553A-59-3). Vesicles within the flows are commonly concentrated into thin bands (cm scale) that variously show grading and inverse grading in vesicle size. These bands show sharp contacts with a markedly less vesicular basalt in which en echelon lenticular veins of smectite are common. Large clasts of vesicular lava showing resorption rims occur sporadically throughout. Some large vesicles are vuggy and infilled with quartz and calcite.

Igneous Petrography

Forty-nine thin sections were made from the section at Site 553. On a petrographical basis and from X-ray mineralogy three major lithotypes can be identified: (1) tholeiitic basalt, (2) lithic volcanic breccia (scoria), and (3) vitric tuff.

1. Tholeiitic basalt. By far the most frequently encountered lithotype is the basalt, which shows little variation in composition over the entire section (except in its degree of alteration, discussed later). The basalts are essentially orthophyric–hypidiomorphic, but in a number of cases there is a minor phenocryst phase, rarely exceeding 5% of the whole rock. Prismatic labradorite, often zoned, up to 5 mm length, and subhedral augite, up to 0.5 mm in length, both occur as phenocrysts (less than 1 mm), and then very rarely, being confined to three flow units only (11, 17, 18). In most cases the phenocrysts are nucleated (glomerophyric texture); individual crystals often display strained extinction or even fracturing. In several flow units the proportion of phenocrysts increases toward the base (excluding the chilled lower margin), suggesting the operation of a differential settling mechanism.

The groundmass of the unaltered basalt is essentially composed of plagioclase (An_{50-70}) laths, augite ($Mg_{42-47}Fe_{17-25}Ca_{33-36}$), and magnesium pigeonite ($Mg_{52}Fe_{34}Ca_{14}$) subhedra and magnetite euhedra (Harrison and Merriman, this volume): grain size varies considerably depending on the position of the sample in the flow. In the finer-grained chilled margins, plagioclase rarely exceeds 0.03 mm, and augite and titanomagnetite 0.01 mm, but in the main mass of the flow plagioclase reaches 0.4 mm, augite 0.15 mm, and titanomagnetite 0.2 mm. Evidence for the order of crystallization is often ambiguous; plagioclase and augite probably crystallized almost simultaneously, with titanomagnetite slightly later. Minor late stage interstitial phases are glass (now completely altered to smectite), quartz, and K-feldspar. In several flow units (11, 12, 13, 14, 17) green brown fibrous hornblende mantles and partially replaces augite, and shows late stage reaction during crystallization.

The general paucity of olivine both as a phenocryst and groundmass phase, and the absence of analcime and nepheline, indicates that the basalts are of tholeiitic type, although several characteristic features of tholeiites are lacking, for example exsolution lamellae in the clinopyroxene. Further shore-based work on the petrography and phase chemistry are required for formal nomenclature.

Groundmass textures are mainly a result of the habits of the plagioclase. Most sections reveal trachytic or subtrachytic texture, and several from chilled margins reveal a variolitic arrangement of the laths, indicating rapid crystallization (e.g., Sample 553A-50-3, 3–26 cm). Some basalts, particularly those higher in the sequence, display distinct textural and mineralogical variations over small distances; boundaries between two distinct areas may be both sharp and gradational in the same section (e.g., Samples 553A-40-2, 55 cm and 41-1, 112 cm). These variations appear to be the result of incorporation of earlier formed basaltic material into the flow, with partial remelting and homogenization along the margins of the "xenoliths."

Most of the basalts are vesicular to some extent, although vesicles are considerably more abundant toward the top and at the very base of flow units. Vesicles are either partially or completely infilled with well-crystallized smectite, toward the top of flow units celadonite may also be developed, often infilling vesicles rimmed with smectite. Celadonite development is obviously a later stage phenomenon than smectite.

Most of the basalts show alteration features to some extent: in all cases glass and olivine are completely argillized, olivine pseudomorphs often being mantled by opaques. An unidentified reddish mineral is also often associated with the olivine pseudomorphs and may be either iddingsite or a ferric-oxide phase (goethite–hematite). Toward the top and in the chilled base of flow units more advanced alteration occurs. Both augite and plagioclase are visibly affected, augite more extensively than plagioclase, with the development of poorly crystallized smectite. The opaque phase also shows some alteration, developing reddish margins (goethite–hematite). Secondary opaque development (of uncertain mineralogy) characterizes the most highly altered basalts and is disseminated through the smectite phase.

Veins were encountered in two basalt sections, one consisting of length-fast chalcedony and pseudo-oolitic and dendritic goethite, the other of fibrous radiating calcite.

2. Lithic volcanic breccia. Five thin sections (Samples 553A-43-1, 62 cm; 45-4, 20 cm; 47-4, 101 cm; 55-2, 77 cm; and 67-1, 60 cm) are characterized by the presence of large angular fragments of altered basalt partially cemented by authigenic clays of subaerial(?) origin. The basalt fragments are commonly vesicular and consist largely of relatively small (0.05 mm) plagioclase laths set in a groundmass which is either wholly opaque or composed of smectite (well-crystallized saponite) with abundant disseminated finely divided opaque minerals. Plagioclase laths often display a variolitic habit, suggesting that the clasts are derived mainly from rapidly cooled basaltic lava.

The absence of glass or palagonite in, and of sediment interbedded with, the breccia strongly suggests that the breccia did not form in the submarine environment but rather by *in situ* fragmentation in a subaerial environment.

3. Vitric tuffs. Two sections (Samples 553A-45-1, 43 cm and 56-1, 73 cm) are characterized by an abundance of volcanic glass shards. The shards consists of brown basaltic glass and are often elongate and streaked out, although many display typical shard morphology. There is no suggestion of welding.

In Sample 553A-45-1, 43 cm, the vitric material is dominant (90%) with only minor lithic grains of basaltic affinity (plagioclase laths set in an opaque groundmass) and of plagioclase crystals, but Sample 553A-56-1, 73 cm contains a higher proportion of lithic material, some of which may be related to the scoriaceous top of the underlying lava flow.

Alteration of the tuffs is minor although development of authigenic smectite (iron-rich beidellite and nontronite) and hematite has occurred. This is in sharp contrast to the volcanogenic material in the overlying marine sediments (see Sediment Lithology), where most of the glass has altered to glauconite or saponite. This is strongly suggestive of a subaerial origin for the tuffs described here and is in accord with the subaerial origin of the basalts, although a subaqueous origin cannot be totally excluded in the grounds of chemical alteration.

Basalt Alteration—Preliminary Results

Two stages of alteration occur in the basalt recovered in Hole 553A, Cores 38 to 46.

1. Hydrothermal alteration, developed in a submarine environment or more probably in relation to the latest stage of consolidation of magma. Secondary products such as quartz, calcite, and clay minerals line or wholly infill vesicles or fractures. Quartz is the main component, with minor low cristobalite in two pieces of "chert" located at the top of the Core 40, and, with calcite, of the fracture infilling in Sample 553A-42-2, 20–24 cm. Calcite infills vesicles, lined with black clay material, mostly in the vesicular upper part of the basalt flow. Ferri-celadonite occurs only in vesicles and its abundance decreases from top to bottom in the basalt flow. It is as well crystallized as a mica, and its habit is different from the ferri-celadonite which has been reported from oceanic basalts (Kempe, 1976). Well crystallized black and green smectites (Mg-saponites) are widespread in the basalt flow, mostly in the middle to lower part and infill vesicles and fractures. These preliminary observations do not show a change in the chemical composition of smectites with color. Paleotemperature estimates obtained by oxygen isotope analyses of the clay minerals indicates that crystallization was at about 100°C for the Mg-saponite and 40°C for the celadonite (Desprairies et al., this volume).

2. Subaerial weathering occurs in volcanogenic sediments interbedded with the lava flows. XRD analyses show, both in the matrix and in the rock fragments, primary minerals (augite, feldspars, magnetite–ilmenite) and secondary products (hematite, ferri–celadonite, dioctohedral and trioctahedral smectites). Some of the latter (ferri–celadonite, trioctahedral smectite (i.e., well-crystallized Mg-saponite) are apparently inherited from the previous "hydrothermal" stage. However, hematite and a part of the smectite (dioctahedral smectites, i.e., nontronite) are poorly crystallized. This, together with a larger amount of "amorphous" matter, suggests subaerial weathering. This weathering would then be superimposed on the earlier hydrothermal stage.

BIOSTRATIGRAPHY

Site 552

Hole 552 was spot-cored to a depth of 108 m, and continuously rotary drilled and cored to a total depth of 314 m below seafloor. Hole 552A was continuously piston cored to a total depth of 183.5 m. The late Neogene and the early Eocene units represent apparently continuous deposition. The transition from preglacial to fully glacial conditions in the Northern Hemisphere is recorded in Hole 552A, and it occurred approximately 2.4–2.5 m.y. ago. The whole glacial sequence appears to be complete, although Core 6 was severely disturbed and not suitable for analysis. Periods of glacial conditions in the Northern Hemisphere are recorded as marls and interglacial conditions as oozes. The marls are to a large extent composed of material of continental origin, thus reflecting the transport of this material by icebergs or possibly, sea-ice, to the oceanic location of Site 552. The alternating climatic and depositional regimes during late Pliocene and Pleistocene times have profoundly affected the abundance and preservation of the microfossil assemblages, phenomena which are discussed at length in other places in this volume.

Throughout the Neogene sequence deposition took place at depths similar to that of the present-day seafloor (2301 m).

Not surprisingly, the HPC-cored Hole 552A recovered a more complete sequence across the Miocene–Eocene transition. Approximately half a meter of Oligocene nannofossil–foraminifer chalk was recorded in the lowermost part of Core 36. A big manganese nodule was found in the top part of Section 552A-37-1. This nodule rests on a mixture of nannofossil–foraminifer chalk and zeolitic mudstones that show severely disturbed stratigraphic relationships.

The only well-established biostratigraphic assignment in Section 552A-37-1 comes from a thin (about 2 cm) bed of chalk within the zeolitic mudstone at the bottom of the section. This chalk contains coccoliths referable to Zone NP15 (CP13b *Chiasmolithus gigas* Subzone) (Okada and Bukry, 1980). This is the only definite sediment of NP15 age recorded during Leg 81. In the upper part of Section 37-2 the biostratigraphic relationships become ordered again, indicating Zone NP14. Hole 552A ends in sediment of NP14 age, whereas the oldest sediments in Hole 552 appear to be close to the NP10/NP11 boundary.

Calcareous Nannofossils

Hole 552

Neogene

Core 552-1 was retrieved from the mudline. Sample 552-1,CC shows a late Pleistocene nannofossil assemblage lacking *Pseudoemiliania lacunosa*, thus placing this sample in Zone NN20 or 21; the assignment is uncertain because of the difficulty of determining the presence or absence of *Emiliania huxleyi* using light microscope techniques.

The NN15/NN16 boundary is present between 48 and 100 cm in Core 2-1.

Continuous coring was performed from Core 3, 108 m down to Core 25 at 314 m. Core 21 is the lowermost core containing nannofossils. The Neogene/Paleogene boundary coincides with a marked change in lithology in Core 8.

Zone NN11 of the upper Miocene encompasses the interval from Sample 552-3-1, 11 cm down to 7-2, 20 cm. *Discoaster quinqueramus* was observed in all investigated samples in that interval. Rare specimens of *Amaurolithus primus* and *A. tricorniculatus* were observed in Sample 552-4,CC, which indicates that this sample is of Messinian age (late late Miocene). Dropstones were found in the top of Core 7. The sediments adjacent to these erratics contain Pliocene (*Discoaster tamalis, Ceratolithus rugosus*) contaminants. The first occurrence of *Discoaster berggrenii* occurs between Samples 552 7-2, 20 cm and 552-7-4, 19 cm. The NN10/NN11 boundary thus occurs between those two samples. Sample 7,CC shows a discoaster association indicative of Zone NN10: *Discoaster bellus, D. calcaris, D. loeblichii, D. pentaradiatus,* and *D. prepentaradiatus.*

Samples 552-8-1, 110 cm and 8-2, 21 cm show essentially identical assemblages, with presence of taxa such as *Cyclicargolithus abisectus, C. floridanus, Coccolithus miopelagicus,* and *Discoaster exilis.* The last two species become extinct within Zone NN8 (Bukry, 1973). According to Muller (1981) the first two become extinct in Zone NN6. Furthermore, *Sphenolithus heteromorphus* is not observed, thus suggesting that these two samples belong to Zone NN6. The last occurrence of *S. heteromorphus* is between 552-8-2, 21 cm and 8-3, 20 cm, indicating the NN5/NN6 boundary. Zone NN5 is present down to 552-8-4, 40 cm, based on the presence of *S. heteromorphus* and absence of *Helicosphaera ampliaperta.* A hiatus of approximately 25 m.y. duration is present in 552-8-4, 40 cm, which separates the overlying middle Miocene sediments from the middle Eocene sediments underneath the unconformity.

Paleogene

The Paleogene sediments in Cores 552-8 through 21 are predominantly of early Eocene (NP11 through NP14) age and show poorly preserved assemblages with abundant nannofossil fragments. The central area cross structures in the chiasmoliths are, for example, commonly completely dissolved. A sample taken from immediately below the unconformity (Sample 552-8-4, 45 cm) contains common or abundant *Cyclicargolithus pseudogammation, Chiasmolithus expansus,* and *Reticulofenestra umbilica,* which suggest that this sample belongs to Zone NP16 (the CP14a *Discoaster bifax* Subzone of Bukry, 1973; Okada and Bukry, 1980). Sample 8,CC does not contain *Reticulofenestra umbilica* (*R. dictyoda* is abundant), but the discoaster association in this sample (*Discoaster keupperi, D. nonaradiatus, D. sublodoensis*), and the presence of *Nannotetrina cristata,* indicates Zone NP14. *Discoaster septemradiatus* and *D. keupperi* were observed in 9,CC. The presence of the former taxon suggests that this sample may be referred to NP14 (Muller, 1979). *Discoaster distinctus, D. sublodoensis* and *N. cristata* are present in 10,CC, again indicating Zone NP14 (Bukry, 1973; Romein, 1979).

No sediments were recovered from Core 11.

The last occurrence of *Tribrachiatus orthostylus,* which defines the NP12/NP13 boundary, is in Section 14-2 between 28 and 56 cm. Zone NP13 is thus represented between 10,CC and 14-2. *Discoaster lodoensis* has its first occurrence between 18-1, 81 cm and 18-2, 24 cm. This datum event defines the NP11/NP12 boundary, which implies that Zone NP12 is represented by the interval between Sections 552-14-2 and 18-1. Within Zone NP12, the first occurrence of reticulofenestrids (Section 15-1) and the last occurrence of *Toweius occultatus* (Section 16-1) were observed. Basalt was encountered in Sample 21-3, 65 cm. In Sample 21-3, 39 cm the first occurrence of *Tribrachiatus orthostylus* was observed. This event closely approximates the NP10/NP11 boundary (e.g., Okada and Thierstein, 1979). In Samples 552 21-3, 60 cm *T. orthostylus* was not observed, whereas *Ellipsolithus macellus,* not present higher in the sequence, occurs. Since the last occurrence of the latter species and the first occurrence of the former species are, at most, separated by one core in any hole drilled in the Rockall area (Leg 48, Sites 403, 404; Leg 81, Sites 552, 553, 554, 555), this may suggest that we are observing the true first occurrence of *T. orthostylus* in Sample 552-21-3, 39 cm. Consequently, the few tens of centimeters of sediments lying on top of the basalts are probably very close to the NP10/NP11 boundary.

Preservation is generally poor, primarily because of partial dissolution but to a lesser extent because of secondary overgrowth of calcite, in the lower Eocene part of Hole 552. It is particularly evident in the interval between Cores 19 and 21, where the frequency of coccoliths is also low. In fact, the frequency is so low below Core 14 that it is very difficult to make estimates of relative abundances of the various taxonomic components.

Hole 552A

Neogene

Cores 1 through 7 represent the Pleistocene. The Pliocene/Pleistocene boundary is placed at the extinction level of *D. brouweri*. The late Pleistocene stratigraphy is excellently resolved by the oxygen isotope stages (see Zimmerman et al., this volume). However, the last occurrence of *Pseudoemiliania lacunosa* (the NN19/NN20 boundary) is in Section 552A-2-3 between 49 and 60 cm. A small gephyrocapsid species, approximately 1 to 3 μm in length, shows a bloom in Sample 552A-4,CC; possibly indicating Gartner's (1977) "small *Gephyrocapsa* Zone." Gartner suggested that the upper boundary of that zone falls within the Jaramillo paleomagnetic event (0.91–0.97 m.y. ago). *Calcidiscus macintyrei* has its last occurrence between 70 and 90 cm in Section 552A-7-1.

The whole sequence of late Pliocene discoaster extinctions is represented in Hole 552A: *Discoaster brouweri* (plus its triradiate form), *D. pentaradiatus, D. surculus* and *D. tamalis*.

Taxon	Last occurrence	Zonal boundary	(Core-Section, level in cm)
Discoaster brouweri	LO	NN18/NN19	8-1, 30 to 8-1, 40
D. pentaradiatus	LO	NN17/NN18	9-2, 120 to 9-3, 20
D. surculus	LO	NN16/NN17	9-3, 40 to 9-4, 10
D. tamalis	LO	—	10-1, 20 to 10-1, 90

Core 13 is disturbed and was therefore neglected for biostratigraphical purposes. *Reticulofenestra pseudoumbilica* s.str. drastically decreases in abundance at the very top of Core 14, although stray specimens were observed in higher cores. The fact that *Discoaster tamalis* is present in the top part of Core 14, but not further down, indicates that the drastic decrease of *R. pseudoumbilica* probably represents the extinction level of this species (see Backman and Shackleton, 1983), and hence the NN15/NN16 boundary, with the few specimens in the higher cores being reworked.

Amaurolithus primus and *Discoaster asymmetricus* cooccur in Sample 552A-16,CC, indicating that this sample belongs to Zone NN14. Zone NN13 is indicated in Sample 18,CC by the presence of *Ceratolithus rugosus*. *Ceratolithus acutus* is present in Sample 22,CC. According to Haq and Berggren (1978) this species has its first occurrence within Zone NN12. Since its last occurrence approximates to the NN12/NN13 boundary, Sample 22,CC may be placed within Zone NN12. Very rare and poorly preserved specimens of *Discoaster quinqueramus* are present in Sample 552A-26,CC, but this species is common in 27,CC, placing the NN11/NN12 boundary between 26,CC and 27,CC. This further implies that the Miocene/Pliocene boundary can be placed between 26,CC–27,CC and 22,CC. Zone NN11 is identified down to Sample 32,CC.

Samples 33,CC and 34,CC both belong to Zone NN10, because of the presence of *Discoaster bellus, D. loeblichii, D. neohamatus*, and *D. pseudovariabilis.*

Sample 35,CC is assigned to Zone NN7, which is based on the presence of *Discoaster kugleri* and *Coccolithus miopelagicus*, and the absence of *Cyclicargolithus abisectus* and *C. floridanus.* The middle Miocene Zone NN7 is represented from 552A-35,CC to the hiatus at 552A-36-3, 139 cm.

The Neogene-Paleogene Transition and the Paleogene

A clear lithologic change occurs in Core 552A-36-3, 139 cm. The coccoliths at 130 cm are dominated by *Coccolithus pelagicus*, but they also show a fairly diversified discoaster association, including *Discoaster bollii, D. exilis, D. kugleri*, and *D. moorei;* thus placing this sample in Zone NN7. An entirely different assemblage characterizes the 141 cm level, with abundant *Zygrhablithus bijugatus, Coccolithus pelagicus*, and *Cyclicargolithus abisectus*, and common *Chiasmolithus altus, Dictyococcites bisectus*, and *D. hesslandii.* Two specimens of *Sphenolithus distentus* were observed. *Cyclicargolithus abisectus* has its first evolutionary appearance at the NP23/NP24 boundary according to Muller (1979), and since *S. distentus* is also present the 141 cm level represents Zone NP24. This indicates the presence of a hiatus at the 139 cm level encompassing approximately 12 m.y.

Considerable lithological changes and signs of intensive burrowing characterize the Paleogene sediments, especially in Sections 552A-36-3 and 37-1. The investigation of a series of closely spaced samples (5 to 20 cm apart) in Sections 36-3 and 4, 37-1 and 2 clearly depict a highly disordered stratigraphic sequence. Samples in Sections 36-3, 36-4, and 36,CC mainly give Oligocene ages (Zones NP21(?), NP22(?), NP23, and NP24). Samples in Sections 37-1 and 2, down to the 66 cm level, contain a mixture of Eocene and Oligocene coccoliths. It is not considered meaningful to establish an ordered stratigraphy in the above-mentioned samples. Apart from the Oligocene taxa mentioned above, major elements in the disordered sequences are: *Chiasmolithus expansus, C. oamaruensis, C. solitus, Cruciplacolithus delus, Cyclicargolithus floridanus, Discoaster bifax, D. distinctus, D. kuepperi, D. sublodoensis, Ericsonia fenestrata, Helicosphaera bramlettei, Isthmolithus recurvus, Reticulofenestra daviesi, R. hillae*, and *R. umbilica.* It is noteworthy that one sample in 552A-37-1, 138 cm shows coccoliths characteristic of Zone NP15, which is the only definite NP15 encountered in the Leg 81 material. *Chiasmolithus gigas* and *Nannotetrina alata* are present in that sample, thus indicating the (CP13b) *C. gigas* Subzone of Okada and Bukry (1980), i.e., the middle part of Zone NP15. Zone NP14 is represented from Samples 552A-37-2, 66 cm down to 38,CC; *Discoaster sublodoensis* and *Nannotetrina cristata* are present in most samples investigated in this interval.

A severely corroded specimen of *Discoaster barbadiensis* was observed from the sedimentary nucleus of a relatively large manganese nodule (Sample 552A 37-1, 20 cm).

Planktonic Foraminifers

Hole 552

Core-catcher 1 was the only Pleistocene sample taken in Hole 552. The diagnostic planktonic foraminifers in Sample 552-1,CC are *Globorotalia truncatulinoides, G. inflata, G. hirsuta, Neogloboquadrina pachyderma* (left coiled), and *Globigerina bulloides cariacoensis*.

Core-catcher 2 is from the upper Pliocene (N21?). The diagnostic planktonic foraminifers include *Neogloboquadrina atlantica* and *Globorotalia puncticulata*, both of which become extinct in the late Pliocene. Sample 552-3,CC appears to be from the lower Pliocene–upper Miocene interval, but there is nothing definitive on which to assign a specific age. The *Neogloboquadrina* plexus overwhelms the planktonic foraminiferal population, whereas *Globorotalia puncticulata, G. margaritae*, and *G. conoidea* are absent.

Core-catchers 4 and 5 appear to be from the upper Miocene because of the presence of *Globorotalia conoidea*, which is characteristic of the upper Miocene in the Rockall area (see Hole 552A). The coiling change in the *Neogloboquadrina* plexus from left coiled above to right coiled below occurs between Samples 6,CC and 7,CC. At or below the coiling change the diversity of the planktonic foraminifers increases and more warm-water species appear, such as *Globigerinoides obliquus, G. quadrilobatus, Sphaeroidinellopsis seminulina*, and *Globigerinopsis aquasrayensis*.

Core-catcher 8 may be in the middle Eocene because *Globigerina eocaena, Acarinina* sp. cf. *A. spinuloinflata*, and *Pseudohastigerina* sp. cf. *P. micra* are present. However, from Sample 9,CC to the lowest foraminiferal sample in Core 21, Section 2 the age of the sediments appears to be early Eocene. This age assignment is based on the occurrence of *Pseudohastigerina wilcoxensis, Acarinina* sp. cf. *A. broedermanni, A. pseudotopilensis, A.* sp. cf. *A. soldadoensis, Globigerina patagonica*, and *Globorotalia* sp. cf. *G. lensiformis*.

Hole 552A

The Pleistocene section can be separated from the Pliocene on the basis of planktonic foraminifers, and it can be divided into an upper and lower part. In general the Pleistocene in this hole can be characterized by the dominance of *Neogloboquadrina pachyderma* (in the broad sense), the abundance of left-coiled *N. pachyderma*, the presence of *Globorotalia inflata*, and a quite variable population of *Globigerina bulloides* with several named "subspecies" or forms. The upper part of the Pleistocene can be distinguished by the general presence of large, well-developed *Globorotalia truncatulinoides*. This species is absent in the lower part of the Pleistocene section.

The Pliocene in Sample 552A-9,CC is distinguished by the absence of *Globorotalia inflata* and by the presence of its ancestor *G. puncticulata*. Sample 9,CC also contains the last occurrence of *Neogloboquadrina atlantica*, a strong if not dominant component of the planktonic foraminiferal assemblage through most of the upper Miocene and Pliocene. The Pliocene planktonic foraminiferal assemblage is noteworthy for its apparent stability and lack of diversity. Going down the section the Pliocene assemblages can be characterized thus: at the top of the Pliocene, *Globorotalia crassaformis* (rare) with sporadic occurrences of *G. crassula* and *G. praehirsuta* are characteristic (probably broadly equivalent to Blow's N21). *Globorotalia crassaformis, G. crassula*, and *G. praehirsuta* apparently do not occur in the lowest upper Pliocene (upper N19).

The top of lower Pliocene can be defined, using planktonic foraminifers, on the first downhole encounter of *Globorotalia margaritae* (within N19 of Blow and PL2 [top] of Berggren). There is a short concurrent range zone of *G. margaritae* and *G. puncticulata* between Samples 552A-16,CC and 19,CC, below which *G. puncticulata* is not found. The lower limit of the Pliocene cannot be defined yet on the basis of planktonic foraminifers. *Globorotalia margaritae* may range down into what must be the upper Miocene (N17) in core-catchers 25, 26, 30, and 31. However, the possibility that some of these forms are those of the ancestor form *Globorotalia cibaoensis* cannot be excluded. The only species that may possibly be useful in delimiting the top of the Miocene is *Globorotalia conoidea*, which does not appear to range into the Pliocene in this area. In this regard it is pointed out that the first definite downhole occurrence of *G. conoidea* is in Sample 23,CC. Therefore, Sample 23,CC possibly represents the top of the Miocene based on planktonic foraminifers.

The planktonic foraminiferal assemblages in the upper part of the upper Miocene (N17) are just as stable and lacking in diversity as the overlying Pliocene assemblages. The only new and consistently present additions to the assemblage appear to be *Globorotalia acostaensis* and *Globigerina parabulloides*. *Globorotalia cibaoensis* and *G. conoidea* occur sporadically and in low abundances throughout most of the upper Miocene. *Globorotalia conoidea*, however, makes its highest consistent appearance in core-catcher 28 and is found through 34,CC. The lowest reasonably certain appearance of *G. cibaoensis* is in 31,CC. The coiling change in the *Neogloboquadrina* plexus occurs between Samples 32,CC and 33,CC.

Tentatively Sample 552A-35,CC is considered to be at the base of the upper Miocene (N16). This is based on the presence and abundance of *Neogloboquadrina* cf. *acostaensis* and *N. continuosa*, with perhaps some *N.* cf. *atlantica* and *N. dutertrei humerosa*. Sample 35,CC also contains *G. panda, G. mayori, G. challengeri*, and *G. miozea miozea* all of which do not occur higher than the middle Miocene. Therefore, it appears that Sample 35,CC contains a reworked and mixed upper and middle

Miocene assemblage. Furthermore, there is definite reworking in Sample 36,CC where the great bulk of the planktonic foraminiferal specimens are of middle Miocene age. Sample 36,CC also contains *Globigerina angiporoides* which is diagnostic of late Eocene and Oligocene age. The middle Miocene faunal components of Sample 36,CC include *Globorotalia panda, G. miozea miozea, G. fohsi peripheroronda, Globorotaloides variabilis, Globoquadrina dehiscens, Sphaeroidinellopsis seminulina, Globigerina wood, G. pseudociperoensis, G. parabulloides, Globigerinoides obliquus*, and *G.* cf. *subquadratus*, suggesting a zonal range of N9 to N12.

Samples 37,CC and 38,CC were barren of planktonic foraminifers.

Benthic Foraminifers

Hole 552

The Neogene is represented by Samples 552-1,CC to 7,CC. All are characterized by a *Planulina wuellerstorfi* fauna which includes *Cibicidoides kullenbergi, Oridorsalis umbonatus*, and *Epistominella exigua.* In the early Pliocene and late Miocene (2,CC to 6,CC) additional forms include *Globocassidulina subglobosa, Laticarinina pauperata*, and *Brizalina subaenariensis.* In 3,CC and 4,CC *Bulimina alazanensis* and *Ehrenbergina serrata* are present. All these assemblages are characteristic of North Atlantic Deep Water at lower mesobathyal depths, i.e., similar to the present site depth (2301 m). The planktonic:benthic ratio is 99:1 or 98:2, and the planktonic tests are large.

Within Core 8 there is a major hiatus between the late Miocene above and the middle Eocene below.

The middle Eocene is represented by Samples 552-8,CC to 10,CC. Preservation is poor to moderate in 8,CC, poor in 9,CC, and moderate in 10,CC. Dissolution has affected these assemblages; there has been almost total loss in 9,CC, and in 8,CC and 10,CC the planktonic:benthic ratio (37:63 in each case) has probably been changed through preferential loss of planktonic tests. Nevertheless, benthic diversity is high in 8,CC ($\propto$20) and moderate in 10,CC ($\propto$14).

Sample 552-8,CC is dominated by *Nodosaria* spp. and *Cibicidoides* spp., and although these forms are present in 10,CC the dominant species are *Oridorsalis ecuadorensis* and *Alabamina wilcoxensis.* By analogy with Hole 552A, this represents a depth greater than 700 m.

The early Eocene assemblages also have poor to moderate preservation. The planktonic:benthic ratio varies from 38:62 to 65:35. If these are true ratios, i.e., unaffected by dissolution modification, they would indicate some degree of isolation from the open ocean. The benthic assemblages are strongly dominated by *Anomalinoides howelli* (20%), and this suggests shelf sea depths, probably middle shelf (75–100 m). The moderate diversity values of $\propto$12–14 are in accordance with this and show the salinity to be normal. There are a few rare occurrences of *Elphidium hiltermanni* and *Protelphidium* sp., which are indicative of not too distant brackish waters.

Hole 552A

The Neogene section, from the topmost Pleistocene (Core 1) to the middle Miocene (Core 36), is characterized by the *Planulina wuellerstorfi* fauna, including among others *Osangularia umbonifera, Epistominella exigua, Oridorsalis umbonatus, Cibicidoides kullenbergi*, and *Melonis* spp.

Two kinds of faunal differentiation can be observed: (1) the strong decrease in abundance of some species (*Stilostomella* spp., *Bulimina alazanensis*) from late Miocene peaks, and the disappearance of others (*Globocassidulina subglobosa, Ehrenbergina serrata, E. trigona*, and *Brizalina subaenariensis*) within Cores 10 and 9 at the onset of "glacial" conditions. *Cassidulina teretis* is present only in the "glacial" late Pliocene part of the section. (2) The quantitative composition of the fauna undergoes strong fluctuations, which occur more or less regularly beginning at least in the late Miocene (Core 30). The amplitude of these fluctuations increase in Cores 10 ("pre-glacial" late Pliocene) and 9 ("glacial" late Pliocene) without showing a distinct reaction to the first occurrence of ice-rafted sediments at the base of Core 9. A further increase in the amplitude of faunal fluctuations, and an increase in cycle length, occurs in the late Pleistocene (Core 3).

The diversity of the benthic fauna is very high in Sample 552A-1,CC ($\propto$30) and is generally high ($\propto$20–24) throughout the Neogene. However, there are some lower values. In Cores 2,CC, 3,CC, 4,CC, and 9,CC, the low values may be indicative of some instability in the bottom water related to the glacial–interglacial cycles. There is no obvious explanation for the lower values in 28,CC and 30,CC, but those of 35,CC and 36-2, 100 cm probably reflect the establishment of the new fauna above the hiatus. The high diversity of 1,CC reflects the presence of fragile species which are normally destroyed fairly early in diagenesis.

The planktonic:benthic ratio is 99:1 throughout and indicates open ocean conditions. The presence of the *Planulina wuellerstorfi* fauna suggests the existence of North Atlantic Deep Water and depths greater than 1500 m. The general rarity of *Sigmoilopsis schlumbergeri* indicates depths greater than 2200 m, while the presence of *Epistominella exigua* in abundances of less than 20% (except in 4,CC; 26%) suggests depths of less than 2900 m.

There is a major hiatus in Core 36 between the middle Miocene and the late Oligocene and in Core 37 between the latter and the middle Eocene.

The late Oligocene assemblages bear some similarity with those of the middle Miocene. The dominant groups are *Nodosaria–Stilostomella* spp., *Gyroidinoides* spp., *Globocassidulina subglobosa*, and *Osangularia* spp. Also present are *Oridorsalis umbonatus, O. ecuadorensis, Bulimina alazanensis*, and *Spiroplectammina spectabilis.* This is clearly a bathyal assemblage and may represent a depth of at least 1500 m. The planktonic:benthic ratio is high and the benthic diversity is moderate to high ($\propto$13–24).

The middle Eocene assemblages, like those of Site 552, have undergone dissolution, and this has probably modified the planktonic: benthic ratio to a greater or lesser extent. The preservation of the benthic forms is generally moderate to good but is poor in Samples 552A-37-2, 137 cm; 37,CC; 38-1, 62 cm; and 38,CC. The assemblages have the following species in common: *Nodosaria–Stilostomella* spp., *Gyroidinoides* spp., *Alabamina wilcoxensis, Pullenia quinqueloba*, and *Lenticulina* spp. Samples 552A-37-1, 65 and 137 cm also have *Spiroplectammina spectabilis, Nuttallides truempyi, Gavelinella semicribrata*, and *Trifarina cuneata*. This suggests epibathyal depths greater than 700 m (cf. Site 116, Berggren and Aubert, 1976). *Nuttallides truempyi* extends down to Sample 552A-37,CC and probably the remainder of this section is epibathyal. The diversity values are moderate, ∝11–13.

Samples 552A-37-1, 65 and 137 cm have essentially the same fauna as Sample 552-8,CC although the depth of recovery is not exactly the same: at Hole 552, 165 m; at Hole 552A, about 174 m (see Operations).

The thin Paleogene succession of Holes 552 and 552A is not only condensed but also reveals the rapid subsidence which was taking place here.

Diatoms

Hole 552

Rare to common diatoms occur in lower Eocene through upper Pliocene sediments at Site 552. Preservation is poor to good, with Eocene sediments generally being dominated by robust forms. Index species are rare, and thus age control throughout the Neogene of Hole 552 is poor.

Core 1 contains rare nondiagnostic fragments. Core 2 is correlated with the *Nitzschia jouseae* Zone represented in Cores 552A-10 through 16. This age assignment is supported by the presence of *Thalassiosira convexa* var. *aspinosa* and *Thalassiosira oestrupii. Nitzschia jouseae* is presumed to be ecologically excluded from this sample.

The occurrence of *T. convexa* var. *aspinosa* and *Thalassiosira miocenica* without *T. oestrupii* allow the placement of Cores 3 through 4-2 into the late Miocene portion of the *Thalassiosira convexa* Zone. The base of this zone coincides with a dissolution interval which is recognized at all sites. In Hole 552 this dissolution interval occurs from Cores 4 through 9. One specimen of *Triceratium castelliferum* was observed in Sample 552-8,CC, suggesting an Eocene age.

Few moderately preserved Eocene diatoms are present in Cores 10 and 12 (Core 11 had no recovery). The presence of *T. castelliferum* and *Stephanopyxis grunowii* without the *Pyrgupyxis, Trinacria*, and *Screptroneis* groups which locally are common within sediments assigned by nannofossils control (see Hole 553A) to the early Eocene suggest a different environment of deposition or a different age. The common occurrence of several species of *Arachnoidiscus* as well as abundant radiolarians and sponge spicules within these samples suggest an outer shelf environment.

Except for Cores 14 and 21, all other samples examined are barren of diatoms. Cores 14 and 21 are late Paleocene–early Eocene in age based on the occurrence of *Pyrgupyxis prolongata, Trinacria pileolus, Trinacria excavata, T. excavata* var. *tetragona, Rhizosolenia interposita*, and *Screptroneis* sp. Numerous varieties of *Stephanopyxis* are common throughout this interval.

Hole 552A

Cores 1 and 2 contain a well-preserved diatom assemblage, including such species as *Pseudoeunotia doliolus, Rhizosolenia bergonii, Hemidiscus cuneiformis, Thalassiosira oestrupii*, and *Nitzschia panduriformis*. These samples are assigned to the Pleistocene *Pseudoeunotia doliolus* Zone.

The interval from the last occurrence of *Nitzschia jouseae* to the first occurrence of *P. doliolus*, which defines the *Nitzschia marina* Zone, is found in Core 3 through Core 10, Section 2. The diatom slides examined within the main part of this zone (Cores 3 to 8) contain a distinct dissolution interval composed of ice-rafted detritus. The extinction of *Thalassiosira convexa* s. ampl. in Core 9 indicates that this interval is in the lower portion of the *Nitzschia marina* Zone and is late Pliocene in age.

Sections 552A-10-2 through 16-4 contain common, moderately to well-preserved diatoms. This interval is assigned to the Pliocene *Nitzschia jouseae* Zone based on the presence of *N. jouseae*. The extinction of *Nitzschia cylindrica* in Section 552A-17-1 supports this age assignment. The assemblage throughout this interval is dominated by *Thalassionema nitzschioides* and *Thalassiothrix longissima*. Other species present include *Nitzschia reinholdii, Nitzschia fossilis, Coscinodiscus nodulifer, Thalassiosira leptopus, Thalassiosira convexa* s. ampl., *Thalassiosira oestrupii*, and *Hemidiscus cuneiformis*.

The interval from Sample 552A-16,CC through Core 28 is placed in the *Thalassiosira convexa* Zone based on the occurrence of *T. convexa, N. cylindrica*, and *Rhizosolenia barboi*. The first occurrence of *Thalassiosira oestrupii*, which is slightly younger than the Miocene/Pliocene boundary (5.3 m.y. ago), occurs in Core 21. Also supporting this boundary placement are the extinctions of *Thalassiosira miocenica* in Core 22 and *Thalassiosira nativa* in Core 21.

Cores 29 and 30 are assigned to Subzone b of the *Nitzschia miocenica* Zone of Burckle (1972, 1977) based on the presence of *Thalassiosira praeconvexa* below the first occurrence of *Thalassiosira convexa* and *Thalassiosira miocenica*. The interval of dissolution, which coincides with the base of this zone at all sites, occurs in Core 31 through Core 37, Section 2. Fragments of *Actinocyclus ingens* in Sample 552A-36-3, 30–32 cm suggest a middle Miocene age.

Core 37, Section 3 through Core 38 are Eocene in age, and contain an assemblage similar to that found in Cores 552-10 through 12. Additional species observed include *Melosira clavegirea, Pterotheca danica*, and *Triceratium* sp. Sponge spicules are common throughout this interval.

Radiolarians

Site 552 presented moderately well-preserved, fairly abundant radiolarian assemblages from the Quaternary, Pliocene, upper Miocene and Eocene.

In the upper Pliocene and Pleistocene, Cores 552-1 and 552A-1 through 11, radiolarians are poorly preserved, rare, and diluted with nonbiogenic components. Many samples in this interval are barren of siliceous fossils. The only age-diagnostic event observed was the extinction of *Stylatractus universus* (0.425 m.y ago, Morley and Shackleton, 1978) between Samples 552A-1-3, 53–54 cm and 552A-2-2, 122–124 cm.

Radiolarians are more abundant and better preserved in the lower Pliocene to upper Miocene Core 552-2 through Core 6, Section 4 and Core 552A-10 through Core 31, Section 1. The last occurrence of *Stichocorys peregrina* occurs between Samples 552A-13,CC and 552A-14-1, 30–31 cm. This datum appears lower than expected, and the species is very rare at the top of this range. The evolutionary transition of *S. delmontensis* to *S. peregrina* happens between Samples 552A-29-3, 54-55 cm and 30,CC.

Below the evolutionary transition of *S. delmontensis* to *S. peregrina*, there is an interval of approximately 30 m (Cores 552-7 through 9, and Sections 552A-31-3, through 37-1), in which radiolarians are all or nearly all dissolved. The shallow-water Eocene sediments of the remaining cores contain rare to common radiolarians diluted with large sponge spicules. *Lophocyrtis norvegiensis, Pterocodon ampla*, and *Phormocyrtis striata striata* are common components of the middle Eocene assemblage in Cores 552-10 and 552A-37 through 38. Cores 552-12 through 21 contain fewer radiolarians but in Section 552-18-2, there are some rather corroded tests that appear to be lower Eocene forms *Amphicraspedum murrayanum* and *Pterocodon lex*, and Sample 552-21-3, 47–49 cm contains the lower Eocene species *Buryella tetradica.*

Dinoflagellates

The dinoflagellate stratigraphy of the Eocene of Hole 552 was studied by Brown and Downie (this volume): their results are summarized here. The dinoflagellate zonation used is that devised by Costa and Downie (1979).

Core 18 contains *Dracodinium condylos* and is referrable to Zone II. Cores 14 to 16 contain assemblages dominated by *Polysphaeridium zohari*, equating with Zone III. Core 13 is barren of palynomorphs. Core 12 is marked by the first occurrence of *Homotryblium oceanicum* and is therefore referred to Zone IV. Cores 8 and 9 are barren of palynomorphs.

Throughout Zones II to IV the percentages of pollen and spores never exceed 35%, and terrestrial organic debris is very sparse, indicating that during this time the shoreline was relatively distant.

Site 553

Pleistocene sediments were recovered in the mudline core (Hole 553) and the four HPC cores of Hole 553B (28.5 m). Glacial–interglacial contrasts are evident from the alternations of nannofossil–foraminifer oozes and darker marls. However, severe drilling disturbance of most of these cores has degraded their biostratigraphic value. Discontinuous rotary drilling (Hole 553A) recovered Pliocene (65.5 to 113 m) and late Miocene (151.0 to 160.5 m) sediments. Continuous coring commenced below 179.5 m. The mid to late Miocene boundary was reached at 200 m (Core 6), the mid to early Miocene boundary at 221.75 m (Core 8), and the early Miocene to late Oligocene boundary at 231.6 m, within Core 9. This Neogene section, however, is incomplete since most of the early Miocene is absent, and represented by a hiatus in Core 8.

Calcareous microfossils are usually abundant and are moderately well preserved in the Neogene sequence of nannofossil–foraminifer oozes. Siliceous microfossils, on the other hand, have been dissolved to various degrees, with radiolarians being somewhat less susceptible than diatoms: radiolarians are absent from Cores 4 and 5 only, whereas diatoms are missing or too poorly preserved for diagnosis from Cores 2 through 6. In the short section of mid-Miocene glauconitic foraminifer oozes and early Miocene nannofossil–foraminifer chalk (Cores 8 and 9, principally) preservation and abundance improves somewhat. Benthic foraminifers indicate that depth of deposition throughout the Neogene took place at depths very close to the actual depth of this site (2329 m).

The 3.25-m-thick section of upper Oligocene foraminifer oozes is rich in moderately well-preserved calcareous and siliceous microfossils and was probably deposited in an environment that continued into the early Miocene. Manganese nodules and stains at the base of this section, perhaps indicative of an incipient hard ground, suggest that initial sedimentation may have been slow.

A major unconformity encompassing the entire early Oligocene, late Eocene, and part of the middle Eocene occurs at 234.8 m (Section 553-9-6). The thin interval (6 m) of middle Eocene sediment may have been deposited in depths greater than 750 m. In these sediments, siliceous biogenic debris is found in great abundance and the planktonic foraminiferal fauna is almost monospecific. A lesser unconformity separates the upper middle Eocene from the lower middle Eocene at 240.5 m (Section 553-10-3), which is characterized by poorly developed planktonic foraminiferal faunas, abundant but mostly poorly preserved biogenic silica, a great increase in volcanogenic sediments, and a decrease in the depth of deposition to probably 100–180 m by Core 553-11,CC. Sediments in Cores 553-14 to 25 contain a rich macrofauna of bivalves, gastropods, bryozoans, echinoids, and serpulids. In the early Eocene and late Paleocene mudstones, radiolarians, and planktonic foraminifers are absent, diatoms are rare or altered beyond recognition, and calcareous nannofossils are absent or poorly preserved. Benthic foraminifers in the interval above the basalt to 11,CC indicate a migration of the shoreline seaward, resulting in brackish lagoons or estuaries. At times of reduced sedimentation, the sea transgressed landward, resulting in an increase in depth to around 100 m, but throughout much of the early Eocene sedimentation and subsidence more or less kept pace with one another.

Calcareous Nannofossils

Hole 553

One core was retrieved from Hole 553, the core catcher sample from which contains an assemblage indicative of Zones NN20-NN21. *Pseudoemiliania lacunosa* is missing in this sample (1,CC).

Hole 553A

Major Unconformities

Thirty-seven cores were retrieved from the sedimentary sequence overlying the basalts in Hole 553A. The Neogene is represented in Cores 1 through 9-4, 90 cm. The nannofossils indicate the presence of an unconformity encompassing a major part of the early Miocene within Core 8-3. The Miocene/Oligocene boundary is present in 9-4. Sediments of late Oligocene age (primarily NP25) are represented in Cores 9-4, -5, and -6. A major hiatus occurs in Core 9-6 between 25 and 35 cm (25 cm: NP25, late Oligocene; 35 cm: NP16, middle Eocene). Another Paleogene unconformity occurs between Core 10-3, 100 cm (NP16, upper part of middle Eocene) and the 130 cm level in the same section (NP14: lower part of middle Eocene). Cores 11 through 24 are all of early Eocene age (NP14 to NP10). Only 4.5 cm of sediment separates the base of NP12 from the base of NP11, indicating a hiatus. Samples 24,CC through 36,CC are barren. Core 37 probably represents the early Eocene (Zone NP10), although a late Paleocene assignment cannot be excluded.

Neogene

A sample from Sample 553A-1,CC shows a late Pliocene (NN16) nannofossil assemblage with abundant *Dictyococcites productus*, common *Coccolithus pelagicus*, rare *Discoaster pentaradiatus* and *D. surculus*, and an absence of *Reticulofenestra pseudodumbilica.* Core 2 is also referred to Zone NN16, again with *Dictyococites productus* and *Coccolithus pelagicus* as dominant forms, but with the addition of *Calcidiscus leptoporus* as a common member of the assemblage. The very rare specimens of *R. pseudoumbilica* observed are considered to represent reworking. Sample 553A-3,CC shows a relatively sparse late Miocene (NN11) assemblage, composed of approximately ten species, in contrast to the fairly diversified early Pliocene assemblage in Core 2 (17–19 species). *Discoaster quinqueramus* is present in Core 3, indicating Zone NN11. The presence of *Discoaster decorus* indicates, however, that Sample 3,CC probably is very close to the NN11/NN12 boundary.

Continuous coring began with Core 4. Cores 4 through 7 are of late and middle Miocene ages. *Dictyococcites perplexus* is the dominant taxon in Cores 4 and 5, whereas *Reticulofenestra pseudoumbilica, Coccolithus pelagicus*, and *D. perplexus* are common to abundant in Cores 6 and 7. The central opening size among the specimens of *R. pseudoumbilica* are in general comparatively small (implying thick collars) in these cores. Sample 4,CC is placed in NN10 on the presence of *Discoaster bellus* and *D. neohamatus* (no *D. quinqueramus*). The assemblage in 5,CC is essentially the same as in 4,CC and is therefore referred to Zone NN10. *Coccolithus miopelagicus* and *Helicosphaera intermedia* are present in 6,CC. The latter form has its last occurrence at the top of Zone NN7. Since *Cyclicargolithus abisectus* and *C. floridanus* are not present, Sample 6,CC is referred to Zone NN7. In 7,CC *C. abisectus* and *C. floridanus* are present, and *Sphenolithus heteromorphus* is absent, which suggests Zone NN6 (see Müller, 1981). Two samples in Core 8, Section 3 (83 cm and 125 cm) contain *S. heteromorphus*, thereby indicating Zone NN5.

The glauconite content gradually increases in Section 8-3 toward a maximum at 130 cm. The sediments at 125 cm, 5 cm above the lithological change, belong to NN5. At 135 cm the nannofossils are represented by abundant *Cyclicargolithus floridanus*, common *Zygrhablithus bijugatus*, few *Coccolithus pelagicus, Helicosphaera obliqua, Triquetrorhabdulus carinatus*, and rare *Chiasmolithus altus* and *Pyrocyclus orangensis:* an assemblage indicative of earliest Miocene times (NN1–NN2). The diatom and radiolarian biostratigraphy of Hole 553A indicates that the sequence immediately below the unconformity in Sample 553A-8-3, 130 cm should be referred to Zone NN1. The last appearance of *Dictyococcites bisectus* closely approximates to the NP25/NN1 boundary at high latitudes (Bukry, 1973) (see Site 552). That extinction event occurs in Section 9-4 between 5 and 15 cm, thus placing the Oligocene/Miocene boundary at this level.

Paleogene

A major hiatus occurs in Section 9-6 between 25 and 35 cm. The 25-cm level contains abundant *Cyclicargolithus abisectus, C. floridanus, Coccolithus pelagicus*, common *Dictyococcites bisectus, Reticulofenestra daviesi*, few *Helicosphaera euphratis, Discoaster deflandrei* and rare *Chiasmolithus altus, Helicosphaera intermedia, Sphenolithus moriformis, Pyrocyclus inversus*, and *Zygrhablithus bijugatus.* According to Müller (1979, see also Site 552) *Cyclicargolithus abisectus* has its first occurrence close to the NP23/NP24 boundary, which suggests that the 25-cm level in Section 9-6 may be referred to either Zone NP25 or NP24, although an uppermost NP23 assignment cannot be excluded.

The upper middle Eocene is present in Section 9-6 from 35 cm to 10-3, 70 cm. *Chiasmolithus nitidus* and *C. solitus* are abundant in this unit. *Reticulofenestra dictyoda, R. umbilica, Rhabdosphaera tenuis*, and *Cyclicargolithus floridanus* are common members of the assemblages. Other taxa in the middle Eocene section are *Chiasmolithus expansus, C. grandis, Coccolithus eopelagicus, Discoaster barbadiensis, D. bifax, D. deflandrei, D. nodifer, Helicosphaera dinesenii, Neococcolithes dubius, Pontosphaera obliquipons, Pyrocyclus inversus, Reticulofenestra minuta, Sphenolithus moriformis, S. spiniger*, and *Zygrhablithus bijugatus.* The presence of

Discoaster bifax strongly suggests that this unit can be referred to NP16 and CP14a of Okada and Bukry, 1890 (the *Discoaster bifax* subzone).

The distinct lithologic change in Sample 553A-10-3, 100 cm is associated with a hiatus encompassing NP15. Zone NP14 is present in Section 10-3 from 130 cm to 10,CC. Approximately 20–25 species were observed in the 12 samples investigated from Zone NP14, including *Discoaster distinctus, D. keupperi, D. nonradiatus, D. septemradiatus, D. sublodoensis, Helicosphaera lophota, Lophdolithus mochlophorus*, and *Nannotetrina cristata*. Zone NP13 is represented in a short interval in Core 11; Sample 11-1, 10 cm to 11-2, 40 cm, which shows an early Eocene assemblage lacking *Discoaster sublodoensis* and *Tribrachiatus orthostylus*.

Discoaster lodoensis and *Tribrachiatus orthostylus* cooccur from Sample 11-2, 80 cm to 11,CC, thus indicating Zone NP12. Sample 12-1, 26 cm does not contain *D. lodoensis*, but has *T. orthostylus*, implying that this sample belongs to Zone NP11. *Tribrachiatus orthostylus* has its first occurrence in 12-1 at the 74 cm level. *Ellipsolithus macellus* and *Chiasmolithus bidens* have their last occurrence in 12,CC. Rare specimens of *Tribrachiatus contortus* are present in 14,CC, which indicates Zone NP10 for this level. The rarity with which *T. contortus* occurs in Leg 81 material makes the last occurrence of this species unsuitable for determination of the NP10/NP11 boundary. Instead, the first occurrence of *T. orthostylus* is chosen to define the NP10/NP11 boundary, which places this boundary in Sample 553A 12-1, 74 cm.

Coccoliths are not present from Sample 15-3, 90 cm to 21,CC. A second barren interval is present from 24,CC to 36,CC. These barren intervals are separated by three cores (22–24) containing coccoliths. *Tribrachiatus nunnii* was observed in several samples between 22-1, 33 cm and 24-1, 60 cm. Furthermore, *Rhomboaster cuspis* is present between 22-1, 33 cm and 23-1, 106 cm. The cooccurrence of these taxa suggests that these three cores can be referred to the lowermost part of Zone NP10, and hence to the lowermost part of the lower Eocene.

Coccolith-bearing sediments are present from the top of Core 37 to Sample 553A 37-4, 116 cm. The basalt–sediment contact occurs at Sample 37-5, 35 cm. Among the coccoliths present in Core 37 are *Chiasmolithus bidens, Discoaster mediosus*, and *Discoaster multiradiatus*. The coccolith assemblage in Core 37 does not provide an unambiguous indication as to whether this core should be referred to NP10 or NP9. The extinction of fasciculiths occurs in the top part of NP9, but this genus is not represented in Site 553. Despite this no positive evidence exists as to whether or not the NP10/NP9 boundary, and hence the Eocene/Paleocene boundary, is reached in Core 37.

Hole 553B

Four cores were retrieved from Hole 553B, two of which were raised from the mudline. Cores 1 and 2 belong to Zones NN20/NN21, but it was not possible to distinguish the two zones using the light microscope techniques available on board. Most of Cores 3 and 4 are assigned to Zone NN19 because of the presence of *Pseudoemiliania lacunosa*. The extinction of this species occurs in Section 553B-3-2 between 75 and 85 cm. The last occurrence of *P. lacunosa* is dated at 485 thousand years ago (Thierstein et al., 1977). The late Pleistocene sedimentation rate is approximately 2.8 cm/1000 yr. in Hole 553B using the *P. lacunosa* datum, which is conceivably higher than that found in Hole 552A (2.1 cm/1000 yr.), using the same datum.

Except for *P. lacunosa* in Cores 3 and 4, the following taxa were observed: *Calcidiscus leptoporus, Coccolithus pelagicus* (large with bridge spanning the central area opening; smaller forms with a closed central area were comparatively rare), *C. radiatus, Dictyococcites productus, Emiliania huxleyi*(?), *Gephyrocapsa oceanica, Gephyrocapsa* sp., *Helicosphaera carteri, H. inversa, Pontosphaera japonica, P. jonesi, Rhabdosphaera clavigera*, and *Syracosphaera* sp.

Minor amounts of reworked nannofossils were observed in all samples. Late Cretaceous forms are most common. A dropstone in Section 2-6 at 30 cm contains some poorly preserved Maestrichtian nannofossils.

Planktonic Foraminifers

Hole 553

Hole 553 is represented by a mudline sample and is Pleistocene in age based on the occurrence of *Globorotalia truncatulinoides* and abundant *Neogloboquadrina pachyderma*. Sample 553-1,CC is thought to be of middle to late Pleistocene age because in this area *G. truncatulinoides* makes its first appearance in the middle part of the Pleistocene.

Hole 553A

In Hole 553A, Sample 553-1,CC is from the upper Pliocene based on the occurrence of *Neogloboquadrina atlantica, Globorotalia puncticulata, G. crassaformis, G. crassula*, and *G. praehirsuta*. Sample 2,CC is early Pliocene in age based on the co-occurrence of *Globorotalia margitae* and *G. puncticulata*. Sample 3,CC is from within the lower part of the range of the left-coiled *N. atlantica*. The occurrence of *G. conoidea* (= *G. conomiozea* of Poore and Berggren, 1975) suggests a late Miocene age for the sample although there is little else definitive in the assemblage to suggest a specific age. Samples 4,CC and 5,CC are probably late Miocene (N16) in age based on the abundance of *Neogloboquadrina acostaensis* and *N. continuosa*. Samples 553A-6,CC and 7-1 through 7-5, 70–72 cm are from an interval of overlap in the ranges of *N. acostaensis* and *G. mayeri*. The ranges of these two taxa have not been known to overlap and the top or extinction of *G. mayeri* is generally accepted as defining the top of N14, whereas the first evolutionary occurrence of *N. acostaensis* is accepted as defining the base of N16. Poore and Berggren (1975) also recognized this zone of overlap in this area, but they attributed it to reworking of middle Miocene sediments during the early part of late Miocene time. However there is no evidence of reworking. Furthermore, the coiling directions of the *N. acostaensis/N. atlantica* plexus in this interval are random in contrast to the coiling directions of right and left which occur throughout the rest of the upper Miocene and Pliocene, suggesting a different, older stratigraphic interval. Finally *N. acostaensis* and *N. atlantica* in this interval differ from the rest of the overlying plexus in having more finely perforated tests and show an evolutionary series into *Globorotalia challengeri* (Kennett and Srinivasan, 1983). It is therefore suggested that the top of *G. mayeri* in this area, and specifically at Sites 552 and 553, may be more stable than the "evolutionary first occurrence" of *N. acostaensis*. On that basis Samples 6,CC through 7-5, 70–72 cm are no younger than Zone N14 and are therefore middle Miocene in age.

Samples 553A-7-6, 70–72 cm and 7,CC are middle Miocene in age based on the occurrence of *Orbulina suturalis, G. miozea miozea, G panda, Globigerina druryi*, and *Globigerinoides subquadratus*. Sample 553A-8,CC is early Miocene, N4 in age, based on the occurrence of *Globoquadrina dehiscens dehiscens, G. dehiscens praedehiscens, Globorotalia* cf. *pseudokugleri*, and *Catapsydrax dissimilis*.

Sample 9,CC contains an almost monospecific fauna of *Globigerina eocaena*. However, two small individuals of *Acarinina* cf. *spinuloinflata* restrict the age of this sample to the middle Eocene. Most of the underlying core-catcher samples are barren of planktonic foraminifers. Of the samples that are not barren (11,CC and 20,CC through 26,CC), the planktonic foraminiferal faunas are all extremely sparse (except for 11,CC) and consist only of *Globigerina linaperta, G. patagonica*, and *G.* cf. *eocaena*. The trace presence of *A. soldadoensis* in 11,CC suggests an early Eocene age for this stratigraphic interval, i.e., from 553A-10,CC to 26,CC.

Hole 553B

Samples 553B-1,CC through 4,CC are all of middle to late Pleistocene age, based on the occurrence of *Globorotalia truncatulinoides* and *Neogloboquadrina pachyderma.*

Benthic Foraminifers

Hole 553

The Neogene assemblages are similar to one another and are characterized by the association of *Planulina wuellerstorfi, Cibicidoides kullenbergi, Oridorsalis umbonatus*, and *Epistominella exigua*. The single Pleistocene sample (Sample 553-1,CC) contains *Hoeglundina elegans* and *Triloculina frigida* not seen lower in the succession. The pre-glacial section contains *Globocassidulina subglobosa, Laticarinina pauperata, Ehrenbergina trigona, E. serrata, Bulimina alazanensis, B. striata, Uvigerina compressa, Brizalina subaenariensis*, and *Siphotextularia catenata*.

The diversity ranges from ∝11 to 23. Although there are some fluctuations, there is overall an increase in diversity from the early Miocene to the Pleistocene.

The planktonic:benthic ratio is generally 99:1, and the lowest value is 96:4 in the early Miocene. These values show the existence of open ocean conditions. The *Planulina wuellerstorfi* fauna is indicative of North Atlantic Deep Water and depths greater than 1500 m. The sporadic occurrence of *Sigmoilopsis schlumbergeri* suggests depths greater than 2200 m, and the low abundance of *Epistominella exigua* suggests depths of less than 2900 m. These two species are present in Samples 553A-2,CC to 7,CC (back to the middle Miocene). The early Miocene (Samples 553A-8,CC, 9-1, 99 cm, and 9-2, 99 cm) lack *Planulina wuellerstorfi. Epistominella exigua* is rare in Sample 553A-9-2, 99 cm and may still be taken as indicating depths of less than 2900 m. Other possible depth indicators include *Bulimina alazanensis* and *Oridorsalis umbonatus*, both of which have an upper limit of about 1500 m. Thus, the depth of the early Miocene could have been in the range 1500–2900 m.

One feature of interest in Sample 553A-5,CC is that the majority of the foraminifers, both planktonic and benthic, are size-sorted and very small. It is clear that they have been winnowed from elsewhere and deposited here, and indeed this level is a contourite deposit of the Hatton Drift.

The Paleogene succession is condensed and there is a major hiatus between the late Oligocene and the middle Eocene.

Samples 553A-9-5, 5 cm and 553A-9-6, 19 cm are from the late Oligocene. Their assemblages closely resemble those of the overlying early Miocene especially in the presence of *Bulimina alazanensis, Globocassidulina subglobosa, Gyroidinoides* spp., *Melonis barleeanus, Nodosaria-Stilostomella* spp., *Oridorsalis umbonatus, O. ecuadorensis, Pullenia bulloides, P. osloensis, Spiroplectammina spectabilis*, and *Cibicidoides kullenbergi.* The diversity is ∝10-20 and the planktonic:benthic ratio is 99:1. These are, therefore, interpreted as representing water depths of at least 1500 m.

The middle Eocene assemblages can be divided into two groups. Samples 553A-9-6, 51 cm to 10-3, 66 cm have a planktonic:benthic ratio of 99:1 and benthic diversity of ∝14–20. The dominant forms are *Nodosaria–Stilostomella* spp. and *Gyroidinoides* spp., with the following species common in some samples: *Oridorsalis ecuadorensis, Cibicidoides* spp., *Alabamina wilcoxensis* and *Nonion* cf. *N. olssoni*. Small individuals of *Nuttallides truempyi* are also present. This suggests epibathyal depths greater than 700 m.

Samples 553A-10-3, 135 cm to 10,CC have planktonic:benthic ratios of 64:36 to 0:100. Certainly the latter value is the result of preferential dissolution of the planktonic tests. Preservation of benthic forms is good in Samples 553A-10-3, 135 cm and 10-4, 14 cm and moderate to poor down to 10,CC. Diversity varies from ∝5 to 10, and these values may also be influenced by dissolution. The assemblages are dominated by *Nodosaria–Stilostomella* spp., *Bulimina parisiensis, Alabamina wilcoxensis* and *Osangularia* spp. Small *Nuttallides truempyi* are common in 10,CC. Thus, if the dissolution effects are taken into consideration, these assemblages are like those described above and may also represent depths greater than 700 m.

The early Eocene assemblages, Sample 553A-11-2, 80 cm to the deepest fossiliferous Sample 553A-37-2, 28 cm, represent much shallower water. Samples 553A-11-2, 80 cm to 12-4, 33 cm are characterized by moderately preserved, moderately diverse (∝9–16) assemblages in which the dominant species are *Anomalinoides howelli, A. danica, Gaudryina hiltermanni*, and *Lenticulina* spp. Subsidiary species include *Bolivinopsis adamsi* and *Cibicidoides* spp. *Pulsiphonina prima* is rare. This is a mid to outer shelf assemblage at depths of 75 to 200 m. The planktonic:benthic ratios of 75:25 to 23:77 are in agreement with this and show some degree of isolation from open ocean waters. The salinity was normal.

Sample 553A-12,CC is a hard agglomerate which yielded only a few *Bolivinopsis adamsi* and *Globocassidulina subglobosa.* Sample 13,CC has a moderately diverse fauna (∝11) dominated by *Lenticulina* spp., *Cibicides* sp., and *Bolivinopsis adamsi.* There are no planktonic forms present. This is considered to represent inner to mid-shelf depths of 50–100 m and waters of normal salinity. The associated macrofauna includes bryozoans, mollusk shell with clionid borings, and spines of echinoids. Sample 553A-14,CC is probably also from this environment, but only a sparse fauna was recovered (*Anomalinoides howelli, A. nobilis*, and *Gyroidinoides angustiumblica*).

Sample 553A-15,CC, a hard agglomerate, could not be broken down. Samples 16,CC and 17,CC have very sparse faunas. Sample 18,CC has a slightly brackish assemblage of *Anomalinoides howelli, Nonion laeve, Elphidium hiltermanni*, and *Pararotalia curryi.* The diversity is ∝4 and no planktonic forms are present. Sample 19,CC has a sparse brackish assemblage of similar composition but with *Protelphidium* sp. also present. Lignitic wood is present in this sample. These two samples represent estuarine or lagoonal conditions.

Sample 20,CC has a moderately diverse assemblage (∝11) of *Nodosaria* spp., *Epistominella vitrea*, and *Praeglobobulimina ovata* indicative of inner-shelf conditions (depth less than 75 m). The salinity was normal and the substrate muddy. The planktonic:benthic ratio is 5:95, suggesting considerable isolation from open oceanic waters. Sample 21,CC has a sparse inner-shelf fauna. Samples 22,CC to 25,CC have assemblages dominated by *Nodosaria* spp., *Alabamina obtusa, Lenticulina* spp., *Cibicidoides alleni*, and *Praeglobobulimina ovata.* Diversity is ∝3 to 11. The low value is that of 22,CC which contains *Cribrostomoides* sp. in 30% abundance. Samples 553A-22,CC and 23,CC are thought to represent inner shelf conditions, generally of normal salinity, but 22,CC may be slight brackish (salinity 30–32‰). Samples 553A-24,CC and 25,CC are mid-shelf, 75–150 m, and of normal salinity.

Samples 26,CC and 27,CC have sparse middle-shelf assemblages. Samples 28,CC, 31,CC, 33,CC, and 34,CC are barren, and 35,CC has a sparse fauna. Sample 36,CC has an assemblage of low diversity (∝4) dominated by *Trochammina* sp. (48%), *Elphidium hiltermanni* (17%), and *Anomalinoides acutus* (13%). This represents a brackish lagoonal tidal flat or marsh. A few shelf forms have been transported in, e.g., *Anomalinoides howelli, Praeglobobulimina ovata.* The lowest sample, Sample 553A-37-2, 28 cm, has a diversity of ∝6, no planktonic foraminifers, and is dominated by *Praeglobobulimina ovata, Cancris subconicus, Anomalinoides howelli*, and *Elphidium hiltermanni.* It represents inner-shelf depths less than 75 m and a salinity of 32–35‰.

Thus, the succession from the basalt to 11,CC represents a period when subsidence and sedimentation were almost in equilibrium. When sedimentation was greater than subsidence, the shoreline migrated seawards and the area was occupied by brackish lagoons or estuaries. At times of reduced sedimentation, the sea transgressed landwards, bringing inner to outer shelf depths. Above 11,CC, sedimentation slowed down, and continued subsidence caused a progressive deepening.

Diatoms

Hole 553

The single mudline core taken at Hole 553 contains few well-preserved Pleistocene diatoms typical of the *Pseudoeunotia doliolus* Zone. Species present include *P. doliolus, Rhizosolenia bergonii, Actinocyclus curvatulus, Thalasiosira leptopus*, and *Coscinodiscus nodulifer.*

Hole 553A

Cores 1 and 2 are placed in the early Pliocene *Thalassiosira convexa* Zone based on the presence of *Thalassiosira convexa* s. ampl. and *Thalassiosira oestrupii.* The interval of dissolution present at the base of this zone occurs in Cores 2 through 7-3. Sample 553A-7,CC through Core 9 extend from the middle Miocene to the middle to late Eocene. The interval from Samples 553A-7,CC to 8-3, 103 cm is assigned to the middle Miocene "*Actinocyclus ingens* Zone" based on the occurrence of *A. ingens* and *Denticulopsis hyalina.* Even though diatoms are rare from Cores 8-4 to 9-3, it is possible to assign the interval of 9-1 to the earliest Miocene on the basis of the rare to few occurrence of *Rocella gelida.* The frequency of *R. gelida* increases downcore, becoming common in Core 9-3, which indicates that the Oligocene/Miocene boundary is very close to this level. Other species present within this section include *Coscinodiscus oligocenicus, Melosira architechuralis, Goniothecium decoratum*, and *Liradiscus* sp. Minor reworking of Eocene species occurs throughout Cores 8 and 9.

Core 9, Section 4 and Core 10 contain rare to common middle Eocene diatoms. Age assignment is based on the presence of *Coscinodiscus oblongus, Brightwellia* cf. *spiralis*, and *Pterotheca danica.*

Core 11 is assigned a late Paleocene–early Eocene age based on the occurrence of *Trinacria pileolus, Rhizosolenia interposita, Stephanopyxis* cf. *superba, Pterotheca aculeifera, Trinacria excavata, Screptroneis* sp. *A., Trinacria simulacrum*, and *Pyrgupyxis prolongata.*

All samples examined below Core 11, with the exception of the following, are barren of diatoms. Samples 553A-18,CC, 21,CC, 22,CC, and 23,CC contain nondiagnostic diatom frustules in which the silica is replaced by calcite; and Samples 553A-14,CC and 37-2, 28 cm contain pyritized diatom frustules of *Triceratium* sp. and *Coscinodiscus* sp.

Hole 553B

Core 1 contains few moderately preserved diatoms typical of the *Pseudoeunotia doliolus* Zone. Cores 2 through 4 either contain nondiagnostic specimens or are completely barren of diatoms. Ice-rafted detritus is present throughout this interval and is correlated to a similar interval occurring within the *Nitzschia marina* Zone at Hole 552A.

Radiolarians

Hole 553

Hole 553 is represented by a single mudline core in which Quaternary radiolarians are common and moderately well preserved.

Hole 553A

In the rotary drilled Hole 553A, radiolarians are common and moderately well preserved in the Pliocene and upper Miocene Cores 553A-1 through 3, apparently dissolved in Cores 4 and 5, few and poorly preserved in the middle Miocene Cores 6 to 8-3, and moderately well preserved in the Oligocene through Eocene Core 8, Section 4 to Core 11, Section 5.

Core 553A-1 contains a moderately well-preserved assemblage in which the presence of *Stylatractus universus* and absence of *Stichocorys peregrina* indicate an age between 425,000 years ago and the late Pliocene. At 113 m, Core 553A-2 is placed in the upper Pliocene *Sphaeropyle langii* Zone (Foreman, 1975) by the presence of *S. langii, Stichocorys peregrina*, and *Didymocyrtis tetrathalamus*. Nearly equal numbers of *S. peregrina* and *S. delmontensis* in Sample 553A-3-2, 32–34 cm (163 m) indicate the proximity of this evolutionary transition which marks the lower boundary of the *S. peregrina* Zone. From 180 m, Hole 553A was continuously cored, and Cores 4 and 5 are barren of siliceous fossils except for rare fragments and sponge spicules. Over most of the mid and low-latitude Atlantic, radiolarians are not preserved at all in sediments younger than mid-Miocene. This is apparently due to the change from an Atlantic silica sink to a carbonate basin, perhaps caused by the closing of the Tethys (Casey and McMillen, 1977), and/or the subsidence of the Iceland–Faeroe Ridge in the middle Miocene. Where radiolarians are preserved in the post mid-Miocene sediments of the Atlantic, they often exhibit provincialism and are difficult to fit into Riedel and Sanfilippo's tropical zonation. Preservation of radiolarians is generally thought to be dependent on (1) productivity, (2) rapid burial, and (3) availability of silica in the interstitial waters. It is unclear which of these factors contribute to the preservation of radiolarians in the late Miocene and Pliocene sediments of this region.

Core 553A-6 contains rare and poorly preserved middle Miocene forms. Samples 553A-7-4, 119–121 cm and 8-1, 62–63 cm are placed in the *Diartus petterssoni* Zone (Riedel and Sanfilippo, 1978) because they appear to be just above the evolutionary transition of *Lithopera renzae* to *L. neotera* which happens at the top of the *Dorcadospyris alata* Zone (Riedel and Sanfilippo, 1978). The boundary event between the *D. petterssoni* Zone and the *D. alata* Zone does not occur here because artiscins are poorly preserved and sparse in these assemblages; however, Samples 553A-8-2, 48–49 cm and 8-3, 103–104 cm are placed in the *D. alata* Zone because *L. renzae* is more abundant than *L. neotera.*

At least four or five radiolarian zones, nearly the entire early Miocene, are missing between the bottom of Section 553A-8-3 and the top of Section 553A-8-4. In the top of Section 4, the radiolarians appear to be older than the early Miocene *Cyrtocapsella tetrapera* Zone (Riedel and Sanfilippo, 1978) because of the absence of *Stichocorys delmontensis* and *Cyrtocapsella tetrapera*, both of which are common in the samples above. It is not possible with the species present to distinguish the earliest Miocene from the Oligocene. *Artophormis gracilis*, which ranges through the Oligocene into the early Miocene, is present in all samples examined between Cores 553A-8-4 and 9-5.

No upper Eocene radiolarians were observed in Hole 553A. Below the Oligocene sediments of Sample 553A-9-5, 102–103 cm, Sample 553A-9,CC through Section 553A-10-2 contain a middle Eocene assemblage with: *Spongatractus pachystylus, Lithocyclia ocellus, Lamptonium pennatum, L. obelix, Lophocyrtis biaurita, L. norvegiensis*, and *Phormocyrtis striata striata.* Samples from Sections 553A-10-3 and 10-4 are barren of siliceous fossils, but Sample 553A-10-5, 98–100 cm contains a few radiolarians, including *Pterocodon ampla* and the middle to upper Eocene forms *Amphicraspedum splendiarmatum* and *Lophocyrtis norvegiensis.* A fairly well-preserved lower Eocene fauna in samples from Core 553A-11 includes *Amphicraspedum prolixum, A. murrayanum, Pterocodon ampla*, and *P. lex.*

Hole 553B

The first two core catchers of Hole 553B at 4.5 and 9.5 m sub-bottom contain a few moderately well-preserved Quaternary radiolarians. These assemblages are probably less than 425,000 years old since they appear to be above the extinction of *Stylatractus universus.* In the terrigenous clays of Samples 553B-3-5, 71–73 cm and 4,CC, radiolarians are completely dissolved, although there are rare, partly dissolved specimens in the carbonate sediments of 553B-3,CC.

Dinoflagellates

Hole 553A

Dinoflagellates from the lower Paleogene of Hole 553A have been studied by Brown and Downie (this volume). The results are summarized here, following the zonal scheme of Costa and Downie (1979).

Cores 13 to 37, although containing many species, lack the forms required to give a precise date to the sediments. However, the occurrence of *Spinidinium* (?)sp. *A*. (Costa and Downie) from Cores 14 to 22 suggests an assignment to Zone Ia or lower Ib (Costa and Downie, 1979), and *Fibrocysta bipolage* (which in Hole 555 is continued to Zone Ia1) occurs between Cores 14 and 37.

This suggests that Cores 13 to 37 are broadly referrable to Zones Ia to Ib. The relatively low species diversity and high content of pollen and spores suggests that an estuarine environment prevailed for much of the depositional phase.

Cores 11 and 12 are much richer in dinoflagellate cysts, both in terms of diversity and ratio to pollen and spores, indicating a major change in environment, to more open-shelf conditions, and the dominance of *Homotryblium tenuispinosum* and increased abundance of *Impagilinium patulum* in Core 11-1 indicates distinct oceanic influences.

The occurrence of *Dracodinium condylos* in Sample 553-12-4, 110–112 cm indicates Zone II: the first appearance of *Kisselovia edwardsii* in Sample 553-11-1, 73–74 cm may indicate Zone III.

All samples above Core 11 were barren of palynomorphs.

ORGANIC GEOCHEMISTRY

Site 552

Introduction

The organic geochemistry for Leg 81 had two purposes: to aid in the pollution-prevention and safety monitoring program, and to study the nature of organic matter in the sediments encountered. The sampling and analysis program was developed progressively through the cruise to satisfy these aims, and instrumental techniques will be described.

METHODS AND SAMPLING

Gases

Core gas pockets were sampled with an evacuated (vacutainer) tube through the plastic core liner. This method has been described previously by Rullkötter (pers. comm., 1981), Claypool (1981), and Patton (1981). The gas samples were analyzed on a Carle gas chromatograph (thermal conductivity detector) for high concentration components (air, methane, and CO_2). Instrumental conditions were described by Rullkötter (pers. comm., 1981) and remain the same. Normally this instrument is calibrated only for C_1, but for this leg it was also calibrated for air and CO_2.

The C_2–C_6 hydrocarbons of gas pockets were analyzed on a FID instrument according to a trapping (−70°C) and valve injection system described in detail by Rullkötter (pers. comm., 1981).

Since only occasional gas pockets were encountered at Site 552, an alternative method was developed for more complete monitoring of the C_1–C_4 hydrocarbons and CO_2. Methods have been described by Claypool (1981) and Shaefer (1978) for extracting or stripping the light hydrocarbons from the sediments.

The method used on Leg 81 consisted of extracting the light hydrocarbons and CO_2 from the interstitial waters squeezed from the cores. Immediately after squeezing, the pore water was extracted with an equal volume of helium (1:1) in a gas tight ("precision, pressure-lok") syringe. The pore water was extruded directly into the syringe, and after the helium had been added, the syringe was vigorously shaken and allowed to stand for several minutes (10 min.) to allow hydrocarbons to enter the gas phase. The C_1–C_4 hydrocarbons will almost completely partition into the gas phase (Claypool, 1975). The gas phase was analyzed for air, CO_2, and the C_1–C_4 hydrocarbons by direct injection.

The lower limit of detection for the hydrocarbons is 0.1 ppm. While this technique does not have the sensitivity of the methods employed by Claypool (1981), Schaefer (1978), and Rullkötter (pers. comm., 1981), it was quite satisfactory in light of the goals and sedimentary conditions of this leg. The sensitivity of this method is many orders of magnitude greater than that necessary to detect potentially hazardous levels of hydrocarbons, and it provides for rapid and continuous monitoring so that anomalous quantities of hydrocarbons may be recognized.

Sediment Samples

Sediment samples were selected to study organic matter for trends in consistent lithologies and differences in environmental settings and to coincide with interstitial water samples. Sediment samples were dried and the organic carbon and nitrogen determined. The carbon and nitrogen analysis is described by Rullkötter et al. (1981).

Pyrolysis analysis of sedimentary organic matter was done by Rock-Eval analysis; the method and theory are described fully by Patton (in press), Clementz et al. (1979), and Espitalié et al. (1977).

Results

Gases

Results of gas analyses are shown in Table 4 and Figure 26. There is no obvious trend in methane values with depth. The methane values range from 2.2–9.3 ppm (V/V) of gas extracted from the pore waters. This is only slightly above the atmospheric C_1 concentration. The low organic matter content (0.01–0.17%) and highly oxidized nature of the sediments probably precludes activity of methane-producing bacteria (Claypool, 1981). The methane observed could result from low-level decomposition reactions (Whelan and Shunji, 1977; Schaefer, 1978; Claypool, 1981), with localized conditions within

Table 4. Gas analyses, Site 552.

Core-Section	Sub-bottom depth (m)	Lithologic unit	C_1^a (ppm)	C_2 (ppm)	CO_2 (%)	Air (%)	Sample
552A-6-3	28.4	I	6.2	nd	0.20	35.2	Pore water
552A-12-3	58.5	II	3.7	nd	0.29	39.2	Pore water
552A-18-3	86.5	II	9.3	nd	0.33	48.6	Pore water
552A-24-2	111.5	II	8.6	nd	0.41	28.8	Pore water
552A-30-2	141.5	II	2.6		0.33	41.0	Pore water
552-36-3	155.7	II			0.23		Pore water
552A-38-3	183.0	IV			0.31	51.5	Pore water
552A-38-3	183.0	IV	(3.5)		(0.12)	100.0	(Core gas)
552-9-4	185.7	IV			0.19	37.4	Pore water
552-12-6	217.5	IV	8.1		0.07	37.2	Pore water
552-16-1	247.5	IV	2.8		0.04	45.0	Pore water
552-21-2	297.0	IV	2.2		0.04	33.4	Pore water

[a] Results are vol./vol. basis in total gas extracted from an equal volume of pore water. Difference from 100% results from use of helium as extraction gas. Blanks in data result from loss of sample.

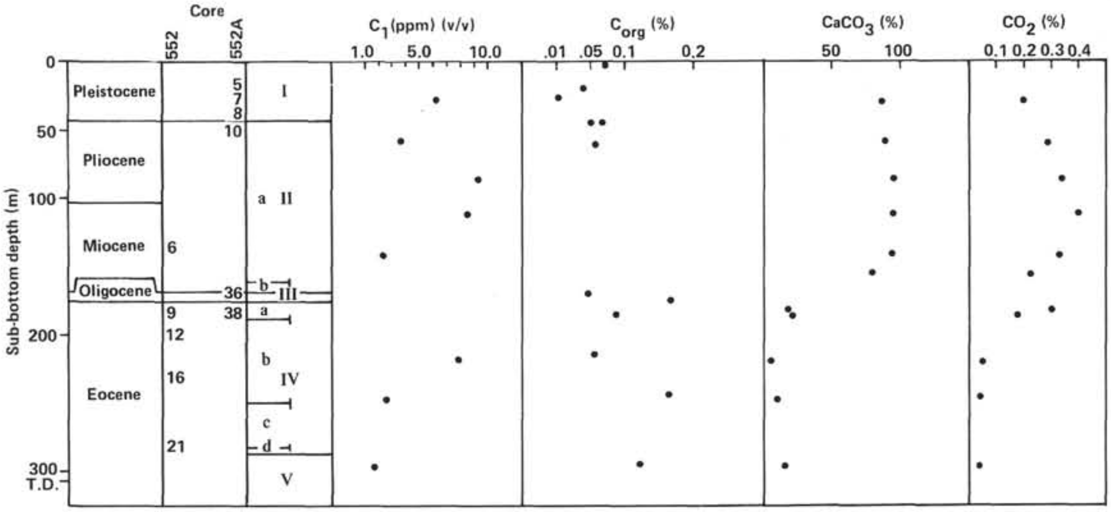

Figure 26. Methane-organic carbon and CO_2–$CaCO_3$ analyses, Site 552.

the sediments accounting for the methane excursions to higher concentrations.

The C_2–C_4 hydrocarbons were present but could not be quantified (0.2 ppm) at this site.

CO_2 appears to follow the pH and alkalinity trends shown in the inorganic chemistry chapter (Gieskes et al., this volume). The large decrease in pore water CO_2 below 180 m is consistent with similar decreases in pore water pH and alkalinity. The carbonate content of the Miocene sediments decreases from 90 to 10% $CaCO_3$ at this depth, and nannofossil oozes to chalks and more lithified sediments grade into mudstones with volcanic ash layers and finally to basalt. The removal of $CaCO_3$ alkalinity and the utilization of CO_2 in neutralizing the alkaline volcanogenic sediment probably accounts for the removal of CO_2 in the deepest segment of the sedimentary column. A similar trend was observed by Gieskes et al. (1979) in Rockall Plateau pore-water alkalinity.

Pyrolysis Analysis of Sediments (Rock-Eval)

Pyrolysis results are given in Table 5 and Figures 27, 28, and 29. The results are consistent with light hydrocarbon and organic carbon data. There is very little organic matter preserved in this sedimentary column, and what is preserved is highly oxidized and immature. However, some interesting observations can be made from the pyrolysis data, which complement our understanding of the sedimentary environment. It should be noted that the concentrations of hydrocarbons present are one to two orders of magnitude lower than that considered "poor" for hydrocarbon generation potential (i.e., 2,500 ppm HC/g rock vs. 20–200 ppm HC/g rock).

Pleistocene Unit I. In the alternating layers of muds and oozes of the Pleistocene (Zone I) (Fig. 29) the oozes (70–90% $CaCO_3$) have smaller amounts of total hydrocarbons than do the muds (20–40% $CaCO_3$). The oxygen-carbon compounds are also somewhat lower in the oozes. The data suggest very low organic production with remnant organic matter being terrestrial or highly oxidized or both.

The Pliocene and Miocene Subunit IIa ooze–chalk interval ($CaCO_3$, 90%) shows a consistently low level of total hydrocarbons and oxygen-carbon compounds and is immature (avg. T_{max} = 390°C). The organic matter is Type III, either terrestrial or highly oxidized or both.

Eocene Unit IV. These sediments show a 20-fold increase in hydrocarbons compared to the overlying sediment, probably reflecting the shallow marine environ-

Table 5. Pyrolysis (Rock-Eval) analysis of sediments, Site 552.

Sample (interval in cm)	Organic carbon (%)	S_1 (mg HC/g rock)	S_2 (mg HC/g rock)	T_{max} (°C)		S_3 (mg CO_2/g rock)	Petroleum potential (S_1+S_2)	(S_2/S_3)	Hydrogen index (mg/g C)	Oxygen index (mg/g C)
552-1-2, 144–146	0.07	0.036	—	—		0.606	0.036	—	—	8.66
552A-5-2, 100–101	0.04	0.068	0.029	—		0.877	0.097	0.03	0.725	21.93
552A-7-2, 8–9	0.01 tr	0.020	0.058	—		0.821	0.078	0.07	(5.8)	82.10
552A-8-2, 36–37	0.06	0.018	—	—		0.714	0.018	—	—	11.90
552A-10-1, 145–146	0.07	0.052	—	—		0.624	0.052	—	—	8.90
552-6-3, 112–114	0.05	0.04	—	385		0.447	0.04	—	—	8.94
552A-36-1, 2–3	0.05	0.029	0.027	398		0.680	0.056	0.04	0.54	13.60
				A	B					
552A-38-2, 47–48	0.17	0.250	0.019	395	550	1.739	0.269	0.01	0.112	10.23
552-9-4, 112–114	0.09	0.036	0.033	412	532	0.844	0.069	0.04	0.366	9.38
552-12-5, 118–120	0.06	0.172	0.072	407	550	0.411	0.244	0.18	1.20	6.85
552-16-1, 10–14	0.17	0.138	0.123	413	550	0.575	0.260	0.23	0.78	3.38
552-21-2, 131–133	0.13	0.146	0.165	420	550	0.581	0.311	0.28	1.27	4.47

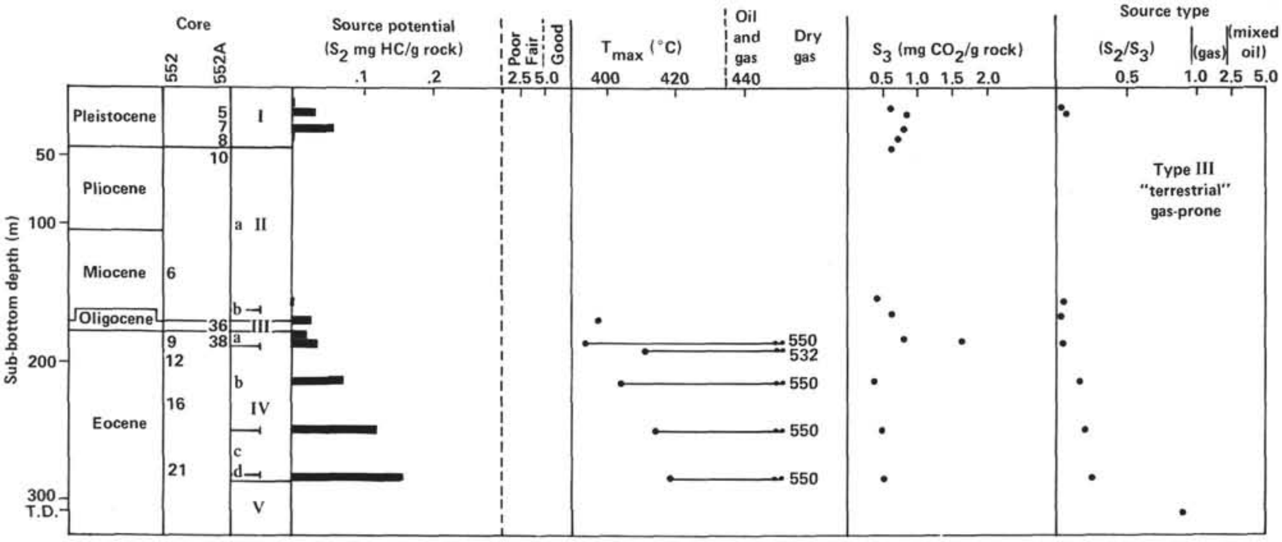

Figure 27. Sediment pyrolysis data (Rock-Eval), Site 552.

ment. The oxygen–carbon organic matter is at its maximum in Subunit IVa, then decreases somewhat through Subunits IVb and IVd. While the organic matter can be generally classified as Type III, terrestrial or highly oxidized, an obvious trend toward Type II indicates a greater proportion of marine organic matter or less weathering (that is, shallower environment or higher sedimentation rates).

The pyrolysis of kerogen in Unit IV yielded two S_2 peaks indicating organic matter of differing maturity. An example is shown in Figure 29. Extreme care has been exercised in the analytical pyrolysis technique because of the high sensitivities (Rock-Eval settings: Attn: X1 FID, X2 TC). All sample crucibles are heated with a torch until they are "glowing red," then carefully blanked (run through 1-3 pyrolysis runs empty). The second S_2 peak has only been observed in one sample from Unit IV.

Boutefeu (1976) has observed a shoulder on the S_2 peak. However, in this case two distinct types of kerogen may be observed because of the very low levels present. The first type shows a gradual increase in maturity to the bottom of Zone IV. The second type shows an abnormally high maturation (T_{max} = 550°C), which could be a contribution from reworked organic matter from erosion of nearby land, e.g., the Mesozoic of East Greenland (see Kaltenback et al., this volume) and deposition in a shallow marine environment.

In summary, the organic content of Site 552 is extremely low and highly oxidized Type III. The pyrolysis studies, however, suggest differences in the Pleistocene (Unit I) and Eocene (Unit IV) sedimentary environments.

Organic Carbon and Nitrogen

The results are given in Table 6. The low levels of organic matter have been discussed above (see also Kaltenback et al., this volume).

Site 553

Gases

The interstitial water–gas-extraction method was improved by experiment at Site 552. The detection limit was improved by increasing sample size to 2 ml and by changing the gas–liquid extraction ratio to 1:2. Although analytical precision at these low levels is limited, hydrocarbons (C_1–C_4) can be detected to about 0.01 ppm in the gas extracted from pore water.

The results, including some core-gas data, are given in Table 7. The sediment pore water yields decreased in Sections 553-18-1, and 21-1, and there was an insufficient amount from which to extract gases. Core "vacutainer" samples were taken but showed only "blank" levels of hydrocarbons.

The hydrocarbon results are similar to those found by Claypool (in press), using a "blender technique." The methane–ethane ratio averaged 14.8 for four samples, and the percentage of wetness C_2–C_4/C_1–C_4 averaged 17.3. This suggests an origin by chemical decomposition rather than a biological source for these hydrocarbons. However, this question of the source of "base-line" levels of light hydrocarbons is still unanswered as (Hunt, 1979) suggests.

The CO_2 in the extracted gas from sediments shows a trend similar to that observed at Site 552 and decreases as carbonates decrease and volcaniclastics increase.

Sediments

Carbon and nitrogen analyses suggest that the sedimentary organic matter at Site 553 is divided into three general types (Table 8). The first group has an average organic carbon content of 0.04% (0–0.08%) and an average C/N of 5 (0–9.3). It includes samples from Cores 4, 7, 10, 11, and 18. Group two has an average organic carbon content of about 0.3% (0.18–0.37%) and an average C/N of 19 (13.3–21.6), and includes samples from

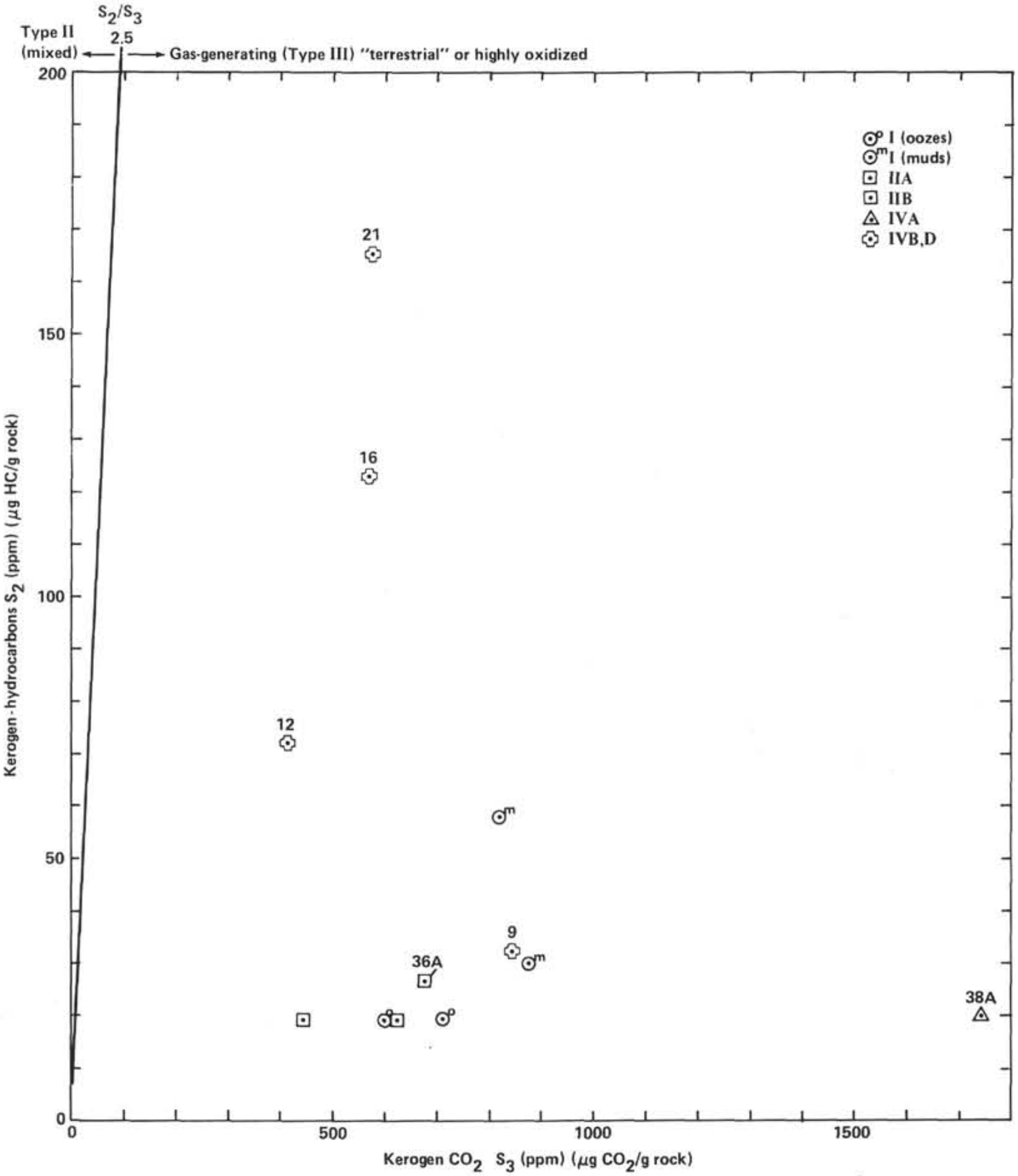

Figure 28. Pyrolysis S_2 versus S_3 plot of kerogen for principal lithologic units and subunits, Site 552.

Cores 21, 24, and 27. The third group has an average organic carbon value of 1.0% (0.76–1.10%) and an average C/N of 31 (29.17–32.08); it includes samples from Cores 14, 22, 36, and 37. These groups can also be distinguished in Figure 30, which shows results of the pyrolysis analyses of these samples.

Pyrolysis (Rock-Eval) analysis results are given in Table 9A and Figures 30–32. The nature of the kerogen present in sediments results from the source of the original organic matter and the environment of deposition. The three different classes of organic matter and the pyrolysis results shown in Figures 30 and 31 suggest that the complex organic matter preserves a record of different source and sedimentary environments.

Miocene Subunit IIa: These nannofossil–foraminifer chalks are similar to those of Site 552, showing low organic carbon, a similar C/N ratio, and a very low hydrocarbon yield by pyrolysis. The organic matter is Type III, either terrestrial or highly oxidized or both.

Eocene Subunit IVa: These sediments are represented by a sample from Section 553-10-2 and are similar to corresponding sediments from Site 552; the organic content of this sample is very low, and yet it has the highest oxygen index of the entire site (Fig. 30, Table 9). This suggests an increase in the production of organic matter which is exceptionally oxidized or humic.

Eocene Subunit IVb: The appearance of two S_2 peaks, also observed at Site 552 in the Eocene, is seen more dramatically at Site 553. Figure 32 shows pyrolysis analyses of several samples from Site 553. The multiple peaks suggest that the kerogen is a mix of different source materials. The source of the organic matter can be sapropelic (algal or pollen), humic, or reworked. It can then be altered chemically (oxidation), biologically, or ther-

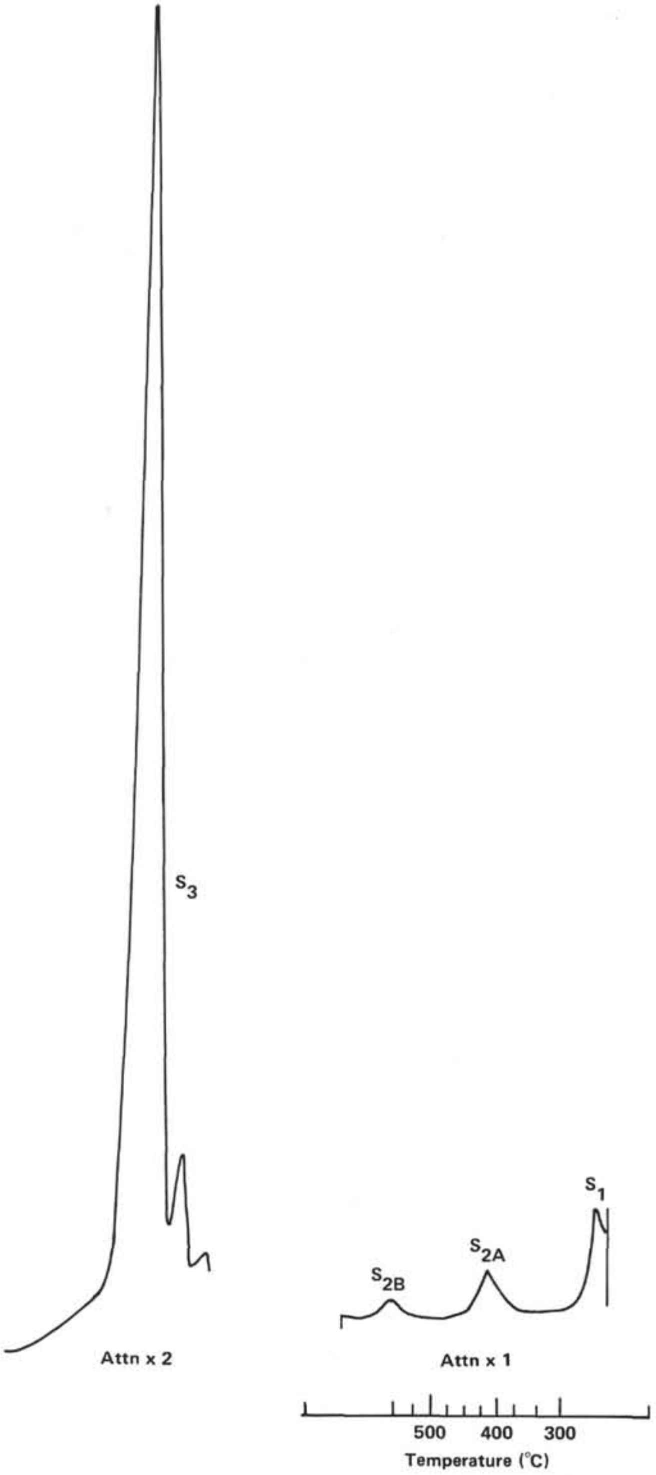

Figure 29. Pyrolysis analysis (Sample 552-16-1, 10–14 cm) showing two S_2 peaks, A and B, of different thermal maturation.

mally through burial or possibly by volcanic activity. Figure 32A shows a pyrolysis analysis of the type observed for this section. There appear to be two types of kerogen of distinctly different maturation (S_{2A}, 378°C, S_{2B}, 550°C). In summary Unit IVb is characterized by low organic content and hydrocarbon yields, and highly oxidized, probably reworked kerogen.

Eocene Subunit IVc: The sediment from Core 14 is a carbonaceous mudstone. The pyrolysis analysis is shown in Figure 32B. Note that the S_{2B} peak with T_{max} = 550°C had not stopped yielding hydrocarbons at 550°C during a normal analysis. The set of rerun data (Table 9) shows the effect of increasing pyrolysis time at 550°C from 2 to 5 minutes. However, this change of instrumental conditions yielded results outside the ranges normally utilized in kerogen studies, and it was therefore abandoned.

The Core 14 sample suggests increased input of organic matter of Type III (humic). The sample from Core 18 shows only one S_2 peak indicating a highly terrestrial origin, T_{max} = 550°C, and only a trace (<0.01%) of organic carbon content. The sample from Core 21 is shown in Figure 32C. It has exceptionally high yields of hydrocarbon and oxygen-carbon for its organic carbon content (Fig. 30). The similarity of the pyrolysis S_2 yields to Figure 32 is noteworthy. The sample from Core 22 is shown in Figures 30 and 32. This sample is from a carbonaceous lamina and is Type III-humic. The setting is shallow marine with a terrestrial or reworked source of organic matter.

Samples from carbonaceous layers in Cores 24 and 27 (IVc and IVd) show kerogen pyrolysis similar to Figure 32A, highly oxidized or reworked, and a bimodal thermal maturation.

The sample from Core 36 (IVf) is from a carbonaceous mudstone and shows a striking Type I (algal) kerogen (Fig. 30). Its pyrolysis is shown in Figure 32C. The hydrocarbon source potential of this sample is "good" (Fig. 31). This would not be the case for a sample "normally" matured to this level. Figure 32 suggests the possibility of a mixture of several different kerogen types, indicated by distinct shoulders of the peak. A minor component of high maturity as observed in other samples could mask the true maturity of the major component of the kerogen. Also, volcanic activity, and the occurrence of this sample only 15 m above the basalt, cannot be ignored as possible causes.

Finally, a sample from the carbonaceous layer in Core 36 (IVf) shows a mix of two kerogen types (Fig. 32) and is considered mature Type III humic.

In summary, the organic matter at Site 553 ranges from very low to high (less than 0.01–1.1%) organic carbon. Sedimentary conditions change from deep marine (Miocene) to shallow nearshore (Eocene). The kerogen source material changes from very minor highly oxidized or terrestrial (Miocene) to carbonaceous sequences of "coaly," terrestrial, and algal (oil-shale). Tissot and Welte (1978) discussed the occurrence of oil shales in association with coal layers being formed in bog and lagoon environments. He also discusses the Eocene occurrence of Green River Type I oil shale and Messel Type II shale. The kerogen in the Eocene sequence at this site is probably a mix of all three types, having been subjected to anaerobic conditions, rapid and slow sedimentation under aerobic conditions, reworking caused by bottom currents, and sea-level variations. The possibility of rapid thermal maturation as a result of volcanic conditions must also be considered. Detailed shore-based

Table 6. Organic carbon and nitrogen data, Site 552.

Sample designation	Sample (interval in cm)	N (%)	C_{org} (%)	H (%)	C/N ratio $\left(\frac{14}{12}\times\frac{C_{org}}{N_{org}}\right)$	$CaCO_3$ bomb (%)
A	552-1-2, 144–146	0.02	0.07		4.08	66
B	552-6-3, 112–114	0.01	0.05		5.83	83
C	552-9-4, 112–114	0.01	0.09		10.50	24
D	552-12-5, 118–120	0.02	0.06		3.50	8
E	552-16-1, 10–14	0.02	0.17		9.92	13
F	552-21-2, 131–133	0.02	0.13		7.58	19
G	552A-5-2, 100–101	0.02	0.04		2.23	44
H	552A-7-2, 8–9	0.02	tr		—	26
I	552A-8-2, 36–37	0.01	0.06		7.00	87
J	552A-10-1, 145–146	0.01	0.07		8.17	87
K	552A-36-1, 2–3	0.01	0.05		5.83	90
L	552A-38-2, 47–48	0.01	0.17		19.83	21

Table 7. Gas analyses, Site 553.

Sample (interval in m)	Air (%)	CO_2 (%)	C_1	C_2	C_3 ppm	$1C_4$	nC_4	C_1/C_2	Wetness (%) C_2-C_4/C_1-C_4	Sample type
553 (mudline) 144–150	49.9	0.18	1.7		nd			—	—	Pore water 1:1 extraction
								Ethylene (?) 0.52		
553-A-1-2	100.0	0.10	4.1	0.26	0.32	—		5.2	13.9	Core—gas
553A-2-2	97.3	0.18	2.0	0.27	0.13	0.35	0.33	7.4	34.	Core—gas
553A-4-4, 144–50	82.2	0.14	2.7	0.11	0.05	0.06	—	24.5	7.5	Pore water 1:2 (g/l) extraction
553A-7-2, 144–150	51.4	0.14	2.6	0.21	—	0.07	0.05	12.4	12.7	Pore water 1:2 (g/l) extraction
553A-11-2, 140–150	29.3	0.05	0.9		nd			—	—	Pore water 1:1[a] extraction
553A-14-6, 140–150	58.7	0.10			nd			—	—	Pore water 1:1 extraction
553A-18-1, 34	96.5	0.04			BLANK			—	—	Core—sample
553A-21-1, 65	89.8	0.05			BLANK			—	—	Core—sample
553A-24-1, 140–150	70.6	0.05			nd			—	—	Pore water 1:1 extraction
553A-27-4, 140–150	49.8	0.04			nd			—	—	Pore water 1:1 extraction
553A-37-5, 140–150	97.4	0.10			nd			—	—	Pore water 1:1

Note: "Core gas"—vacutainer air blank (subtract from core gas HC samples only): C_1 = 2.12 ppm, C_2 = 0.01, C_3 = 0.20 ppm, $1C_4$ = —, nC_4 = 0.01, air = 98.7%, CO_2 = 0.06%.

[a] Not enough pore water for 1:2 extraction.

Table 8. Organic carbon and nitrogen data, Hole 553A.

Sample designation	Sample (interval in cm)	N (%)	C_{org} (%)	H (%)	C/N ratio $\left(\frac{14}{12}\times\frac{C_{org}}{N_{org}}\right)$	$CaCO_3$ bomb (%)
M	4-1, 125	0.01	0.06		7.00	91
N	7-2, 90–94	0.01	0.08		9.33	91
O	10-2, 25	0.01	0.01		1.17	71
P	11-2, 125	0.01	0.05		5.83	12
Q	14-5, 106	0.03	0.76		29.56	2
R	18-1, 128	0 (tr)	0 (tr)		—	—
S	21-1, 125	0.01	0.18		21.00	1
T	22-5, 104	0.04	1.09		31.79	—
U	24-1, 23	0.02	0.37		21.58	2
W	36-1, 114–116	0.04	1.10		32.08	1
X	27-4, 125–127	0.02	0.31		13.29	—
Y	37-4, 123–125	0.04	1.00		29.17	3

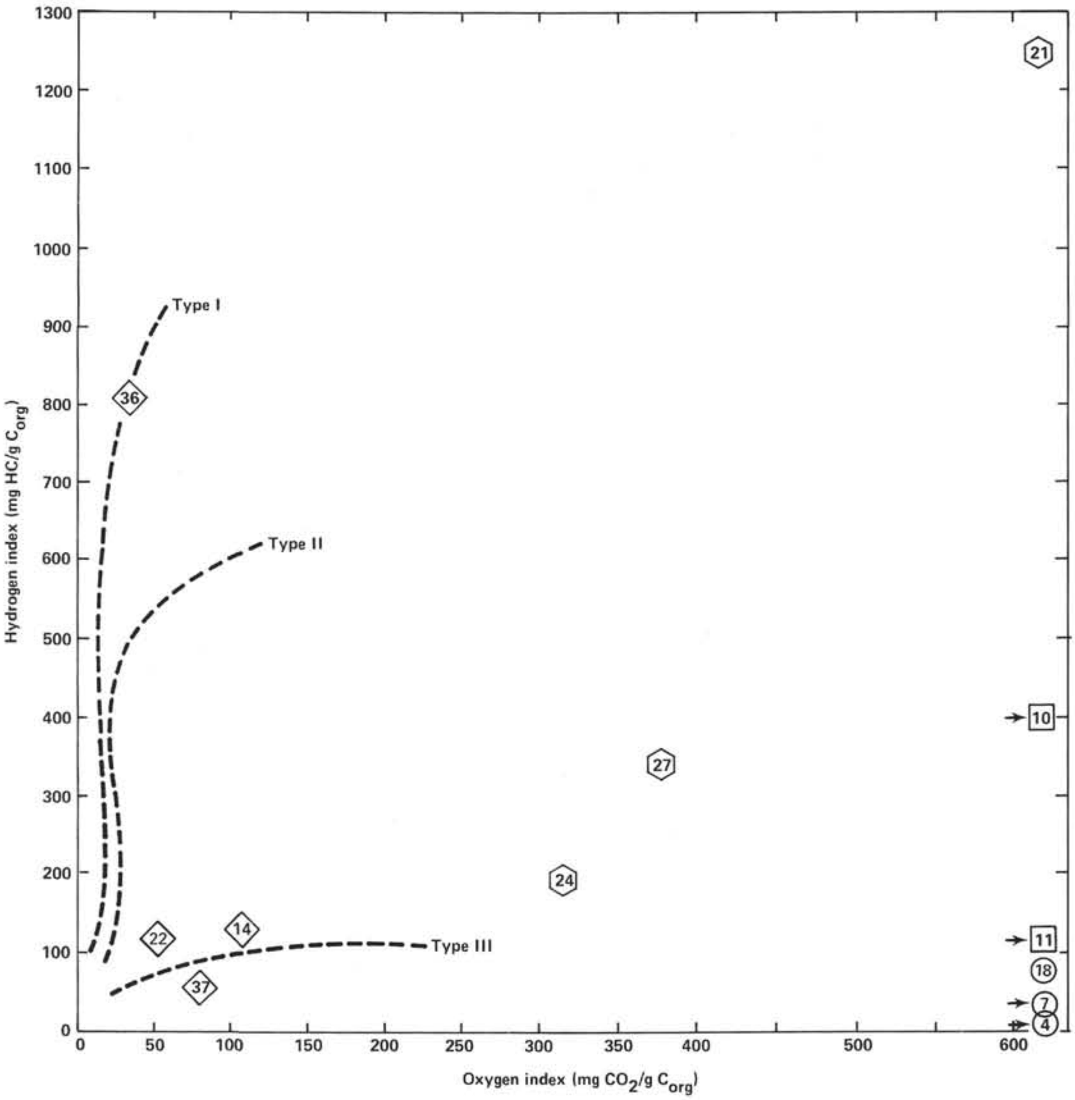

Figure 30. Kerogen-type plot of sediments, Site 553.

studies are reported in this volume by Kaltenback et al. (this volume).

Hole 553B

A series of samples (9) from the HPC in Hole 553B were analyzed by pyrolysis (Rock-Eval) to determine if there were distinguishable differences in the organic matter in glacial versus interglacial sediments. The results are shown in Table 9B and Figures 33–35. The organic carbon, $CaCO_3$, and organic nitrogen contents were determined on board and are shown in Table 10. The amount of organic matter present in this sequence is low (0.05–0.17% OC), although distinct differences are discernable between glacial and interglacial organic matter by pyrolysis analysis within the precision of the method.

Figures 34 and 35 show the qualitative difference in pyrolysis-analysis scans of glacial (a) and interglacial (b) samples. This was first observed at Site 552 and initiated this work. The "interglacial" organic matter (Fig. 34) yields a small amount of hydrocarbons and is very immature as expected. The "glacial" sample yields pyrolyzable hydrocarbons through the entire maturity range with a maximum at 550°C, indicating some very mature, possibly reworked organic matter.

There are several differences in organic matter suggested by this study: the quantitative yield of hydrocarbons from glacial organic matter is greater than that from interglacial organic matter (S_1 and S_2, Fig. 34 and Table 9B); the S_2/S_3 ratio in glacial organic matter (see Figs. 33, 34 and Table 9B) is three to eight times larger than interglacial. While both types of organic matter would be considered Type III (terrestrial) on a Van Krevelen diagram, their S_2/S_3 ratios are distinct, and the difference appears to increase with depth. Possible explanations could be that the humic and reworked organic matter carried to the oceans during glacial periods is more resistant to decomposition than the marine-type organic matter produced during interglacial periods. Other environmental factors, such as lower temperatures or decreased biological activity, could also account for the observed differences in organic matter.

The production index $S_1/S_1 + S_2$ (Table 9B) may also suggest that the organic matter of interglacial periods is more easily converted to hydrocarbons. This suggests

Table 9A. Pyrolysis (Rock-Eval) analysis of sediments, Hole 553A.

Sample (interval in cm)	Organic carbon (%)	S_1 (mg HC/g rock)	S_2 (mg HC/g rock)	S_2 (T_{max})°C Peak A	Peak B	S_3 (mg CO_2/g rock)	Production index (S_1/S_1+S_2)	Approximate source (S_2/S_3)	Hydrogen index (mg HC/g C)	Oxygen index (mg CO_2/g C)	Remarks
4-1, 125	0.06	0.04	—	—		0.53	—	—	—	883	
7-2, 90–94	0.08	0.02	—	—		0.79	—	—	—	988	
10-2, 20	0.01	0.03	0.04	417		0.95	0.42	0.04	390	9480	
11-2, 125	0.05	0.29	0.05	378–550		1.26	0.86	0.04	96	2512	
14-5, 106	0.76	0.27	0.98	422–550		0.80	0.22	1.22	129	106	
18-1, 128	0 (tr)	0.19	0.12	550		0.92	0.61	0.13	—	—	
21-1, 125	0.18	0.21	2.23	529		1.32	0.08	1.70	1239	731	
22-5, 104	1.09	0.28	1.23	408–550		0.56	0.19	2.20	113	51	Organic layer
24-1, 23	0.37	0.33	0.67	423–550		1.15	0.18	0.58	181	310	
27-4, 125–127	0.31	0.20	1.03	413–550		1.16	0.16	0.89	332	374	
36-1, 114–116	1.10	0.16	8.94	550		0.44	0.02	35.5	813	23	Organic layer
37-4, 123–125	1.0	0.40	0.60	418–542		0.79	0.40	0.76	60	79	
[reruns: changing Δtf from 2 min.→5 min.]											
10-2, 25	0.01	0.19	0.11	405		1.33	0.63	0.08	1130	13330	
11-2, 125	0.05	0.53	0.47	367–550		1.37	0.53	0.34	936	2734	
14-5, 106	0.76	0.80	2.27	418–550		1.13	0.26	2.00	299	149	
18-1, 128	0 (tr)	0.61	0.37	550		1.16	0.61	0.33	—	—	
21-1, 125	0.18	0.15	2.96	533		1.80	0.05	1.64	1643	998	
22-5, 104	1.09	0.52	2.45	412–550		0.94	0.18	2.70	223	86	
24-1, 23	0.37	0.78	1.28	427–550		1.28	0.38	1.00	345	346	
27-4, 125–127	0.31	0.42	2.01	427–550		1.44	0.17	1.43	649	465	
36-1, 114–116	1.10	0.21	11.14	486–550		0.44	0.02	25.2	1013	40	

Table 9B. Pyrolysis (Rock-Eval) analysis of sediments, Hole 553B.

Sample (interval in cm)	S_1 (mg HC/g rock)	S_2 (mg HC/g rock)	S_2 (T_{max})°C Peak A	Peak B	S_3 (mg CO_2/g rock)	$S_1 + S_2$ $\frac{\text{mg HC}}{\text{g rock}}$	Production index (S_1/S_1+S_2)	Approximate source (S_2/S_3)	Hydrogen index mg HC/g C)	Oxygen index (mg CO_2/g C)	Remarks
1-1, 124–128	0.06	0.08			1.59	0.14	0.43	0.05	72	1446	Percent OC, 36% $CaCO_3$, mud line
1-3, 10–14	0.08	0.05			1.57	0.13	0.62	0.03	71	2243	Percent OC, 81% $CaCO_3$, interglacial
1-3, 47–52	0.10	0.19			1.60	0.29	0.35	0.12	211	1778	Percent OC, 20% $CaCO_3$, glacial
2-5, 80–83	0.04	0.09	300		1.41	0.13	0.31	0.06	53	829	Percent OC, 84% $CaCO_3$, interglacial
2-6, 105–108	0.18	0.25		500	1.39	0.43	0.42	0.18	417	2317	Percent OC, 8% $CaCO_3$, glacial
4-3, 92–96	0.11	0.06			1.16	0.17	0.65	0.05	120	2320	Percent OC, 79% $CaCO_3$, interglacial
4-3, 127–131	0.27	0.35		500	1.15	0.62	0.44	0.30	219	719	Percent OC, 12% $CaCO_3$, glacial
4-6, 63–67	0.08	0.07			1.27	0.15	0.53	0.06	100	1814	Percent OC, 73% $CaCO_3$, interglacial
4-6, 108–111	0.17	0.39		550	0.87	0.56	0.30	0.45	325	725	Percent OC, 4% $CaCO_3$, glacial

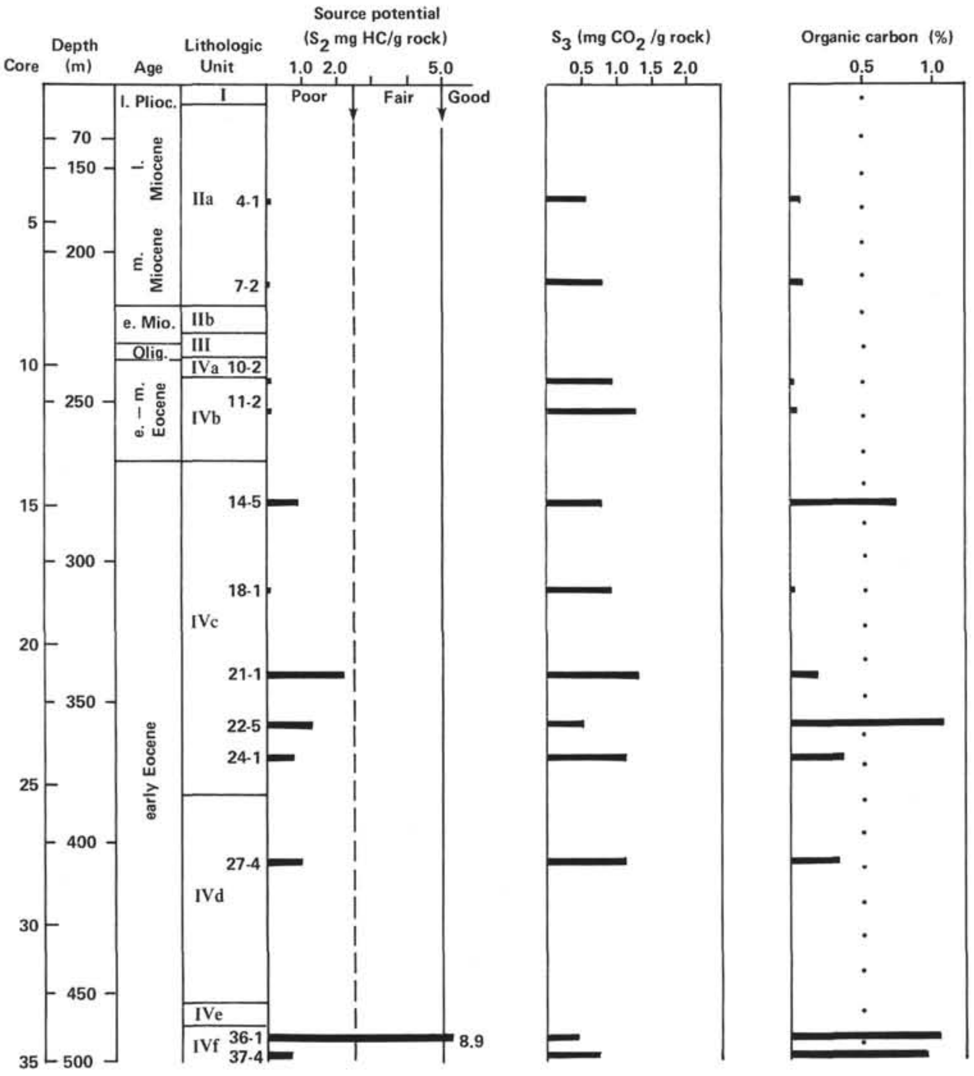

Figure 31. Sediment pyrolysis data, Hole 553.

that the interglacial organic matter at this site is primarily marine, but it is highly degraded before preservation in the sediments. This scenario is similar to the oceanic sedimentation of organic matter described by Huc (1980). These results may be applicable to the occurrence of "terrestrial" "highly" oxidized organic matter found in recent deep ocean sediments. The possibility of differentiating between terrestrial and highly oxidized marine organic matter is suggested by Figure 35.

The oxygen-containing organic compounds are quantitatively similar in glacial and interglacial organic matter and show a gradual decrease with depth in the sediments, an effect probably caused by the initial hydrolysis decomposition of organic matter (Huc, 1980).

Table 9B also shows that the oxygen-carbon pyrolysis yield (S_3) for sediments from the same depth, containing greatly varying amounts of carbonate, is approximately the same. This suggests that the S_3 pyrolysis peak is not affected by carbonates, as some workers have feared, because of the high S_3 values.

In summary there are clear differences in organic matter deposited in glacial versus interglacial sediments. It is possible that the difference is caused by higher terrestrial input and preservation during glacial times in contrast to a "normal" marine highly oxidized source of organic matter during interglacial periods. The possibility of distinguishing between these sources will be the focus of further shore-based research.

PHYSICAL PROPERTIES

Site 552

Physical properties measured on sediments and basalts recovered in Hole 552 and on sediments penetrated in Hole 552A include shear strength, compressional-wave velocity, 2-minute GRAPE wet-bulk density, continuous GRAPE wet-bulk density and wet-bulk density, wet water content, and porosity by traditional gravimetric techniques. The gravimetric measurements were carried out in the shipboard chemistry laboratory. Shear-strength measurements were made on soft undisturbed sediments of HPC cores from Hole 552A down to 182.7 m in split core liners. All measurements and calculations were made as described in the Introduction and Explanatory Notes.

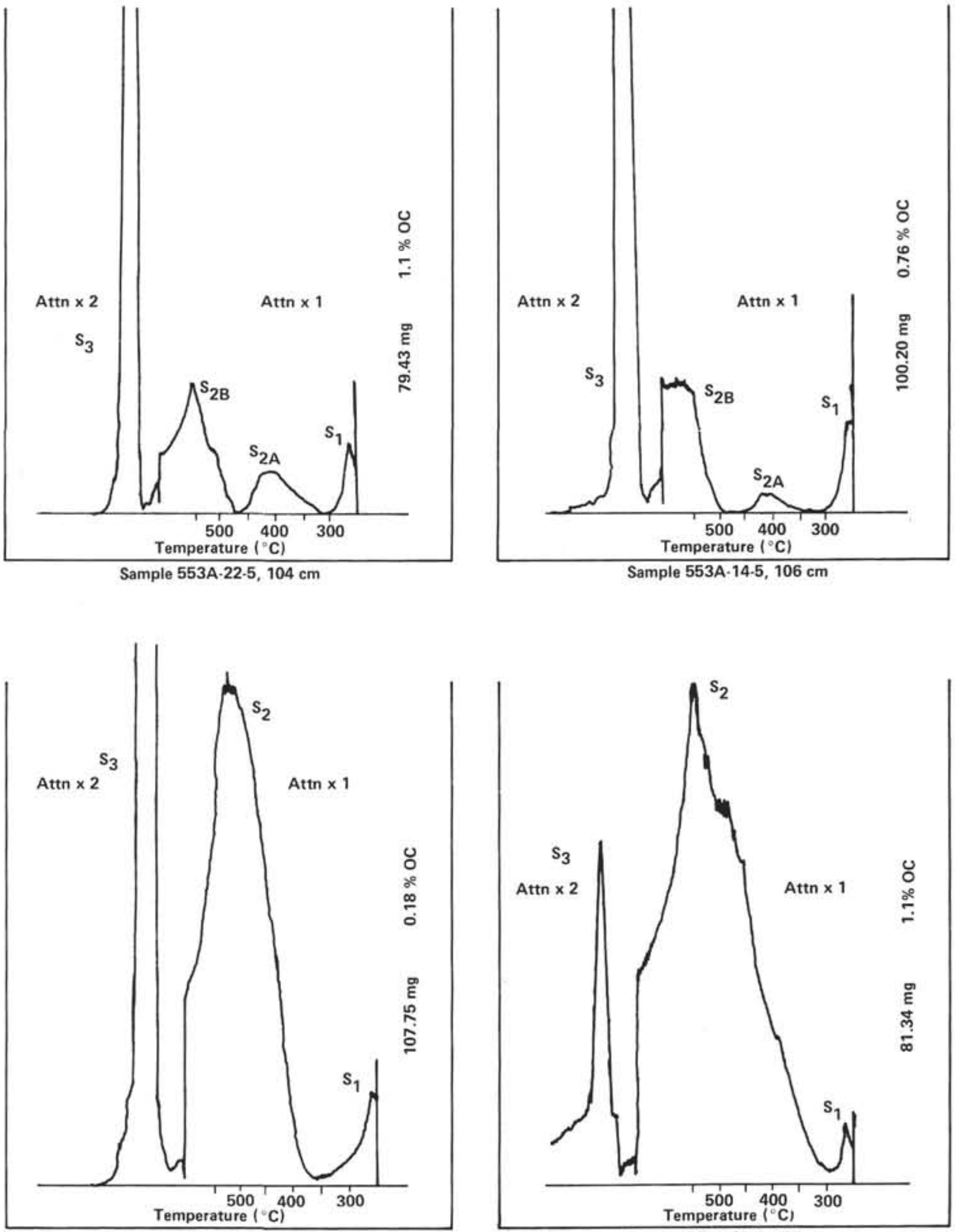

Sample 553A-22-5, 104 cm

Sample 553A-14-5, 106 cm

Sample 553A-36-1, 114 cm

Sample 553A-21-1, 125 cm

Figure 32. Sediment pyrolysis analyses, Hole 553.

Table 10. Organic carbon and nitrogen data, Hole 553B.

Sample designation	Sample (interval in cm)	N (%)	C_{org} (%)	H (%)	C/N ratio $\left(\frac{14}{12} \times \frac{C_{org}}{N_{org}}\right)$	$CaCO_3$ bomb (%)	Remarks
A	1-3, 10–14	0.01	0.07		8.2	81	
B	1-3, 47–52	0.03	0.09		3.5	20	
C	1-1, 124–128	0.03	0.11		4.3	36	
D	2-5, 80–83	0.02	0.17		9.9	84	
E	2-6, 105–108	0.03	0.06		2.3	8	
F	4-3, 92–96	0.01	0.05		5.8	79	
G	4-3, 122–127	—	—		—	—	Lost
	4-3, 127–131	0.04	0.16		4.7	12	Resample
H	4-6, 63–67	0.01	9.07		8.2	73	
I	4-6, 108–111	0.03	0.12		4.7	4	

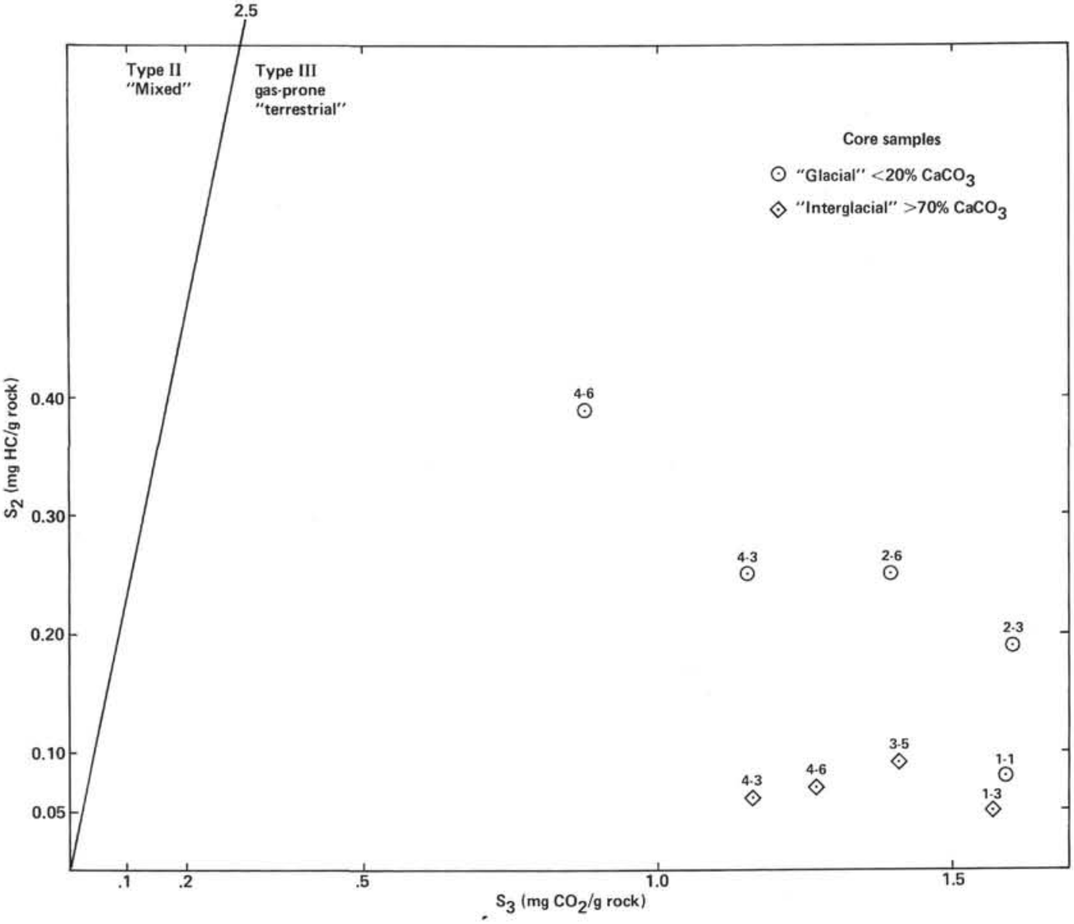

Figure 33. Pyrolysis S_2 versus S_3 of Hole 553B.

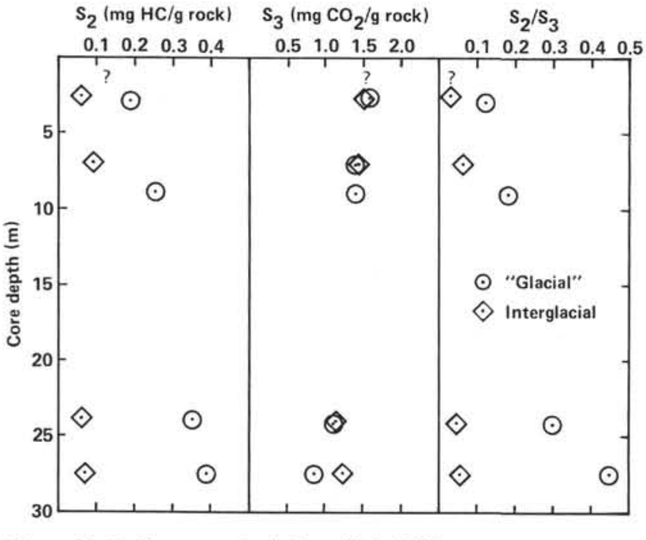

Figure 34. Sediment pyrolysis data, Hole 553B.

All the data measured and calculated are given in Table 11 and plotted in Figure 36.

Main Results

Although core recovery in Hole 552 was very poor and physical properties could be measured only sporadically, three different units can be depicted by their physical properties.

Unit A: Quaternary–Middle Eocene

Unit A, which covers lithologic Units I through IVa, is characterized by sonic velocities of about 1.5 km/s throughout and a correspondingly homogeneous acoustic impedance of around 2.8 [g(cm^2 s)]10^5 (see Fig. 37, Physical Properties summary chart, which appears in the back pocket of this volume). The other physical properties measurements show no discernible trend.

Unit B: Early Eocene

Unit B, which overlies altered basalts at 282.7 m, includes lithologic Units IVb through IVd. Because of the poor core recovery below 193 m and the bad drilling disturbances of the sediments, only the measured sonic velocities and the acoustic impedance are shown in the summary chart. The velocities range between 1.6 and 2.3 km/s and are characteristic for a heterogeneous sequence of biosiliceous volcanic tuffs, tuffaceous chalks, mudstones, and nannofossil chalk.

Unit C: Probably Early Eocene

The basalts penetrated below 282.7 m have sonic velocities going up to 3.55 km/s. These relatively low velocities are typical of altered basalts.

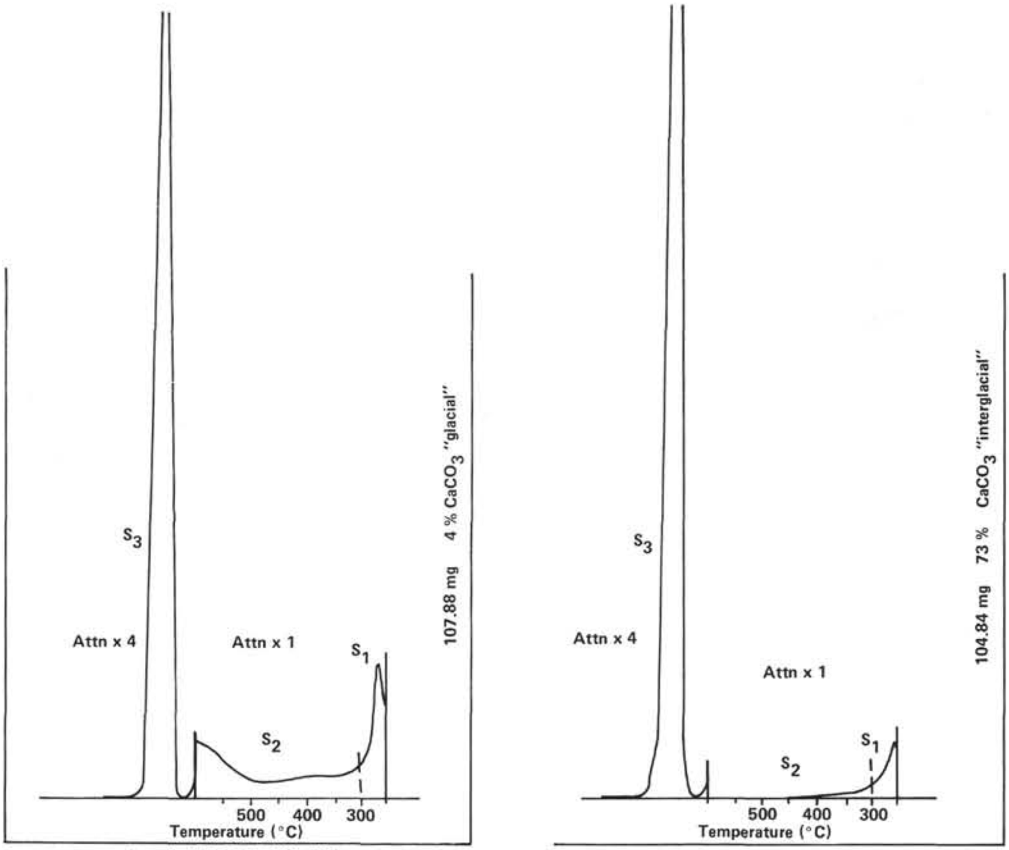

Sample 553B-4-6, 108–111 cm

Sample 553B-4-6, 63–67 cm

Figure 35. Pyrolysis analyses, Hole 553B.

Site 553

Physical properties measured on sediments and basalts recovered in Hole 553A include shear strength, compressional-wave velocity, 2-minute GRAPE wet-bulk density, continuous GRAPE wet-bulk density and wet-bulk density, wet water content, and porosity by gravimetric techniques.

The gravimetric measurements were carried out in the shipboard chemistry laboratory.

Shear-strength measurements were made on soft sediments in split liners down to a depth of 221.88 m. Because the recovered material was disturbed to a great extent, the measurements have not been plotted against depth but the values are given in Table 12.

The sonic velocities were measured as described in the Introduction and Explanatory Notes. These measurements are summarized in Table 12 and shown in Figure 37. The highest velocities were measured on massive basalts and range up to 6.00 km/s.

For the calculation of the wet-bulk density of the sediments and the basalts by the 2-minute GRAPE technique, grain densities were calculated from the gravimetric determinations. The grain density values vary widely between 2.42 (volcaniclastic sediments) and 3.05 g/cm^3 (massive basaltic lava flows).

For the determination of the wet-bulk density, the wet water content, and the porosity of soft sediments by the gravimetric technique, samples were taken with "Boyce-Cylinders" so that 2-minute GRAPE measurements could be carried out on the same samples. From the firmer sediments (mainly volcaniclastic sediments) and the basalts, samples of 3 to 4 cm thickness were taken and treated the same way.

Main Results

Seven lithological units can be distinguished according to the physical properties. The boundaries between the units correlate well with the lithological units given in this site chapter.

The boundary between Unit A and B was drawn at about 235 m. Unit A (Quaternary–early Miocene), which includes sedimentological Units I to III, is characterized by sonic velocities between 1.48 and 1.72 km/s, by porosities as high as about 60%, and by acoustic impedance values not exceeding 2.86 [g/(cm^2 s)]10^5. Unit B extending down to about 269.5 m shows approximately the same sonic velocity values as Unit A but could be defined by very high porosities (going up to 78%). This unit includes lithologic Units IVa and IVb: volcanic tuffs with interbeds of zeolitic–biosiliceous nannofossil–foraminifer chalk of early to late Eocene age.

The interval between 261.5 and 388 m, referred to as Unit C, shows fluctuations in all the physical properties determined (see Fig. 37, back pocket). The sonic velocities vary between 1.68 and 2.9 km/s and porosities decrease from 65.5 to 31.5%. These values reflect the alternating sequence of tuffaceous layers and volcani-

Table 11. Physical property data, Holes 552 and 552A.

Sample (level in cm)	Depth in hole (m)	Sound velocity			GRAPE "Special" wet-bulk density 2-min. count (g/cm^3)		Gravimetric			Acoustic Impedance $\left(\frac{g\ 10^5}{cm^2 s}\right)$	Vane shear strength (g/cm^2)
		∥ Beds (km/s)	⊥ Beds (km/s)	Temp. (°C)	∥ Beds	⊥ Beds	Wet bulk density (g/cm^3)	Wet-water content (salt corr.) (%)	Porosity (%)		
Hole 552											
1-1, 122	1.22			19.0	1.86			44.46			
1-2, 121	2.71	1.4813		19.0	1.69			41.40		2.509	
2-1, 60	51.60	1.462		19.0	1.66			38.86		2.433	
3-1, 90	108.90	1.530		19.0	1.90			32.51		2.913	
3-3, 95	111.95	1.539		19.0	1.85			32.38		2.841	
3-4, 88	113.38	1.559		19.0							
3-5, 72	114.75			19.0	1.94			29.27			
4-1, 123	118.73	1.542		19.0	1.85			29.99		2.857	
4-2, 96	119.96	1.508		19.0							
4-3, 61	121.11	1.490		19.0	1.85			32.20		2.758	
4-4, 90	122.90	1.492		19.0							
5-2, 105	129.55	1.510		19.0	1.85			31.62		2.795	
5-4, 120	132.70			19.0	1.81			33.73			
5-5, 43	133.43	1.516		19.0							
6-1, 110	137.60	1.504		19.0							
6-2, 101	139.01			19.0	1.79			33.64			
6-3, 73	140.23	1.355		19.0							
6-4, 81	141.81			19.0	1.79			32.76			
7-1, 132	147.32	1.410		19.0	1.72			37.46		2.428	
7-2, 135	148.75	1.562		19.0							
7-3, 132	150.32			19.0	1.71			38.82			
7-4, 56	151.06	1.515		19.0							
8-2, 81	157.80	1.487		19.0	1.69			38.75		2.519	
8-4, 75	160.75	1.524		19.0							
9-1, 125	166.25			19.0	1.33			62.90			
9-3, 43	168.43			19.0	1.37			61.00			
9-3, 138	169.38	1.511		19.0							
9-5, 106	172.06	1.534		19.0	1.59			44.96		2.441	
12-1, 130	194.80			19.0	1.66			44.04			
12-2, 104	196.04	1.499		19.0	2.05			25.90		3.073	
12-3, 100	197.50	1.485		19.0	1.64			42.76		2.429	
12-4, 127	199.27	1.595		19.0							
12-5, 100	200.50			19.0	1.58			40.80			
12-6, 132	202.32	1.586		18.0	1.56			40.25		2.474	
12-7, 18	202.68	1.582		18.0							
13-1, 120	204.20	2.049	2.144	18.0		1.57				3.221	
14-1, 15	212.65			18.0		1.56		36.09		3.336	
14-1, 95	213.45	2.303		18.0		1.67				3.837	
14-2, 28	214.28	2.279		18.0		1.72				3.920	
14-3, 141	216.91	1.654	2.021	18.0	1.63					2.701	
14-4, 37	217.37			18.0		1.50		33.90		3.034	
14, CC (16)	217.58	1.982	1.971	18.0	1.55					3.002	
15-1, 40	222.40			18.0	1.57					3.096	
15-1, 50	222.50	3.36	2.031	19.0							
16-1, 67	232.17	2.113	2.788	19.0		1.47		31.48		3.115	
17-1, 21	241.21		2.287	19.0		1.95		4.74		5.440	
18-2, 75	252.75		1.585	19.0		1.56		27.73		3.561	
21-1, 124	280.24			19.0		1.48		31.41		2.352	
21-2, 105	281.55	1.489	2.280	19.0							
21-3, 77	282.77		3.177	18.5		2.40					5.474
22-1, 20	284.20	3.087	3.546	18.5		2.61					8.301
22-1, 100	285.00	3.43		18.5		2.74					9.720
Hole 552A											
1-2, 65	2.15	1.504		18.5	1.57		1.52	45.55	69.05	2.361	0.140
1-3, 85	3.85	1.320		18.5	1.61		1.58	42.05	66.46	2.119	0.210
2-2, 97	6.47	1.529		18.5	1.63		1.60	40.40	64.49	2.492	0.380
2-3, 58	7.58	1.484		18.5	1.54		1.55	44.42	68.92	2.279	0.230
3-2, 107	11.57	1.554		18.5	1.70		1.72	34.53	59.35	2.642	0.200
3-3, 78	12.78	1.548		18.5	1.62		1.59	42.00	66.89	2.508	0.305
4-2, 58	16.08	1.489		18.5	1.65		1.62	39.50	64.03	2.457	0.245
4-3, 109	18.09	1.507		18.5	1.70		1.71	34.95	59.67	2.562	0.350
5-1, 68	19.68	1.455		18.5	1.63		1.71	36.81	63.04	2.372	0.300
5-3, 88	22.88	1.516		18.5	1.62		1.59	42.25	67.24	2.461	0.365
7-2, 37	30.87	1.512		18.5	1.72		1.70	35.11	59.21	2.604	
7-3, 138	33.38	1.529		18.5	1.61		1.54	43.07	66.23	2.462	0.410
8-1, 128	35.28	1.514		18.5	1.63		1.64	39.58	64.83	2.468	0.410
8-2, 97	36.47	1.542		18.5	1.65		1.60	39.94	64.11	2.551	0.420
8-3, 119	38.19	1.473		18.5	1.67		1.72	35.29	60.60	2.467	0.460

Table 11. (Continued).

Sample (level in cm)	Depth in hole (m)	Sound velocity			GRAPE "Special" wet-bulk density 2-min. count (g/cm3)		Gravimetric			Acoustic Impedance $\left(\frac{g\ 10^5}{cm^2 s}\right)$	Vane shear strength (g/cm^2)
		∥ Beds (km/s)	⊥ Beds (km/s)	Temp. (°C)	∥ Beds	⊥ Beds	Wet bulk density (g/cm^3)	Wet-water content (salt corr.) (%)	Porosity (%)		
Hole 552A (Cont.)											
9-1, 38	39.38	1.616		18.5	1.66		1.66	37.35	61.84	2.687	0.250
9-3, 88	42.88	1.550		18.5	1.70		1.68	36.39	61.09	2.641	0.570
10-1, 99	44.89	1.937		18.5	1.71		1.64	37.82	61.85	3.312	0.450
10-3, 128	48.28	1.507		18.5	1.63		1.57	41.54	65.03	2.462	0.280
11-2, 98	51.48	1.540		18.5	1.68		1.68	36.33	60.86	2.590	0.195
11-3, 139	53.39	1.524		18.5	1.70		1.68	35.37	59.46	2.591	0.230
12-3, 79	57.79	1.513		18.5	1.73		1.68	36.29	60.88	2.673	0.515
14-3, 98	65.98	1.519		18.5	1.82		1.77	31.43	55.51	2.769	0.115
15-2, 88	69.38	1.519		18.5	1.79		1.76	31.68	55.85	2.724	0.615
15-3, 99	70.99	1.531		18.5	1.82		1.71	33.82	57.87	2.786	0.600
16-3, 118	76.18	1.576		18.5	1.79		1.75	31.66	55.53	2.821	0.460
17-2, 99	79.18	1.570		18.5	1.81		1.75	30.86	53.93	2.842	0.700
18-2, 129	84.79	1.573		18.5	1.77		1.76	31.02	54.72	2.791	0.545
18-3, 88	85.88	1.534		18.5	1.75		1.76	31.73	55.74	2.685	0.450
19-2, 99	89.49	1.570		18.5	1.79		1.78	29.99	53.52	2.81	0.630
20-2, 109	94.59	1.531		18.5	1.85		1.81	29.02	52.48	2.832	0.745
21-3, 59	98.59	1.534		18.5	1.83		1.79	29.91	53.41	2.807	0.640
22-2, 139	101.89	1.567		18.5	1.86		1.81	29.18	52.76	2.910	0.715
23-1, 139	105.39	1.575		18.5	1.86		1.83	27.94	50.38	2.93	0.785
23-3, 49	107.49	1.574		18.5	1.82		1.76	31.61	55.66	2.86	0.630
24-2, 79	110.79	1.538		18.5	1.86		1.75	31.82	55.60	2.867	0.800
24-3, 139	102.89	1.555		18.5	1.78		1.73	32.72	56.71	2.77	0.630
25-1, 99	114.49	1.510		18.5	1.84		1.75	31.44	54.89	2.77	0.630
25-3, 79	117.29	1.542		18.5	1.86		1.78	30.12	53.55	2.86	0.855
26-2, 99	120.99	1.534		18.5	1.82		1.76	31.36	55.33	2.79	0.680
27-1, 99	124.49	1.486		18.5	1.77		1.73	33.90	56.78	2.63	0.520
27-3, 89	127.39	1.538		18.5	1.81		1.73	32.94	56.90	2.78	0.745
28-2, 58	130.58	1.530		18.5	1.80		1.72	33.02	56.85	2.754	0.580
29-2, 79	135.79	1.518		18.5	1.75		1.71	33.94	58.10	2.66	0.750
30-2, 79	140.79	1.498		17.5	1.74		1.73	33.39	57.76	1.597	0.640
31-2, 89	145.89	1.525		17.5	1.76		1.77	32.14	56.73	2.69	0.700
32-2, 99	150.99	1.535		18.5	1.74		1.77	33.62	59.39	2.67	0.860
33-2, 89	155.89	1.535		18.5	1.72		1.74	32.88	57.22	2.64	0.765
34-2, 99	160.99	1.529		18.5	1.71		1.68	34.89	58.69	2.64	0.550
35-2, 89	165.89	1.550		18.5	1.77		1.74	33.24	57.94	2.74	0.480
36-2, 79	170.79	1.541		18.5	1.70		1.68	36.42	61.15	2.615	0.865
36-3, 119	172.69	1.575		18.5	1.70		1.81	33.35	60.49	2.671	0.965
37	Could not be measured because of liner quality										
38-1, 112	179.62	1.525	No other measurements								
38-2, 90	180.90	1.522									

Note: Heat conductivity at 21°C cal · X^{-3} cm°C s.

clastic sediments with varying contents of detrital terrigenous material.

Another break in the physical properties occurs at about 406 m. The overlying sequence (Unit D) consists of clastic sediments with an average porosity of about 50% and a water content of 27% in which we have a fairly good core recovery. We interpret the underlying sequence (Unit E) to be more porous but having the same overall mineralogical composition. Core recovery in this interval is very poor and only the more tightly calcite cemented layers were recovered and hence measured.

Sonic velocities of these tightly calcite-cemented siliceous sandstones range up to 4.6 km/s and porosities as low as 10%. The high velocities cause high values in the acoustic impedance of those layers which affects the interpretation of the seismic profiles. Units D and E correlate with lithological Unit IVd, which is early Eocene in age.

Samples of Unit F (about 465 to 499 m), comprising mainly lapilli tuffs and tuffaceous mudstones of lithologic Units IVe and IVf (late Eocene), have sonic velocities of about 1.7 km/s and porosities up to 63%. Although there are only a few measurements on samples of that unit the lower boundary at 499 m is very well established.

This boundary separates the volcaniclastic sedimentary sequence from the top of the basaltic lava flows, which are characterized by higher sonic velocities, grain densities, and acoustic impedances, as well as by a sharp decrease in porosities and water contents. The basalt sequence is divided into Units G1 and G2.

Within the different lava flows, three different rock types can be distinguished by their physical properties:

1. Weathered and to a variable extent altered tops of single lava flows—low velocities, high porosities, and high water contents.

2. Vesicular layers of the different lava flows—intermediate velocities, porosities, and water contents.

3. Massive basalt varieties with very high velocities (greater than 5 and up to 6.0 km/s) and very low porosities and water contents.

Moreover, a very distinct boundary within the basalts can be identified from the physical properties: below 603 m a sequence of lava flows was penetrated whose sonic velocities are distinctly lower than those of the directly overlying massive lava flow.

This boundary may be the top of the dipping reflector sequence.

The physical properties measured on samples of Hole 553A correlate very well with the downhole measurements; the correlation is obvious in the physical properties correlation chart.

SEDIMENT ACCUMULATION RATES

Site 552

The sedimentation rates for Holes 552 and 552A are shown in Figure 38. It is apparent that there is an artificial depth difference between the two holes. Biostratigraphic data (Table 13) indicate that this discrepancy may occur in the spot-cored interval of Hole 552 (ca. 3.5 to ca. 108.0 m). For this reason, the Neogene sedimentation rate for Hole 552 is not plotted.

Accumulation at Site 552 appears to be continuous from the present to the late Miocene (about 6.0–6.5 m.y. ago). The glacial sequence in Hole 552A, Cores 1 through 9 probably has a greater internal variation in accumulation rates than that apparent from Figure 38. Backman (this volume) and Baldauf (this volume) present a more detailed account of the late Pliocene and Pleistocene sedimentation rates. The available biostratigraphic information does not exclude the possibility of a number of minor breaks in the Neogene record between approximately 6.5 and 13 m.y ago. The rate deduced in that interval (0.6 cm/1000 yr.) may thus be too low. A major hiatus separates the middle Miocene from the early Eocene and has a duration of approximately 35 m.y. Traces of late Oligocene and middle Eocene sediments are, however, preserved at the level of the hiatus. The early Eocene accumulation appears continuous and virtually linear. It should be noted that the above sedimentation rates have not been corrected for compaction.

Accumulation Rates

The accumulation rates of foraminifers, nannoplanktons, and noncalcareous sedimentary components have been determined using a method developed by Shackleton during Leg 74. For each time slice, average foraminifer–nannofossil ratios have been calculated, using physical properties data from the core together with observations on 35 core-catcher samples. At least double this number of $CaCO_3$ bomb determinations and bulk-density measurements from lithologies compatible with the sample from the core catcher have also been used in the calculation. The data tabulated in Table 14 have been calculated as follows:

Column	
A	Average accumulation (cm/10^3 yr.)—the sedimentation rate
B	Average bulk density—GRAPE from the physical properties data
C	Average dry weight in g/wet water content corrected $\frac{\text{Column B} \times (100 - \text{wet water content})}{100}$
D	Total accumulation g/cm^2/10^3 yr.: Column A × Column C
E	Average percent $CaCO_3$: from carbonate bomb data
F	$CaCO_3$ accumulation: $\frac{\text{Column A} \times \text{Column E}}{100}$
G	Average percent, foram g/wet g: samples were weighed wet, washed on a 63 μm sieve, and the dry >63 μm fraction was weighed. $\frac{\text{Weight of dry residue}}{\text{Weight of wet sediment}} \times 100$
H	Foram accumulation g/cm^2/10^3 yr.: $\frac{\text{Column A} \times \text{Column B} \times \text{Column G}}{100}$
I	Nanno accumulation g/cm^2/10^3 yr: Column F – Column H
J	Non-$CaCO_3$ accumulation g/cm^2/10^3 yr: Column D – Column F

The accumulation rates are shown in Figure 39 and Table 14. The slow sedimentation rates of the middle Miocene and earlier part of the late Miocene are reflected in low accumulation rates of all components. Most of the carbonate is contributed by the nannoflora. In the later late Miocene and Pliocene there was a four-fold increase in the sedimentation rate. Most of this is accounted for by a great increase in the carbonate component, but there is also a cyclic variation in the noncarbonate component (cf. the total and $CaCO_3$ accumulation curves, Fig. 39). There is a pronounced cyclic variation in both the nannofossil and foraminifer components, the two groups showing reciprocal changes in abundance. The first glacial sediments occur in the Core 9 core catcher. A major change in the pattern of sediment accumulation is shown at this level with a reduction in carbonate deposition (by chance the core-catcher samples are from interglacials). Although there is variation within the Pleistocene, the $CaCO_3$ accumulation values are significantly lower than those of the preglacial Pliocene and late Miocene succession.

The interpretation of these results hinges on the relative importance of productivity rates of both nannofossils and foraminifers (especially the planktonic foraminifers) and sediment transport. It does not seem possible to attribute all these variations to productivity differences. It is, however, clear that transport has played a

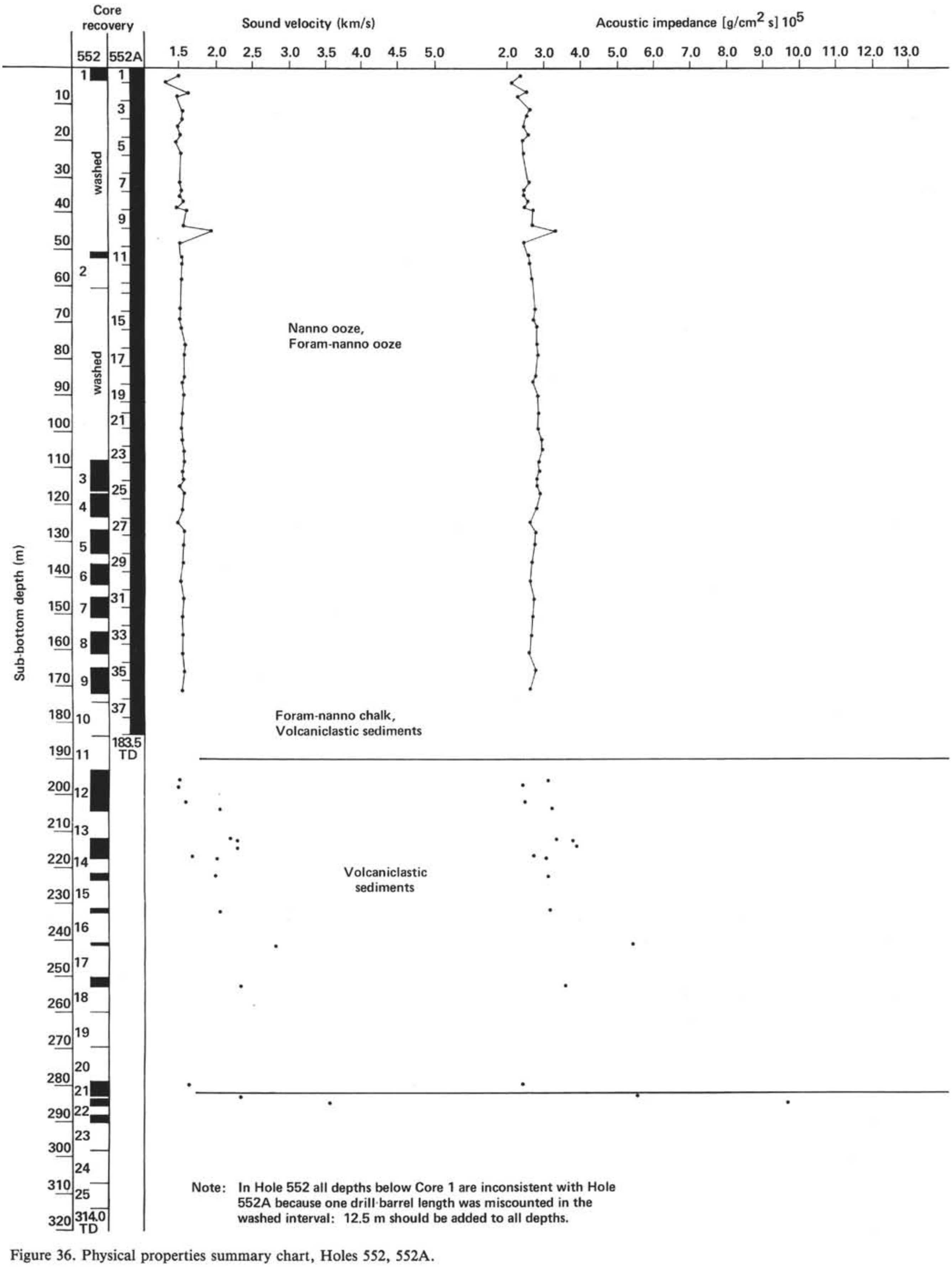

Note: In Hole 552 all depths below Core 1 are inconsistent with Hole 552A because one drill-barrel length was miscounted in the washed interval: 12.5 m should be added to all depths.

Figure 36. Physical properties summary chart, Holes 552, 552A.

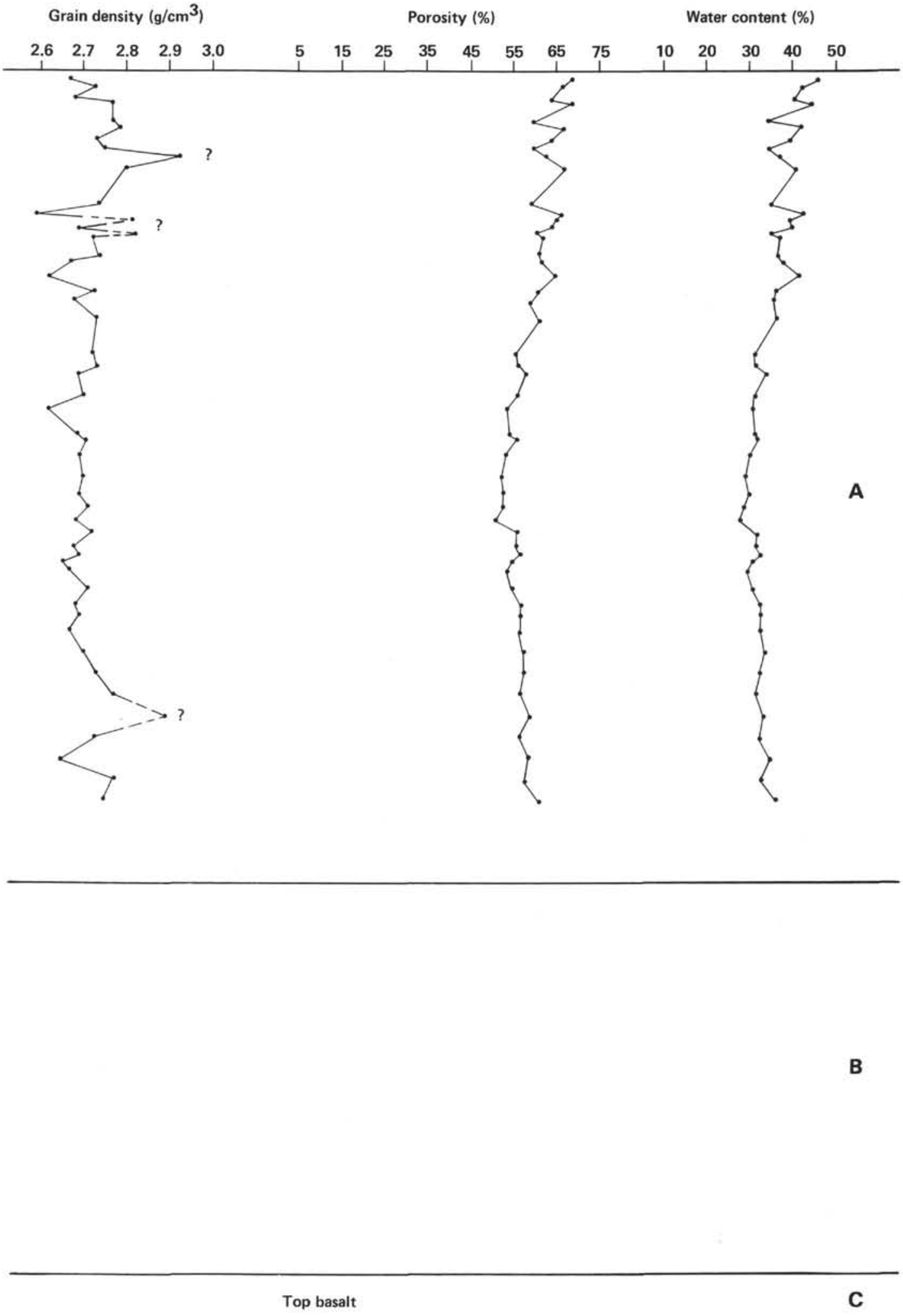

Figure 36. (Continued).

Table 12. Physical property data, Hole 553A.

Sample (level in cm)	Depth in hole (m)	Sound velocity		Temp. (°C)	GRAPE "special" wet-bulk density 2-min. count (g/cm^3)		Gravimetric			Acoustic impedance $\left(\frac{g\ 10^5}{cm^2 s}\right)$	Vane shear strength (g/cm^2)
		‖ Beds (km/s)	⊥ Beds (km/s)		‖ Beds	⊥ Beds	Wet bulk density (g/cm^3)	Wet-water content (salt corr.) (%)	Porosity (%)		
Hole 553A											
1-1, 48	65.98	1.541		18.0	1.743		1.68	35.42	59.49	2.686	0.135
2-1, 128	104.78	1.552		18.0	1.697		1.71	34.52	58.99	2.634	0.210
2-5, 58	110.08	1.554		18.0	1.741		1.70	35.31	59.92	2.706	0.390
3-1, 128	152.28	1.530		18.0	1.802		1.76	32.40	56.94	2.757	0.325
3-4, 98	156.48	1.520		18.0							0.610
3-6, 98	159.48	1.482		18.0	1.795		1.70	34.56	58.85	2.660	0.410
4-2, 128	182.28	1.557		18.0	1.724		1.66	36.39	60.44	2.684	0.330
4-5, 88	186.30	1.562		18.0	1.757		1.76	32.24	56.80	2.744	0.635
4-6, 138	188.38	1.618		18.0	1.742		1.70	34.92	59.33	2.819	0.675
5-3, 78	192.78	1.563		18.0	1.741		1.75	33.14	58.03	2.720	0.340
5-5, 128	196.28	1.569		18.0	1.823		1.78	30.92	55.09	2.860	0.255
5-6, 58	197.08	1.572		18.0	1.772		1.70	33.35	56.67	2.786	0.485
6-3, 108	203.58	1.717		18.0	1.666		1.62	37.82	61.29	2.860	0.450
6-5, 108	205.08	1.576		18.0	1.742		1.71	34.32	58.54	2.745	0.655
7-2, 79	210.29	1.556		18.0	1.754		1.79	30.82	55.04	2.730	0.250
7-6, 89	216.39	1.588		18.0	1.689		1.72	34.68	59.81	2.682	0.980
8-2, 118	220.18	1.545		18.0	1.741		1.72	33.33	57.31	2.69	0.120
8-3, 138	221.88	1.582		18.0							0.870
9-1, 65	227.65	1.600		18.0							
9-3, 85	230.85	1.634		18.0	1.634		1.54	41.73	64.25	2.671	
9-5, 98	233.98	1.661		18.0							
9-6, 60	235.10	1.594		18.0							
9,CC (12)	235.35		1.703	18.0	1.567		1.586	42.84	66.32	2.669	
10-2, 140	239.40	1.654		18.0	1.642		1.635	39.06	62.15	2.716	
10-3, 90	240.40	1.921	1.872	18.0	1.545						
10-5, 10	242.60	1.546		18.0	1.545		1.44	50.99	73.50	2.389	
10-7, 43	245.93	1.596		18.0	1.410		1.37	56.95	78.24	2.250	
11-1, 128	247.68	1.602		18.0	1.562		1.61	43.59	70.19	2.50	
11-3, 68	249.68	1.622		18.0	1.601		1.46	46.49	67.78	2.597	
11-4, 78	251.28	1.649		18.0	1.608		1.59	43.52	69.36	2.652	
11-5, 102	253.02	1.587		18.0	1.572		1.46	49.02	71.50	2.495	
12-2, 126	258.26	1.786	2.089	18.0		1.494	1.458	52.40	74.56	3.121	
12-3, 103	259.53	1.796	1.779	18.0		1.486	1.542	47.00	70.76	3.195	
12,CC (6)	261.80	2.146	2.240	18.0		1.944	1.939	26.34	49.85	4.355	
13-1, 84	265.84	2.041	2.021	18.0		1.759	1.773	33.44	57.89	3.590	
14-3, 26	277.76	1.893	1.950	18.0		1.655	1.606	42.38	66.45	3.227	
15-2, 79	286.29	2.020	2.013	18.0		1.683	1.721	35.86	60.22	3.40	
15-3, 96	287.96	2.047		18.0		1.774	1.838	31.18	55.95	3.631	
18-1, 106	313.56	2.382		18.0		1.860	1.860	28.73	52.16	4.431	
19-1, 135	323.35	2.131	2.224	18.0		1.817	1.757	31.37	53.78	4.041	
19,CC 7	328.07	2.214	2.253	18.0		1.753	1.719	33.60	56.37	3.950	
20-2, 119	334.19	1.994	2.084	18.0		1.792	1.722	34.42	57.87	3.735	
20-5, 104	338.54	1.748	1.839	18.0		1.693	1.666	37.90	61.63	3.113	
21-5, 135	345.35	1.945		18.0		1.694	1.646	39.25	63.09	3.295	
22-2, 87	352.87	1.564	1.658	18.0		1.777	1.750	33.26	56.81	2.946	
22-6, 58	358.58	1.679	1.671	18.0		1.696	1.689	36.98	60.97	3.848	
23-2, 4	361.54	1.676	1.737	18.0		1.621	1.623	39.87	64.73	2.816	
23-4, 44	364.94	2.214		18.0		1.873	1.340	27.61	52.29	4.147	
24-1, 28	369.78	1.721	1.282	18.0		1.626	1.620	41.43	65.50	2.898	
24-2, 29	371.29	1.940		18.0		1.764	1.739	35.84	60.83	3.422	
25-2, 84	381.34	2.909	3.452	18.0		2.244	2.264	14.27	31.52	7.073	
26-1, 109	389.59	1.980	2.073	18.0		1.919	1.904	25.94	48.21	3.978	
27-2, 49	400.00	1.679		18.0	1.809		1.87	27.99	52.42	3.04	
27-5, 90	404.90	1.651		18.0	1.886		1.82	27.55	50.18	3.114	
28,CC	407.60	4.203		18.0	2.497		6.512	5.65	13.84	10.415	
29,CC	417.05	4.587		18.0	2.593		2.516	4.69	11.51	11.894	
31,CC	436.03	2.889		18.0	2.316		2.234	13.09	28.34	6.691	
32,CC	445.05	4.316		18.0	2.597		2.534	4.02	9.93	11.209	
35-1, 90	474.90	2.223	2.337	18.0		1.893	1.817	28.46	50.49	4.424	
36-3, 110	487.60	1.683	1.838	18.0		1.722	1.784	33.80	58.84	3.165	
37-3, 60	496.60	1.684	1.719	18.0		1.667	1.696	38.29	63.39	2.866	
37,CC	499.60	3.336		18.0		2.277	2.350	12.94	29.68	7.596	
38-1, 10	503.00	3.440		18.0		2.27	2.435	11.14	26.48	7.812	
47-2, 78	582.78	4.801		18.0		2.592	2.79	3.82	10.41	12.44	
47-3, 140	584.90	4.712		18.0		2.595	2.76	3.77	10.16	12.23	
47-4, 100	586.00	2.828		19.0		2.087	2.27	15.78	34.95	5.90	
48-1, 90	588.40	5.018		19.0		2.576	2.78	3.80	10.32	12.93	
48-2, 130	590.30	5.611		19.0		2.658	2.92	1.75	4.98	14.91	
48-3, 140	591.90	5.655		19.0		2.611	2.91	1.91	5.43	14.77	
48-4, 145	593.45	5.712		19.0		2.646	2.93	1.75	5.00	15.11	

Table 12. (Continued).

		Sound velocity			GRAPE "special" wet-bulk density 2-min. count (g/cm^3)		Gravimetric			Acoustic impedance	Vane shear strength
Sample (level in cm)	Depth in hole (m)	‖ Beds (km/s)	⊥ Beds (km/s)	Temp. (°C)	‖ Beds	⊥ Beds	Wet bulk density (g/cm^3)	Wet-water content (salt corr.) (%)	Porosity (%)	$\left(\frac{g\ 10^5}{cm^2 s}\right)$	(g/cm^2)
Hole 553A (Cont.)											
48-5, 140	594.90	6.004		19.0		2.65	2.94	1.84	5.29	15.91	
48-6, 85	595.85	5.78		19.0		2.65	2.93	1.80	5.14	15.32	
49-1, 43	596.93	5.466		19.0		2.646	2.93	1.71	4.89	14.46	
49-2, 90	598.90	5.616		19.0		2.66	2.97	1.21	3.50	14.94	
49-3, 38	599.88	5.902		19.0		2.65	2.97	1.30	3.76	15.64	
49-4, 5	601.05	5.39		19.0		2.609	2.95	1.52	4.37	14.06	
49-5, 35	602.85	5.66		19.0		2.64	2.93	1.60	4.57	14.94	
49-6, 100	604.50	3.696		19.0		2.362	2.45	9.99	23.92	8.73	
50-1, 124	606.74	4.424		19.0		2.52	2.64	5.87	15.11	11.15	
50-2, 108	608.08	5.103		19.0		2.61	2.82	2.46	6.93	13.32	
50-3, 52	609.02	2.476		19.0		2.096	2.13	18.73	39.82	5.19	
51-1, 30	614.80	4.707		19.0		2.59	2.73	4.17	11.40	12.19	
51-2, 145	617.45	5.477		19.0		2.684	2.88	1.85	5.34	14.70	
52-1, 120	619.20	5.406		19.0		2.677	2.94	1.52	4.48	14.47	
52-3, 55	621.55	3.325		19.0		2.300	2.39	11.63	27.76	7.65	
53-1, 102	624.52	5.164		19.0		2.556	2.79	3.66	10.22	13.20	
53-2, 145	626.45	3.645		19.0		2.241	2.40	11.35	27.20	8.17	
54-1, 105	633.55	4.356		19.0		2.48	2.66	4.82	12.84	10.80	
54-2, 125	635.25	4.455		19.0		2.401	2.60	7.10	18.49	10.70	
54-3, 67	636.17	4.642		19.0		2.494	2.73	4.26	11.66	11.58	
54-4, 40	637.40	4.713		19.0		2.516	2.69	4.69	12.64	11.86	
55-1, 45	641.95	3.297		19.0		2.204	2.43	11.21	27.24	7.27	
55-2, 115	644.15	4.25		19.0		2.497	2.58	6.40	16.48	10.61	
55-3, 85	645.35	4.03		19.0		2.43	2.58	7.00	18.08	9.79	
55-4, 85	646.15	4.86		19.0		2.58	2.78	3.78	10.50	12.54	
55-5, 58	647.03	5.543		19.0		2.578	2.87	2.27	6.51	14.29	
55-6, 50	648.00	5.727		19.0		2.645	2.93	1.59	4.64	15.15	
56-1, 130	651.80	3.812		19.0		2.376	2.52	8.41	21.18	9.06	
56-2, 22	652.22	3.806		19.0		2.40	2.60	6.78	17.63	9.13	
56-3, 17	653.07	4.651		19.0		2.463	2.54	8.92	22.66	11.46	
57-1, 60	660.10	3.149		19.0		2.236	2.33	12.86	29.98	7.04	
58-1, 50	669.00	4.389		19.0		2.463	2.66	5.29	14.09	10.81	
58-2, 90	670.90	4.627		19.0		2.498	2.71	4.28	11.61	11.56	
59-1, 112	674.12	3.990		19.0		2.317	2.35	11.35	26.70	9.24	
59-3, 126	676.76	5.894		19.0		2.656	2.90	1.66	4.83	15.65	

Note: Heat conductivity at 21°C cal · X^{-3} cm°C s.

major role in determining the level of maximum accumulation rates; the nannofossil oozes of the preglacial Pliocene and late Miocene are contourite deposits showing preferential concentration of fine particles (especially nannofossils but also juvenile planktonic tests). In the period preceding this (middle to early late Miocene) productivity may have been low; nannofossils still greatly exceed the foraminifers, suggesting that the bottom currents were not so powerful that all fine material was winnowed away. In the glacial part of the succession, productivity would have varied with the amount of ice cover, but changes in bottom water circulation may also have taken place.

Site 553

Sedimentation Rates

Spot-coring to a depth of 179.5 m at Site 553 has resulted in a poorly constrained age-depth control for that part of the sequence (Fig. 40). The biostratigraphic data used to construct Figure 40 are presented in Table 15. The sedimentation rate in the Pliocene and Pleistocene sequence is approximately 3.0 cm/1000 yr. The average rate over the same time-stratigraphic interval is 1.7 cm/1000 yr. in Hole 552A. Given the small distance between the two sites it appears likely that the difference in accumulation rate reflects a difference in influence of bottom currents rather than differences in microplankton productivity. This conclusion is supported by the different topographic positions of Sites 552 and 553. The latter site is situated close to the crest of Hatton Drift where accumulation rates would be higher, while Site 552 is situated on the inner edge of a marginal channel separating the drift from the slope.

As at Site 552 a change in deposition rate occurs close to the Miocene/Pliocene boundary. The average accumulation rates for the late (552, 553) and middle Miocene (553) are as low as a 0.6 cm/1000 yr., suggesting a change from more vigorous to less erosive bottom currents at the two sites at around the Miocene/Pliocene boundary. This is supported by the fact that the average Atlantic Ocean accumulation rate (see Davies et al., 1977) is considerably higher during the late Miocene interval than at Sites 552 and 553, whereas the difference between the average Atlantic rates and those at Sites 552 and 553 is lesser during Pliocene times.

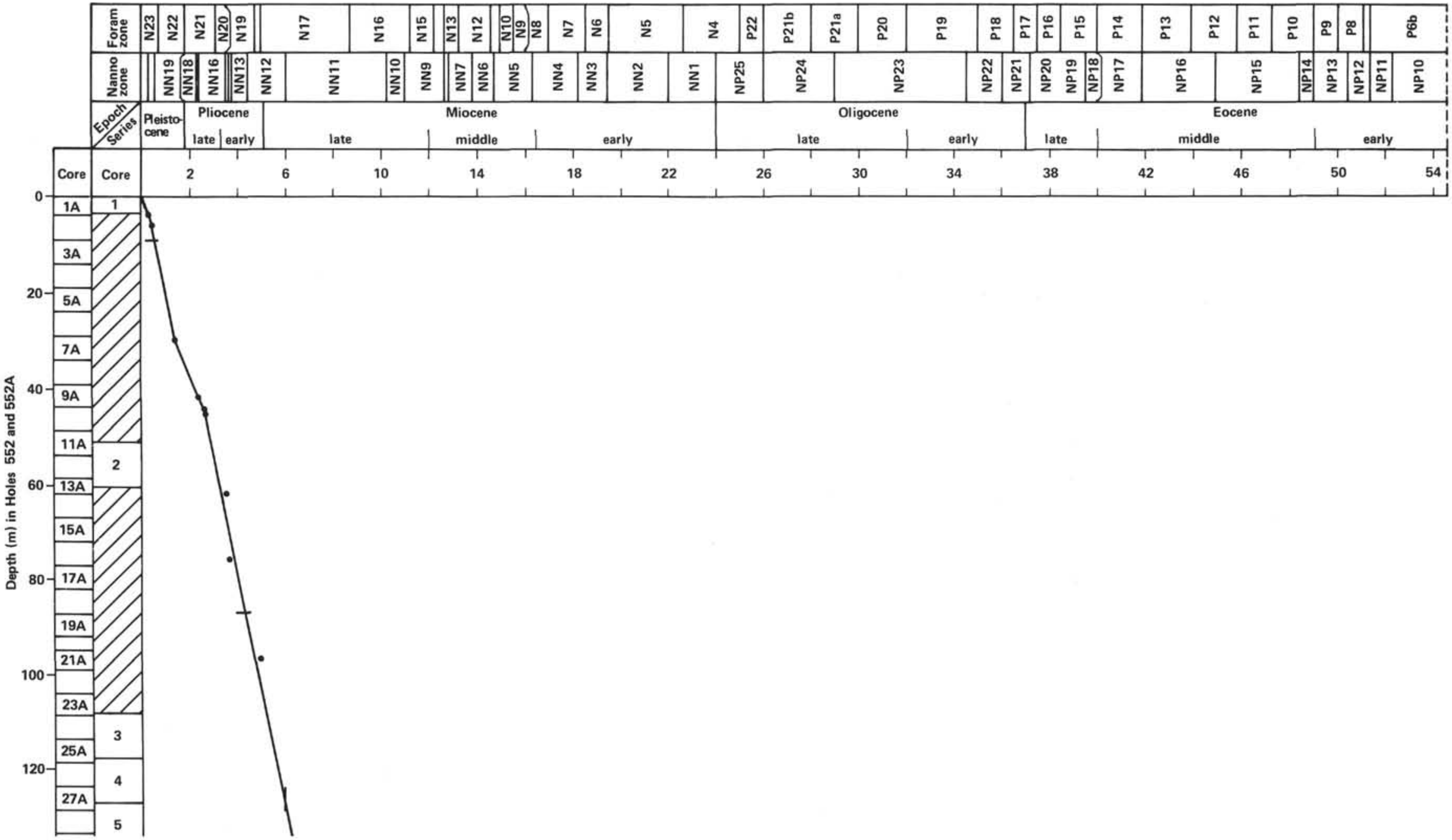
Foram zone
N23
N22
N21
N20
N19
N17
N16
N15
N13
N12
N10
N9
N8
N7
N6
N5
N4
P22
P21b
P21a
P20
P19
P18
P17
P16
P15
P14
P13
P12
P11
P10
P9
P8
P6b
Nanno zone
NN19
NN18
NN16
NN13
NN12
NN11
NN10
NN9
NN7
NN6
NN5
NN4
NN3
NN2
NN1
NP25
NP24
NP23
NP22
NP21
NP20
NP19
NP18
NP17
NP16
NP15
NP14
NP13
NP12
NP11
NP10
Epoch Series
Pleistocene
Pliocene
late
early
Miocene
late
middle
early
Oligocene
late
early
Eocene
late
middle
early
Core
Core
2
6
10
14
18
22
26
30
34
38
42
46
50
54
0
20
40
60
80
100
120
1A
3A
5A
7A
9A
11A
13A
15A
17A
19A
21A
23A
25A
27A
1
2
3
4
5
Depth (m) in Holes 552 and 552A

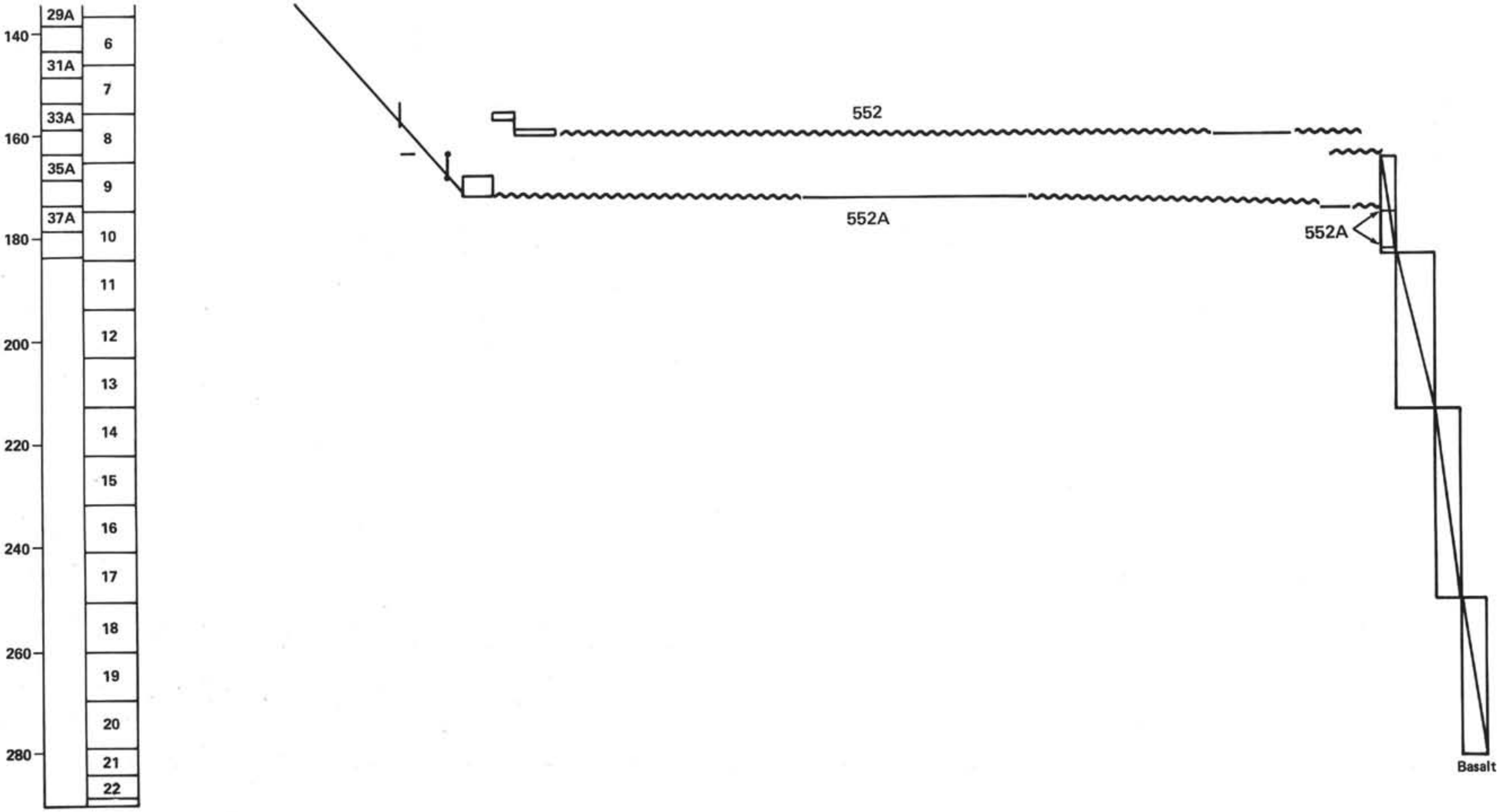

Figure 38. Sedimentation rates, Site 552.

Table 13. Biostratigraphic data used to derive sedimentation rates for Site 552 (Fig. 38).

Paleontologic event	Depth (m)	Million years ago	Sedimentation rate (cm/1000 yr.)
L.O. *S. universus*	4	0.425	0.9
L.O. *P. lacunosa*	6	0.458	
R. curviostris	9	0.125–0.750	2.1
L.O. *C. macintyrei*	30	1.45	
L.O. *D. brouweri*	34	1.88	
L.O. *T. convexa*	39	2.2	
L.O. *D. pentaradiatus, D. surculus*	42	2.4–2.45	1.3
L.O. *D. tamalis*	44	2.65	
L.O. *N. jouseae*	45.5	2.65	
L.O. *R. pseudoumbilica*	62	3.53	
Co-occurrence *A. primus* and *D. asymmetricus*	77	3.8	
C. rugosus	87	<4.6	
L.O. *T. nativa* F.O. *T. oestrupii*	96–97	5.0	2.5
L.O. *D. quinqueramus*	123–128	6.0	
F.O. *T. convexa*	133.5	6.2	
NN10/NN11	153–158	10.3	
NN10	163	10.3–10.9	
L.O. *G. mayeri*	163–165	12.2	0.6
NN7	168–172	12.8–13.9	
NP23/NP24	172.5–173.5	26–34.5	
NP15 *C. gigas* sub-zone	175	46–47	
NP14	176–183	48.4–49.3	4.8
Site 552			
NN6	156–157	13.9–14.7	
NN5/NN6 L.O. *S. heteromorphus*	157–159	14.7	
NN5	159–160	14.7–16.3	
NP16	160.5	39.9–44.9	
NP14 F.O. *D. sublodoensis*	165–184	48.4–49.3	4.8
NP13	184–214	49.3–50.4	
NP13/NP12 L.O. *T. orthostylus*	214.5	50.4	
NP11/NP12 F.O. *D. lodoensis*	251–252.5	51.4	
NP10/NP11 F.O. *T. orthostylus*	282	52.2	

Approximately 15 m of lowermost Miocene and uppermost Oligocene sediments are separated from the middle Miocene by a hiatus of a duration of approximately 7 m.y. Another hiatus spanning some 16 m.y. separates the late Oligocene from the underlying middle Eocene sediments (NP16), which has a thickness of about 5 m. A third hiatus, encompassing Zone NP15, separates the overlying thin beds of Eocene and Oligocene sediments from the underlying sequence of apparently continuous deposition of predominantly early Eocene and late Paleocene sediments. The sequence in Site 553 which comprises Zones NP11 through NP14 is rather condensed, especially if compared to the equivalent sequence in Site 552 where a comparatively good representation of these zones is evident.

The top of the basalt is overlain by sediments, being close to the NP10/NP9 boundary, which is in accord with the magnetostratigraphy of Site 553 (see Krumsiek and Roberts, this volume). A hiatus must be present in view of the subaerial origin of the basalt. The sediment on top of the basalts at Site 555 is likewise close to the NP10/NP9 boundary. The age of the sediments overlying the basalt at Site 552 (Zone NP11) is not easily explained if one assumes a synchronous age of the top of the basalt pile. However, the basalts are submarine and may be a later event. It is noteworthy that the oldest sediments at Site 552 correspond in age with the major early Eocene transgression in this area.

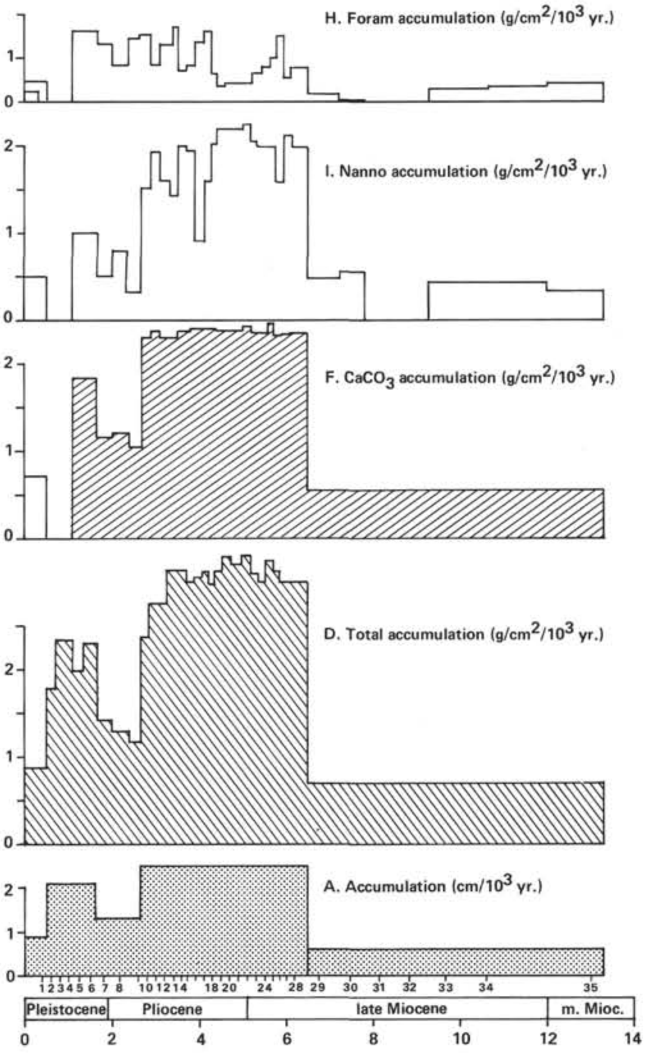

Figure 39. Neogene accumulation rates, Hole 552A.

Sediment Accumulation Rates

Only a few samples were available at this site (Fig. 41; Table 16). Nevertheless, the pattern of sediment accumulation shows many similarities with that at Hole 552A. Accumulation rates were low in the middle and late Miocene and high in the preglacial Pliocene. No samples were taken from the late late Miocene, but it seems likely that contourite deposition proceeded here just as at Hole 552A.

CORRELATION OF SEISMIC REFLECTORS WITH DRILLING RESULTS

Site 552

Seismic reflection data in the vicinity of Sites 552 and 553 consisted principally of a number of multichannel

Table 14. Data for the sediment accumulation rates, Hole 552A (see Fig. 39).

Core	A	B	C	D	E	F	G	H	I	J
1,CC	0.9	1.605	0.93	0.84	80	0.72	15.63	0.23	0.49	0.12
2,CC	2.1	1.536	0.85	1.79						
3,CC	2.1	1.700	1.11	2.34						
4,CC	2.1	1.700	1.10	2.32						
5,CC	2.1	1.623	0.94	1.97	87	1.83	24.25	0.83	1.00	0.14
6,CC	2.1	1.610	1.09	2.30	87	1.83	23.67	0.80	1.03	0.47
7,CC	1.3	1.610	1.09	1.42	89	1.15	32.20	0.67	0.49	0.26
8,CC	1.3	1.654	0.99	1.29	92	1.20	19.33	0.41	0.79	0.09
9,CC	1.3	1.704	1.08	1.17	80	1.04	33.12	0.73	0.31	0.13
10,CC	2.5	1.634	0.95	2.37	91	2.28	18.65	0.76	1.52	0.09
11,CC	2.5	1.700	1.10	2.75	93	2.33	9.65	0.41	1.92	0.42
12,CC	2.5	1.732	1.10	2.75	91	2.28	14.75	0.64	1.64	0.47
13,CC	2.5	1.823	1.25	3.12	91	2.28	18.83	0.86	1.42	0.84
14,CC	2.5	1.823	1.25	3.12	93	2.33	7.71	0.35	1.98	0.79
15,CC	2.5	1.820	1.20	3.0	93	2.33	8.73	0.40	1.93	0.67
16,CC	2.5	1.790	1.22	3.05	95	2.38	15.01	0.67	0.9	0.67
17,CC	2.5	1.810	1.25	3.12	95	2.38	17.72	0.80	1.58	0.74
18,CC	2.5	1.750	1.19	2.99	96	2.40	8.31	0.36	2.04	0.57
19,CC	2.5	1.790	1.25	3.12	94	2.35	3.83	0.17	2.18	0.77
20,CC	2.5	1.850	1.31	3.27	95	2.38	4.66	0.22	2.16	0.89
21,CC	2.5	1.830	1.28	3.2	95	2.38	4.67	0.21	2.17	0.82
22,CC	2.5	1.860	1.32	3.3	97	2.43	4.26	0.20	2.23	0.87
23,CC	2.5	1.820	1.24	3.1	94	2.35	7.09	0.32	2.03	0.75
24,CC	2.5	1.781	1.20	3.0	94	2.35	8.64	0.38	1.97	0.65
25,CC	2.5	1.857	1.30	3.25	99	2.48	10.86	0.50	1.98	0.77
26,CC	2.5	1.820	1.25	3.12	93	2.33	16.69	0.76	1.57	0.79
27,CC	2.5	1.810	1.21	3.0	95	2.38	5.83	0.26	2.12	0.62
28,CC	2.5	1.800	1.21	3.0	94	2.35	8.40	0.38	1.97	0.65
29,CC	0.6	1.750	1.16	0.7	93	0.56	8.45	0.09	0.47	0.14
30,CC	0.6	1.740	1.16	0.7	95	0.57	2.40	0.03	0.54	0.13
33,CC	0.6	1.720	1.15	0.7	95	0.57	13.57	0.14	0.43	0.13
34,CC	0.6	1.710	1.11	0.7	94	0.56	17.44	0.18	0.46	0.14
35,CC	0.6	1.770	1.18	0.71	92	0.55	20.26	0.22	0.33	0.16

seismic lines made by Seismograph Services (U.K.) Ltd. under contract to the Institute of Oceanographic Sciences, U.K. The IPOD 76 numbered lines were acquired using a 2160 in.^{3} air-gun array and 48-channel hydrophone with 50 m between traces. The digitized data were resampled at 4 ms and subjected to true amplitude recovery prior to 24-fold processing using deconvolution before and after stack, and time varied filtering. Line IPOD 76-8 was further processed by diffraction stack migration. Lines numbered IOS-1, etc. were shot in 1981 using Maxipulse and a 60-channel hydrophone and have not been fully processed. An additional IFP-CEPM line RH115 crosses the vicinity of the sites (see Fig. 42). A few NAVOCEANO and LDGO single-channel seismic lines were available in the area. In addition, the single-channel seismic profiles obtained during the site approach by *Glomar Challenger* using two air guns (5 and 120 in^3) and a single-channel streamer towed at 300 m were also available.

Hole 552A was drilled near SP 15440 on IOS multichannel seismic line IPOD 76-8 and close to its crossing with line IPOD 76-4 (Fig. 43).

Seismic Stratigraphy

Hole 552A was located in the Edoras Basin near Sites 403 and 404 previously drilled during Leg 48 (Montadert, Roberts et al., 1979). Two principal reflectors called 1 and 2 (Fig. 43) divide the seismic sequences within the basin as follows:

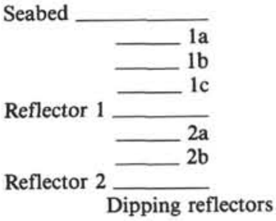

Reflector 1 defines the base of a comparatively transparent interval characterized NW of SP 15460 by weak laterally impersistent reflectors. Evidence of a lateral change in this interval to the southeast of SP 15475 is shown by the greater transparency of the interval and the presence of mud waves in the seabed. Southeast of SP 15460, Reflector 1a defines the base of the transparent unit and downlaps northwestward onto Reflector 1. Two reflectors, 1b and 1c, are present in the interval between Reflectors 1 and 2. Reflector 1a varies in strength and is associated with small diffractions that are not due to faults (see Fig. 43) but may arise from small-scale topography in the horizon causing the reflection. Underlying Reflector 1b is laterally impersistent but may be truncated by Reflector 1a although it is conformable with Reflector 1c. Reflector 1c is more persistent and downlaps westward against Reflector 1. It is also truncated by Reflector 1a.

The interval between Reflector 1 and 2 is thickest west of Hole 552A. In this region the 1–2 interval includes several reflectors (2a and 2b) that arise from the

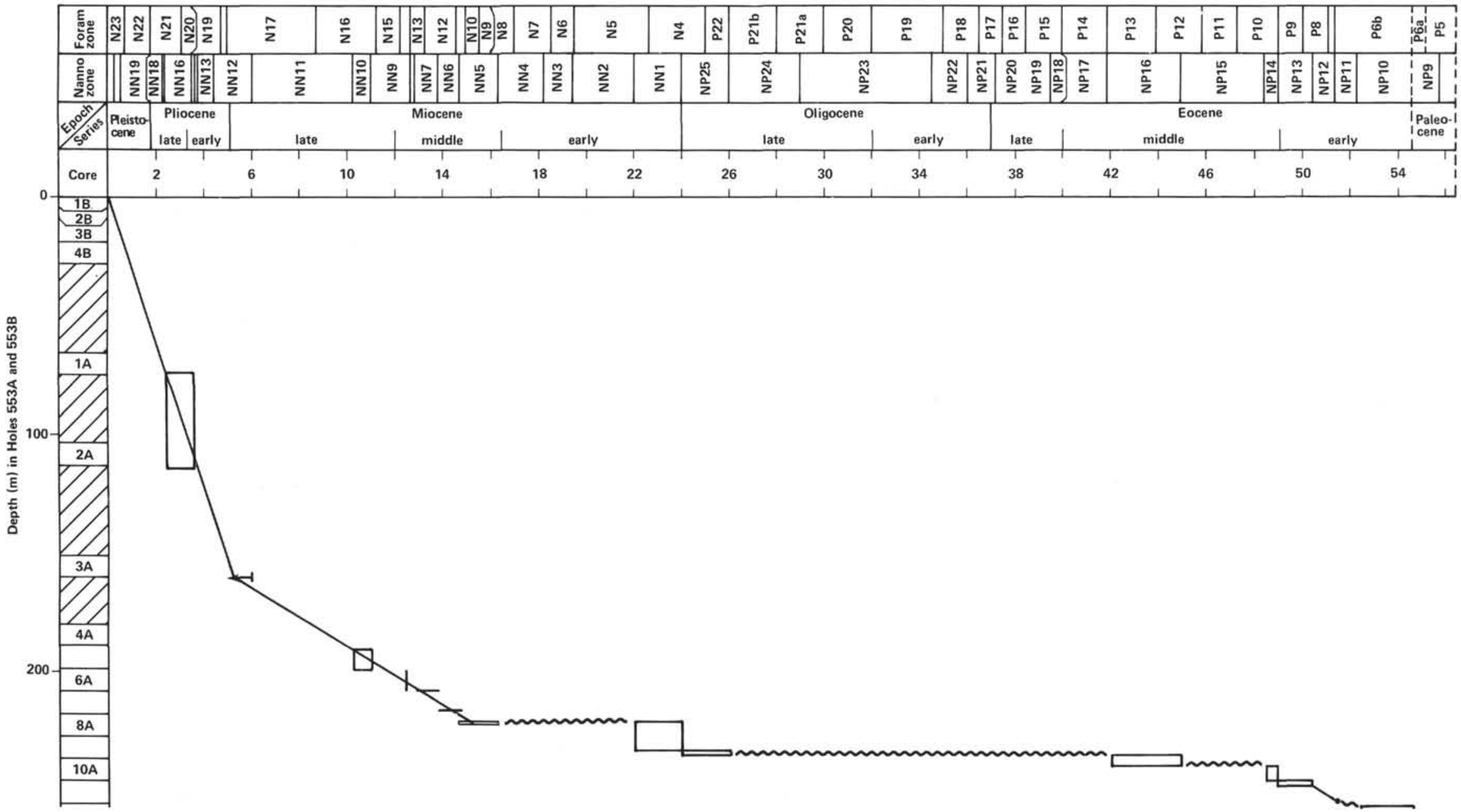
Foram zone
N23
N22
N21
N20
N19
N17
N16
N15
N13
N12
N10
N9
N8
N7
N6
N5
N4
P22
P21b
P21a
P20
P19
P18
P17
P16
P15
P14
P13
P12
P11
P10
P9
P8
P6b
P6a
P5
Nanno zone
NN19
NN18
NN16
NN13
NN12
NN11
NN10
NN9
NN7
NN6
NN5
NN4
NN3
NN2
NN1
NP25
NP24
NP23
NP22
NP21
NP20
NP19
NP18
NP17
NP16
NP15
NP14
NP13
NP12
NP11
NP10
NP9
Epoch
Series
Pleisto-cene
Pliocene
late
early
Miocene
late
middle
early
Oligocene
late
early
Eocene
late
middle
early
Paleo-cene
Core
2
6
10
14
18
22
26
30
34
38
42
46
50
54
0
100
200
Depth (m) in Holes 553A and 553B
1B
2B
3B
4B
1A
2A
3A
4A
6A
8A
10A

Figure 40. Sedimentation rates, Site 553.

Table 15. Biostratigraphic data used to derive sedimentation rates for Site 553 (Fig. 40).

Paleontologic event	Depth (m)	Million years ago	Sedimentation rate (cm/1000 yr.)
L.O. *P. lacunosa*	(Hole 553B) 13	0.458	
NN16	(Hole 553A) 75–113	2.4–3.4	3.0
NN12	160.5	<6	
NN10	189–198.5	10.3–10.9	
L.O. *G. mayeri*	198.5–208	12.2	
NN7	208	12.8–13.8	0.62
NN6	217.5	13.9–14.7	
>N13 *G. druryi* present	217.5	>12.6	
NN5	221.5–222	14.7–16.3	
NN1	222–231.5	22–24	
NP25 L.O. *D. bisectus*, common *R. gelida*	231.5–235	24–26	
NP16	235–240	41.9–44.9	0.8
NP14 (F.O. *D. sublodoensis* in 10CC)	240.5–246.0	48.4–49.3	
NP13	246–248	49.3–50.4	
NP12/13 L.O. *T. orthostylus*	248–248.5	50.4	
F.O. *D. lodoensis*	255.5	51.4	1.5
F.O. *T. orthostylus*	255.5–256	52.2	
NP10	379	52.2–54.6	5.5
NP9	493–502.5	54.6–56.6	

tuffs previously drilled at Sites 403 and 404. This interval onlaps and thins southeastward against Reflector 2 from 0.2 to 0.08 m/s at SP 15500. Site 552 was chosen to take advantage of this decrease in thickness to ensure penetration into the upper, flat-lying part of the dipping reflector sequence, the prime objective of the site, at shallow depth. In the vicinity of the site, there is an abrupt decrease in the thickness of the 1–2 interval coupled with a marked change in the character of Reflector 1 so that southeast of SP 14560 Reflectors 1 and 2 appear to have merged to form a double reflector (cf. SP 15500 and SP 15450).

Correlation of Seismic Reflectors

For Site 552, correlation between the seismic reflectors and the cored section has been made by comparison at the multichannel interval velocities and depths with velocity and density data measured on the cores as described in the Physical Properties section.

In Figure 44, a plot of acoustic impedance versus depth is given, showing possible reflectors.

In Figure 45, two-way travel time is correlated against major changes in lithology observed downhole. Reflector 1a probably arises from the cherts lying just below the hard ground at the Eocene–Oligocene contact. Reflector 1a lies in a zone of poor recovery but where a significant drop in acoustic impedance was recorded (see Fig. 44). Well-cemented volcaniclastics recovered in this zone may cause Reflector 1b. A second increase in acoustic impedance near 250 m is followed by a sharp drop and corresponds to the boundary between volcaniclastics above and calcareous sediments below. Reflector 1c is interpreted as arising from this lithological break. The slope of the time-depth curve from Reflector 1a to the basalt gives a mean velocity of $2.5\ \mathrm{km/s^{-1}}$, in good agreement with shipboard measurements of velocities (see Physical Properties section).

The correlation between reflectors, predicted depth from multichannel seismic velocities, lithology, and age, appear in Table 17. Depths predicted from velocity analyses, assuming that Hole 552A is midway between V_3 and V_4, appear in Tables 18A and 18B.

Site 553

Site 553 was located near SP 15590 on Line IPOD 76-8 and close to SP 13600 on the intersecting profile IPOD 76-5 (Fig. 46).

Seismic Stratigraphy

The multichannel profiles across the site show several reflectors of contrasting acoustic character discussed here in order of increasing depth. The nomenclature used for the reflectors at Site 552 has been followed again here. The principal reflectors are shown in Table 19.

The seismic stratigraphic relationship and character of these reflectors and the intervening seismic units can be summarized as follows:

Seabed Reflector 1a

The seismic interval is acoustically transparent in comparison to those below. On the dip Profile IPOD 76-8, laterally impersistent reflectors within the unit downlap westward onto Reflector 1a. On the strike Profile IPOD 76-5, however, these reflectors are essentially conformable with Reflector 1a. Within the sequence, cross-cutting reflectors hint at minor unconformities. The sequence is less transparent than its lateral equivalent at Site 552. The interval thins southeastward towards the intervening channel between Holes 553A and 552 after which the interval becomes more transparent. Northwestward thinning of the interval is also evident. The seismic sequence exhibits many of the characteristics of sediment drifts and probably represents a less well-developed equivalent of the Hatton Drift known in the

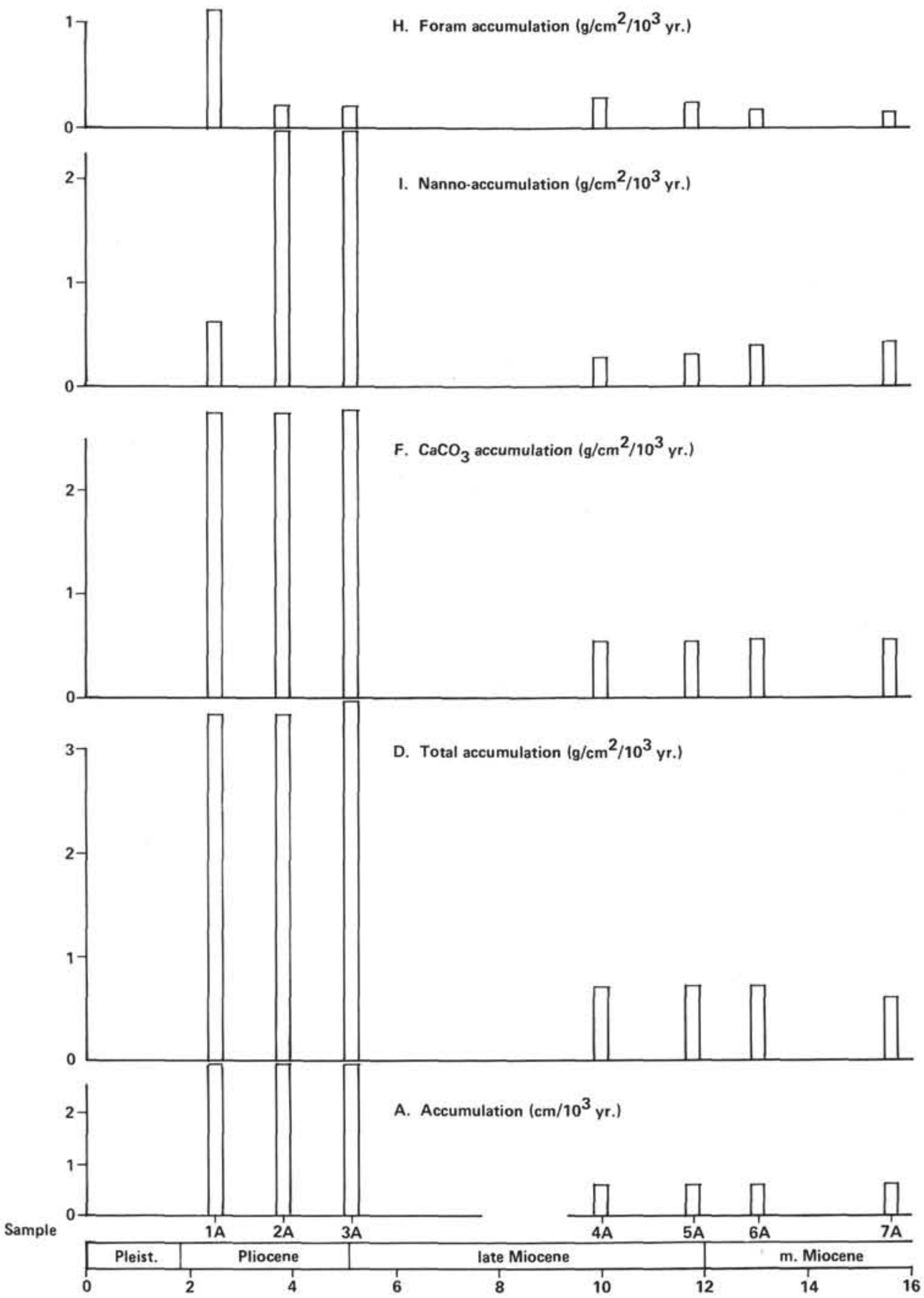

Figure 41. Neogene accumulation rates, Site 553.

Table 16. Data for the sediment accumulation rates (Fig. 41).

Core	A	B	C	D	E	F	G	H	I	J
Hole 553										
1,CC	3.0	1.743	1.11	3.33	91	2.73	11.9	0.62	2.11	0.60
Hole 553A										
1,CC	3.0	1.743	1.11	3.33	91	2.73	21.2	1.11	0.62	0.60
2,CC	3.0	1.741	1.13	3.39	91	2.73	4.0	0.20	2.53	0.66
3,CC	3.0	1.795	1.18	3.54	92	2.76	3.4	0.18	2.58	0.78
4,CC	0.62	1.757	1.14	0.71	91	0.56	26.2	0.28	0.28	0.18
5,CC	0.62	1.772	1.18	0.73	91	0.56	21.7	0.24	0.32	0.17
6,CC	0.62	1.742	1.14	0.71	90	0.56	16.0	0.17	0.39	0.15
7,CC	0.62	1.689	1.00	0.62	91	0.56	12.5	0.13	0.43	0.06

same position on the slope further north (Ruddiman, 1972; Roberts et al., 1979).

Reflector 1a

Underlying Reflector 1a downlaps toward Reflector 1 in the vicinity of the site thinning the 1a–1 interval from 0.12 s at Hole 552 to 0.03 s at Site 553 and cutting out Reflectors 1b and 1c observed at the latter site. Northwest of Site 553, the 1a–1 interval thickens and there are suggestions of clinoforms (progradation?) within the thicker 1a–1 interval. The intersecting Profile IPOD 76-5 (Fig. 47) shows that the interval pinches out to the

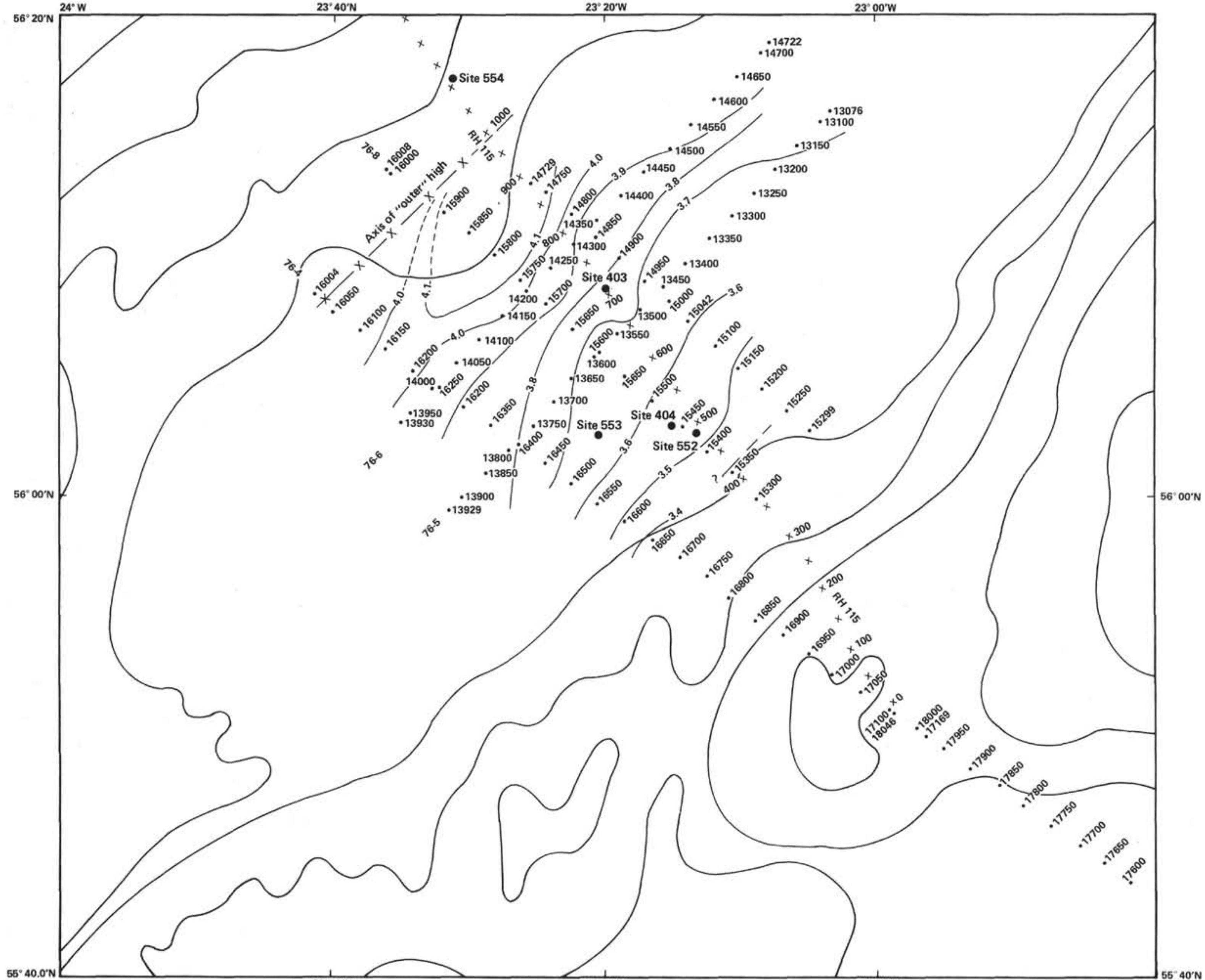

Figure 42. Location of seismic profiles around Sites 552 and 553. (Contours labelled 3.6 s are in two-way time on Reflector 2.)

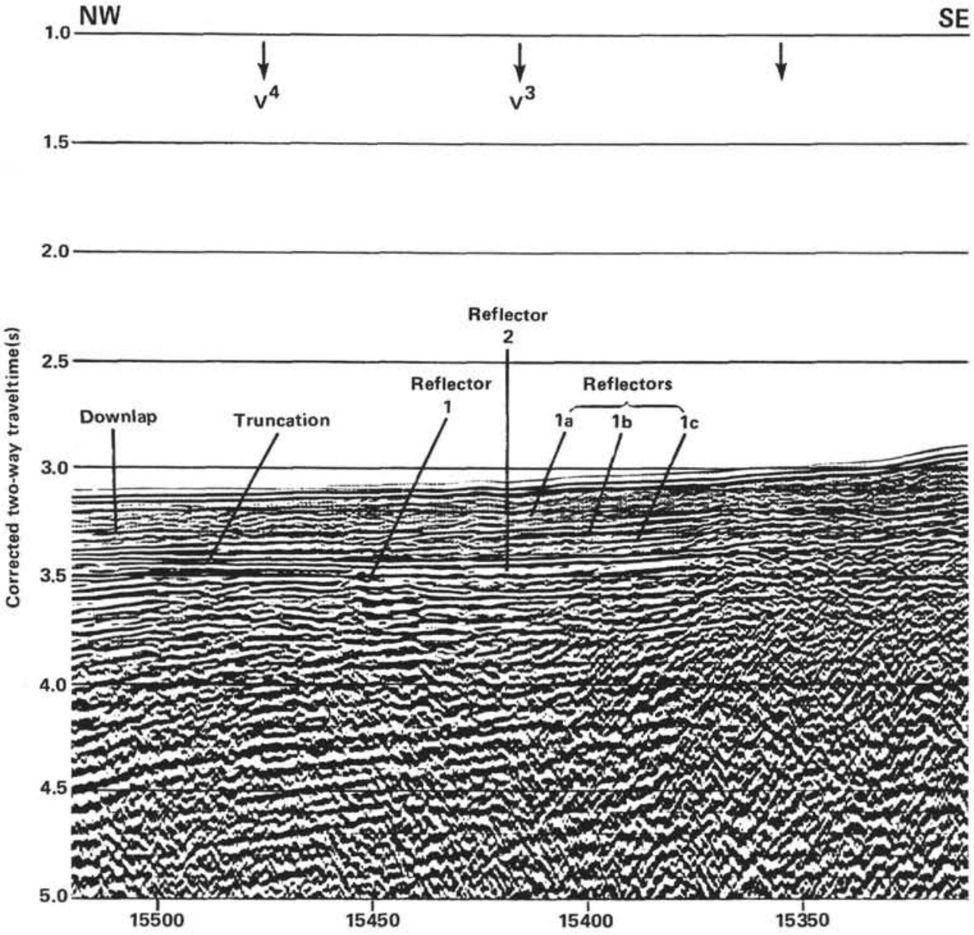

Figure 43. Multichannel seismic profile IPOD 76-8 through Site 552.

northeast where Reflector 1 may have been eroded; to the southwest, the 1a–1 interval thickens.

Reflector 1

Reflector 1 is broadly arched in profile, increasing in relief to a maximum of about 0.03 s between SP 15500 and 15600: the crest of the arch lies just west of Hole 553A. From the crest Reflector 1 dips gently westward. The intersecting Profile 76-5 also shows that Reflector 1 is gently arched and dips very gently to the northwest and more appreciably to the southwest. Erosion of Reflector 1 is evident near SP 13550 on IPOD 76-5.

Reflector 1–2

This interval thins southeastward and is overlapped by Reflector 1a. Thickening of the interval is clear beneath the culmination of Reflector 1. Northwestward, Reflector 2a becomes impersistent. The intersecting profile suggests southwestward thickening of the interval.

Reflector 2a

Reflector 2a becomes laterally impersistent toward the northwest. The intersecting profile shows a very convincing channel-like feature in the reflector just beneath the culmination in Reflector 1. Toward the southwest, Reflector 2a downlaps toward Reflector 2b.

Interval 2a–2b

On Profile 76-8, the interval thickens southwestward. An increase in thickness of the interval beneath the culmination of Reflector 1 suggests that the latter is depositional in origin. Downlap of the overlying Reflector 2A against the reflectors within the 2a–2b interval suggests that the interval may comprise a depositional (progradational?) lobe.

Reflector 2b

Reflector 2b onlaps Reflector 2 near SP15500 and is itself overlapped in Profile 76-8 by Reflector 1 and perhaps Reflector 2a.

Internal Reflector 2b–2

The interval 2b–2 exhibits a small increase in thickening beneath Site 553 as part of an overall thickening to the northwest. On intersecting Profile 76-5, reflectors within the interval downlap onto Reflector 2 and resemble clinoforms. Channels are also present.

Reflector 2 and the Dipping Reflectors

Reflector 2 is an extremely high-amplitude reflector that can be correlated throughout the "basin" and is the seismic event defining the top of the dipping reflectors

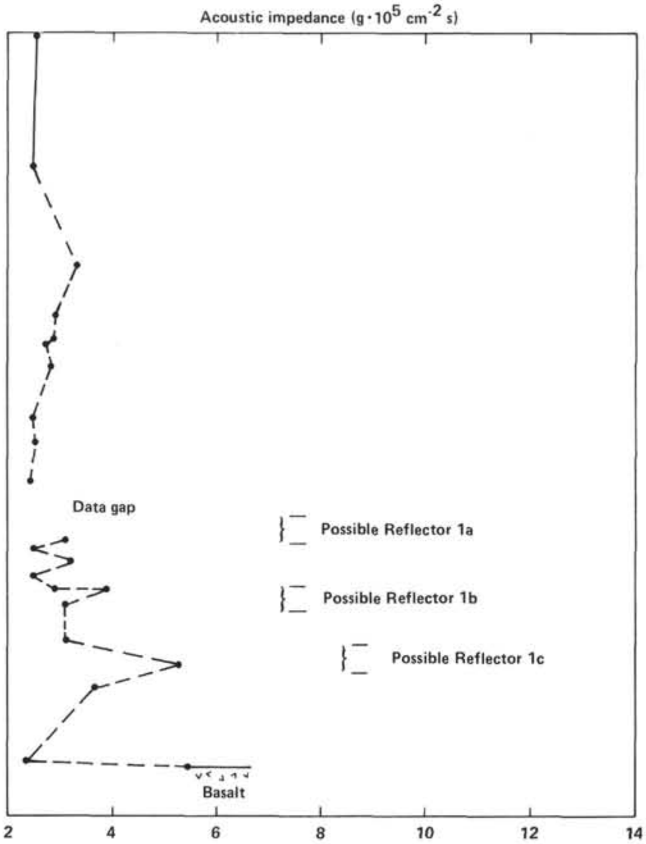

Figure 44. Variation in acoustic impedance downhole Site 552.

below. The reflector shows distinct irregularities (SP 15600-SP 15625) that presumably arise from the morphology of the reflecting interface. Hints that the single reflector may be a more complex event are given by divergent events appearing towards the base of the main reflection. Below Reflector 2, there is a complete change in reflection character. The section is characterized by many small low-amplitude reflectors showing suggestions of faulting. These dip northwestward as Profile 76-8 but dip more gently to the northeast on Profile 76-5. The latter profile also shows clearly that the dipping events are laterally impersistent and cannot be traced with confidence beyond an average of 10–15 km.

Correlation of Seismic Reflectors

Correlation of the seismic reflectors has been done using the interval transit time data provided by the sonic log.

The interval transit data requires a small correction since sonic logging did not begin until the tool left the drill stem at 126 m subsea. Assuming a mean V_p of 1.5 km/s^{-1}, this missing section corresponds to an interval of 0.08 s.

The data below and Figure 47 summarize the reflector–lithologic log correlation.

Reflector 1a: probably arises from the contrast in density and velocity between Oligocene nannofossil–foraminifer chalks and middle Eocene biosiliceous chalks and tuffs (see Core 10).

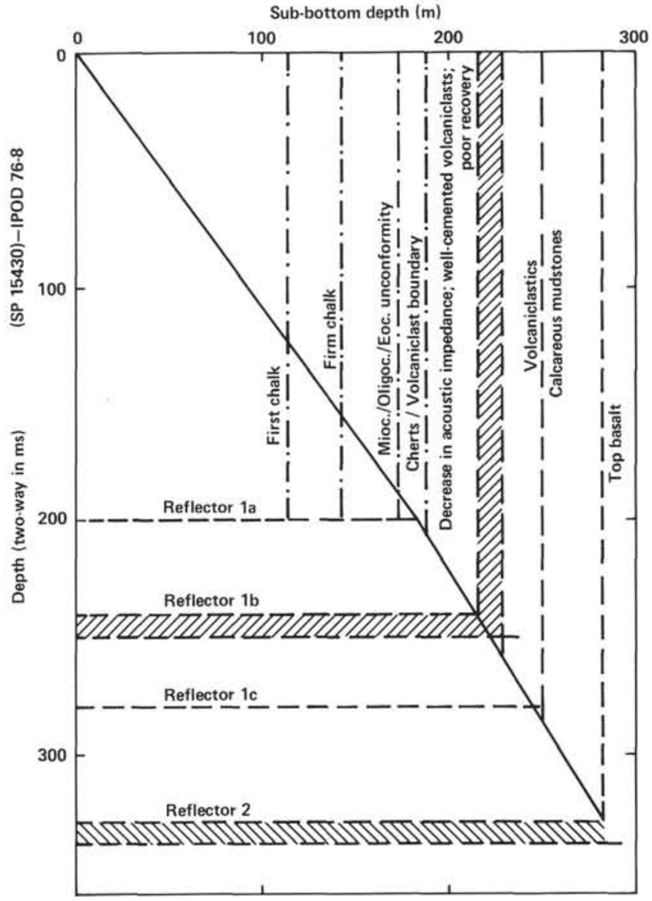

Figure 45. Correlation of seismic reflectors, Site 552.

Reflector 1: coincides with the boundary between tuffs interbedded with zeolite biosiliceous nannofossil–foraminifer chalk above (Subunit IVb) and tuffs interbedded with sandstones and mudstones below (Subunit IVc).

Reflector 2b: appears to occur just above the boundary between Subunits IVc and IVd in a zone of poor recovery. It may mark the transition from tuffaceous mudstones above to micaceous sandstones below of which little was recovered in cores.

Reflector 2: arises from the velocity and density contrast between tuffaceous mudstones and the underlying basalt. The base of Reflector 2 may correspond to the change from the more massive flow basalt (lithostratigraphic Subunit Vb) to the thinner and more extensively fractured flows of Subunit Vc below.

The Dipping Reflectors

The log data obtained at Hole 553A show that the uppermost part of the dipping reflector sequence was penetrated to a depth of about 71.5 (2950.0–3021.5 m T.D.), indicating that the main objective of the hole was achieved despite loss of the drill bit, although deeper penetration would clearly have been desirable.

The strong Reflector 2 undoubtedly results from the sequence of basalts comprising basalt Subunits Va and Vb. The base of the reflection probably arises from the acoustic impedance contrast between the massive flows of Subunit Vb and the thinner flows below. Flows in

Table 17. Correlation between reflectors, predicted depth, lithology, and age.

Reflection	Two-way time	Predicted sub-bottom depth (m)	Observed depth (m)	Lithology
Seabed	0 (3.08)			
Reflector 1a	0.20 (3.28)	184	185	Miocene and Oligocene chalks Eocene cherts
Reflector 1b	0.25 (3.33)	207–220	210–225	Well-cemented volcaniclastics—poor recovery
Reflector 1c	0.28 (3.36)	252	250	Volcaniclastics Calcareous mudstones
Reflector 2	0.34 (3.42)	289	285	Basalt

Table 18A. Depths of the principal reflectors from nearby velocity analyses.

		V_4 (SP. 15475)				V_3 (SP.15417)		
Reflection	Two-way time	Depth (m)	Interval thickness (m)	Sub-bottom depth (m)	Two-way time	Depth (m)	Interval thickness (m)	Sub-bottom depth (m)
Seabed	3.1	2294	—	0	3.060	2264	—	0
	(0.05)			37	(0.07)		52	
?	3.150	2331	37		3.130	2316		52
	(0.20)			201	(0.17)		126	178
Reflector 1a	3.350	2495	164		3.300	2442		
	(0.08)			261	(0.13)		139	
Reflector 1	3.430	2555	60		3.430	2581		317
	(0.12)			380				
Reflector 2	3.550	2674	119 ←					

Reflectors 1 and 2 merge SP 15467

Table 18B. Depths predicted from velocity analyses, on assumption that Hole 552A is midway between V_3 and V_4.

	Depth (m)	Interval	Sub-bottom depth (m)
Seabed	2279	—	0
		44	
Velocity analysis only	2323		44
Reflector 1a	2463		184
		150	
Reflector 1/2	2568		289

Table 19. Principal reflectors, Site 553.

	Two-way time		
	Total (s)	Sub-bottom (s)	
Reflector 1a	3.39	0.29	
Reflector 1	3.43	0.32	
Reflector 2a	3.48	0.38	
Reflector 2b	3.52	0.42	
Reflector 2	3.64	0.515	} Dipping reflector sequence
Base reflector 2	3.67	0.57	
Reflector 3	3.82	0.71	

Subunit Vb are characterized by high sonic velocities and densities, but interbeds of sediments are tentatively suggested by low velocities, low densities, and high porosities and particularly by the higher gamma response. Similar but sharper variations in these parameters are present in Subunit Vc. The impedance contrast between these interbeds (tuffs, volcaniclastics, paleosols?) and the basalts may cause the dipping reflectors. However, large contrasts in acoustic impedance occur between the scoriaceous (weathered?) tops (low velocity 2.5–3.5 km/s and wet-bulk density (ca. 2.28 (g/cm^3) (acoustic impedance 6.0–8.0 g 10^5 cm^{2}s) and the base of the succeeding

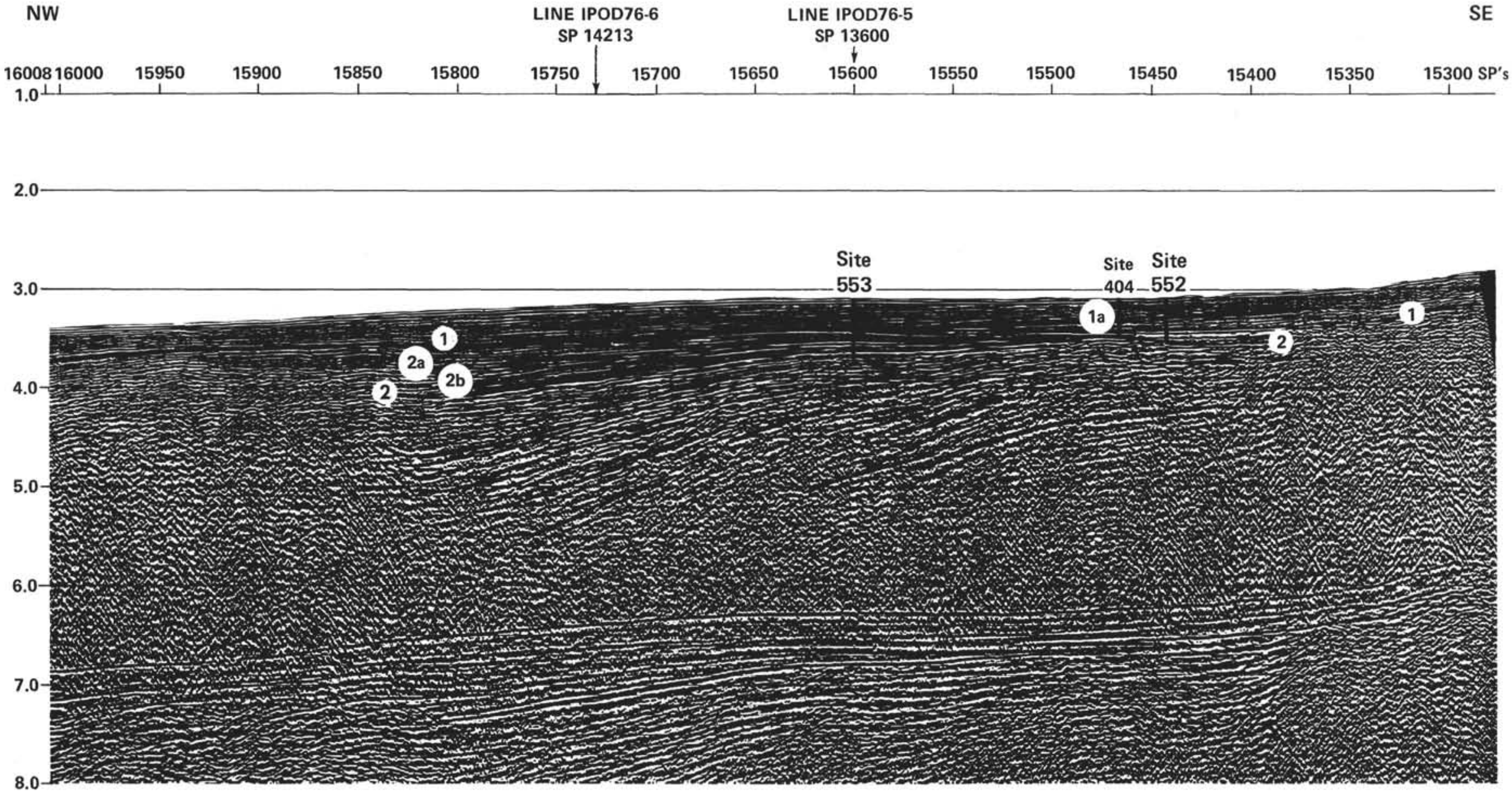

Figure 46. Intersecting multichannel seismic Profile IPOD 76-5 through Site 553.

flow (high velocity 4–6 km/s and high density 2.6 g/cm^3). The contrasts in these values at 6.0 to 8.0 to the 13–16 g 10^5 cm^{2}s of the massive basalt may be sufficient to cause the reflections. However, at the wavelengths of the seismic source in use (= 170 m), it seems probable that only a few units (thickest and greatest impedance contrast?) are being sensed by the seismic technique. The presence of interbedded sediments (e.g., tuffs, volcaniclastics, paleosols, continental sediments?) indicated by the log response would enhance the impedance contrast further, and this possibility cannot be excluded from the data.

In this initial report of the site, it would be premature to discuss the cause of the reflectors in detail without recourse to the necessary synthetic seismograms and models of the seismic-reflection response of the effects of lava flows or lava flows interbedded with sediments.

SUMMARY AND CONCLUSIONS

Sites 552 and 553

Sites 552 and 553 were drilled on the southwest margin of the Rockall Plateau in 2301 and 2329 m, respectively. Hole 552 bottomed in basalt at 282.7 m but was then aborted by bad weather. Hole 552A was hydraulically piston cored to a depth of 183.5 m. Hole 553 was a pilot hole for re-entry Hole 553A where 181.5 m of basalt were drilled above total depth before the hole was aborted by bit loss. Hole 553B was an attempt to again HPC the Pliocene–Pleistocene section and penetrated to 28.5 m before failure of the HPC.

The west margin of the Rockall Plateau is thought to have formed by rifting and spreading beginning at about Anomaly 24B time. Unlike other rifted margins such as the Bay of Biscay (DeCharpal et al., 1978) the classical pattern of tilted and rotated fault blocks is absent. By contrast, the west Rockall margin consists of three structural units consisting of Zone IV, the shallow Edoras and Hatton banks; Zone III, characterized by a prominent series of oceanward dipping reflectors; and Zone II, an outer high (see Fig. 6). The latter varies considerably in relief but the feature trends subparallel to and is partly overlapped by magnetic Anomaly 24B, the oldest anomaly recorded in the adjacent ocean crust.

Sites 552 and 553 were drilled to penetrate the oceanward dipping reflectors. Closely comparable reflectors are now known to occur widely beneath many passive margins (in the Norwegian Sea, off Antarctica and southwest Africa; Hinz, 1982; Roberts et al., this volume) but their origin has not been understood. One hypothesis is that they comprise a sequence of lavas and pyroclastics interbedded with sediments respectively extruded and deposited contemporaneously with rifting (Roberts et al., 1979). Another hypothesis (Talwani et al., 1981; Mutter et al., 1982) considers that the reflectors comprise a sequence of subaerial lava flows formed by subaerial seafloor spreading in a manner akin to Iceland.

In the instance of west Rockall, the presence of a thin Neogene section made the sites ideally suited to penetrate the dipping reflectors at shallow depth.

Basaltic Lava Flows

Basaltic lava flows were recovered in Holes 552 and 553A from (Site 552) and below (Hole 553A) the level of Reflector 2 corresponding to the top of the dipping reflector sequence.

At Site 552, only 7.95 m of deeply altered, reversely magnetized basalt overlain by reddened marine sediments was cored before we abandoned the site. A submarine origin is thought most likely. The basalt is younger than the basalts at Hole 553A and lies in the lower NP11 interval.

At Hole 553A, 181.5 m of basalt were drilled and cored to total depth at 682.5 m. Thirty-four lava flows were tentatively identified from the logs, of which 27 were recognized in the cores. Typical flow units consist of a weathered scoriaceous agglomeratic top passing gradationally downward into vesicular basalt, massive foliated basalt, and then the highly vesiculated base of the flow in which vertical streaming of the vesicles is common above the basal chilled margin. Trachytic and glomerophyric textures occur throughout. Petrographical study shows the basalts to be essentially uniform in composition and of tholeiitic type.

Three basalt subunits were identified from the physical properties data, downhole logs, and paleomagnetic measurements. The top of lowermost Subunit Vc is tentatively identified as the top of the sequence of dipping reflectors. The subunit is characterized by its higher gamma response compared to the overlying units and by an increase in both susceptibility and intensity of magnetization with depths. Within the unit, the unrecovered intervals between the flows are characterized by higher gamma response and porosity, and by a lower sonic velocity and density compared to the flows that may indicate sediment interbeds of unknown origin or paleosols. Flows within the subunit exhibit the typical structure discussed above but in addition are thinner and characterized by more slickensided fracturing than overlying Subunit Vb.

Subunit Vb is characterized by lower gamma response, low susceptibilities, and higher intensities of magnetization. Five lava flows were identified from the logs of which four were recovered. Individual flows are thicker than those in Units Vc and Va and the lower gamma response suggests that sedimentary interbeds are sparse. A deeply reddened vitric tuff (hyaloclastite?) is present in Core 45 at the top of the unit (Fig. 21).

Subunit Va, comprising the top of the basalt sequence, contains 12 flow units. Wider zones of increased gamma and porosity response as well as decreasing density and sonic velocity may indicate interbeds of sediment. Two small pebbles of ferriceladonite-bearing chert from Core 40 are probably of hydrothermal origin (see also below).

Paleomagnetic measurements show that the basalts are all reversely magnetized. Susceptibilities seem to be lower than values obtained on the Reykjanes Ridge during Leg 49 (Leg 81: 1.03×10^{-4} G/Oe; Leg 49: 1.1×10^{-3} G/Oe) but a correction needs to be made for sample volume. Five cyclical variations in inclination possi-

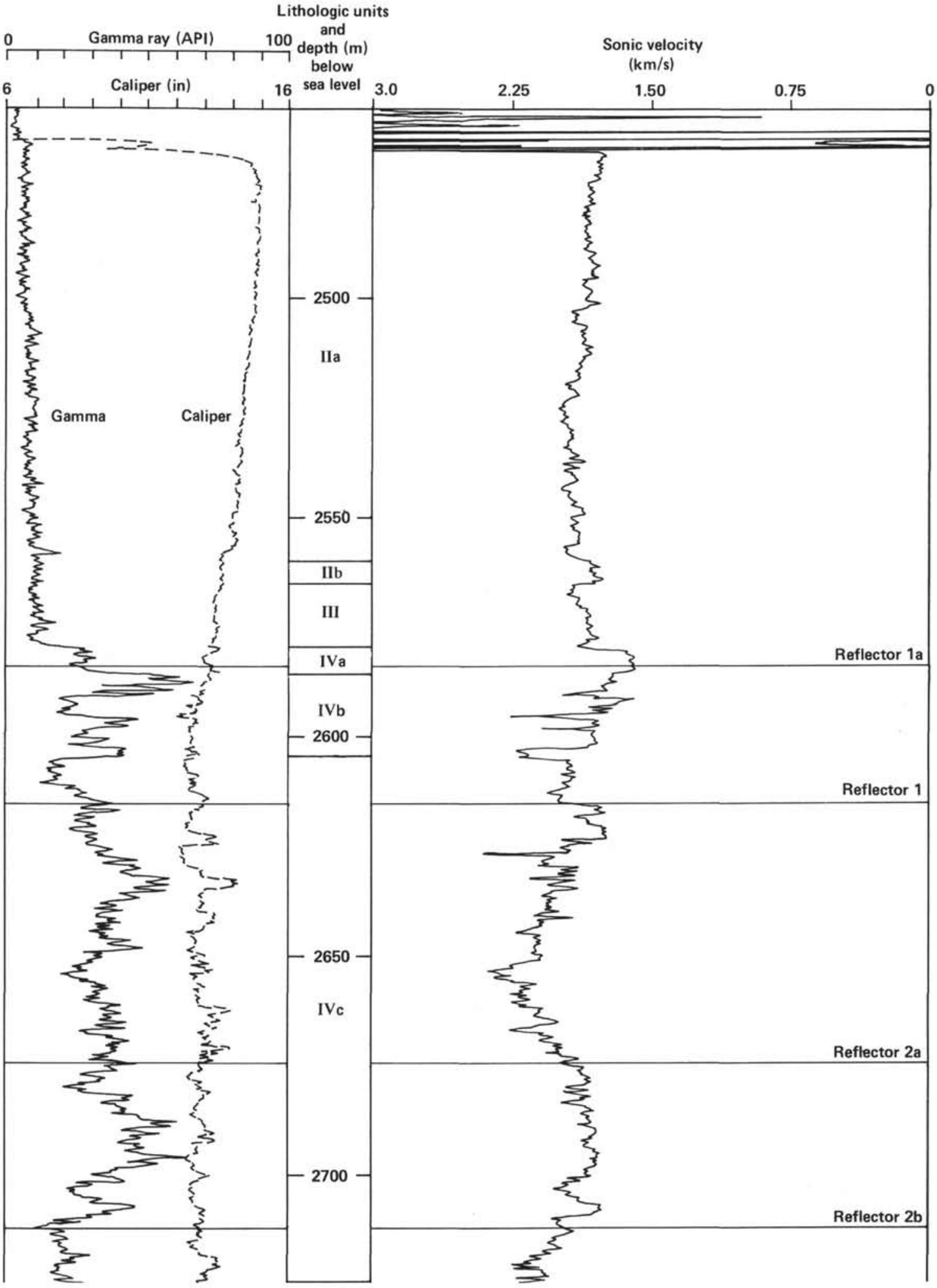

Figure 47. Correlation of reflectors with sonic-gamma caliper log and principal lithologic units, Site 553.

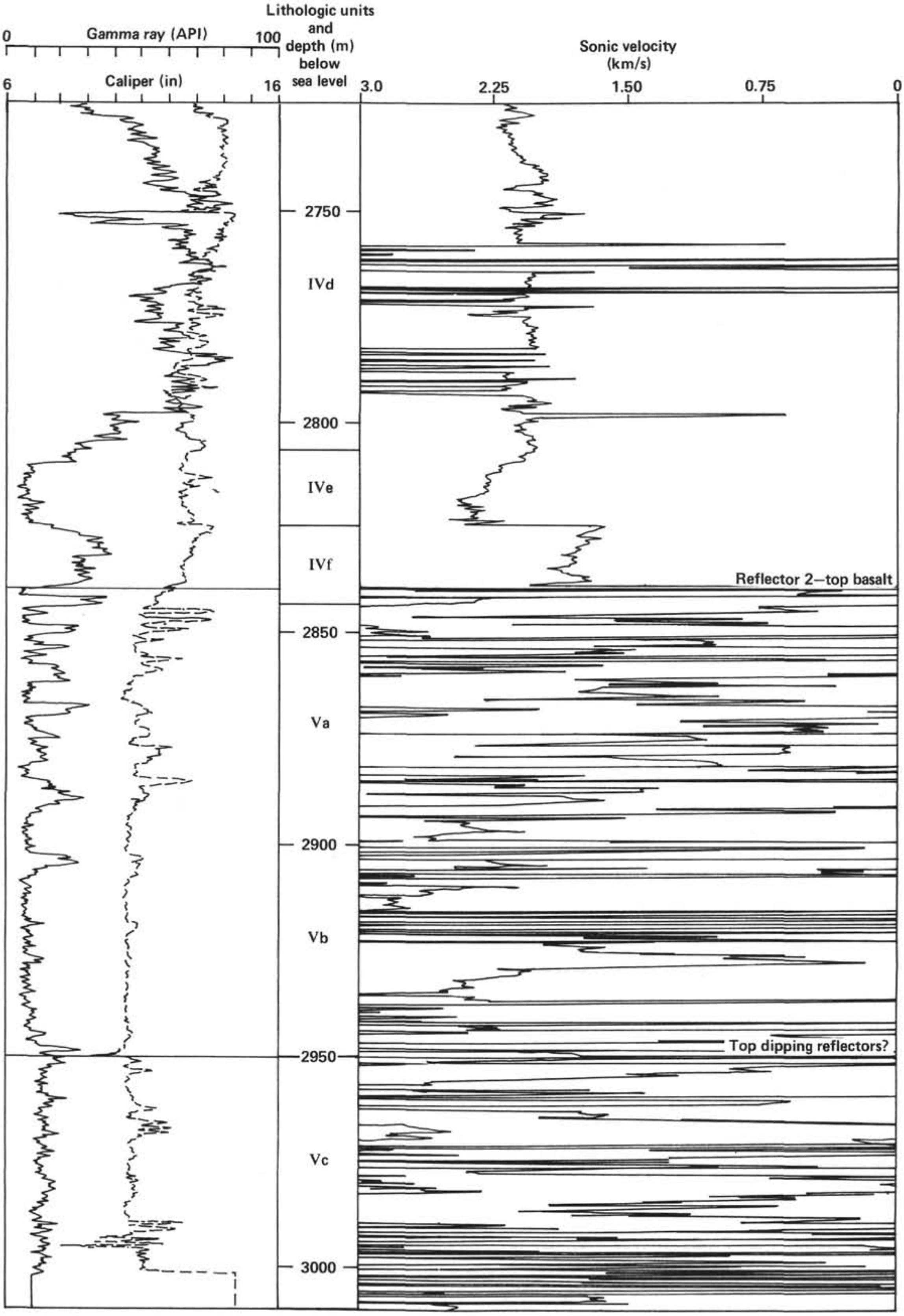

Figure 47. (Continued).

bly resulting from secular variation characterize the flows. Assuming a secular variation period of about 2800 yr. (Stuiver, 1978), the frequency of eruption can be found. Thus, the flows in Subunits Vc, Vb, and the lower part of Unit Va were produced in about 10,000 yr. (142 m thickness) and the remaining part of the basalt flows were extruded in about 1400 yr. The upward increase in number and thickness of flows per secular variation cycle may reflect accelerated extrusion during the terminal phases of volcanic activity.

Precise determination of the age of the basalts must await geochronologic studies onshore but an age older than 52.3 m.y for the top of the basalt can be tentatively inferred from the paleomagnetic stratigraphy of the overlying late Paleocene–early Eocene section (Hailwood et al., 1979).

Late Paleocene–Early Eocene

Sediments of early Eocene age or possibly latest Paleocene were found overlying the basalt at Site 553 and early Eocene at Site 552. At Site 552, only 108.5 m of early and middle Eocene, representing Zones NP11–16, was present in contrast to 264.52 m of early and middle Eocene sediments in Hole 553A (NP10–16).

Correlation on the basis of biostratigraphy and heavy mineral analyses shows that the whole of Unit IV of Site 552 is equivalent to Unit IVb of Site 553. Thus between Site 552 and Hole 553A, Unit IVb thins from 108.5 m to 37.2 m in Hole 553A. In contrast, the underlying 227.85 m of section at Site 553 is absent at Site 552 but possibly underlies the basalt cored at total depth. For convenient review of the early Eocene at these sites, the lowermost subunits (IVc through IVf) of the early Eocene at Hole 553A are described first.

In Hole 553A, the sediments (Subunit IVf) immediately overlying the basalt are close to the NP10/NP9 boundary and reversely magnetized. They were thus deposited during the reversed polarity interval between Anomaly 24–25. Three short intervals of normal polarity, identified in Cores 19, 25–26, and 35–37 in this otherwise reversely magnetized interval, may correspond to hitherto unreported short normal polarity intervals in the 24–25 reversed polarity interval. If confirmed by further work, this indicates a tentative age of the base of the early Eocene section of younger than 54–56 m.y. (Hailwood et al., 1979, time scale) and a minimum sedimentation rate of approximately 10.6 cm/1000 yr.

The earliest early Eocene sediments of Unit IVf are sandy tuffaceous mudstones, possibly representing a basal transgressive deposit, and are succeeded by tuffaceous mudstones deposited in inner shelf depths that changed to a brackish marsh environment by Core 36.

The succeeding subunit (IVe), which is clearly identified in the gamma log, consists in contrast almost wholly of volcanic lapilli, altered glass, and zeolites. Deposition took place in inner shelf depths.

Very poor recovery was obtained in succeeding Subunit IVd (Cores 26–33). The few fragments consist of micaceous arkosic sandstones, often highly carbonaceous with a minor volcanogenic component (Cores 26 and 27 only). The clear high gamma response suggests that the sandstones are probably the principal lithology. A decrease in temperature gradient through the interval may indicate flushing of the formation by connate water. Deposition took place in inner to mid-shelf water depths.

The overlying subunit (IVc) is marked by a sharp increase in the abundance of tuff with two maxima in Cores 12 to 16 and 21 to 25. The tuffaceous components are largely vitric and typically palagonitized but are clearly more silicic than those of Subunits IVe and IVb. An early Eocene (NP10/11 boundary) nannoflora occurs near the base of the subunit (24-1, 60 cm). A rich macrofauna comprising bivalves, including oysters, gastropods, and serpulids, is present and thick shelled oysters occur in Core 19. Scour structures, cross laminae, and intraclasts are common, with disseminated carbonaceous matter along laminae. A heavy mineral assemblage characterized by metamorphic hornblende and epidote (also found at nearby Site 403) is present throughout. Benthic forams indicate brackish lagoonal or estuarine conditions in Cores 18 and 19 and inner shelf elsewhere. The top of the unit is placed beneath a highly glauconitic unit, marking a major transgression, which dramatically alters the sediment type.

Unit IVb is marked by the appearance of nannofossil–foraminifer chalk, the disappearance of common detrital quartz, and the change in heavy mineral content from epidote–hornblende to the augite–iddingsite above occurring within the upper part of Zone NP11(?). The succeeding Unit IVb is equivalent to the whole of Unit IV of Site 552. In Hole 553A, the subunit is composed principally of tuffs reworked and interbedded with zeolitic nannofossil–foraminifer chalk. The tuffs are mainly vitric, often unaltered and of basaltic type. Grading is present together with a small slump (Core 11), microfaults, and sedimentary dykes. Macrofossils, including serpulids, gastropods, bryozoans, and in situ bivalves, are common in the lower part but become less common upward. The benthic foram assemblage is tentatively interpreted to show a depth change from 100–180 m to greater than 700 m by Core 10. The age of the top of the subunit is NP14.

The thicker IVb equivalent at Site 552 has an age range from NP11 at the base to NP14 at the top. The basal section (Subunit IVd) is a terrigenous diatomaceous claystone. The overlying beds (Subunit IVc) are glauconitic and contain echinoid spines, bryozoan, and gastropod fragments. Deposition took place in mid-shelf depths of 75–100 m. The overlying subunit (IVb) consists of calcareous biosiliceous volcanic ash of basaltic composition and tuffaceous biosiliceous chalk. Ripple drift cross laminae, intraclasts, small microfaults, and contorted beds occur throughout. Deposition took place in mid-outer shelf depths.

Middle Eocene

A hiatus representing NP15 is present within the middle Eocene at both Holes 553A and 552 and at least part of the middle Eocene is missing above (NP17-18?). Benthic foraminifers indicate depths of deposition were greater than 700 m. The middle Eocene section at both sites consists of a characteristic pale brown biosiliceous nannofossil-foraminifer chalk with sparse volcanic ash. At Hole 552A scouring, cross laminae and thin beds of sponge spicules are present.

Late(?) Eocene–Oligocene

At both sites, a condensed sequence (maximum 1.75 m) containing several hiatuses bridges the 30 m.y. of geological time between the middle Eocene and the early Miocene. At Site 553, 0.75 m of late Oligocene (NP25) nannofossil-foraminifer chalk with palagonitized ash rests on the middle Eocene. Manganese nodules and fish remains at the base suggest a period of prolonged nondeposition and/or erosion. In Hole 552A in contrast, a more complete section was cored using the HPC. Here, 1.5 m of Oligocene foraminifer-nannofossil chalk pass down into a chalk containing complete and broken manganese nodules together with angular clasts of the underlying unit. The manganese nodules contain lithified volcanogenic sediments, and evidence of both erosion and nondeposition are clearly shown. The Oligocene section (1 m) in Hole 552A contains Zones NP21–24 compared to NP 25 at Site 553. Depths of deposition in Oligocene time increased from about 700 m to in excess of 1400 m in late Oligocene time.

Miocene to Late Pliocene

Sedimentation was continuous only between the Miocene and Oligocene in Hole 553A where a thin (4 m) nannofossil-foraminifer chalk represents the early Miocene (NN1). A hiatus encompassing NN2–N4 separates those beds from overlying early Miocene (NN5) glauconitic foraminifer chalk. In Hole 552A the early Miocene is absent and the Oligocene is succeeded by middle Miocene (NN7) glauconitic foraminifer chalk. At both sites a hiatus is present within the middle Miocene above which the principal lithology is a uniform nannofossil-foraminifer chalk that passes upward into nannofossil ooze, the transition from chalk to ooze occurring at about 142 m. Faint bluish gray laminae and thin bands of well-sorted forams are present in the lower part of this unit. Water depths of greater than 2200 m are comparable to those at present.

Late Pliocene–Pleistocene

A complete Pliocene–Pleistocene section (in which the preglacial–glacial transition occurs at 44 m) was cored in Hole 552A and the equivalent interval was washed and in part cored by HPC in Hole 553A. The average accumulation rate of 1.4 cm/1000 yr. was determined in Hole 552A and deposition took place in depths closely comparable to those at present.

The base of the section is defined by the appearance of alternating beds of foraminifer–nannofossil ooze and calcareous mud with dropstones as well as an abrupt change in the variation in $CaCO_3$ content. Below 44 m, uniform carbonate values of about 90% are characteristic. Above 44 m, cyclical variations in carbonate content are apparent, increasing abruptly in amplitude near 43 m and in length near 16 m. These carbonate cycles correlate with the lithologic cycles of which 34 were identified visually. Assuming a 2.1 cm/1000 yr. sedimentation rate, cycles above 16 m are longer (c. 130,000 yr.) than those below (20,000–30,000 yr.). Within each lithologic cycle, smectites dominate in the carbonates while illite, kaolinite, detrital quartz, and feldspar predominate in the muds and marls. Dropstones occur throughout. Diatoms are abundant in the carbonate zones but absent in the intervening muds. These cycles correlate rather well with the oxygen isotope cycles recognized by Shackleton and Opdyke (1976) in the Pleistocene of the Pacific. This preliminary correlation demonstrates that a complete Pliocene–Pleistocene record is present. This is the first complete record obtained in the northern North Atlantic and will thus be invaluable in interpreting the evolution of Pleistocene climate and ocean circulation through magnetic and biostratigraphic studies complemented by studies of the lithostratigraphy and oxygen isotope stages.

REFERENCES

Backman, J., and Shackleton, N. J., 1983. Quantitative nannofossil correlation to open-ocean deep sea sections from Plio/Pleistocene boundary at Vrica, Italy. *Nature*, 304:156–158.

Berggren, W. A., and Aubert, J., 1976. Late Paleogene (late Eocene and Oligocene) benthonic foraminiferal biostratigraphy and paleobathymetry of Rockall Bank and Hatton-Rockall Basin. *Micropaleontology*, 22:307–326.

Bott, M. H. P., et al., 1983. *Structure and development of the Greenland-Scotland Ridge:* New York (Plenum Press).

Bott, M. H. P., Browitt, C. W. A., and Stacey, A. P., 1971. The deep structure of the Iceland-Faeroe Ridge. *Mar. Geophys. Res.*, 1: 328–351.

Bott, M. H. P., Sunderland, J., Smith, P. J., Casten, U., and Saxon, S., 1974. Evidence for continental crust beneath the Faeroe Islands. *Nature*, 248:20–204.

Boutefeu, A., 1976. Pyrolysis study of organic matter from DSDP Sites 370 (Leg 41), 415 and 416 (Leg 50). *In* Lancelot, Y., Winterer, E. L., et al., *Init. Repts. DSDP*, 50: Washington (U.S. Govt. Printing Office), 555–567.

Brooks, C. K., 1973. Tertiary of Greenland—A plutonic and volcanic record of continental breakup. *Mem. Am. Assoc. Pet. Geol.*, 19: 150–160.

Bukry, D., 1973. Coccolith and silicoflagellate stratigraphy, Tasman Sea and southwestern Pacific Ocean. *In* Burns, R. E., Andrews, J. E,. et al., *Init. Repts. DSDP*, 21: Washington (U.S. Govt. Printing Office), 885–893.

Bullard, E. C., Everett, J., and Smith, A. G., 1965. The fit of the continents around the Atlantic. *Phil. Trans. Roy. Soc. London*, 258: 41–51.

Burckle, L. H., 1972. Late Cenozoic planktonic diatom zones from the eastern equatorial Pacific. *Nova. Hedwig. Beih.*, 39:217–246.

________, 1977. Pliocene and Pleistocene diatom datum levels for the equatorial Pacific. *Quat. Res.*, 7:330–340.

Cande, S. C., and Kristoffersen, Y., 1977. Late Cretaceous magnetic anomalies in the North Atlantic. *Earth Planet. Sci. Lett.*, 35: 215–224.

Casey, R. E., and McMillen, K. J., 1977. Cenozoic radiolarians of the Atlantic Basin and margins. *Development Paleo. Stratigr.*, 6: 521–544.

Casten, U., 1973. The crust beneath the Faeroe Islands. *Nature*, 241(108):83–84.

Claypool, G., 1975. JOIDES manual on pollution prevention and safety. *JOIDES J.*, Appendix C.

________, in press. Diagenesis of organic matter, isotopic composition of calcite veins in basement basalt and pore water in sediment—Barbados Ridge Complex, Deep Sea Drilling Project Leg 78A. *In* Biju-Duval, B., Moore, J. C., et al., *Init. Repts. DSDP*, 78A: Washington (U.S. Govt. Printing Office), 385–392.

Clementz, D. M., Daly, A. R., and Demaison, J. J., 1979. Well site geochemistry by programmed pyrolysis. *Off. Tech. Conf. Pap.*, OTC-3410(1):465–470.

Cline, R. M., and Hays, J., 1976. Investigation of late Quaternary paleoceanography and paleoclimatology. *Geol. Soc. Am. Mem.*, 145.

Costa, L., and Downie, C., 1979. Cenozoic dinocyst stratigraphy of Sites 403 and 406, Rockall Plateau. *In* Montadert, L., Roberts, D. G., et al., *Init. Repts. DSDP*, 48: Washington (U.S. Govt. Printing Office), 513–529.

Davies, T. A., Hay, W. W., Southam, J. R., and Worsley, T. R., 1977. Estimates of Cenozoic sedimentation rates. *Science*, 197:53–55.

de Charpal, O., Guennoc, D., Montadert, L., and Roberts, D. G., 1978. Rifting, crustal attenuation and subsidence in the Bay of Biscay. *Nature*, 275(5682):706–711.

Detrick, R. S., Sclater, J. G., and Thiede, J., 1977. Subsidence of aseismic ridges. *Earth Planet. Sci. Lett.*, 34:185–196.

Duddy, I. R., in press. *Stratigraphy of the Otway Group, Southeast Australia* [Ph.D. dissert.]. University of Sydney.

Espitalié, J., LePlat, P., Madec, M., Menning, J. J., and Tissot, B., 1977. Source rock characterization method for petroleum exploration. *Off. Tech. Conf. Pap.*, OTC2935(3):439–444.

Featherstone, P. S., Bott, M. H. P., and Peacock, J. H., 1976. Structure of the continental margin of southeastern Greenland. *Geophys. J.*, 48:15–40.

Foreman, H. P., 1975. Radiolaria from the North Pacific. *In* Larson, R. L., Moberly, R., et al., *Init. Repts. DSDP*, 32: Washington (U.S. Govt. Printing Office), 579–676.

Gartner, S., 1977. Calcareous nannofossil biostratigraphy and revised zonation of the Pleistocene. *Mar. Micropaleontol.*, 2:1–25.

Gerard, I., and Smith, G. C., 1983. Post-Palaeozoic succession and structure of the southwestern African continental margin. *Mem. Am. Assoc. Pet. Geol.*, 34:49–76.

Gieskes, J., Ellis, R., and Pine, J., 1979. Interstitial water studies, Leg 48. *In* Montadert, L., Roberts, D. G., et al., *Init. Repts. DSDP*, 48: Washington (U.S. Govt. Printing Office), 297–304.

Gleadow, A. J. W., and Duddy, I. R., 1980. Early Cretaceous volcanism and the early breakup history of southeastern Australia: Evidence from volcaniclastic sediments. *In* Vella, P., and Cresswell, M. M. (Eds.), *Gondwana Five:* (Wellington), pp. 295–300.

Grow, J. A. 1981. The Atlantic continental margin of the United States. *Geology of Passive Continental Margins* (AAPG Education Course Note Series) 19;4-1:4–60.

Hailwood, E. A., Bock, W., Costa, L., Dupeuble, P. A., Müller, C., and Schnitker, D., 1979. Chronology and biostratigraphy of northeast Atlantic sediments, DSDP Leg 48. *In* Montadert, L., Roberts, D. G., et al., *Init. Repts. DSDP*, 48: Washington (U.S. Govt. Printing Office), 1119–1142.

Haq, B. U., and Berggren, W. A., 1978. Late Neogene calcareous plankton biochronology of the Rio Grande Rise (South Atlantic Ocean). *J. Paleontol.*, 52:1167–1194.

Harrison, W., and La Porte, J., 1979. Shipboard organic geochemistry. *In* Montadert, L., Roberts, D. G., et al., *Init. Repts. DSDP*, 48: Washington (U.S. Govt. Printing Office), 959–964.

Hinz, K., 1981. A hypothesis on terrestrial catastrophes: Wedges of very thick oceanward dipping layers beneath passive continental margins—Their origin and paleoenvironmental significance. *Geol. Jahrbuch. Ser. E.*, 22:3–28.

Huc, A. A., 1980. Origin of organic matter in recent marine sediments. *In* Durand, B. (Ed.), *Sedimentary Organic Matter and Kerogen:* Paris (*Editions Techniq.*), pp. 445–466.

Hunt, J., 1979. *Petroleum Geochemistry and Geology*: New York (McGraw-Hill).

Jones, E. J. W., Ewing, M., Ewing, J. I., and Eittreim, S. L., 1970. Influences of Norwegian Sea overflow water on sedimentation in the northern North Atlantic and Labrador Sea. *J. Geophys. Res.*, 75:1655–1680.

Jones, M. T., and Roberts, D. G., 1975. *Marine Magnetic Anomalies in the North Atlantic Ocean:* Reading (Mtg. Europ. Geol. Soc.). (Abstract)

Kempe, D. R. C., 1976. Petrological studies on DSDP Leg 34 basalts: Nazca Plate, Eastern Pacific Ocean. *In* Yeats, R. S., Hart, S. R., et al., *Init. Repts. DSDP*, 34: Washington (U.S. Govt. Printing Office), 189–214.

Kennett, J. P., and Srinivasan, M. S., 1983. *Neogene Planktonic Formaminfera: A Phylogenetic Atlas:* Stroudsburg, Pa. (Huchinson-Ross).

Kristoffersen, Y., 1978. Sea-floor spreading and the early opening of the North Atlantic. *Earth Planet. Sci. Lett.*, 38:273–290.

Kristoffersen, Y., and Talwani, M., 1978. Extinct triple junction south of Greenland and the Tertiary motion of Greenland relative to North America. *Geol. Soc. Am. Bull.*, 88:1037–1049.

Laughton, A. S., 1971. South Labrador sea and the evolution of the North Atlantic. *Nature*, 232(5313):612–617.

Laughton, A. S., Berggren, W. A., et al., 1971. *Init. Repts. DSDP*, 12: Washington (U.S. Govt. Printing Office).

Le Pichon, X., Hyndman, R., and Pautot, G., 1972. Geophysical study of the opening of the Labrador Sea. *J. Geophys. Res.*, 76: 2891–2895.

Matthews, D. J., 1939. *Tables of the Velocity of Sound in Pure Water and in Seawater*: London (Hydrographic Dept., Admiralty).

McKenzie, D. P., 1978. Remarks on the evolution of sedimentary basins. *Earth Planet. Sci. Lett.*, 40:25–32.

Miller, J. M., Roberts, D. G., and Matthews, D. H., 1973. Rocks of Grenville Age from Rockall Bank. *Nature*, 246:61.

Montadert, L., Roberts, D. G., and the Shipboard Scientific Party, 1979. Sites 403 and 404. *In* Montadert, L., Roberts, D. G., et al., *Init. Repts. DSDP*, 48: Washington (U.S. Govt. Printing Office), 165–209.

Moorbath, S., and Welke, H., 1969. Isotopic affinity for the continental affinity of Rockall Bank, North Atlantic. *Earth Planet. Sci. Lett.*, 79:2059–2072.

Morley, J. J., and Shackleton, N. J., 1978. Extension of the radiolarian *Stylatractus universus* as a biostratigraphic diatom to the Atlantic Ocean. *Geology*, 6:309–311.

Müller, C., 1979. Calcareous nannofossils from the North Atlantic DSDP Leg 48. *In* Montadert, L., Roberts, D. G., et al., *Init. Repts. DSDP*, 48: Washington (U.S. Govt. Printing Office), 589–640.

________, 1981. Beschreibung neuer Helicosphaera-Arten ausdem Miozan und Revision biostratigraphischer Reichweiten einiger neogener Nannoplanken-Arten. *Senck. Lethaia*, 61 (3/6):427–435.

Mutter, J. C., Talwani, M., and Stoffers, P. L., 1982. Origin of seaward-dipping reflectors in the oceanic crust of the Norwegian margin by "subaerial seafloor spreading." *Geology*, 10:353–357.

Noe-Nygaard, A., 1976. Tertiary igneous rocks between Shannon and Scoresby Sund. *In* Noe-Nygaard, A., et al. (Eds.), *Geology of East Greenland:* Copenhagen (Groen. Geol. Undersol.), pp. 386–402.

Okada, H., and Bukry, D., 1980. Supplementary modification and introduction of code numbers to the low latitude coccolith biostratigraphic zonation (Bukry, 1973, 1975). *Mar. Micropaleontol.*, 5(3): 321–325.

Okada, H., and Thierstein, H. 1979. Calcareous nannoplankton Leg 43, DSDP. *In* Tucholke, B. E., Vogt, P. R., *Init. Repts. DSDP*, 43: Washington (U.S. Govt. Printing Office), 507–573.

Olivet, J. L., Le Pichon, X., Monti, S., and Sichler, B., 1974. Charlie-Gibbs Fracture Zone. *J. Geophys. Res.*, 79:2059–2073.

Palmason, G., 1979. A continuum model of crustal growth in Iceland: Kinematic aspects. *J. Geophys.*, 47:7–18.

Patton, J., Croquette, P. W., Guennel, G. K., Kaltenback, A. J., and Moore, A., in press. Organic geochemistry and sedimentology of lower to mid-Cretaceous deep sea carbonates, Sites 535 and 540, Leg 77. *In* Schlager, W., Buffler, R. T., et al., *Init. Repts. DSDP*, 77: Washington (U.S. Govt. Printing Office).

Poore, R. Z., and Berggren, W. A., 1975. Late Cenozoic planktonic foraminifera biostratigraphy and paleoclimatology: Hatton-Rockall Basin, DSDP Site 116. *J. Foram. Res.*, 5(4):279–293.

Rasmussen, J., and Noe-Nygaard, A., 1969. Beskrivelse for geologisk kost over Faeroerne. *Dan geol. Unders., I. Rk.*, 24:1–370.

Riedel, W., and Sanfilippo, A., 1978. Stratigraphy and evolution of tropical Cenozoic radiolarians. *Micropaleontology*, 24(1):61–96.

Roberts, D. G., 1970. Recent geophysical studies on the Rockall Plateau and adjacent areas. *Proc. Geol. Soc. Lond.*, 1662:87–93.

________, 1971. New geophysical evidence on the origins of the Rockall Plateau and trough. *Deep-Sea Res.*, 19:353–359.

________, 1975. Marine geology of the Rockall Plateau and trough. *Phil. Trans. Roy. Soc. London* (Ser. A), 278:447–509.

Roberts, D. G., Ardus, D. A., and Dearnley, R., 1973. Pre-Cambrian rocks drilled from the Rockall Bank. *Nature Phys. Sci.*, 244:21–23.

Roberts, D. G., Bott, M. H. P., and Uruski, C., 1983. Structure and origin of the Wyville-Thomson Ridge. *In* Bott, M. H. P., et al. (Eds.), *Structure and Development of the Greenland-Scotland Ridge:* New York (Plenum Press), pp. 133–158.

Roberts, D. G., Masson, D. G., and Miles, P. R., 1981. Age and structure of the southern Rockall trough: New evidence. *Earth Planet. Sci. Lett.*, 52:115–128.

Roberts, D. G., Matthews, D. H., and Eden, R. A., 1972. Metamorphic rocks from the southern end of Rockall Bank. *J. Geol. Soc. London*, 128:501–506.

Roberts, D. G., Montadert, L., and Searle, R. C., 1979. The western Rockall Plateau: Stratigraphy and crustal evolution. *In* Montadert, L., Roberts, D. G., et al., *Init. Repts. DSDP*, 48: Washington (U.S. Govt. Printing Office), 1061–1088.

Roberts, D. G., and Scrutton, R. A., 1971. Structure of Rockall Plateau and Trough, Northeast Atlantic. *Inst. Geol. Sci. Rep.*, No. 70114:77–87.

Romein, A. J. T., 1979. Lineages in early Palaeogene calcareous nannoplankton. *Utrecht Micropalaeontol. Bull.* 22:1–231.

Royden, L., Sclater, J,. and Von Herzen, R. P., 1980. Continental margin subsidence and heat flow: Important parameters information of petroleum. *Am. Assoc. Pet. Geol. Bull.*, 64(2):173–187.

Ruddiman, W., 1972. Sediment distribution on the Reykjanes Ridge: New evidence. *Geol. Soc. Am. Bull.*, 83:2039–2062.

Scrutton, R. A., 1970. Results of a seismic refraction experiment on Rockall Bank. *Nature*, 227(5260):826–827.

________, 1972. The crustal structure of Rockall Plateau microcontinent. *Geophys. J.*, 27(3):259–275.

Shackleton, N. J, and Opdyke, N., 1976. Oxygen isotope and paleomagnetic evidence for early northern hemisphere glaciation. *Nature*, 270:216–219.

Schaefer, R., Leythaeuser, D., and Weiner, B., 1978. Single step capillary column GC method for extraction and analysis of sub-ppb (10^6) amounts of hydrocarbons (C_2–C_6) from rock and crude oil samples and its application to geochemistry. *J. Chromatography*, 167:355–363.

Scrutton, R. A., and Roberts, D. G., 1971. Structure of the Rockall Plateau and Trough, North East Altantic. ICSU/SCOR WG31 Symposium, Cambridge, 1970. The Geology of the East Atlantic Continental Margin, Europe. Rept. 70/14, *Instit. Geol. Sci.*, 12: 77–78.

Srivastava, S., 1978. Evolution of the Labrador Sea and its bearing on the early evolution of the North Atlantic. *Geophys. J.*, 52:313–357.

Talwani, M., Udintsev, G. et al,. 1976. *Init. Repts. DSDP*, 38: Washington (U.S. Govt. Printing Office).

Talwani, M., Muller, J. C., and Eidholm, O., 1981. The initiation of opening of the Norwegian Sea. *Oceanologica Acta*, No. Sp., 23–30.

Thiede, J., 1980. Paleoceanography, margin stratigraphy and paleophysiography of the Tertiary North Atlantic and Norwegian-Greenland Seas. *Phil. Trans. Roy. Soc. London*, 345:177–185.

Thierstein, H. R., Geitzenauer, K. R., Molfino, B., and Shackleton, N. J., 1977. Global synchroneity of late Quaternary coccolith datum levels: Validation by oxygen isotopes. *Geology*, 5:400–404.

Tissot, B., and Welte, D., 1978. Petroleum Formation and Occurrence: Berlin (Springer-Verlag).

van Hinte, J,. 1979. Subsidence of the Iceland-Faeroes Ridge. *Abstr. Geol. Soc. London*, 133:159. (Abstract)

Vogt, P. R., 1972. The Faeroe-Iceland-Greenland seismic ridge and the western boundary undercurrent. *Nature*, 239:79–81.

Vogt, P. R., and Avery, O. E., 1974. Detailed magnetic surveys in the Northeast Atlantic and Labrador Sea. *J. Geophys. Res.*, 76:363.

Vogt, P. R., Avery, O. E., Schneider, E. D., Anderson, C. N., and Bracey, D. R., 1969. Discontinuities in seafloor spreading. *Tectonophysics*, 8(4–6):285–317.

Vogt, P. R., Johnson, G. L., Holcombe, T. L., Gilg, J. G., and Avery, O. E., 1979. Episodes of seafloor spreading recorded in North Atlantic basement. *Tectonophysics*, 12:211–234.

Watts, A. B., Schreiber, B. D., and Habib, D., 1975. Dredged rocks from the Hatton Bank, Rockall Plateau. *J. Geol. Soc. London*, 131:639–646.

Whelan, J., and Shunji, S., 1977. C_1–C_7 volatile organic compounds in sediments from DSDP Legs 56 and 57, Japan Trench. *In* Langseth, M., von Huene, R., et al., *Init. Repts. DSDP*, 56-57, Pt. 2: Washington (U.S. Govt. Printing Office), 1349–1366.

APPENDIX A
Smear Slide Summary, Hole 552

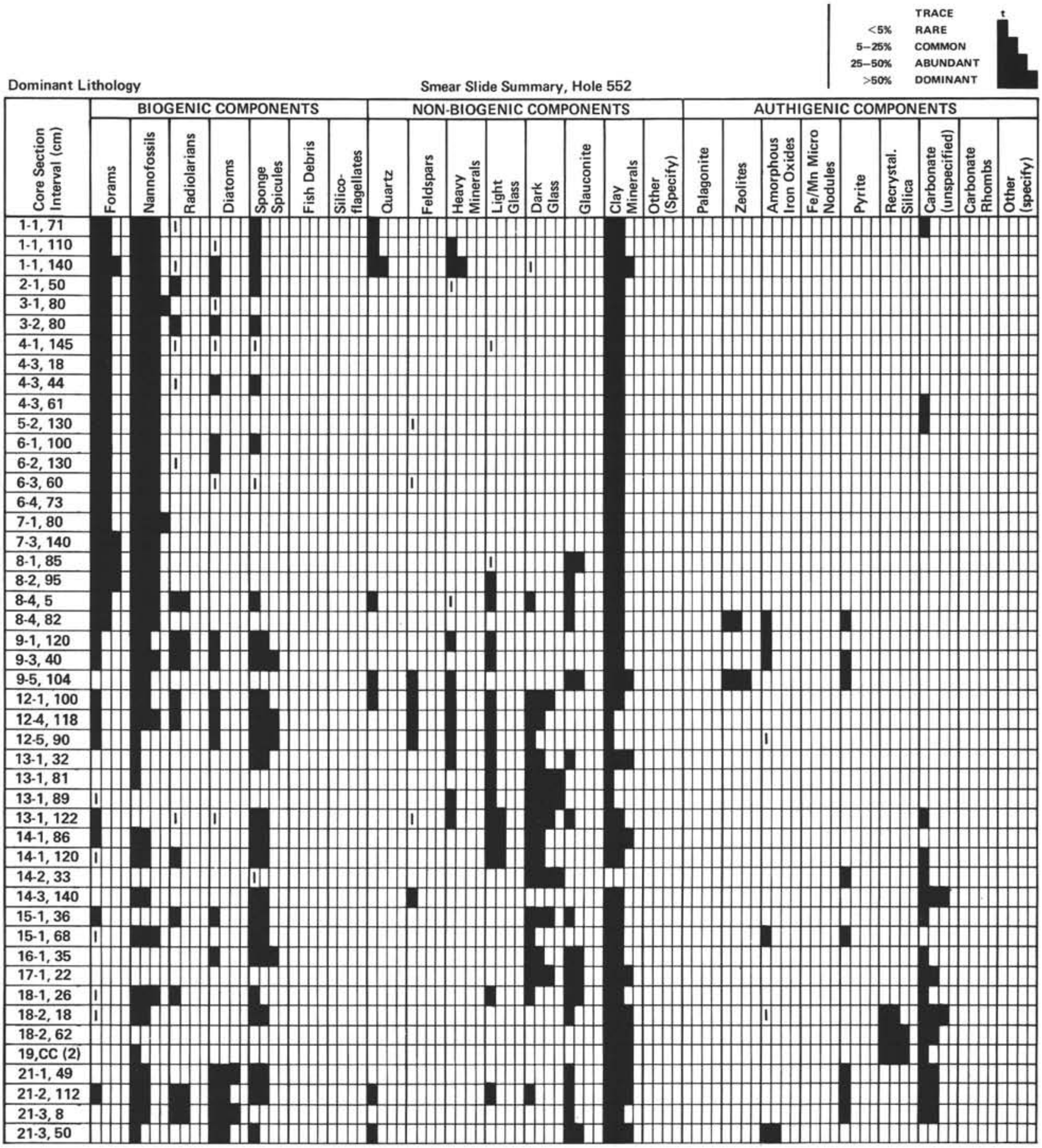

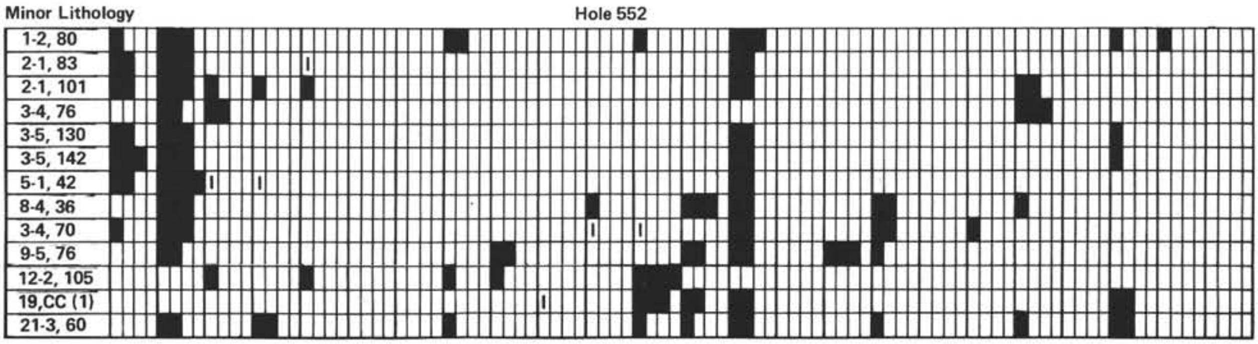

Appendix A. (Continued).

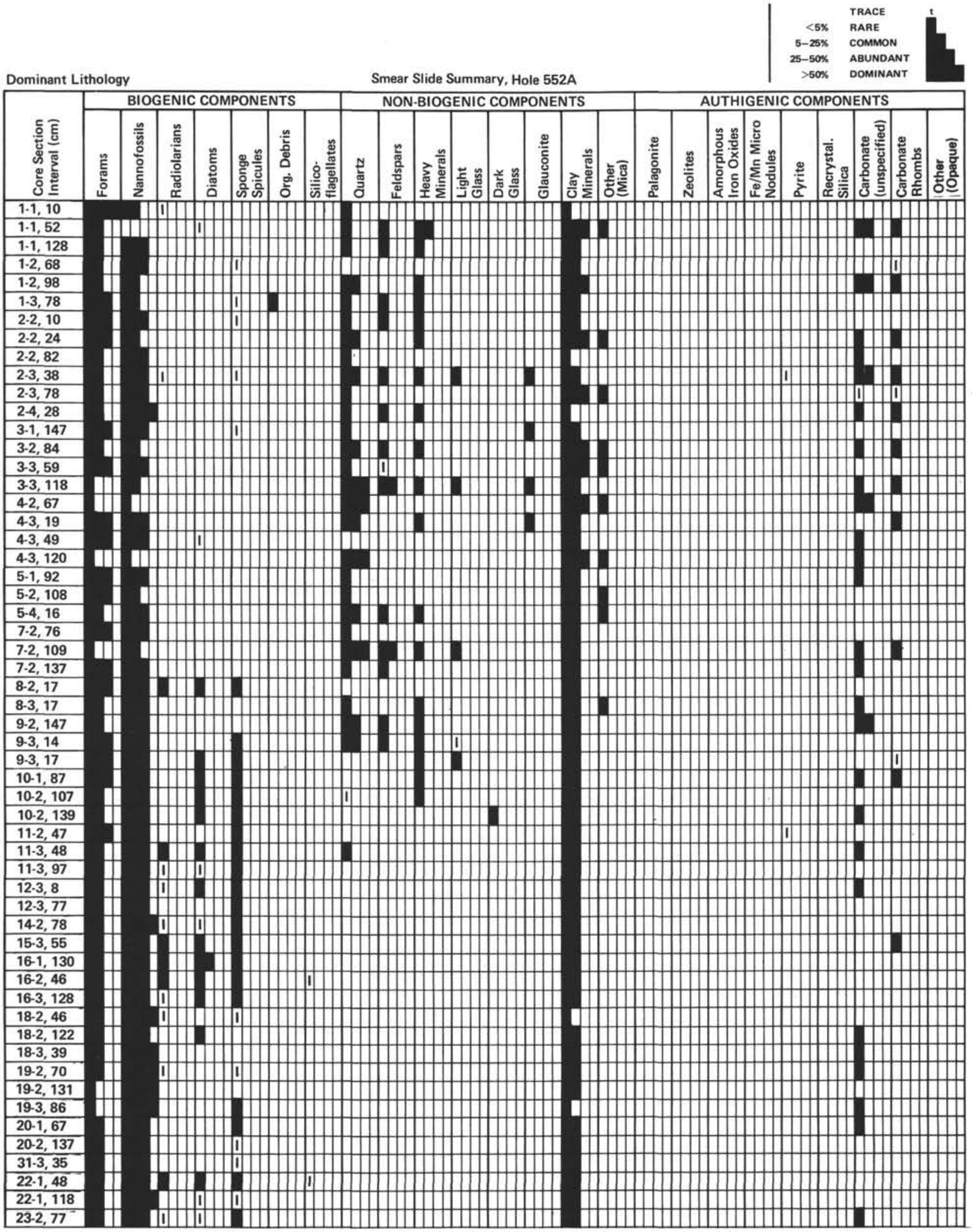

Appendix A. (Continued).

Dominant Lithology

Smear Slide Summary, Hole 552A

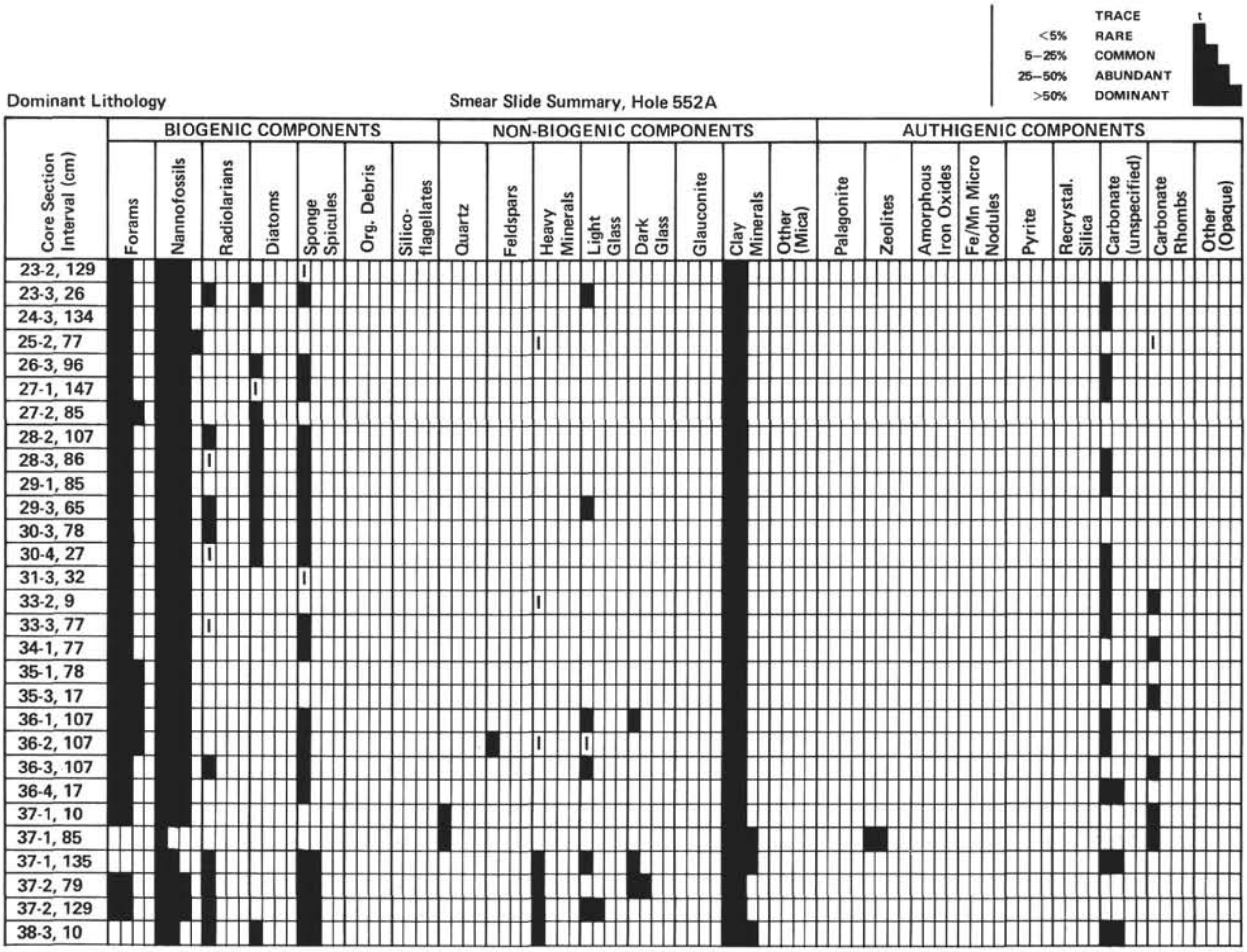

Minor Lithology

Hole 552A

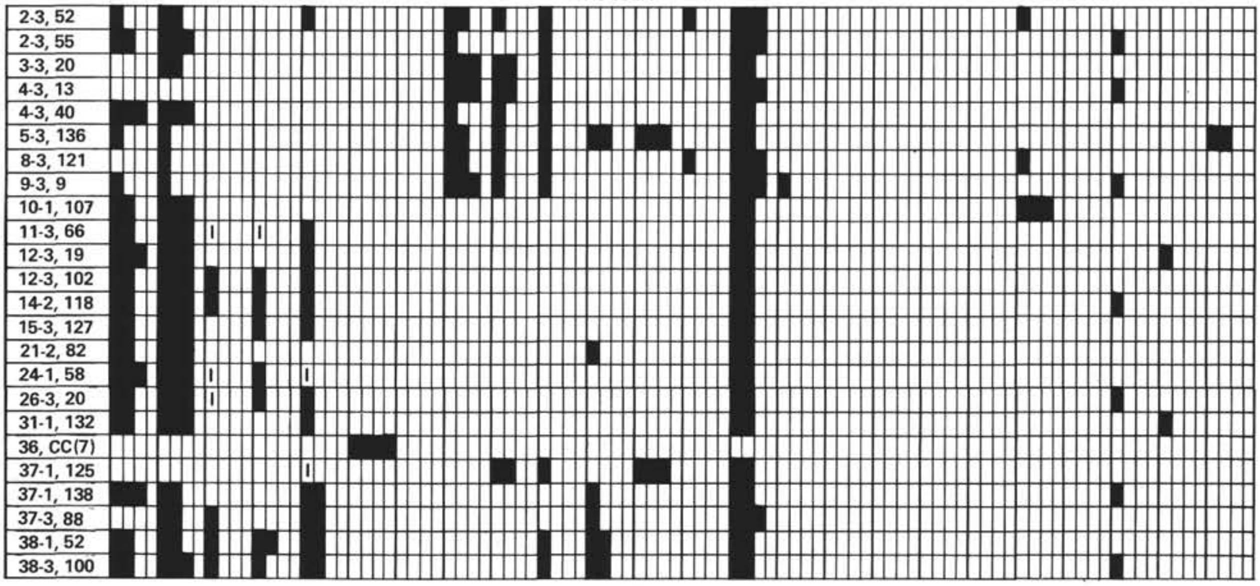

APPENDIX B
Smear Slide Summary, Hole 553

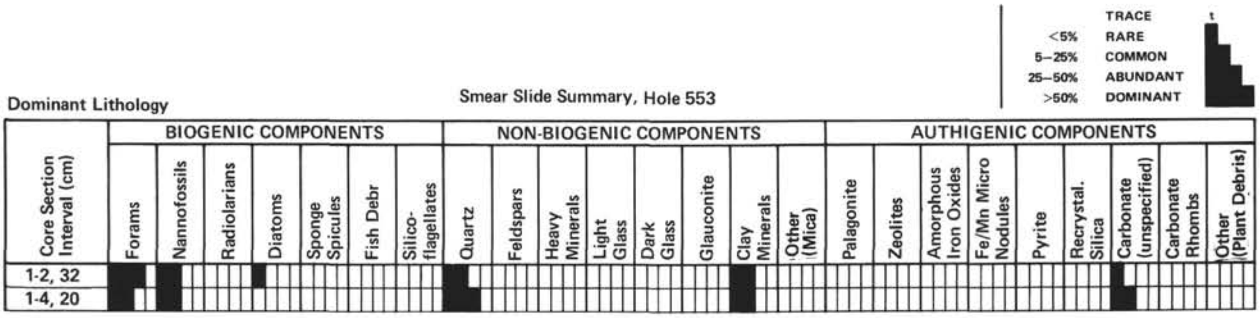

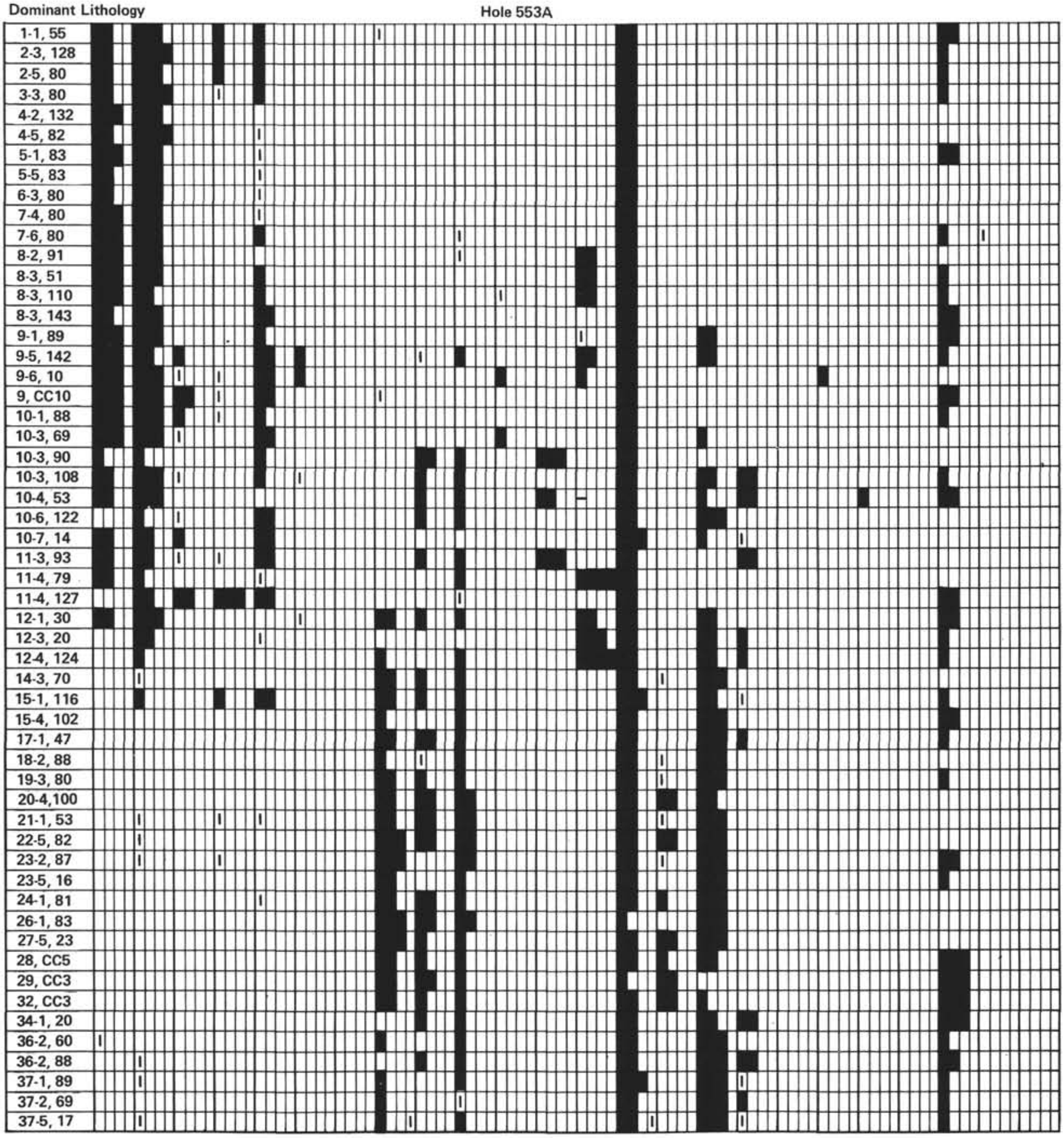

Appendix B. (Continued).

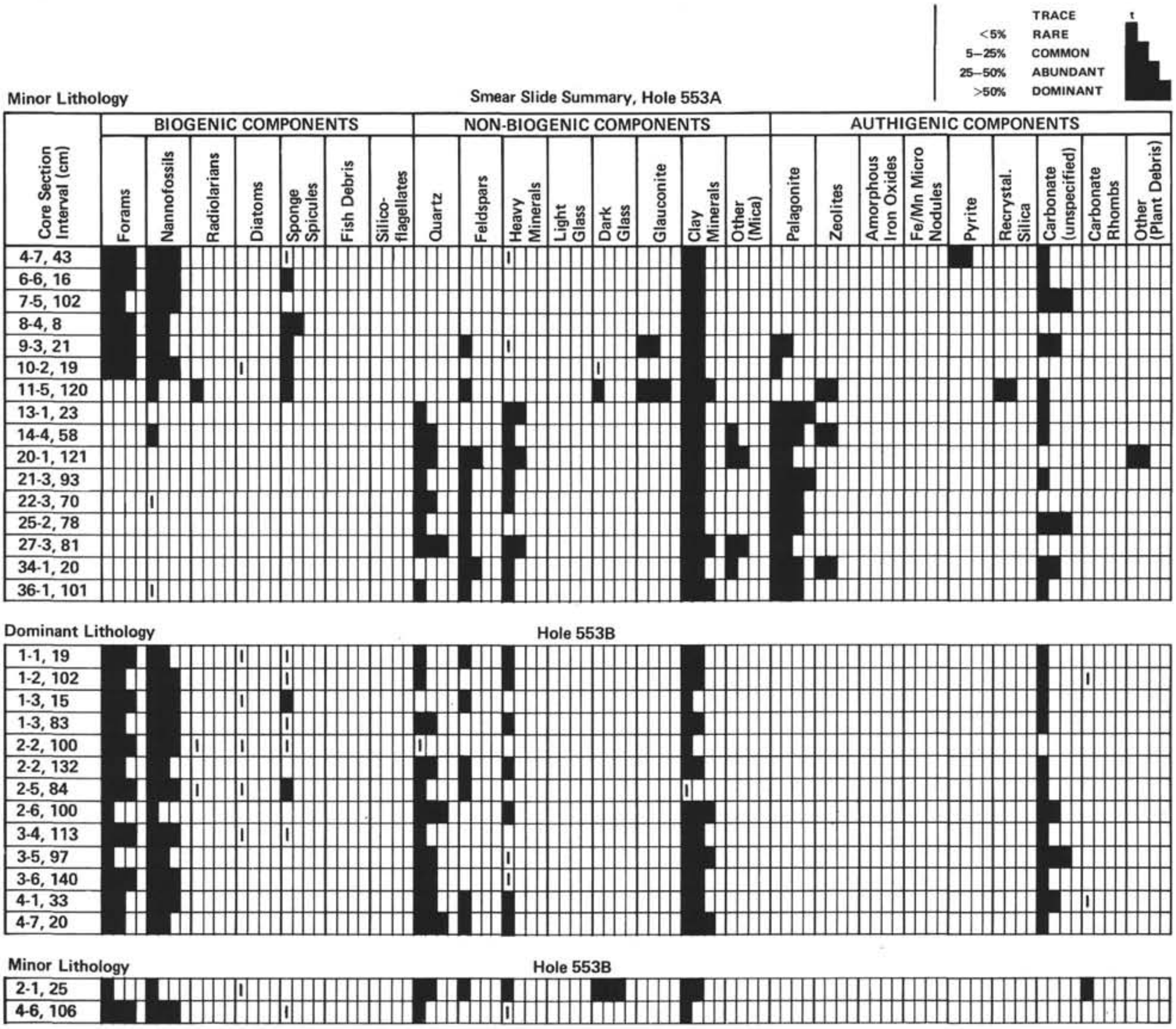

SITE 552 HOLE CORE 1 CORED INTERVAL 0.0–3.5 *m*

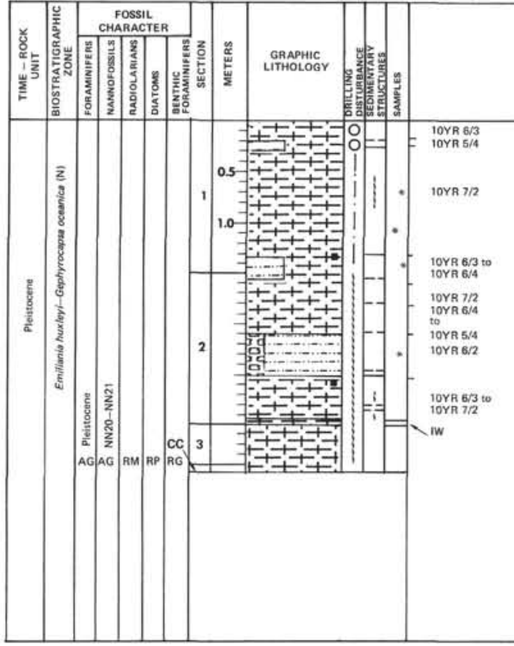

LITHOLOGIC DESCRIPTION

FORAM-NANNO OOZE with NANNO-FORAM MARL and CALCAREOUS MUD

Color is alternating pale brown (10YR 6/3) and light gray (10YR 7/2), with mottled transitional boundaries. Core is very disturbed by drilling. Distorted laminations present. Granule and sand-size black lithic clasts throughout. Angular pebbles of quartzite and *phyllite also present. Bioturbation present in light colored layers.* Boundary between marl and overlying ooze is sharp.

SMEAR SLIDE SUMMARY (%):

	1, 71	1, 110	1, 140	2, 80
	D	D	D	M
Texture:				
Sand	10	10	15	15
Silt	10	15	25	20
Clay	80	75	60	65
Composition:				
Quartz	5	5	10	15
Heavy minerals	–	2	5	–
Clay	15	10	25	30
Volcanic glass	–	–	Tr	2
Carbonate unspec.	2	–	–	10
Foraminifers	20	20	25	5
Calc. nannofossils	55	61	30	33
Diatoms	–	Tr	3	–
Radiolarians	Tr	–	Tr	–
Sponge spicules	3	2	2	–
Dolomite	–	–	–	5

CARBONATE BOMB: $CaCO_3$ (%):
1, 71 = 74
2, 81 = 28
2, 145 = 66
3, 24 = 66

SITE 552 HOLE CORE 2 CORED INTERVAL 51.0–60.5 m

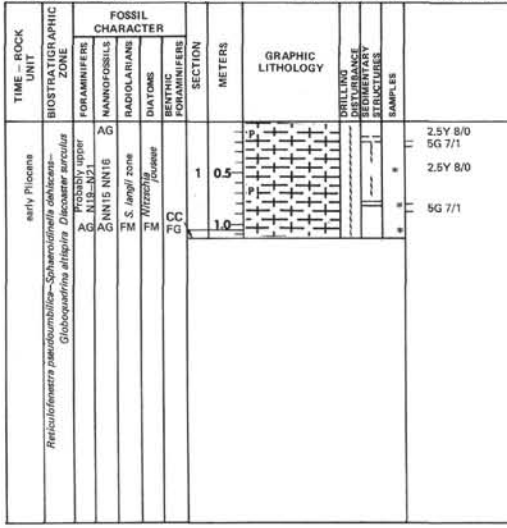

LITHOLOGIC DESCRIPTION

FORAM NANNO OOZE

Very deformed by drilling. Mainly white (2.5Y 8/0) with minor laminations of grayish green (5G 7/1), gray (5Y 5/1), and black (5Y 2.5/1) patches and spots represent burrows and disseminated pyrite.

SMEAR SLIDE SUMMARY (%):

	1, 50	1, 83	1, 101
	D	M	M
Texture:			
Sand	15	5	15
Silt	15	10	20
Clay	70	85	65
Composition:			
Heavy minerals	Tr	–	–
Clay	5	10	10
Pyrite	–	–	15
Foraminifers	10	10	20
Calc. nannofossils	76	80	47
Diatoms	3	–	3
Radiolarians	3	–	2
Sponge spicules	3	Tr	3

CARBONATE BOMB: $CaCO_3$ (%):
1, 50 = 88

SITE 552 HOLE CORE 3 CORED INTERVAL 108.0–117.5 m

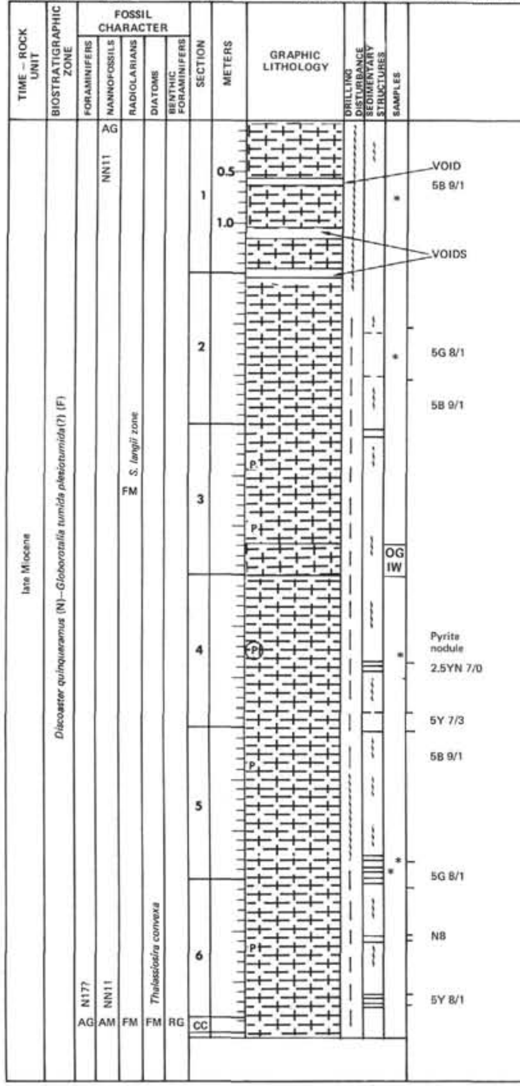

LITHOLOGIC DESCRIPTION

FORAM NANNO OOZE

Color is mainly bluish white (5B 9/1) with laminations of light gray (2.5Y N7) and minor layers of pale yellow (5Y 7/3). Core is moderately disturbed by drilling. Bioturbation is common throughout with some disseminated pyrite. Sediment becomes *firmer below* Section 3. Texture is sandy mud.

SMEAR SLIDE SUMMARY (%):

	1, 80	2, 80	4, 76	5, 130	5, 142
	D	D	M	M	M
Texture:					
Sand	5	10	30	10	25
Silt	5	10	50	15	10
Clay	90	80	20	75	65
Composition:					
Clay	10	20	–	20	20
Pyrite	–	–	70	–	–
Carbonate unspec.	–	–	–	10	10
Foraminifers	10	10	–	15	25
Calc. nannofossils	80	64	20	55	45
Diatoms	Tr	1	–	–	–
Radiolarians	–	3	10	–	–
Sponge spicules	–	2	–	–	–

CARBONATE BOMB: $CaCO_3$ (%):
1, 20 = 94
3, 80 = 92

Information on core description sheets, for ALL sites, represents field notes taken aboard ship under time pressure. Some of this information has been refined in accord with post-cruise findings, but production schedules prohibit definitive correlation of these sheets with subsequent findings. Thus the reader should be alerted to the occasional ambiguity or discrepancy.

SITE 552 HOLE CORE 4 CORED INTERVAL 117.5–127.0 m

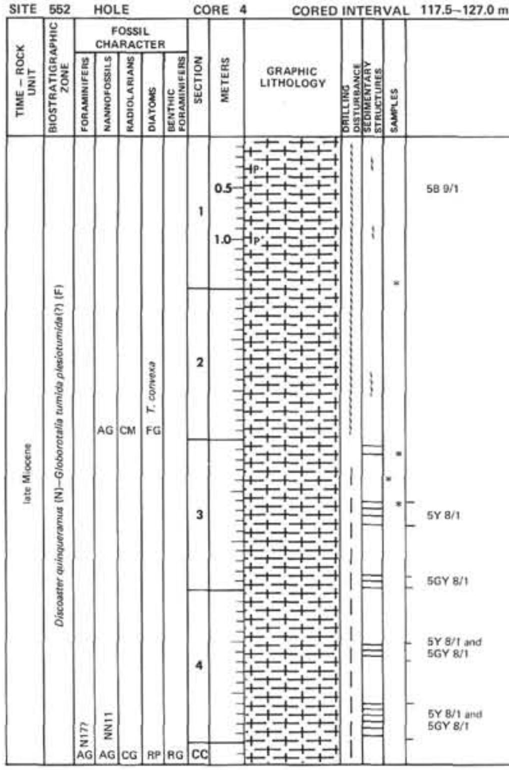

LITHOLOGIC DESCRIPTION

FORAM NANNO OOZE
Color is mainly bluish white (5B 9/1) with zones and laminations below Section 2 of yellowish gray (5Y 8/1) and light greenish gray (5GY 8/1). Sharp contact at base of some gray layers. Other contacts are gradational.

Ooze is a firm sandy mud. Minor bioturbation.

SMEAR SLIDE SUMMARY (%):

	1, 145	3, 18	3, 44	3 61
	D	D	D	D
Texture:				
Sand	10	5	5	Tr
Silt	10	15	25	15
Clay	80	80	70	85
Composition:				
Clay	15	15	15	15
Volcanic glass	Tr	–	–	–
Carbonate unspec.	–	–	–	5
Foraminifers	15	15	10	10
Calc. nannofossils	70	70	71	70
Diatoms	Tr	–	2	–
Radiolarians	Tr	–	Tr	–
Sponge spicules	Tr	–	2	–
Silica unspec.	–	Tr	–	–

CARBONATE BOMB: $CaCO_3$ (%):
1, 145 = 92

SITE 552 HOLE CORE 5 CORED INTERVAL 127.0–136.5 m

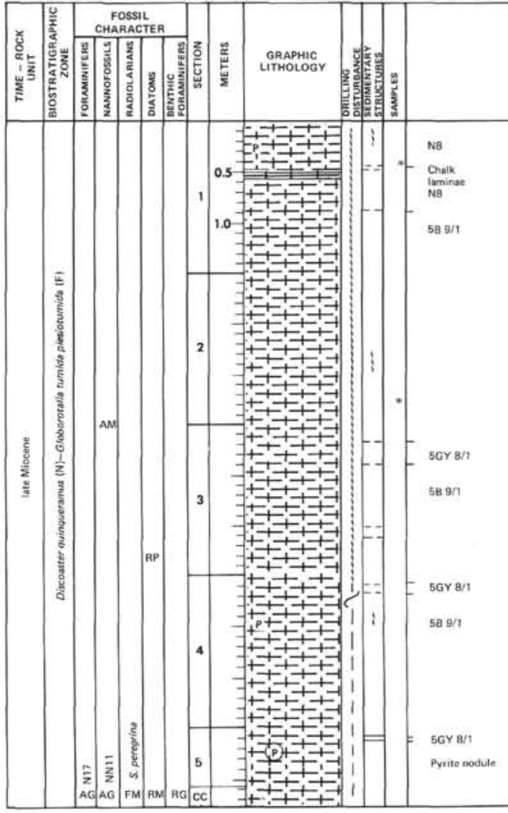

LITHOLOGIC DESCRIPTION

FORAM NANNO OOZE and MINOR FORAM NANNO CHALK
Color is mainly bluish white (5B 9/1) with very light gray (N8) Minor laminations of light greenish gray (5GY 8/1).

Drilling disturbance may have destroyed some laminations. Bioturbation is rare with some disseminated black pyrite and an authigenic pyrite nodule.

Alternating firm and soft ooze with thin chalk layer (1 cm) in Section 1.

SMEAR SLIDE SUMMARY (%):

	1, 42	2, 130
	M	D
Texture:		
Sand	0	5
Silt	10	15
Clay	90	80
Composition:		
Feldspar	–	Tr
Clay	10	15
Carbonate unspec.	–	5
Foraminifers	10	10
Calc. nannofossils	80	70
Diatoms	Tr	–
Radiolarians	Tr	–

CARBONATE BOMB: $CaCO_3$ (%):
2, 115 = 92

SITE 552 HOLE CORE 6 CORED INTERVAL 136.5–146.0 m

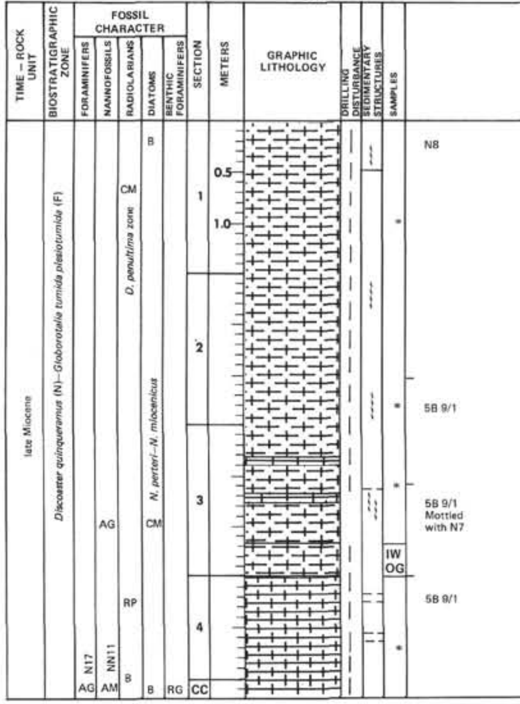

LITHOLOGIC DESCRIPTION

FORAM NANNO OOZE and FORAM NANNO CHALK

Color is mainly bluish white (5B 9/1) and very light gray (N8). Minor burrow mottling with light gray (N7) and faint laminae of light greenish gray (5G 8/1) and very light gray (N8).

Section 4 is much firmer and is classified as a chalk.

SMEAR SLIDE SUMMARY (%):

	1, 100 D	2, 130 D	3, 60 D	4, 73 D
Texture:				
Sand	5	0	5	0
Silt	10	10	15	10
Clay	85	90	80	90
Composition:				
Feldspar	–	–	Tr	–
Clay	15	10	15	10
Foraminifers	10	10	10	10
Calc. nannofossils	71	75	75	80
Diatoms	2	4	Tr	–
Radiolarians	–	1	–	–
Sponge spicules	2	–	Tr	–

CARBONATE BOMB: $CaCO_3$ (%):
3, 60 = 88
3, 112 = 83

SITE 552 HOLE CORE 7 CORED INTERVAL 146.0–155.5 m

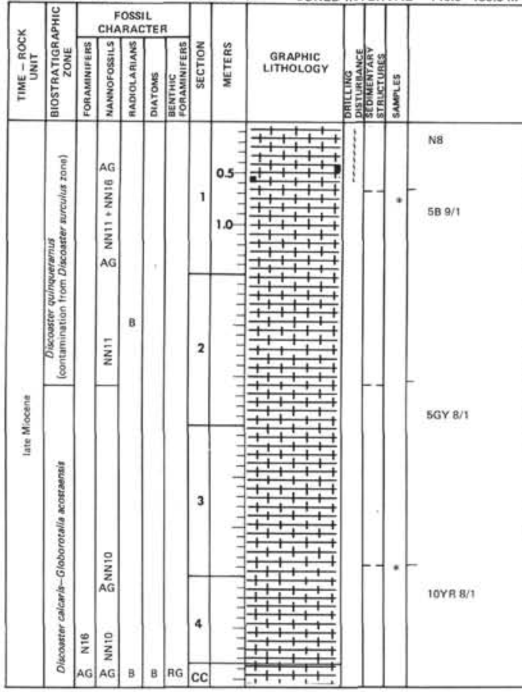

LITHOLOGIC DESCRIPTION

FORAM NANNO CHALK overlying NANNO FORAM CHALK

Color is bluish white (5B 9/1) grading to light greenish gray (5GY 8/1) with depth. There is a sharp change in sediment color in the base of Section 3 to white (10YR 8/1). Rare laminae and no visible bioturbation. (Top of Section 1 is very disturbed by drilling and is mainly downhole contamination).

Sediment becomes sandy in texture and foram-rich below Section 3.

SMEAR SLIDE SUMMARY (%):

	1, 80 D	3, 140 D
Texture:		
Sand	0	10
Silt	10	20
Clay	90	70
Composition:		
Quartz	–	Tr
Clay	10	10
Volcanic glass	–	Tr
Foraminifers	10	25
Calc. nannofossils	80	65

CARBONATE BOMB: $CaCO_3$ (%):
1, 80 = 91
3, 144 = 91

SITE 552 HOLE CORE 8 CORED INTERVAL 155.5–165.0 m

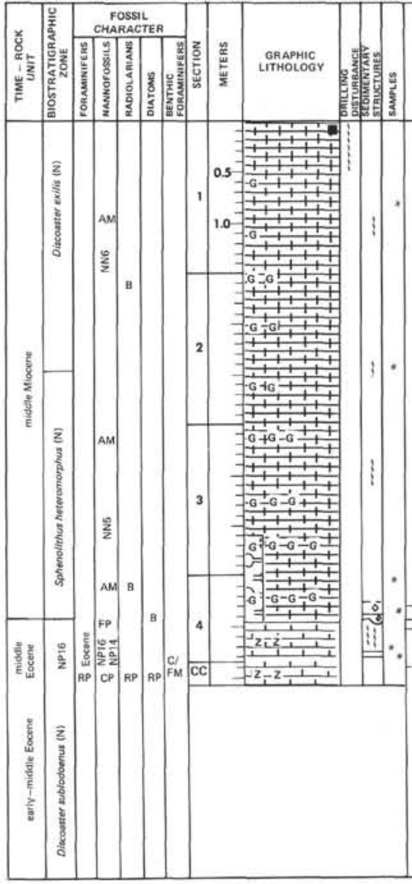

LITHOLOGIC DESCRIPTION

5GY 8/1

Mottled
5G 8/1
and
5GY 2/1

and
5Y 8/1

5GY 4/1
10YR 5/4
10YR 5/4

10Y 5/4

(Downhole contamination in very disturbed top of Section 1.)

Glauconitic nanno foram chalk and glauconitic biosiliceous chalk overlying zeolitic nanno chalk.

Color is light greenish gray (5GY 8/1) with minor mottling of 5G 8/1 and sand grains colored greenish black (5GY 2/1) throughout and increasing with depth. Some yellowish gray (5Y 8/1) mottling above sharp contact in Section 4. Abundant sand-size glauconite above this contact (dark greenish gray [5GY 4/1]) and below is a thin lens of light olive (10Y 5/4) nanno clay overlying (with a sharp, uneven contact) moderate yellow brown (10YR 5/4) burrow mottled layer.

Lithified clasts near contact in Section 4 may be drilling breccia.

SMEAR SLIDE SUMMARY (%)

	1, 85	2, 95	4, 5	4, 36	4,70	4, 82
	D	D	D	M	M	D
Texture:						
Sand	10	10	15	25	5	5
Silt	35	35	25	45	35	25
Clay	55	55	60	30	60	70
Composition:						
Quartz	–	–	2	–	–	Tr
Heavy minerals	–	–	Tr	–	–	–
Clay	15	15	10	10	15	10
Volcanic glass	Tr	2	5	2	2	Tr
Glauconite	5	3	5	50	–	5
Pyrite	–	–	–	5	–	5
Micronodules	–	–	–	–	1	2
Zeolites	–	–	–	5	25	20
Foraminifers	45	30	20	–	5	10
Calc. nannofossils	35	50	48	28	52	48
Radiolarians	–	–	7	–	–	–
Sponge spicules	–	–	3	–	–	–
Barite	–	–	–	–	Tr	–

CARBONATE BOMB: $CaCO_3$ (%):
2, 95 = 78
4, 4 = 73
4, 80 = 40

X. R. D. BULK SAMPLE ANALYSES:

	Calc.	Feld.	Crist.	Zeol.	Clays :	Sm	K+C
4, 34 =	84	–	–	9	7	: 100	–
4, 38 =	48	7	13	26	6	: 50	50
4, 56 =	68	6	8	11	7	: 100	–

SITE 552 HOLE CORE 9 CORED INTERVAL 165.0–174.5 m

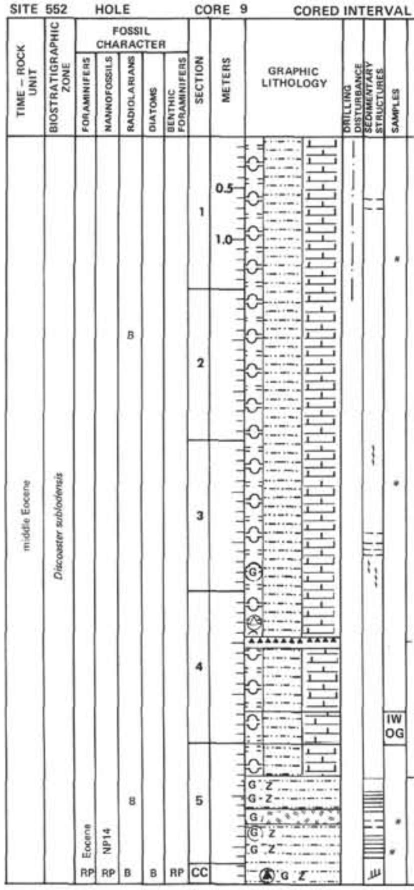

LITHOLOGIC DESCRIPTION

10YR 5/4

Glauconite nodule

Porcellanite nodule

10YR 7/4 and
5Y 5/6

10YR 4/4

Volcanic ash layer

Biosiliceous nanno marlstone with minor porcellanite and chert overlying glauconitic zeolitic mudstone and minor volcanic ash.

Color is mainly moderate yellowish brown (10YR 5/4) with burrows, lenses and laminae of paler (grayish orange [10YR 7/4]) and minor light olive brown (5Y 5/6). Below a sharp contact in Section 5 the sediment is coarser grained (sand) and colored dark yellowish brown (10YR 4/4) with minor light olive brown (2.5Y 5/6) and glauconite grains. Some laminations and cross-beds in Core-Catcher. Chert is brecciated with fractures filled with secondary chalcedony. Ash layer is palagonitized.

SMEAR SLIDE SUMMARY (%):

	1, 120	3, 40	5, 76	5, 104
	D	D	M	D
Texture:				
Sand	15	25	70	10
Silt	35	25	10	30
Clay	50	50	20	60
Composition:				
Quartz	–	–	–	5
Feldspar	–	–	20	2
Heavy minerals	5	–	–	3
Clay	20	10	10	30
Volcanic glass	5	4	–	–
Palagonite	–	–	40	–
Glauconite	–	–	15	20
Pyrite	–	5	–	5
Fe-oxide	5	3	–	–
Zeolite	–	–	5	25
Foraminifers	5	4	–	–
Calc. nannofossils	25	42	10	10
Diatoms	5	2	–	–
Radiolarians	10	5	–	–
Sponge spicules	20	25	–	–
Barite	–	–	–	Tr

CARBONATE BOMB: $CaCO_3$ (%):
3, 40 = 15
4, 112 = 24
5, 104 = 6

X. R. D. BULK SAMPLE ANALYSES:

	Calc.	Crist.	Zeol.	Clays :	I.	Sm
5, 20 =	31	23	17	29	: 40	60

SITE 552 HOLE CORE 10 CORED INTERVAL 174.5–184.0 m

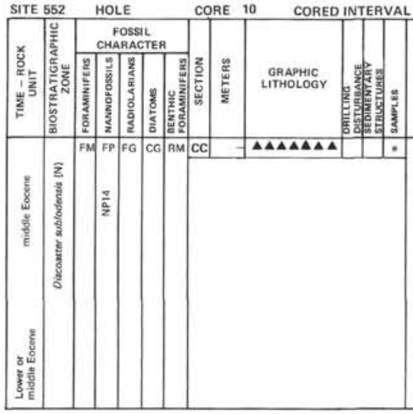

LITHOLOGIC DESCRIPTION

CHERT
Four pieces of chert (lengths 4, 4, 5, 4 cm). Two are tuffaceous and grayish blue green (5BG 5/2) to dusky blue green (5BG 3/2) Bedded with minor PORCELLANITE on margins.

Other two pieces are light olive brown (5Y 5/6) and are breccias resilicified by clear quartz. Botryoidal chalcedony lines a cavity 2 cm in size.

CARBONATE BOMB: $CaCO_3$ (%):

CC (1) = 2

NOTE: Core 11, 184.0–193.5 m: No recovery.

SITE 552 HOLE CORE 12 CORED INTERVAL 193.5–203.0 m

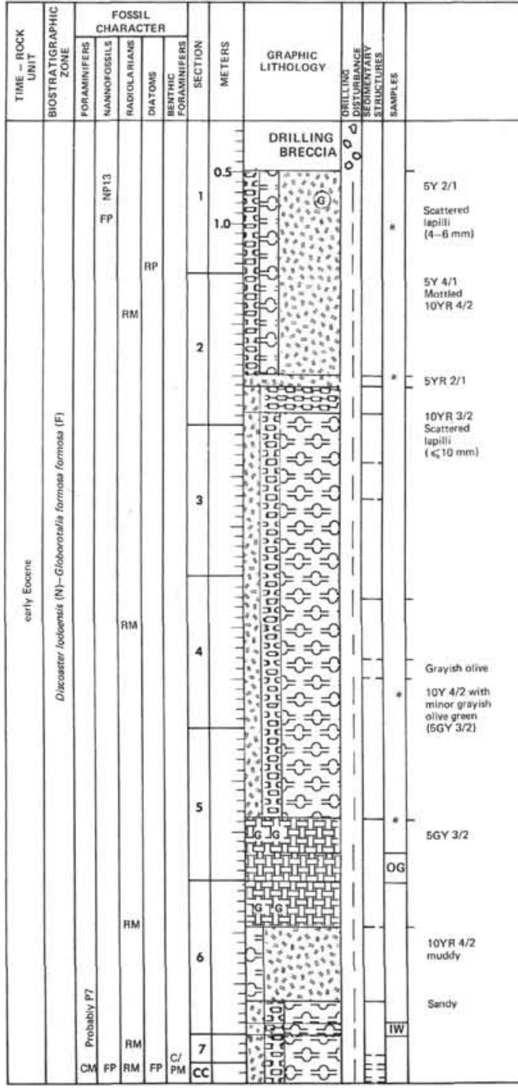

LITHOLOGIC DESCRIPTION

Calcareous biosiliceous tuff, volcanic tuff, tuffaceous chalk and tuffaceous calcareous biosiliceous ooze. Minor glauconitic spiculite, and biosiliceous tuff.

Slightly disturbed by drilling. Color is olive black (5Y 2/1), with black lapilli becoming olive gray (5Y 4/1) with depth. Mottled with dark grayish brown (10YR 4/2). Tuff layer is brownish black (5YR 2/1). Section 3 is sandy mud texture (very dark grayish brown, 10YR 3/2). Sections 4 and 5 are sandy texture, grayish olive (10Y 4/2) grading down to grayish olive green (5GY 3/2).

SMEAR SLIDE SUMMARY (%):

	1, 100	2, 105	4, 118	5, 90
	D	M	D	D
Texture:				
Sand	40	50	30	45
Silt	40	40	40	25
Clay	20	10	30	30
Composition:				
Quartz	3	3	–	–
Feldspar	3	2	3	3
Heavy minerals	3	–	2	3
Clay	10	–	5	5
Volcanic glass	36	90	15	6
Glauconite	–	–	–	35
Micronodules	–	–	–	Tr
Foraminifers	3	–	5	3
Calc. nannofossils	22	–	30	5
Diatoms	2	–	5	5
Radiolarians	3	2	5	–
Sponge spicules	15	3	30	35

CARBONATE BOMB: $CaCO_3$ (%):
1, 100 = 4
4, 118 = 11
5, 118 = 8

X. R. D. BULK SAMPLE ANALYSES:

	Calc.	Feld.	Crist.	Zeol.	Clays :	I.	Sm
2, 105 =	30	40	–	20	10 :	–	100
5, 95 =	40	27	10	5	18 :	46	54

SITE 552 HOLE CORE 13 CORED INTERVAL 203.0–212.5 m

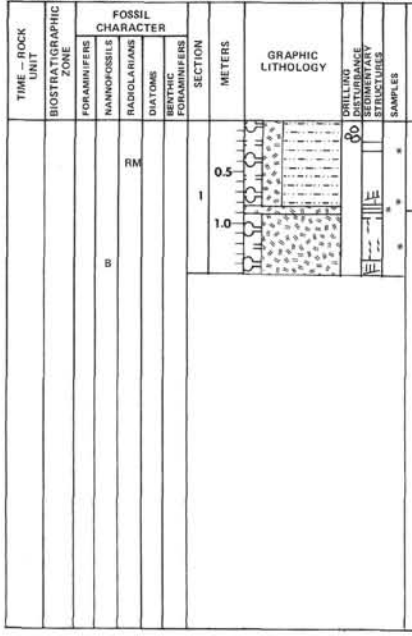

LITHOLOGIC DESCRIPTION

5GY 2/1

5G 4/1

5G 3/2

5GY 2/1

Biosiliceous tuffaceous mudstone, vitric tuff and biosiliceous vitric tuff.

Core is badly brecciated by drilling. Color is mainly greenish black (5GY 2/1) with minor dark greenish gray (5G 4/1).

The rocks are well lithified, with bedding, laminations and minor ripple-drift cross laminations and burrows. Mottled light olive gray (5Y 5/2).

SMEAR SLIDE SUMMARY (%):

	1, 32 D	1, 81 D	1, 89 D	1, 122 D
Texture:				
Sand	40	–	50	50
Silt	30	95	30	30
Clay	30	5	20	20
Composition:				
Feldspar	–	–	–	Tr
Heavy minerals	5	–	5	5
Clay	30	5	5	10
Volcanic glass	30	93	90	50
Glauconite	5	–	–	5
Carbonate unspec.	–	–	–	5
Foraminifers	–	–	Tr	5
Calc. nannofossils	5	2	–	–
Diatoms	–	–	–	2
Radiolarians	–	–	–	2
Sponge spicules	25	–	–	15

CARBONATE BOMB: $CaCO_3$ (%):
1, 83 = 2
1, 117 = 12

SITE 552 HOLE CORE 14 CORED INTERVAL 212.5–222.0 m

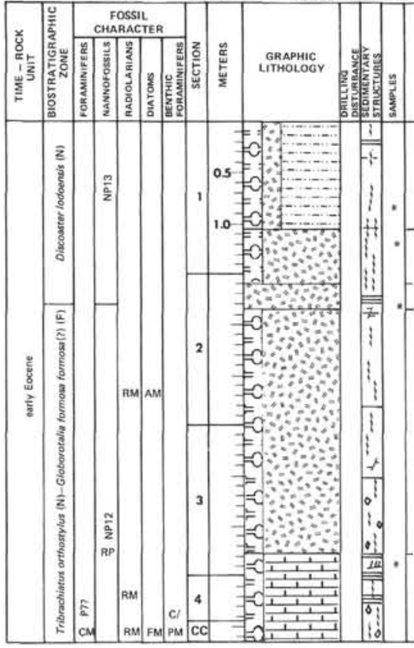

LITHOLOGIC DESCRIPTION

5GY 4/1,
5G 4/1,
and
5G 2/1

5GY 6/1
mottled
5Y 5/2

5G 2/1

5GY 6/1
mottled
5Y 5/2

5Y 5/2

Biosiliceous vitric mudstone, biosiliceous tuff, volcanic tuff, and biosiliceous nanno chalk.

Colors are dark greenish gray (5GY 4/1), greenish black (5G 2/1), olive black (5Y 2/1), greenish gray (5GY 6/1) with mottling of light olive gray (5Y 5/2). Bioturbation throughout. Soft sediment deformation (slump?) base of Section 3.

Broken up by drilling. Well-cemented. Texture sandy mud. Laminations and ripple-drift cross-laminations base of Section 3.

SMEAR SLIDE SUMMARY (%):

	1, 86 D	1, 120 D	2, 33 D	3, 140 D
Texture:				
Sand	15	50	30	20
Silt	20	30	70	40
Clay	45	20	0	40
Composition:				
Feldspar	–	–	–	5
Clay	35	10	–	15
Volcanic glass	35	50	95	–
Pyrite	–	–	2	–
Carbonate unspec.	–	5	3	50
Foraminifers	2	Tr	–	–
Calc. nannofossils	8	10	–	10
Radiolarians	–	5	–	–
Sponge spicules	20	20	Tr	20

CARBONATE BOMB: $CaCO_3$ (%):
4, 37 = 5

SITE 552 HOLE CORE 15 CORED INTERVAL 222.0–231.5 m

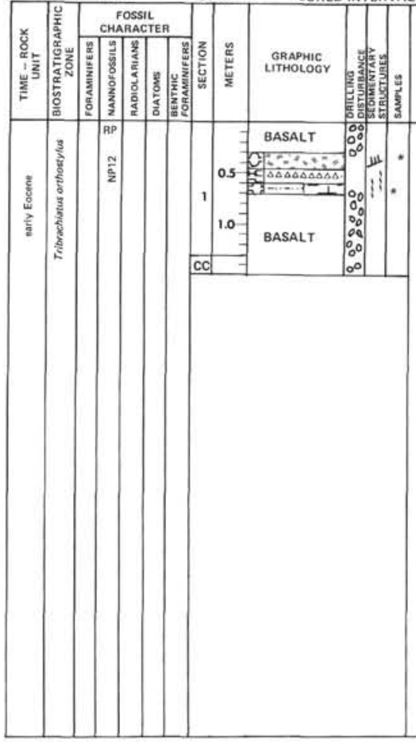

LITHOLOGIC DESCRIPTION

Biosiliceous vitric tuff, calcareous tuffaceous porcellanite and minor biosiliceous nanno marl.

(Five broken pieces in a drilling breccia of downhole cavings.)

Tuff: weakly cemented layers (1–2 cm) interbedded with finer silt-size laminae. Intensely burrowed, including a large (1 cm diameter) vertical burrow filled with volcanoclastic sand. Major color is olive gray (5Y 4/1), minor: brownish black.

Porcellanite: dark greenish gray (5G 4/1) with burrows surrounded by dark reaction rims.

SMEAR SLIDE SUMMARY (%):

	1, 36 D	1, 68 D
Texture:		
Sand	50	10
Silt	30	30
Clay	20	60
Composition:		
Clay	10	18
Volcanic glass	70	3
Palagonite	–	2
Gluconite	1	–
Pyrite	–	2
Carbonate unspec.	1	–
Foraminifers	1	Tr
Calc. nannofossils	–	50
Diatoms	2	–
Radilolarins	5	–
Sponge spicules	10	25

CARBONATE BOMB: $CaCO_3$ (%):
1, 36 = 3

X. R. D. BULK SAMPLE ANALYSES:

	Calc.	Feld.	Crist.	Zeol.	Clays	: I.	Sm.
1, 36 =	18	20	21	12	29	: 40	60
1, 89 =	8	21	12	–	59	: 28	72

SITE 552 HOLE CORE 16 CORED INTERVAL 231.5–241.0 m

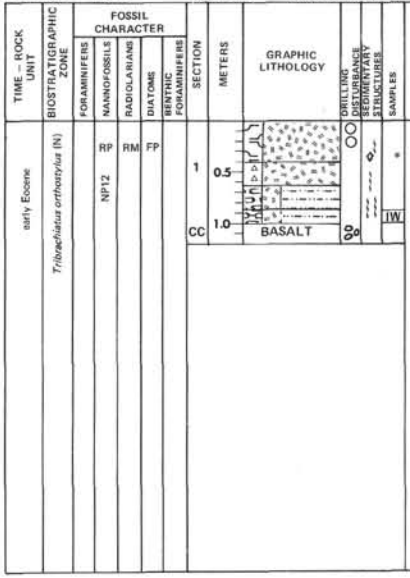

LITHOLOGIC DESCRIPTION

Cave in

Biosiliceous volcanic tuff, silicified tuff and calcareous tuffaceous mudstone.

(Lithified sediment brecciated by drilling – not a stratigraphically continuous section.)

Principal colors are:
Tuff: grayish olive green (5GY 3/2) and grayish olive (10Y 4/2)
Mudstone: olive gray (5Y 3/2), bioturbated and mottled (10Y 4/2) with intraclasts.

SMEAR SLIDE SUMMARY (%):

	1, 35 D
Texture:	
Sand	50
Silt	30
Clay	20
Composition:	
Clay	20
Volcanic glass	30
Glauconite	10
Carbonate unspec.	5
Diatoms	5
Sponge spicules	30

CARBONATE BOMB: $CaCO_3$ (%):
1, 10 = 13
1, 76 = 4

SITE 552 HOLE CORE 17 CORED INTERVAL 241.0–250.5 m

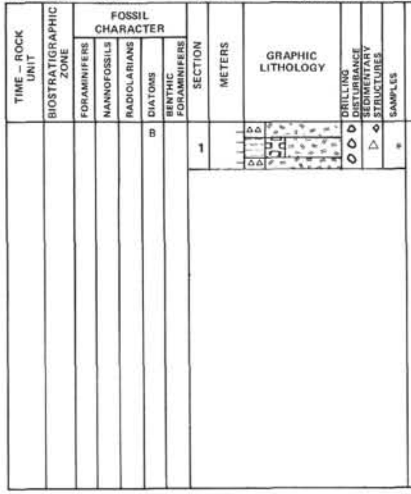

LITHOLOGIC DESCRIPTION

Silicified tuff and clayey calcareous volcanic tuff.

(Breccia due to drilling.)

Color: silicified tuff is dusky yellow green (5GY 5/2).
Clayey tuff: slightly graded with minor granule size intraclasts at base. Grayish olive green (5GY 3/2) with lenticular fine-grained laminae of olive gray (5Y 3/2).

SMEAR SLIDE SUMMARY (%):

	1, 22 D
Texture:	
Sand	40
Silt	30
Clay	30
Composition:	
Clay	30
Volcanic glass	45
Glauconie	10
Carbonate unspec.	15

CARBONATE BOMB: $CaCO_3$ (%):
1, 28 = 15

SITE 552 HOLE CORE 18 CORED INTERVAL 250.5–260.0 m

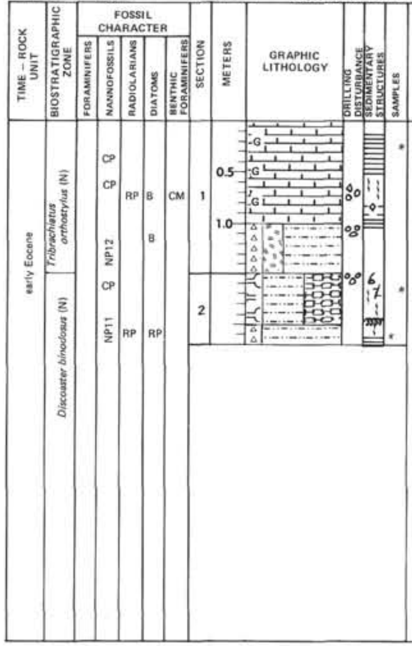

LITHOLOGIC DESCRIPTION

Lapilli

Glauconitic nanno chalk, biosiliceous marlstone and silicified mudstone.

(Broken up by drilling.)

Chalk: lenticular laminae throughout of grayish olive (10Y 4/2) and grayish olive green (5GY 3/2). Minor burrowing and some intraclasts and devitrified volcanic lapilli. Piece of bivalve.
Mudstone: olive black (5Y 2/1) and dark gray (10YR 4/1). Finely laminated greenish gray (5GY 6/1) and dark greenish gray (5GY 4/1). Soft sediment deformation (slump fold) and burrowing.

SMEAR SLIDE SUMMARY (%):

	1, 26 D	2, 18 D	2, 62 D
Texture:			
Sand	10	10	0
Silt	30	30	10
Clay	60	60	90
Composition:			
Clay	10	30	40
Volcanic glass	8	–	–
Palagonite	–	Tr	–
Glauconite	20	3	–
Carbonate unspec.	5	30	10
Foraminifers	Tr	Tr	–
Calc. nannofossils	50	12	–
Radiolarians	5	–	–
Sponge spicules	2	15	–
Silica cement	–	10	50

CARBONATE BOMB: $CaCO_3$ (%):
1, 15 = 37

SITE 552 HOLE CORE 19 CORED INTERVAL 260.0–269.5 m

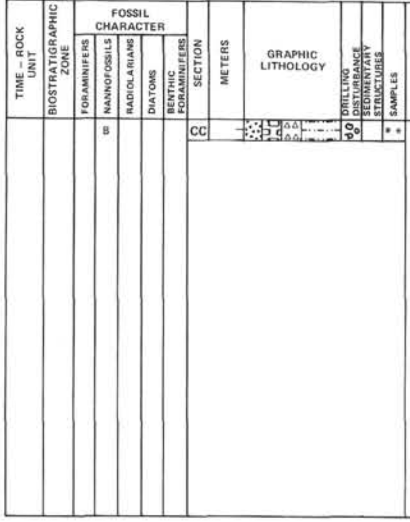

LITHOLOGIC DESCRIPTION

Pumice and calcareous silicified mudstone.

Pumice: vesicular with r. i. = 1.52. Color: greenish gray (5GY 6/1) with dark greenish gray (5GY 4/1).
Mudstone: laminated, color is gray (10YR 5/1).

SMEAR SLIDE SUMMARY (%):

	CC (1) M	CC (2) D	CC, no. 2 D
Texture:			
Sand	40	0	
Silt	40	10	
Clay	20	90	
Composition:			
Heavy minerals	Tr	–	
Clay	15	50	
Volcanic glass	60	–	
Glauconite	10	–	
Carbonate unspec.	15	5	
Calc. nannofossils	–	5	
Silica cement	–	40	

NOTE: Core 20, 269.5–279.0 m: No recovery.

SITE 552 HOLE CORE 21 CORED INTERVAL 279.0–284.0 m

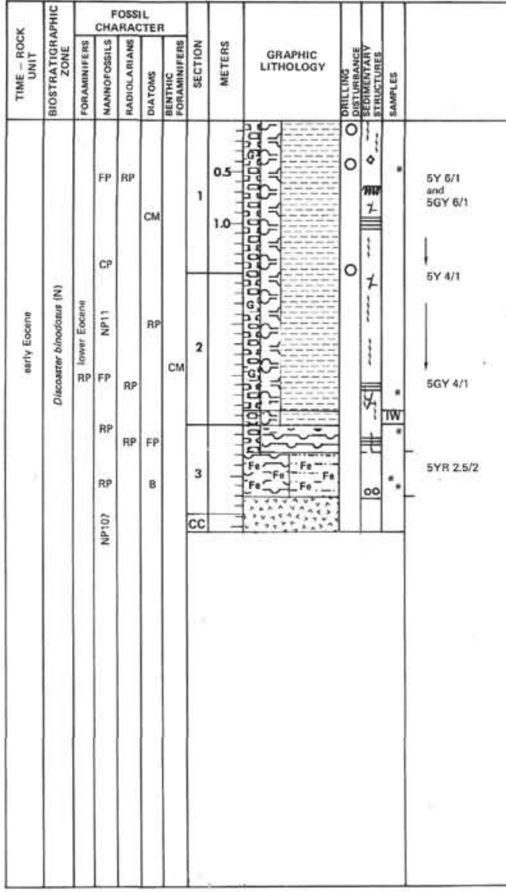

LITHOLOGIC DESCRIPTION

Calcareous biosiliceous claystone, calcareous diatomite and ferruginous diatomaceous claystone. Basalt.

(Brecciated by drilling in parts.)

Color dominantly light olive gray (5Y 6/1) to greenish gray (5GY 6/1) overlying olive gray (5Y 4/1) and dark greenish gray (5GY 4/1). Green glauconite grains throughout and burrow mottled and laminated. Intraclasts disturbed bedding and microfaults also present.

Section 3: color is dark reddish brown (5YR 2.5/2) with minor mottles of dark yellowish brown (10YR 4/2) and dark reddish brown (2.5YR 2.5/4) overlying basalts. Basalt fragments in base of overlying sediment.

SMEAR SLIDE SUMMARY (%):

	1, 49 D	2, 112 D	3, 8 D	3, 50 D	3, 60 M
Texture:					
Sand	10	20	10	10	5
Silt	40	30	60	40	30
Clay	50	50	30	50	65
Composition:					
Quartz	–	2	–	2	2
Clay	31	25	20	48	25
Volcanic glass	–	7	–	–	2
Palagonite	–	–	–	10	–
Glauconite	2	2	5	10	5
Pyrite	2	2	2	–	1
Zeolite	–	–	–	–	5
Carbonate unspec.	15	10	15	–	25
Foraminifers	–	2	–	–	–
Calc. nannofossils	15	15	10	5	15
Diatoms	25	15	43	20	20
Radiolarians	–	10	10	–	–
Sponge spicules	10	10	–	5	–

CARBONATE BOMB: $CaCO_3$ (%):
1, 48 = 28
2, 112 = 18
2, 131 = 19
3, 30 = 3

X. R. D. BULK SAMPLE ANALYSES:

	Calc.	Feld.	Crist.	Clays	:	I.	Sm.
1, 43 =	14	–	–	86	:	–	100
3, 39 =	17	–	40	43	:	–	100
3, 46 =	10	8	53	29	:	11	89
3, 58 =	54	–	30	16	:	–	100

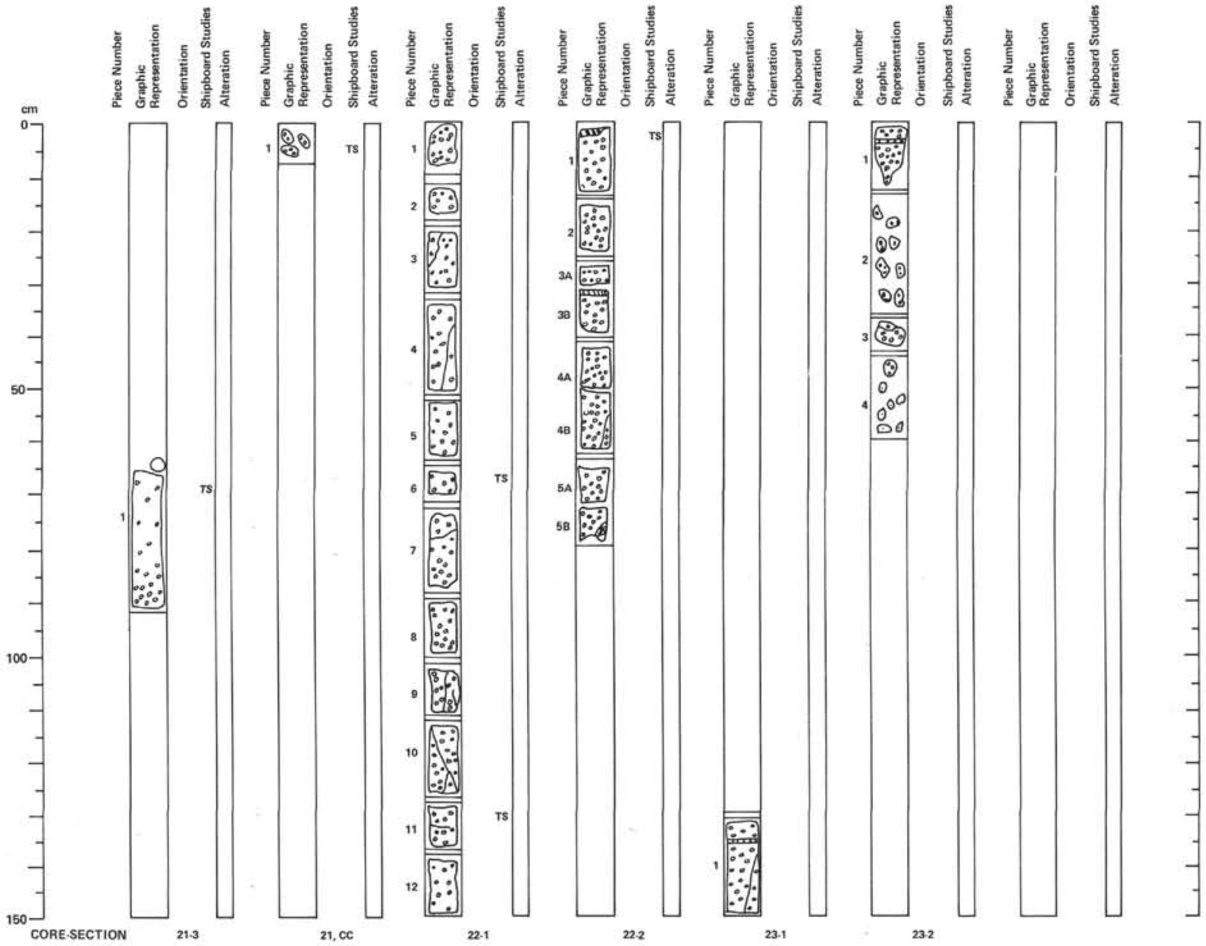

LEG 81, HOLE 552

CORE 21, SECTION 3 and Core-Catcher — Depth 283.6–284.0 m

Phyric vesicular basalt (full description see 552-22-1) differing in that vesicles are largely infilled and are less common. One piece lies within sediment and has chilled margins surrounding central zone with visible plagioclase laths (small pillow?). Grain size is generally finer than underlying section, and vesicles range up to 5 mm in diameter.

CORE 22, SECTION 1 — Depth 284.0–285.5 m

Dark gray to grayish black (N3–N2) phyric vesicular BASALT. Visible plagioclase laths (up to 3 mm length) and pyroxenes(?) numerous in fine-grained groundmass. Vesicles up to 8 mm widespread throughout, but Piece 1 has 2 cm band with vesicles rare. Vesicles infilled with black (N1) mineral identified on XRD as Fe-Mg saponite (smectite); also brassy yellow pyrite. Occasional fractures (Pieces 3, 4, 7, 9, 10, and 11) also infilled with black mineral.

CORE 22, SECTION 2 — Depth: 285.5–286.3 m

Phyric vesicular BASALT as 552-22-1 but with fractures infilled by white fibrous calcite (Pieces 1, 3B, and 5B) in addition.

CORE 23, SECTION 1 — Depth: 288.5–290.0 m

0–130 cm: Drilling breccia of basalt, chert, and drilling mud. Clasts up to 1 cm.

130–150 cm: Phyric vesicular basalt with calcite veining as before.

CORE 23, SECTION 2 — Depth: 290.0–290.6 m

Phyric vesicular basalt as before.

SITE 552 HOLE A CORE (HPC) 1 CORED INTERVAL 0.0–4.0 m

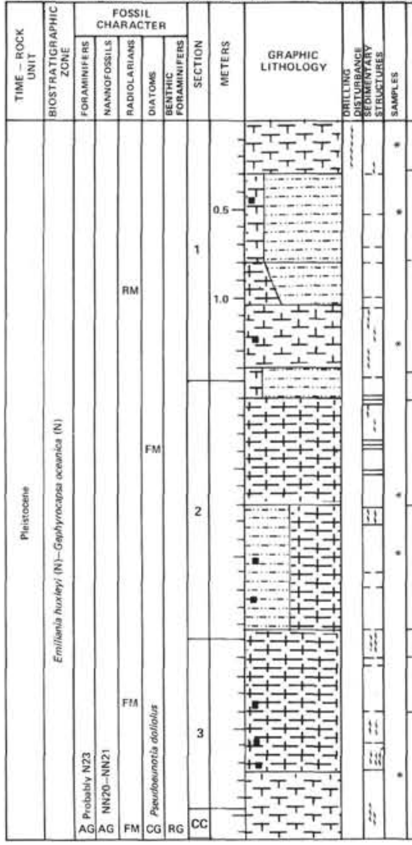

LITHOLOGIC DESCRIPTION

10YR 7/3
10YR 5/4
Mottled with 10YR 7/3 and 10YR 6/3
10YR 5/3
10YR 8/2
10YR 5/4
10YR 7/3
10YR 5/4
10YR 7/3

Foram-nanno ooze interbedded with foram-nanno marl. Minor interbeds of foram-ooze, nanno-ooze and foram mud.

Color is white (10YR 8/2) interbedded with brown (10YR 5/3) and yellowish brown (10YR 5/4). Burrow mottling is intense at the boundaries.

Relatively undisturbed with some coarser foram-rich, laminae preserved. Dropstones and sand and granule size terrigenous clasts are common throughout.

SMEAR SLIDE SUMMARY (%)

SMEAR SLIDE SUMMARY (%):

	1, 14 D	1, 52 D	1, 128 D	2, 68 D	2 98 D	3, 78 D
Texture:						
Sand	70	35	15	20	25	50
Silt	20	25	25	8	15	30
Clay	10	40	60	80	60	20
Composition:						
Quartz	5	15	5	–	15	4
Feldspar	–	5	2	–	–	3
Mica	–	5	–	–	–	–
Heavy minerals	–	10	3	–	5	1
Clay	5	35	15	10	30	12
Carbonate unspec.	–	15	–	–	10	–
Foraminifers	80	13	10	20	10	65
Calc. nannofossils	10	–	65	70	25	10
Diatoms	–	Tr	–	–	–	–
Radiolarians	Tr	–	–	–	–	–
Sponge spicules	–	–	–	Tr	–	Tr
Fish remains	–	–	–	–	–	5
Dolomite	–	2	–	Tr	5	–

CARBONATE BOMB: $CaCO_3$ (%):

1, 7 = 80 2, 68 = 83
1, 48 = 34 2, 98 = 28
1, 128 = 51 3, 88 = 72

X. R. D. BULK SAMPLE ANALYSES:

	Calc.	Feld.	Qtz.	Clays :	K+C	I.	Sm.
1, 10 =	86	4	8	2 :	–	–	100
1, 56 =	40	8	40	12 :	32	37	31
2, 69 =	83	2	12	3 :	–	–	100

SITE 552 HOLE A CORE (HPC) 2 CORED INTERVAL 4.0–9.0 m

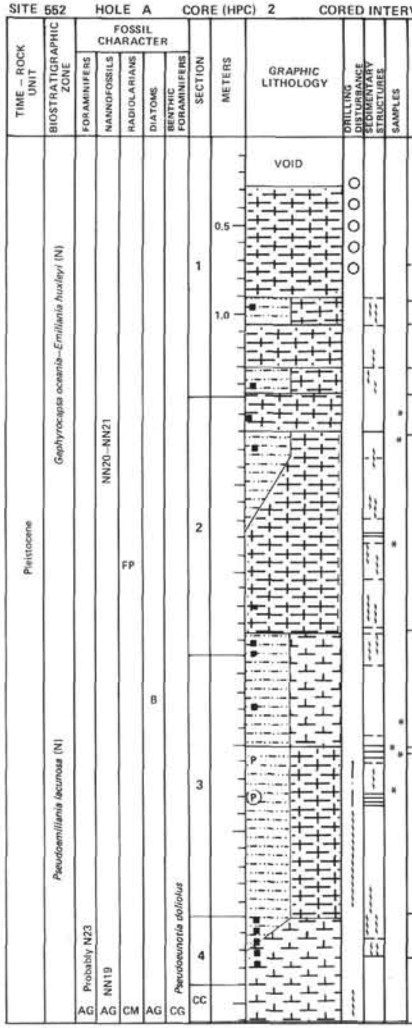

LITHOLOGIC DESCRIPTION

10YR 6/4
10YR 7/2
10YR 6/3
10YR 7/2
10YR 7/3
10YR 7/2 sandy
10YR 6/4
10YR 7/2
10YR 8/1 Foram laminae
N9
Pebble (angular 5 mm)
Pebbles (angular (1–2 cm)
10YR 5/3
5Y 4/1 and 5GY 4/1
5GY 6/1 mottled with 5Y 4/2
N9 mottled 10YR 6/1
Pebble, granite (1 cm) 5B 9/1

Foram-nanno ooze interbedded with foram-nanno marl. Minor interbeds of nanno-foram ooze, nanno ooze and nanno marl. Relatively undisturbed.

Color is white (N9 and 10YR 8/1) and light gray (10YR 7/2) interbedded with brown (10YR 5/3) and light yellowish brown (10YR 6/4). Sharp color change below Section 3, 50 cm to greenish gray (5GY 6/1) and olive gray (5Y 4/1 and 5Y 4/2) overlying bluish white (5B 9/1).

Bioturbation is common; sharp contacts and laminae are also preserved. Dark terrigenous sand is common in some laminae and forams are concentrated in others. Pebbles (some faceted) of igneous and metamorphic origin are common. Below Section 3, 50 cm get authigenic pyrite as nodules and disseminated.

SMEAR SLIDE SUMMARY (%):

	2, 10 D	2, 24 D	2, 82 D	3, 38 D	3, 52 M
Texture:					
Sand	30	20	5	10	10
Silt	20	30	10	30	30
Clay	50	50	85	60	60
Composition:					
Quartz	5	15	2	10	15
Feldspar	2	–	–	3	3
Mica	–	3	–	–	–
Heavy minerals	1	2	–	2	2
Clay	15	30	5	20	48
Volcanic glass	–	–	–	1	–
Glauconite	–	–	–	1	3
Pyrite	–	–	–	Tr	5
Carbonate unspec.	–	2	5	10	5
Foraminifers	35	35	15	15	2
Calc. nannofossils	42	10	73	35	20
Radiolarians	–	–	–	Tr	–
Sponge spicules	Tr	–	–	Tr	2
Dolomite	–	3	–	3	–

	3, 55 M	3, 78 D	4, 28 D
Texture:			
Sand	5	25	5
Silt	10	25	10
Clay	85	50	80
Composition:			
Quartz	3	5	2
Feldspar	–	–	1
Mica	–	5	–
Heavy minerals	2	–	1
Clay	40	25	5
Carbonate unspec.	5	–	5
Foraminifers	10	20	10
Calc. nannofossils	40	45	80
Dolomite	–	Tr	1

CARBONATE BOMB: $CaCO_3$ (%):

2, 25 = 52 3, 78 = 32
2, 99 = 87 4, 28 = 88
3, 38 = 34

X. R. D. BULK SAMPLE ANALYSES.

	Calc.	Feld.	Qtz.	Clays :	K+C	I.	Sm.
1, 38 =	57	3	32	8 :	45	24	31
3, 38 =	41	11	42	6 :	35	27	38
3, 80 =	61	6	25	8 :	31	34	35

SITE 552 HOLE A CORE (HPC) 3 CORED INTERVAL 9.0–14.0 m

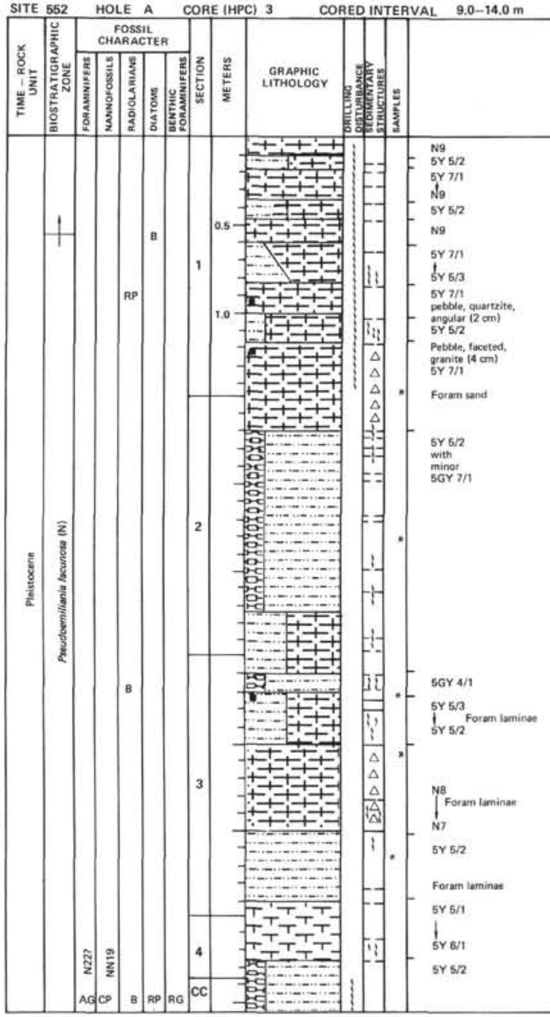

LITHOLOGIC DESCRIPTION

Nanno-foram ooze interbedded with foram-nanno marl and calcareous mud. Minor interbeds of foram-nanno ooze, foram ooze and mud.

Color is either olive gray (5Y 5/2) and dark greenish gray (5GY 4/1) interbedded with light gray (N7), very light gray (N8), gray (5Y 6/1) and white (N9).

Top section is very disturbed. Pebbles, granules and sand are scattered throughout, particularly in the darker layers. Contacts generally gradational due to bioturbation. Burrows below contacts are filled with overlying lithology and some with foram sand.

Suggestion of grading in the calcareous oozes.

SMEAR SLIDE SUMMARY (%):

	1, 147	2, 84	3, 20	3, 59	3, 118
	D	D	M	D	D
Texture:					
Sand	30	35	40	30	10
Silt	20	15	35	10	60
Clay	50	50	25	60	30
Composition:					
Quartz	5	15	40	4	50
Feldspar	–	1	20	–	10
Mica	–	1	–	1	–
Heavy minerals	–	2	5	–	3
Clay	10	30	25	10	10
Volcanic glass	–	–	–	–	6
Glauconite	2	–	–	–	1
Carbonate unspec.	–	5	–	–	1
Foraminifers	33	20	–	35	5
Calc. nannofossils	50	25	10	50	10
Sponge spicules	Tr	–	–	–	–
Dolomite	–	1	–	Tr	4

CARBONATE BOMB: $CaCO_3$ (%):
2, 88 = 24
3, 57 = 89
3, 118 = 8

X. R. D. BULK SAMPLE ANALYSES:

	Calc.	Feld.	Qtz.	Clays	: K+C	I.	Sm.
3, 59 =	87	4	4	5	: –	38	62
3, 117 =	13	12	62	13	: 41	36	23

SITE 552 HOLE A CORE (HPC) 4 CORED INTERVAL 14.0–19.0 m

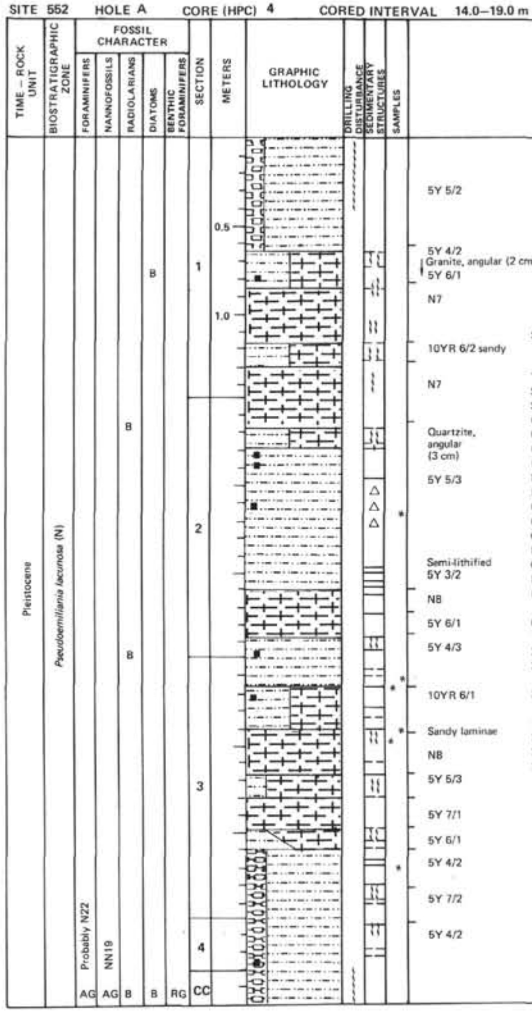

LITHOLOGIC DESCRIPTION

Nanno-foram ooze interbedded with nanno-foram marl, calcareous mud and mud. Minor interbeds of foram-nanno ooze and foram marl.

Color is olive gray to dark olive gray (5Y 5/2, 5Y 4/2, 5Y 5/3) interbedded with light gray (N7, N8, 5Y 7/1). In general thin core is undisturbed and quite firm. The darker olive laminae are semilithified. Scattered terrigenous dropstones and sand throughout. Burrow mottling common. Laminae of coarser forams and terrigenous sand occur in marls and muds.

SMEAR SLIDE SUMMARY (%):

	2, 67	3, 13	3, 19	3, 40	3, 49	3, 120
	D	M	D	M	D	D
Texture:						
Sand	40	50	35	50	15	50
Silt	10	40	35	15	25	10
Clay	50	10	30	35	60	40
Composition:						
Quartz	35	45	15	5	–	35
Feldspar	–	15	–	1	–	–
Mica	3	–	–	–	–	5
Heavy minerals	–	5	2	1	–	–
Clay	45	30	15	10	10	50
Glauconite	–	–	2	–	–	–
Carbonate unspec.	10	5	–	–	5	5
Foraminifers	5	–	35	50	30	3
Calc. nannofossils	2	–	33	38	55	2
Diatoms	–	–	–	–	Tr	–
Dolomite	–	–	3	–	–	–

CARBONATE BOMB: $CaCO_3$ (%):

1, 129 = 76	3, 19 = 50
2, 68 = 7	3, 48 = 88
3, 9 = 4	4, 17 = 11

X. R. D. BULK SAMPLE ANALYSES:

	Calc.	Feld.	Qtz.	Clays	:	K+C	I.	Sm
1, 7 =	85	–	12	3	:	–	–	100
2, 66 =	11	8	65	17	:	40	40	20
2, 139 =	24	16	47	13	:	36	39	25
2, 147 =	7	12	64	17	:	44	35	21

SITE 552 HOLE A CORE (HPC) 5 CORED INTERVAL 19.0–24.0 m

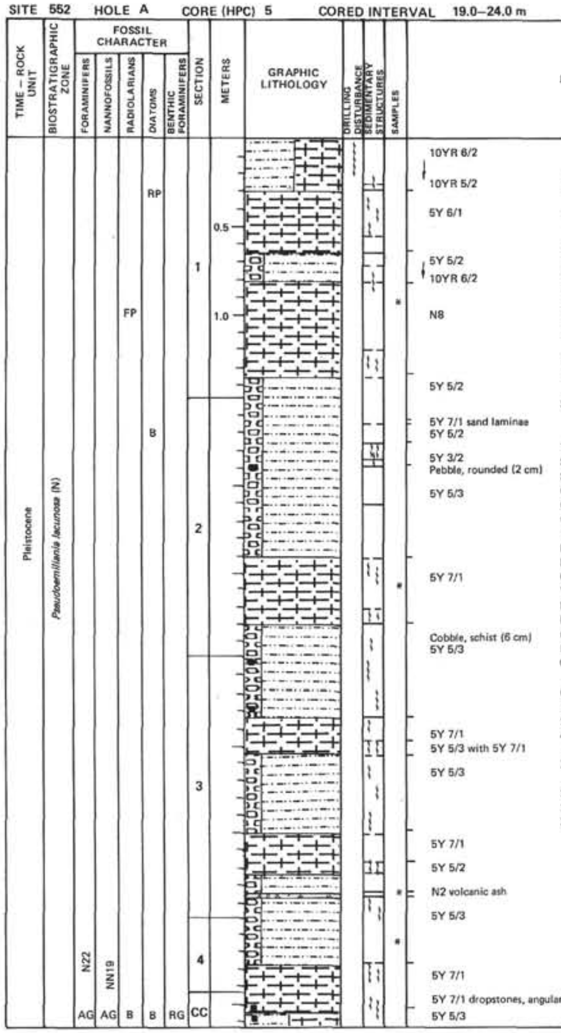

LITHOLOGIC DESCRIPTION

Nanno-foram ooze interbedded with calcareous mud and nanno-foram marl. Minor interbeds of foram-nanno ooze.

Volcanic ash bed in Section 3 (grayish black [N2]).

Color is olive and olive gray (5Y 5/3, 5Y 3/2, 5Y 5/2) interbedded with very light gray (N8) and light gray (5Y 7/1). Burrow mottling results in transitional colors between the layers. Relatively undisturbed, a few thin beds rich in sand-size particles (foram and clastics) have sharp contacts. Most contacts are gradational. Pyrite streaks (?burrows) are common in calcareous ooze layers.

Pebble, granule and sand-size lithoclasts are common throughout.

SMEAR SLIDE SUMMARY (%):

	1, 92	2, 108	3, 136	4, 16
	D	D	M	D
Texture:				
Sand	20	50	50	20
Silt	30	10	40	30
Clay	50	40	10	50
Composition:				
Quartz	3	4	10	25
Feldspar	–	–	5	4
Mica	–	1	–	1
Heavy minerals	–	–	3	2
Clay	10	15	10	20
Volcanic glass	–	–	10	–
Palagonite	–	–	42	–
Pyrite	–	–	15	–
Carbonate unspec.	2	–	–	–
Foraminifers	35	55	3	10
Calc. nannofossils	50	25	2	38

CARBONATE BOMB: $CaCO_3$ (%).
1, 96 = 89
2, 107 = 85
4, 16 = 12

X. R. D. BULK SAMPLE ANALYSES:

	Calc.	Feld.	Qtz.	Clays :	K+C	I.	Sm.
2, 37 =	3	13	62	22 :	40	27	33
2, 87 =	42	13	37	8 :	42	–	58
2, 107 =	85	–	12	3 :	–	–	100

SITE 552 HOLE A CORE (HPC) 6 CORED INTERVAL 24.0–29.0 m

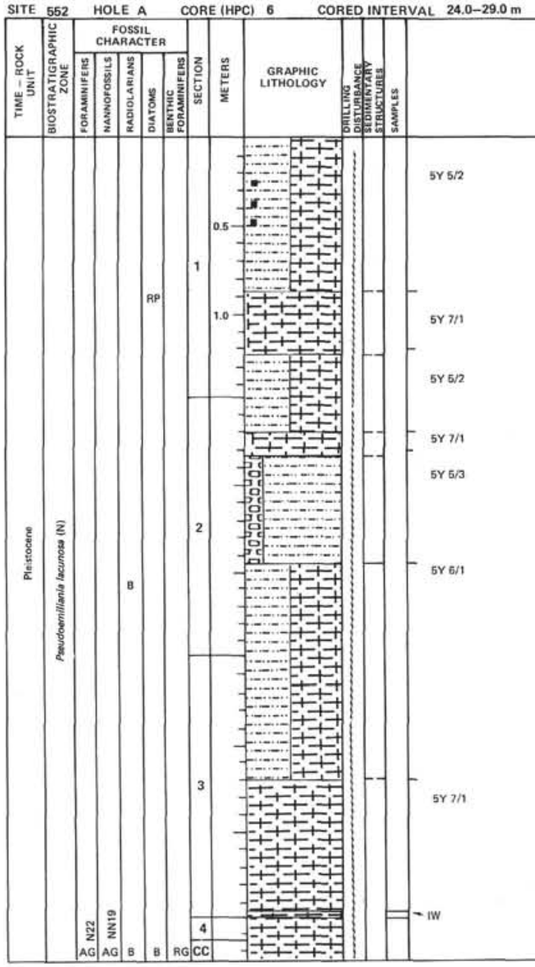

LITHOLOGIC DESCRIPTION

Very disturbed core consisting of nanno-foram ooze interbedded with nanno-foram marl and calcareous mud.

Principal colors are olive gray (5Y 5/2) alternating with light gray (5Y 7/1) and olive gray (5Y 5/2) and light gray (5Y 6/1).

Several pebbles and granules of terrigenous origin occur at top of Section 1.

SITE 552 HOLE A CORE (HPC) 7 CORED INTERVAL 29.0–34.0 m

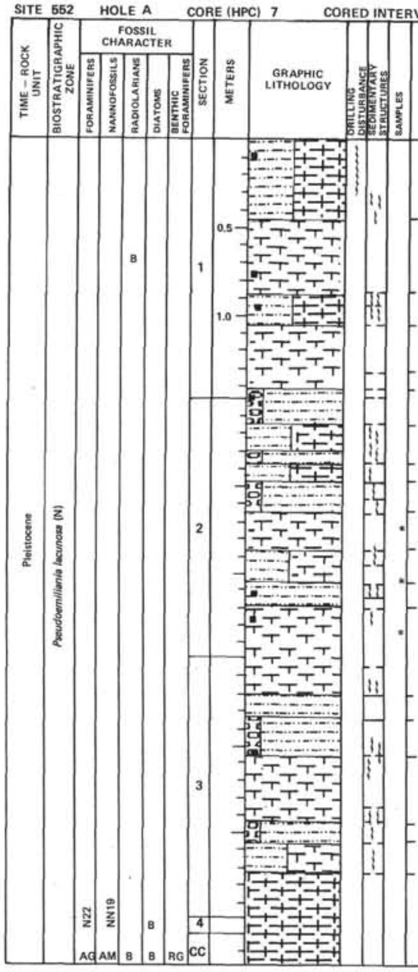

Pebble, quartzite, rounded (2 cm)
5Y 4/2
10YR 7/1
Dropstone, faceted (5 mm)
5Y 5/3
10YR 7/1
5Y 6/2
5Y 5/2 Lithified laminae
5Y 5/4
5Y 5/3
mottled
5Y 5/2
5Y 7/1
5Y 4/2
5Y 7/1
5Y 4/2
5Y 6/1 sandy
5Y 5/2 sandy
5Y 8/1
5Y 7/1
5Y 5/2 stiff mud
5Y 5/3
5Y 7/1
5Y 5/2
5Y 7/1 pyrite
5Y 8/1

LITHOLOGIC DESCRIPTION

Foram ooze interbedded with nanno-foram marl, foram marl, calcareous mud and mud.

Color is light gray (10YR 7/1) and white (5Y 8/1) alternating with olive (5Y 5/3), olive gray (5Y 5/2, 5Y 4/2). *Bioturbation leads to mottling of these colors and gradational boundaries.*

The light colored layers have a sandy texture (foram rich). Dark colored terrigenous grains occur throughout as do dropstones. Pyrite is associated with some burrows.

SMEAR SLIDE SUMMARY (%):

	2, 76 D	2, 109 D	2, 137 D
Texture:			
Sand	25	20	40
Silt	20	50	15
Clay	55	30	45
Composition:			
Quartz	5	40	1
Feldspar	–	10	1
Heavy minerals	–	5	–
Clay	10	10	10
Volcanic glass	–	5	–
Carbonate unspec.	–	5	3
Foraminifers	40	5	50
Calc. nannofossils	45	15	35
Dolomite	–	5	–

CARBONATE BOMB: $CaCO_3$ (%):
2, 77 = 84
2, 108 = 7
2, 137 = 89

SITE 552 HOLE A CORE (HPC) 8 CORED INTERVAL 34.0–39.0 m

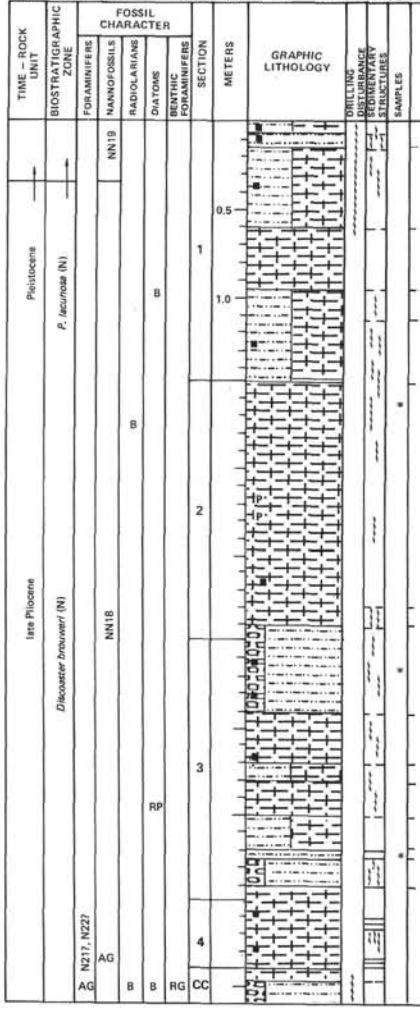

5Y 6/1
5Y 5/2
5Y 6/1
5Y 7/1
5Y 6/1
5Y 7/1
N8
5Y 7/1 and 5Y 4/2
5Y 4/2
5Y 7/1
5Y 5/1
5Y 7/1
5Y 5/2
5Y 3/2 semilithified mud
5Y 4/3–5Y 5/2
N8
laminations of light gray (5Y 6/1)
5Y 3/2

LITHOLOGIC DESCRIPTION

Nanno-foram ooze and foram-nanno ooze interbedded with nanno marl, calcareous mud and minor mud.

Color is very light gray (N8), light gray (5Y 7/1, 5Y 6/1) interbedded with olive gray (5Y 5/2, 5Y 4/2) and dark olive gray (5Y 3/2). Bioturbation has resulted in gradational contacts between the major lithologies. The core is relatively undisturbed and there is a semilithified mud layer in Section 3. Faint laminations occur in the calcareous ooze in Section 4.

The alternating light and dark colored cycles are clear and *on two scales in this core (~2 m and < 0.5 m).*

Dropstones and dark colored sand grains occur throughout.

SMEAR SLIDE SUMMARY (%):

	2, 17 D	3, 17 D	3, 121 M
Texture:			
Sand	20	20	15
Silt	20	10	25
Clay	60	70	60
Composition:			
Quartz	–	5	25
Feldspar	–	–	5
Mica	–	1	–
Heavy minerals	–	1	5
Clay	20	15	60
Glauconite	–	–	1
Pyrite	–	–	1
Carbonate unspec.	–	3	–
Foraminifers	30	15	–
Calc. nannofossils	45	60	3
Diatoms	2	–	–
Radiolarians	1	–	–
Sponge spicules	2	–	–

CARBONATE BOMB: $CaCO_3$ (%):
2, 17 = 92
3, 17 = 29

SITE 552 HOLE A CORE (HPC) 9 CORED INTERVAL 39.0–44.0 m

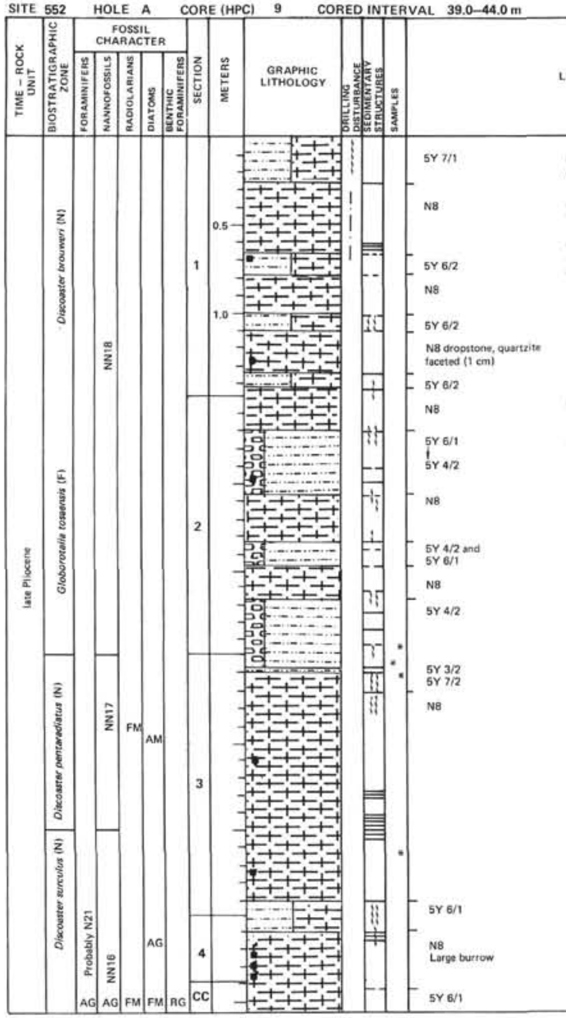

LITHOLOGIC DESCRIPTION

Nanno-foram ooze interbedded with nanno-foram marl, calcareous mud and minor mud.

Alternating color (and carbonate content) cycles are distinct (as with all overlying cores).

Color is very light gray (N8) and light gray (5Y 6/1) alternating with light olive gray (5Y 6/2), olive gray (5Y 4/2) with minor dark olive gray (5Y 3/2).

The core is relatively undisturbed with minor burrow mottling and generally sharp contacts between layers. Laminae are well developed in the calcareous oozes.

Dropstones and black sand and granule size terrigenous clasts common.

SMEAR SLIDE SUMMARY (%):

	2, 147	3, 9	3, 14	3, 117
	D	M	D	D
Texture:				
Sand	30	30	10	20
Silt	20	15	40	30
Clay	50	55	50	50
Composition:				
Quartz	15	30	12	–
Feldspar	2	3	2	–
Mica	–	1	–	–
Heavy minerals	3	3	1	1
Clay	15	50	10	15
Volcanic glass	–	–	Tr	1
Carbonate unspec.	10	5	–	–
Foraminifers	20	5	35	35
Calc. nannofossils	35	3	40	42
Diatoms	–	–	–	2
Sponge spicules	–	–	1	2
Dolomite	–	–	Tr	2

CARBONATE BOMB: $CaCO_3$ (%):
2, 147 = 23
3, 17 = 92
3, 117 = 67

X. R. D. BULK SAMPLE ANALYSES:

	Calc.	Feld.	Qtz.	Clays :	K+C	I.	Sm.
1, 28 =	95	–	2	3 :	–	–	100
2, 127 =	22	12	51	15 :	37	28	35
2, 138 =	44	6	44	6 :	37	33	30

SITE 552 HOLE A CORE (HPC) 10 CORED INTERVAL 44.0–49.0 m

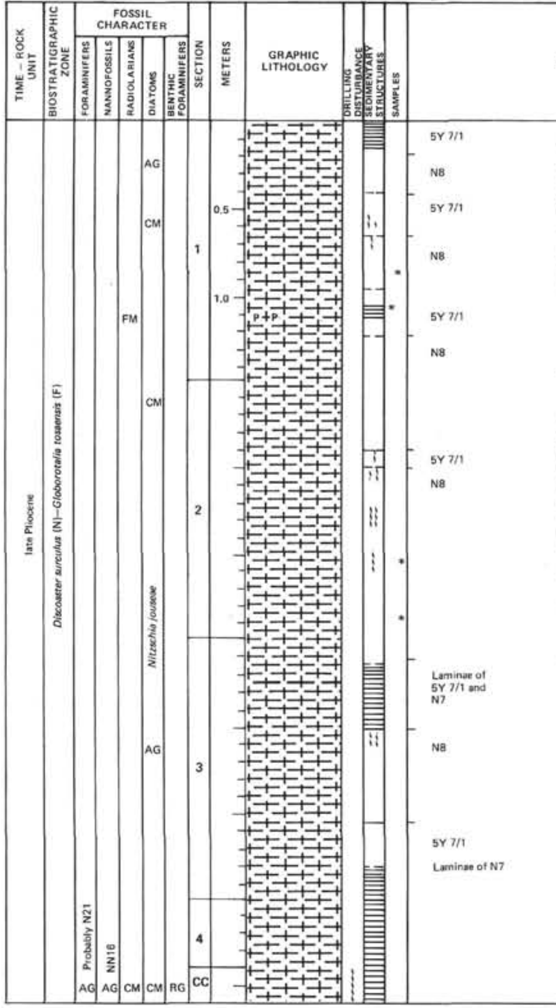

LITHOLOGIC DESCRIPTION

Nanno-foram ooze and foram-nanno ooze.

Color is mainly very light gray (N8) alternating with light gray (5Y 7/1, N7) . Slight color variations indicate burrow mottling and laminations.

The core is undisturbed and the laminations are confined to the slightly darker layers in the core. The boundaries of the color changes are gradational. The faint color alternations (or cycles) cannot be distinguished in the smear slides or carbonate bomb data.

Black pyrite patches in Section 1. The darker layers (5Y 7/1) are foram rich. Rare granule and sand size terrigenous clasts.

SMEAR SLIDE SUMMARY (%):

	1, 87	1, 107	2, 107	2, 139
	D	M	D	D
Texture:				
Sand	20	–	25	10
Silt	30	50	5	20
Clay	50	50	70	70
Composition:				
Quartz	–	–	Tr	–
Clay	20	20	15	10
Volcanic glass	1	–	–	1
Pyrite	–	30	–	–
Carbonate unspec.	5	–	–	5
Foraminifers	35	20	25	20
Calc. nannofossils	35	30	55	54
Diatoms	1	–	2	5
Sponge spicules	3	–	3	5

CARBONATE BOMB: $CaCO_3$ (%):
1, 87 = 92
1, 107 = 92
2, 107 = 90
2, 137 = 92

SITE 552 HOLE A CORE (HPC) 11 CORED INTERVAL 49.0–54.0 m

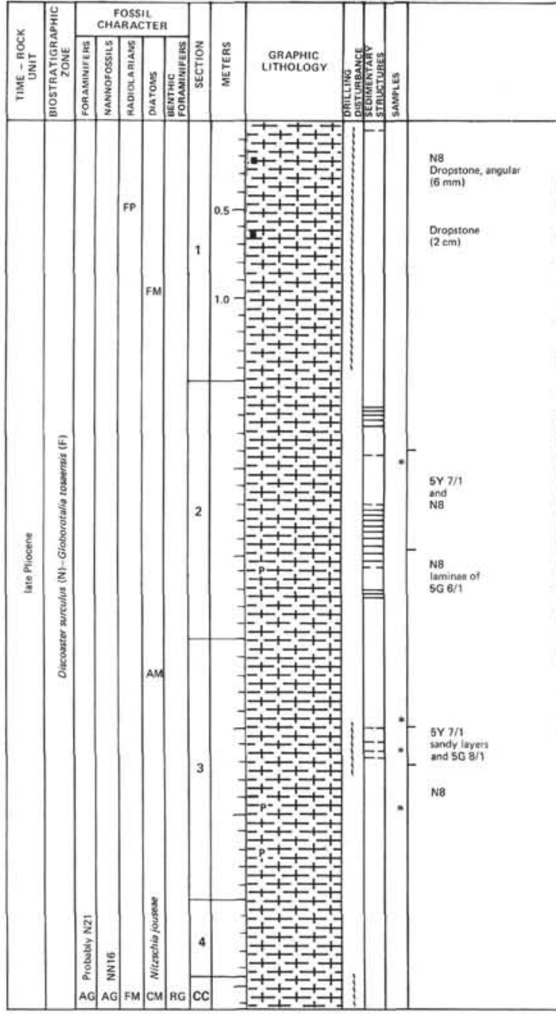

LITHOLOGIC DESCRIPTION

Foram-nanno ooze and nanno-foram ooze.

Color is dominated by very light gray (N8) grading into slightly darker layers of light gray (5Y 7/1). These alternatives are faint. Very disturbed in Section 1.

Minor burrowing and some black pyrite patches.

The laminations are due to slight changes in texture (foram:nanno ratio) and color (greenish gray [5G 6/1]).

Rare dropstones. In general less forams and terrigenous mud compared with overlying cores.

SMEAR SLIDE SUMMARY (%):

	2, 47 D	3, 48 D	3, 66 M	3, 97 D
Texture:				
Sand	25	10	20	10
Silt	20	10	5	10
Clay	55	80	75	80
Composition:				
Quartz	–	1	–	–
Clay	15	10	20	15
Pyrite	Tr	–	–	–
Carbonate unspec.	–	1	–	–
Foraminifers	35	10	25	20
Calc. nannofossils	45	70	53	60
Diatoms	–	1	Tr	Tr
Radiolarians	–	2	Tr	Tr
Sponge spicules	5	5	2	5

CARBONATE BOMB: $CaCO_3$ (%).
2, 47 = 91
3, 47 = 93
3, 97 = 93

X. R. D. BULK SAMPLE ANALYSES:

	Calc.	Feld.	Qtz.	Clays : K+C	I.	Sm.
3, 8 =	95	–	3	2 : –	–	100
3, 18 =	97	–	–	3 : –	–	100

SITE 552 HOLE A CORE (HPC) 12 CORED INTERVAL 54.0–59.0 m

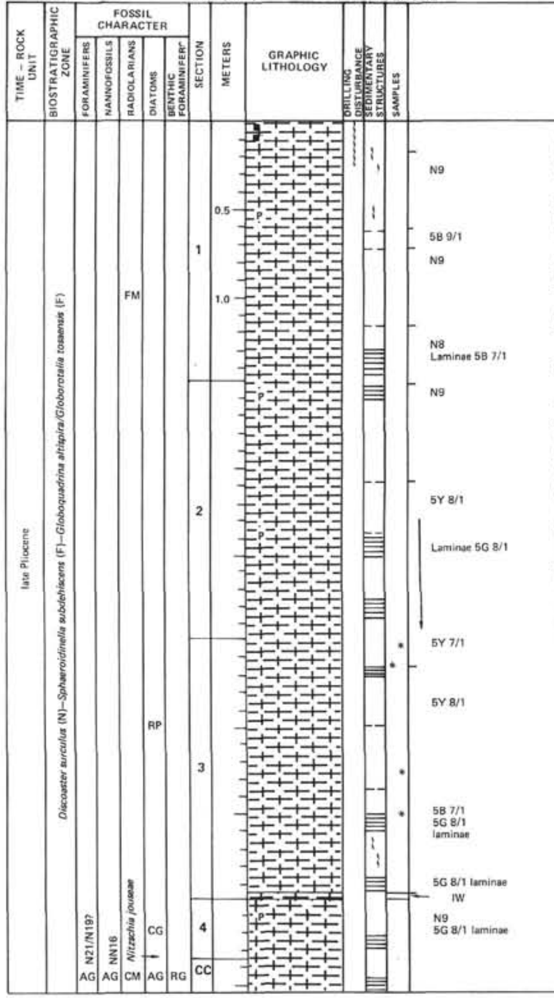

LITHOLOGIC DESCRIPTION

Foram-nanno ooze with minor nanno-foram ooze. (Granite dropstones in badly disturbed top of core are downhole contaminants.)

Color is mainly white (N9, 5Y 8/1) with laminations of light bluish gray (5B 7/1), light greenish gray (5G 8/1) and light bluish gray (5B 7/1).

Minor burrowing with pyrite (black) associated with burrows in white layers (as black halos around burrow and as a filling).

Dominant texture is sandy mud and the laminae are muddy sand.

SMEAR SLIDE SUMMARY (%):

	3, 8 D	3, 19 M	3, 77 D	3, 102 M
Texture:				
Sand	10	25	10	10
Silt	10	25	5	10
Clay	80	50	85	80
Composition:				
Clay	15	25	20	20
Carbonate unspec.	2	–	–	–
Foraminifers	20	35	10	15
Calc. nannofossils	60	35	68	60
Diatoms	1	–	–	2
Radiolarians	Tr	–	–	1
Sponge spicules	2	2	2	2
Dolomite	–	3	–	–

CARBONATE BOMB: $CaCO_3$ (%):
3, 8 = 88
3, 77 = 94

SITE 552 HOLE A CORE (HPC) 13 CORED INTERVAL 59.0–62.0 m

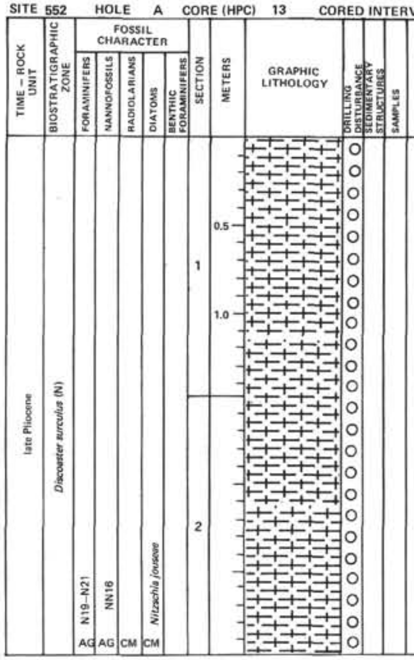

LITHOLOGIC DESCRIPTION

Foram-nanno ooze.

All structures and textures completely destroyed by drilling.

SITE 552 HOLE A CORE (HPC) 14 CORED INTERVAL 62.0–67.0 m

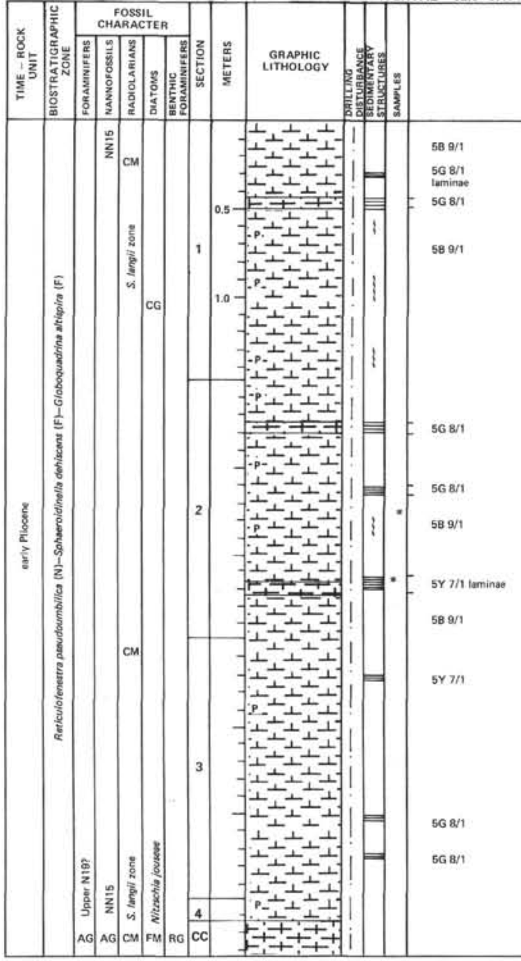

LITHOLOGIC DESCRIPTION

Nanno ooze with minor foram-nanno ooze.

Color is bluish white (5B 9/1) with laminations of light greenish gray (5G 8/1) and light gray (5Y 7/1). Patches and streaks of black pyrite are common (probably burrows).

Core is moderately disturbed and the sediment is soft with a sandy mud texture.

SMEAR SLIDE SUMMARY (%):

	2, 78	2, 118
	D	M
Texture:		
Sand	10	10
Silt	5	10
Clay	85	80
Composition:		
Clay	10	20
Carbonate unspec.	–	2
Foraminifers	10	15
Calc. nannofossils	77	60
Diatoms	Tr	1
Radiolarians	Tr	1
Sponge spicules	3	1

CARBONATE BOMB: $CaCO_3$ (%):
2, 77 = 95

SITE 552 HOLE A CORE (HPC) 15 CORED INTERVAL 67.0–72.0 m

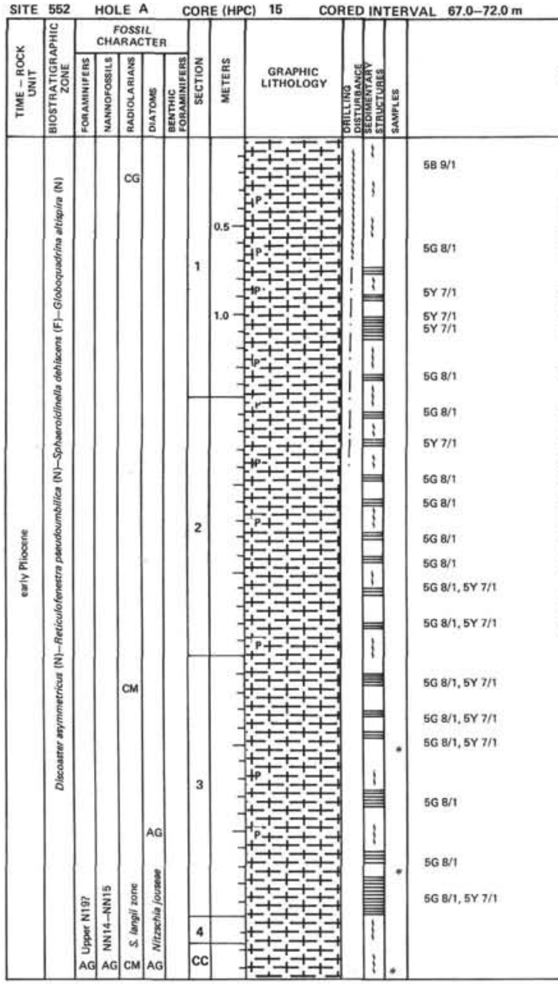

LITHOLOGIC DESCRIPTION

Foram-nanno ooze.

Color is bluish white (5B 9/1) with laminations of light greenish gray (5G 8/1) and light gray (5Y 7/1). Patches, streaks and mottling of light bluish gray (5B 7/1) occur throughout and represent pyrite associated with bioturbation.

Section 1 is moderately disturbed. Most laminae have gradational boundaries with the more homogeneous layer on either side. Texturally the sediment is a sandy mud throughout.

SMEAR SLIDE SUMMARY (%):

	3, 55 D	3, 127 M
Texture:		
Sand	10	20
Silt	20	5
Clay	70	75
Composition:		
Clay	10	15
Foraminifers	20	20
Calc.mannofossils	65	59
Diatoms	1	2
Radiolarians	1	–
Sponge spicules	2	4
Dolomite	1	–

CARBONATE BOMB: $CaCO_3$ (%):
3, 56 = 93
3, 126 = 93

SITE 552 HOLE A CORE (HPC) 16 CORED INTERVAL 72.0–77.0 m

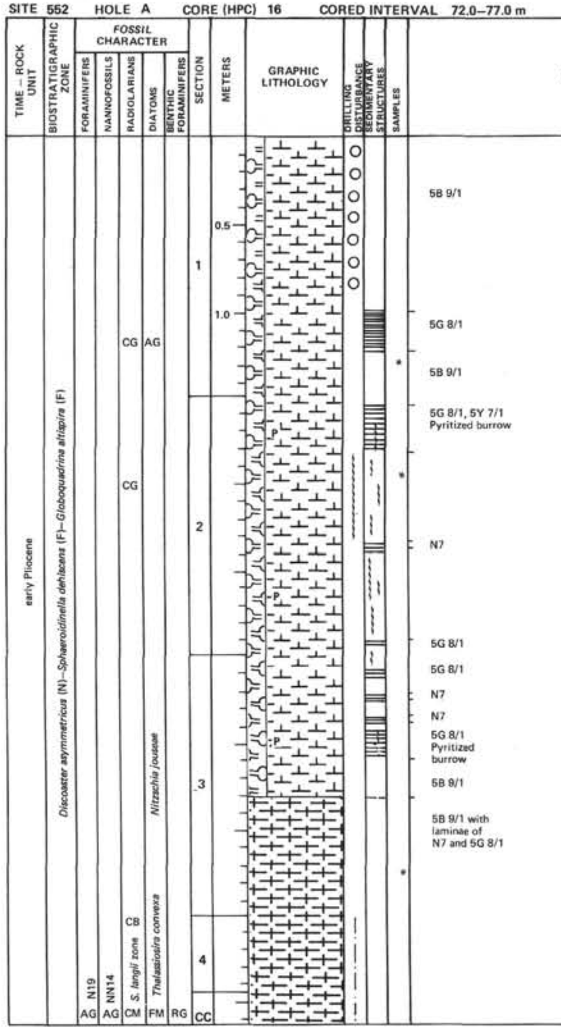

LITHOLOGIC DESCRIPTION

Biosiliceous nanno-ooze overlying foram nanno ooze.

Color is dominantly light bluish white (5B 9/1) with burrow mottling of light bluish gray (5B 7/1) and light gray (5Y 7/1) and laminations of light greenish gray (5G 8/1) and light gray (N7).

The top meter is very disturbed. Below Section 3, 80 cm sediment becomes uniform, more sandy, less burrows with very faint laminae throughout.

SMEAR SLIDE SUMMARY (%):

	1, 130 D	2, 46 D	3, 128 D
Texture:			
Sand	5	5	10
Silt	10	15	10
Clay	85	80	80
Composition:			
Clay	20	10	10
Foraminifers	10	10	10
Calc. nannofossils	60	70	75
Diatoms	7	3	3
Radiolarians	3	2	Tr
Sponge spicules	5	5	2
Silicoflagellates	–	Tr	–

CARBONATE BOMB: $CaCO_3$ (%):
3, 127 = 95

SITE 552 HOLE A CORE (HPC) 17 CORED INTERVAL 77.0–82.0 m

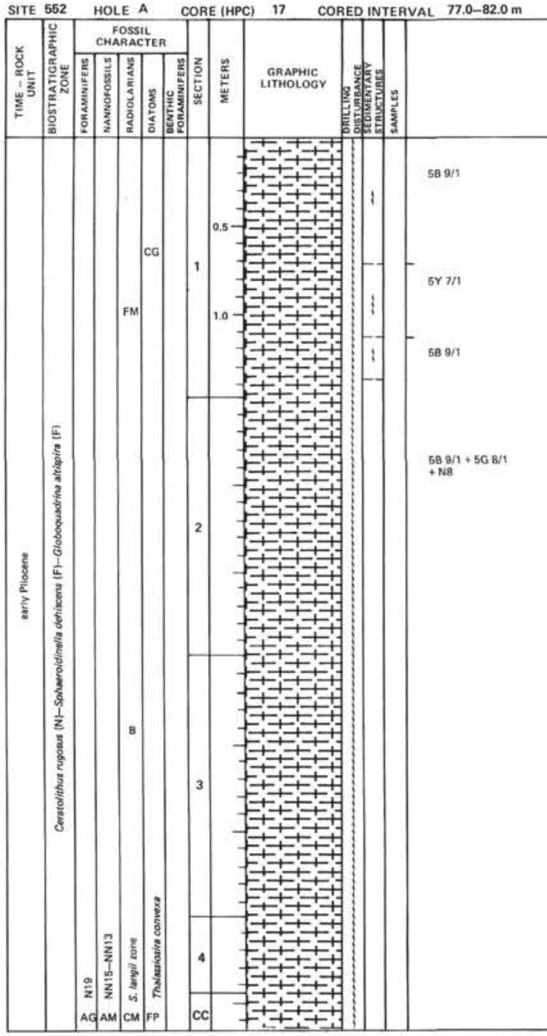

LITHOLOGIC DESCRIPTION

Foram-nanno ooze.

Core is very disturbed.

Color is alternating light and slightly darker layers. The lighter layers are bluish white (5B 9/1) and the darker layers are light gray (5Y 7/1). Some burrow mottling is present in the top section. Below Section 1 the sediment is laminated but badly deformed by drilling. The laminae, or thin beds, are greenish gray (5G 8/1) and very light gray (N8). Core is probably laminated below Section 1.

CARBONATE BOMB: $CaCO_3$ (%):
2, 117 = 95

SITE 552 HOLE A CORE (HPC) 18 CORED INTERVAL 82.0–87.0 m

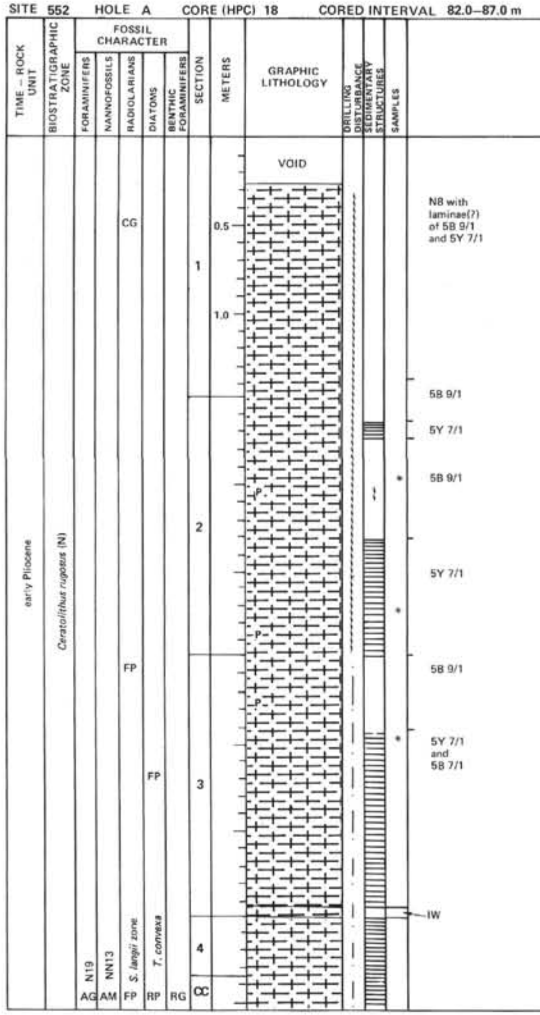

LITHOLOGIC DESCRIPTION

Foram-nanno ooze.

Core is very disturbed. Laminations are steeply inclined and contorted.

Color is bluish white (5B 9/1) with minor mottling due to burrowing, and laminations of light gray (5Y 7/1) and light bluish gray (5B 7/1).

Disseminated pyrite is assoicated with burrows.

Texture is sandy mud with more sand in the laminated zones.

SMEAR SLIDE SUMMARY (%):

	2, 47 D	2, 122 M	3, 38 D
Texture:			
Sand	5	25	10
Silt	5	5	5
Clay	90	70	85
Composition:			
Clay	5	15	10
Carbonate unspec.	–	1	2
Foraminifers	10	25	10
Calc. nannofossils	85	58	78
Diatoms	–	1	–
Radiolarians	Tr	–	–
Sponge spicules	Tr	–	–

CARBONATE BOMB: $CaCO_3$ (%).
2, 46 = 95
3, 36 = 97

SITE 552 HOLE A CORE (HPC) 19 CORED INTERVAL 87.0–92.0 m

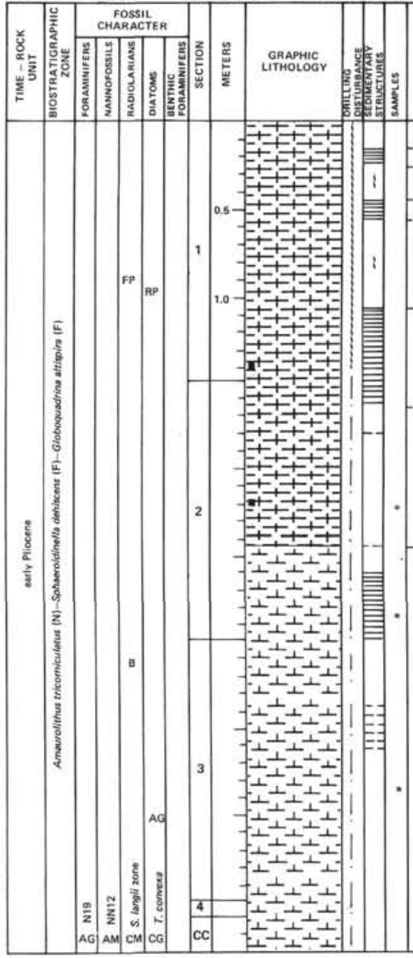

LITHOLOGIC DESCRIPTION

5B 9/1
5Y 7/1
5B 9/1
5Y 7/1
5B 9/1
5Y 7/1
Granule
(contamination?)
5B 9/1
N8
sandy dropstone
(contamination?)
(1 cm)
5B 9/1
Firm
layers

Foram nanno ooze overlying nanno-ooze.

Core is moderately disturbed but some original laminations obvious throughout.

Color is mainly bluish white (5B 9/1) with minor burrow mottling of light bluish gray (5B 7/1). The lamine are light gray (5Y 7/1) and a zone in Section 2 is very light gray (N8).

Foram-nanno ooze has a sandy mud texture becoming a muddy sand in Section 2.

Laminations are less distinct in the nanno ooze (texture: mud). Three firm layers present in Section 3.

Terrigenous dropstones are probably downhole contamination.

SMEAR SLIDE SUMMARY (%):

	2, 70	2, 139	3, 86
	D	D	D
Texture:			
Sand	10	5	5
Silt	5	5	5
Clay	85	90	90
Composition:			
Clay	10	15	5
Carbonate unspec.	2	–	1
Foraminifers	10	5	5
Calc. nannofossils	78	80	88
Radiolarians	Tr	–	–
Sponge spicules	Tr	–	1

CARBONATE BOMB: $CaCO_3$ (%):
2, 68 = 95
3, 87 = 93

SITE 552 HOLE A CORE (HPC) 20 CORED INTERVAL 92.0–95.0 m

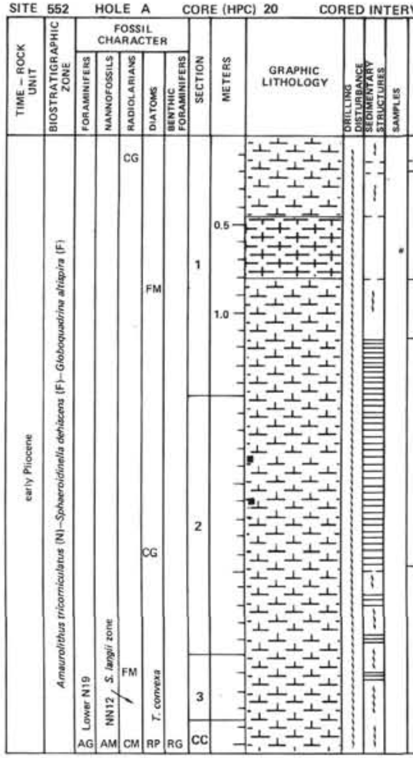

LITHOLOGIC DESCRIPTION

5B 9/1
5Y 7/1
5B 9/1
5Y 7/1
5B 9/1
5Y 7/1
and
5B 7/1
Granules (?cavings)
5B 9/1

Nanno ooze with minor foram-nanno ooze.

Core is soft and very disturbed.

Principal color is bluish white (5B 9/1) with minor mottling of light bluish gray (5B 7/1). Laminae of light gray (5Y 7/1) and light bluish gray (5B 7/1).

The texture is dominantly mud with sandy mud (foram rich layers).

SMEAR SLIDE SUMMARY (%):

	1, 67	1, 139
	D	D
Texture:		
Sand	20	5
Silt	10	5
Clay	70	90
Composition:		
Clay	15	15
Carbonate unspec.	1	–
Foraminifers	20	10
Calc. nannofossils	63	75
Sponge spicules	1	Tr

CARBONATE BOMB: $CaCO_3$ (%):
1, 67 = 95
2, 137 = 96

SITE 552 HOLE A CORE (HPC) 21 CORED INTERVAL 95.0–99.0 m

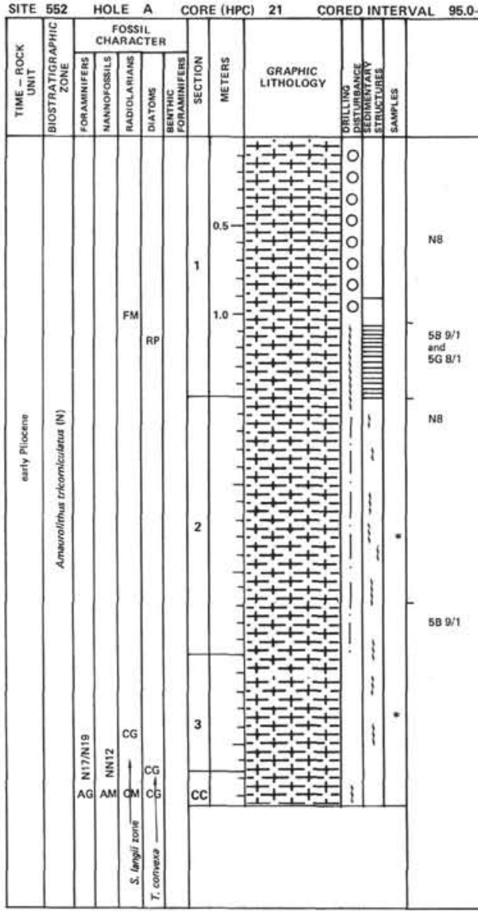

LITHOLOGIC DESCRIPTION

Foram-nanno ooze.

Top section is very disturbed and contains pebbles and angular grit. This is downhole contamination.

Color grades from very light gray (N8) to light bluish white (5B 9/1). Burrow mottling of light bluish gray (5B 7/1), yellowish gray (5Y 8/1) and light gray (5Y 7/1) Laminations of light greenish gray (5G 8/1) in Section 1.

SMEAR SLIDE SUMMARY (%):

	2, 82	3, 35
	M	D
Texture:		
Sand	5	5
Silt	15	5
Clay	80	90
Composition:		
Clay	15	15
Volcanic glass	1	–
Foraminifers	15	15
Calc. nannofossils	69	70
Sponge spicules	–	Tr

CARBONATE BOMB: $CaCO_3$ (%):
3, 38 = 95

SITE 552 HOLE A CORE (HPC) 22 CORED INTERVAL 99.0–104.0 m

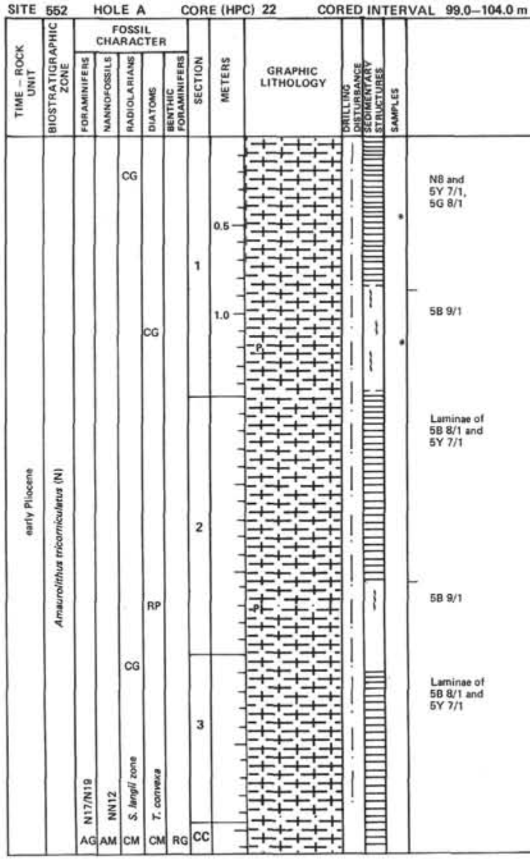

LITHOLOGIC DESCRIPTION

Foram-nanno ooze.

Principal colors are very light gray (N8) and bluish white (5B 9/1) with laminations of light gray (5Y 7/1) and light greenish gray (5G 8/1). More homogeneous zones are mottled with light bluish gray (5B 7/1) due to burrowing. Disseminated pyrite near some burrows.

Sediment is firm but moderately disturbed due to drilling.

SMEAR SLIDE SUMMARY (%):

	1, 48	1, 118
	D	D
Texture:		
Sand	5	5
Silt	15	5
Clay	80	85
Composition:		
Clay	10	10
Foraminifers	10	10
Calc. nannofossils	73	80
Diatoms	3	Tr
Radiolarians	1	–
Sponge spicules	2	Tr
Silicoflagellates	1	–

CARBONATE BOMB: $CaCO_3$ (%):
1, 116 = 97

X. R. D. BULK SAMPLE ANALYSES:

	Calc.	Feld.	Qtz.	Clays:	:	K+C	I.	Sm.
1, 36 =	96	–	2	2	:	–	–	100
1, 87 =	95	–	2	3	:	–	–	100

SITE 552 HOLE A CORE (HPC) 23 CORED INTERVAL 104.0–108.5 m

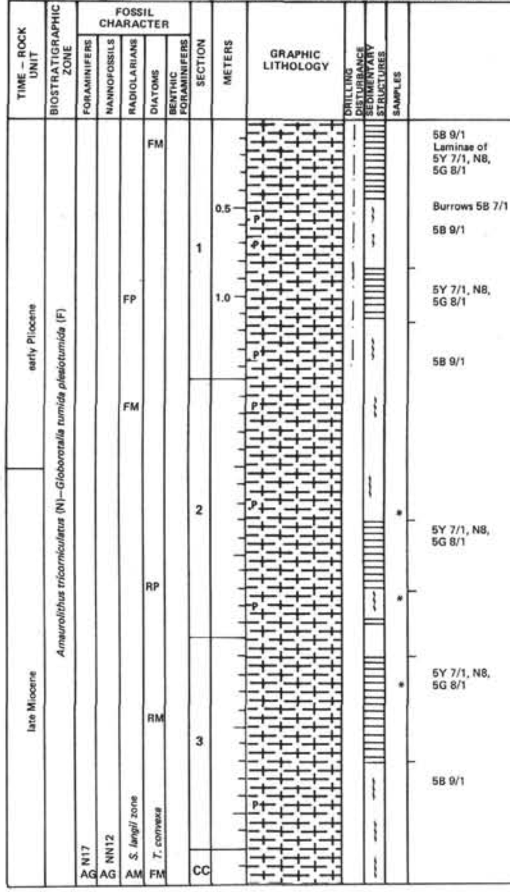

LITHOLOGIC DESCRIPTION

Foram-nanno ooze.

Principal color is bluish white (5B 9/1) with laminations of light gray (5Y 7/1), very light gray (N8) and light greenish gray (5G 8/1).

Less laminated zones are mottled with light bluish gray (5B 7/1) and contain disseminated pyrite.

The core is only slightly disturbed and the laminations are very distinct.

SMEAR SLIDE SUMMARY (%):

	2, 77	2, 129	3, 26
	D	D	D
Texture:			
Sand	10	10	10
Silt	10	20	20
Clay	80	70	70
Composition:			
Clay	15	15	20
Volcanic glass	–	–	1
Carbonate unspec.	2	–	5
Foraminifers	10	15	25
Calc. nannofossils	70	70	40
Diatoms	Tr	–	4
Radiolarians	Tr	–	3
Sponge spicules	3	Tr	2
Dolomite	–	Tr	–

CARBONATE BOMB: $CaCO_3$ (%):
2, 77 = 94

SITE 552 HOLE A CORE (HPC) 24 CORED INTERVAL 108.5–113.5 m

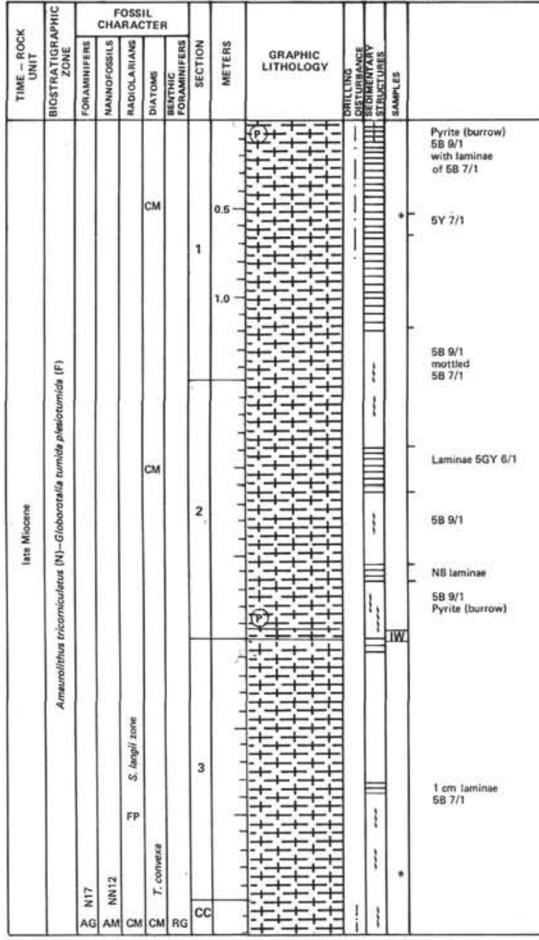

LITHOLOGIC DESCRIPTION

Foram nanno ooze with minor nanno-foram ooze.

Color is dominantly bluish white (5B 9/1) with laminae of light bluish gray (5B 7/1), light gray (5Y 7/1), greenish gray (5GY 6/1), very light gray (N8).

Core is relatively undisturbed and laminae vary in thickness from mm scale up to 2 cm.

Sediment is firm throughout. Textures is a sandy mud. Adjacent to the pyrite filled burrows the sediment is greenish (5G 6/1).

SMEAR SLIDE SUMMARY (%):

	1, 58	3, 134
	M	D
Texture:		
Sand	30	–
Silt	10	15
Clay	60	85
Composition:		
Clay	10	10
Carbonate unspec.	–	5
Foraminifers	30	15
Calc. nannofossils	60	70
Diatoms	Tr	–
Radiolarians	Tr	–
Sponge spicules	Tr	–

CARBONATE BOMB: $CaCO_3$ (%):
3, 127 = 94

SITE 552 HOLE A CORE (HPC) 25 CORED INTERVAL 113.5–118.5 m

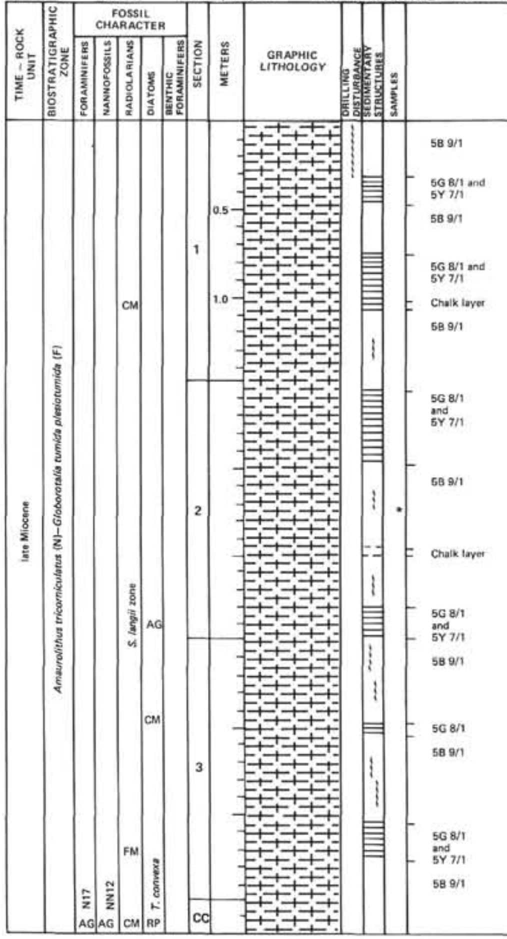

LITHOLOGIC DESCRIPTION

Foram-nanno ooze.

Color is dominantly bluish white (5B 9/1) with burrow mottling of light bluish gray (5B 7/1). Less distinct zones are laminated light greenish gray (5G 8/1) and light gray (5Y 7/1).

The sediment is undisturbed and firm with more lithified chalk layers (1 cm thick) in Sections 1 and 2.

Laminations become less distinct down the core.

SMEAR SLIDE SUMMARY (%):

	2, 77
	D
Texture:	
Sand	–
Silt	10
Clay	90
Composition:	
Heavy minerals	Tr
Clay	10
Foraminifers	10
Calc. nannofossils	80
Dolomite	Tr

CARBONATE BOMB: $CaCO_3$ (%):
2, 77 = 99

SITE 552 HOLE A CORE (HPC) 26 CORED INTERVAL 118.5–123.5 m

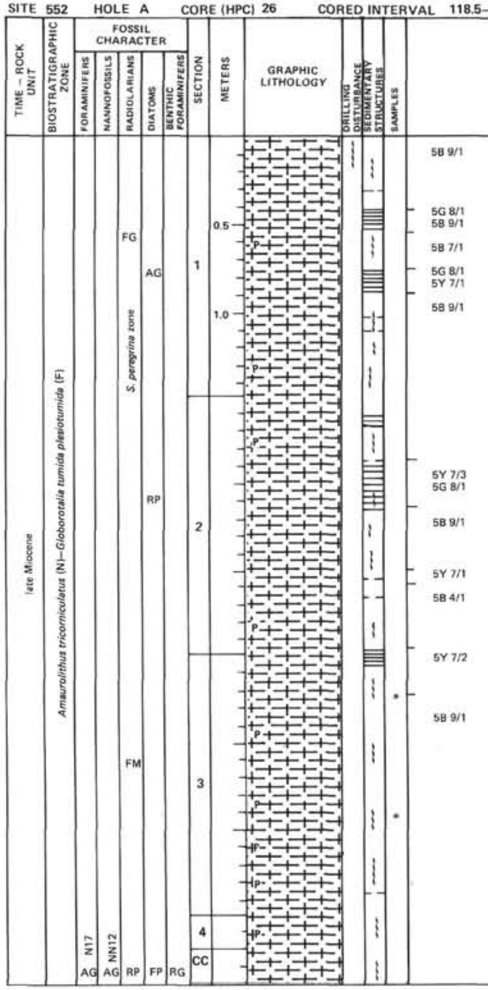

LITHOLOGIC DESCRIPTION

Foram nanno ooze.

Color is mainly bluish white (5B 9/1) with burrow mottling of light bluish gray (5B 7/1). Laminated layers are light greenish gray (5G 8/1), light gray (5Y 7/1), and pale yellow (5Y 7/3).

Very little drilling disturbance. Gradational contacts between laminated and non-laminated zones. Laminae are alternating mud (nanno) and foram-rich layers.

Large burrows (? echinoderm) with 1–2 cm diameter are filled with light gray (5Y 7/1 or 5Y 7/2) sandy mud and have diagenetic alteration halos of disseminated pyrite (light bluish gray [5B 7/1]).

The brownish (clay rich?) laminated interbeds are firmer.

SMEAR SLIDE SUMMARY (%):

	3, 20	3, 96
	M	D
Texture:		
Sand	20	10
Silt	10	10
Clay	70	80
Composition:		
Clay	15	10
Carbonate unspec.	2	2
Foraminifers	20	10
Calc. nannofossils	60	75
Diatoms	1	1
Radiolarians	Tr	–
Sponge spicules	2	2

CARBONATE BOMB: $CaCO_3$ (%):
2, 17 = 94
2, 77 = 91

X. R. D. BULK SAMPLE ANALYSES:

	Calc.	Feld.	Qtz.	Clays	:	K+C	I.	Sm.
3, 27 =	94	–	2	4	:	–	–	100

SITE 552 HOLE A CORE (HPC) 27 CORED INTERVAL 123.5–128.5 m

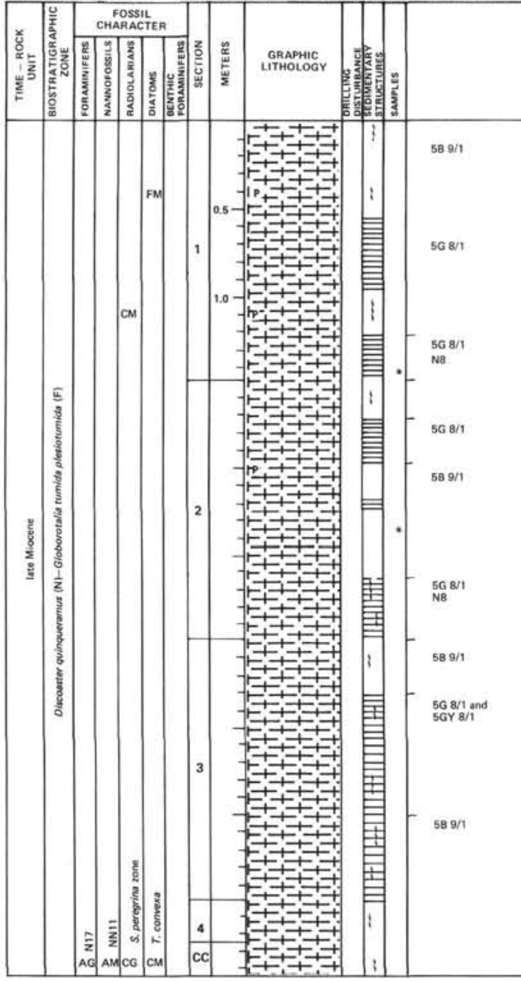

LITHOLOGIC DESCRIPTION

Foram nanno ooze and minor nanno foram ooze.

Color is alternations of homogeneous bluish white (5B 9/1) with laminated layers which are light greenish gray (5G 8/1) and light gray (N8) with bluish white. Moderate bioturbation (mottled medium dark gray [N4]).

No drilling disturbance.

Texture is a sandy mud. Some disseminated pyrite associated with burrows.

Laminations in Section 3 are yellow gray (5Y 8/1).

SMEAR SLIDE SUMMARY (%):

	1, 147 D	2, 85 D
Texture:		
Sand	20	5
Silt	10	25
Clay	70	70
Composition:		
Clay	10	10
Carbonate unspec.	1	–
Foraminifers	25	30
Calc. nannofossils	63	57
Diatoms	Tr	3
Sponge spicules	1	–

CARBONATE BOMB: $CaCO_3$ (%):
2, 87 = 95

X. R. D. BULK SAMPLE ANALYSES:

	Calc.	Feld.	Qtz.	Clays	:	K+C	I.	Sm.
2, 147 =	96	–	2	2	:	–	–	100

SITE 552 HOLE A CORE (HPC) 28 CORED INTERVAL 128.5–133.5 m

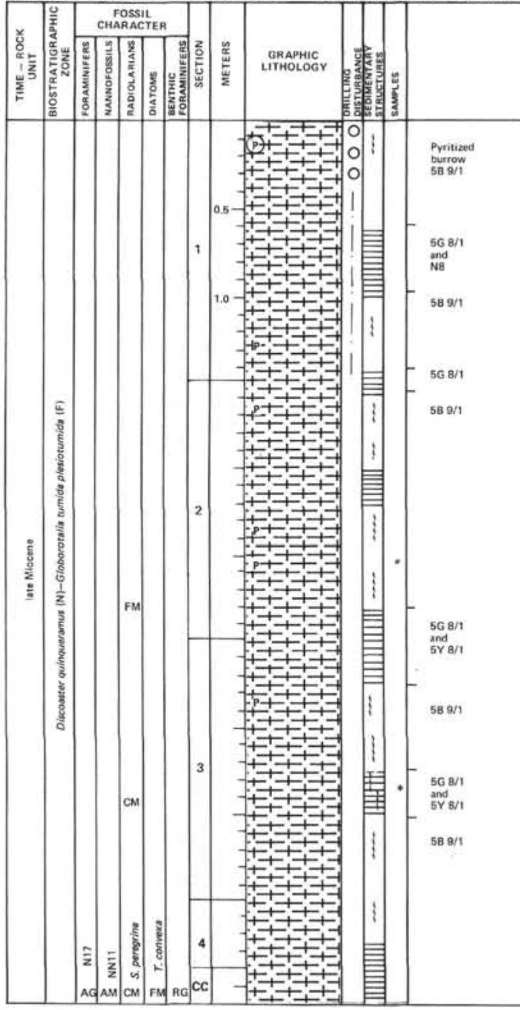

LITHOLOGIC DESCRIPTION

Foram nanno ooze.

Color is alternations of homogeneous bluish white (5B 9/1) with laminated layers which are light greenish gray (5G 8/1), very light gray (N8), yellowish gray (5Y 8/1).

The core is relatively undisturbed by drilling.

Moderate bioturbation (mottled medium dark gray [N4]) with authigenic pyrite.

Laminated zones are darker in color and firmer.

SMEAR SLIDE SUMMARY (%):

	2, 107 D	3, 86 D
Texture:		
Sand	–	10
Silt	20	20
Clay	80	70
Composition:		
Clay	10	15
Carbonate unspec.	–	3
Foraminifers	10	20
Calc. nannofossils	75	60
Diatoms	2	1
Radiolarians	1	Tr
Sponge spicules	2	1

CARBONATE BOMB: $CaCO_3$ (%):
2, 78 = 94

SITE 552 HOLE A CORE (HPC) 29 CORED INTERVAL 133.5–138.5 m

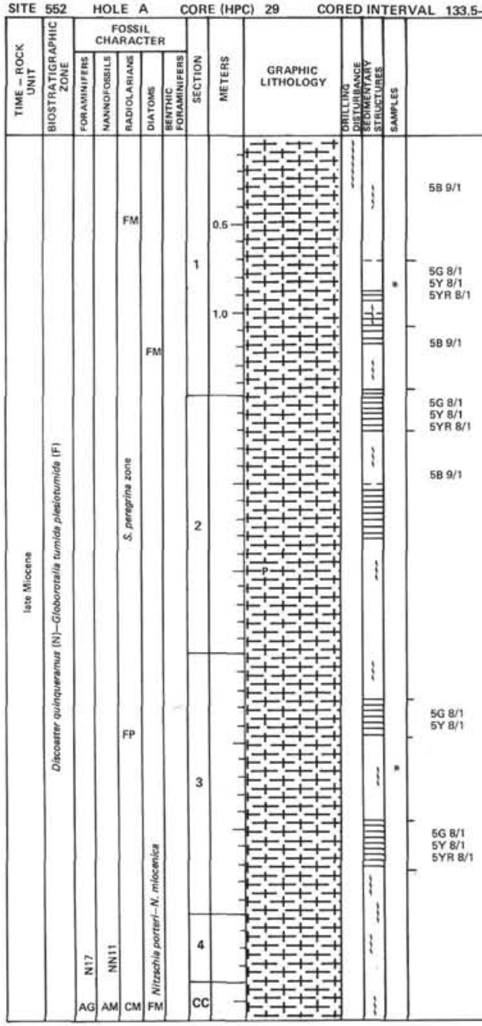

LITHOLOGIC DESCRIPTION

Foram nanno ooze.

Color is alternations of homogeneous bluish white (5B 9/1) with laminated layers which are light greenish gray (5G 8/1), yellowish gray (5Y 8/1) and very light gray (5YR 8/1).

The core is relatively undisturbed by drilling.

Faint laminae and bioturbation occur in the 5B 9/1 zones. Burrow (1 cm diameter) in Section 2 has halo of pyrite.

Laminated zones are darker in color and firmer.

SMEAR SLIDE SUMMARY (%):

	1, 85	3, 65
	D	D
Texture:		
Sand	20	5
Silt	10	15
Clay	70	80
Composition:		
Clay	20	15
Volcanic glass	–	1
Carbonate unspec.	2	–
Foraminifers	20	10
Calc. nannofossils	55	70
Diatoms	1	2
Radiolarians	–	1
Sponge spicules	2	1

CARBONATE BOMB: $CaCO_3$ (%):
1, 85 = 90
2, 65 = 95

SITE 552 HOLE A CORE (HPC) 30 CORED INTERVAL 138.5–143.5 m

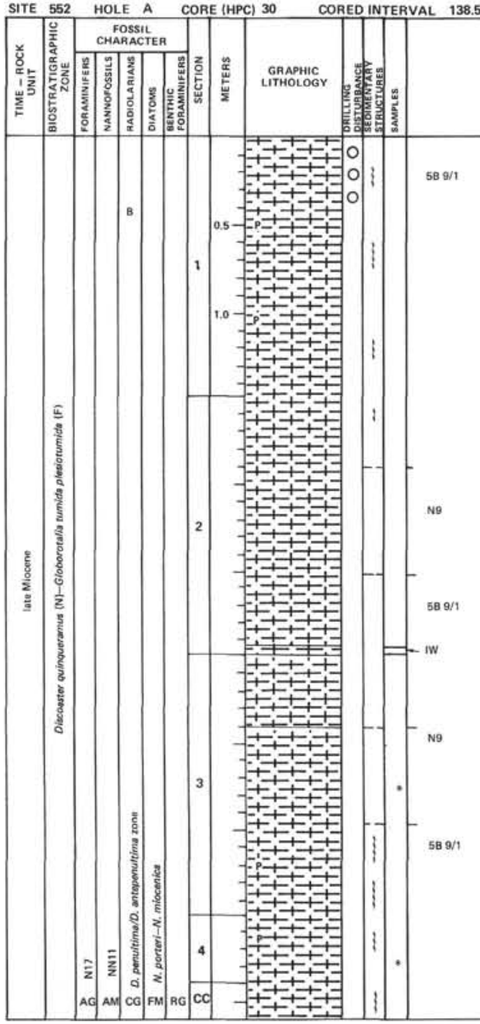

LITHOLOGIC DESCRIPTION

Foram nanno ooze with foram nanno chalk. (Gradational boundary into underlying chalk.) Downhole contamination in top of Section 1.

Color is generally uniform, grading between bluish white (5B 9/1) and white (N9).

Very faint occasional laminae of light greenish gray (5GY 8/1) and light gray (N8).

Rare bioturbation with minor disseminated pyrite (light bluish gray [5B7/1]).

SMEAR SLIDE SUMMARY (%):

	3, 78	4, 27
	D	D
Texture:		
Sand	5	20
Silt	15	10
Clay	80	70
Composition:		
Clay	10	15
Carbonate unspec.	–	3
Foraminifers	10	20
Calc. nannofosils	75	60
Diatoms	3	1
Radiolarians	1	Tr
Sponge spicules	1	1

CARBONATE BOMB: $CaCO_3$ (%):
3, 78 = 92
4, 26 = 97

SITE 552 HOLE A CORE (HPC) 31 CORED INTERVAL 143.5–148.5 m

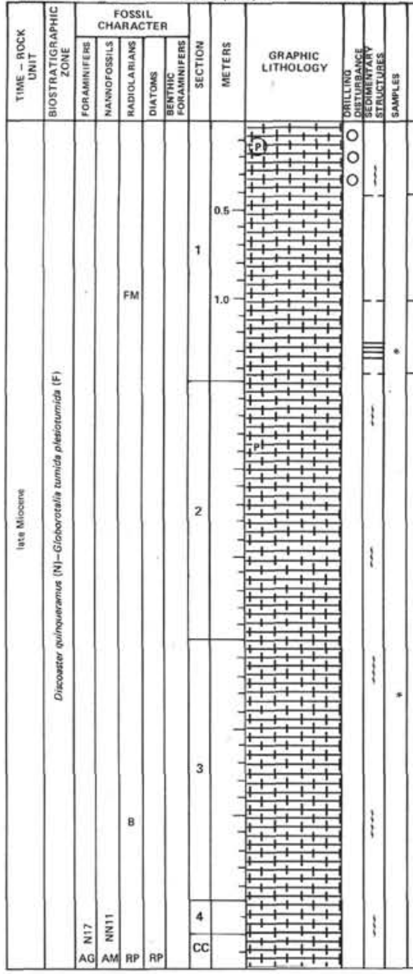

LITHOLOGIC DESCRIPTION

Pyritized burrow
5B 7/1

5B 9/1

N8
laminae of
5G 8/1, 5B 7/1, and
N6

N9

Foram-nanno chalk (downhole contamination in top of Section 1).

Color is generally uniform, grading between bluish white (5B 9/1) and white (N9). Exception is very fine color laminations at base of Section 1; laminae of light greenish gray (5G 8/1), light bluish gray (5B 7/1), and medium light gray (N6). Also occasional faint laminae of greenish gray (5GY 8/1) and very light gray (N8).

Firm chalk with rare burrows and minor pyrite.

SMEAR SLIDE SUMMARY (%):

	1, 132	3, 32
	M	D
Texture:		
Sand	10	10
Silt	10	10
Clay	80	80
Composition:		
Clay	20	15
Carbonate unspec.	–	5
Foraminifers	20	20
Calc. nannofossils	55	10
Sponge spicules	2	Tr
Dolomite	3	–

CARBONATE BOMB: $CaCO_3$ (%):
3, 37 = 94

SITE 552 HOLE A CORE (HPC) 32 CORED INTERVAL 148.5–153.5 m

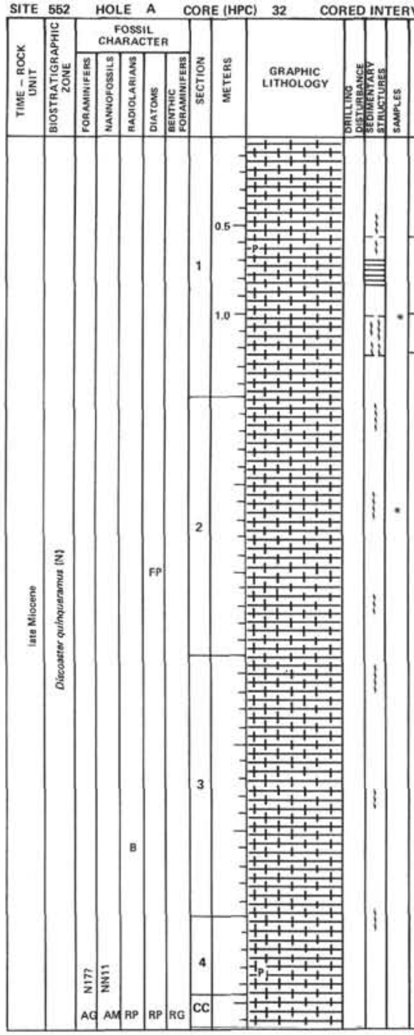

LITHOLOGIC DESCRIPTION

5Y 8/1

N9

2.5YN 7/1

5Y 8/1

Foram-nanno chalk.

Color is generally uniform, grading between shades of white (5Y 8/1 and N9) with occasional laminae of very light gray (N8). Burrow mottled zone in Section 1 is light gray (2.5YN 7/1).

Firm chalk with rare burrows and minor pyrite.

SMEAR SLIDE SUMMARY (%):

	1, 107	2, 67
	M	D
Texture:		
Sand	20	10
Silt	10	10
Clay	70	80
Composition:		
Heavy minerals	Tr	–
Clay	20	10
Carbonate unspec.	3	4
Foraminieers	20	15
Calc. nannofossils	55	70
Diatoms	1	–
Sponge spicules	1	1

CARBONATE BOMB: $CaCO_3$ (%):
2, 67 = 94

SITE 552 HOLE A CORE (HPC) 33 CORED INTERVAL 153.5–158.5 m

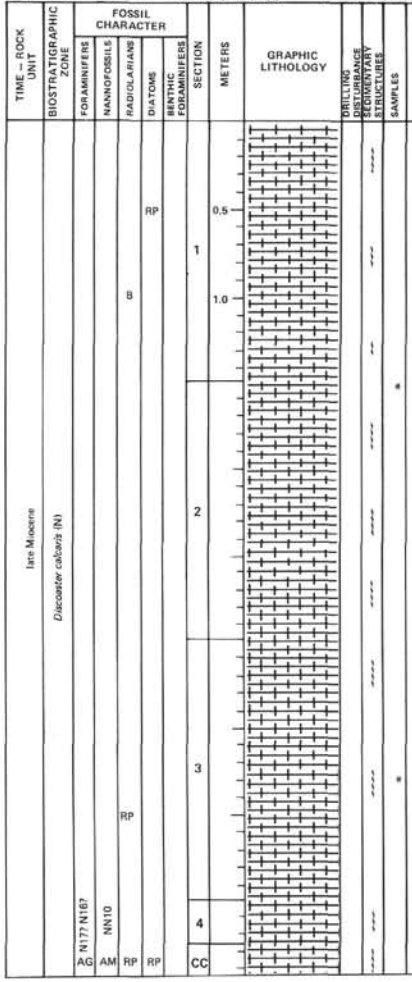

LITHOLOGIC DESCRIPTION

5Y 8/1

Foram-nanno chalk.

Color is uniform white (5Y 8/1) with rare mottling and faint laminae of light gray (N7).

Undisturbed by drilling. Firm chalk with rare burrows and minor softer layers (~5 cm). Texture is mud.

SMEAR SLIDE SUMMARY (%):

	2, 9 D	3, 77 D
Texture:		
Sand	5	10
Silt	15	10
Clay	80	80
Composition:		
Heavy minerals	Tr	–
Clay	15	10
Carbonate unspec.	5	4
Foraminifers	10	15
Calc. nannofossils	68	70
Radiolarians	–	Tr
Sponge spicules	–	1
Dolomite	2	–

CARBONATE BOMB: $CaCO_3$ (%):
2, 7 = 95

SITE 552 HOLE A CORE (HPC) 34 CORED INTERVAL 158.5–163.5 m

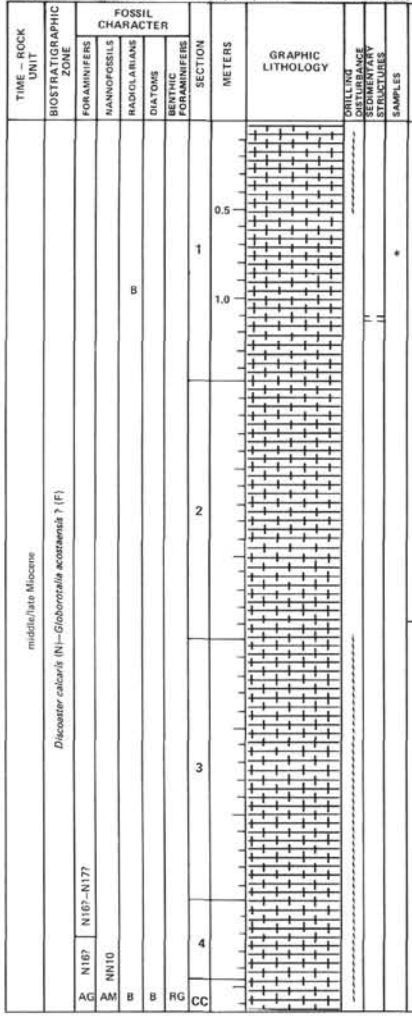

LITHOLOGIC DESCRIPTION

5Y 8/1

Foram-nanno chalk. (Downhole contamination, top of Section 1.)

Color is uniform white (5Y 8/1) gradually becoming darker (light gray [N8]) with depth.

Parts of core very disturbed by flowin.

Laminations and burrows are rare.

SMEAR SLIDE SUMMARY (%):

	1, 77 D
Texture:	
Sand	10
Silt	10
Clay	80
Composition:	
Clay	20
Foraminifers	20
Calc. nannofossils	56
Sponge spicules	1
Dolomite	3

CARBONATE BOMB: $CaCO_3$ (%):
2, 67 = 94

5Y 8/1
and
N8

SITE 552 HOLE A CORE (HPC) 35 CORED INTERVAL 163.5–168.5 m

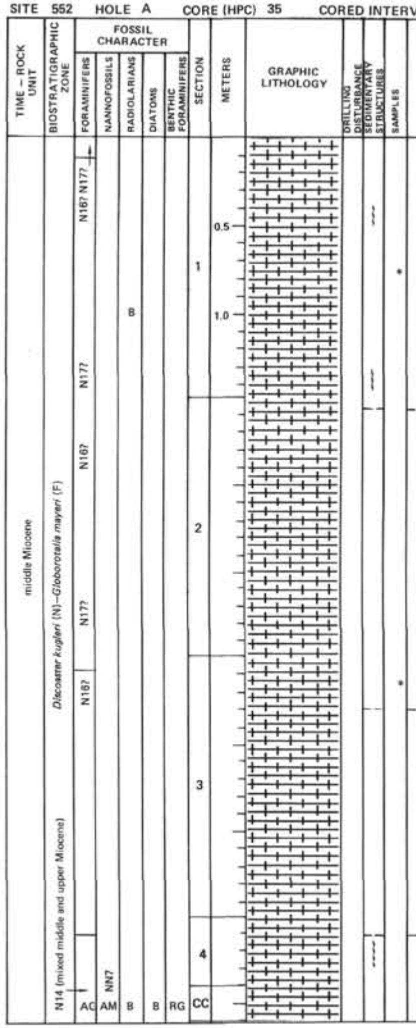

N8

10YR 8/1

5Y 8/1

5Y 8/1
mottled
5GY 8/1

LITHOLOGIC DESCRIPTION

Nanno-foram chalk.

Color is very light gray (N8) grading to white (10YR 8/1 and 5Y 8/1).

Uniform sandy mud texture with rare burrows, becoming mottled with light greenish gray (5GY 8/1) at base.

No drilling disturbance.

SMEAR SLIDE SUMMARY (%):

	1, 78	3, 17
	D	D
Texture:		
Sand	30	20
Silt	10	20
Clay	60	60
Composition:		
Clay	10	15
Carbonate unspec.	5	–
Foraminifers	30	35
Calc. nannofossils	55	47
Dolomite	–	3

CARBONATE BOMB: $CaCO_3$ (%):
1, 77 = 92
3, 17 = 92

SITE 552 HOLE A CORE (HPC) 36 CORED INTERVAL 168.5–173.5 m

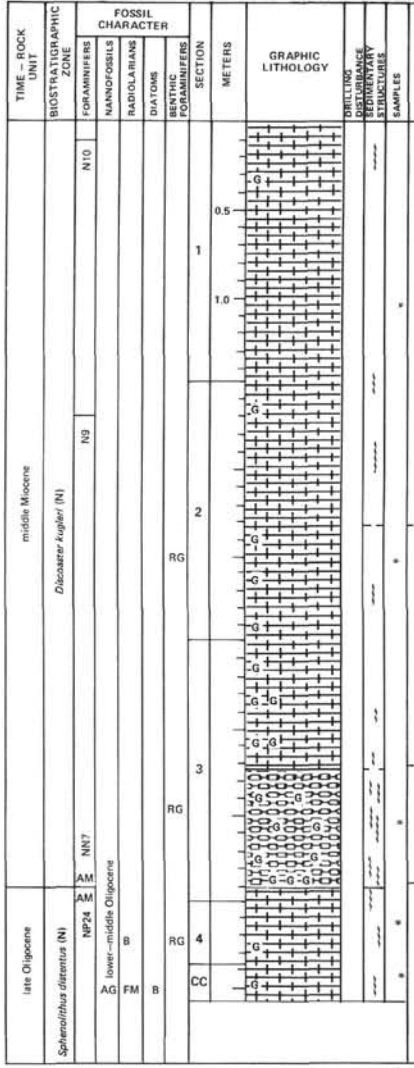

N9

5Y 8/1

5Y 3/2

Sharp, uneven contact

5Y 8/1 and 5Y 8/2
and 5Y 7/3
burrow (3 cm diameter)

and 10YR 5/6

LITHOLOGIC DESCRIPTION

Nanno foram chalk and glauconitic chalk.

Uniform white (N9) becoming yellowish gray (5Y 8/1) and then mottled with dark olive gray (5Y 3/2) as the glauconite content increases with depth.

Major sharp contact in base of Section 3 Some large burrows below this contact are filled with sediment from above. Nanno foram chalk underlies the contact and is mottled pale yellow (5Y 7/3), yellowish brown (10YR 5/6) and olive (5Y 5/6) with a white (5Y 8/1) background. Bioturbation throughout.

Above contact texture is sandy and below is sandy mud.

No drilling disturbance.

SMEAR SLIDE SUMMARY (%):

	1, 107	2, 107	3, 107	4 17	CC, 7
	D	D	D	D	M
Texture:					
Sand	20	35	20	20	–
Silt	20	5	30	30	–
Clay	60	60	50	50	100
Composition:					
Feldspar	–	1	–	–	–
Heavy minerals	–	Tr	–	–	–
Clay	15	20	10	25	100
Volcanic glass	6	Tr	5	–	–
Glauconite	–	3	30	–	–
Carbonate unspec.	5	4	–	10	–
Foraminifers	30	30	10	25	–
Calc. nannofossil	41	40	35	35	–
Radiolarians	–	–	2	–	–
Sponge spicules	3	2	5	5	–
Dolomite	–	–	3	–	–

CARBONATE BOMB: $CaCO_3$ (%):
1, 107 = 94
2, 107 = 81
3, 107 = 53
4, 35 = 88

X. R. D. BULK SAMPLE ANALYSES:

	Calc.	Feld.	Qtz.	Clays	: K+C	I.	Sm.
3, 137 =	95	–	–	5	: –	–	100
CC, 7 =	50	–	33	17	: –	–	100

SITE 552 HOLE A CORE (HPC) 37 CORED INTERVAL 173.5–178.5 m

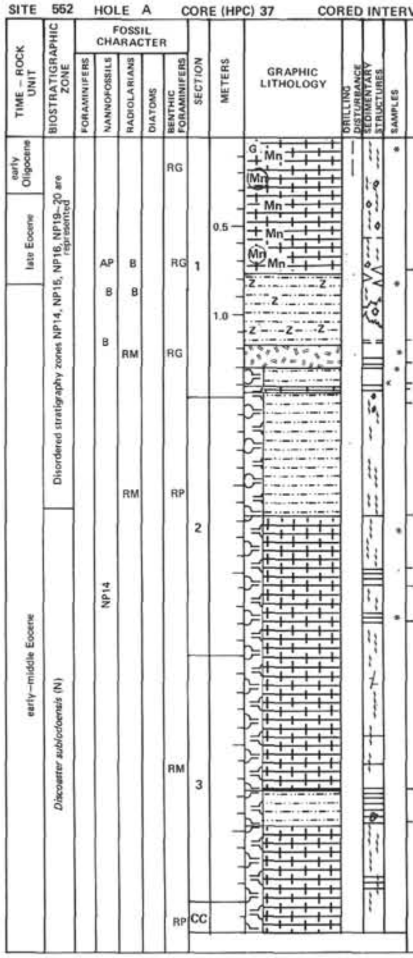

10YR 8/3
10YR 7/1
mottled
10YR 8/4
10YR 6/3
10YR 4/2

5Y 5/4
and
10YR 7/4
2.5Y 5/4

5Y 4/2 tuff

5Y 5/6
10YR 8/4

2.5Y 5/4

2.5Y 7/4

2.5Y 5/4

5Y 5/6, 2.5Y 6/4

2.5Y 5/4

2.5Y 6/4 and
2.5Y 6/2

5Y 5/6
fecal pellets

2.5Y 6/4
and
2.5Y 6/2

LITHOLOGIC DESCRIPTION

Foram nanno chalk, zeolitic mudstone, volcanic tuff, manganese nodules, biosiliceous mudstone and nanno-foram chalk, biosiliceous foram nanno chalk, and biosiliceous mud.

Colors: Section 1: very pale brown (10YR 8/3) mottled with light gray (10YR 7/1), pale brown (10YR 8/4, 10YR 6/3), dark grayish brown (10YR 4/2) overlying olive (5Y 5/4) with lenses of very pale brown (10YR 7/4) and mottled light olive brown (2.5Y 5/4). Olive gray (5Y 4/2) layer overlies olive (5Y 5/6) and olive gray (5Y 4/2). Section 2–Core-Catcher: mainly light olive brown (2.5Y 5/4) and pale yellow (2.5Y 7/4).

Mn nodules, intraclasts and soft sediment deformation common in Section 1.

Bioturbation intense throughout.

Sharp, erosive contacts also present.

Some laminae preserved. No drilling disturbance.

Texture is sandy mud.

SMEAR SLIDE SUMMARY (%):

	1, 10 D	1, 85 D	1, 135 D	1, 138 M
Texture:				
Sand	25	0	5	50
Silt	25	10	35	20
Clay	50	90	60	30
Composition:				
Quartz	1	5	–	–
Heavy minerals	–	–	5	–
Clay	20	65	45	15
Volcanic glass	–	–	10	5
Glauconite	5	–	–	–
Zeolite	–	25	–	–
Carbonate unspec.	–	–	10	5
Foraminifers	20	–	–	45
Calc. nannofossils	49	2	15	15
Radiolarians	–	–	5	–
Sponge spicules	–	–	10	15
Dolomite	5	3	–	–

	2, 19 D	2, 129 D	3, 88 M
Texture:			
Sand	15	30	10
Silt	35	20	15
Clay	50	50	75
Composition:			
Heavy minerals	5	2	–
Clay	10	15	73
Volcanic glass	10	8	5
Foraminifers	10	15	–
Calc. nannofossils	40	30	10
Radiolarians	5	5	2
Sponge spicules	20	25	10

SITE 552 HOLE A CORE (HPC) 38 CORED INTERVAL 178.5–183.5 m

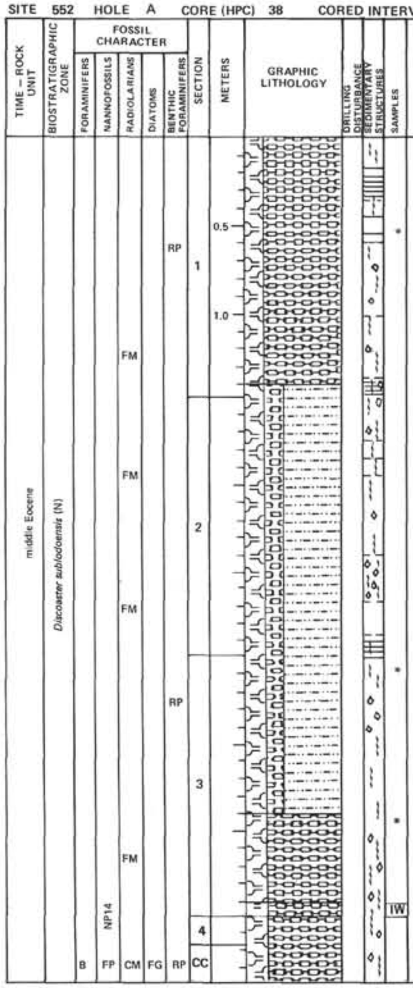

2.5Y 6/4
with
5Y 5/6
0.5 cm sand layers

LITHOLOGIC DESCRIPTION

Biosiliceous chalk and biosiliceous calcareous mudstone.

Color is dominantly light yellowish brown (2.5Y 6/4) with mottling and lenses of olive (5Y 5/6).

Bioturbation is common throughout with many darker (muddy) intraclasts. Thin beds (2 cm) with a sandy texture are also present and composed mainly of sponge spicules. Lenticular and laminated units are also present.

No drilling disturbance.

SMEAR SLIDE SUMMARY (%):

	1, 52 M	3, 10 D	3, 100 M
Texture:			
Sand	50	10	10
Silt	30	20	40
Clay	20	70	50
Composition:			
Heavy minerals	2	2	5
Clay	20	48	10
Volcanic glass	10	–	10
Carbonate unspec.	–	20	4
Foraminifers	15	–	10
Calc. nannofossils	23	20	30
Diatoms	8	3	1
Radiolarians	2	2	5
Sponge spicules	20	10	25

SITE 553 HOLE CORE 1 CORED INTERVAL 0.0–9.0 m

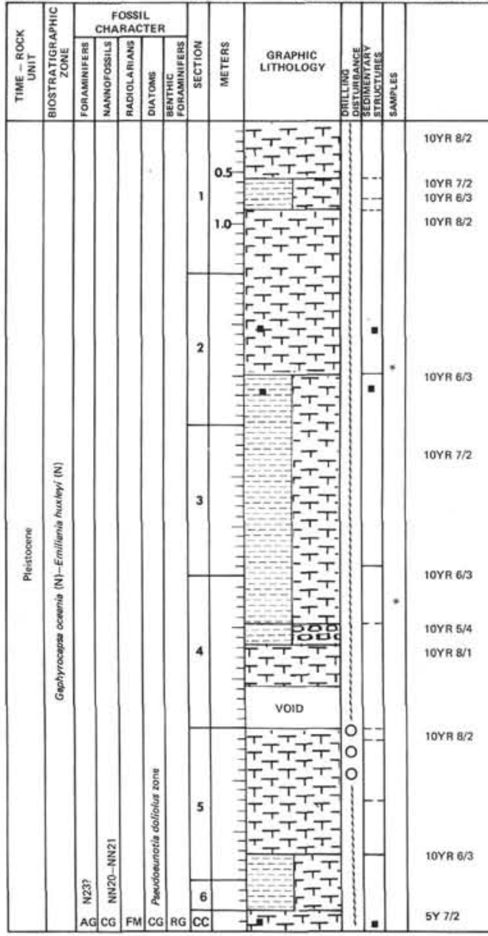

LITHOLOGIC DESCRIPTION

Foram marl, foram ooze and marl interbeds with terrigenous sand and granule-sized particles scattered throughout.

Color is mainly white (10YR 8/2, 10YR 8/1) with very pale brown (10YR 7/2) pale brown (10YR 6/3) yellowish brown (10YR 5/4) and light gray (5Y 7/2).

Sandy texture but brown horizons contain more mud. Core very disturbed to soupy causing blurring of sedimentary boundaries and obliteration of sedimentary structures, but units seem to have muddy bases and grade into white foram ooze.

SMEAR SLIDE SUMMARY (%):

	2, 92 D	4, 20 D
Texture:		
Sand	50	40
Silt	5	20
Clay	45	40
Composition:		
Quartz	10	30
Clay	35	35
Carbonate unspec.	3	20
Foraminifers	40	5
Calc. nannofossils	10	10
Diatoms	2	–
Dolomite	Tr	Tr

SITE 553 HOLE A CORE 1 CORED INTERVAL 65.5–75.0 m

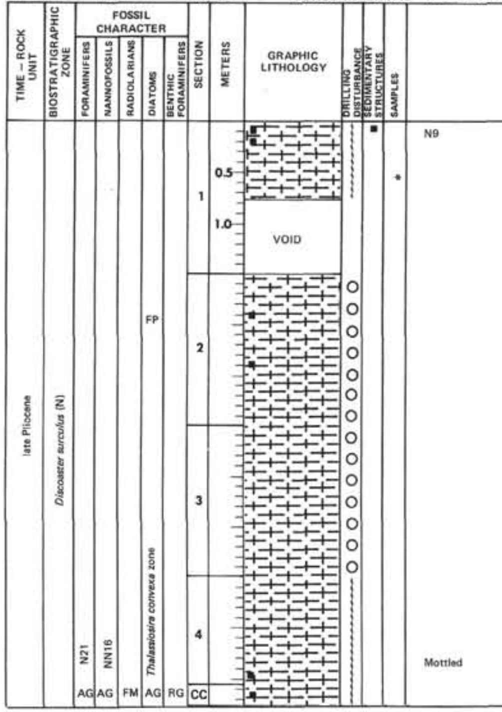

LITHOLOGIC DESCRIPTION

Foram-nanno ooze with scattered angular dropstones up to 2 cm of granite and quartzite.

Color is entirely white (N9) with rare mottles of light greenish gray (5GY 8/1), possibly originally burrows.

Texture slightly sandy mud throughout.

Intense disturbance throughout has obliterated any signs of structure or bedding.

SMEAR SLIDE SUMMARY (%):

	1, 55 D
Texture:	
Sand	10
Silt	10
Clay	80
Composition:	
Quartz	Tr
Heavy minerals	5
Carbonate unspec.	5
Foraminifers	10
Calc. nannofossils	75
Diatoms	2
Sponge spicules	3

CARBONATE BOMB (%):
1, 22 = 91

SITE 553 HOLE A CORE 2 CORED INTERVAL 103.5–113.0 m

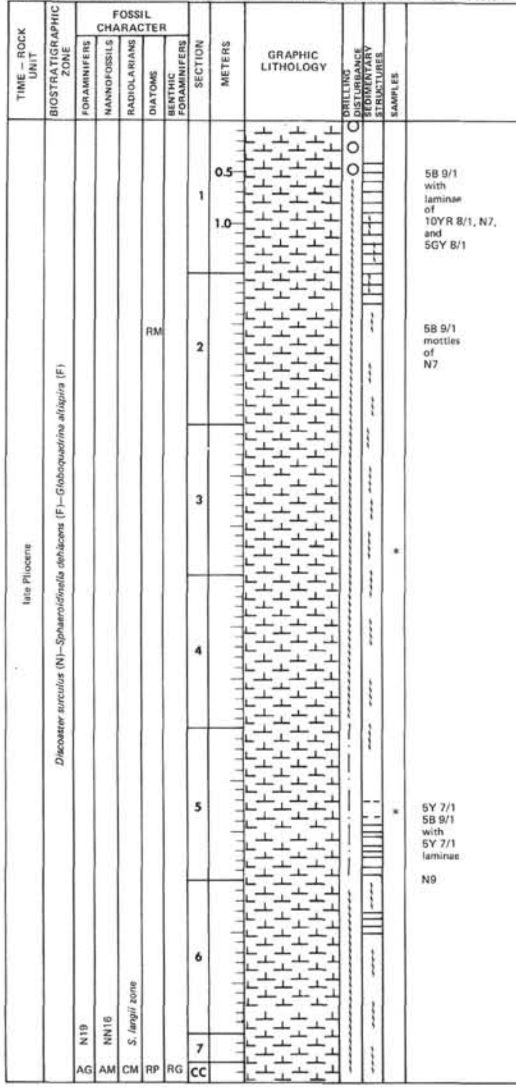

LITHOLOGIC DESCRIPTION

Nannofossil ooze, mainly white (N9) or bluish white (5B 9/1) with laminae of light gray (5Y 7/1), white (10YR 8/1) and light greenish gray (5GY 8/1). Mottles of light gray (N7) (burrows).

Mud texture throughout, some laminated with units, burrowed throughout.

Core is moderately or very disturbed.

SMEAR SLIDE SUMMARY (%):

	3, 128	5, 80
	D	M
Texture:		
Sand	5	10
Silt	5	10
Clay	90	80
Composition:		
Clay	10	10
Carbonate unspec.	3	2
Foraminifers	5	10
Calc. nannofossils	80	75
Diatoms	1	1
Sponge spicules	1	2

CARBONATE BOMB (%):
5, 26 = 91

SITE 553 HOLE A CORE 3 CORED INTERVAL 151.0–160.5 m

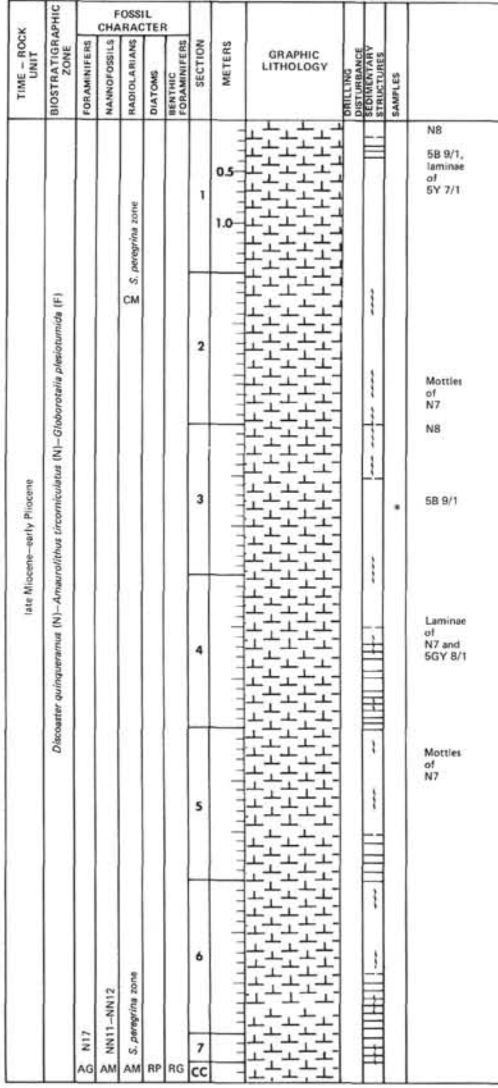

LITHOLOGIC DESCRIPTION

Nannofossil ooze, varying from bluish white (5B 9/1) to very light gray (N8). Some laminae of light gray (N7), light greenish gray (5GY 8/1) and light gray (5Y 7/1). Mottles of light gray (N7).

Mud dominates, distinctly firmer than Core 2. Alternation of burrowed and laminated units, boundaries essentially gradational.

Core relatively undisturbed.

SMEAR SLIDE SUMMARY (%):

	3, 80
	D
Texture:	
Sand	5
Silt	5
Clay	90
Composition:	
Clay	5
Carbonate unspec.	3
Foraminifers	5
Calc. nannofossils	85
Diatoms	Tr
Sponge spicules	2

CARBONATE BOMB (%):
4, 100 = 92
5, 90 = 92

SITE 553 HOLE A CORE 4 CORED INTERVAL 179.5–189.0 m

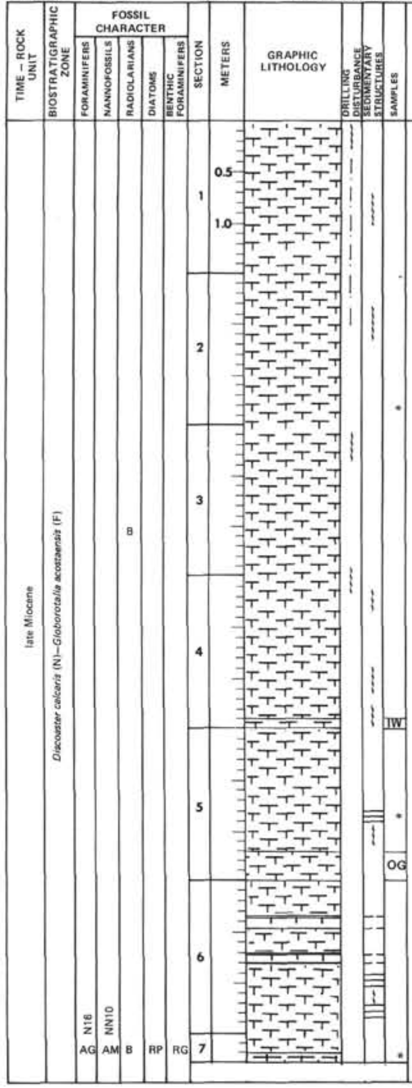

5B 9/1

N7 mottles

N9

N7 laminae

5B 9/1

Chalk, N8

Chalk, N8

N7 laminae

5B 7/1

LITHOLOGIC DESCRIPTION

Foraminiferal ooze with rare chalky zones; mainly bluish white (5B 9/1) with subordinate white (N9). Minor light bluish gray (5B 7/1) nanno-foram ooze. Mottles and laminations of light gray (N7).

Texturally sandy mud. Rare laminae and burrows. Sequences shows development of chalky interbeds towards base.

Relatively undisturbed throughout.

SMEAR SLIDE SUMMARY (%):

	2, 132 D	5, 82 D	7, 43 M
Texture:			
Sand	50	10	30
Silt	10	10	10
Clay	40	80	60
Composition:			
Clay	10	5	10
Foraminifers	50	15	30
Calc. nannofossils	40	80	60
Sponge spicules	–	Tr	Tr

CARBONATE BOMB (%):
1, 125 = 91

SITE 553 HOLE A CORE 5 CORED INTERVAL 189.0–198.5 m

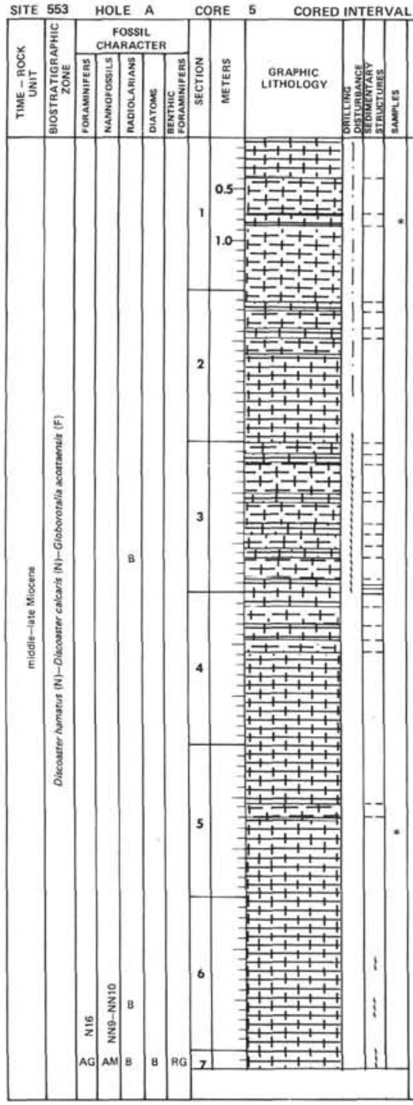

5B 9/1

Laminae of N7

Mottles of N7

LITHOLOGIC DESCRIPTION

Foram-nanno ooze and chalk interbeds, bluish white (5B 9/1) throughout. Minor burrow mottling of lighter gray (N7), also laminae.

Slightly sandy mud texturally, with interbeds of chalk and ooze.

Ooze sections tend to show some deformation.

SMEAR SLIDE SUMMARY (%):

	1, 83 D	5, 83 D
Texture:		
Sand	30	10
Silt	10	10
Clay	60	80
Composition:		
Clay	15	15
Carbonate unspec.	–	5
Foraminifers	30	15
Calc. nannofossils	55	65
Sponge spicules	Tr	Tr

CARBONATE BOMB (%):
5, 80 = 91

SITE 553 HOLE A CORE 6 CORED INTERVAL 198.5–208.0 m

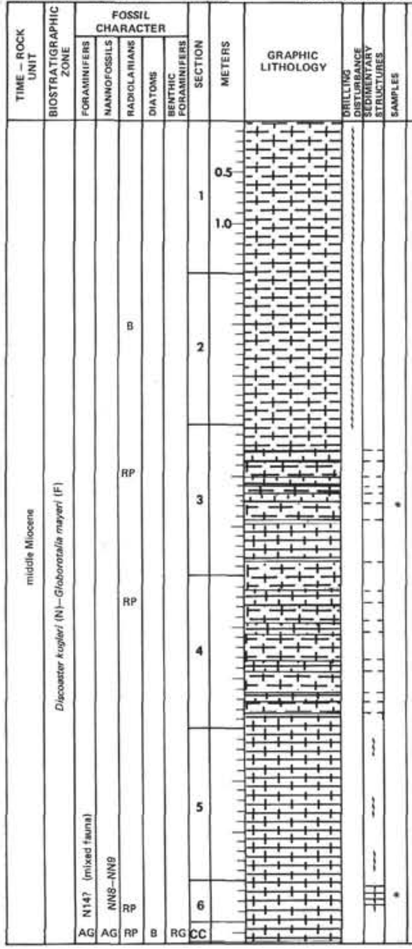

LITHOLOGIC DESCRIPTION

5Y 8/1

Predominantly foram-nanno ooze and chalk, with minor nanno-foram ooze. Foram nanno ooze is white (5Y 8/1) with rare light gray (N7) mottles. Nanno-foram ooze is very light gray (N8) with medium gray (N6) mottles and laminae, related to pyrite concentration.

Largely composed of sandy mud, with chalk and ooze interbeds. Rare laminations and burrows visible.

Core largely undisturbed except first two sections, which also contains angular pebbles, probably caved.

SMEAR SLIDE SUMMARY (%):

	3, 80	6, 16
	D	M
Texture:		
Sand	15	40
Silt	5	20
Clay	80	40
Composition		
Heavy minerals	–	Tr
Clay	10	20
Pyrite	–	10
Carbonate unspec.	–	4
Foraminifers	20	30
Calc. nanoofossils	70	35
Sponge spicules	Tr	1

CARBONATE BOMB (%):
3, 80 = 90

N7
mottles

N8 with
N6 laminae
5Y 8/1

SITE 553 HOLE A CORE 7 CORED INTERVAL 208.0–217.5 m

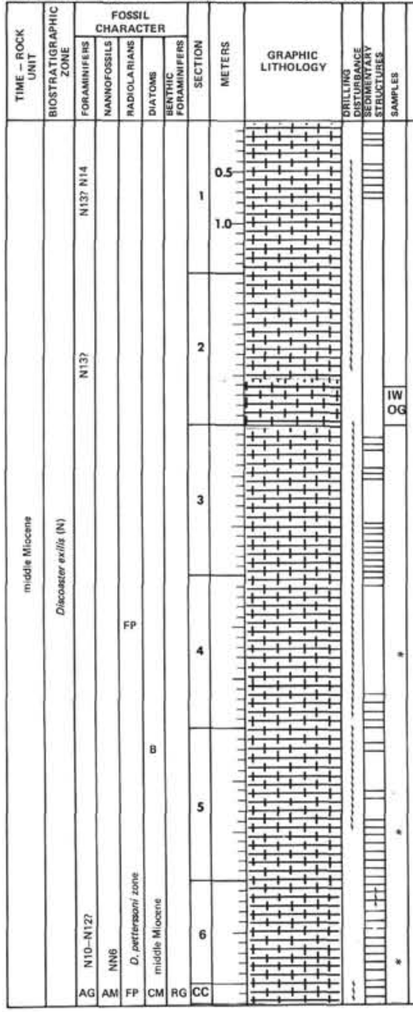

LITHOLOGIC DESCRIPTION

N9

Laminae
of 5GY 8/1,
N7, and
5Y 8/1

Nanno foram chalk with minor foram-nanno chalk, grading from white (N9, 5Y 8/1) to bluish white (5B 9/1), and containing laminae of light greenish gray (5GY 8/1), light gray (N7) and white (5Y 8/1, 5Y 8/2).

Dominantly sandy mud, some zones less sandy. Common laminations, rare burrows. Still some variations in firmness but essentially all chalk here.

Much of core is extremely disturbed.

SMEAR SLIDE SUMMARY (%):

	4, 80	5, 102	6, 80
	D	M	D
Texture:			
Sand	40	10	40
Silt	10	5	10
Clay	50	85	50
Composition:			
Heavy minerals	–	–	Tr
Clay	15	25	20
Carbonate unspec.	–	2	4
Foraminifers	40	8	35
Calc. nannofossils	45	65	40
Sponge spicules	Tr	– 1	

CARBONATE BOMB (%):
2, 90 = 91
4, 80 = 93
6, 80 = 90

5B 9/1

N9

5Y 8/1

N9

5B 9/1

5Y 8/1
with
5Y 8/2
laminae

SITE 553 HOLE A CORE 8 CORED INTERVAL 217.5–227.0 m

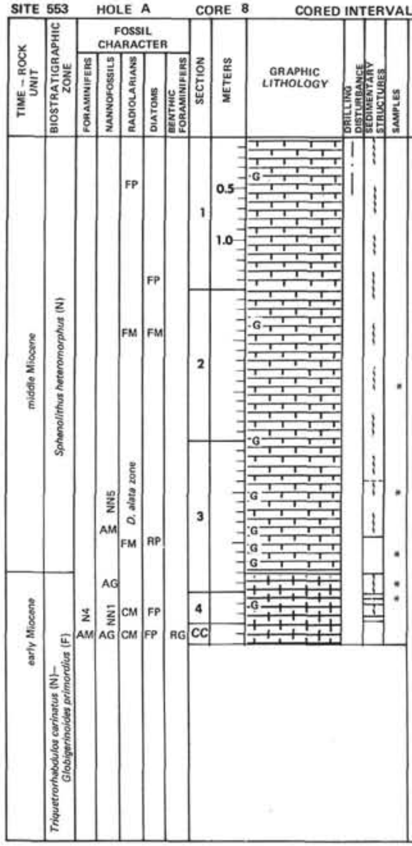

5B 9/1

N7
burrow
mottles

5GY 8/1

5G 8/1

5GY 8/1
with
5G 8/1
laminae

LITHOLOGIC DESCRIPTION

Above Section 3, 128 cm: Foram chalk and nanno foram chalk becoming increasingly glauconitic downhole, to glauconitic foram chalk. This gradation marked by change from bluish white (5B 9/1) through light greenish gray (5GY 8/1) to greenish gray (5G 6/1). Sharp contact at Section 3, 128 cm, with nanno-foram chalk below, of light greenish gray (5GY 8/1) color, with greenish gray (5G 8/1) laminae.

Texture above Section 3, 128 cm, largely sandy: below, sandy mudstone. Section shows extensive burrowing throughout, but disconformity at Section 3, 128 cm associated with extensive burrowing into underlying sediment. Minor laminations below Section 3, 128 cm.

Core relatively undisturbed.

SMEAR SLIDE SUMMARY (%):

	2, 91	3, 51	3, 110	3, 143	4, 8
	D	D	D	D	M
Texture:					
Sand	50	30	70	40	40
Silt	20	10	10	20	30
Clay	30	60	20	40	30
Composition:					
Heavy minerals	Tr	–	–	–	–
Clay	20	10	15	15	20
Volcanic glass	–	–	Tr	–	–
Glauconite	5	5	15	–	–
Carbonate unspec.	–	2	3	20	30
Foraminifers	40	30	40	25	35
Calc. nannofossils	35	50	25	30	10
Sponge spicules	–	3	2	5	5
Dolomite	Tr	–	–	–	–

CARBONATE BOMB (%):
3, 112 = 51

SITE 553 HOLE A CORE 9 CORED INTERVAL 227.0–230.5 m

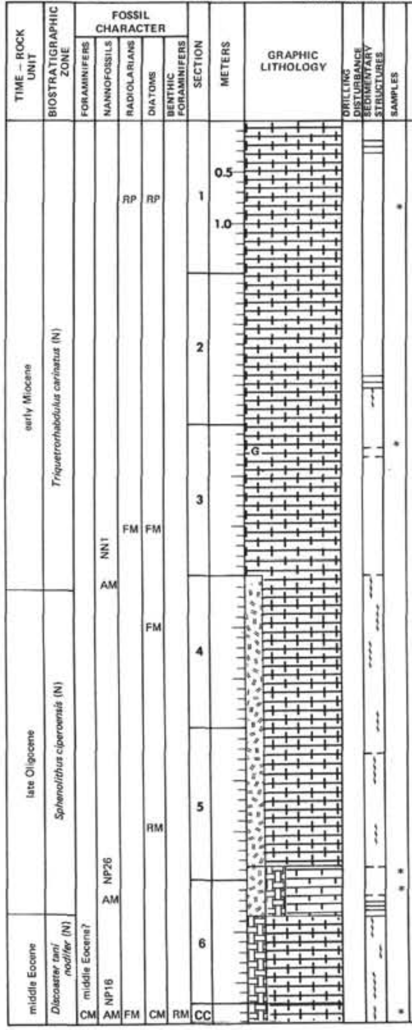

5GY 8/1
rare
laminae
of
5G 8/1

Burrow
fills
of
2.5Y 8/2

5Y 8/2
with
5Y 8/1
burrows

5Y 8/2
10YR 8/3 with
10YR 8/4 laminae

10YR 8/4

LITHOLOGIC DESCRIPTION

Nanno-foram chalk with increasing content of palagonitized ash towards contact at Section 6, 35 cm; colors grade from light greenish gray (5GY 8/1) to white (5Y 8/2). Rare laminae of greenish gray (5G 8/1) in this unit, as well as burrows filled with white (5Y 8/1 and 2.5Y 8/2). Minor biosiliceous component immediately overlying the break, black Mn nodules also. Below Section 6, 35 cm: biosiliceous foram chalk, pale brown (10YR 8/4) burrowed extensively.

Texture slightly sandy to sandy mudstone. Minor laminations, extensive burrowing both within each unit and from the overlying unit into the underlying.

Important development of Mn nodules at the break. Core essentially undisturbed.

SMEAR SLIDE SUMMARY (%):

	1, 89	3, 21	5, 142	6, 10	CC, 10
	D	M	D	D	D
Texture:					
Sand	30	60	60	60	–
Silt	20	20	10	5	–
Clay	50	20	30	45	–
Composition					
Quartz	–	–	–	–	Tr
Feldspar	–	1	Tr	–	–
Heavy minerals	–	Tr	1	–	–
Clay	10	10	5	9	5
Volcanic glass	–	–	–	1	–
Palagonite	5	8	20	–	–
Glauconite	Tr	15	10	3	–
Micronodules	–	–	–	1	–
Carbonate unspec.	9	5	1	–	10
Foraminifers	30	40	30	45	30
Calc. nannofossils	45	20	20	35	30
Diatoms	–	–	–	Tr	Tr
Radiolarians	–	–	1	Tr	5
Sponge spicules	1	1	10	5	15
Fish remains	–	–	2	1	–

CARBONATE BOMB (%):
2, 122 = 80
5, 100 = 79
6, 47 = 72

X. R. D. BULK SAMPLE ANALYSES:

	Calc.	Feld.	Clay :	Sm.
5, 145 =	88	6	6	: 100

SITE 553 HOLE A CORE 10 CORED INTERVAL 236.5–240.0 m

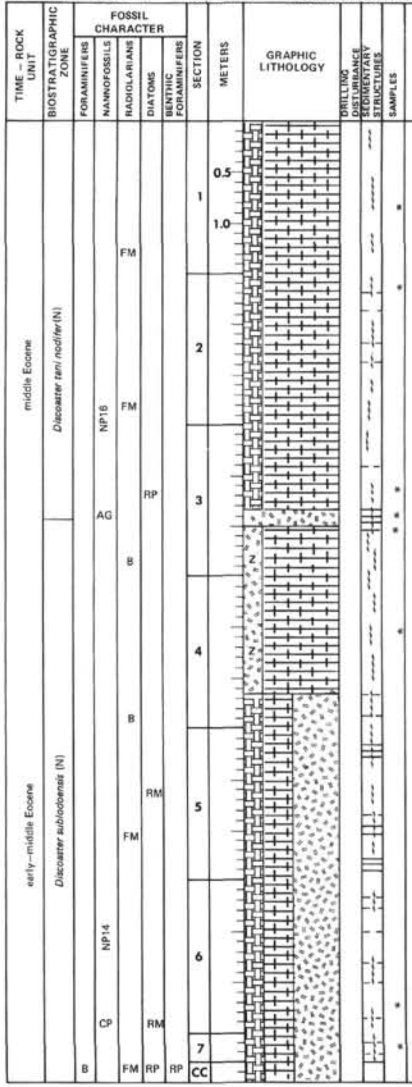

LITHOLOGIC DESCRIPTION

2.5YR 8/4

Burrows of
2.5Y 8/2
and
10Y 8/2

Green
(10Y 6/2)
mottled

Mottles
10Y 6/2

2.5Y 7/4

5Y 7/4 with
5Y 6/2 laminae

2.5Y 5/4
with
2.5Y 6/4
and
2.5Y 7/4
burrows

5Y 5/3
with
10Y 5/4
mottles
and
laminae

Two units.

Unit 1: Sections 1–3, 85 cm is pale yellow (2.5Y 8/4 and 2.5Y 7/4) biosiliceous nanno-foram chalk, with some pale olive (10Y 6/2) mottles. Texturally is sandy mudstone, intensely burrowed, mainly horizontally.

Unit 2: Below Section 3, 85 cm is vitric tuff, zeolitic tuffaceous nanno-foram chalk, zeolitic nanno-foram chalk and biosiliceous palagonitic tuff. Tuffs are fine-grained; some clasts reach 1–2 mm, set in sandy mudstones background. Colors range from pale yellow (5Y 7/4) through light olive brown (2.5Y 7/4) to olive (5Y 5/3), with burrows mottles of light olive brown (2.5Y 6/4 and 2.5Y 7/4) and light olive (10Y 5/4). Lapilli are light olive (10Y 5/4) through palagonitization.

Texturally sandy mudstone, extensively burrowed both within the unit and from the overlying unit.

Core undisturbed.

SMEAR SLIDE SUMMARY (%):

	1, 88 D	2, 19 M	3, 69 D	3, 90 D	3, 108 D
Texture:					
Sand	30	60	40	10	30
Silt	20	10	20	70	25
Clay	50	30	40	20	45
Composition:					
Feldspar	–	–	–	5	1
Heavy minerals	–	–	–	1	1
Clay	10	15	10	15	5
Volcanic glass	–	Tr	2	75	–
Palagonite	–	2	3	–	15
Clinoptilolite	–	–	–	–	15
Carbonate unspec.	2	–	–	–	2
Foraminifers	30	50	35	2	20
Calc. nannofossils	55	30	40	1	40
Diatoms	Tr	Tr	Tr	–	–
Radiolarians	1	–	Tr	–	Tr
Sponge spicules	2	3	10	1	1
Fish remains	–	–	–	–	Tr

	4, 53 D	6, 122 D	7, 14 D
Texture:			
Sand	25	50	20
Silt	30	30	20
Clay	45	20	60
Composition:			
Feldspar	2	1	–
Heavy minerals	2	2	–
Clay	13	15	35
Volcanic glass	5	–	–
Palagonite	2	70	3
Glauconite	1	–	–
Pyrite	1	–	–
Clinoptilolite	20	–	Tr
Carbonate unspec.	6	–	–
Foraminifers	15	–	15
Calc. nannofossils	30	2	25
Radiolarians	–	Tr	2
Sponge spicules	–	10	20

CARBONATE BOMB (%):
2, 25 = 71

X. R. D. BULK SAMPLE ANALYSES:

	Calc.	Zeol.	Clay	:	Sm.
3, 110 =	87	10	3	:	100
6, 121 =	38	–	62	:	100

SITE 553 HOLE A CORE 11 CORED INTERVAL 246.0–255.5 m

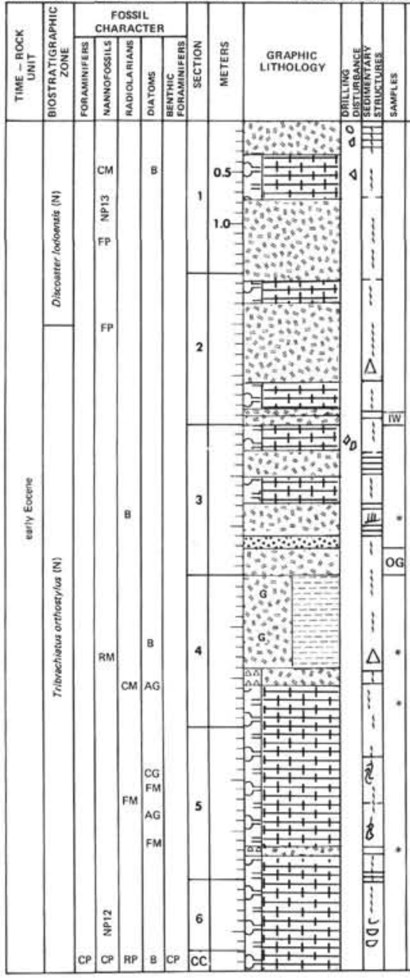

LITHOLOGIC DESCRIPTION

5Y 5/3
with
10Y 5/4
laminae

5GY 2/1

Burrows of
5Y 5/3

5Y 5/3

5GY 2/1
with
5G 2/1

5Y 5/3
5GY 2/1
5Y 5/3

5Y 3/2 +
5GY 2/1
laminae
5Y 5/3

5Y 3/2

5GY 2/1

5G 4/1

2.5Y 4/2,
burrows of
5Y 6/2

10Y 4/2

2.5Y 4/2,
burrows of
10Y 4/2

5Y 4/2
5Y 5/2

Volcanic tuff and volcanic lapilli, predominantly greenish black (5GY 2/1, 5G 2/1) or dark olive gray (5Y 3/2), minor dark greenish gray (5G 4/1), interbedded with biosiliceous nannofossil chalk, grading from pale olive (5Y 5/3), through dark grayish brown (2.5Y 4/2), light olive gray (5Y 6/2), grayish olive (10Y 4/2) to olive gray (5Y 5/2, 5Y 4/2) and glauconitic mudstone (5GY 2/1).

Volcanic tuffs are generally fine- to medium-grained but occasional grains > 4 mm (lapilli) are encountered. Chalk is mudstone texture but has common reworked volcanic clasts throughout. Some graded tuffs but disturbed by interior burrowing (echinoid feeding burrows recognized). Some scouring and minor cross-bedding and slumping. Macrofossils appear – echinoid and serpulid worms. Some drilling breccia but mainly intact.

SMEAR SLIDE SUMMARY (%):

	3, 93 D	4, 79 D	4, 127 D	5, 120 M
Texture:				
Sand	40	70	0	0
Silt	45	25	60	10
Clay	15	5	40	90
Composition:				
Feldspar	1	–	–	1
Heavy minerals	1	1	Tr	–
Clay	10	5	–	35
Volcanic glass	65	–	–	4
Glauconite	–	85	–	25
Zeolite	5	–	–	5
Carbonate unspec.	–	–	5	–
Foraminifers	5	7	–	–
Calc. nannofossils	5	2	20	4
Diatoms	Tr	–	30	–
Radiolarians	Tr	–	15	2
Sponge spicules	8	Tr	15	2
Opal-CT	–	–	–	20

CARBONATE BOMB (%):
2, 100 = 6
2, 125 = 12
6, 62 = 41

X. R. D. BULK SAMPLE ANALYSES:

	Calc.	Feld.	Crist.	Clay	: Sm.
4, 78 =	32	–	–	68	: 100
4, 96 =	62	8	26	4	: 100

SITE 553 HOLE A CORE 12 CORED INTERVAL 255.5–265.0 m

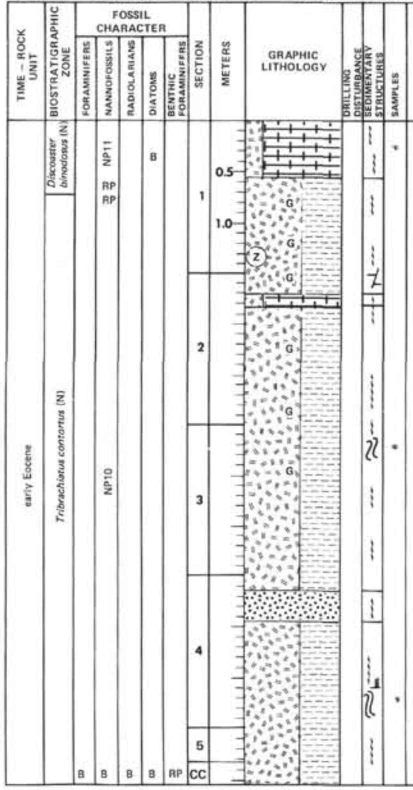

LITHOLOGIC DESCRIPTION

5G 6/1
burrows of
5Y 6/1 +
5G 4/1

5GY 2/1
and
5G 2/1

5G 6/1

5GY 2/1

Burrows
of
5GY 4/1

5G 4/1

5GY 2/1

5G 2/1

Tuffaceous glauconitic mudstone predominant, ranging from greenish black (5GY 2/1, 5G 2/1) to dark greenish gray (5G 4/1). Minor interbeds of tuffaceous nanno-foram chalk, greenish gray (5G 6/1). Extensive burrowing throughout burrows filled by light olive gray (5Y 6/1) and dark greenish gray (5G 4/1 and 5GY 4/1).

Below Section 4, lapilli tuff, with angular to rounded lapilli up to 1 cm. Range from brownish gray (5YR 2/1) to greenish black (5G 2/1).

Soft-sediment deformation common including slumping, micro-faulting and sedimentary dykes.

Core essentially undisturbed.

SMEAR SLIDE SUMMARY (%):

	1, 30 D	3, 20 D	4, 124 D
Texture:			
Sand	50	60	80
Silt	20	20	10
Clay	30	20	10
Composition:			
Quartz	8	–	3
Feldspar	2	–	–
Heavy minerals	2	–	2
Clay	10	20	5
Palagonite	5	10	5
Glauconite	10	60	80
Zeolite	–	1	2
Carbonate unspec.	8	4	1
Foraminifers	20	–	–
Calc. nannofossils	35	5	2
Sponge spicules	–	Tr	–
Fish remains	Tr	–	–

CARBONATE BOMB (%):
1, 12 = 47
4, 25 = 3

SITE 553 HOLE A CORE 13 CORED INTERVAL 265.0–274.5 m

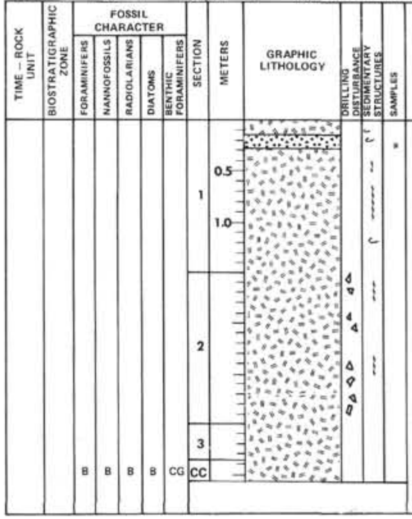

LITHOLOGIC DESCRIPTION

5G 2/1

Volcanic ash and lapilli, greenish black (5G 2/1). Mainly sand-size particles with scattered lapilli but one bed of coarser lapilli-sized material occurs.

Extensive burrowing has destroyed any original grading.

Macrofossils increase gastropods, bryozoa and bivalves, the latter both as fragments and in place, both valves occurring.

Core brecciated in parts.

SMEAR SLIDE SUMMARY (%):

	1, 23 D
Texture:	
Sand	80
Silt	10
Clay	10
Composition:	
Quartz	3
Heavy minerals	5
Clay	10
Palagonite	80
Carbonate unspec.	2

CARBONATE BOMB (%):
1, 126 = <1%

SITE 553 HOLE A CORE 14 CORED INTERVAL 274.5–284.0 m

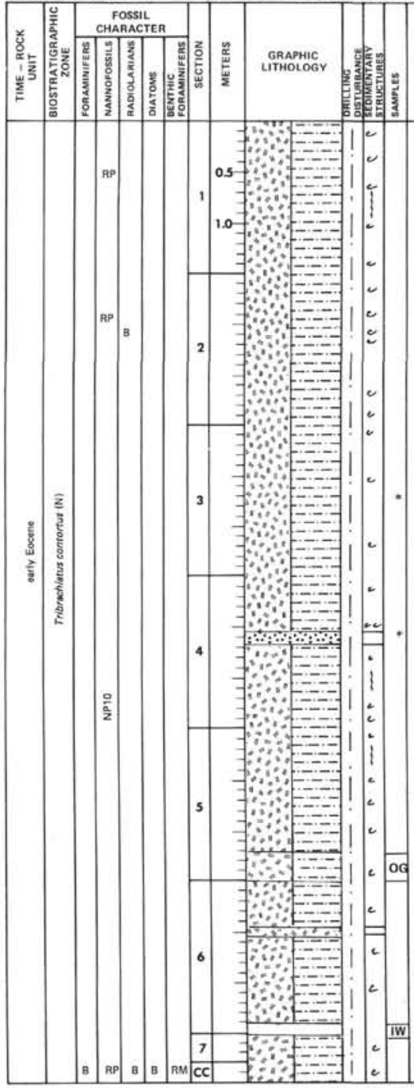

LITHOLOGIC DESCRIPTION

5G 2/1

5Y 4/1

5G 2/1

Tuffaceous sandy mudstone, greenish black (5G 2/1) with minor volcanic ash or lapilli interbeds, ranging from greenish black (5G 2/1) to olive gray (5Y 4/1).

Sandy mudstone texture except for ash beds – one is argillized, with mudstone texture, the other is coarse grained (lapilli-size, up to 1 cm). Abundant macrofossils, including in situ and re-worked bivalves, serpulids, and gastropods (turritella). Sequence essentially homogeneous with minor burrowing.

Core is moderately disturbed throughout – drilling biscuit.

SMEAR SLIDE SUMMARY (%):

	3, 70 D	4, 58 M
Texture:		
Sand	80	60
Silt	10	30
Clay	10	10
Composition:		
Quartz	20	6
Feldspar	3	–
Mica	Tr	1
Heavy minerals	2	1
Clay	10	10
Palagonite	65	60
Zeolite	–	20
Carbonate unspec.	–	1
Calc. nannofossils	Tr	1

CARBONATE BOMB (%):
2, 10 = 2
5, 106 = 2

X. R. D. BULK SAMPLE ANALYSES:

	Zeol.	Clay	:	Sm.
4, 58 =	64	36	:	100

SITE 553 HOLE A CORE 15 CORED INTERVAL 284.0–293.5 m

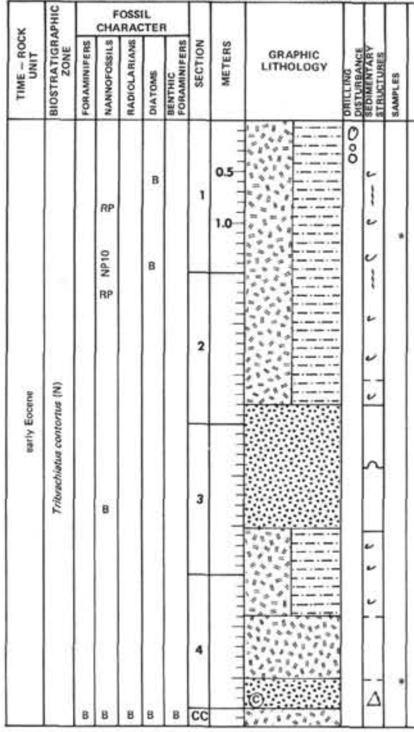

LITHOLOGIC DESCRIPTION

5G 2/1

Tuffaceous sandy mudstone, greenish black (5G 2/1, 5GY 2/1) with volcanic tuff and volcanic lapilli interbeds, also greenish black (5GY 2/1). Base of one tuff is calcite cemented with a white matrix (5Y 8/1). Lapilli range from black (N4), through greenish black (5G 2/1) to dusky red (2.5YR 3/2).

Tuffs are mainly sand sized but some are coarser, ranging up to 2 cm lapilli. Background sediment has sandy mudstone texture. Some grading discernible in the tuffs, and one has a slumped contact.

Macrofossils common particularly in the mudstone – mainly bivalves and serpulids.

5GY 2/1

SMEAR SLIDE SUMMARY (%):

	1, 116 D	4, 102 D
Texture:		
Sand	40	60
Silt	20	10
Clay	40	30
Composition:		
Quartz	20	3
Feldspar	2	–
Heavy minerals	1	2
Clay	35	25
Palagonite	30	60
Zeolites	Tr	–
Carbonate unspec.	–	10
Calc. nannofossils	3	–
Diatoms	3	–
Sponge spicules	6	–

CARBONATE BOMB (%):
2, 30 = 4

5Y 8/1

SITE 553 HOLE A CORE 16 CORED INTERVAL 293.5–303.0 m

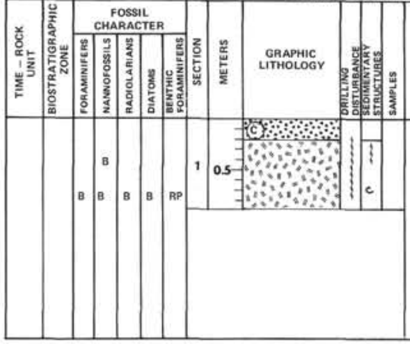

LITHOLOGIC DESCRIPTION

5Y 8/1
5GY 2/1

Volcanic tuff and volcanic lapilli, greenish black (5GY 2/1), minor burrow mottling of olive (5Y 4/3). White (5Y 8/1) matrix to lapilli.

Mainly medium-grained tuffs, with coarser lapilli in top section. Macrofossils include serpulids and bivalves.

Core moderately or intensely disturbed.

CARBONATE BOMB (%):
1, 32 = 14

SITE 553 HOLE A CORE 17 CORED INTERVAL 303.0–312.5 m

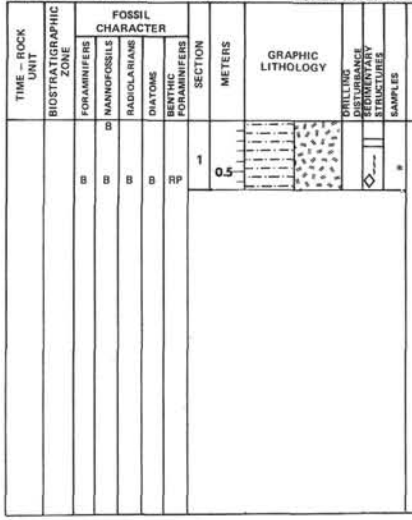

LITHOLOGIC DESCRIPTION

5GY 2/1

Sandy volcanic tuff, greenish black (5GY 2/1).

Reworked and burrowed locally. Sand-sized particles mainly.

Core undisturbed.

SMEAR SLIDE SUMMARY (%):

	1, 47 D
Texture:	
Sand	70
Silt	20
Clay	10
Composition:	
Quartz	15
Feldspar	5
Heavy minerals	4
Clay	10
Palagonite	60
Zeolite	4
Carbonate unspec.	2

CARBONATE BOMB (%):
1, 32 = <1

SITE 553 HOLE A CORE 18 CORED INTERVAL 312.5–322.0 m

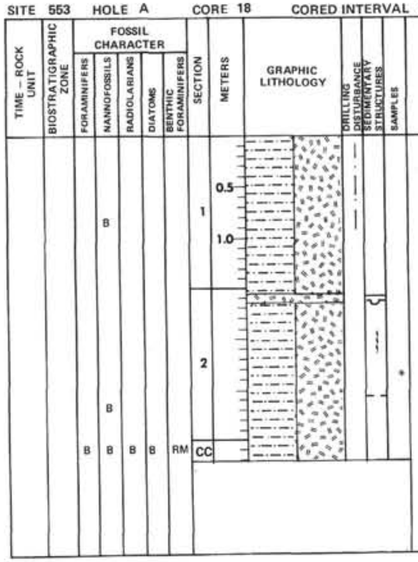

LITHOLOGIC DESCRIPTION

5GY 2/1

Sandy volcanic tuff with minor volcanic tuff interbeds, all greenish black (5GY 2/1).

Tuff particles fairly coarse but rarely grade to lapilli.

Local scours evident, minor burrowing.

Core undisturbed except for drilling biscuit in first 80 cm.

SMEAR SLIDE SUMMARY (%):

	2, 88 D
Texture:	
Sand	80
Silt	10
Clay	10
Composition:	
Quartz	3
Feldspar	Tr
Mica	Tr
Heavy minerals	2
Clay	20
Palagonite	75

CARBONATE BOMB (%):
1, 91 = 1
1, 128 = <1

SITE 553 HOLE A CORE 19 CORED INTERVAL 322.0–331.5 m

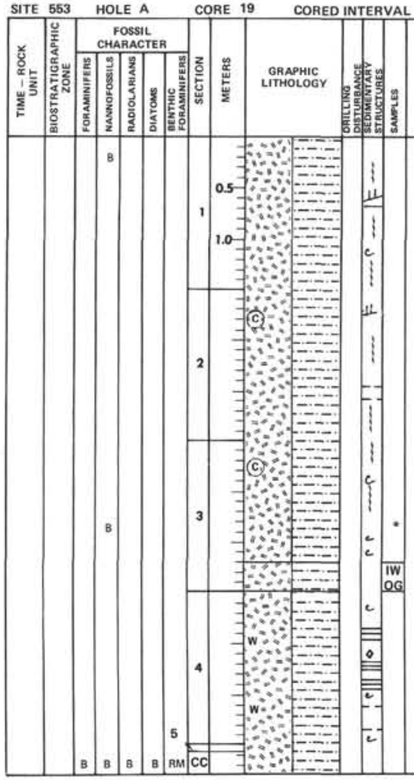

LITHOLOGIC DESCRIPTION

5GY 2/1

Sandy volcanic tuff throughout, greenish black (5GY 2/1). Carbonaceous fragments appear toward base. Well-sorted, probably reworked; extensive burrowing (vertical and horizontal) minor cross-lamination and rip-up clasts. Some laminations.

Macrofauna includes serpulid worms and thick-shelled bivalves (c.f. higher in the sequence).

Calcite cementation locally. Core relatively undisturbed.

SMEAR SLIDE SUMMARY (%):

	3, 80
	D
Texture:	
Sand	60
Silt	20
Clay	20
Composition:	
Quartz	10
Feldspar	2
Mica	Tr
Heavy minerals	2
Clay	15
Palagonite	70
Carbonate unspec.	1

CARBONATE BOMB (%):
2, 57 = <1

X. R. D. BULK SAMPLE ANALYSES:

	Feld.	Qtz.	Zeol.	Clay	:	Illite	Sm.
4, 52	19	42	9	30	:	33	67

SITE 553 HOLE A CORE 20 CORED INTERVAL 331.5–341.0 m

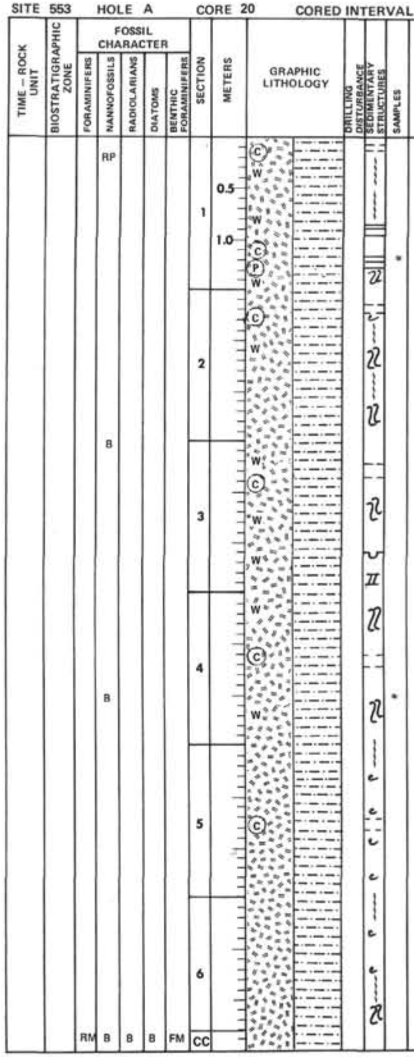

LITHOLOGIC DESCRIPTION

5GY 2/1

Tuffaceous sandy mudstone throughout, abundant carbonaceous material concentrated in laminae. Color uniform greenish black (5GY 2/1).

Material fine- to medium-grained. Evidence of slumping, scouring, cross-lamination and extensive burrowing.

Rich macrofauna, mainly thin-shelled bivalves.

Calcite and pyrite concretions.

Core relatively undisturbed.

SMEAR SLIDE SUMMARY (%):

	1, 121	4, 100
	M	D
Texture:		
Sand	50	70
Silt	40	10
Clay	10	20
Composition:		
Quartz	20	30
Feldspar	5	10
Mica	15	15
Heavy minerals	5	5
Clay	15	25
Palagonite	25	15
Plant debris	15	–

SITE 553 HOLE A CORE 21 CORED INTERVAL 341.0–350.5 m

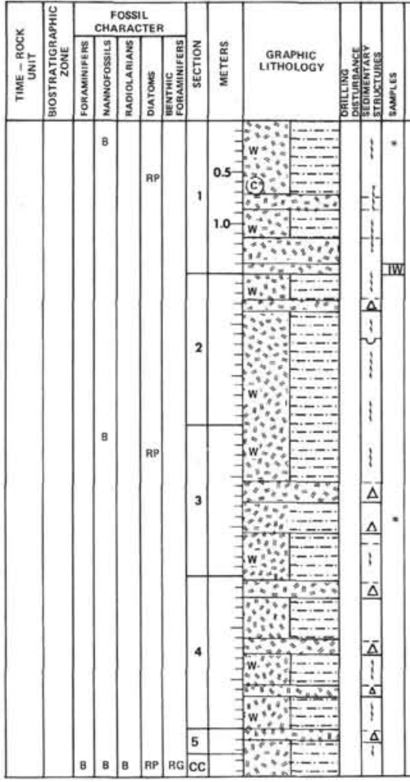

LITHOLOGIC DESCRIPTION

5Y 2/1

Tuffaceous sandy mudstone with common interbeds of volcanic tuff and volcanic lapilli, all olive black (5Y 2/1).

Tuffs and lapilli are sharp-based and graded, but sometimes this is obscured by burrowing. Mudstone has fine-grained sand and silt-size particles. Local scours and extensively burrowed throughout. Carbonaceous matter common. Some calcite cementation. Lapilli commonly olive-gray vesicular pumice.

Core essentially undisturbed.

SMEAR SLIDE SUMMARY (%):

	1, 21	3, 93
	D	D
Texture:		
Sand	70	85
Silt	10	5
Clay	20	10
Composition:		
Quartz	20	4
Feldspar	5	2
Mica	Tr	–
Heavy minerals	5	2
Clay	25	10
Palagonite	45	80
Carbonate unspec.	–	2
Calc. nannofossils	Tr	–
Diatoms	Tr	–
Sponge spicules	Tr	–

CARBONATE BOMB (%):
1, 125 = 1
3, 85 = 1
4, 50 = 2

SITE 553 HOLE A CORE 22 CORED INTERVAL 350.5–360.0 m

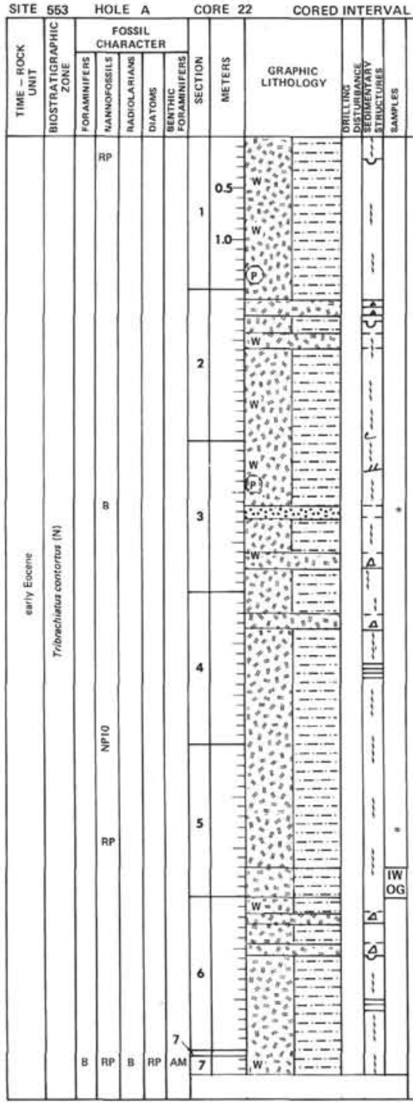

LITHOLOGIC DESCRIPTION

5Y 2/1

Tuffaceous sandy mudstone with volcanic tuff and volcanic lapilli interbeds, all olive black (5Y 2/1). Carbonaceous fragments disseminated throughout.

Tuff beds graded and sharp-based except where obscured by burrowing. Some evidence of scouring, lamination and cross-laminations. Becoming extensive, some burrows pyritized.

Macrofossils confined to serpulids.

Core undisturbed.

SMEAR SLIDE SUMMARY (%):

	3, 70	5, 82
	D	D
Texture:		
Sand	70	70
Silt	10	10
Clay	20	20
Composition:		
Quartz	10	35
Feldspar	2	5
Mica	–	5
Heavy minerals	3	5
Clay	25	20
Palagonite	60	30
Calc. nannofossils	Tr	Tr

CARBONATE BOMB (%):
5, 104 = <1

X. R. D. BULK SAMPLE ANALYSES:

	Feld.	Qtz.	Zeol.	Clay	:	Illite.	Sm.
4, 88 =	53	26	5	16	:	58	42

SITE 553 HOLE A CORE 23 CORED INTERVAL 360.0–369.5 m

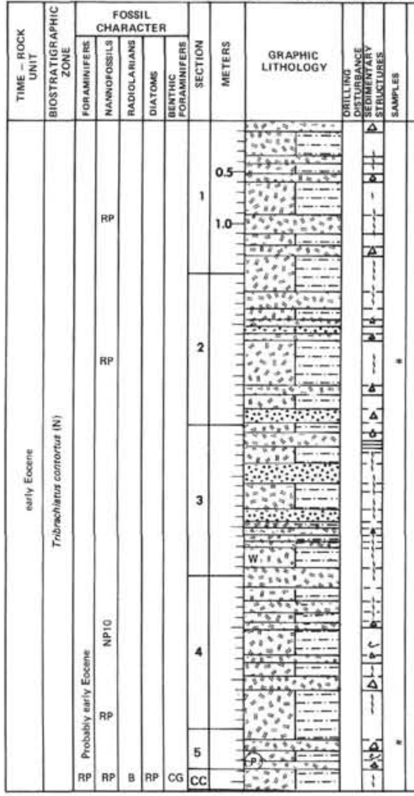

LITHOLOGIC DESCRIPTION

5Y 2/1

Common volcanic tuff and lapilli units in background of tuffaceous sandy mudstone, all olive black (5Y 2/1).

Volcanic units are sharp based and graded: interbedded sediment. are sandy mudstone texture with abundant burrowing. Minor woody material.

Some macrofossils, largely serpulids; one gastropod noted.

Core undisturbed.

SMEAR SLIDE SUMMARY (%):

	2, 87	5, 16
	D	D
Texture:		
Sand	70	70
Silt	10	10
Clay	20	20
Composition:		
Quartz	30	10
Mica	Tr	–
Heavy minerals	5	3
Clay	20	25
Palagonite	40	60
Carbonate unspec.	5	2
Calc. nannofossils	Tr	–
Diatoms	Tr	–

CARBONATE BOMB (%):
2, 19 = 2

SITE 553 HOLE A CORE 24 CORED INTERVAL 369.5–379.0 m

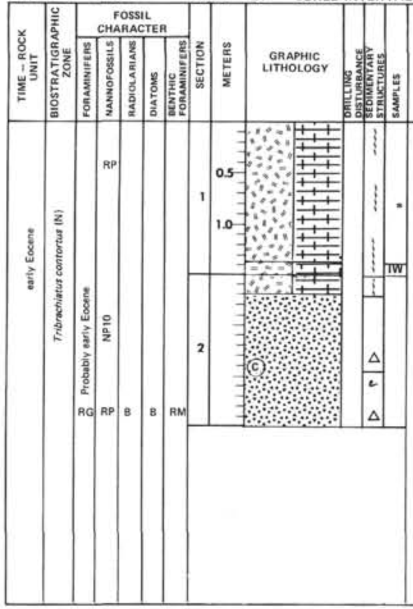

LITHOLOGIC DESCRIPTION

5Y 4/1

Tuffaceous sandy mudstone with volcanic tuff and volcanic lapilli interbeds, olive black (5Y 4/1).

Tuff and lapilli units contain fairly coarse material (up to 1 cm), sandy mudstone texture for remaining sediments.

Volcanogenic units show grading: burrowing common, Serpulids rare; bivalve observed.

Lapilli are vesicular pumice mainly.

Core undisturbed.

SMEAR SLIDE SUMMARY (%):

	1, 81
	D
Texture:	
Sand	70
Silt	10
Clay	20
Composition:	
Quartz	20
Feldspar	5
Mica	1
Heavy minerals	4
Clay	25
Palagonite	45
Sponge spicules	Tr

CARBONATE BOMB (%):
1, 23 = 2

SITE 553 HOLE A CORE 25 CORED INTERVAL 379.0–388.5 m

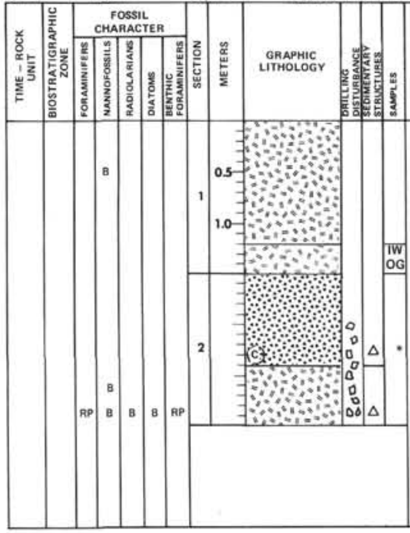

LITHOLOGIC DESCRIPTION

5G 2/1

Volcanic tuff and volcanic lapilli, greenish black (5G 2/1).

Dominantly coarse grained volcanogenic, lapilli up to 8 mm. Base of graded unit is calcite cemented.

No macrofauna observed.

Core brecciated towards base.

SMEAR SLIDE SUMMARY (%):

	2, 78
	M
Texture:	
Sand	50
Silt	40
Clay	10
Composition:	
Quartz	4
Feldspar	1
Clay	10
Palagonite	55
Carbonate unspec.	30

CARBONATE BOMB (%):
2, 57 = 4

SITE 553 HOLE A CORE 26 CORED INTERVAL 388.5–398.0 m

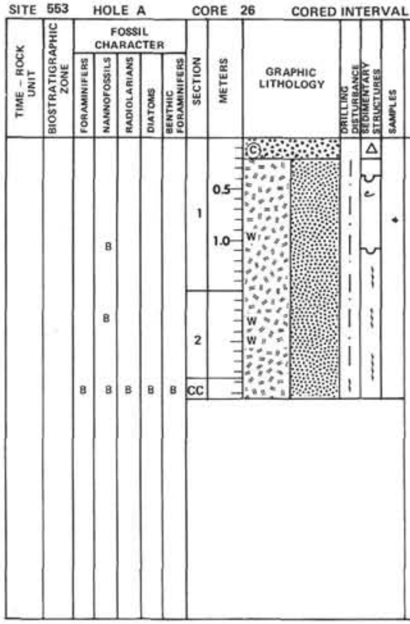

LITHOLOGIC DESCRIPTION

5G 2/1

5GY 2/1

Tuffaceous sandstone with minor lapilli units, greenish black (5G 2/1, 5GY 2/1). Some burrows of pale brownish gray (5YR 6/1). Carbonaceous material common. One volcanogenic unit present – shows grading. Lapilli up to 1 cm, ranging from olive black (5Y 2/1), through dark olive gray (5Y 3/2) to dusky red (2.5YR 3/2). Base is calcite-cemented.

Sandstones are extensively burrowed, and show scoured bases. Some reworked lapilli occur along some bedding planes – current sorting.

Burrows
of
5YR 6/1

Macrofauna – rare thin-shelled bivalves, serpulids.

Core broken into drilling biscuit.

SMEAR SLIDE SUMMARY (%):

	1, 83 D
Texture:	
Sand	80
Silt	15
Clay	5
Composition:	
Quartz	35
Feldspar	10
Heavy minerals	5
Clay	5
Palagonite	45

CARBONATE BOMB (%):
1, 42 = <1

SITE 553 HOLE A CORE 27 CORED INTERVAL 398.0–407.5 m

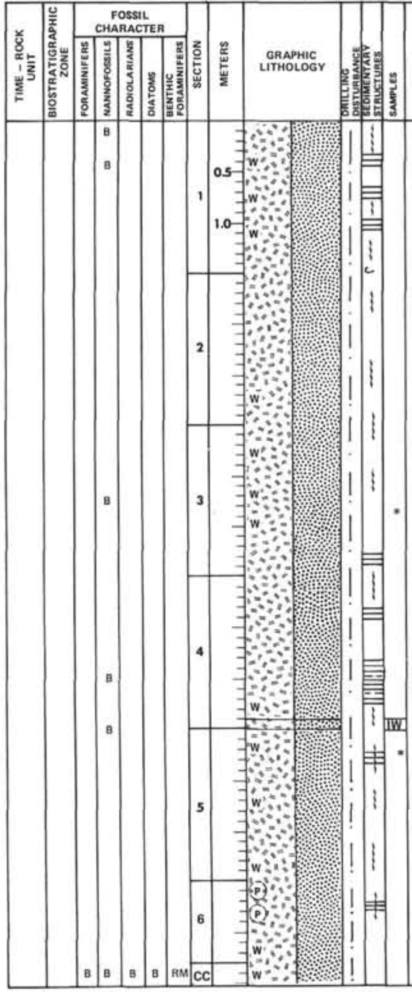

LITHOLOGIC DESCRIPTION

5GY 2/1

Tuffaceous sandstone, greenish black (5GY 2/1) grading to dark greenish gray (5GY 6/1), with burrows of olive black (5Y 2/1). Very carbonaceous and micaceous.

Faint laminations picked out by concentrations of woody detritus. Burrowing extensive, mainly horizontal: some burrows pyritized.

Serpulids rare.

Core broken into drilling biscuit.

Burrows
of
5Y 2/1

SMEAR SLIDE SUMMARY (%):

	3, 81 D	5, 23 M
Texture:		
Sand	60	50
Silt	10	10
Clay	30	40
Composition:		
Quartz	40	30
Feldspar	2	3
Mica	15	10
Heavy minerals	5	2
Clay	30	25
Palagonite	8	30

CARBONATE BOMB (%):
2, 50 = <1
4, 125 = <1

} 5GY 6/1

SITE 553 HOLE A CORE 28 CORED INTERVAL 407.5–417.0 m

TIME – ROCK UNIT	BIOSTRATIGRAPHIC ZONE	FOSSIL CHARACTER: FORAMINIFERS	NANNOFOSSILS	RADIOLARIANS	DIATOMS	BENTHIC FORAMINIFERS	SECTION	METERS	GRAPHIC LITHOLOGY	DRILLING DISTURBANCE	SEDIMENTARY STRUCTURES	SAMPLES	LITHOLOGIC DESCRIPTION
		B	B	B	B	B	CC			¦		*	5GY 6/1

Calcite-cemented tuffaceous sandstone, greenish black (5GY 6/1).

Sandstone medium-grained, volcanic component conspicuous. Micaceous.

Serpulid present.

Core is brecciated.

SMEAR SLIDE SUMMARY (%):

	CC, 5 D
Texture:	
Sand	40
Silt	40
Clay	20
Composition:	
Quartz	10
Feldspar	3
Mica	4
Heavy minerals	3
Clay	15
Palagonite	20
Carbonate unspec.	45

SITE 553 HOLE A CORE 29 CORED INTERVAL 417.0–426.5 m

TIME – ROCK UNIT	BIOSTRATIGRAPHIC ZONE	FOSSIL CHARACTER: FORAMINIFERS	NANNOFOSSILS	RADIOLARIANS	DIATOMS	BENTHIC FORAMINIFERS	SECTION	METERS	GRAPHIC LITHOLOGY	DRILLING DISTURBANCE	SEDIMENTARY STRUCTURES	SAMPLES	LITHOLOGIC DESCRIPTION
							CC		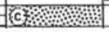	¦ ¦		*	N6

Calcite-cemented sandstone. Light gray (N6). Mica conspicuous. Sandstone medium grained.

Core is brecciated.

SMEAR SLIDE SUMMARY (%):

	CC, 3
Texture:	D
Sand	30
Silt	50
Clay	20
Composition:	
Quartz	8
Feldspar	5
Mica	15
Heavy minerals	2
Clay	5
Carbonate unspec.	65

NOTE: Core 30, 426.5–436.0 m: No recovery.

SITE 553 HOLE A CORE 31 CORED INTERVAL 436.0–445.5 m

TIME – ROCK UNIT	BIOSTRATIGRAPHIC ZONE	FOSSIL CHARACTER: FORAMINIFERS	NANNOFOSSILS	RADIOLARIANS	DIATOMS	BENTHIC FORAMINIFERS	SECTION	METERS	GRAPHIC LITHOLOGY	DRILLING DISTURBANCE	SEDIMENTARY STRUCTURES	SAMPLES	LITHOLOGIC DESCRIPTION
		B	B	B	B	B	CC		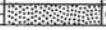	○			

Sandstone slump – disaggregated micaceous medium-grained sand, dark greenish gray (5G 6/1) in color.

Core intensely disturbed.

SITE 553 HOLE A CORE 32 CORED INTERVAL 445.5–455.0 m

TIME – ROCK UNIT	BIOSTRATIGRAPHIC ZONE	FOSSIL CHARACTER: FORAMINIFERS	NANNOFOSSILS	RADIOLARIANS	DIATOMS	BENTHIC FORAMINIFERS	SECTION	METERS	GRAPHIC LITHOLOGY	DRILLING DISTURBANCE	SEDIMENTARY STRUCTURES	SAMPLES	LITHOLOGIC DESCRIPTION
							CC		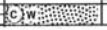		¦	*	

Calcite-cemented fine-grained micaceous sandstone, light gray (N6).

Burrowing evident; common woody detritus.

SMEAR SLIDE SUMMARY (%):

	CC, 3 D
Texture:	
Sand	20
Silt	60
Clay	20
Composition:	
Quartz	12
Feldspar	2
Mica	5
Heavy minerals	3
Clay	20
Palagonite	3
Carbonate unspec.	55

NOTE: Core 33, 455.0–464.5 m: No recovery.

SITE 553 HOLE A CORE 34 CORED INTERVAL 464.5–474.0 m

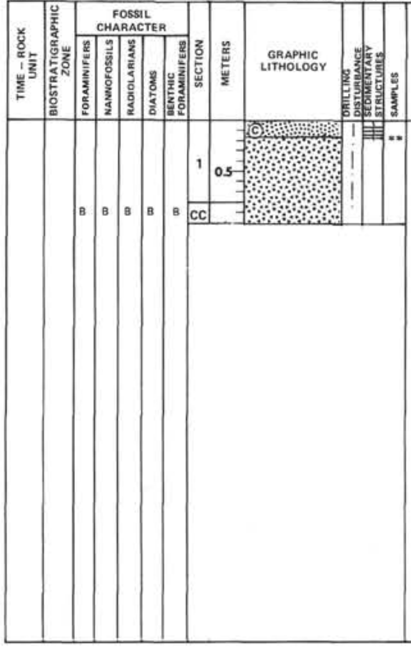

LITHOLOGIC DESCRIPTION

N6
5Y 2/1

Calcite-cemented fine-grained sandstone, light gray (N6) overlying volcanic lapilli, olive black (5Y 2/1). Volcanic lapilli is also calcite-cemented in part, with fragments of vesicular pumice dominating, and is highly zeolitic.

Sandstone contains minor woody material, and is laminated, *with minor burrowing. Lapilli shows no grading.*

Core broken into drilling biscuit.

SMEAR SLIDE SUMMARY (%):

	1, 20 D	1, 20 M
Texture:		
Sand	40	0
Silt	35	80
Clay	25	20
Composition:		
Feldspar	2	5
Mica	–	1
Heavy minerals	2	4
Clay	15	10
Palagonite	42	50
Zeolite	9	10
Carbonate unspec.	30	20

CARBONATE BOMB (%):
1, 46 = <1

X. R. D. BULK SAMPLE ANALYSES:

	Feld.	Clay	:	Sm.
1, 50	18	82	:	100

SITE 553 HOLE A CORE 35 CORED INTERVAL 474.0–483.5 m

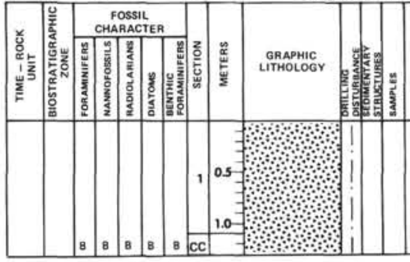

LITHOLOGIC DESCRIPTION

5Y 2/1

Volcanic lapilli, olive black (5Y 2/1), with pumice lapilli up to 2 cm. Some lapilli show alteration haloes.

Core is broken into drilling biscuit.

CARBONATE BOMB (%):
CC = 5

SITE 553 HOLE A CORE 36 CORED INTERVAL 483.5–493.0 m

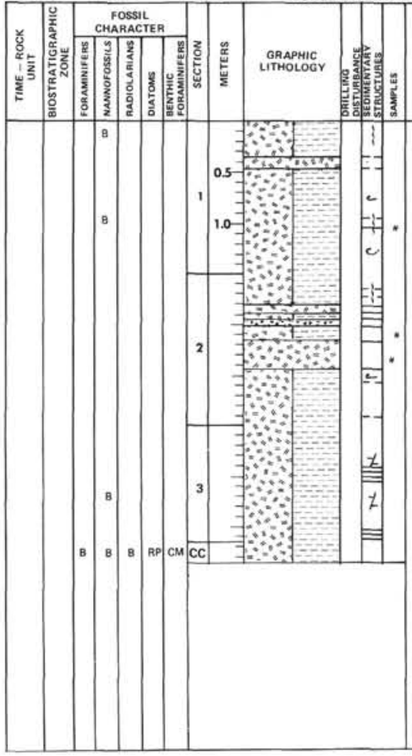

LITHOLOGIC DESCRIPTION

10YR 3/2

10YR 5/3
10YR 3/2

10YR 4/2
5G 2/1
10YR 4/2
5G 2/1
10YR 4/2

Tuffaceous mudstone, very dark grayish brown (10YR 3/2), grading to dark grayish brown (10YR 4/2) and brown (10YR 5/3), with interbeds of volcanic tuff and lapilli, greenish black (5G 2/1).

Mudstone very fine grained. Volcanics are medium to coarse. Mudstones show laminations, with very little evidence of current activity – one minor channel noted. Faults are associated with slickensides and are post-depositional. Calcite-cementation of tuffs. Macrofossils include thin-shelled bivalves, gastropods and serpulids.

Core undisturbed.

SMEAR SLIDE SUMMARY (%):

	1, 101 D	2, 60 D	2, 88 D
Texture:			
Sand	60	70	60
Silt	10	10	20
Clay	30	20	20
Composition:			
Quartz	2	2	–
Feldspar	1	–	1
Heavy minerals	1	1	1
Clay	30	25	18
Palagonite	65	70	50
Zeolite	–	–	10
Carbonate unspec.	1	2	20
Foraminifers	–	Tr	–
Calc. nannofossils	Tr	–	Tr
Calc. nannofossils	Tr	–	Tr

CARBONATE BOMB (%):
1, 76 = 1
1, 114 = 1

X. R. D. BULK SAMPLE ANALYSES:

	Calc.	Feld.	Qtz.	Zeol.	Clay	:	Sm.
1, 75 =	–	–	48	9	43	:	100
2, 80 =	32	6	–	25	37	:	100

SITE 553 HOLE A CORE 37 CORED INTERVAL 493.0–502.5 m

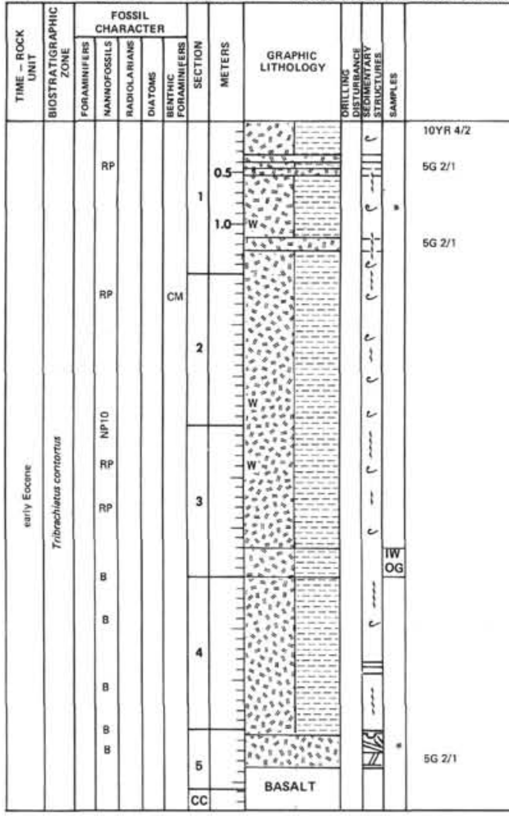

LITHOLOGIC DESCRIPTION

Tuffaceous mudstone, dark grayish brown (10YR 4/2) with minor volcanic tuff or lapilli interbeds (greenish black [5G 2/1]) Mudstones contain common carbonaceous detritus.

Extensive burrowing throughout, many burrows exhibiting palagonite and pyrite rims. Burrowing has destroyed much original structures but laminae preserved locally.

Abundant thin-walled bivalves: gastropods and serpulids also present.

Immediately overlying basalt a coarse grained cross-bedded and slumped reworked(?) tuff present; large clast of overlying mudstone incorporated into this unit.

Core essentially undisturbed.

SMEAR SLIDE SUMMARY (%):

	1, 89 D	5, 17 D
Texture:		
Sand	70	70
Silt	5	5
Clay	25	25
Composition:		
Quartz	2	1
Feldspar	–	Tr
Mica	–	Tr
Heavy minerals	Tr	1
Clay	25	25
Palagonite	70	70
Zeolite	1	Tr
Carbonate unspec.	2	3
Calc. nannofossils	–	Tr

CARBONATE BOMB (%):
1, 129 = 8
4, 123 = 3

X. R. D. BULK SAMPLE ANALYSES:

	Calc.	Qtz.	Zeol.	Clay	:	Sm.
1, 98 =	17	63	6	14	:	100

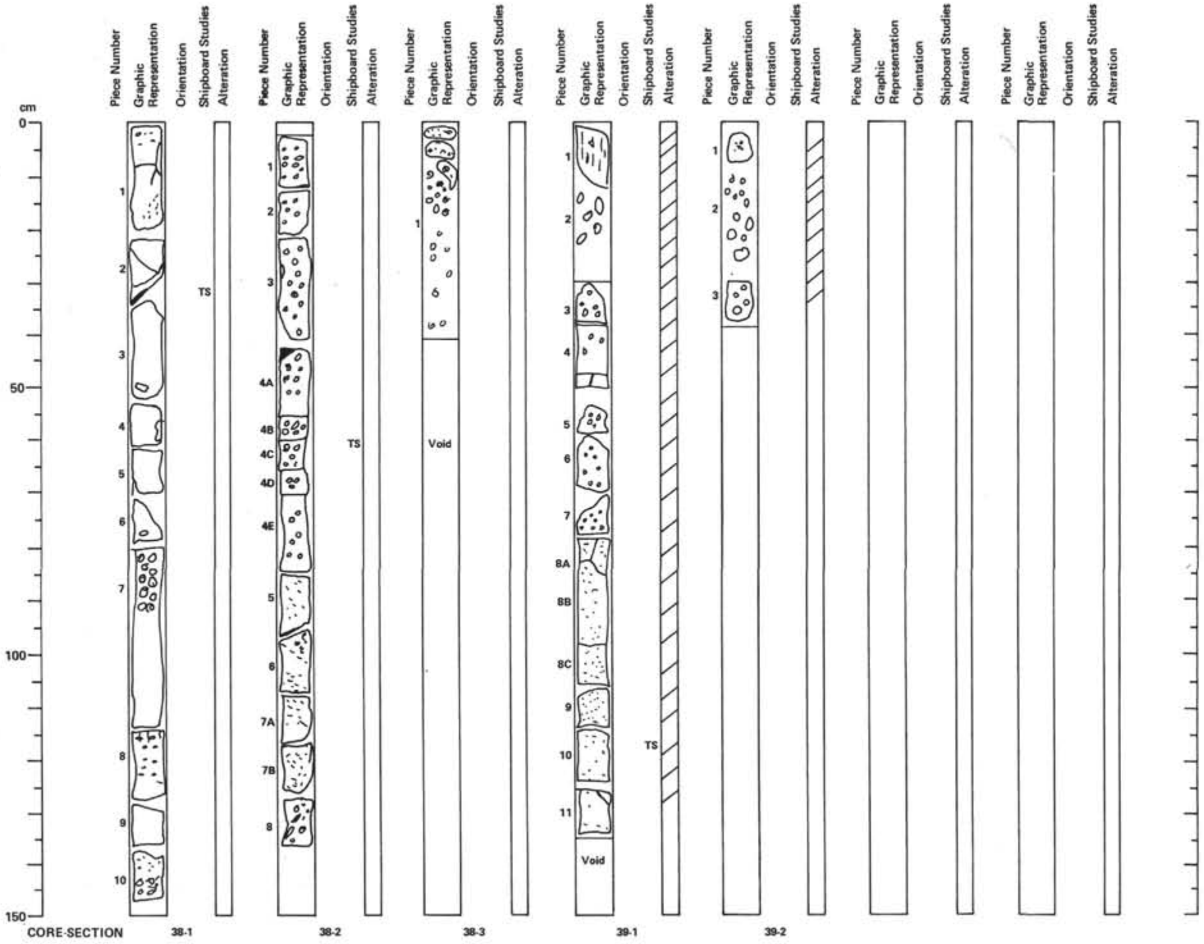

LEG 81, HOLE 553A

CORE 38, SECTION 1 — Depth 502.5–504.0 m

Pieces 1 and 2: Dark gray (N3) vesicular basalt uniform size distribution of vesicles ~1 cm or less. Yellowish gray (5Y 8/1) to light gray (N7) irregular patches of calcite and quartz. Vesicles are filled with smectite. At 3 cm vesicles dip at 45°. At 25 cm calcite(?) vein inclined at 60°.

Piece 3: Large angular 'clast' with diffuse rim exhibiting markedly less vesicularity. Basalt fracture pieces covered in calcite. Veins dip at 50° and 30°. Groundmass: plagioclase laths, etc.

78 cm: Base of unit/top of unit.

Piece 7: Medium-dark grgy (N4) vesicular phyric basalt. Abundant dusky blue green patches, irregularly veining rock, and vesicles (celadonite?).

Piece 8: Medium gray (N5) highly vesicular phyric basalt. Vesicles highly irregular but towards top of unit show preferred vertical orientation. Occasional vesicles filled with grayish blue green (5BG 5/2).

Markedly less vesicular, but vesicles commonly filled with grayish blue green mineral. Sparse unfilled vesicles. No apparent difference in groundmass – plagioclase laths and pyroxene.

Piece 10: Abundant large (0.5 cm) vesicle filled with light gray (N6–N7) mineral. Vesicles inpart unfilled.

Thin Section – 33 cm: Altered tholeiitic basalt (orthophyric-hypidiomorphic, vesicular, trachytic).

CORE 38, SECTION 2 — Depth 504.0–505.5 m

Pieces 1–5: Medium light gray (N7) vesicular phyric basalt.

0–100 cm: General trend is a downward decrease in vesicle size from sizes of 0.5 cm at top to 0.2 cm towards 95 cm. Infilling of vesicles also progressively increases over this interval. Infilling of yellowish gray (5Y 8/1) may be quartz and calcite. Smaller vesicles are nearly completely infilled by smectite and quartz. Gradational boundary at 100 cm.

Pieces 6 and 7: Medium light gray (N7) vesicular phyric basalt – abundant small vesicles (>0.1 cm). Unfilled vesicles sparse.

Piece 8: Vesicular basalt. Vesicle size larger (possible contact in overlying pebble?). Some indication of near vertical preferred circulation. Larger vesicles infilled by bluish white (5B 9/1) mineral (quartz and calcite).

Thin Section – 60 cm: Tholeiitic basalt (orthophyric-hypidiomorphic, vesicular, trachytic).

CORE 38, SECTION 3 — Depth 505.5–505.9 m

Vesicular phyric basalt, medium gray (N7). Small pebbles of basalt extensively colored light blue green (5BG 6/6). Base of unit at 10 cm.

CORE 39, SECTION 1 — Depth 512.0–513.5 m

Piece 1: Basalt, phyric, medium gray with vertically oriented vesicles which are filled with blue green and black smectite.

Pieces 2–11: Basalt, medium gray (N5) aphyric to phyric with different sized vesicles which according to diameter show black (N1) rims which are void, filled with white, bluish green (5BG 4/6) and black micro-cryptocristalline mineral identified by XRD as smectite. With depth vesicles become less and smaller in size.

Thin Section – 115 cm: Altered tholeiitic basalt (orthophyric-hypidiomorphic, vesicular, trachytic).

CORE 39, SECTION 2 — Depth 513.5–513.88 m

Basalt, medium gray as above but as seen in Piece 3 with few vesicles up to 8 mm in diameter.

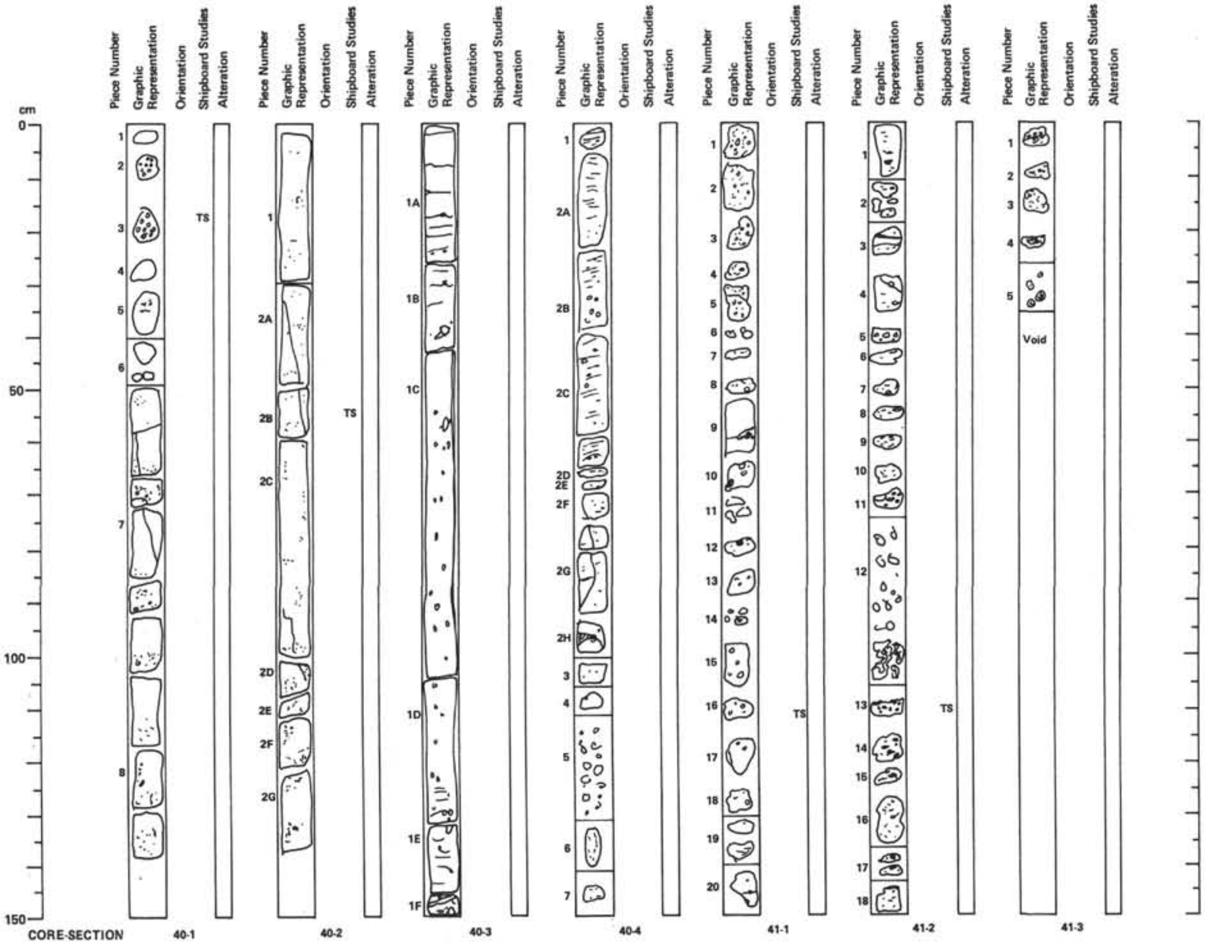

LEG 81, HOLE 553A

CORE 40, SECTION 1

Depth 521.5–523.0 m

Piece 1: Grayish green (5G 5/2) piece of 'chert' (quartz and low crystobalite). Highly vesicular basalt, medium gray (N4).

Pieces 2 and 3: Veiscular basalt, dark gray (N5) vesicles (0.3–0.7 mm) with green (5G 5/2) amorphous(?) lining.

Piece 4: Grayish green (10G 4/2) chert (quartz, low crystobalite and celadonite) lining black patches.

Pieces 5–8: Basalt is phyric and a uniform gray (N5) in color. Major variations are in the presence of infilled vesicles especially in Pieces 6, 7B and E. Towards the base (Piece 8C) vesicles become more abundant and are partially open (size 1–3 mm). Vesicles in Pieces 6, 7B and E are concentrated in water patches within which there is some suggestion of a preferred concentration perpendicular to the axis of the core. Vesicles are infilled with black (N2.5) mineral. Part infilled vesicles are used with black mineral forming amygdules. Occasional white mineral completely infills amygdules (quartz and calcite).

In more uniform phyric basalt smaller vesicles (1 mm or less) predominate. Laths of feldspar are apparent and pyroxenes(?) or altered pyroxenes (10Y 6/6) in groundmass. Occasional specks of pyrite.

Extremely vesicular basalt at top of section probably represents top of flow. Presence of celadonite in chert indicates submarine environment.

Thin Section – 16 cm: Altered tholeiitic basalt (orthophyric, hypidiomorphic, trachytic, vesicular).

CORE 40, SECTION 2

Depth 523.0–524.5 m

Pieces 1 and 2: Gray to dark gray (N4–N5) phyric vesicular basalt.

Principle vesicle variations down section are of two types: 1) Vesicles from two size populations. First group less than 0.5 mm scattered uniformly throughout basalt. 2) Second group concentrated in circular patches (1–2 mm). These patches vary in size from 2–3 cm down to 1 cm. Some have (e.g. Piece 2G) clear reaction rims around them.

The patches of infilled vesicles show no preferred orientation. *One prominent band of vesicles (Pieces 2E and F)* shows a distinct horizontal orientation although some kind of 'flow line' defines its upper surface.

Basalt groundmass consists of laths of plagioclase (1 mm in length) and green minerals (pyroxenes).

Vesicles generally composed of olive gray (5Y 3/2) mineral with sparse rare minute white nuclei.

Thin Section – 55 cm: Altered tholeiitic basalt (orthophyric-hypidiomorphic, vesicular, trachytic).

CORE 40, SECTION 3

Depth 524.5–526.0 m

Piece 1: Dark gray to gray (N5–N4) phyric vesicular basalt. Vesicles scattered partly informly throughout core. Vesicles range in size from 1 mm to 3 cm. Larger vesicles have thin (1 mm) lining and green (montmorillonite?) core. Large vesicle in Core 40, Section 2 has black lining and light brownish gray (2.5Y 6/2) infill smectite. A vein adjoining the vesicle and just below is filled with a light gray (N6) mineral (quartz and calcite). In some vesicles, the black mineral seems to be ungrowing at the expense of the green montmorillonite. In Piece 1F, a light gray (N6) vein (5 mm) dips at 45°; probably quartz and calcite. Below this vein there is an oblate patch of the vesicles described from Core 40, Section 2.

The most remarkable fracture of the section is the presence of a well developed set of horizontal and dipping fractures now infilled with smectite. These fractures are most abundant in Pieces 4A and B where they are regularly spaced at about 3 mm. Below Piece 4B, the fractures decrease in abundance but are also inclined at about 30° (Piece 4C). Sparse sub-horizontal fractures are present down Piece 4A but increase in abundance in the lower part where they have the same spacing as above. Vesicle infilling and veining post-dates these fractures.

Groundmass composed of laths of plagioclase and green phenocrysts of pyroxene(?).

CORE 40, SECTION 4

Depth 526.0–527.5 m

Pieces 1–7: Dark gray to gray (N5–N4) phyric vesicular basalt.

Vesicles ranging in size from 1 mm to 4 mm are scattered uniformly throughout the basalt. As before, the vesicles are typically lined with black and have dusky green centers (5G 3/2). Vesicles decrease dramatically in size below Piece 2F. Vesicles in Piece 2D and below are commonly only partly infilled. Fracturing is again apparent in Pieces 1 and 2. Fracturing is horizontal in Pieces 1 and 2A but becomes inclined in Piece 2B decreasing in abundance from Piece 2D downward.

The change in fracture pattern down section is accompanied by a general decrease in crystal size so that Pieces 2H, 3 and the upper part of 5 may be aphyric (aphanitic?) vesicular basalt. As before the groundmass of the basalt consists of feldspar laths and(?) pyroxene cyrstals.

The change in fracture abundance and lath size may indicate proximity to the base of the flow (see description for Piece 4 and below).

Piece 4, a number of small fragments of brown (5YR 3/4) to dark reddish brown (2.5YR 3/4). Open fractures(?) in individual fragments are lined with a grayish green (5G 5/2) mineral (smectite?). These fragments are interpreted as the top of the lower flow below (+ celadonite).

Pieces 6 and 7 are dark gray (5Y 4/1) phyric vesicular basalt with large (3–4 mm) elongate irreulgar vesicles whose long axes are vertical. Vesicles are partly filled with dark gray (5Y 4/1) mineral.

Groundmass: plagioclase laths (>1 mm) and green phenocrysts (pyroxene?).

CORE 41, SECTION 1

Depth 531.0–532.5 m

Pieces 1–5: Dark gray to gray (N4–N5) phyric vesicular basalt and green pyroxene(?) grains. Groundmass: plagioglase laths.

Abundant vesicles filled and part-filled ranging in size from 5 mm to less than 1 mm. Vesicles typically consist of black rim with white or part-filling of medium gray (N5) mineral. Minor sub-horizontal fracturing apparent and mixes vesicles in several cases.

Pieces 6–20: Dark gray to gray (N4–N5) phyric vesicular basalt sparse large vesicles (2–5 mm) and rare to absent small vesicles (1 mm). Subhorizontal fracturing apparent in Pieces 7, 8, and 9. Near vertical fracturing in Pieces 12, 13, and 15. Becomes sub-horizontal in Piece 20.

Vesicles typically unfilled with black rim. Interior of vesicles shows white mineral (calcite?) in black lining. Large vein in Piece 9 probably related in fractures and may be infilled with calcite and quartz. Fractures are infilled with black mineral.

Thin Section – 112 cm: Altered tholeiitic basalt (orthophyric-hypidiomorphic, trachytic).

CORE 41, SECTION 2

Depth 532.5–534.0 m

Pieces 1–8: Dark gray to gray phyric vesicular basalt. Fracturing clear to Piece 8. Piece 1 shows sinking change in inclination of fractures from 45° to sub-horizontal progressively. Pieces 4 and 5 also show veins. At 22 cm fractures inclined at 45°. Fracturing in some cases closely related to long axes of vesicles. Vesicles range from 5 mm to 0.3 mm. Normally lined with black mineral and infilled with calcite or quartz. Well developed vein has light gray (N4) rim and pale yellow (2.5Y 7/4) mineral (XRD quartz + calcite).

Pieces 9–11: Dark gray to gray phyric vesicular basalt with minor fracturing only. Minor fracturing only but some vesicles apparently deformed. Also vesicles flattened parallel to fractures. Vesicles increase in size and abundance downward and also become more flattened. Large vesicle (5 mm) in Piece 11 infilled with calcite. Possibly basal part of flow.

Piece 12: Vesicular pale red (5R 6/2) to grayish red (5R 4/2) basalt. Vesicles and fractures in fragment coated with light blue green (5BG 6/6) mineral. Pebbles become more vesicular toward base. Top of next lava unit.

Pieces 13–18: Dark gray to gray (N5–N4) vesicular basalt. Vesicles show round vesicles 0.2–0.5 cm (Piece 13) systematic downward change.

Groundmass becomes coarser downward with plagioclase laths and green mineral grains (altered pyroxenes?).

Pieces 14 and 15: Flattened vesicles 0.2–1.0 cm apparently vertical.

Piece 16: Small vesicles (0.5 cm–0.1 cm) flattened, mineral.

Piece 17: Irregular vesicles infilled with grayish blue green (5BG 5/2) and light gray (N7), some open.

Piece 18: Irregular vesicles infilled with gray and grayish blue green (50% infilled).

Thin Section – 112 cm: Altered tholeiitic basalt, orthophyric-hypidiomorphic, vesicular.

CORE 41, SECTION 3

Depth 534.0–534.4 m

Dark gray to gray vesicular phyric basalt. Groundmass as above. Irregular vesicles (0.5 mm maximum) infilled with grayish blue green mineral inside black lining. Vein (1–2 mm) in Piece 1 filled with same(?) material. Not all vesicles are infilled. Piece 3 is dark gray vesicular phyric basalt with no green infilling of vesicles – strong possibility that not in place. Contrast in lithology with Core 42, Section 1 suggests base of unit lies in unrecovered interval between Cores 41 and 42.

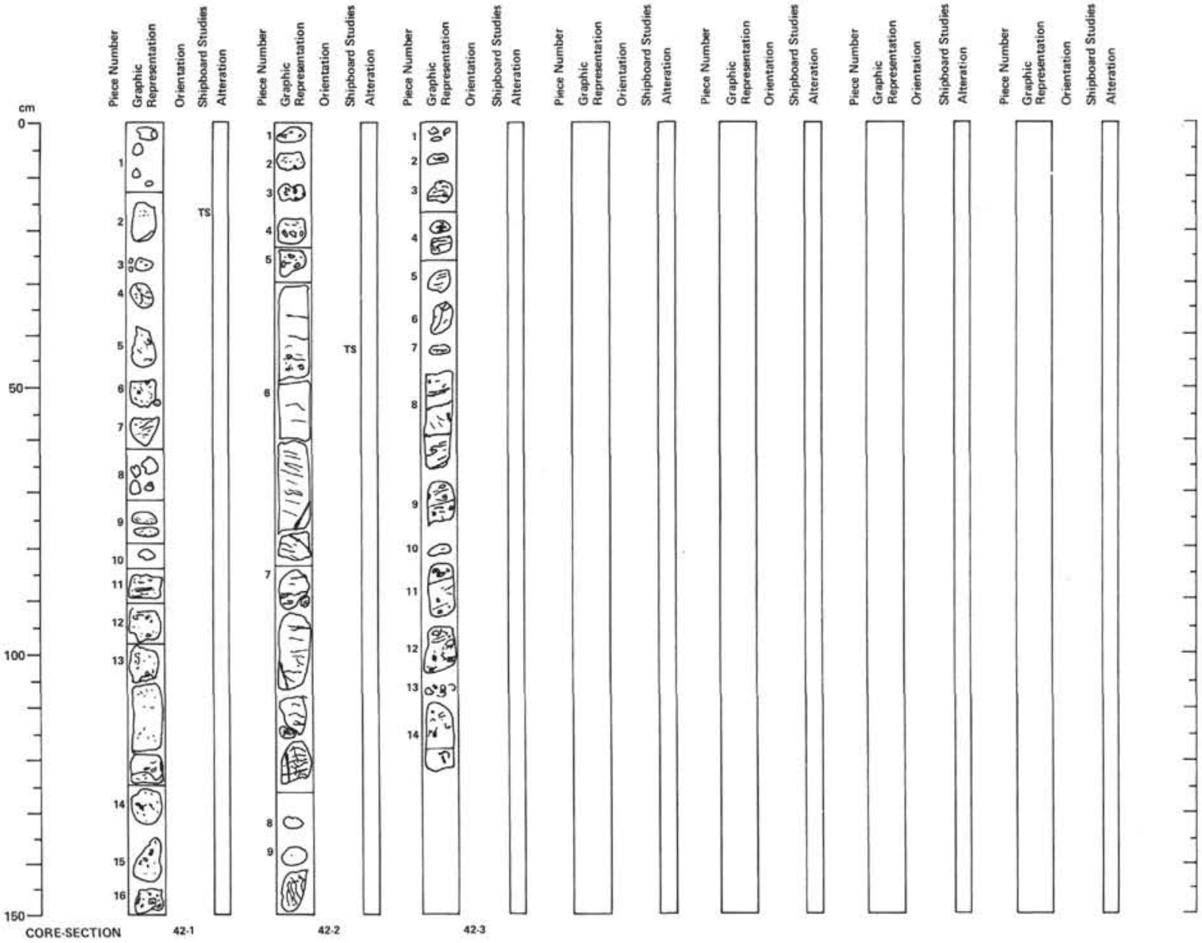

CORE 42, SECTION 1 Depth 540.5–542.0 m

Piece 1: Phyric basalt, dark gray to gray (N5–N4) minor vesicles (>0.1 mm).

Pieces 2–4: Dark gray to gray basalt. Several large 'clasts' with dusky bluish green vesicular cores. Surrounded by phyric basalt separated by black partly corroded rim(?) from adjacent groundmass. Groundmass: feldspar laths and pyroxenes.

Piece 5: Vesicular phyric basalt. Vesicles open or partly infilled with light gray (N5 quartz?) and show flow structure. Sample possibly not in place.

Pieces 6–8: Gray (N5–N6) phyric vesicular basalt. Vesicles (0.1–0.2 mm – occasionally 4 mm), 75% infilled, 25% open; infilling black lining – light gray core. Sparse green infilling. Binocular examination shows green also in light gray (5BG 5/2) cores. Vesicles irregular.

Pieces 9 and 10: Phyric vesicular basalt vesicles less than 0.1 mm and infilled with black clay (smectite?).

Pieces 11 and 12: Phyric vesicular basalt. Vesicles disposed in horizontal zones (vesicle size 0.2 mm) separated by zone in which vesicles smaller in size (0.1 mm).

Pieces 13–15: Fine-grained vesicular basalt.

Sharp increase in abundance of vesicles and appearance of discrete oblate zones of high infilled vesicle concentration. Some suggestion of flow concentration of vesicles.

Piece 16: Large clast of vesicles with clear rim. Large vesicle shown is not filled and contains(?) quartz crystals.

Thin Section – 16 cm: Tholeiitic basalt: porphyritic, trachytic.

CORE 42, SECTION 2 Depth 542.0–543.5 m

Pieces 1–5: Dark gray to gray (N5–N6) vesicular phyric basalt. Groundmass of feldspar laths and pyroxenes. Pieces 1–3 show 'vesicle clasts' with part rims and large open (5 mm) vesicles with black rims and quartz(?). Pieces 4 and 5 show larger flattened vesicles in part infilled with quartz and calcite.

Piece 6: Gray (N5) phyric vesicular basalt. Thinner vesicular clasts present. Vesicles decrease downward to 10% and are infilled by smectite (black). Dominated by horizontal to sub-horizontal fractures (>0.1 cm) infilled by black mineral. At 75 cm black (N2.5) vein with quartz(?) 0.2 mm stringer. Vein possibly associated with minor movement.

Pieces 7–9: Gray (N5) phyric vesicular basalt. Dominated by fracturing – here more irregular but larger. Fractures both horizontal and vertical and infilled by black mineral. Some evidence in Piece 7D of minor movement along fractures. Groundmass plagioclase laths and green pyroxene crystalls.

Thin Section – 44 cm: Orthophyric-hypidiomorphic, trachytic, tholeiitic basalt.

CORE 42, SECTION 3 Depth 543.5–544.7 m

Pieces 1–12: Gray (N5) phyric basalt, well developed fractures – altitude not determinate as fragments possibly rotated. Occasional 'vesicle clasts'. At 53 cm: Vein (0.2 cm). Some increment as basalt fragments included in vein. Vein black (2.5Y) with light gray (N5/N6) stringer (quartz). Fractures present as above but dip at 45° and cross at vein. At 63 cm veins en-echelon pattern. At 70–80 cm vesicles increase in abundance. At 96 cm: large vesicle clast with clear rim. Minor fracturing only from 96 cm to base of Section 3. At 100 cm: 1 cm vesicle.

Piece 13 (110 cm): Sparse large vesicles.

Piece 14: Abundant small black vesicle in N4 phyric basalt. Change in color possibly related to abundance of plagioclase laths. Gradation decreasing size and abundance of vesicles. Bottom portion has sparse vesicle in N5 phyric basalt.

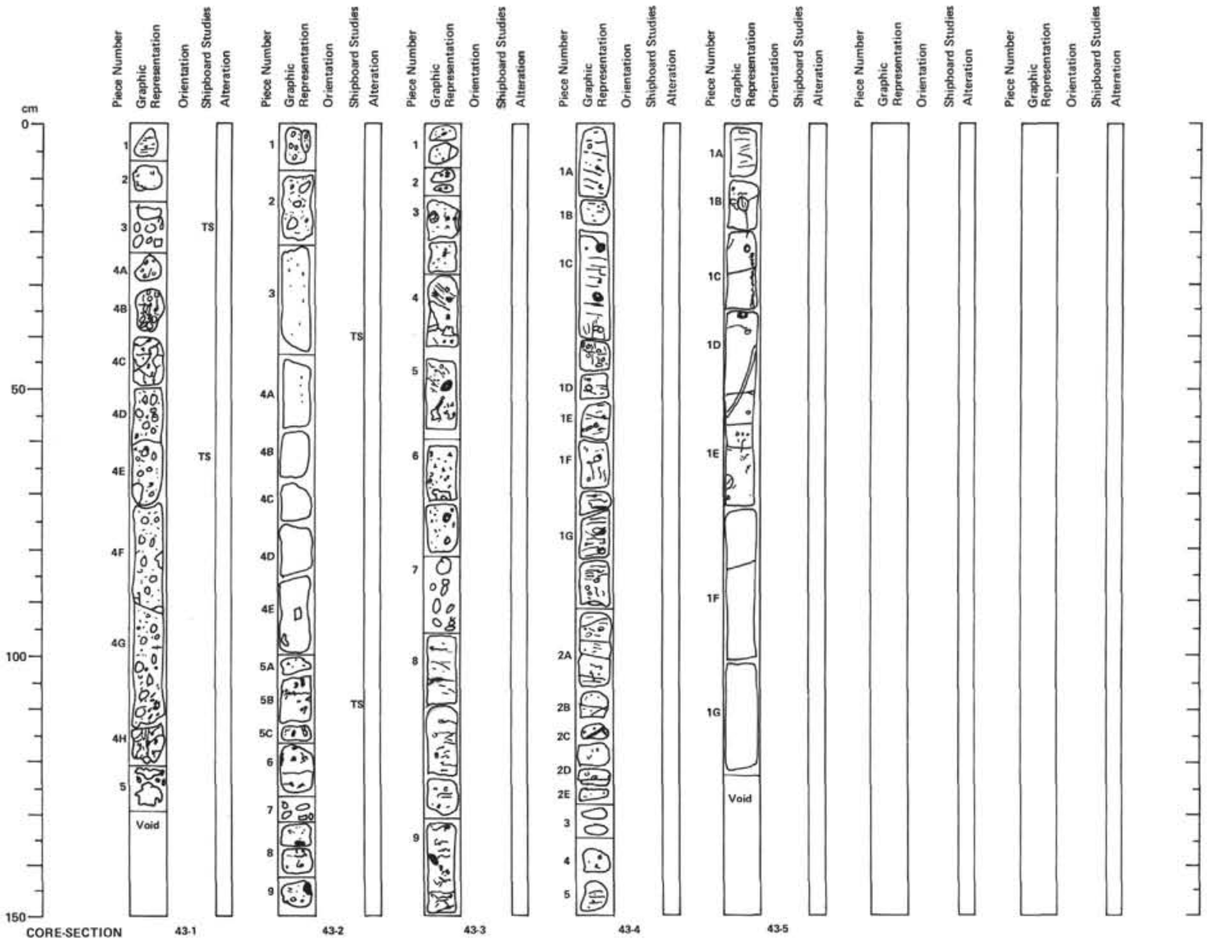

CORE 43, SECTION 1 Depth 550.0–551.5 m

Piece 1: Dark gray to gray (N5—N6) vesicular phyric basalt with minor fracturing (near base of unit?).

Piece 2: Grayish red (10R 4/2) vesicular phyric basalt. Sparse plagioclase phenocrysts. Bluish green (5BG 4/6) alteration. Vesicles contain blue green (5BG 4/6) mineral (smectite) and light gray (quartz?). Red color due to alteration of plagioclase and pyroxene in groundmass.

Piece 3: Grayish red (10R 4/2) and dark gray (N6) vesicular basalt. Vesicles in part infilled blue green (5BG 4/6).

Piece 4: Basaltic breccia, angular to rounded clasts of gray (N6) to reddish gray (10R 5/1) phyric vesicular basalt. Sparse gray (N5) and grayish purple (5PB 2/2) clasts. Clast size range 5 cm to 2 mm. Clasts set in green (smectite?) matrix. Clasts probably several different lithologic types. Clasts are polymict shown by contrasting lithologies (e. g. vesicular basalts with green infilling of vesicles. Phyric basalts. Different degree of red alteration rim around basalt clasts. Note: Some clasts show suggestion of corrosion and penetration by the matrix (contemporaneous deformation?).

Piece 4C: Vesicular agglomerate – vesicles concentrated sub-vertically.

Pieces 4G and H: Reddening of whole rock becomes more pervasive (red – 10R 3/6) vesicularity begins at same level and becomes more intense downward as does the reddening. Green in matrix probably celadonite.

Piece 5: Dark red (2.5YR 3/6), greenish black (5GY 2/1) pebbles of above.

Thin Section – 20 cm: Altered tholeiitic basalt: orthophyric-hypidiomorphic, trachytic.

Thin Section – 62 cm: Lithic volcanic breccia – scoriaceous top of basalt flow.

CORE 43, SECTION 2 Depth 551.5–553.0 m

Pieces 1 and 2: Gray (N5) to reddish brown (10R 3/6) clasts of phyric basalt in dusky green (5GY 2/1) to green black matrix. At 22 cm: Base of unit(?) but gap possible.

Pieces 3 and 4: Medium gray (N5) phyric vesicular basalt. Vesicles 0.1–0.2 cm exhibit preferred vertical circulation and increase in abundance downward. Vesicles infilled by black mineral (smectite?). Groundmass: plagioclase and altered pyroxenes. Distinct reddening (10R 4/6) related to alteration of pyroxene as well as vesicles(?). At 30–65 cm: Vertical concentration of vesicles. Some basalt lithology continues but no preferred circulation in vesicles (size range: 0.1 cm–0.5 cm).

Piece 4E: Large vesicles infilled with light gray (N7) mineral quartz(?).

Piece 5: Medium gray (N5) phyric basalt with large vesicles (0.75 cm) and large vesicle clasts (3.5 cm) with reaction rim of smectite(?).

Pieces 6–9: Medium gray (N5) phyric basalt with rare to absent vesicle clasts. Vesicles (size 0.2 cm–0.5 cm) normally infilled with smectite but rare quartz and calcite(?) also.

Thin Section – 40 cm: Altered tholeiitic basalt: orthophyric-hypidiomorphic, trachytic.

Thin Section – 109 cm: Tholeiitic basalt: orthophyric-hypidiomorphic, vesicular, trachytic.

CORE 43, SECTION 3 Depth 553.0–554.5 m

Pieces 1–4: Medium gray (N5) vesicular phyric basalt. At 19 cm large vesicles (2 cm) with quartz(?) core.

Piece 4: Fractures inclined at 50° with preferred circulation of vesicles along fractures. Large vesicle infilled with quartz and calcite with black rims.

Pieces 5–7: Occasional large vesicles filled with quartz (N8) and or calcite (5Y 8/1) in medium gray (N5) vesicular phyric basalt.

Pieces 8 and 9: Medium gray (N5) vesicular basalt with sparse smectite filled vesicles (0.2 cm). Fracturing abundant, spaced at 0.5 cm and sub-horizontal. Fractures (sub-horizontal) infilled by smectite. Megascopic examination shows preferred circulation of plagioclase and pyroxene grains in groundmass.

CORE 43, SECTION 4 Depth 554.5–556.0 m

Pieces 1–5: Medium gray (N5) phyric basalt with sparse vesicles. At 0–35 cm: Horizontal sub-horizontal fractures infilled with smectite. At 34 cm: Sharp contact. At 35–45 cm: Vertical fractures, medium gray (N4) phyric basalt, large (0.3 cm) vesicles filled with quartz. At 45–65 cm fractures at 45° in medium gray (N4) basalt. At 65–100 cm sub-horizontal fractures in medium gray (N4) phyric basalt vesicles rare – when present size 0.3 cm with grayish bluish green (5BG 5/2) matrix. At 105 cm: Fractures decrease in abundance to rare. At 114 cm black (N1) vein with light gray stringer. At 120–130 cm groundmass: uniform plagioclase laths and pyroxene phenocrysts, possible slight upward decrease in grain size. At 145 cm: horizontal to sub-horizontal fractures.

CORE 43, SECTION 5 Depth 556.0–557.2 m

Pieces 1A–E: Medium dark gray (N4) vesicular phyric basalt. Vesicles are light gray (N7). At 5 cm: Fractures induced at 20°. At 15 cm: Large vesicle infilled with calcite. Medium to irregular vein of quartz and calcite induced at 70° . Fractures rare to absent. At 22 cm: Black halo (alteration) around green core. At 30 cm: Vertical contact, medium gray (N5) phyric basalt with sparse inclined fractures. At 50 cm: Vein inclined at 70°, light gray (N7) and yellowish gray (5Y 8/1) infilling. At 66 cm: Large partly assimulated clasts.

Pieces 1F and G: Medium gray (N5) phyric basalt with sparse vesicles. Fractures generally sub-horizontal but some show changes in dip from horizontal to about 20° . Groundmass: plagioclase laths and pyroxenes(?). Plagioclase laths show preferred circulation approximately parallel to fractures.

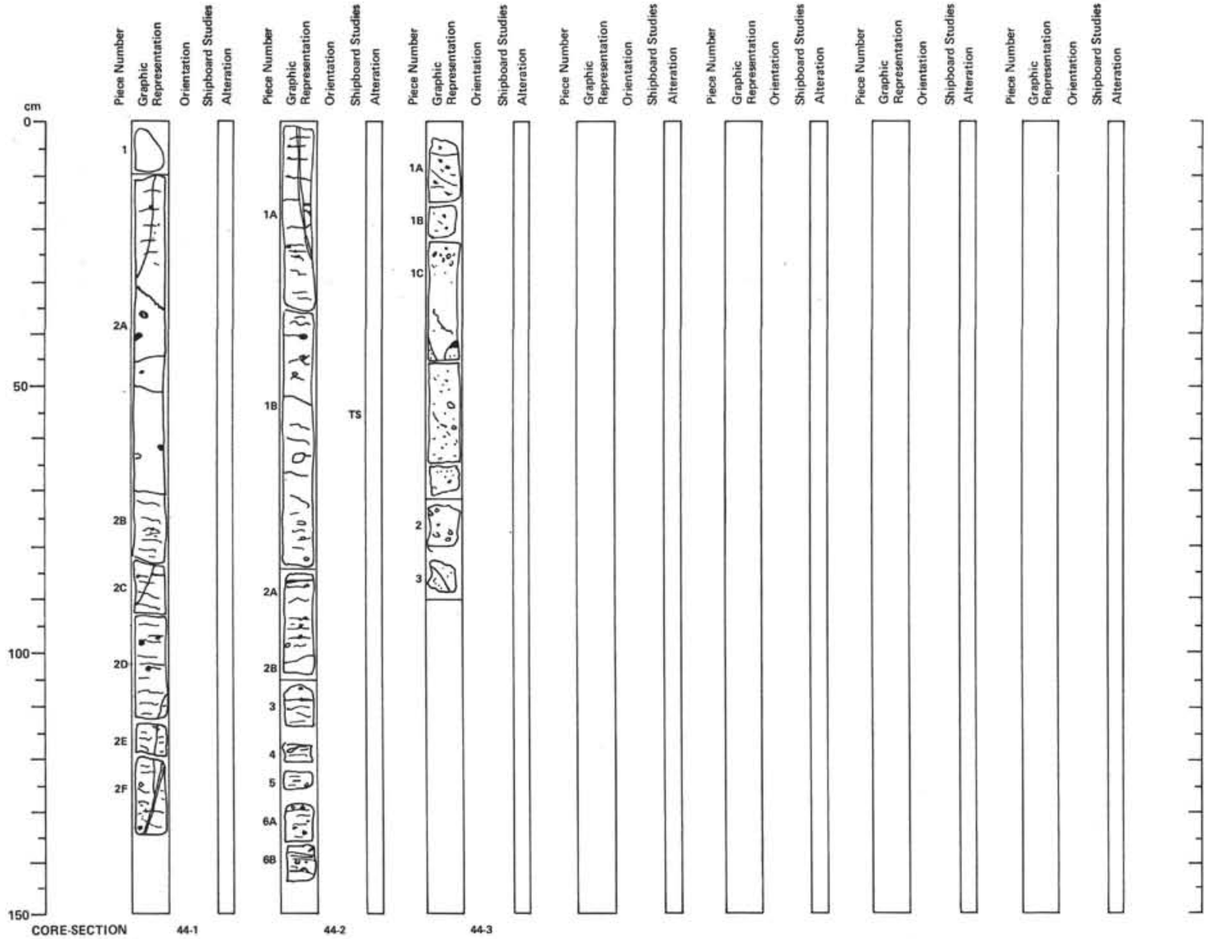

CORE 44, SECTION 1 Depth 559.5–561.0 m

Pieces 1 and 2: Medium gray (N5) phyric basalt throughout. Whole section cut by sub-horizontal fractures. Typically spaced at 0.3–0.5 cm. Fractures filled by black clay mineral (smectite?). Sparse vesicles occur throughout ranging in size from 1 cm–0.1 cm. Vesicles infilled with: 1) yellowish gray (5Y 8/1) (quartz and calcite?) and 2) dusky green (5G 3/2) to dusky blue green (5BG 3/2). Prominent veins in Piece 2A (dip 40°) and Pieces E and F (dip 70°). Infilling is grayish black (N1) with near complete massive infilling of light olive gray (5Y 5/2) (quartz and calcite?). Also light olive gray appears as discrete blebs (0.5 mm). No indication of displacement of fracture pattern by veins. Binocular examination shows very fine-grained groundmass (aphyric) of plagioclase and a green mineral.

CORE 44, SECTION 2 Depth 561.0–562.5 m

Pieces 1–6: Medium gray (N5) phyric vesicular basalt. Sparse vesicles (size 0.5 cm–0.2 cm) occur throughout and are infilled with: 1) grayish green (10G 4/2) to greenish black (5GY 2/1) and 2) light gray (N7). Black linings common to both. Entire section shows well developed sub-horizontal fractures that increase in abundance and spacing down section. (Spacing 0.5–1.0 cm at top to 0.3 cm at base.) Vein at top dips 87° and is walled black (N7) with vein infill of light olive gray. Veins at base inclined at 10°. Veins lined with black (N2) but with light gray (N7) to yellowish gray infilling (quartz and calcite?). Groundmass: predominantly some plagioclase laths with sparse green patches (pyroxene?).

Thin Section – 56 cm: Tholeiitic basalt, orthophyric-hypidiomorphic.

CORE 44, SECTION 3 Depth 562.5–563.4 m

Piece 1: Medium gray (N5) phyric vesicular basalt. Vesicles more abundant than in lowest part of Core 44, Section 2. Size range 0.3–0.1 cm. Vesicles infilled with dusky green (5G 3/2) commonly or sparse yellowish gray (5GY 8/1). Fracturing continues down to the top 5 cm of Piece 1C but then becomes minor. Vesicles also grade out at this level. Also a marked contrast in groundmass size. At 38 cm: Irregular vein that closes up and downward and confined to zone of coarser groundmass. Irregularities on opposite sides match. Possible cooling crack.

Pieces 2 and 3: Medium dark gray (N4) phyric vesicular basalt. Main difference from overlying basalt in color and appearance of open vesicles (absent above). Vesicles lined with black and infilled with or internally lined with light gray. Groundmass much greater abundance of green mineral (refer to above). Plagioclase laths more subordinate. This is probably cause of different color.

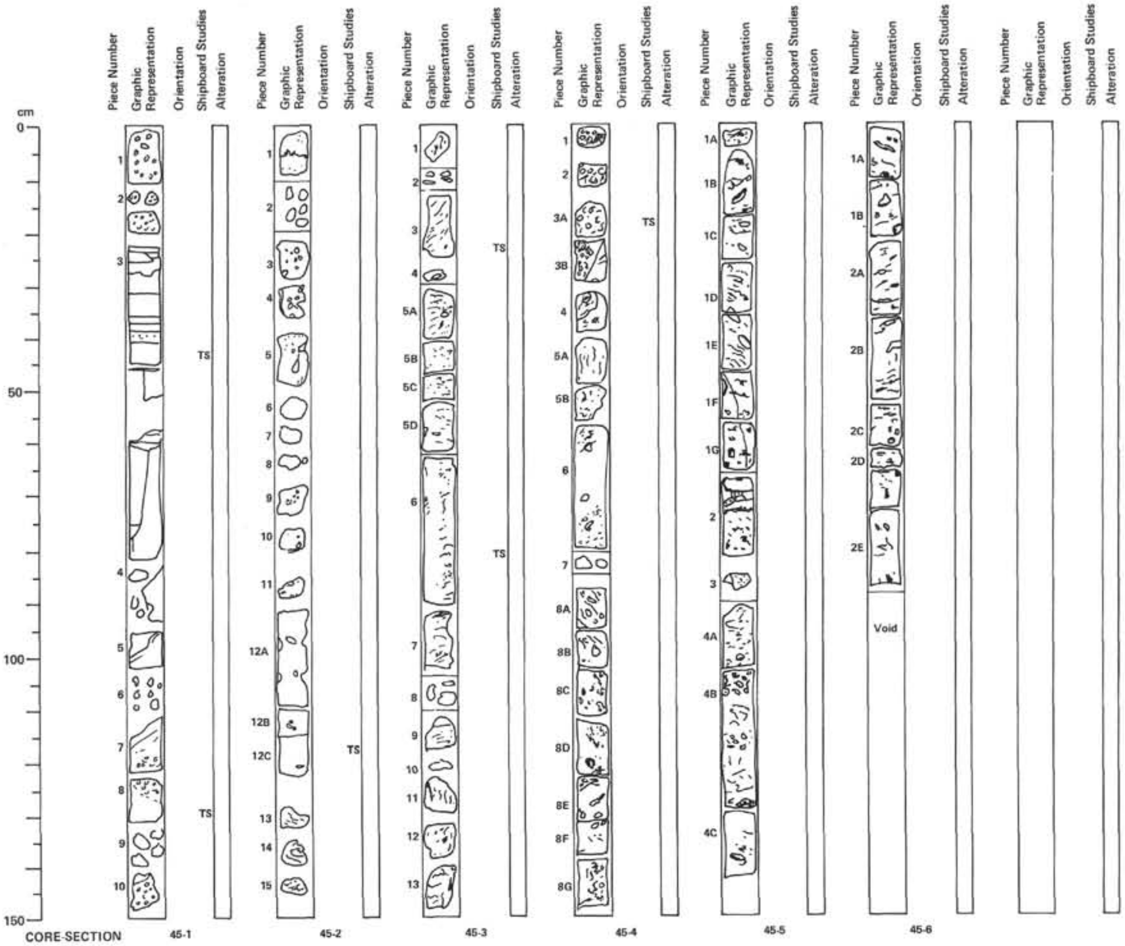

CORE 45, SECTION 1 Depth 562.0–563.5 m

Pieces 1 and 2: Blackish red (5R 2/2) vesicular phyric basalt, very fine grained red groundmass of plagioclase laths. Three mm vesicle size vesicles decrease in size downward.

Piece 2: Irregular smectite patches and other green minerals, occasional pyrite. Note: reddening does not affect vesicles. At 19 cm: Vesicle size 0.1 mm or less.

24 cm: Contact between vesicular basalt and underlying tuff.

24–27 cm: Uppermost part of tuff. Dark reddish brown (10R 3/4) contains polymict fragments 1–3 mm of phyric basalt, vesicular basalt.

27 cm: Faint irregular contact separates this piece from main part of tuff.

27–32 cm: Grayish red to dark reddish brown (5R 4/2–10R 3/4) tuff. Small > 0.1 cm laths of white plagioclase showing subparallel orientation to reddening. Irregular green traces of smectite also elongated in same sense. Lithic fragments sparse.

32–36 cm: Laminated grayish red (5R 4/2) and thin dusky red (10R 3/4) interbeds. Dark lamination due to thin beds of dusky red (dark green mineral).

36–38 cm: Upturned grayish red (5R 4/2) laminae with thicker dusky red interbed. Possible large red clast and gas escape structure – vertical orientation of green mineral on opposite side of core.

38–42 cm: Graded bed, dark reddish brown (10R 3/4) in upper part becoming dark reddish gray (10R 4/1) below. Distinct zone of 2 mm lithic fragments at base.

Below 45 cm: Grayish red (10R 4/2) to minor convoluted base near 50 cm. Distinct sub-horizontal circulation of black/dark green minerals. Large altered grayish green (5BG 5/2) with light blue green (5BG 6/6) flecks. At 53–57 cm: Coarser zone with 2–3 mm altered clasts. Zone is dark reddish gray (10R 3/1). At 57–77 cm: Distinctly laminated (mm scale) interbeds are dark reddish gray (10R 3/1) and dark reddish brown (10R 3/4) laminae emphasized by black mineral. Grading also present in thicker beds. Angular calcite evident, especially at 77.5 cm. Below 77.5 cm: reddening decreases markedly to blackish red (5R 2/2). Sedimentary contact at 75 cm between finer grained tuff and coarser grained below. Basal part of unit is very dark gray (N3) with sparse red (2.5YR /2) patches. Small feldspar(?) phenocrysts and grayish bluish green (5BG 2/2) clay mineral. Occasional large lithic fragment.

Pieces 7–10: At top has chilled edge and contact with overlying lithic tuff – contact has light blue green (5BG). Vesicular phyric basalt with vesicles becoming larger and more open toward base. Color is variegated from week red (2.5YR 4/2) to dark greenish gray (5GY 4/1) in irregular patches and infilling vesicles. 'Normal' color occasionally seen in dark gray (N2). Groundmass appears deeply altered and is reddened.

Thin Section – 43 cm: Vitric tuff.

Thin Section – 128 cm: Altered tholeiitic basalt (orthophyric-hypidiomorphic; vesicular).

CORE 45, SECTION 2 Depth 563.5–565.0 m

Pieces 1 and 2: Dark olive gray (5Y 3/2) vesicular phyric basalt. Groundmass red and probably altered. Large lithic clast surrounded by 'chilled(?)' margin at 5 cm. At 20 cm: Possible base of flow?

Pieces 3–12B: Grayish red purple (5RP 4/2) to medium gray (N4) agglomerate. Large clasts are gray (N5) and typically angular (size up to 5 cm). Clasts seem to be polymict and show evidence of fracturing and penetration by the matrix. Matrix consists of smaller (mm) size particles. Reddening decreases downward. Vesicles occur throughout this unit and occur in both the clasts as well as the matrix. Vesicles lined with grayish blue green(5BG 5/2) mineral or light gray (N7) mineral. Both also seem to occur in matrix.

115 cm: Contact with basalt. Contact shows progessive fracture of surface of flow and peeling off of clasts of all sizes and incorporation into matrix of agglomerate above clasts are medium gray (N5) with dark greenish gray (5GY 4/1) interstices.

Pieces 12C–15: Basalt. Medium gray (N5) phyric vesicular basalt. Upper surface of basalt is chilled. Vesicles are vertical and probably due to gas streaming. Cooling cracks occur – Pieces 13 and 14.

Thin Section – 116 cm: Altered tholeiitic basalt (orthophyric-hypidiomorphic, vesicular, trachytic).

CORE 45, SECTION 3 Depth 565.0–566.5 m

Pieces 1–13: Medium gray (N5–N6) vesicular phyric basalt.

Piece 3: Vesicles (mm scale) oriented vertically.

Pieces 5B and C: Randomly converted vesicles.

Piece 6: Sub-horizontal fractures spaced at 3 mm. At 85 cm: Large clast of medium dark gray (N4) vesicular basalt (exotic) with vesicles flow banded in host basalt which is chilled against clast.

Piece 7 and 8: Vesicles inclined at 70°. Groundmass: predominately fine laths of plagioclase with green mineral. Possibly deeply altered.

Piece 9: Sparse vesicles.

Piece 11: Vertical vesicles.

Piece 13: Sparse inclined fractures grain size of groundmass decreases downward to chilled contact at base of unit. Small pebble of agglomerate from top of underlying unit is at edge of pebble. Vertical fractures near base of pebble infilled with dusky green (5G 3/2) mineral.

Thin Section – 23 cm: Tholeiitic basalt (orthophyric-hypidiomorphic, trachytic).

Thin Section – 81 cm: Altered tholeiitic basalt (orthophyric-hypidiomorphic, trachytic, vesicular).

CORE 45, SECTION 4 Depth 566.5–568.0 m

Pieces 1–8: Dark reddish brown (2.5YR /8) matrix with vesicular basalt clasts, grayish red purple (5RP 4/2) to pale red purple (5RP 6/2). Reddening decreases downward so clasts above flow are predominantly grayish red purple (5RP 4/2) to medium gray (N5). At 20 cm: Contact agglomerate/basalt irregular near vertical. Fragments clearly being broken off basalt and incorporated in agglomerate chilling of flow surface. Also evidence of flow banding and folding of vesicles.

Piece 5A: Vertical vesicles (gas streaming).

53 cm: Gap in vesicles.

60 cm: Steeply inclined vesicles preferred circulation (80° dip). Groundmass: fine grained predominantly plagioclase laths. Vesicles generally black (N2) to greenish black (5GY 2/1). Sparse large vesicles (1 cm), light gray (N7) to yellowish gray (5Y 8/1).

Piece 8A and B: Inclined vesicles and wisps of medium gray (N5) indicate flow folding. Also present within limbs of fold are several large vesicular clasts showing partial incorporation into the flow.

Piece 8E: Vertical vesicles abundant.

Piece 8F: Sparse vesicles. Fractures inclined at 45°.

Piece 8G: Abundant 3 mm irregular vesicles becoming sub-horizontal in base of last pebble.

Thin Section – 20 cm: Lithic volcanic breccia – scoriaceous top of basalt flow.

CORE 45, SECTION 5 Depth 568.0–569.5 m

0–7 cm: Medium gray phyric basalt with sparse irregular large vesicles. Groundmass: fine plagioclase laths and green mineral and pyrite(?) grains. Sub-horizontal vesicles.

7–20 cm: Near vertical vesicles.

20–55 cm: Sparse vesicles oriented parallel to fracturing, inclined at 30°. Large (3 cm) vesicles inclined along fractures. These have light gray (N7) to yellowish gray (5Y 8/1) and fill (quartz and calcite).

70 cm: Two large veins lined with smectite. Lower vein infilled with pale purple (5P 6/2) to light gray (N7) mineral, upper yellowish gray (5Y 8/1). Several generations of mineral growth apparent.

80 cm: Irregular large vesicles (2–4 mm).

90–100 cm: Abundant vesicles (mm scale with sparse 0.5 cm vesicles). Vesicles black (N7) to dusky green (5G 3/2).

105 cm: Irregular large vesicles.

110 cm: Vertical fractures.

115–140 cm: Sub-horizontal to 10° fractures. Sparse vesicles occasionally concentrated in patches.

CORE 45, SECTION 6 Depth 569.5–570.4 m

Pieces 1 and 2: Medium light gray (N5) phyric vesicular basalt. Groundmass: fine plagioclase and pyroxene. Sparse larger laths of plagioclase. Green mineral too small to be resolved with binoculars (altered pyroxene?). At 5 cm: inclined vein black lining infilled with light gray (N7).

Piece 1B: Inclined to sub-horizontal fractures.

Piece 2A: Sub-horizontal – inclined fracture.

42 cm: Vein light gray (N7) to yellowish gray (5Y 8/1) – some suggestion of growth of smectite lining at expense of mineral (quartz and calcite?).

Piece 2C: Large elongate inclined vesicles.

Piece 2E: Complex pattern of sub-horizontal and near vertical fractures.

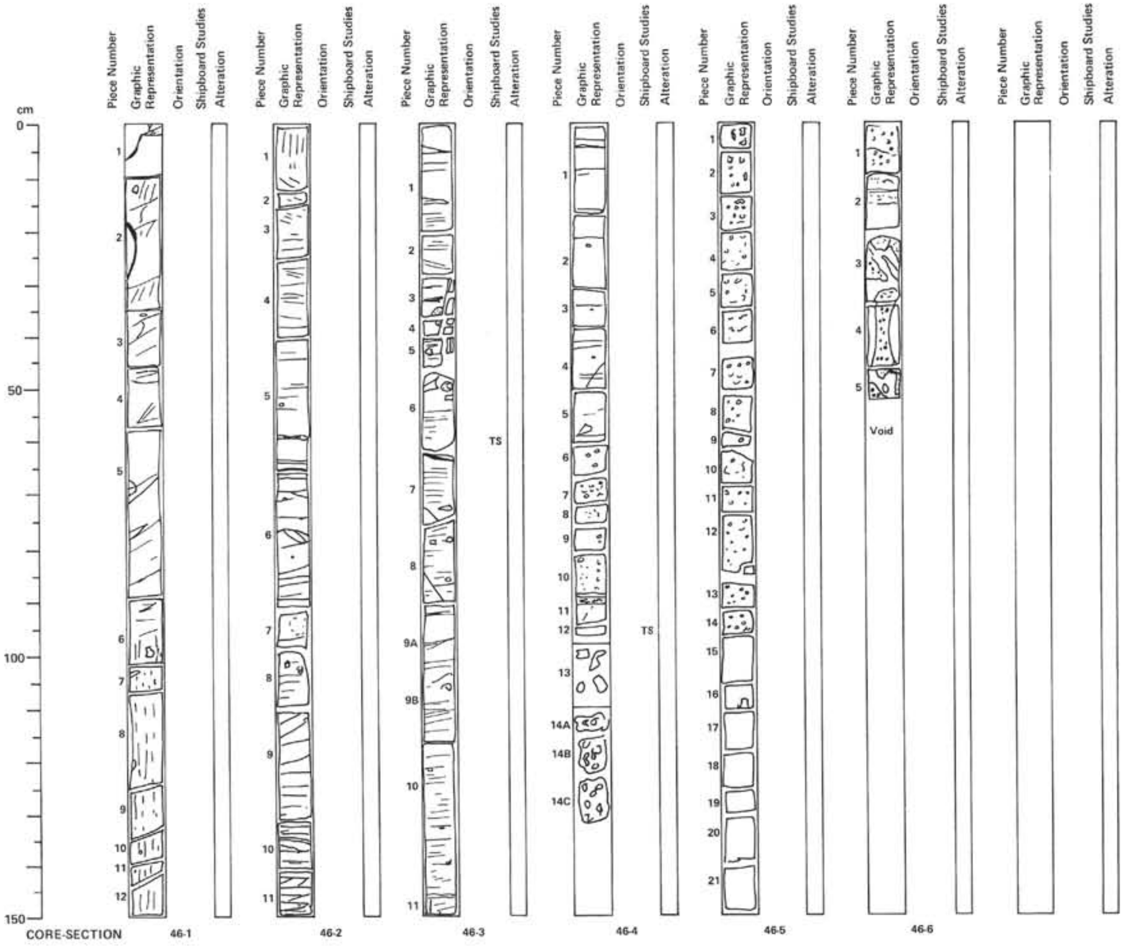

CORE 46, SECTION 1 Depth 571.5–573.0 m

Medium light gray (N6) phyric vesicular basalt throughout. Principle feature of the section is the abundant fracturing. Several clasts exhibiting abundant unfilled vesicles occur sporadically and show varying degrees of incorporation into the basalt. Groundmass: uniform fine grained plagioclase and pyroxene. Texture probably closely to aphyric. At 20 cm: black vein – possible cooling crack.

CORE 46, SECTION 2 Depth 573.0–574.5 m

Medium gray phyric vesicular basalt. Principle variation in section is in altitude of fractures. Groundmass uniform throughout; plagioclase laths and pyroxene. Fracture filling – altered pyroxenes? Fracture spacing 2 cm.
5 cm: Fracture inclined.
20 cm: 20° to sub-horizontal.

30 cm: Horizontal to sub-horizontal.

50 cm: Sub-horizontal to horizontal, 0.5 cm spaced fracture.

75 cm: Fractures exhibit cross cutting (imbrication?).

92 cm: Vesicular clast.

100 cm: Large vesilces infilled with light gray (N5) core surrounded by greenish black (5GY 2/1).

110 cm: 25° inclination.

140 cm: Sub-horizontal.

CORE 46, SECTION 3 Depth 574.5–676.0 m

Pieces 1–11: Medium gray phyric – aphyric basalt. Principle variation in this section is in braided aspect of the fractures. Braiding seems to reflect streaking out of black mineral. Vesicles are sparse and also present core filled with: 1) always lined with black and 2) core may be dusky green (5G 3/2) or a combination of light gray (N7) and yellowish gray (5Y 8/1).

10–30 cm: Fractures sub-horizontal with braided aspect, spacing 1–3 cm.

45–90 cm: Sub-horizontal to horizontal braiding minor, spacing >0.5 cm.

90–110 cm: Braided sub-horizontal to horizontal fractures.

110–150 cm: Sub-horizontal to horizontal fractures, spacing 0.5 cm or less.

Thin Section – 61 cm: Tholeiitic basalt: orthophyric-hypidiomorphic, trachytic.

CORE 46, SECTION 4 Depth 576.0–577.5 m

Pieces 1–13: Medium gray (N6/N5) phyric – aphyric basalt. Suggestion of progressive decrease in grain size towards top of vesicle zone. At 0–20 cm horizontal fractures with some braiding decrease in abundance downward. At 50 cm fractures are minor. At 58 cm large vesicle infilled with light gray (N6) and olive gray (5Y 4/1) flecks at edges of black lining. At 60–100 cm progressive increase in vesicle (rounded) abundance. Individual vesicles have long axes oriented vertically. Oblate vesicles part open and where filled are grayish black (N6) to olive gray (5Y 4/1). At 105 cm: base of unit.

Piece 14: Grayish red (5R 4/2) vesicular basalt. Vesicles irregular and up to 1.5 cm in size. Piece 14A has moderate red (5R 5/4) top with moderate green (5G 5/6) coating. Groundmass: reddened plagioclase laths and pyroxene(?). Vesicles infilled with quartz and smectite(?). All have characteristic black lining.

Thin Section – 94 cm: Tholeiitic basalt, orthophyric-hypidiomorphic, trachytic.

CORE 46, SECTION 5 Depth 577.5–579.0 m

Pieces 1–12: Grayish red (10R 4/2) vesicular basalt. Reddened groundmass – probably altered. Vesicles of all sizes (1.5 cm to mm) persist throughout core both open and filled. Filling: grayish black (N2) with light olive gray (5Y 6/1) core. Smaller vesicles are concentrated and may be vesicular from 'vesicle clasts'. Obvious vesicle clasts are present throughout below Piece 6. At 85 cm approximate unit of downward reddening (gradational).

Pieces 13–21: Medium gray (N5) vesicular basalt. Groundmass distinctly flow banded and finer in size than in non-banded areas. Composition: plagioclase laths with banding highlighted by black/dark green grains. Probably no compositional difference between reddened basalt and gray basalt below.

Piece 18: Shows distinct flow banding between two partly assimilated 'vesicle clasts'.

Pieces 20 and 21: Show distinct light gray (N7) bands free of vesicles inclined at 50°. Intervening bands show vesicles oriented at same angle. In Piece 21 one band is near vertical and may be related to gas streams in Core 46, Section 6.

CORE 46, SECTION 6 Depth 579.0–579.5 m

Pieces 1–5: Medium gray (N5) phyric vesicular basalt.

0–15 cm: vesicles are horizontal banded and separated by bands (N5) containing fewer vesicles. Vesicle rich bands also differ in size population. Below 15 cm, the basalt contains sparse minor vesicles.

Below 22 cm (Pieces 3, 4, and 5), there is a spectacular vertical structure. It consists of almost vesicle free medium light gray (N6) basalt separating zones in which vesicles (1 mm) are highly concentrated.

The vesicle free basalt is finer grained towards its contact with the vesicle rich segmation and becomes coarser towards its center. Foliation is also evident.

Probably two phases present. Phase 1 – vesicular basalt then magma streamed upward from below.

Groundmass: plagioclase laths and pyroxene(?).

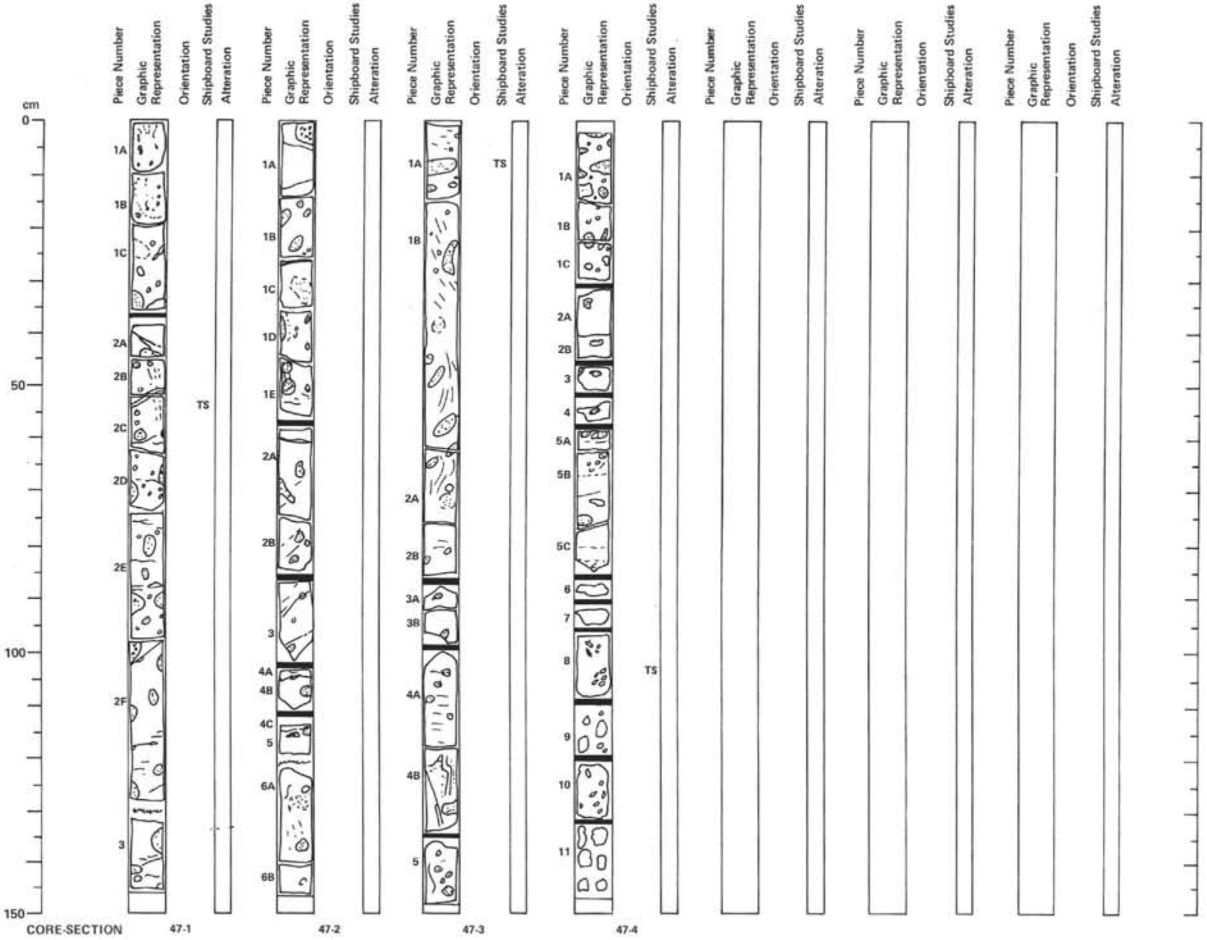

CORE 47, SECTION 1 Depth: 580.5–582.0 m

Medium light gray (N6) phyric vesicular basalt.

Pieces 1A, B, and C: Veins of vertically elongated filled and open vesicles up to 7 mm in length. Also vertical changes in grain size between Piece 1A and B. Piece 1B defined also by marked change in vesicularity. Suggestion of decrease in grain size towards vesicular area. Vesicular clasts appear in Piece 1C but vertical filaments and flow structures are also present with open vesicles up to 1 cm. Vesicles typically have black lining (smectite) and lined (open) or infilled with medium gray (N5) quartz or calcite. Several large vesicles (5 cm) infilled with grayish blue green (5BG 5/2) present.

52 cm: 3 mm vein partially infilled with grayish blue green (5BG 5/2) with matrix and lining of grayish red (5R 4/2).

Pieces 2 and 3: Principle difference here overlying 35 cm is an increase in the size and abundance of 'vesicular clasts'. Vertical structures revealed as filaments of oriented dark mineral grains are common in the upper part but become random with depth. There is a suggestion that the vesicular clasts may be separated by sub-vertical flow structures. Reaction rims are common around the clasts but the smaller ones show partial assimilation. Reddening (5R 4/2) associated with the host rock around the grayish blue vein at 89 cm evident. Vein at 117 cm is infilled by light bluish gray (5B 7/1) – medium gray mineral (calcite?). Host basalt as well as vein reddened (5R 4/2) – vein is sub-horizontal. Large open vesicles (up to 0,5 cm) common in the matrix between 'clasts' and sparsely within clasts.

Groundmass: trachytic texture composed of elongated plagioclase laths common with suggestion of flowage between clasts. Green minerals (pyroxene) smaller.

Vesicular clasts: coarse groundmass here of plagioclase laths and pyroxenes with rare evidence of trachytic structure.

CORE 47, SECTION 2 Depth 582.0–583.5 m

Pieces 1–5: Medium light gray (N6) vesicular basalt: predominantly plagioclase laths showing pronounced trachytic texture. Piece 4A: coarser plagioclase/pyroxene, no trachytic texture. Lighter olive patches are predominantly plagioclase. Reddening apparent toward edge of vesicle.

The same lithology observed with lower part of Core 47, Section 1 continues down to 105 cm. The only differences of significance are an increase in the size of the vesicle clasts up to 5 cm. Reddening associated with sub-horizontal veins and diffusing into the groundmass is evident. The top of a vesicular clast at 30 cm has been reddened. The veins show a light bluish gray (5B 7/1) infill – calcite(?). Reddening is absent below 50 cm.

25 cm: Vein.

Vertical filaments are evident between 35 and 54 cm, but are replaced down section by filaments dipping at 50°.

104 cm: Contact. Brownish gray (5YR 4/1) vesicular basalt containing irregular black patches and light olive gray patches. Top of piece is dark gray (N3) to grayish black (N2) irregular lining of 5 cm diameter vesicle. Crystals(?) lining vesicle seem to be coated black with light gray core. A second 3 cm long open vesicle occurs in the outside of the core.

Pieces 6A and B: Medium light gray (N6) vesicular basalt with vesicular clasts (5 cm–0.5 cm). The large vesicular clast shows inverted grading. Olive gray filaments are vertical to sub-vertical.

There is a possibility that Pieces 4 or 5 may be wrong way up.

CORE 47, SECTION 3 Depth: 583.5–585.0 m

Medium gray (N5) phyric basalt – vesicular. Groundmass: predominantly plagioclase laths showing trachytic texture. Pyroxene also oriented into filaments.

Vesicular clasts ranging in size from 6 cm to 1 cm or less occur commonly throughout. Several clasts – the larger ones show a distinctive graded structure shown by the black patches. Open and infilled vesicles occur throughout.

The dominant feature is the ubiquitous presence of vertical to near vertical filaments of dark minerals shown also by the trachytic texture.

A distinct 1 cm zone of finer grained nearly vesicle free basalt vertical and 5 cm in length occurs in Piece 3B. It is truncated downward by an irregular olive gray (5Y 4/1) patch.

Thin Section – 9 cm: Tholeiitic basalt.

CORE 47, SECTION 4 Depth 585.0–586.5 m

Medium gray (N5) phyric vesicular basalt. Vesicular clasts decrease in size and abundance below. Grading clear in several clasts.

Below 40 cm vesicle clasts become smaller and seem to be more assimilated by the groundmass. Vertical filament structures become rare. The impression is also of a subtle decrease in grain size. Vesicles also decrease in size. Large open vesicles are absent below 50 cm and small irregular filled vesicles are more abundant though concentrated in irregular patches.

80 cm: Contact fine grained phyric vesicular basalt (medium gray – N4–N5) above coarser vesicular basalt. Fine (0.5 mm) infilled vesicles (black – N2) grade down into open vesicles (1 mm). Open and infilled vesicles have paler cores – this in base of unit between Pieces 5C and 6.

Pieces 7 and 8: Grayish red (5R 4/2) to dusky red (5R 3/4) scoriaceous lava. Extremely vesicular in patches. Vesicles elongate (sub-horizontal – flattened?). Suggestion of several large lithic clasts in finer groundmass. Sparse to rare dusky green (5G 3/2) infills to vesicles.

Piece 10: Very dusky red (10R 2/2) with very dark red (5R 2/6) patches. Scoriaceous. Several large lithic clasts of vesicular basalt in finer groundmass. Note clasts differ in vesicularity.

Thin Section – 101 cm: Altered lithic volcanic breccia – scoriaceous lava flow top.

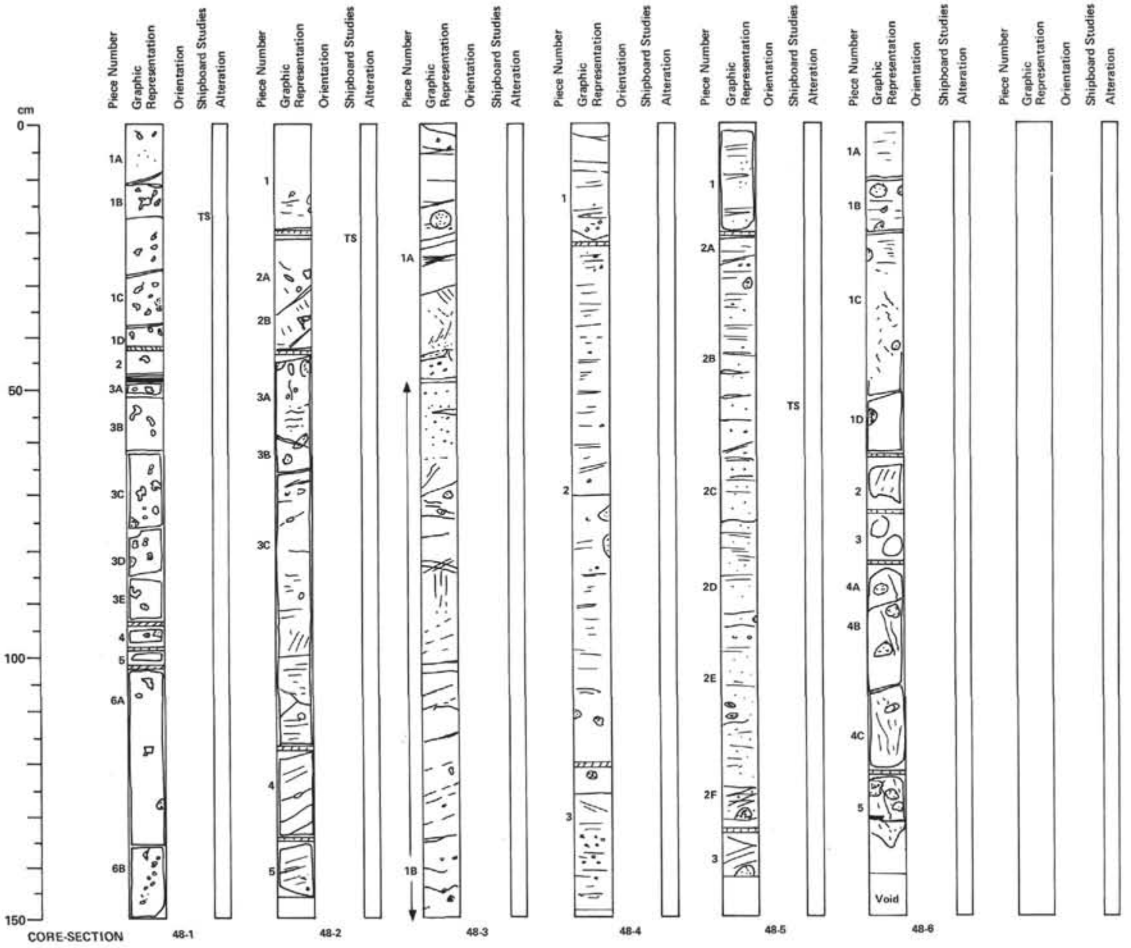

CORE 48, SECTION 1 Depth 587.5–589.0 m

0–12 cm: Medium gray (N5) phyric vesicular basalt. Vesicles range in size from 0.3 mm down and are open and filled. Open lined with light gray (N5) and black (N6) which is also seen in filled vesicles. One vesicle clast.

12–38 cm: Medium gray (N5) phyric vesicular basalt. Vesicles larger (2 cm–0.1 cm) predominently filled. Largest vesicle inclined and flattened along 45°. Vesicles infilled with black lining and white core. One vesicle clast.

38–100 cm: Medium gray (N5) phyric vesicular basalt. Vesicles decrease in abundance by 50% compared to above. Maximum size 0.7 cm. Some vesicles infilled with grayish yellow (5Y 8/4) and very light gray (N8) – quartz and calcite(?). Otherwise vesicles generally closed with black infill. Vesicles in Piece 3D apparently inclined at 60°. Groundmass: predominantly plagioclase laths with smaller grains of pyroxene(?) locally concentrated into irregular lensoid trachytic texture sparse to core. Black infill to vesicles under binocular commonly has dusky green core often with complex white filigree structure.

100–150 cm: Medium gray (N5) vesicular phyric basalt. Vesicles sparse and about 1 cm in diameter. Typically very light gray (N8) core and black lining. Horizontal streaks towards base of Piece 6A and sparsely in Piece 6B. Vesicles in Piece 6B roughly inclined at 60°.
Thin Section – 17 cm: Tholeiitic basalt.

CORE 48, SECTION 2 Depth 589.0–590.5 m

Medium gray (N5) phyric basalt.

15–25 cm: Reddened zone (pale red – 5R 6/2).

Principal variation is the continued (from Core 48, Section 1) decrease in vesicle abundance. Veins at 60 cm are inclined at 50–60°. Below 60 cm only sparse large (0.5 cm) vesicles are present. The change is more or less coincident with an increase in prominence of late stage fractures. These are inclined at high angles or are horizontal; the change from one to the other is abrupt (e. g. at 99 cm).

Small veins (sub-horizontal and parallel to fractures are infilled with a black (N6) mineral but a large vein (2 cm) in Piece 3C has a black lining and is color banded from yellowish gray (5Y 8/1) to light greenish gray (5G 8/1) towards the center. Both boundaries are sharp. The black lining appears to have ingrown into the inner yellowish gray core.

Vesicle clasts are spare to rare.

Groundmass: 1) Reddened zone, plagioclase laths and pyroxenes – these concentrated in patches. Red mineral grains (altered pyroxene) account for the red color. 2) Outside the reddened zone, the groundmass consists of plagioclase laths with the pyroxenes concentrated in small irregular patches or concentrated in thin layers.

Thin Section – 21 cm: Tholeiitic basalt.

CORE 48, SECTION 3 Depth 590.5–592.0 m

The principal variation in the altitude of the fractures and in the presence of a zone of abundant vesicles. Vesicle clasts occur sparsely. A faint reddening is present above the vesicular zone.

30–40 cm: Diffuse red color (groundmass – sparse red mineral – altered pyroxene?).

40–63 cm: Abundant unfilled vesicles (black or black and light gray (N2) core).

Groundmass: Predominantly plagioclase laths with pyroxenes typically concentrated within streaks. Trachytic texture sparse.

Veins typically infilled with black (N2) mineral.

CORE 48, SECTION 4 Depth 592.0–593.5 m

Medium gray (N5) phyric basalt.

15 cm: Diffuse boundary.

15–36 cm: reddened (10R 6/2). Groundmass: diffuse patches of red and discrete grains of a red mineral (altered pyroxene?).

36 cm: relatively sharp boundary.

The principle variations are the reddened zone. Vesicles are sparse to common between 10 and 30 cm. Sparse to 115 cm and sparse to common below. The vesicles between 10 and 30 cm are slightly larger in mean size 1–3 cm than those at the base.
Ubiquitous are sub-horizontal to horizontal black laminae composed of pyroxene.

Groundmass: equigranular laths of plagioclase and pyroxene. Pyroxene is concentrated in streaks.

CORE 48, SECTION 5 Depth 593.5–595.0 m

Medium gray (N5) phyric basalt – vesicular.

Vesicles (0.15 m–0.5 mm) occur throughout. Horizontal to sub-horizontal fractures with pyroxenes streaked out along them occur throughout. Vesicle clasts are sparse.

Groundmass: Predominantly plagioclase laths with smaller pyroxene grains. Pyroxene grains concentrated in darker layers. In variety of dark layers, there is a suggestion also of preferred orientation of plagioclase laths.

Thin Section – 57 cm: Tholeiitic basalt.

CORE 48, SECTION 6 Depth 595.0–596.4 m

Medium gray (N5) phyric basalt.

Vesicles are small (0.5 mm or less) and sparse to rare throughout the section. Vesicle clasts (up to 3 cm) occur sporadically and show varying degree of reaction with the groundmass.

The principle variation is in the altitude of the fractures. These are 0–25 cm: sub-horizontal, 25–63 cm: approximately at random, 63–70 cm: ~60°, 70–117 cm: ~70°, and 117–130 cm: ~70°.

Groundmass: plagioclase laths and pyroxenes (subordinate). There suggestion that the plagioclase laths may be oriented perpendicular to the horizontal streaks of pyroxene(?).

46 cm: is slickensided.

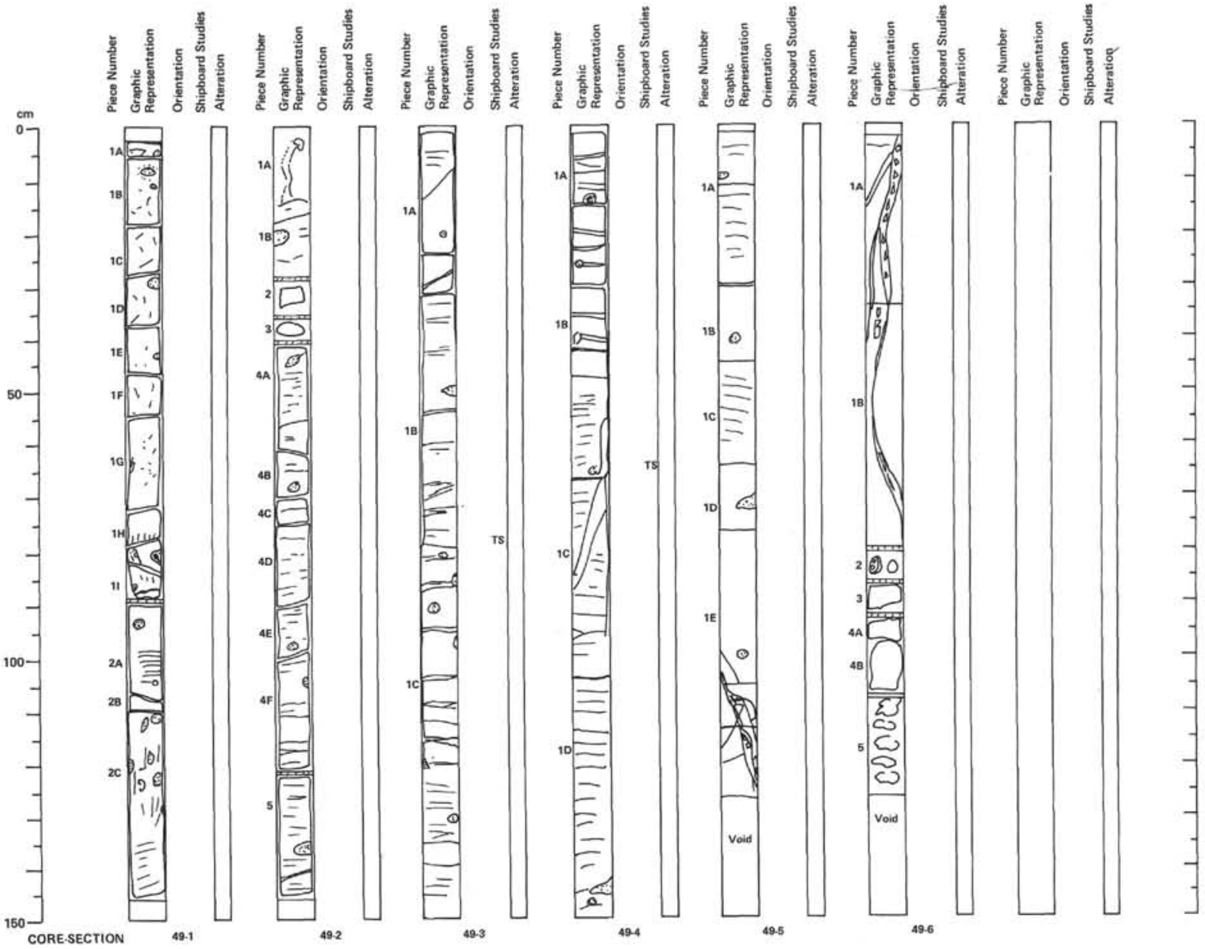

CORE 49, SECTION 1

Depth 596.5–598.0 m

Medium gray (N5) phyric vesicular basalt.

Down to 80 cm there are major variations in lithology. Vesicle clasts up to 1 cm occur sporadically. Black patches of pyroxene show a random to rare sub-horizontal orientation. The base of this interval is defined by a 2 mm dark gray band near 80 cm.

Below this level, the vesicle clasts are more abundant and larger (2 cm) showing sharp and diffuse contacts with the matrix. Between 90 and 106 cm, a series of 3 mm medium gray (N5) at medium dark gray (N4) bands are present. Below this level, the dark bands are cracked vertically but cross-cut inclined (10°) bands near the base.

Note: Just above the contact at 80 cm, binocular examinations shows a strong vertical preferred orientation of the plagioclase and pyroxenes in the groundmass.

Groundmass: plagioclase laths and pyroxenes locally showing a strong preferred orientation parallel or perpendicular to the pyroxene streaks.

CORE 49, SECTION 2

Depth 598.0–599.5 m

Medium gray (N5) phyric basalt.

Vesicle clasts (up to 1 cm) occur sparsely through the section. Vesicles are small (0.5 mm or less) and minor. The principle variation is a subtle variation in color from medium gray (N5) towards medium dark gray (N5) reflecting the abundance of the darker (5Y 4/1) horizontal layers.

Some evidence of vertical streaking of the pyroxenes in Piece 1A.

Groundmass: Plagioclase laths with minor pyroxenes concentrated in the darker layers.

CORE 49, SECTION 3

Depth 599.5–601.0 m

Only significant difference from Core 49, Section 2 is tendency for pyroxene to be concentrated in 3 mm layers of horizontal to sub-horizontal altitude down core. Vesicle clasts sparse and typically without reaction rims.

Groundmass: plagioclase laths and pyroxenes. Suggestions that laths and long axes of dark minerals are oriented perpendicular to the darker layers which appear different (smaller?) in grain size then intervening groundmass.

115 cm: 2 mm smectite vein with thin streaks of light gray (N7) – calcite(?).

Thin Section – 77 cm: Tholeiitic basalt.

CORE 49, SECTION 4

Depth 601.0–602.5 m

Medium gray (N5) phyric basalt.

Vesicles sparse throughout.

Occasional 1 mm veins infilled with smectite are present and sparse vesicle clasts of up to 1 cm size.

Horizontal to slightly inclined beds of pyroxene occur throughout.

The most prominant feature in the 1 cm wide vein is Piece 1C inclined at approximately 70°.

Grayish black (N7) vein lining also penetrates host rock black vein lining contains light gray (N6) and dusky green patches that penetrate main vein filling. Sparse dusky red patches also present.

Groundmass: plagioclase laths predominate with pyroxenes concentrated in irregular patches or horizontal sub-horizontal layers.

Thin Section – 64 cm: Vein quartz – chalcedony and goethite.

CORE 49, SECTION 5

Depth 602.5–604.0 m

Medium gray (N5) phyric basalt.

Sparse vesicles (0.5 mm) occur throughout infilled with black vesicle clasts sparse. Principle variations in abundance of dark streaks which increase into lower part of the section which is closer to medium dusky gray (N4).

Groundmass: plagioclase laths with pyroxenes. Sparse trachytic texture.

Principle texture of the section is the braided vein structure between 95 and 124 cm. One 5 mm thick and one 1 mm thick vein are parallel and inclined at 70°. The veins cut and truncate center veins parallel to the foliation in the basalt. Included with black (N2) infill of the vein are 3 cm angular fragments of medium gray (N5) basalt. Their presence and a suggestion of slickensides in the face of one of the veins suggests a small fault.

CORE 49, SECTION 6

Depth 604.0–605.3 m

Medium gray (N5) phyric vesicular basalt.

Principle feature is an increase in vesicle size and abundance towards the base of the unit.

The principle feature is the complex system of fractures extending the length of Pieces 1A and B. The fractures have a vein infilling ranging from black (N2) to black with light olive brown (2.5Y 5/6) patches and light gray (N7) infilling. Angular and ruptured basalt fragments occur throughout the length of the vein. Horizontal vein in the host basalt truncate against the vein.

Groundmass: plagioclase laths and pyroxene without preferred orientation. No downward change in grain size apparent. Note: Fault continues into top of next flow unit where it is seen in the scoriaceous top of the underlying unit.

78 cm: Top of next unit.

Pieces 3 and 4: Dusky blue (5PB /2) deferred layer resting in dark gray (N3) of lapilli passing down into (Pieces 4A and B) scoriaceous unit consisting of dark gray (N3) and dark reddish brown (10R 3/4) fragments of vesicular basalt showing all grades between these extremes. Numerous angular lithic fragments in the groundmass. Veiscles in basalt infilled with dusky blue green (5BG 3/2).

Piece 5: Extremely vesicular basalt. Large vesicles (>1 cm) and small infilled vesicles contain light blue green (5BG 6/6) mineral.

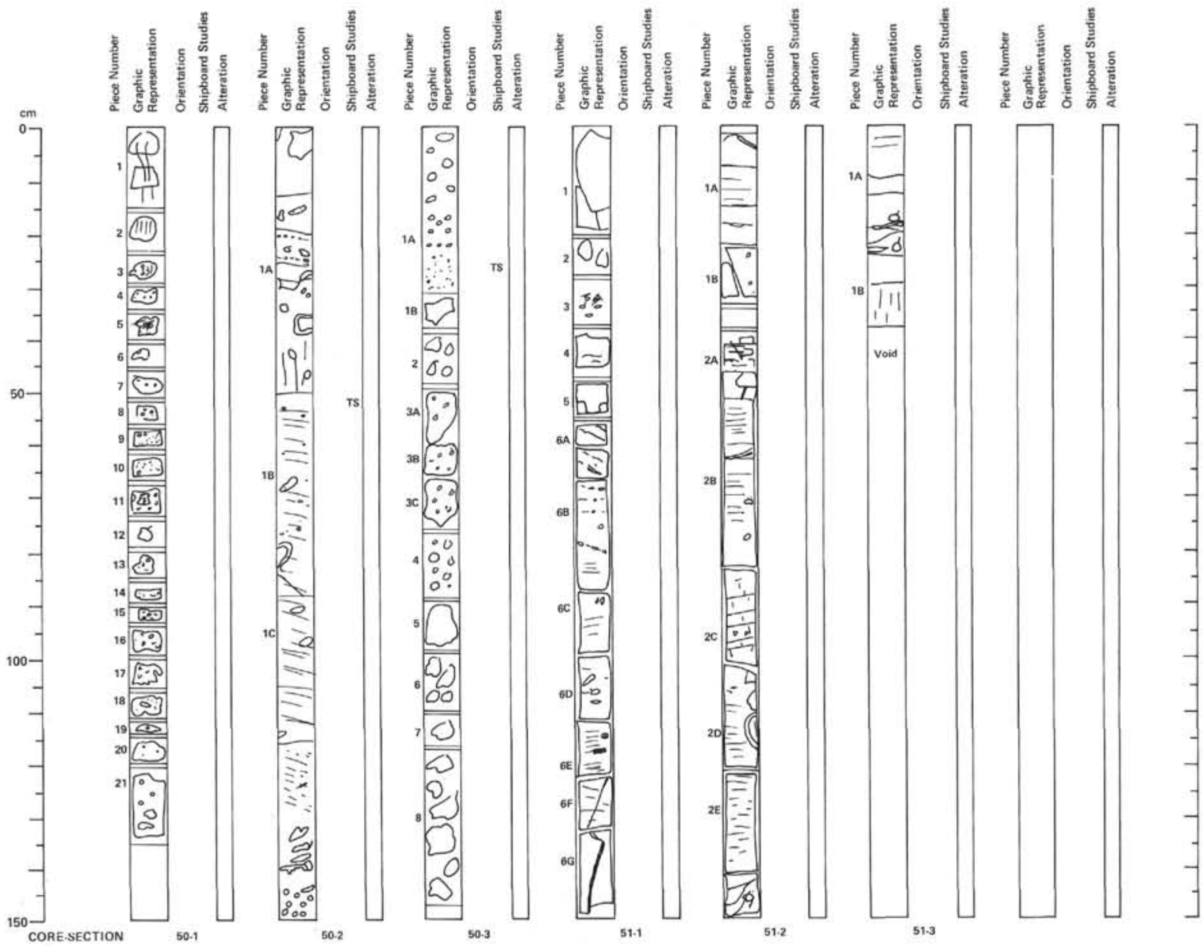

CORE 50, SECTION 1

Depth 605.5–607.0 m

Medium gray (N5) phyric vesicular basalt.

Pieces 1, 2, and 3 have split naturally along a slickensided surface. Slickensides vertical with pale olive (10Y 6/2) fibrous patches also slickensided. Not present below Piece 3. Possible fault.

Pieces 4–9: Abundant large open vesicles (0.5 + cm) in medium gray (N5) phyric basalt.

Pieces 10–15: Sharp decrease in abundance of large vesicles and sharp increase in abundance of small vesicles to common. Transition is in Piece 9. Small vesicles are 0.5 mm or less in size. Large vesicles unfilled. Both contain light gray (N7) and light blue green (5BG 6/6) in lining of black mineral.

Pieces 16–21: Decrease in abundance of small vesicles to sparse. Larger vesicles still present but largely infilled. Light gray (N7) common in larger vesicles. Large vesicle size (1 cm).

Groundmass: plagioclase laths with smaller pyroxene grains. General impression is of increasing grain size with decreasing abundance of small vesicles.

CORE 50, SECTION 2

Depth 607.0–608.5 m

Medium gray (N5) phyric vesicular basalt.

0–13 cm: Sparse vesicles. Large vesicle at 5 cm black (N2) lining and infilled with grayish yellow (5Y 8/4) and light gray (N7).

13–27 cm: Zone of abundant vesicles apparently stratified. Largest vesicles (0.5+ cm) random but smaller vesicles crowded. Clear contact with basalt above and below lava with smaller vesicles larger in grain size than the smaller size associated with the larger vesicles.

29 cm: Vein(?) lined with black – predominantly light gray (N7) core with minor light olive gray (5Y 6/1).

40–50 cm: Fractures vertical.

50–130 cm: Abundant fractures spaced at 1 cm interval. No small vesicles. Sparse large vesicles (1.5 cm) have black lining and light gray (N7) core intergrown with minor black (N7) medium gray (N5) phyric basalt.

Groundmass: plagioclase laths with pyroxenes. Tendency for pyroxenes to be oriented along horizontal planes.

130–150 cm: Sharp but gradational increase in vesicle size. Vesicles mean size 0.3 cm.

Thin Section – 51 cm: Tholeiitic basalt.

CORE 50, SECTION 3

Depth 608.5–610.0 m

Medium gray (N5) phyric vesicular basalt.

0–37 cm: Increasing abundance and decreasing vesicle size (1 cm–0.5 mm). Unfilled vesicles rare. Vesicles typically infilled with black (N2) with light gray (N7) flecks.

37 cm: Base of flow unit. Top of next flow unit.

Piece 2: Grayish red (5R 4/2) vesicular basalt.

Pieces 3 and 4: Blackish red (5R 2/2) scoriaceous vesicular basalt. Vesicles lined with dark dusky green (5BG 3/2).

Upper part of a flow unit extends to base of section. It is a blackish red (very light) scoriaceous vesicular basalt. A dark dusky green (5BG 3/2) to light grayish green (5BG 5/2) mineral typically lined many of the small vesicles. Impression is of a decrease in vesicle size downward. Groundmass is very grained aphyric to aphanitic.

Thin Section – 26 cm: Altered tholeiitic basalt.

CORE 51, SECTION 1

Depth 614.5–616.0 m

Medium gray (N5) phyric basalt. Apart from the zones of inclined vesicles and the flowage in Piece 6, the principle variation down section is a decrease in the abundance of vesicles and the apperance of the characteristic sub-horizontal location. Vesicles predominatly black (N2) with light gray (N7) core.

10 cm: Vein with horizontal slickensides and fibrous calcite, black mineral is saponite.

38 cm: Light gray (N7) yellowish (5Y 8/1) vesicle infill.

45 cm: Contact between basalt with vesicles flattened parallel to location and below.

Piece 5: Zone showing complex flow similar in vesicle concentration. Base of this lithology seen in top of Piece 6A and base of Piece 5. In the lithology, vesicles typically fractured between vesicle clasts. Vesicle in flow zone has unusual 'red green' color and may be present in smaller vesicles (nearest is 5BG 3/2).

55–65 cm: Vesicles inclined along 60°.

80 cm: Vesicles inclined at 40°.

125 cm: Calcite vein (fibers perpendicular to vein edge). Vein inclined at 80° but late stage fracture not displaced although slickensides present.

CORE 51, SECTION 2

Depth 616.0–617.5 m

Medium gray (N5) phyric basalt.

Predominant variation downcore is in the abundance and inclination of the late stage fracture foliation.

Piece 1A, the foliation is sub-horizontal and consists of discrete 1–2 mm wide medium dark gray (N5) bands composed of pyroxenes(?).

In Piece 2C, the foliation has a orthogonal pattern but then becomes sub-horizontal mainly to the base of the core. More steeply inclined foliation (60°) is evident in Piece 2D at 110 cm and in Piece 2E.

Lined with a black mineral. The center is either an intergrowth of black (N2) and light gray (N7) or a mixture of light olive gray (5Y 6/2).

Groundmass: predominantly plagioclase laths with altered(?) pyroxene disposed in irregular patches or foliation.

120 cm: Calcite vein.

140 cm: Light gray (N7) and olive (5Y 4/4) vein.

CORE 51, SECTION 3

Depth 617.5–617.87 m

Medium gray (N5) phyric basalt.

Sparse vesicles infilled with light gray (N7).

Principle variation is sharp change in altitude of foliation from horizontal to vertical downhole.

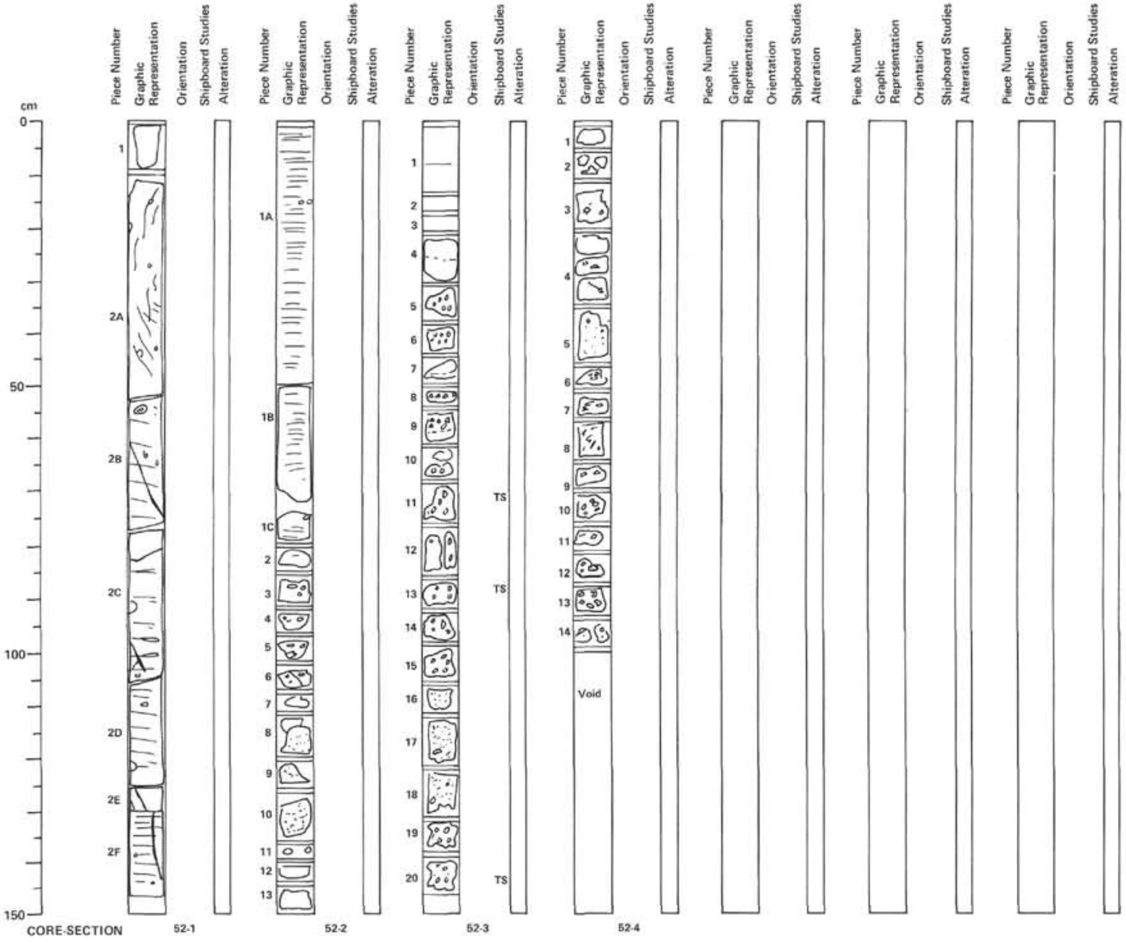

CORE 52, SECTION 1 Depth 618.0–619.5 m

Piece 1: Dusky blue (5PB 3/2), light brownish gray (5YR 6/1) to medium gray (N5) altered vesicular basalt.

10 cm: Base and top – section probably missing?

Piece 2: Principle variation down core is in number and abundance of foliation. In Piece 2A foliation is irregular but near vertical in the upper part to cross cut. A sequence of inclined (50) foliation in the lower part.

In Pieces 2B–F the foliation decreases in induration to become sub-horizontal and also the spacing decreases from around 1.0 cm above to 0.2 cm in the lower part.

Sparse vesicles present and infilled with black (N2) or black intergrown with light gray (N7) occasional light olive gray (5Y 6/1) patches.

Veins are lined with black and infilled with light gray (N7) to bluish white (5B 9/1) crystals (not fibrous) – calcite? Slickensides absent.

Groundmass: plagioclase laths and pyroxenes, these disposed in foliation or in small irregular patches.

CORE 52, SECTION 2 Depth 619.5–621.0 m

Medium gray (N5) phyric basalt.

Principle variation well developed foliation is present in the top of Piece 1A (spacing 3 mm) but decreases in spacing down piece to 0.5 cm becoming inclined. In the series of small pieces below, large (1 cm) open vesicles appear in Piece 3 and continue through Piece 5. Below Piece 5, small (2 mm or less) size vesicles becomes more abundant with an accompanying decrease in size to less than 1 mm lowered the base of the flow. Vesicles rare to absent in Pieces 1A–2.

Groundmass: Typically from plagioclase laths and pyroxene. Much lower grained thin in Core 52, Section 1.

Vesicles: black (N2) lining with typical light gray euhedral crysts in open ones.

68 cm: Foliation ends and sparse foliation begins below.

85–95 cm: Large vesicles.

100–135 cm: Increasing abundance and decrease in size of vesicles downwards.

130 cm: Broken along slickensided fracture (slickensides near vertical).

140 cm: Base of flow and top of flow.

CORE 52, SECTION 3 Depth 621.0–622.5 m

Piece 1: Scoriaceous dusky red (5R 3/4) to medium gray (N5) vesicular basalt. Irregular clasts of vesicular basalt showing different degrees of reddening and are set in a matrix of smaller angular clasts. Sparse large vesicles present.

Piece 2: Angular clasts of medium gray (N5) basalt reddened grayish red (5R 4/2).

Piece 3: Medium gray (N5) vesicular (0.5 cm) basalt.

26 cm: Contact between agglomeratic top of flow and vesicular basalt below medium gray (N5) vesicular (0.5 mm) passes upward then reddened (5R 4/2) zone to agglomerate.

Pieces 5, 6, and 7: Grayish red (5R 4/2) to medium gray vesicular basalt. Vesicles show strong vertical orientation. Brecciated basalt at base of Piece 7. Clasts 0.3 cm.

Pieces 8 and 9: Brecciated (agglomerate) grayish red (5R 4/2) basalt. Clasts 1 cm–0.3 cm with contact (gradational) to medium dark gray (N5) vesicular basalt at 68 cm.

Pieces 10–15: Weak red (10R 5/2) highly vesicular basalt. Vesicles typically 0.3 cm and flattened with large axes vertical. Flattening decreases downward to Pieces 14 and 15 does not show preferred orientation and has only round to subround vesicles. Abrupt change to small vesicles between Pieces 15 and 16.

Pieces 16–18: Grayish red (5R 4/2) vesicular (0.1 mm) basalt typical. Sparse large (late stage?) 1 cm vesicles.

130 cm: Base of flow and top of flow.

Piece 19: Extremely vesicular (1 cm) basalt.

Piece 20: Predominantly medium dark gray (N4) to grayish red purple (5RP 4/2) agglomerate. Large clasts of vesicular basalt with vesicles often showing strong preferred circulation.

Thin Section – 71 cm: Tholeiitic basalt.

Thin Section – 88 cm: Tholeiitic basalt.

Thin Section – 143 cm: Altered tholeiitic basalt.

CORE 52, SECTION 4 Depth 622.5–623.5 m

Pieces 1–5: Very dusky red purple (5RP 2/2) vesicular basalt. Principal trend down to transition at 45 cm is a decrease with purple color and a change to a medium gray (N5) vesicular basalt. Vesicle size (0.5 mm) uniform throughout with sparse open (1 cm) vesicles. Some induration of preferred orientation of vesicles in Piece 5.

Pieces 6–14: Transition to medium light gray (N6) vesicular basalt. Large irregular partly open and infilled vesicles (0.5 cm) have long axes near vertical. Vesicles typically lined with black (N2) and light gray (N8) cores common but occasional pale blue green (5BG 7/2) present.

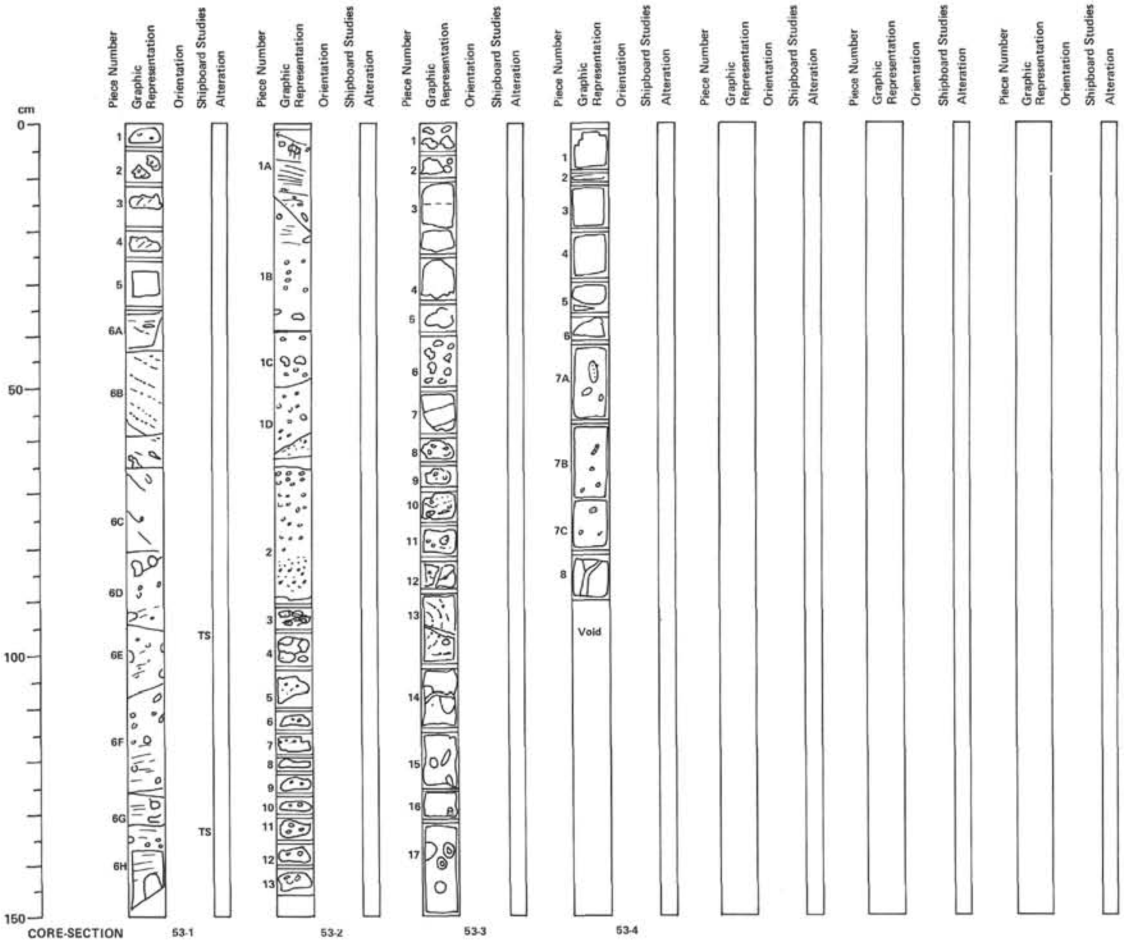

CORE 53, SECTION 1 Depth 623.5–625.0 m

Pieces 1–6B: Medium gray (N5) to medium light gray (N6) phyric vesicular basalt. Principle variation is in the appearance of strings of vesicles linked by black (N2) veins. These are prevalent down to 65 cm. Within this interval, they vary in inclination from 60° to 40°. The vesicles range in size from 1 mm to 1 cm and typically infilled by black (N2) smectite. Some partly open vesicles have a light gray (N7) core. Piece 6A is cut by a slickensided fracture inclined at 60°. Slickensides across the fracture plane at 50°.

Pieces 6C–H: Below 65 cm, large vesicles are common and the horizontal foliation becomes important. The large vesicles form small geodes lined with calcite and quartz, but occasionally completely filled by light bluish gray (5B 7/1) and light greenish gray (5G 8/1) minerals.

107 cm: Slickensided fracture.

Thin Section – 96 cm: Tholeiitic basalt.

Thin Section – 132 cm: Altered tholeiitic basalt.

CORE 53, SECTION 2 Depth 625.0–626.5 m

Pieces 1–3: Medium gray (N5) phyric vesicular basalt. Principle variation is a downward increase in vesicle abundance. Foliation dies out downward at 25 cm. Vesicles become especially abundant down from 48 cm. Between 48 and 62 cm, the vesicles average 1 cm–0.2 cm diameter. Below a sharp transition at 62 cm, vesicles decrease in size to become sparse downward. Below a transitional contact at 84 cm. Small vesicles (1–2 mm) and sparse large vesicles become abundant to the base of the flow.

Vesicles: Typically infilled with black (N2) smectite. Larger vesicles have black (N2) intergrown with light gray (N7) and yellowish gray (5Y 8/1) patches.

Groundmass: plagioclase laths and pyroxenes.

18 cm: Fracture with slickensides(?).

95 cm: Base of flow and top of flow.

Pieces 4–13: Blackish red (5R 2/2) to dark gray (N4) vesicular basalt. Small vesicles in upper part grade downward to large (1 cm) open vesicles in lower part (Pieces 11, 12, and 13) associated with increase in gray color.

Vesicles lined with black and infilled wholly or partly with light gray (N7) or moderate blue green (5BG 4/6).

CORE 53, SECTION 3 Depth 626.5–628.0

Pieces 1–4: Medium dark gray (N4) basalt breccia. Small angular basalt fragments (1 mm) interbedded with vesicular basalt. Top of unit (Piece 2) much more vesicular.

33 cm: Base of unit and top of unit?

Pieces 5 and 6: Blackish red (5R 2/2) vesicular basalt. Vesicles infilled with light gray and dusky greenish gray, but also latter color is basalt.

Piece 7: Blackish red (5R 2/2) to dusky purple (5RP 2/2) to medium grav (N5). Veiscular basalt dusky green band at 55 cm. Impression is of downward decrease in reddening. Green color also decreases downward and is absent in medium gray basalt. Green color concentrated in vesicles.

Pieces 8–17: Medium gray (N5) vesicular phyric basalt.

Vesicles are abundant down to 101 cm and show folding indicating late stage deformation of flow. Vesicles decrease below this level and become sparse.

Large (2 cm) vesicles are developed in Piece 17 where incipient foliation is present. One nice geode is present. Vesicles have a light bluish gray (5B 7/1) or bluish white (5B 9/1) core. Some have a light blue green (5BG 6/6) or dusky blue green (5BG 3/2) core. Concentric growth evident. All have black lining.

108 cm: Large vesicle lined with black with light gray (N7) and yellowish gray (5Y 8/1) amygdaloidal core.

Groundmass: plagioclase laths and pyroxenes.

CORE 53, SECTION 4 Depth 628.0–628.9 m

Pieces 1–5: Medium dark gray (N1) phyric vesicular basalt. Predominantly 1 mm vesicles in sub-horizontal bands. Patches 1–2 mm of black and white intergrown crystals.

33 cm: Base of unit. Top of unit. Contact with brecciated top of underlying flow is grayish red (5R 4/2) and sharp.

Piece 6: Abundant small (1–2 mm) fractured and corroded vesicular basalt clasts with dusky green (5BG 3/2) in matrix.

Piece 7: Main body of flow: medium gray (N5) phyric basalt. Vesicles are sparse and a weak horizontal foliation is present. Vesicle clasts are present in Piece 7B.

85 cm: 5 mm vein lined with black (N2) smectite. Center predominantly in intergrowth of light bluish gray (5B 7/1) and bluish white (5B 9/1) with yellowish gray (5Y 8/1) occurring more sparsely.

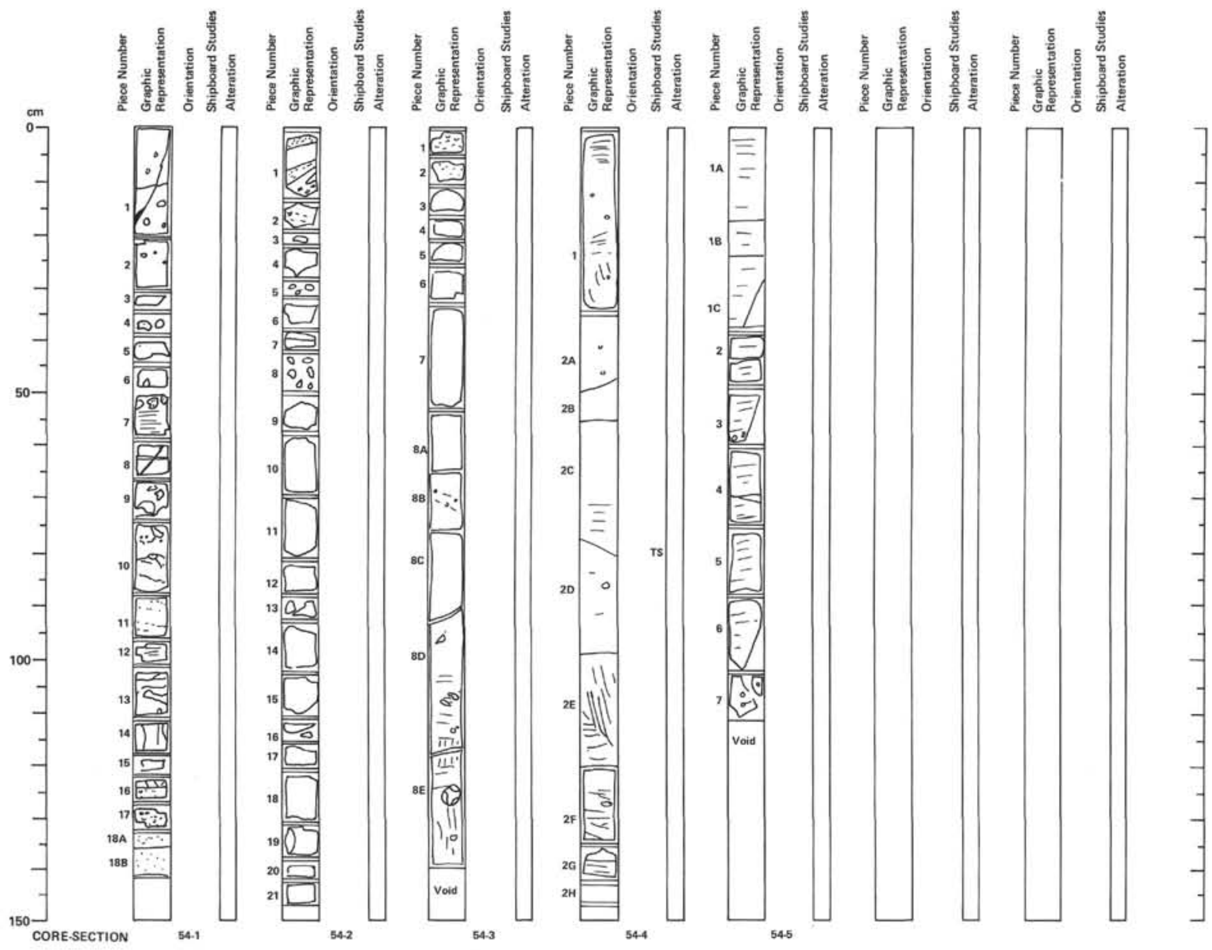

CORE 54, SECTION 1 Depth 632.5–634.0 m

Medium gray (N5) phyric vesicular basalt.

Slickensided fracture (63°). Slickensided oriented occurance along fault plane in Piece 1. Clasts (3 mm) of basalt are in fault breccias.

Between 0–75 cm: A weakly developed sub-horizontal foliation is present. Only sparse large vesicles (0.5 cm) are present and are both open and infilled. Vesicle clasts (2 cm) occur in Piece 7. Vesicle infill in either black (N2) smectite or a mix of light bluish gray (5B 7/1) and yellowish gray (5Y 8/1).

Below 75 cm: Vesicles increase in abundance and are arranged in layers often 'graded' and inclined at 30° . Below 110 cm (Piece 14) vesiculation is in vertical bands with light gray (N6) almost vesicle free bands (0.5 cm) separating wide (3 cm) bands continuing randomly distributed small (1 mm) vesicles.

80 cm: Horizontal fracture with basalt clasts.

At 128 cm: A sharp contact defines the base of the above. Below abundant vesicles are present.

Groundmass: 52 cm – having random plagioclase laths and pyroxene granules; 105 cm – as at 52 cm but occasional xenoliths of plagioclase and pyroxene phenocrysts; and 135 cm – a phyric(?) very small plagioclase laths and pyroxenes.

CORE 54, SECTION 2 Depth: 634.0–635.5 m

Pieces 1–6: Medium gray (N4) phyric vesicular basalt. Principle variation toward base of flow is a decrease in vesicle size and grain size. Contact with underlying flow evident in Piece 6 and apparently chilled vesicles in Piece 1 flattened and concentrated in inclined bands (30°) with intervening vesicle free bands. Some suggestion if inverted grading.

Groundmass: small plagioclase laths and pyroxenes.

38 cm: Base of flow and top of flow.

Pieces 6–13: Agglomerate, blackish red (5R 2/2), very dusky red (10R 2/2), very dusky purple (5RP 2/2) fragments of vesicular basalt. Frequently angular and ranging in size from cm to mm. Vesicles often vertical orientation. Sparse large cm vesicles. Grayish blue green (5BG 5/2) common in upper part but minor below Piece 11.

92 cm: Base of agglomerate.

Pieces 14–21: Medium dark gray (N4) highly vesicular basalt. Abundant often elongate vesicles (1–3 mm) throughout. A large grayish black (N2) clast (4 cm) with reaction rim present in Piece 19.

CORE 54, SECTION 3 Depth 635.5–637.0 m

Pieces 1 and 2: Medium gray (N5) phyric vesicular basalt. Abundant small vesicles (1 mm or less). Large vesicles rare to absent.

Pieces 3–8: Medium gray (N5) phyric vesicular basalt. Groundmass: having random plagioclase laths and pyroxene crysts. Irregular to sub-rounded large (2–5 mm) vesicles abundant. Vesicle infill: black (N2) dusky blue green (5BG 3/2), bluish white (5B 9/1) with minor yellowish gray (5Y 8/1).

Piece 8A and B: Small vesicles sparse. Large 1–5 cm vesicles present. Black (N2) lining infilled with dusky blue green (5BG 3/2). Strong geodal structure. One large vesicle infilled with light bluish gray (5B 7/1) with yellowish gray (5Y 8/1).

70 cm: Vesicles inclined at 40° .

Pieces 8C–E: Vesicles sparse. Principal variation in appearance of horizontal foliation and a weak vertical foliation in Piece 8E.

90 cm: Slickensided fracture (30° inclination).

125 cm: Large 1.5 cm vesicle, yellowish gray (5Y 8/1) and light gray (N7).

CORE 54, SECTION 4 Depth 637.0–638.5 m

Medium gray (N5) phyric basalt. Vesicles rare to absent throughout. Principal variation is in the degree of development of the weak foliation. A nice contact between near vertical foliation and sub-horizontal braided foliation clear in Piece 2E.

Groundmass: Plagioclase laths and pyroxenes in nearly equal proportions showing occasional trachytic texture.

78 cm: Slickensided fracture (40°) with fibrous calcite.

Thin Section – 78 cm: Tholeiitic basalt.

CORE 54, SECTION 5 Depth 638.5–639.6 m

Medium gray (N5) phyric basalt.

12 cm: Slickensided fracture (inclined 60°). Slickensides parallel to vertical axis.

30 cm: Slickensided fracture (inclined 70°). Slickensides inclined at 50° to horizontal.

Piece 2: Face of fracture in these pieces.

Principle feature is the well developed braided foliation seen in the lower part of Core 54, Section 4.

Groundmass: plagioclase laths predominate with suborfinate pyroxene.

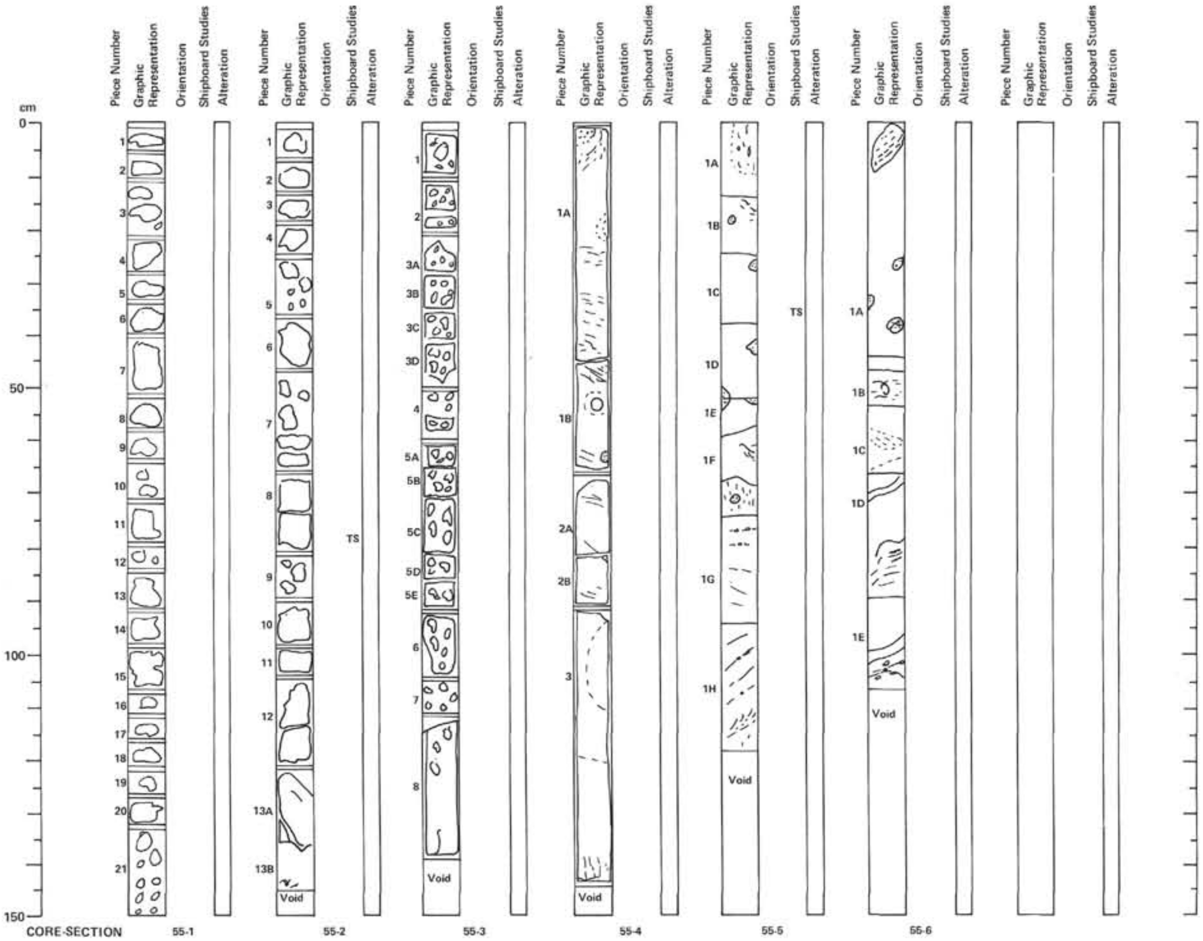

CORE 55, SECTION 1 Depth 641.5–643.0 m

Pieces 1–5: Grayish red (5R 4/2) vesicular basalt. Piece 2 contains an angular clast of grayish red basalt and a very dusky red (10R 2/2) matrix – a similar lithology is in Piece 6 (agglomerate?).

Pieces 6–8: Very dusky red (10R 2/2) agglomerate to grayish red purple (5RP 4/2) agglomerate clasts are vesicular basalt reddened at edges. Interstices amygdaloidal an infilled with grayish blue green (5BG 5/2) to moderate blue green (5BG 4/6) mineral. Edges of clasts have welded aspect?

Pieces 9–17: Vesicular very dusky red (10R 2/2) to grayish red purple (5RP 4/2) basalt. Vesicle sizes 1–2 cm but occasional larger vesicles (3–4 cm) present. Vesicles infilled with outer black (N2) lining. Then moderate blue green (5BG 4/6) layer. Thin amygdular core at light greenish gray (5G 8/1) euhedra.

Pieces 17–21: Medium gray (N5) phyric vesicular basalt characterized by 1–2 cm vesicle clasts.

Groundmass: plagioclase laths and pyroxenes. Vesicles show same color pattern as above.

CORE 55, SECTION 2 Depth 643.0–644.5 m

Pieces 1–12: Dusky blue (5PB 3/2), very dusky purple (5RP 2/2) and grayish red purple (5RP 4/2) clasts (3–5 cm) of basalt in matrix of smaller angular clasts (3 mm or less) of same. Agglomerate/scoriaceous top of flow?

Reddening (5R 4/2) apparent around basalt clasts. Large irregular vesicles represent unfilled interstices in clasts. Vesicles typically infilled with olive (5Y 5/4).

110 cm: Gradational base of agglomerate.

Piece 13: Medium dark gray (N4) phyric basalt. Vertical to inclined joints present infilled with black (N2) or olive (5Y 5/4) mineral. Becomes brecciated again towards the base.

Thin Section – 77 cm: Lithic volcanic breccia – scoriaceous top of lava.

CORE 55, SECTION 3 Depth: 644.5–646.0 m

Pieces 1–7: Scoria/agglomerate. Dusky blue (5PB 3/2), very dusky purple (5RP 2/2) and grayish red purple (5RP 4/2) vesicular clasts of basalt. Clasts are rounded to sub-rounded. Larger clasts up to 3 cm in diameter with an abundance of smaller 5 mm clasts in a matrix of smaller clasts of the same. Clasts show corrosion and fracturing. Vesicles present throughout and have formed in the interstices. Dusky blue green mineral common in interstices, vesicles and veining clasts.

110 cm: Base of scoria/agglomerate.

Piece 8: Medium gray (N5) phyric vesicular basalt. Abundant small vesicles (0.5 mm). Several 1 cm size vesicle clasts with reaction rims in the upper part of Piece 8.

CORE 55, SECTION 4 Depth 646.0–647.5 m

Medium gray (N5) phyric vesicular basalt.

Principle variation is in the distribution of vesicles and veined microfractures.

At 5 cm vesicles exhibit flow circulation around large clast and again at 20 cm. Vesicles also disposed in an incline (40°) at 32 cm. A preferred inclination of the vesicles also at 86 cm (inclined 40°).

Between 33 and 70 cm, abundant anastomosing vein filled fractures inclined at 30–50°.

Below 90 cm the structure is more uniform. A large zone of more vesicular basalt between 98 and 110 cm is banded by phyric basalt in which vesicles are minor.

Faint vertical foliation is present towards the base of Piece 3.

70 cm: Slickensided fracture inclined at 40°.

Groundmass: plagioclase laths and pyroxenes (altered?). Some trachytic texture developed between 100 and 110 cm and around clast between 0 and 10 cm.

CORE 55, SECTION 5 Depth 647.5–649.0 m

Medium gray phyric basalt. Principle variation down section is in the abundance of minor concentrations of vesicles and the development of vein fracture filling.

0–6 cm: Vertical trains of vesicles.

6–67 cm: Vesicles rare, sparse vesicle clasts. No foliation.

Groundmass: Altered plagioclase laths and pyroxene grains.
67 cm: Sharp contact between unfractured basalt and zone of vertical fracture vein filling.

75–94 cm: Inclined foliation and vein linking sparse vesicles (inclined 30°). Below 100 cm prominent vein (spacing 0.5 cm) thickness 1 mm inclined at 45° seperated by 3 cm band of unfractured unveined phyric basalt.

Thin Section – 36 cm: Tholeiitic basalt.

CORE 55, SECTION 6 Depth 649.0–650.05 m

Medium gray (N5) phyric basalt. Principal variation in the section is in the appearance of a well developed foliation often showing flow texture frequently followed by flattened vesicles. Foliation also flows around the sparse vesicle clasts.

Vesicles increase in abundance to sparse towards base and are filled with black (N2) or dusky blue green (5BG 3/2) inside black lining. Occasional light bluish gray infill with yellowish gray (5Y 8/1) patches intergrown with black (N2) both of lining and within vesicle center.

Groundmass: Plagioclase laths and pyroxenes that are altered to brown?

5 cm: Large vesicular clast showing well developed 'grading'.

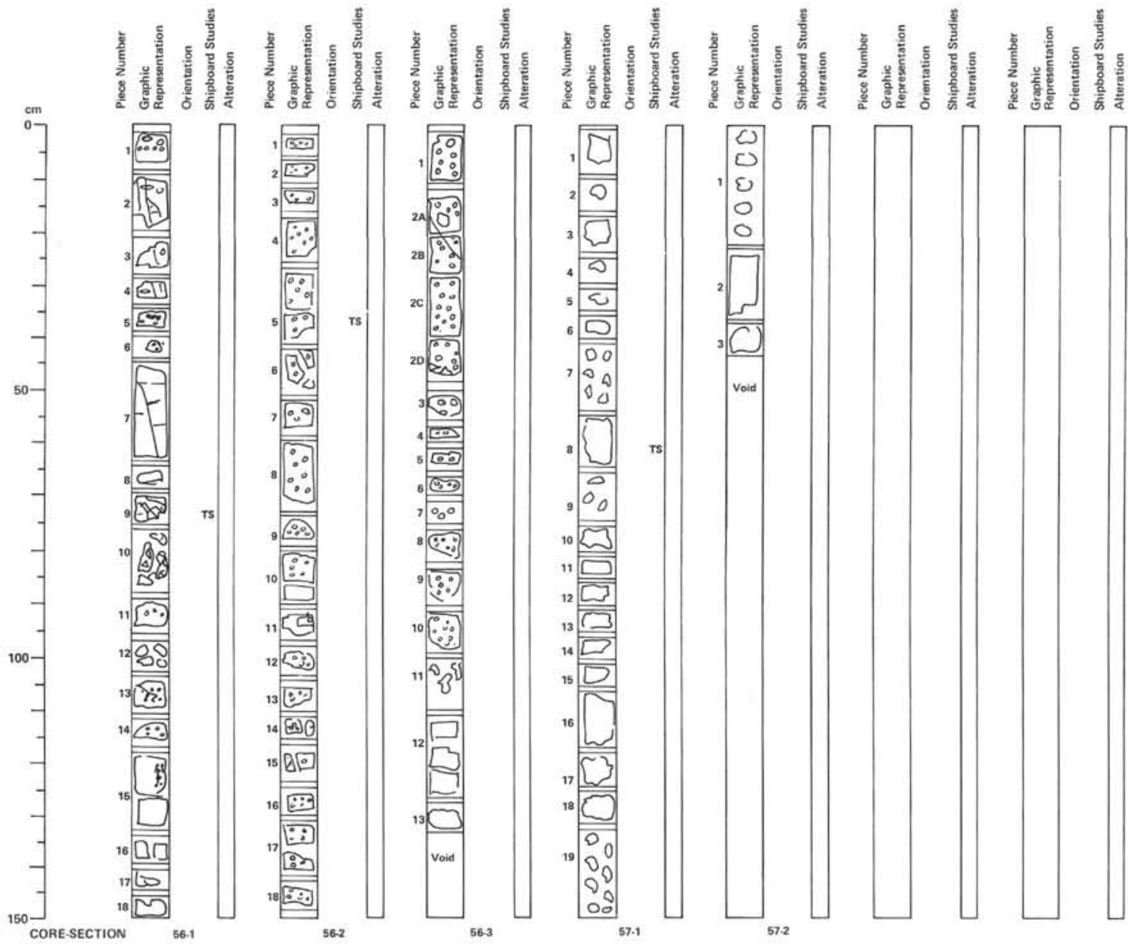

CORE 56, SECTION 1 Depth 650.5–652.0 m

Pieces 1–8: Medium gray (N5) phyric basalt. Principle lithologic variation in top 49 cm is a gradual increase in number of vesicles. The sparse vesicles are generally 0.5 cm in size and typically flattened. Weak foliation is present. Small 1 cm vesicle clasts in Section 1. Veining associated with brecciation of the basalt extends through Pieces 2, 3, 4, and 5.

49 cm: Sharp transition from sparse large vesicles to abundant vesicles of uniform 1 mm size. Towards base of Piece 7, vesicles decrease in size to 0.1 mm. Vein inclined at 80°. Slickensides at 70° to cut piece of core.

70 cm: Base of flow and top of flow.

Pieces 8–10: Contact in Pieces 8 and 9, appears chilled. Aphyric medium gray basalt rests on grayish red brown (5R 4/2) scoriaceous agglomeratic very dusky purple (5RP 2/2), grayish purple (5RP 4/2) and medium gray (N5) basalt. Matrix between angular corroded and fractures clasts (size 1–2 cm) is very dark red (5R 2/6). Sparse vesicles developed in interstices are infilled with pale olive (5Y 6/1) intergrown with black (N2) and light bluish gray (5B 7/1) crystals.

Grayish red purple (5RP 4/2) diminishes downward through dusky blue (5PB 3/2) to medium gray (N5) basalt. Vesicular throughout with vesicles entrained either horizontally (Pieces 15B) or vertically (Piece 15A). Minor reddening present in Piece 16.

Pieces 11–18: Medium gray (N5) phyric vesicular basalt. Groundmass: aphyric to aphantic. Not resolvable with binoculars.

Thin Section – 73 cm: Lithic – vitric volcanic breccia.

CORE 56, SECTION 2 Depth 652.0–653.5 m

Medium gray (N5) phyric vesicular basalt.

No veining or faulting is present. Principle variation is an increase in vesicle size in Pieces 1 and 2 to reach a uniform 3 mm size that continues down to the base of the section. Vesicles are typically infilled with black (N2) smectite but light bluish gray (5B 7/1) and grayish blue green (5BG 8/2) infills are also present.

Groundmass: predominantly plagioclase laths and pyroxene crystals showing trachytic texture.

Thin Section – 37 cm: Tholeiitic basalt.

CORE 56, SECTION 3 Depth 653.5–654.8 m

Pieces 1–10: Medium gray (N5) phyric vesicular basalt.

20 cm: Abundant 3 mm vesicles occur down to 50 cm but then decrease in number to 90 cm. Piece 10 shows a sharp increase in vesicle abundance with an associated decrease in size to 1 mm. This is probably the vesiculated zone at the base of the flow. Vesicles are predominantly infilled with black (N2) smectite. Some have light bluish gray (5B 7/1) and black (N2) intergrowth with sparse light olive gray (5Y 6/1) intergrowth. Fracture (inclined 60°) and slickensides but no displacement visible in crosscut vesicles.

100 cm: Base of flow and top of flow. Nominal only – small pieces in this section and top of Core 57, Section 1 suggest not in place to within 3 m or so.

Pieces 11–13: Pieces of brecciated vesicular basalt, medium gray (N5) to grayish red (5R 4/2). Vesicles and fracture vein filling in breccia, pale blue green (5BG 7/2) color.

CORE 57, SECTION 1 Depth 659.5–661.0 m

Pieces 1–7 are a mixture of medium gray (N5) phyric vesicular basalts and the blackish red (5R 2/2) and grayish red (5R 4/2) scoriaceous basalt. These pieces are not in place. The medium gray basalt probably derives from the overlying basalt flow and the highly vesicular Pieces 1, 2, 3, and 5 (small vesicles size) probably represent its base. The remaining scoriaceous Pieces 4 and 7 probably represent the top of the underlying flow.

Piece 8: Scoriaceous/agglomeratic grayish red (5R 4/2), dusky red (5R 3/4) and angular basaltic clasts set in a blackish red (5R 2/2) matrix. Vesicular interstices part infilled with olive (5Y 5/6).

Pieces 9, 10, 11, and 12: Medium gray (N5) vesicular basalt. Vesicles show gas streaming and are typically 3–1 mm in size with light olive gray (5Y 6/1) centers.

Pieces 13, 14, and 15: Medium gray (N5) vesicular basalt vesicles are much smaller (less than 1 mm).

Pieces 16, 17, and 18: Coarsely vesicular medium gray (N5) basalt. Large 0.5–1.0 cm open vesicles partly infilled with light olive gray (5Y 6/1).

Groundmass: plagioclase laths and altered pyroxene (reddened) – sparse glomerophyric patches of plagioclase and pyroxene phenocrysts.

Thin Section – 60 cm: Lithic volcanic breccia – scoriaceous top.

CORE 57, SECTION 2 Depth 661.0–661.5 m

Piece 1: Not in place. Four pebbles of medium gray (N5) phyric vesicular basalt and 1 pebble of scoriaceous lava (Core 57, Section 2).

Pieces 2 and 3: Medium gray (N5) phyric vesicular basalt. Some segregation of vesicle size evident.

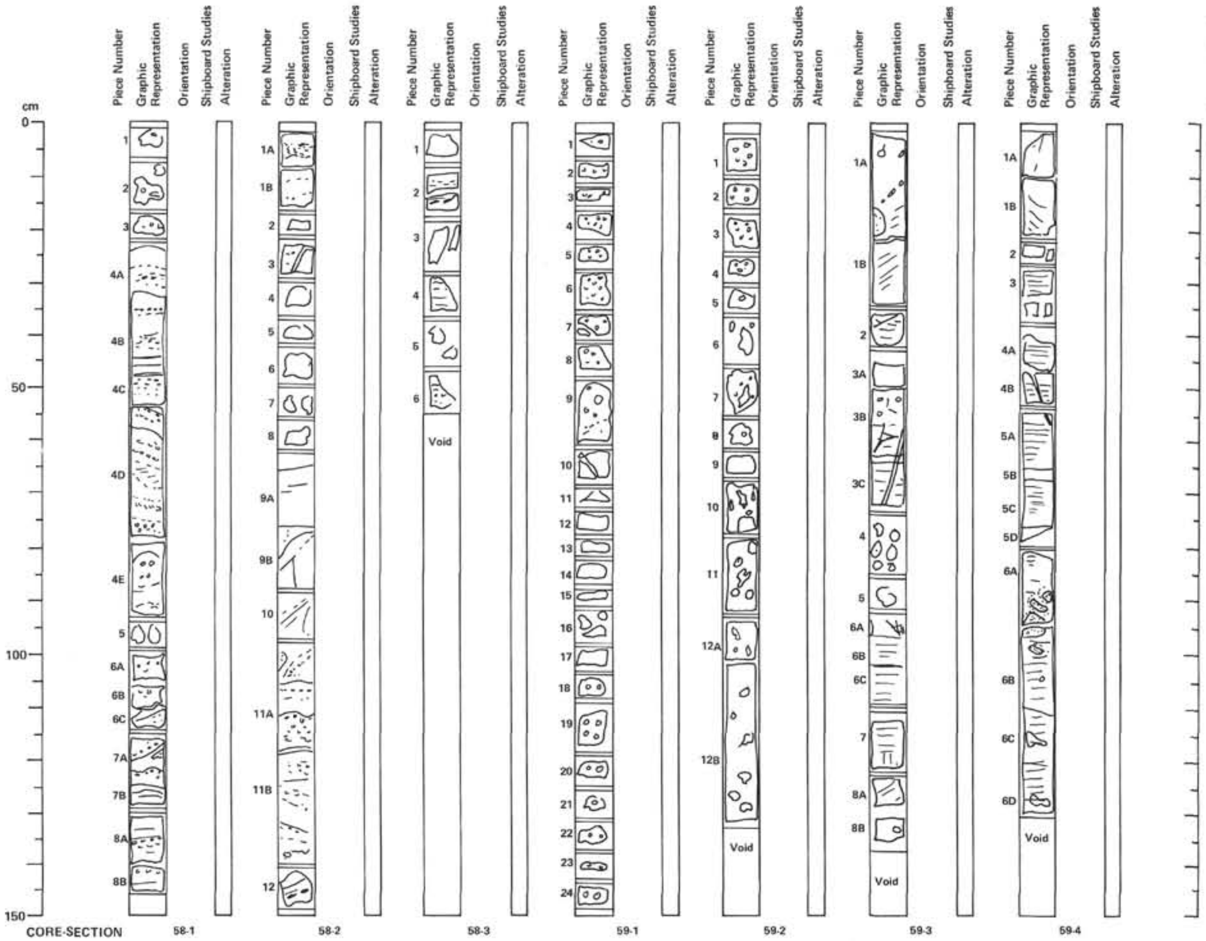

CORE 58, SECTION 1 Depth 668.5–670.0 m

Top of flow.

Pieces 1–3: Grayish red (5R 4/2) vesicular basalt. Vesicles lined with grayish blue green (5BG 5/2) reddened groundmass of pure plagioclase laths and altered pyroxenes. Plagioclase phenocrysts (laths) common and glomerophyres of plagioclase and pyroxene.

27 cm: Contact not recovered.

Pieces 4–8: Medium gray (N5) phyric vesicular basalt. The principle characteristic is the variation in abundance of vesicles and their concentration in discrete zones. Zones of high vesicle concentration (vesicle size typically 1–3 mm) show both grading and inverted grading. These zones are separated by vesicle free zones of finer grain size in which veins composed of black (N2) smectite have a distinct en-echelon appearance. Faithfully following the line of contact between the vesicle rock and poor zones. The pattern is reminiscent of Riedel showing.

The zonation with vesicle rich/poor zones is generally sub-horizontal to inclined at 10° but an inclined zone (50°) is present in Piece 6C.

Groundmass: Vesicular basalts consist of coarser plagioclase laths and pyroxenes. Sparse phenocrysts are glomerophyres. Vesicles typically lined with black (N2) then dusky blue green (5BG 3/2) then brownish gray (5YR 4/1) core.

Vesicle free area finer in grain but with same mineral composition. Riedel fractures have same color composition and banding as vesicles.

CORE 58, SECTION 2 Depth 670.0–671.5 m

Pieces 1–3: Medium gray (N5) phyric vesicular basalt.

0–30 cm: Vesicles (1 mm) concentrated in horizontal bands with vesicle free material between.

25 cm: Traces of slickenside on fracture, dark greenish yellow (10Y 6/6) developed along face.

30 cm: Top of flow unit.

Pieces 4–6: Dark gray vesicular basalt showing some reddening, thick finer grain. Groundmass: plagioclase laths and pyroxenes.

Pieces 7–8: Scoriacoous dusky red (5R 3/4) vesicular basalt with grayish green (5G 5/2) infill to vesicles.

Pieces 9–12: Medium gray (N5) phyric vesicular basalt. Principle feature is concentration of vesicles into discrete bands separated by zones with minor vesicles. These zones are generally horizontal but occasionally are steeply inclined ostensibly cross cutting the horizontal zones. Distinct grading also apparent in vesicle rich zones.

Groundmass: plagioclase laths and pyroxene. Some suggestion of a decrease in grain size across vesicle rich/poor transition. Within vesicle poor zone veining is parallel to contact and may be related to Riedel shows above.

CORE 58, SECTION 3 Depth 671.5–672.05 m

Medium gray (N5) phyric basalt. Major lithologic variation is again the presence of zoning into vesicle rich and poor zones. Distinct size zonation is present within and between vesicle rich zones.

Distinct 'Riedel show' pattern developed in Pieces 2 and 6 and always are found in vesicle free zone.

Curvature of zone boundaries strongly suggest comtemporaneous formation.

22 cm: Slickensides?

CORE 59, SECTION 1 Depth: 673.0–674.5 m

Medium gray (N5) phyric vesicular basalt. Principle variation down section is an increase in the size of the vesicles (from 1 mm–3 mm) and in the proportion of open vesicles. The change occurs at about 100 cm. Foliation is absent. There are hints of a preferred vesicle orientation in Pieces 7 and 9.

Groundmass: plagioclase laths and altered pyroxenes(?) locally glomerophyric.

0–95 cm: Small vesicles, large open vesicles rare.

95–150 cm: More open large vesicles.

CORE 59, SECTION 2 Depth 674.5–676.0 m

Medium gray (N5) phyric vesicular basalt. Pieces 1, 2, 3, and 4 vesicular (1–2 mm) basalt with occasional glomerophyres – coarser in grain than Piece 5. Vesicles lined with black in the light olive (10Y 5/4) cores.

Piece 5: Fine grained medium gray basalt with glomerophyres and sparse large vesicles.

35 cm: Base of flow(?) and top of flow(?).

Pieces 6–8: Grayish purple (5P 4/2) vesicular basalt characterized by large (3 cm) open vesicles lined with dark greenish gray (5GY 4/1). Smaller vesicles (1–2 mm) infilled with black (N2) and reddened at edges. Microfracturing present. Groundmass: plagioclase laths and reddened (altered) pyroxenes.

Pieces 9–12: Medium dark gray (N4) phyric vesicular basalt gradational downward into medium gray (N5) vesicular phyric basalt.

Piece 10: Small black (N2) vesicles and large (2 cm) vugs. Vugs lined with black and have amygdaloidal structure of light bluish gray (5B 7/1) and pale olive (10Y 6/2).

100 cm: Inclined fracture (50°) – not slickensided.

Vugs become sparse in Piece 11. Below this level, sparse 3 cm vesicles are common. Some vesicles are aligned along vein filled fractures.

Groundmass: plagioclase laths and pyroxenes with sparse glomerophyres.

Large vesicles have black (N2) lining with core of intergrown light bluish gray (5B 7/1) and pale olive (10Y 6/2) to light olive (10Y 5/4) and black (N2).

CORE 59, SECTION 3 Depth 676.0–677.5 m

Medium gray (N5) phyric vesicular basalt.

Large vesicles (0.2 cm–1 cm) predominate down to 15 cm and are filled with black lining with dusky green (5G 3/2) core or intergrowth of black (N2), light bluish gray (5B 7/1) and light olive gray (5Y 6/1).

Below this level, vesicles occur sporadically and the major structure is a marked horizontal foliation that persists down to the base of the section. Vertical foliation occurs in Piece 7.

Pieces 3B, 3C, 4, and 6A: Fault. Brecciated basalt fragments occurs along fault. Vein infill along fault consists of black lining which has penetrated host rock, elongate angular light bluish gray. Fibrous light olive (10Y 5/4) mineral along slickensided face.

Inclination of fault (80°). Slickensides (70°) to cut face of core.

Groundmass: plagioclase laths and small pyroxenes. Occasional plagioclase phenocrysts.

CORE 59, SECTION 4 Depth 677.5–678.8 m

Medium gray (N5) phyric basalt.

Principle variation is in the presence of sub-horizontal foliation. Foliation first appears in Piece 1B becoming most pronounced (3 mm spacing) in Piece 5 and upper part of Piece 6 to become less pronounced in Pieces 6C and D.

Vesicles are minor but occur throughout and are typically less than 1 mm in size. Large vesicles reappear in Pieces 6C and D. The largest vuggy vesicle has 1 cm light bluish gray blebs with pale olive (10Y 6/2) mineral in the interstices. Black lining has thin gray (N7) layers. Black (N2) mineral also present as phenocrysts within light bluish gray. Some suggestion that black lining has been fractured and partly incorporated into bluish gray area – angular black (N2) fragments and penetration of bluish gray into black lining.

Groundmass: plagioclase laths and pyroxenes.

50 cm: Vein inclination 70°.

115 cm: large (3 cm) vesicle.

SITE 553 HOLE B CORE 1 CORED INTERVAL 0.0–4.6 m

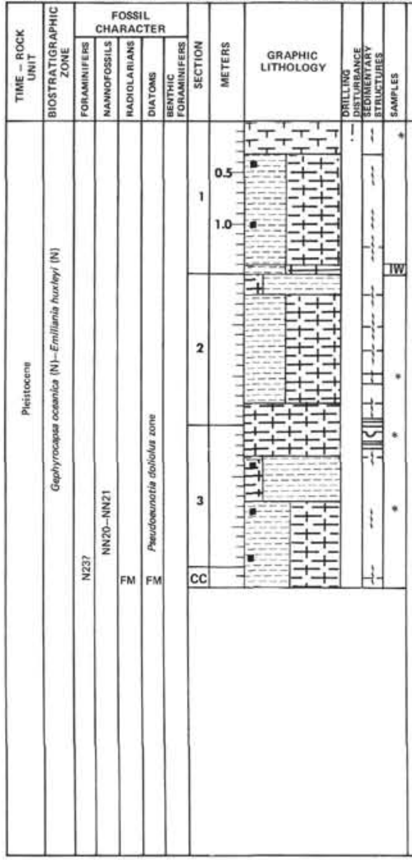

LITHOLOGIC DESCRIPTION

2.5Y 7/2
2.5Y 7/4
mottles
of
10YR 6/3
and
10YR 3/2
2.5Y 6/2
2.5Y 5/4
2.5Y 7/2
2.5Y 6/2
2.5Y 6/2
2.5Y 7/4
2.5Y 5/4
2.5Y 7/2
Lamine of
2.5Y 6/2
2.5Y 8/2
2.5Y 5/4
2.5Y 7/2

Foram ooze and nanno-foram ooze interbedded with nanno-foram marl and calcareous mud is cyclic sequences. Calcareous oozes are sharp based and grade through marls into calcareous muds. Color grades from light gray (2.5Y 7/2) and white (2.5Y 8/2) in the oozes, to pale yellow (2.5Y 7/4) and light brownish gray (2.5Y 6/2) in the marls and light olive brown (2.5Y 5/4) in the muds.

Oozes are sandy in texture: muds largely clay with coarse sand or granule size dropstones (pumice, sandstone).

Burrowing has caused mottling of pale brown (10YR 6/3) and very dark grayish brown (10YR 3/2) and has disturbed some contacts.

Core is undisturbed.

SMEAR SLIDE SUMMARY (%):

	1, 19 D	2, 102 D	3, 15 D	3, 83 D
Texture:				
Sand	70	20	40	30
Silt	10	10	10	20
Clay	20	70	50	50
Composition:				
Quartz	5	5	–	10
Feldspar	1	–	1	–
Heavy minerals	1	2	–	1
Clay	10	15	5	20
Carbonate unspec.	3	3	3	4
Foraminifers	60	10	40	15
Calc. nannofossils	20	65	50	50
Diatoms	Tr	–	Tr	–
Sponge spicules	Tr	Tr	1	Tr
Dolomite	–	Tr	–	–

CARBONATE BOMB: $CaCO_3$ (%):

1, 1 = 83
1, 28 = 55
1, 60 = 30
1, 87 = 32
1, 119 = 32
2, 1 = 21
2, 28 = 45
2, 61 = 51
2, 89 = 34
2, 117 = 35
2, 134 = 64
3, 1 = 79
3, 28 = 71
3, 89 = 36
3, 117 = 41
3, 61 = 19
CC, 1 = 45

SITE 553 HOLE B CORE 2 CORED INTERVAL 0.0–9.5 m

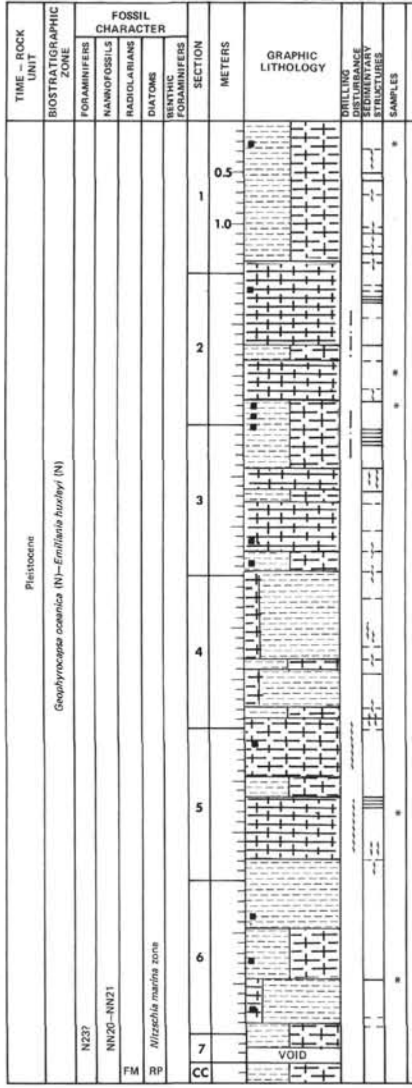

LITHOLOGIC DESCRIPTION

2.5Y 7/4
Mottles
of
2.5Y 6/2
2.5Y 7/2
2.5Y 6/2
2.5Y 5/4
2.5Y 6/4
2.5Y 4/2
2.5Y 7/2
2.5Y 8/2
Laminae of
2.5Y 5/4
2.5Y 7/2
2.5Y 8/2
2.5Y 6/4
2.5Y 8/2
2.5Y 5/4 with
2.5Y 8/2 mottles
2.5Y 5/4
2.5Y 7/2
2.5Y 7/2
2.5Y 5/4
2.5Y 8/2
2.5Y 6/4
2.5Y 7/4
2.5Y 8/2
2.5Y 5/4
2.5Y 6/4
5Y 6/3
2.5Y 6/4
10YR 7/3
2.5Y 5/4
2.5Y 7/4
2.5Y 8/2
2.5Y 6/4
2.5Y 8/2
with minor
laminae
of 2.5Y 6/4
2.5Y 5/4
5Y 5/3
2.5Y 5/4
2.5Y 7/2
Mottles of
5Y 5/2

Nanno-foram ooze interbedded with nanno-foram marl, mud and calcareous mud in cyclic sequence. Oozes are sharp based and grade into marls, calcareous muds and muds. Color grades from white (2.5Y 8/2), light gray (2.5Y 7/2), pale yellow (2.5Y 7/4) and light yellow brown (2.5Y 6/4) in the oozes, to pale yellow (2.5Y 7/4), light brownish gray (2.5Y 6/2), very pale brown (10YR 7/3), light olive brown (2.5Y 5/4) and light yellow brown (2.5Y 6/4) in the marls, to light olive brown (2.5Y 5/4), light yellow brown (2.5Y 6/4) in the marls and light olive (5Y 6/3) and olive (5Y 6/3) in the muds. Texture grades from sand to mud through 1 cycle. Angular dropstones (pumice, mudstone, quartzite in mud units.

Core essentially undisturbed.

SMEAR SLIDE SUMMARY (%):

	1, 25 M	2, 100 D	2, 132 D	5, 84 D	6, 100 D
Texture:					
Sand	80	40	50	40	50
Silt	10	10	20	10	10
Clay	10	50	30	50	40
Composition:					
Quartz	10	Tr	15	1	30
Feldspar	3	–	1	1	–
Heavy minerals	1	–	1	–	2
Clay	10	5	20	Tr	40
Volcanic glass	65	–	–	–	–
Carbonate unspec.	4	–	3	3	25
Foraminifers	2	40	30	40	1
Calc. nannofossils	5	55	30	54	2
Diatoms	Tr	Tr	–	Tr	–
Radiolarians	–	Tr	–	Tr	–
Sponge spicules	–	Tr	–	1	–

CARBONATE BOMB: $CaCO_3$ (%):

1, 1 = 29
1, 30 = 37
1, 58 = 40
1, 90 = 53
1, 122 = 35
1, 130 = 21
2, 1 = 65
2, 30 = 67
2, 59 = 78
2, 90 = 81
2, 130 = 31
3, 1 = 49
3, 30 = 41
3, 58 = 62
3, 70 = 39
3, 92 = 71
3, 124 = 52
4, 1 = 29
4, 30 = 27
4, 59 = 26
4, 90 = 28
4, 110 = 22
4, 123 = 35
5, 30 = 63
5, 80 = 54
5, 66 = 74
5, 90 = 82
6, 1 = 6
6, 31 = 9
6, 58 = 34
6, 90 = 37
6, 124 = 16
7, 1 = 46
CC, 35 = 48

SITE 553 HOLE B CORE 3 CORED INTERVAL 9.5–19.0 m

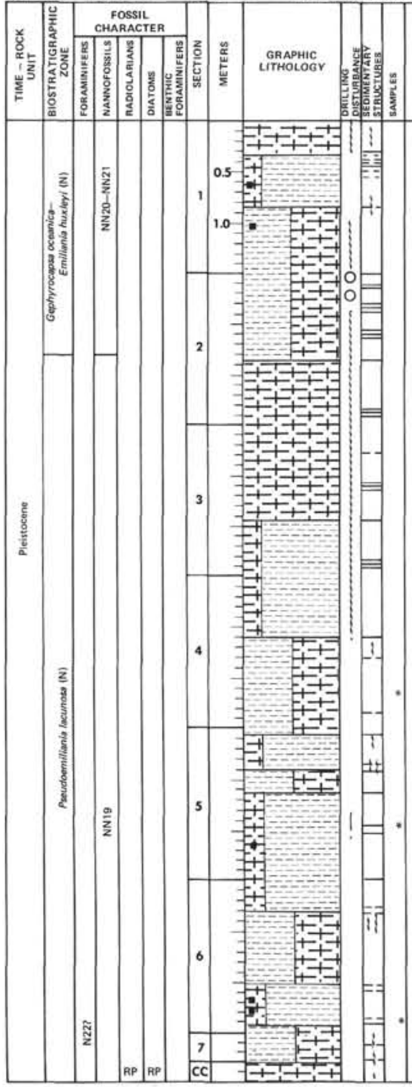

LITHOLOGIC DESCRIPTION

5B 9/1

5Y 4/2
5Y 5/2
5Y 3/2
5Y 5/2

5Y 8/1

Laminae
of
5Y 6/1

5Y 7/1
with laminae
of 5Y 6/1

5B 9/1

Laminae
of 5Y 6/1

5Y 8/1

N8

Laminae of
5GY 8/1

5Y 5/2

?laminae of
5G 6/1 and
5Y 4/1, 5Y 3/1

5Y 8/1
5Y 7/1 mottles
5Y 6/1
↓
5Y 7/1
5GY 6/1

5Y 6/2
mottled
with 5Y 4/2
5GY 6/1
5Y 6/1
5Y 5/2

5Y 4/2
5Y 5/2

5Y 4/1

Mottles of
5Y 4/1
5Y 5/2

5Y 4/1
5Y 5/2
5Y 4/1
5Y 7/1
5Y 5/2

N8 mottled with
5B 7/1

Nanno-foram ooze interbedded with marls and calcareous muds in cyclic sequence. Oozes are sharp-based and grade through marls into muds. Colors in oozes are very light gray (N8) and bluish white (5B 9/1); in marls are white (5Y 8/1), light gray (5Y 7/1), gray (5Y 6/1), light greenish gray (5GY 6/1) and olive gray (5Y 5/2); in muds are olive gray (5Y 5/2, 5Y 4/2), dark gray (5Y 4/1) and dark olive gray (5Y 3/2). Textures range from sandy muds in the oozes to mud with angular granules or cobbles in the mud units. Dropstones are sharp and quartzite.

Some sections (oozes) are laminated, and burrow mottling occurs in some intervals.

Core intensely disturbed or soupy.

SMEAR SLIDE SUMMARY (%):

	4, 113	5, 97	6, 140
	D	D	D
Texture:			
Sand	60	20	40
Silt	10	40	10
Clay	30	40	50
Composition:			
Quartz	1	15	10
Heavy minerals	–	Tr	1
Clay	10	30	20
Carbonate unspec.	4	40	4
Foraminifers	55	5	30
Calc. nannofossils	30	10	35
Diatoms	Tr	–	–
Sponge spicules	Tr	–	–

SITE 553 HOLE B CORE 4 CORED INTERVAL 19.0–28.5 m

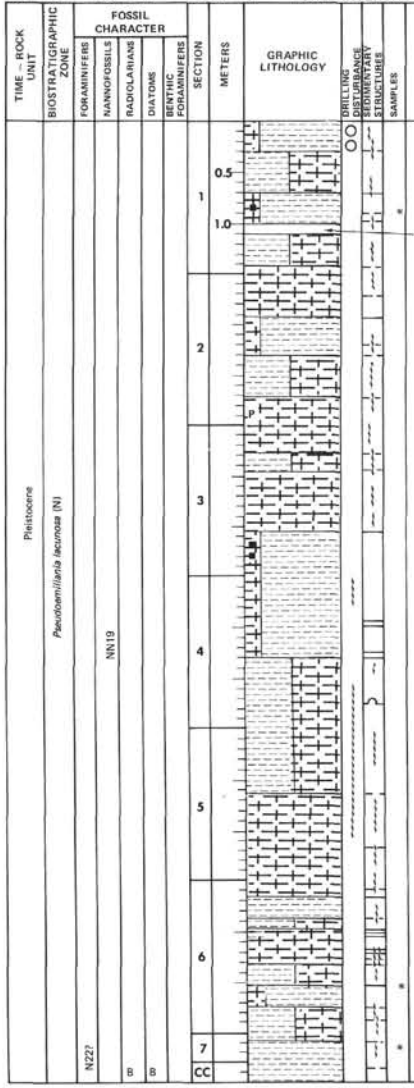

LITHOLOGIC DESCRIPTION

5Y 4/1

5Y 6/1

5Y 4/2
5Y 5/2

Void

5Y 6/1

5Y 8/1

5Y 4/2

5Y 5/1
5Y 6/1

5Y 8/1
mottled with
5B 5/1

5Y 5/3

5Y 8/1

5Y 4/3

5Y 6/1
5Y 4/2
5Y 3/2

5Y 4/2

5Y 5/2

5Y 7/1

N8

5Y 7/1
5Y 5/2

5Y 7/2
5Y 7/1
5Y 5/2 mottles
5Y 6/1
5Y 4/2

5Y 7/2

5GY 6/1

5Y 4/2
5Y 5/3

Alternations of nanno-foram ooze, nanno-foram marl, mud and calcareous mud in cyclic fashion: sharp-based oozes grade through marls to calcareous muds and muds. Colors grade from white (5Y 8/1), light gray (5Y 7/1) and gray (5Y 6/1) in the ooze, gray (5Y 6/1), olive gray (5Y 5/2, 5Y 4/2), olive (5Y 5/3), light gray (5Y 7/2) and greenish gray (5GY 6/1) in the marls, and to dark gray (5Y 4/1) and olive gray (5Y 4/2, 5Y 4/3, 5Y 5/2) in the muds. Textures grade from sandy muds (oozes) to muds with coarse dropstones (muds). Dropstones are mainly quartzite.

Rare laminae; burrows are common and have disturbed some contacts. Core partially disturbed.

SMEAR SLIDE SUMMARY (%):

	1, 93	6, 106	7, 20
	D	M	D
Texture:			
Sand	40	50	30
Silt	20	20	40
Clay	40	30	30
Composition:			
Quartz	10	5	35
Feldspar	4	–	5
Heavy minerals	1	Tr	2
Clay	25	5	30
Carbonate unspec.	15	–	5
Foraminifers	15	50	15
Calc. nannofossils	30	40	8
Sponge spicules	–	Tr	–
Dolomite	Tr	–	–

CARBONATE BOMB: $CaCO_3$ (%):

2, 27 = 82 4, 21 = 26
3, 27 = 74 6, 29 = 8

SITE 553 HOLE B CORE M1 CORED INTERVAL 1.0–10.5 m

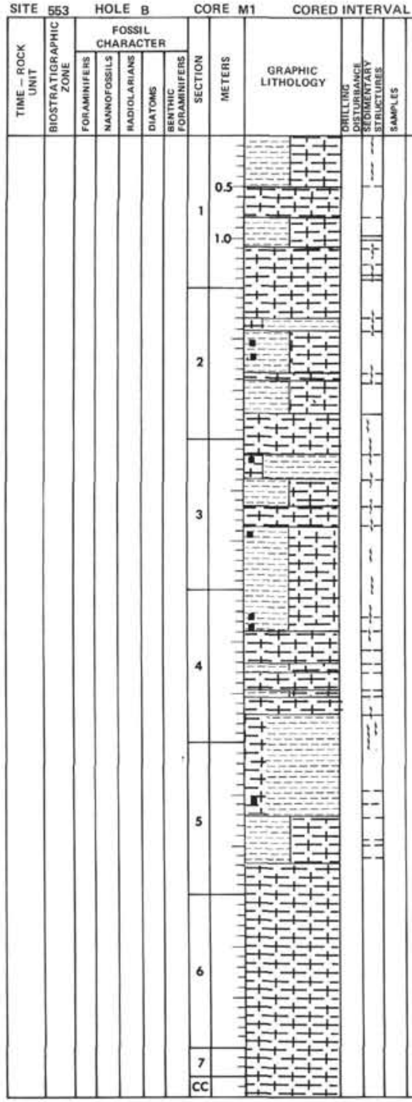

2.5Y 6/2

2.5Y 7/2

2.5Y 6/2
2.5Y 7/4
2.5Y 5/4
2.5Y 7/2
Laminae of
2.5Y 5/4

2.5Y 5/4

2.5Y 7/2
2.5Y 5/4

2.5Y 7/2

2.5Y 5/4

2.5Y 7/4

2.5Y 7/2

2.5Y 5/4

Mottles of
5Y 6/3

2.5Y 5/4
2.5Y 7/4
2.5Y 8/2

2.5Y 6/4
2.5Y 8/2
2.5Y 6/4
2.5Y 8/2

2.5Y 5/4
mottles of
2.5Y 4/2

5Y 5/3
2.5Y 5/4

2.5Y 6/2

5GY 6/1
2.5Y 6/2
5Y 7/1

LITHOLOGIC DESCRIPTION

Nanno-foram ooze interbedded with nanno foram marl and calcareous mud in cyclic fashion; sharp based oozes grade through marls to calcareous mud. Oozes are white (2.5Y 8/2) and light gray (2.5Y 7/2, 5Y 7/1); marls are pale yellow (2.5Y 7/4), light yellowish brown (2.5Y 6/4), light brownish gray (2.5Y 6/2) and light olive brown (2.5Y 5/4); muds are light olive brown (2.5Y 5/4).

Texture of ooze is sandy mud, and of mud is mud with scattered angular granule or cobble-sized dropstone clasts, ranging from pumice to quartzite.

Some laminated zones; burrowing, locally extensive, has disturbed many contacts.

Core essentially undisturbed.

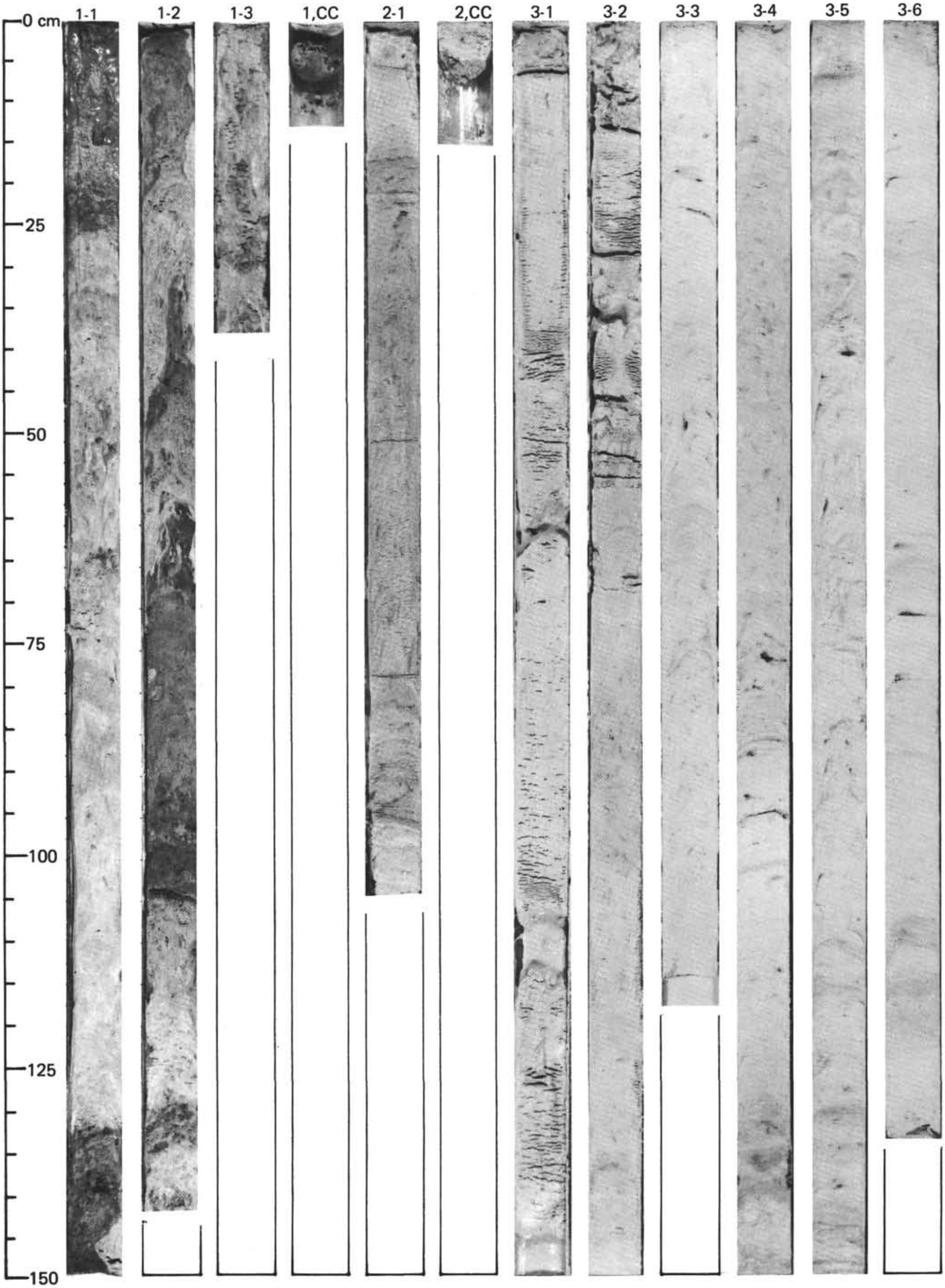
0 cm
25
50
75
100
125
150
1-1
1-2
1-3
1,CC
2-1
2,CC
3-1
3-2
3-3
3-4
3-5
3-6

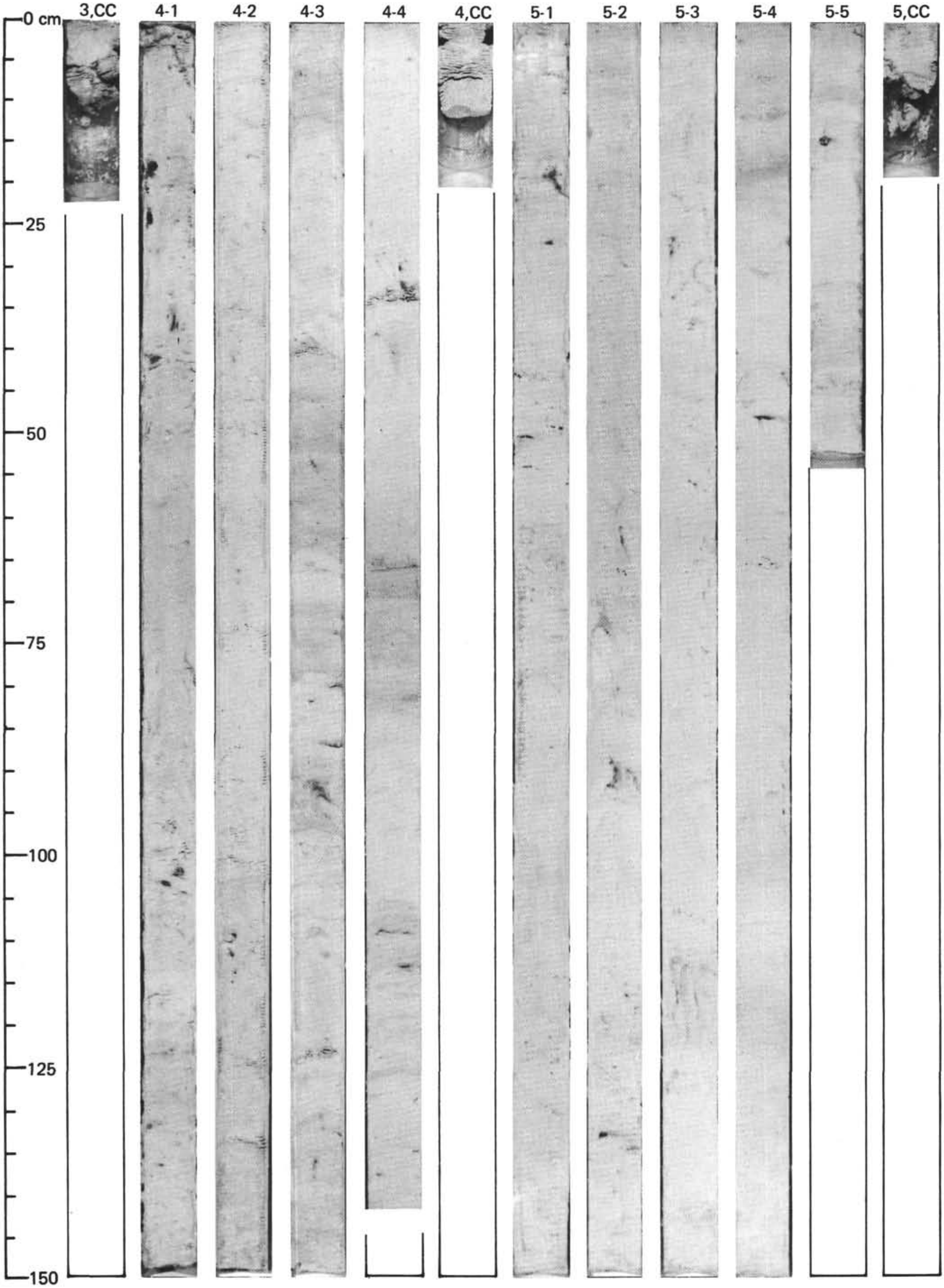
0 cm
25
50
75
100
125
150
3,CC
4-1
4-2
4-3
4-4
4,CC
5-1
5-2
5-3
5-4
5-5
5,CC

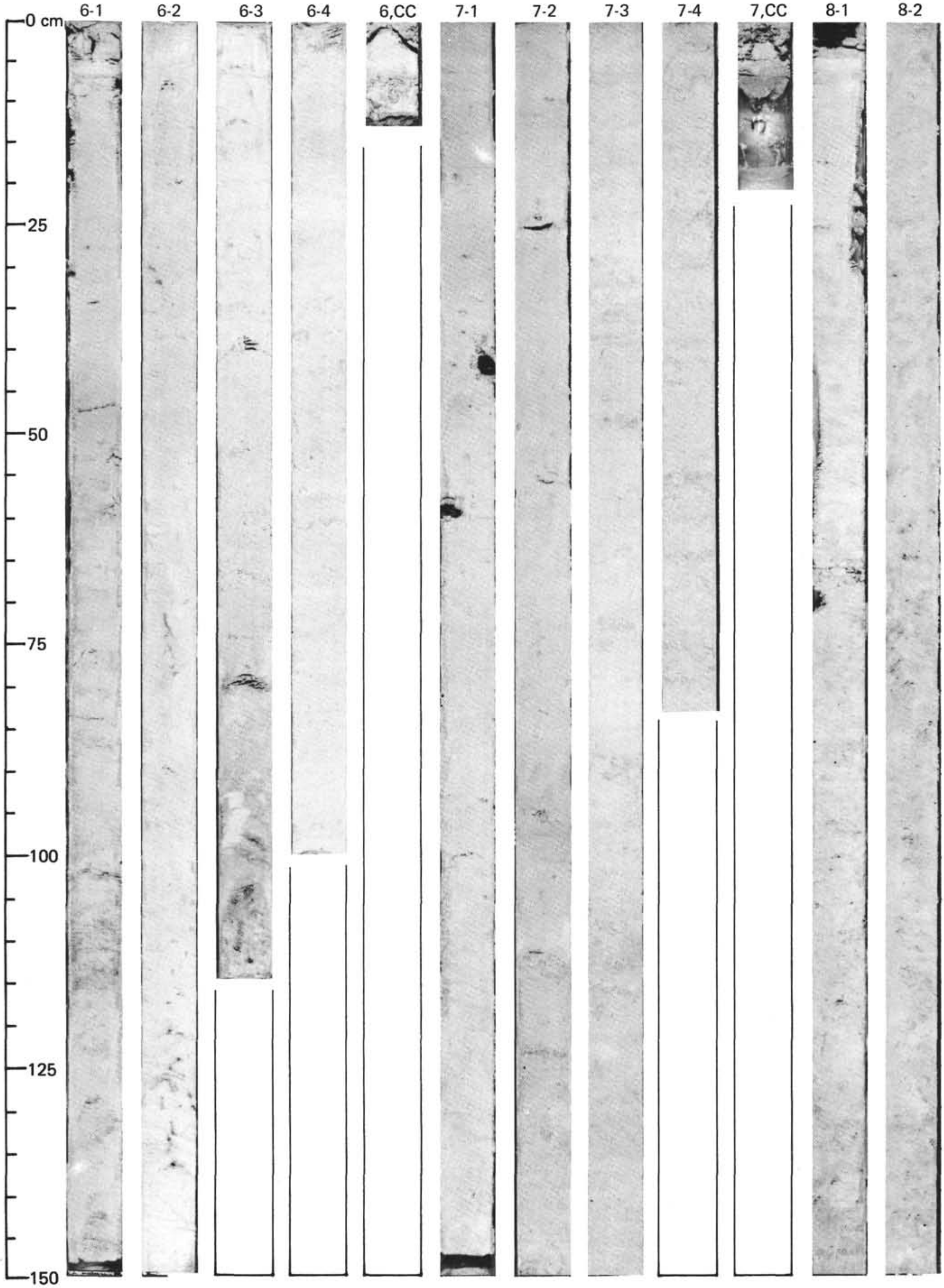
0 cm
25
50
75
100
125
150
6-1
6-2
6-3
6-4
6,CC
7-1
7-2
7-3
7-4
7,CC
8-1
8-2

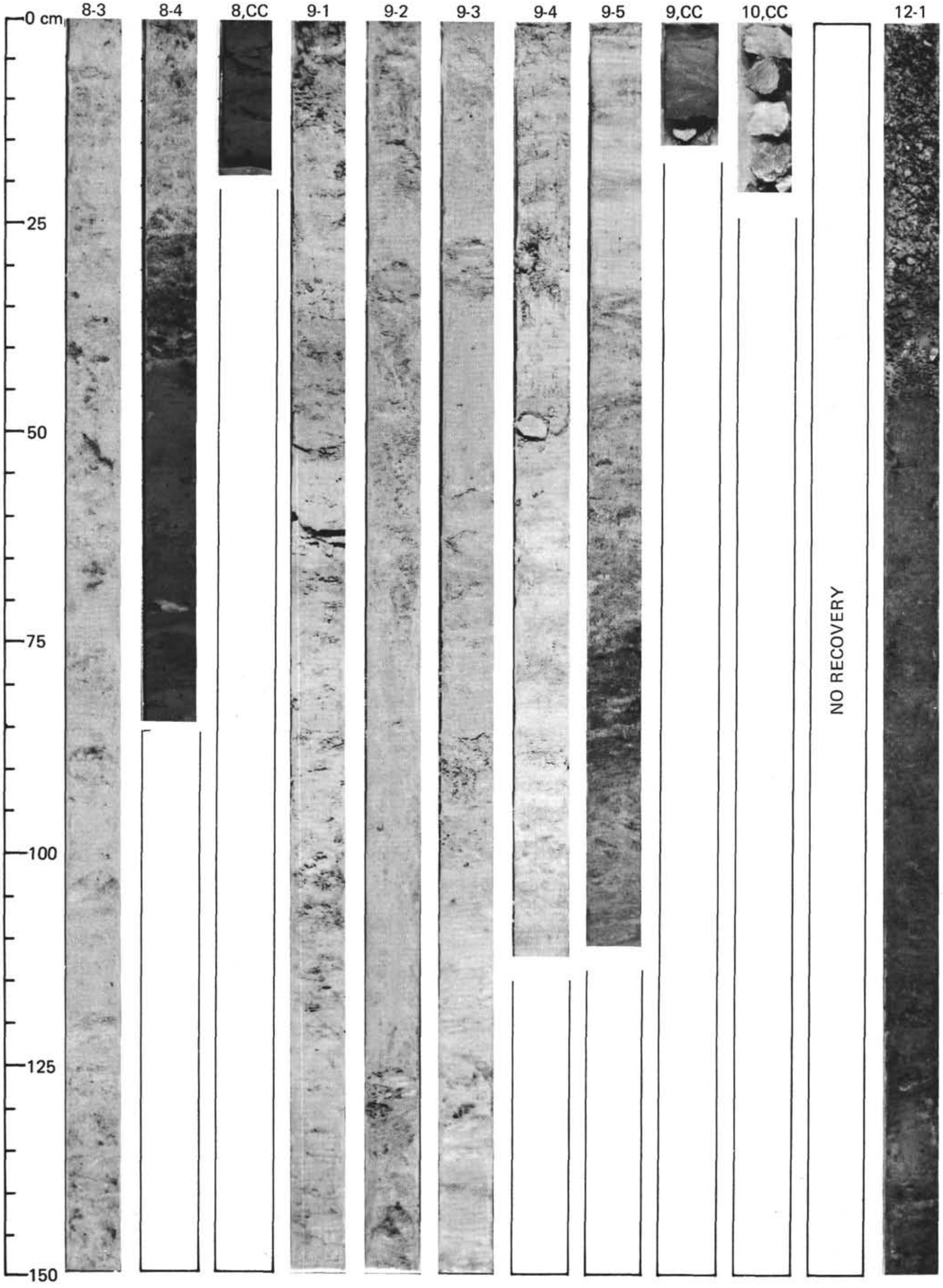
0 cm
25
50
75
100
125
150
8-3
8-4
8,CC
9-1
9-2
9-3
9-4
9-5
9,CC
10,CC
NO RECOVERY
12-1

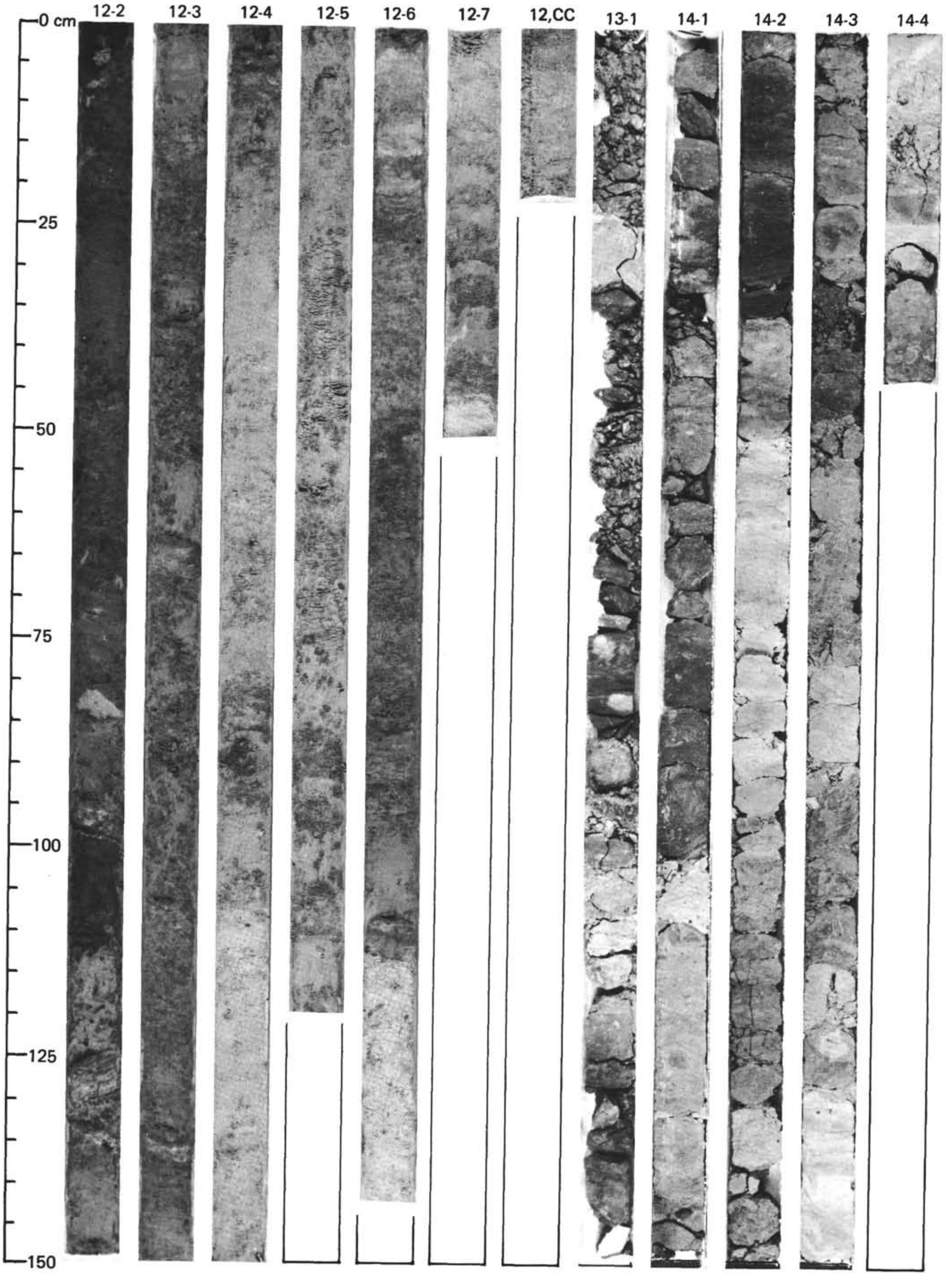
0 cm
25
50
75
100
125
150
12-2
12-3
12-4
12-5
12-6
12-7
12,CC
13-1
14-1
14-2
14-3
14-4

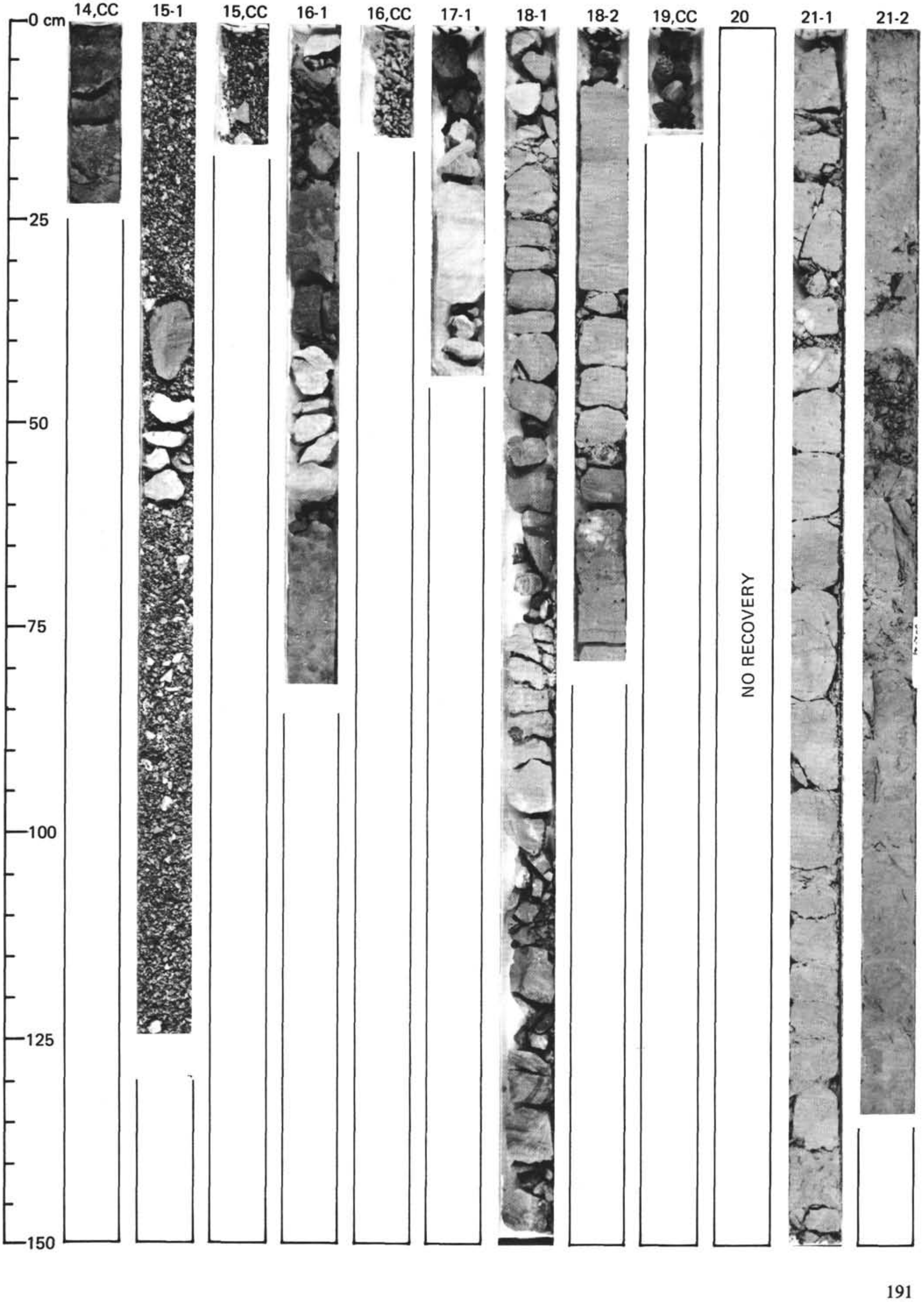
0 cm
25
50
75
100
125
150
14,CC
15-1
15,CC
16-1
16,CC
17-1
18-1
18-2
19,CC
20
NO RECOVERY
21-1
21-2

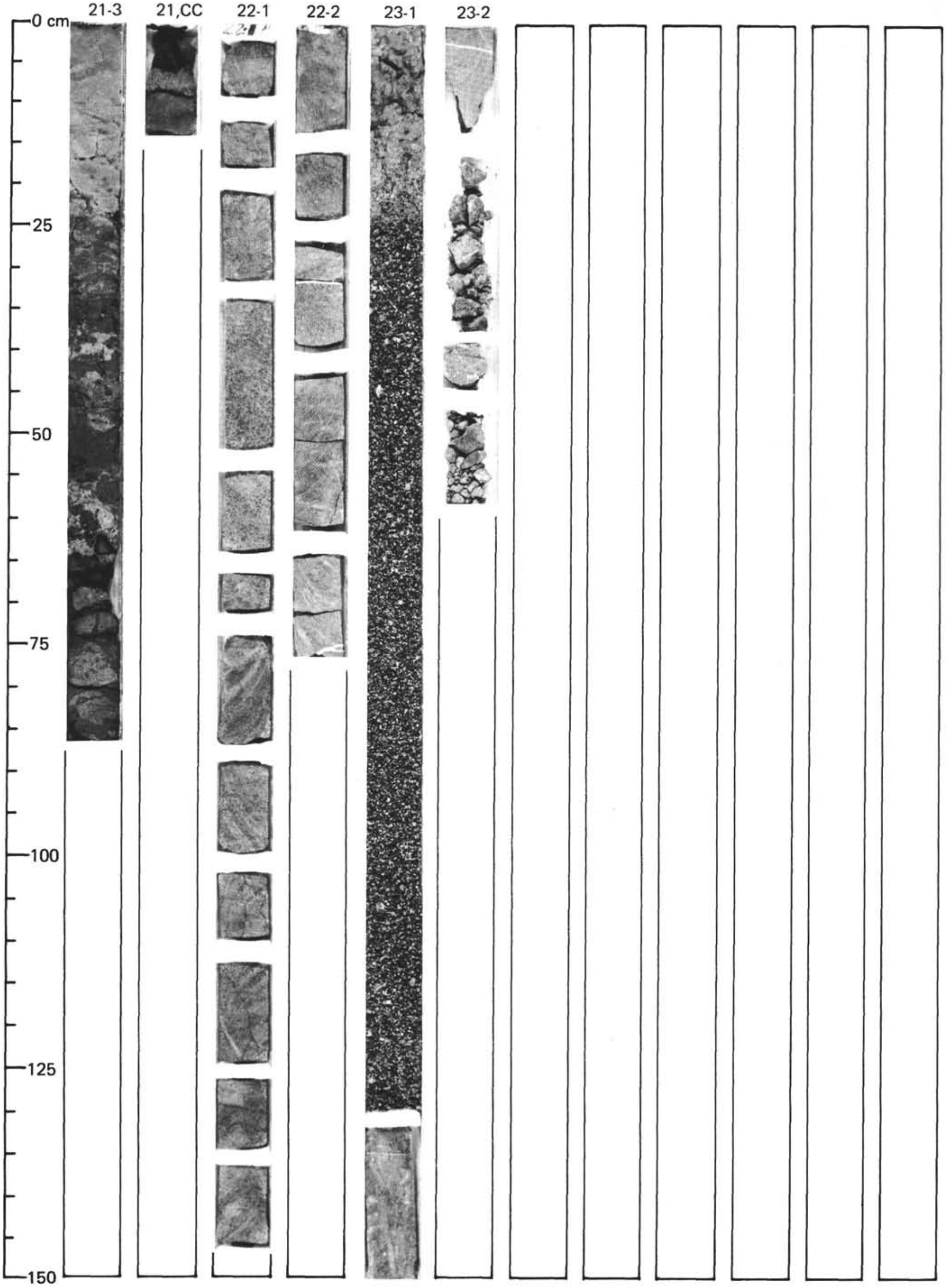
21-3
21,CC
22-1
22-2
23-1
23-2
0 cm
25
50
75
100
125
150

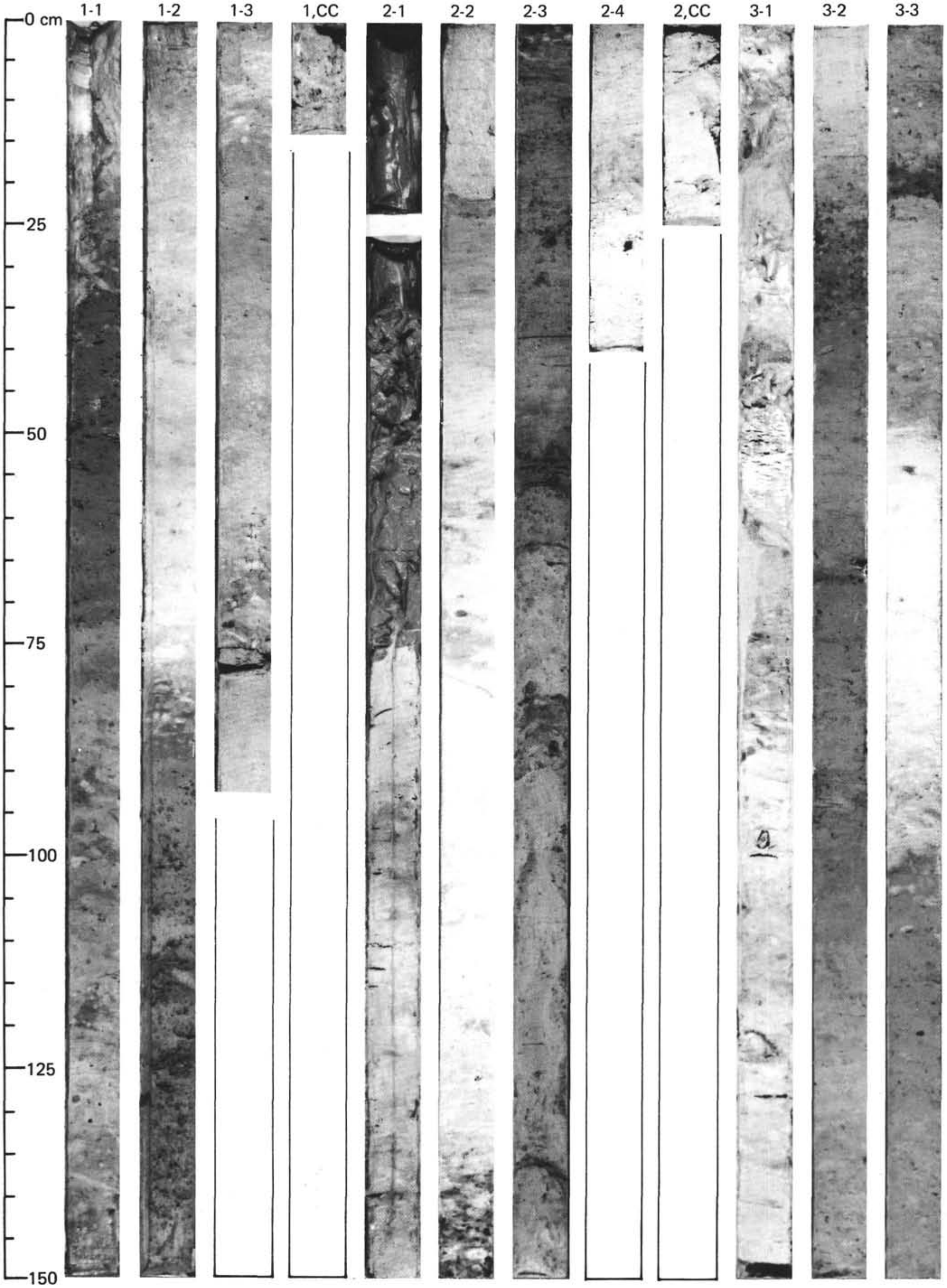
0 cm
25
50
75
100
125
150
1-1
1-2
1-3
1,CC
2-1
2-2
2-3
2-4
2,CC
3-1
3-2
3-3

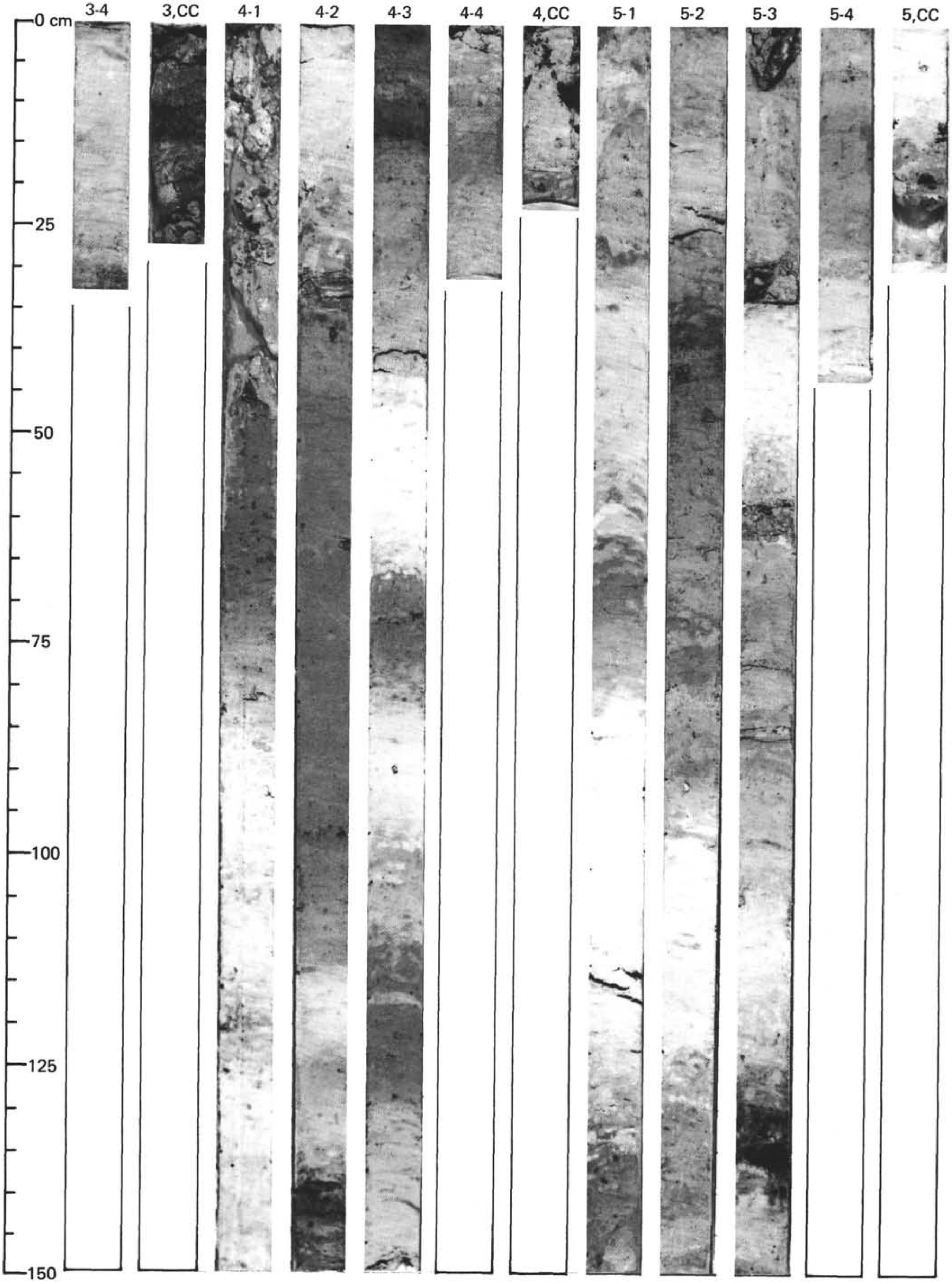
3-4
3,CC
4-1
4-2
4-3
4-4
4,CC
5-1
5-2
5-3
5-4
5,CC
0 cm
25
50
75
100
125
150

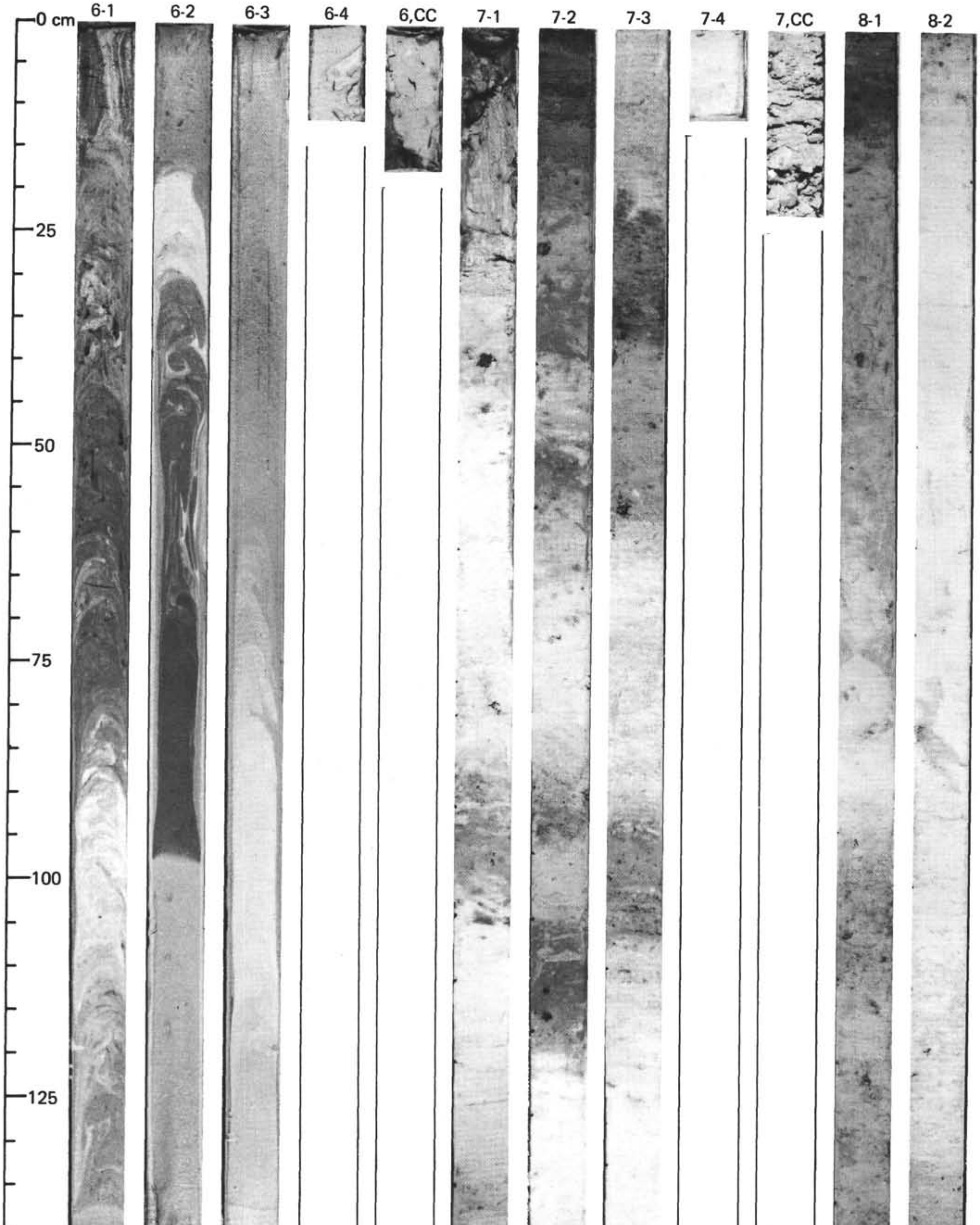
0 cm
25
50
75
100
125
150
6-1
6-2
6-3
6-4
6,CC
7-1
7-2
7-3
7-4
7,CC
8-1
8-2

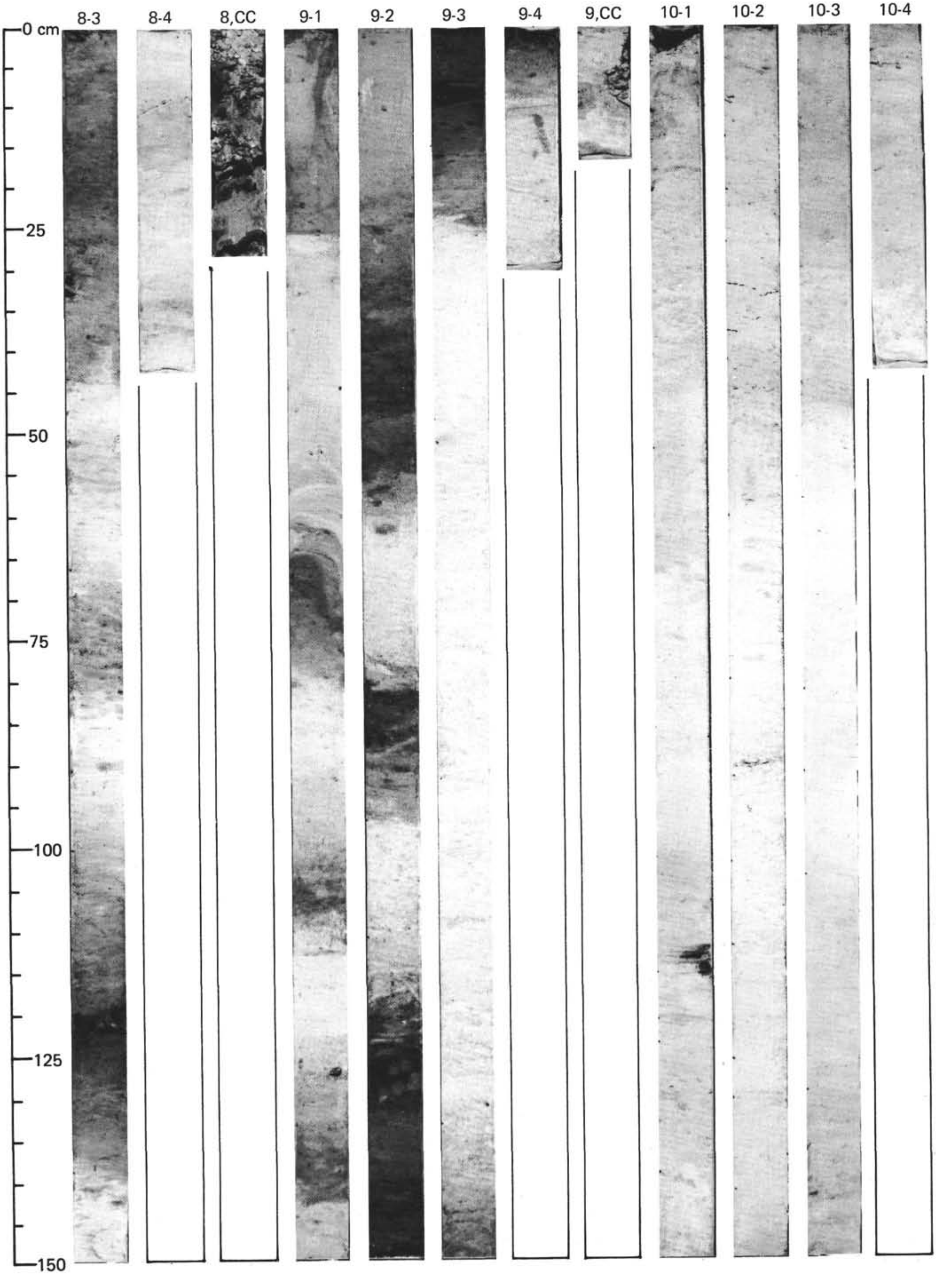
8-3
8-4
8,CC
9-1
9-2
9-3
9-4
9,CC
10-1
10-2
10-3
10-4
0 cm
25
50
75
100
125
150

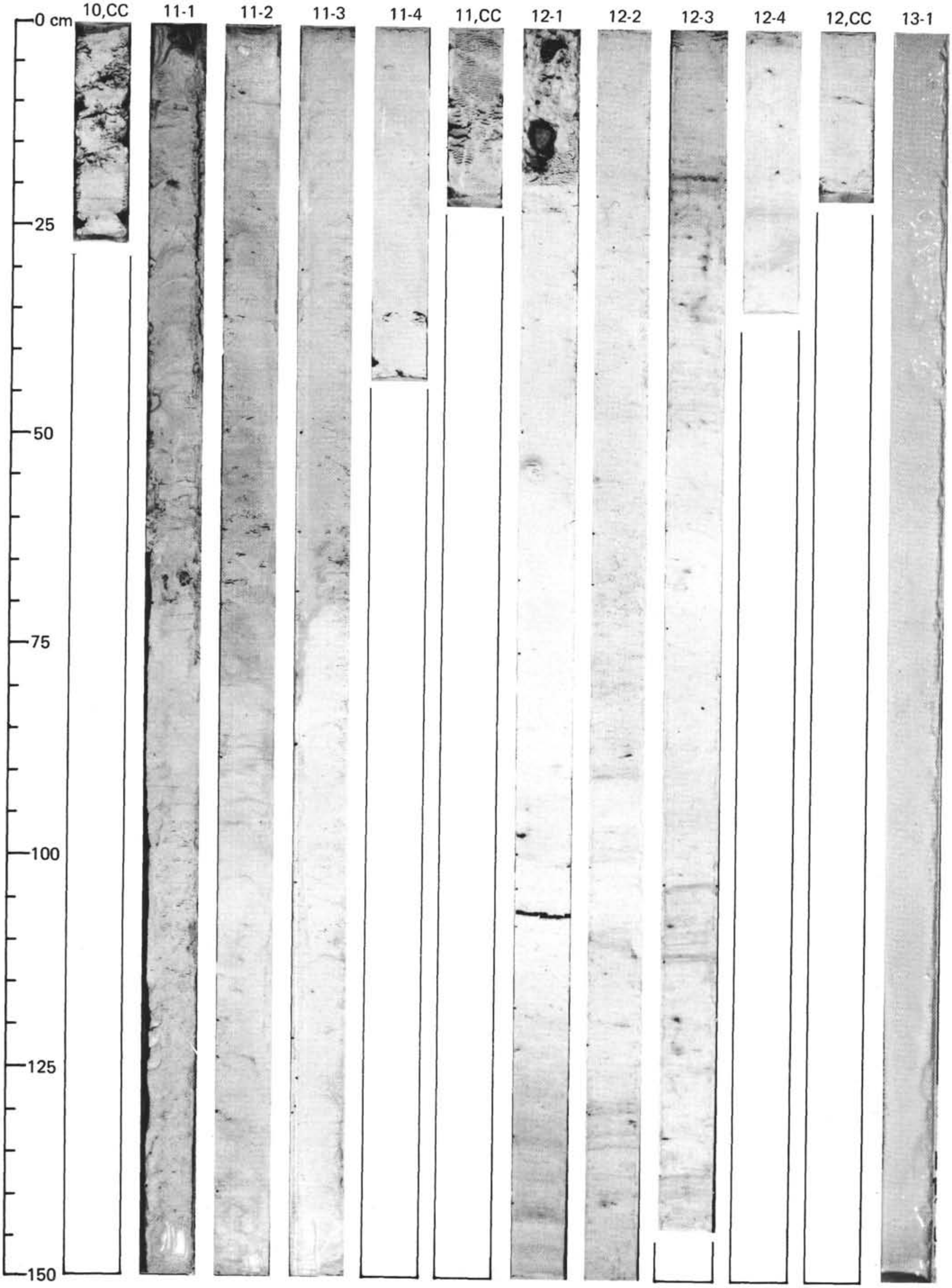
0 cm
25
50
75
100
125
150
10,CC
11-1
11-2
11-3
11-4
11,CC
12-1
12-2
12-3
12-4
12,CC
13-1

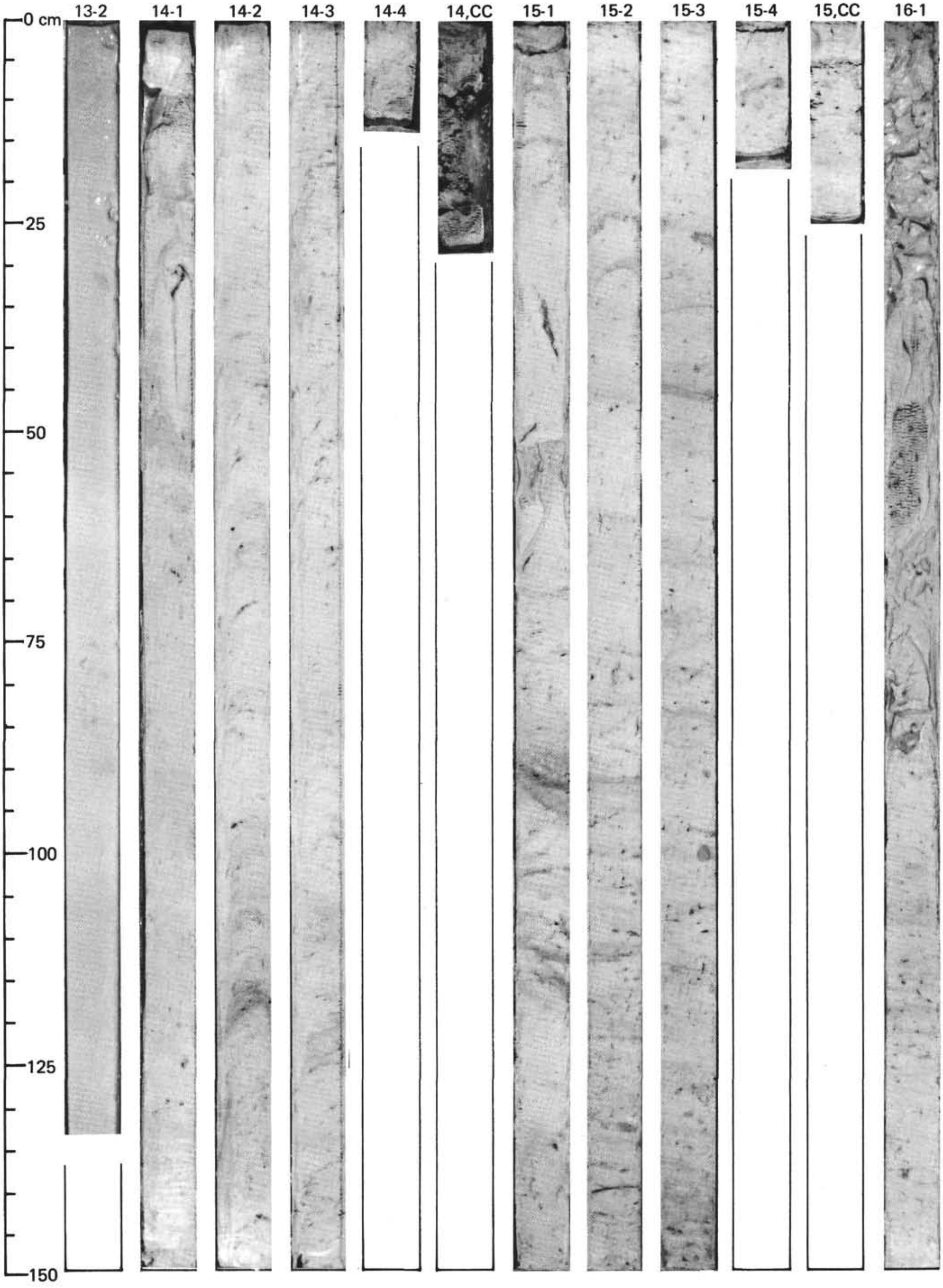
0 cm
25
50
75
100
125
150
13-2
14-1
14-2
14-3
14-4
14,CC
15-1
15-2
15-3
15-4
15,CC
16-1

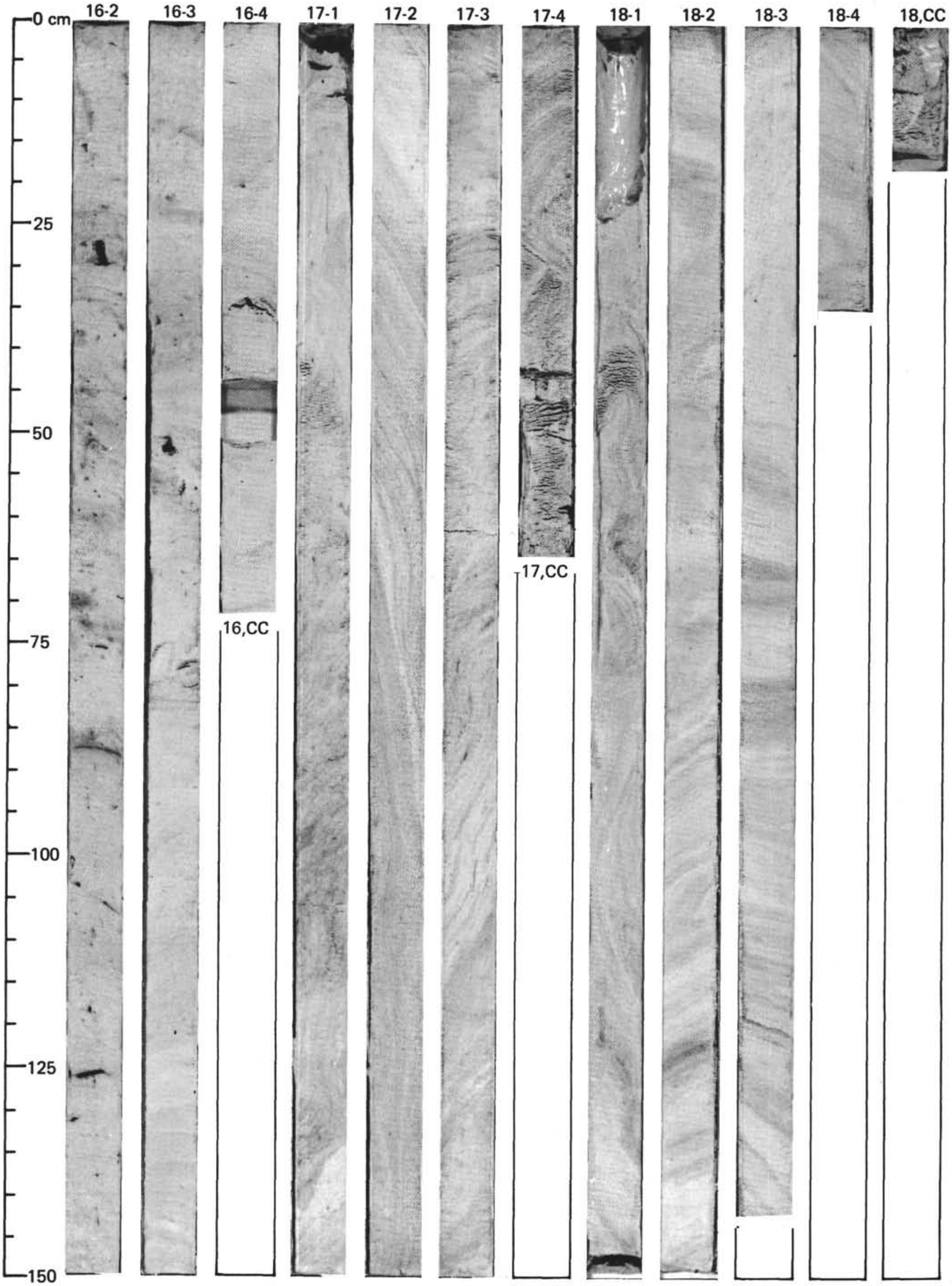
0 cm
25
50
75
100
125
150
16-2
16-3
16-4
16,CC
17-1
17-2
17-3
17-4
17,CC
18-1
18-2
18-3
18-4
18,CC

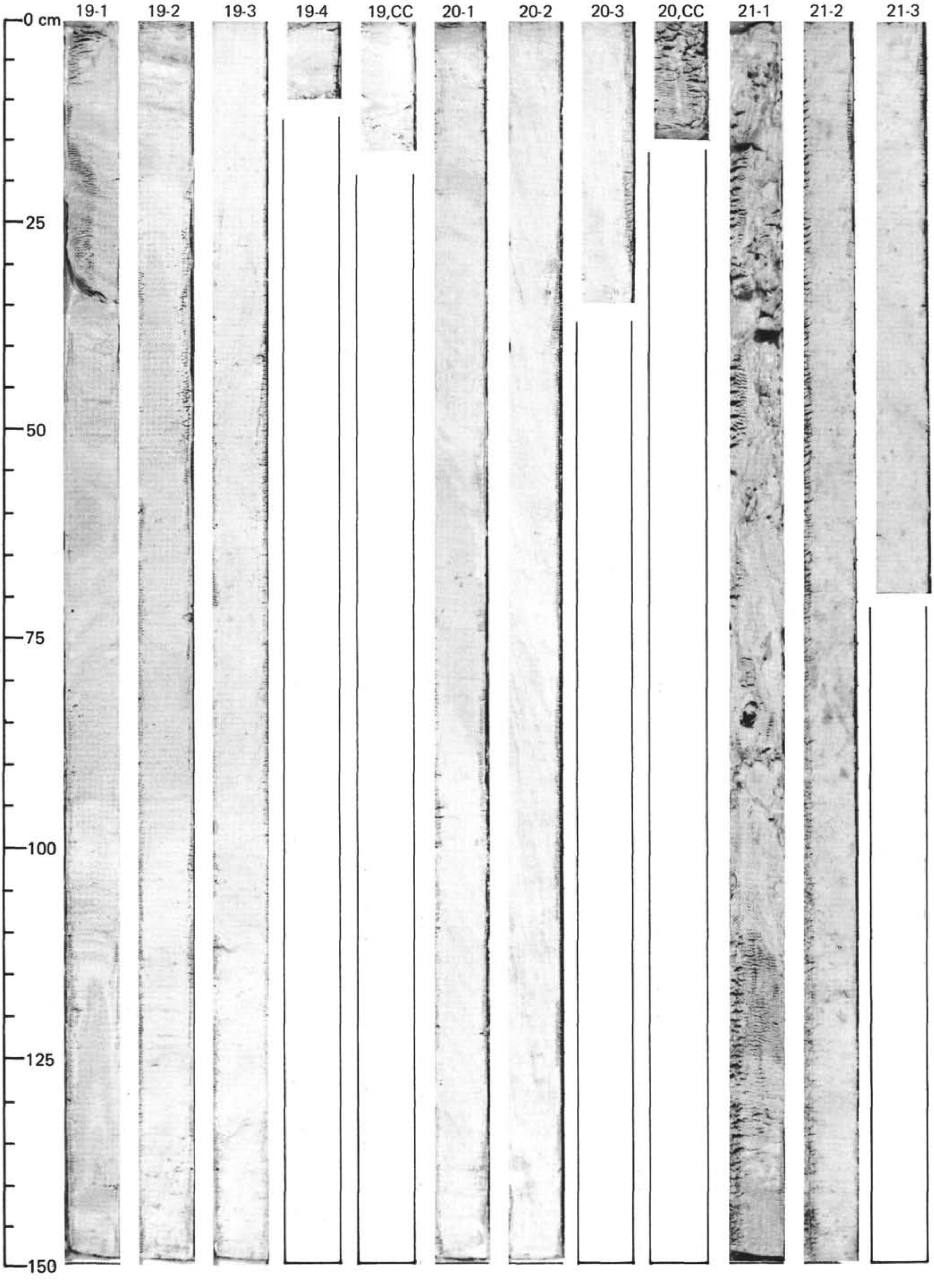
0 cm
25
50
75
100
125
150
19-1
19-2
19-3
19-4
19,CC
20-1
20-2
20-3
20,CC
21-1
21-2
21-3

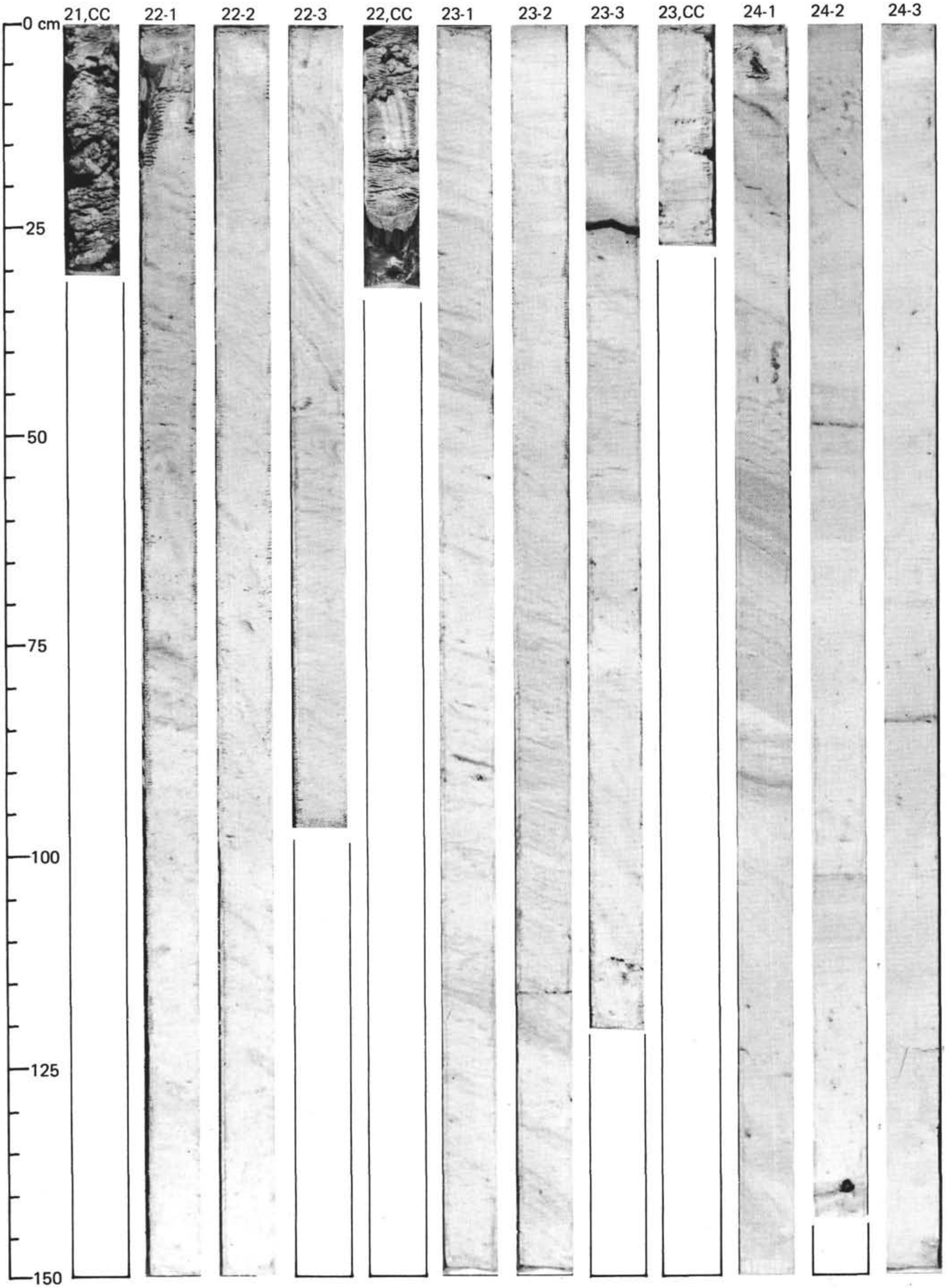
0 cm
25
50
75
100
125
150
21,CC
22-1
22-2
22-3
22,CC
23-1
23-2
23-3
23,CC
24-1
24-2
24-3

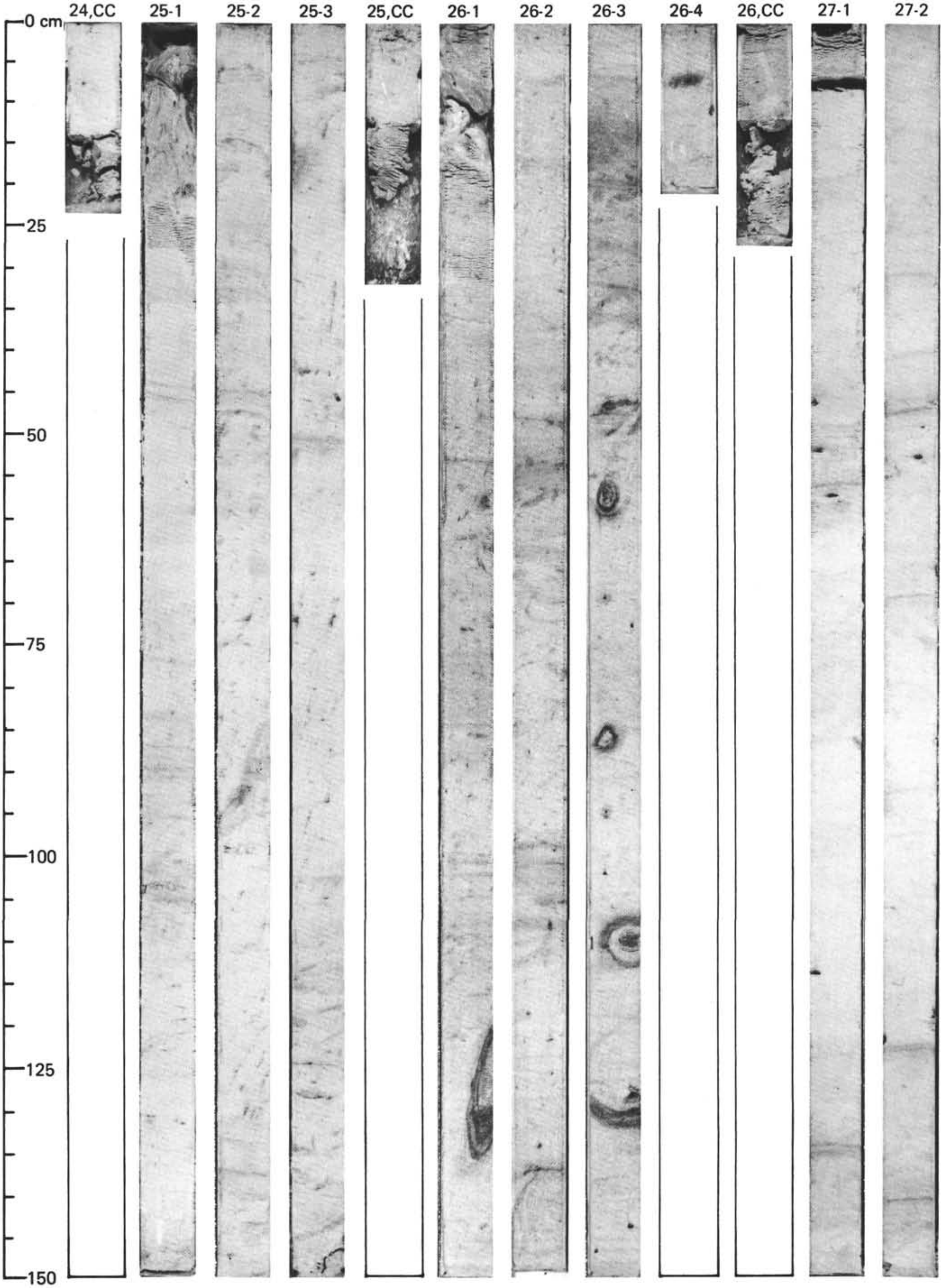
24,CC
25-1
25-2
25-3
25,CC
26-1
26-2
26-3
26-4
26,CC
27-1
27-2
0 cm
25
50
75
100
125
150

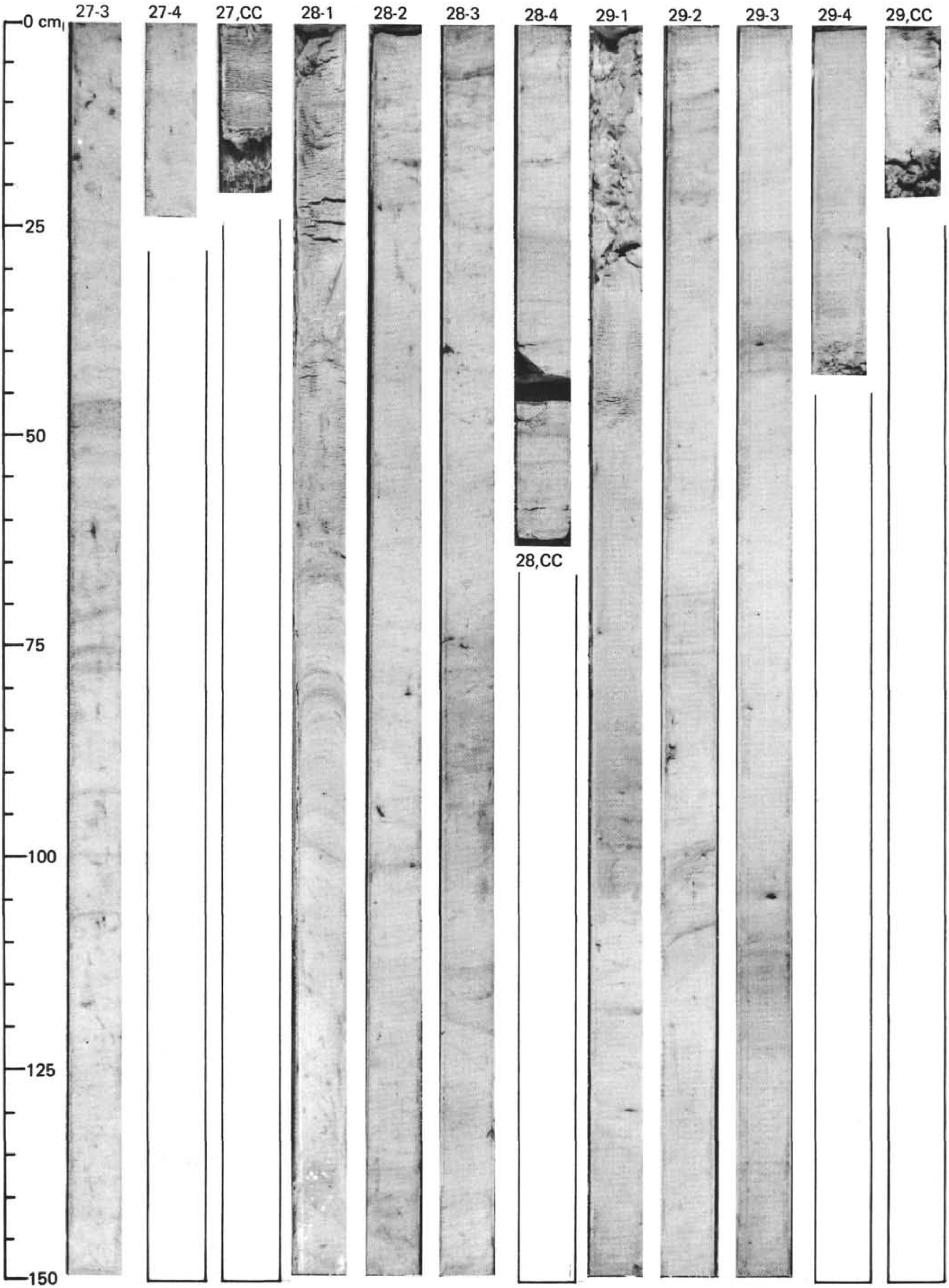
27-3
27-4
27,CC
28-1
28-2
28-3
28-4
28,CC
29-1
29-2
29-3
29-4
29,CC
0 cm
25
50
75
100
125
150

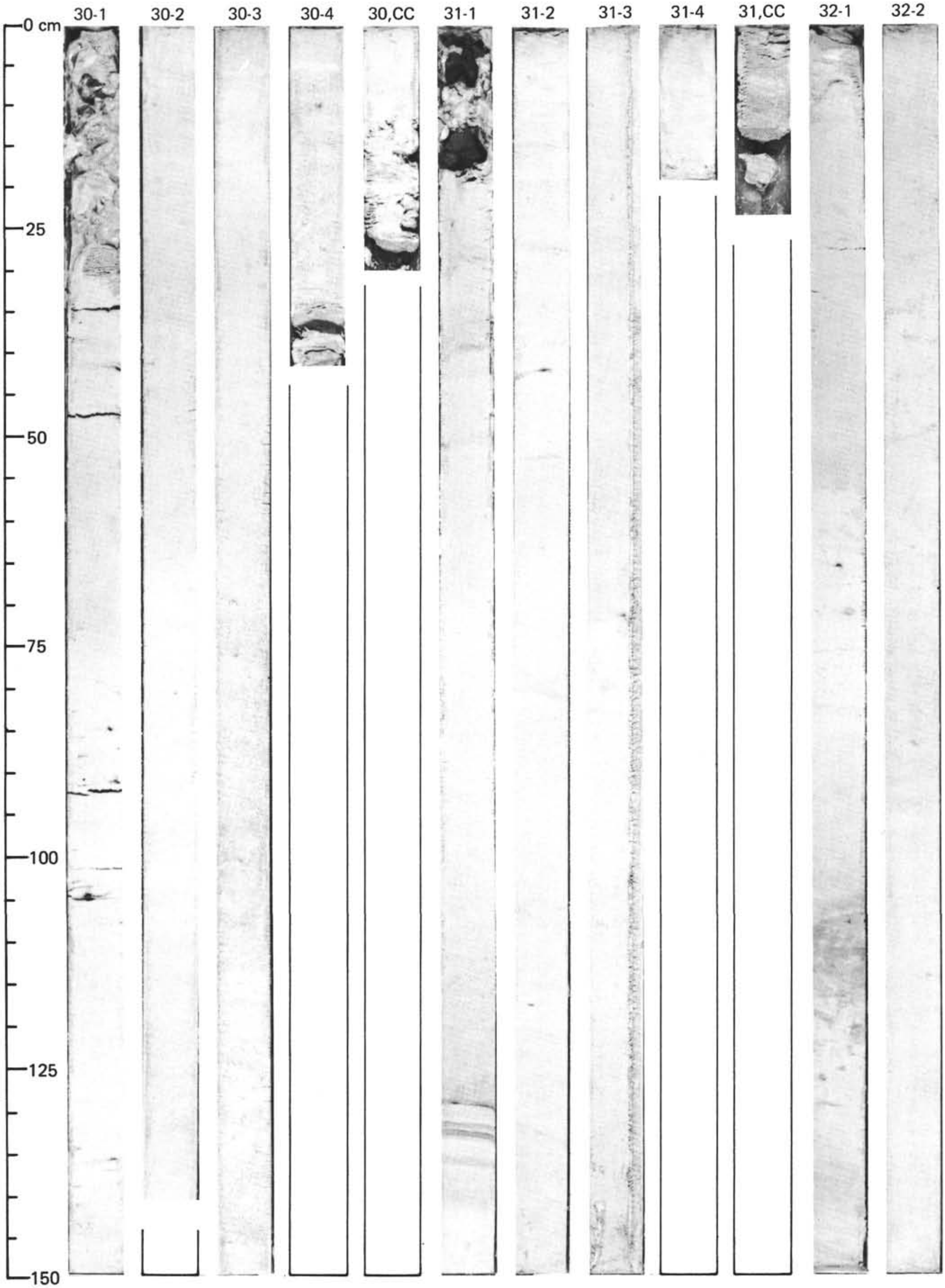
30-1
30-2
30-3
30-4
30,CC
31-1
31-2
31-3
31-4
31,CC
32-1
32-2
0 cm
25
50
75
100
125
150

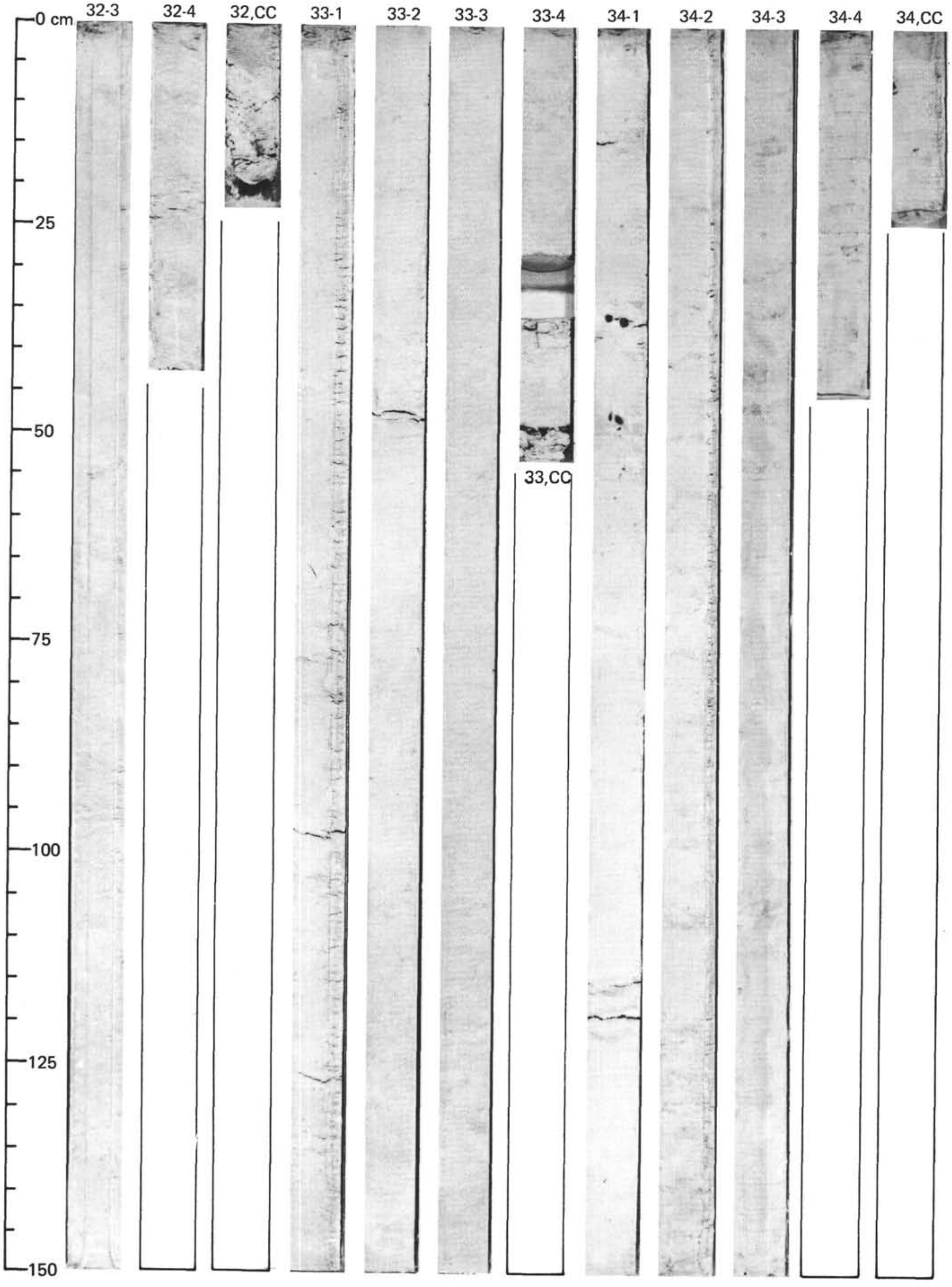
0 cm
25
50
75
100
125
150
32-3
32-4
32,CC
33-1
33-2
33-3
33-4
33,CC
34-1
34-2
34-3
34-4
34,CC

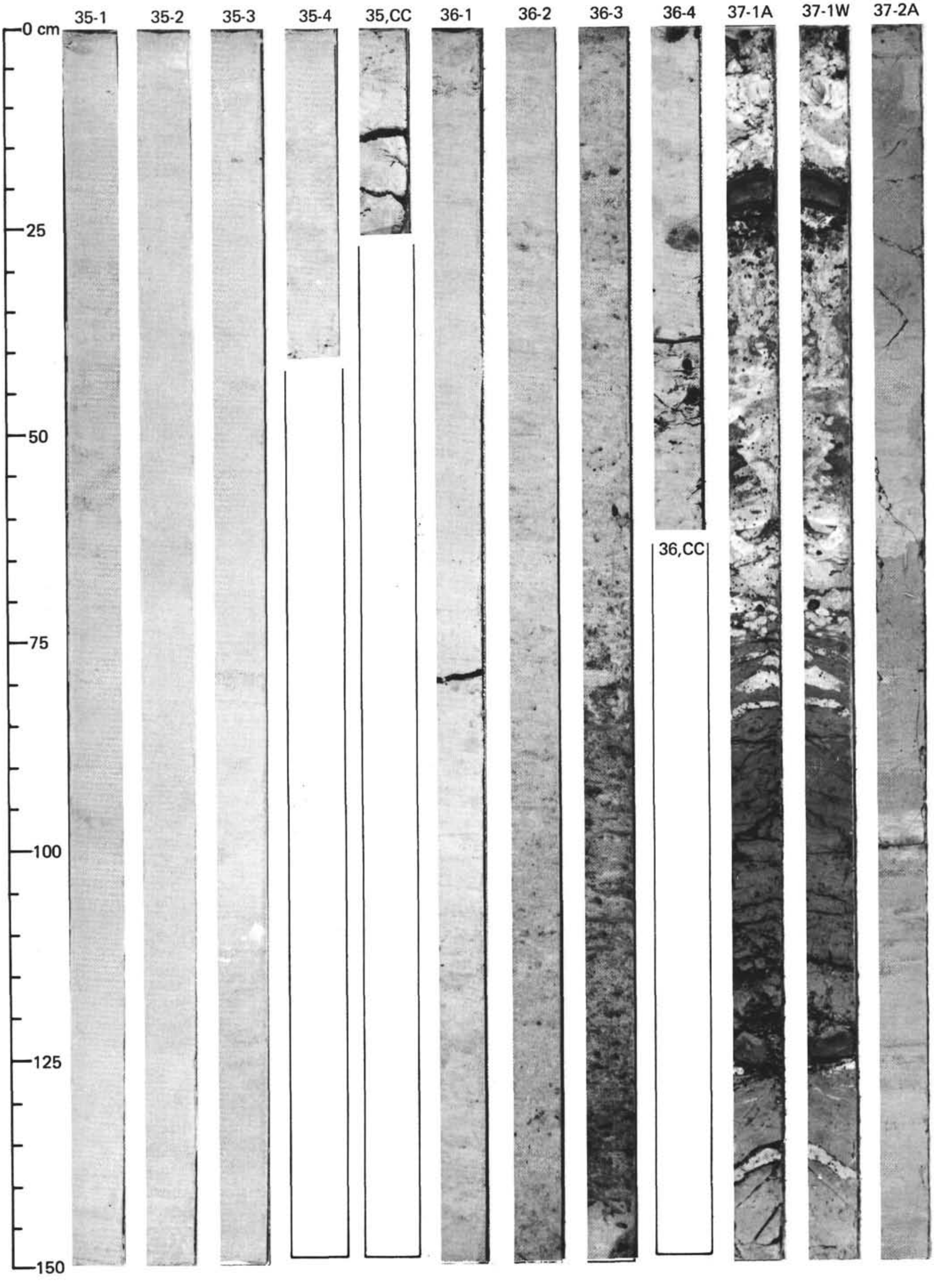
35-1
35-2
35-3
35-4
35,CC
36-1
36-2
36-3
36-4
37-1A
37-1W
37-2A
36,CC
0 cm
25
50
75
100
125
150

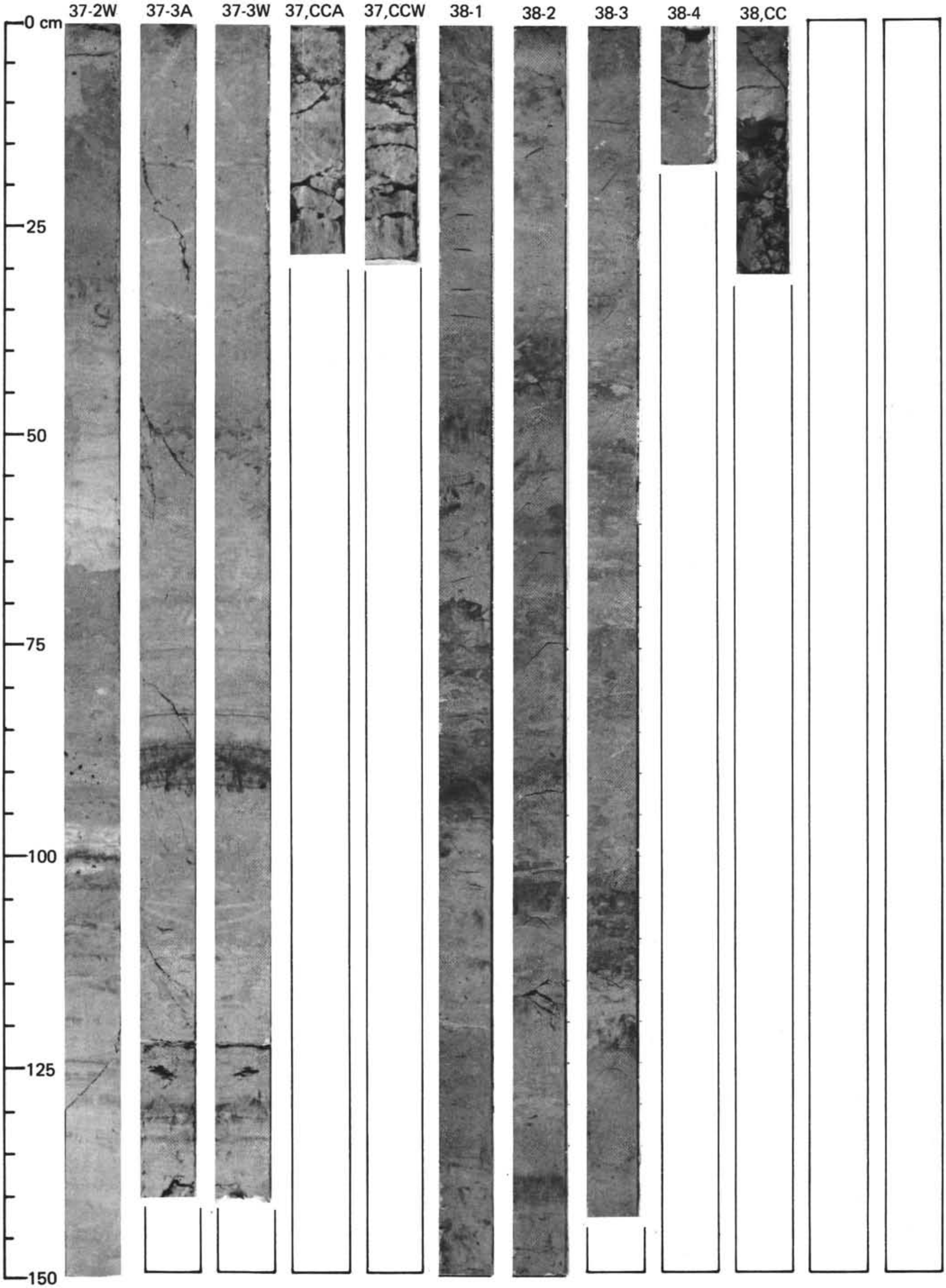
37-2W
37-3A
37-3W
37,CCA
37,CCW
38-1
38-2
38-3
38-4
38,CC
0 cm
25
50
75
100
125
150

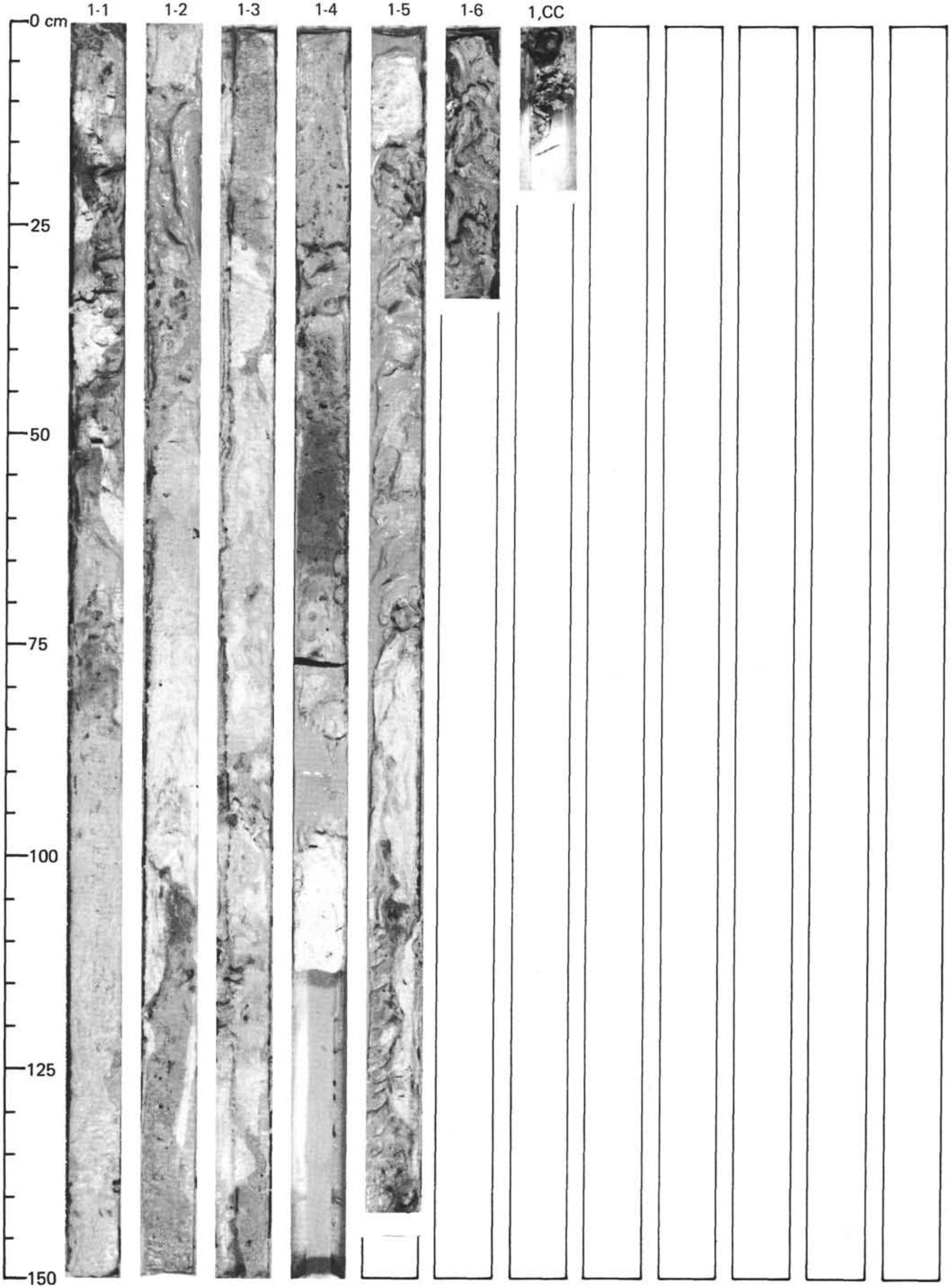
0 cm
25
50
75
100
125
150
1-1
1-2
1-3
1-4
1-5
1-6
1,CC

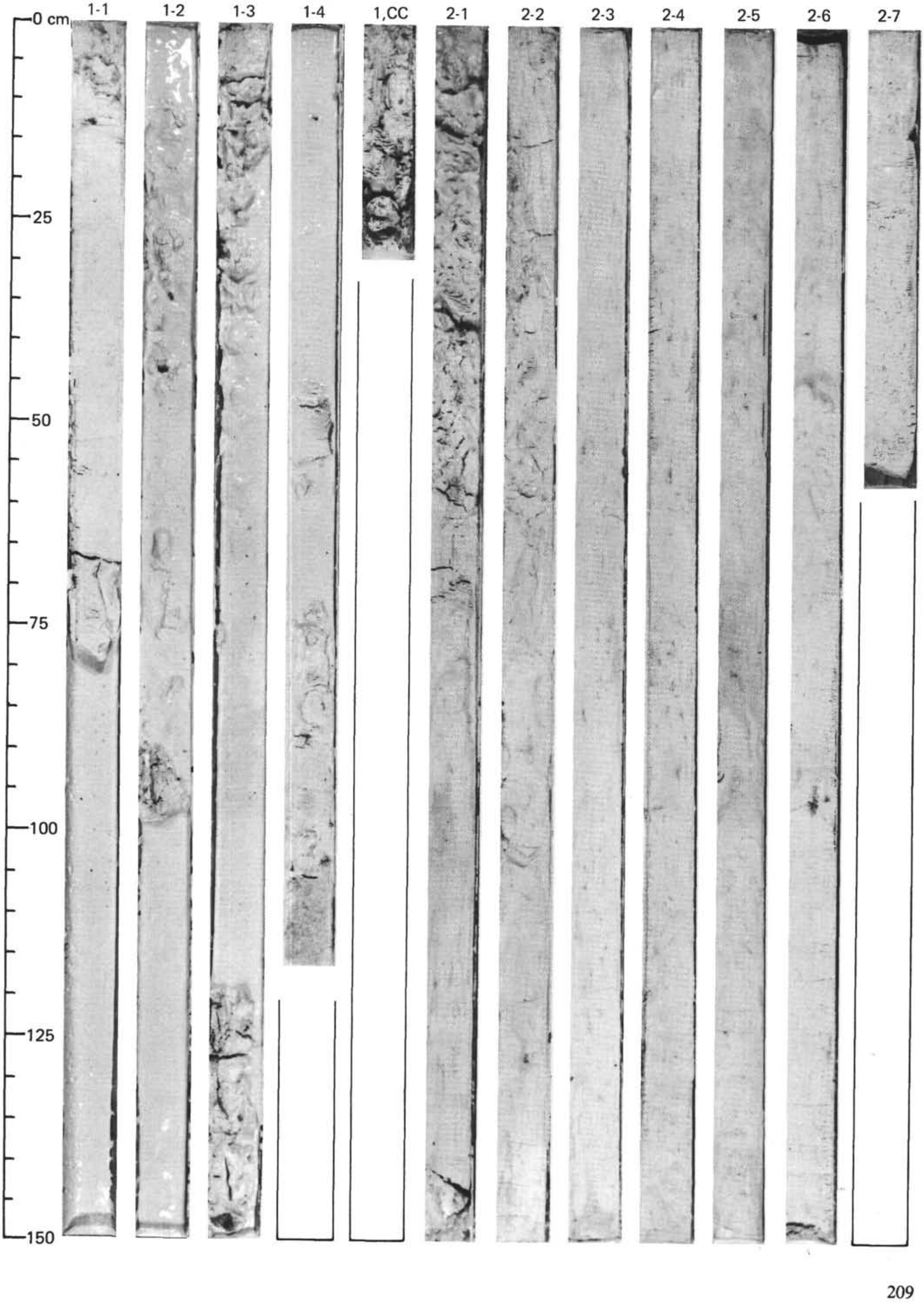
0 cm
25
50
75
100
125
150
1-1
1-2
1-3
1-4
1,CC
2-1
2-2
2-3
2-4
2-5
2-6
2-7

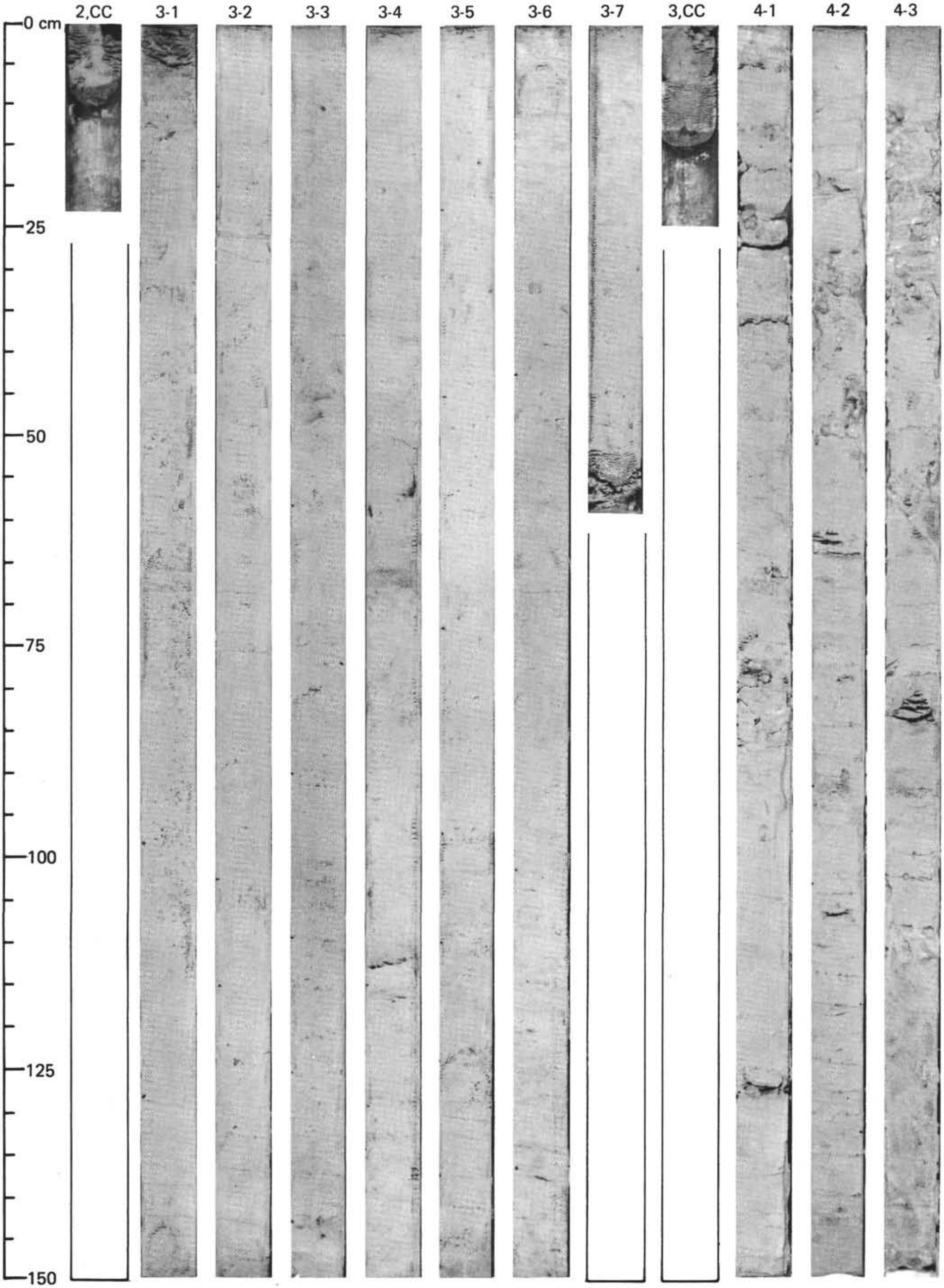
2,CC
3-1
3-2
3-3
3-4
3-5
3-6
3-7
3,CC
4-1
4-2
4-3
0 cm
25
50
75
100
125
150

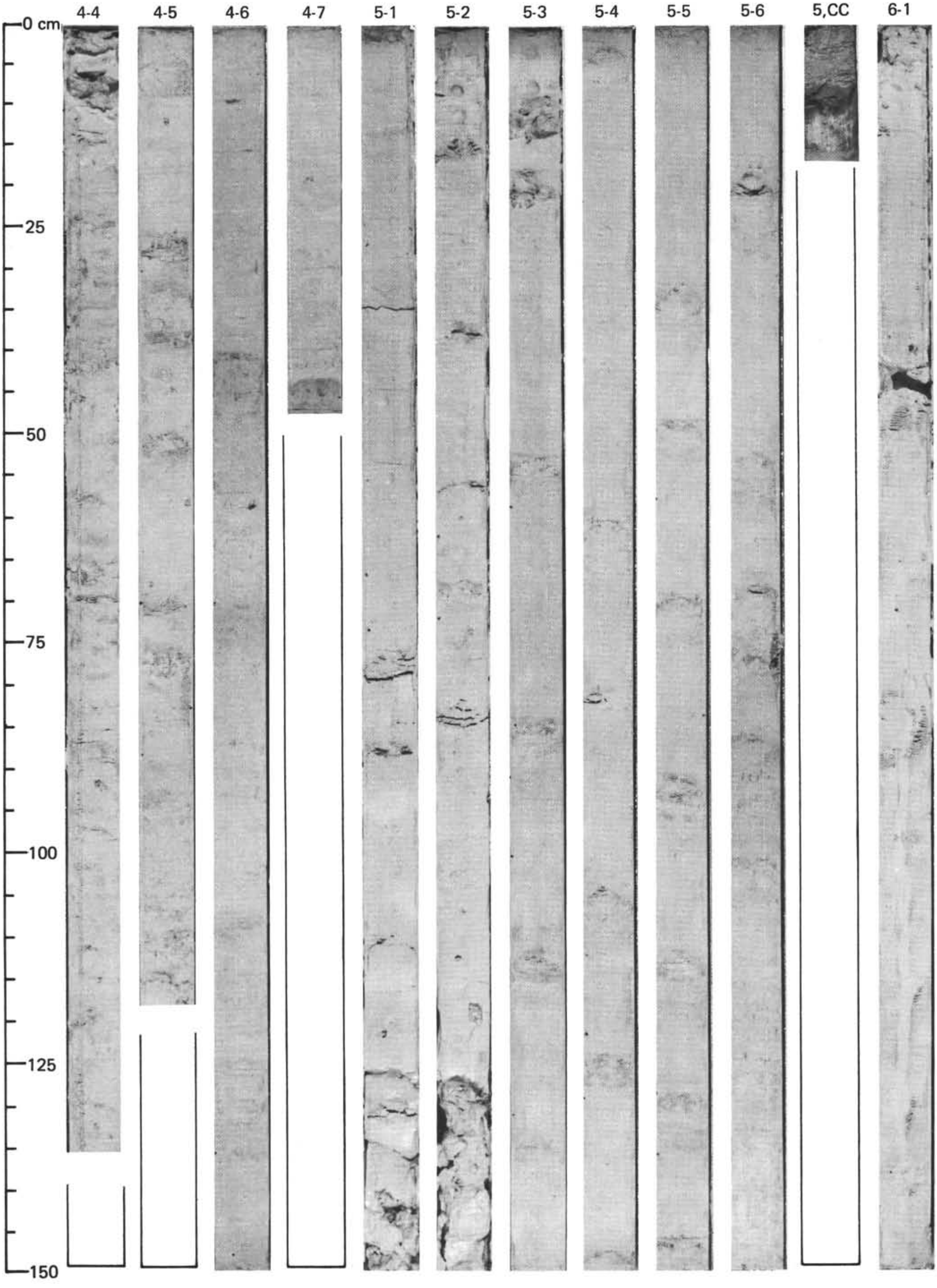
4-4
4-5
4-6
4-7
5-1
5-2
5-3
5-4
5-5
5-6
5,CC
6-1
0 cm
25
50
75
100
125
150

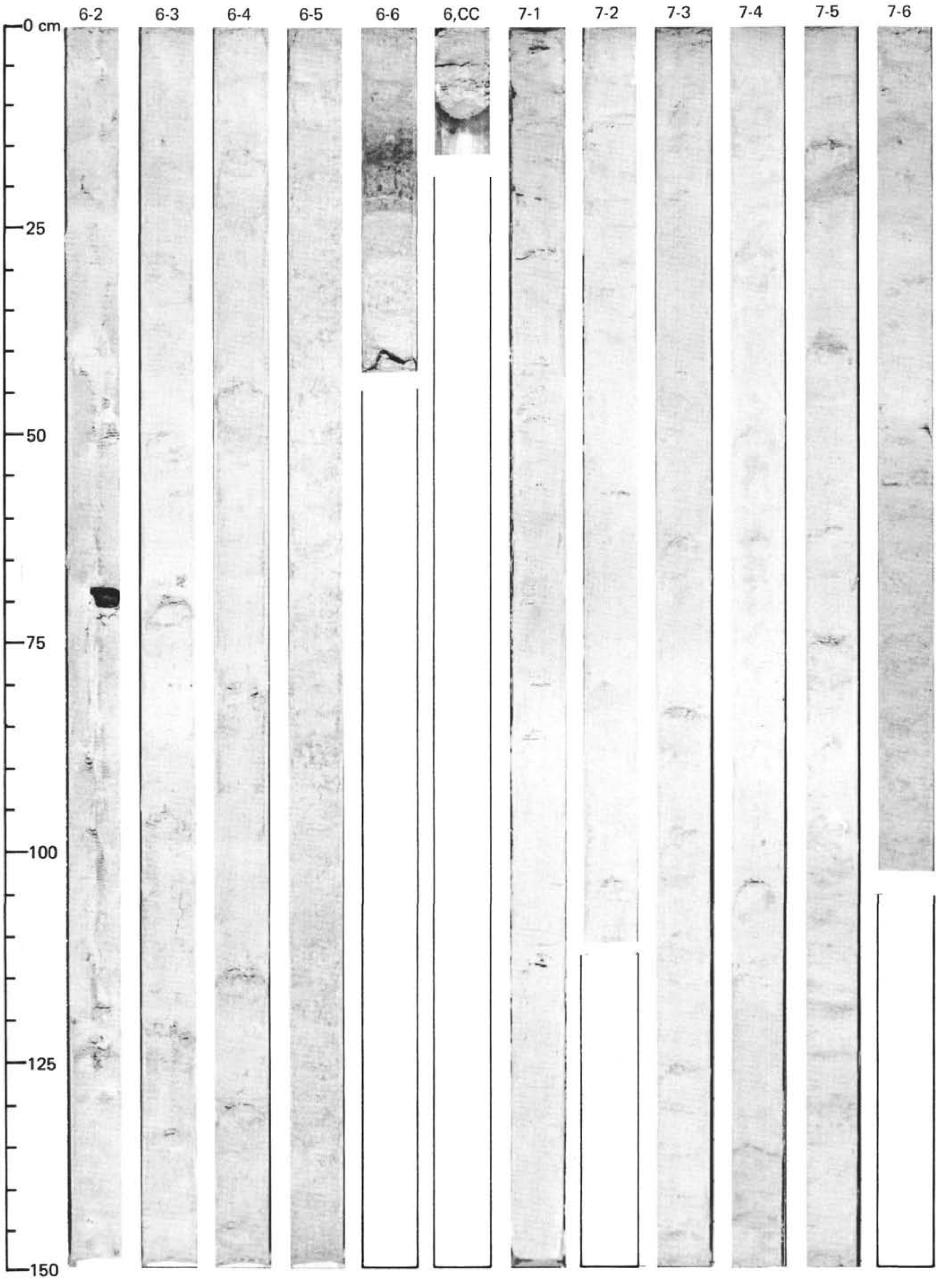
6-2
6-3
6-4
6-5
6-6
6,CC
7-1
7-2
7-3
7-4
7-5
7-6
0 cm
25
50
75
100
125
150

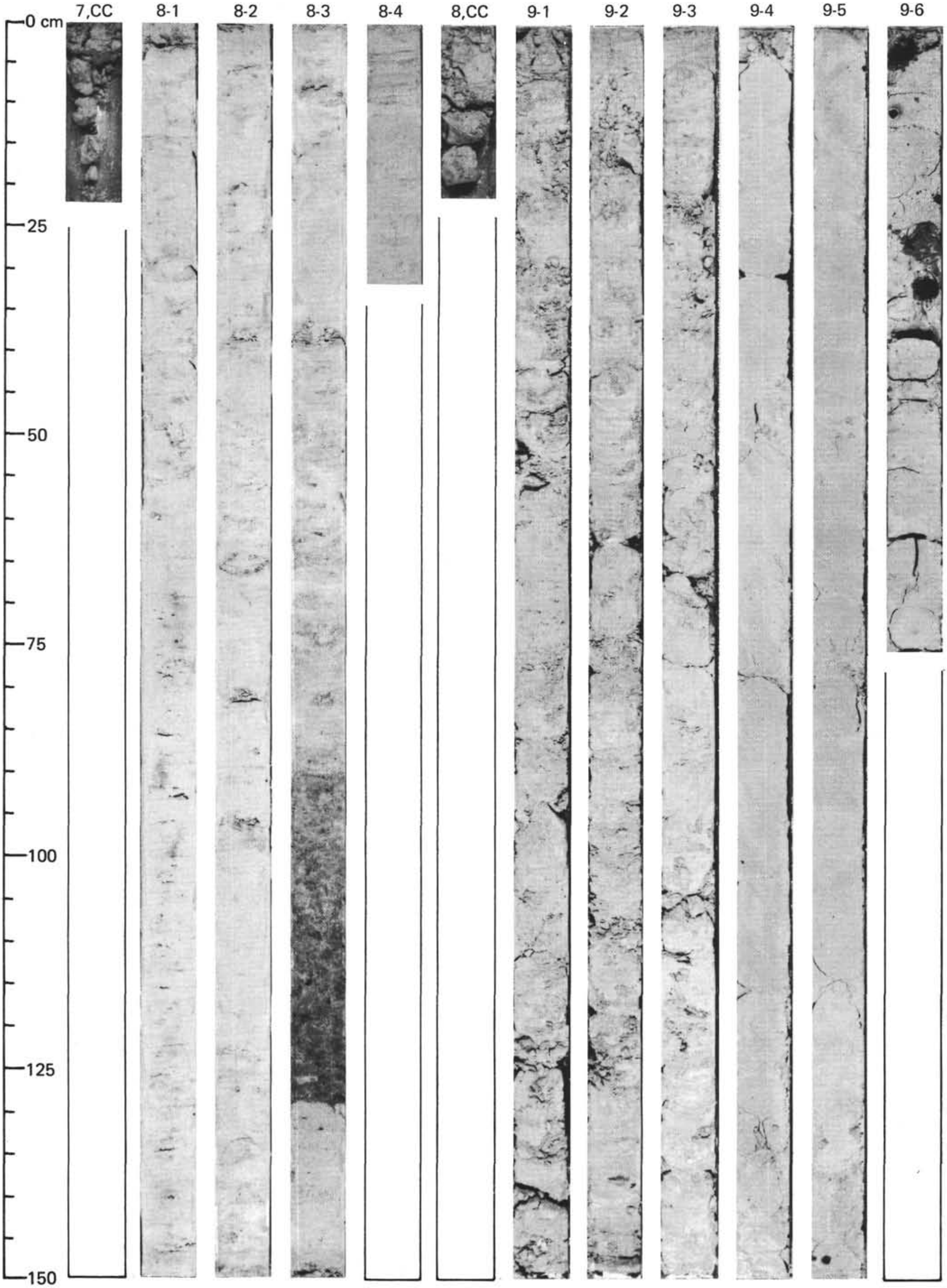
7,CC
8-1
8-2
8-3
8-4
8,CC
9-1
9-2
9-3
9-4
9-5
9-6
0 cm
25
50
75
100
125
150

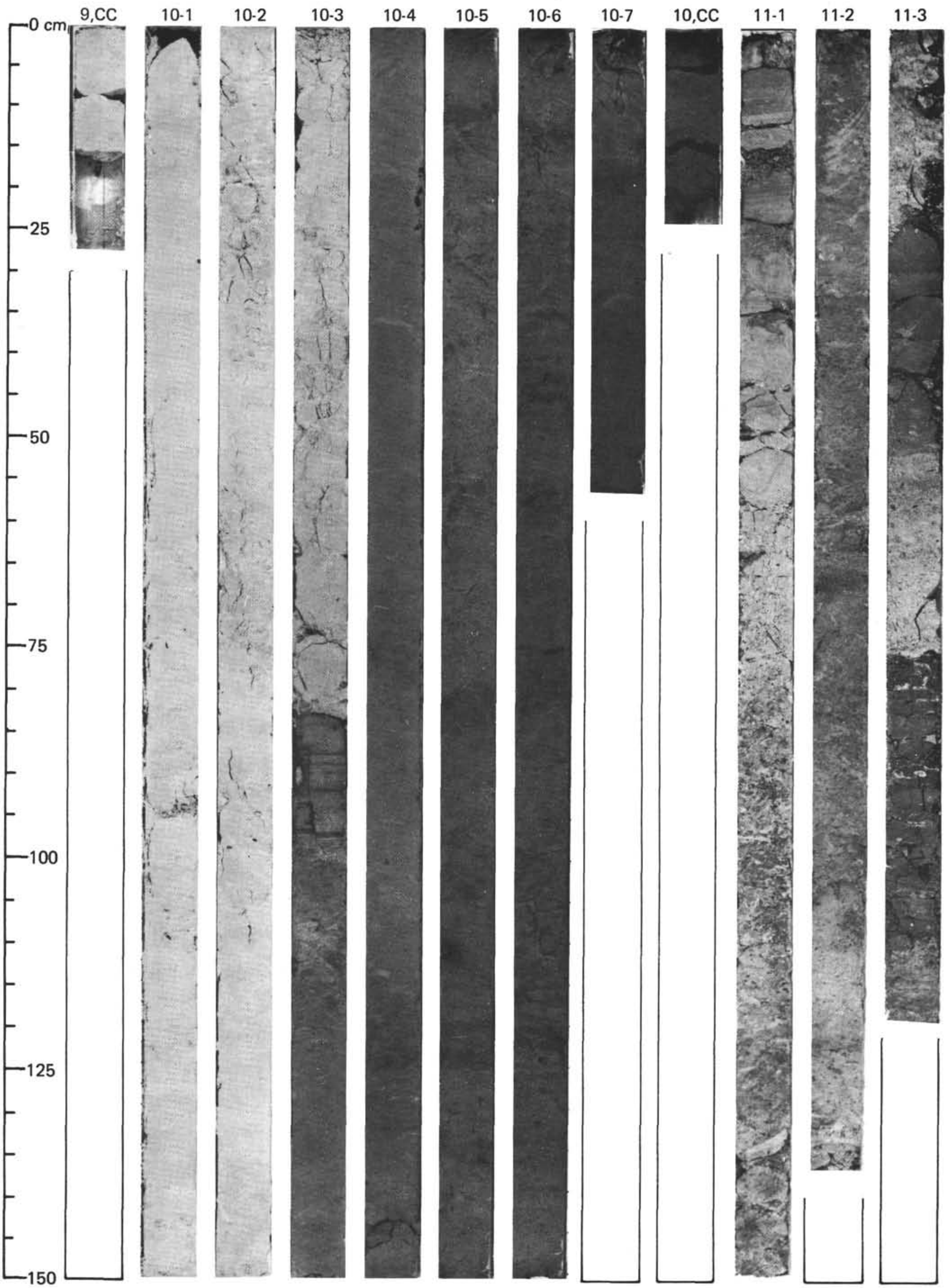
0 cm
25
50
75
100
125
150
9,CC
10-1
10-2
10-3
10-4
10-5
10-6
10-7
10,CC
11-1
11-2
11-3

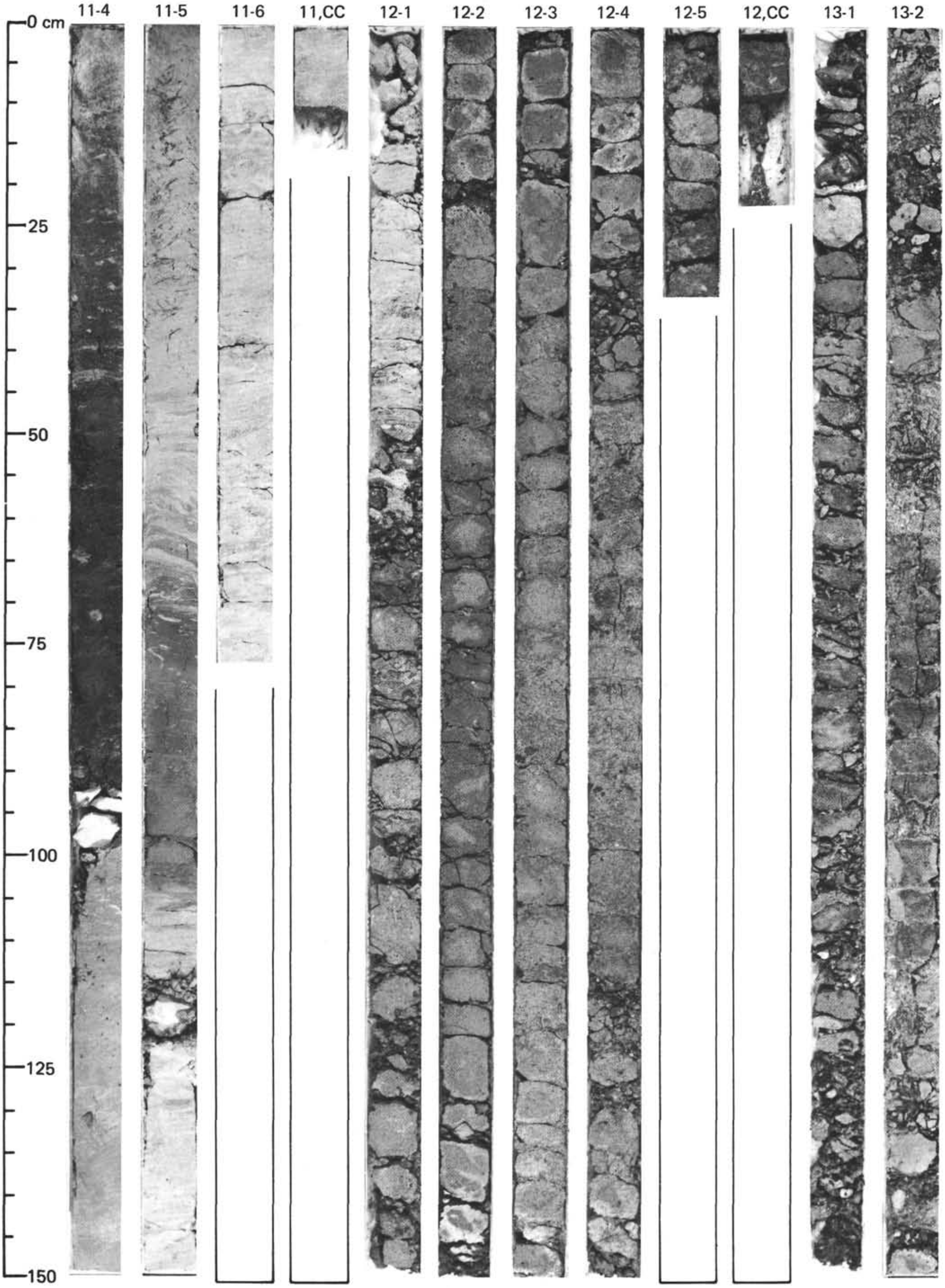

0 cm
25
50
75
100
125
150
11-4
11-5
11-6
11,CC
12-1
12-2
12-3
12-4
12-5
12,CC
13-1
13-2

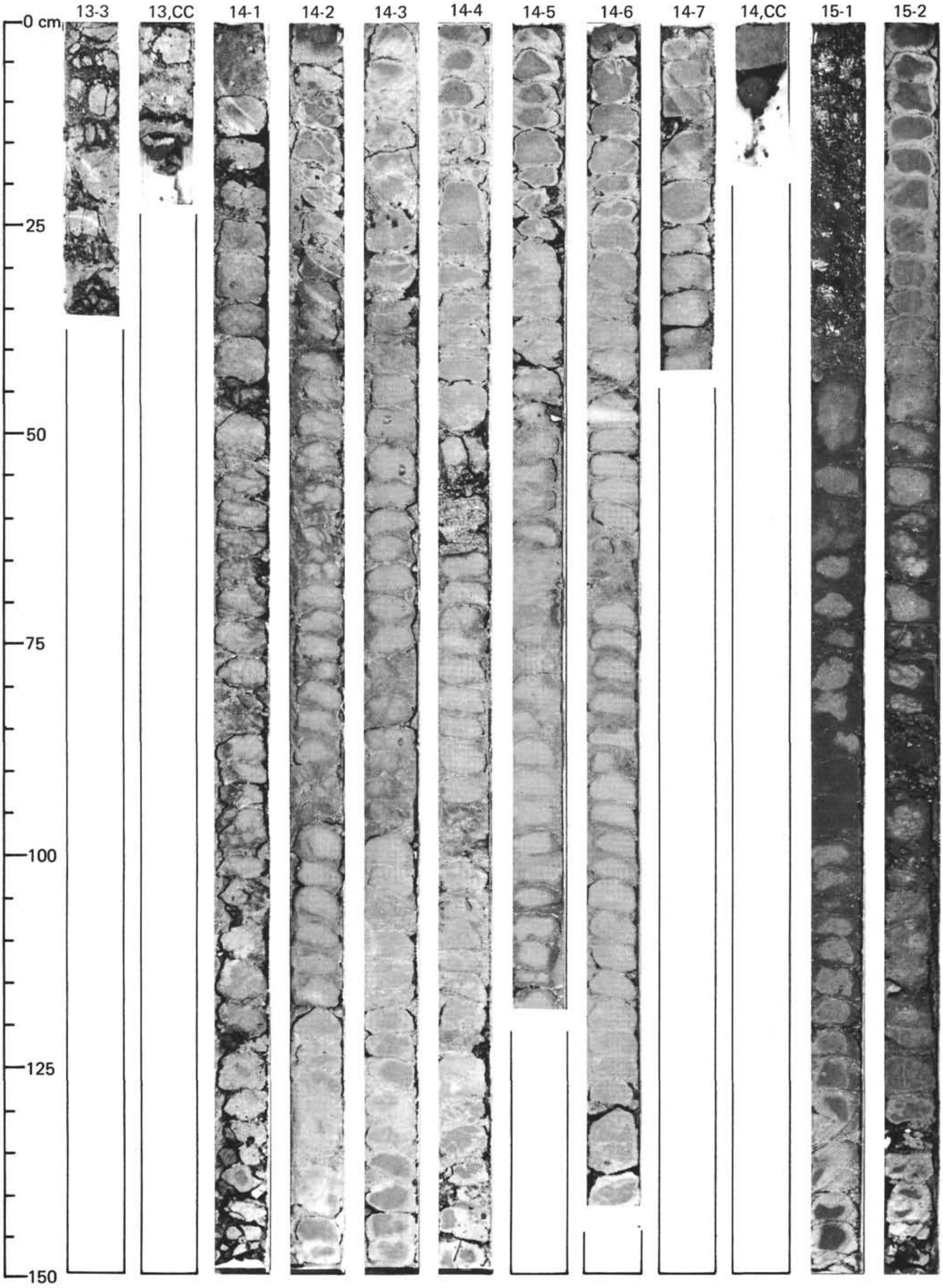
13-3
13,CC
14-1
14-2
14-3
14-4
14-5
14-6
14-7
14,CC
15-1
15-2
0 cm
25
50
75
100
125
150

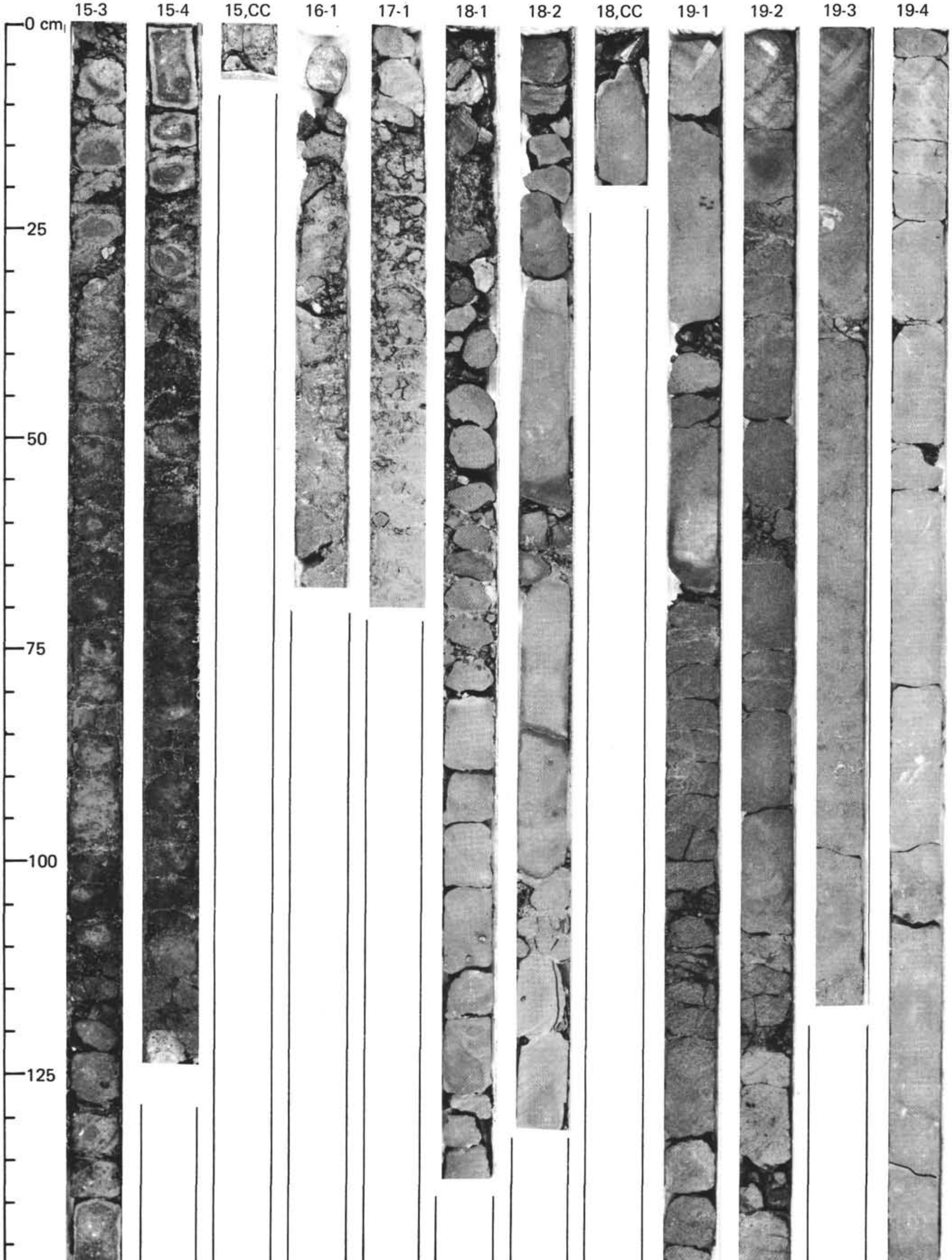
15-3
15-4
15,CC
16-1
17-1
18-1
18-2
18,CC
19-1
19-2
19-3
19-4
0 cm
25
50
75
100
125
150

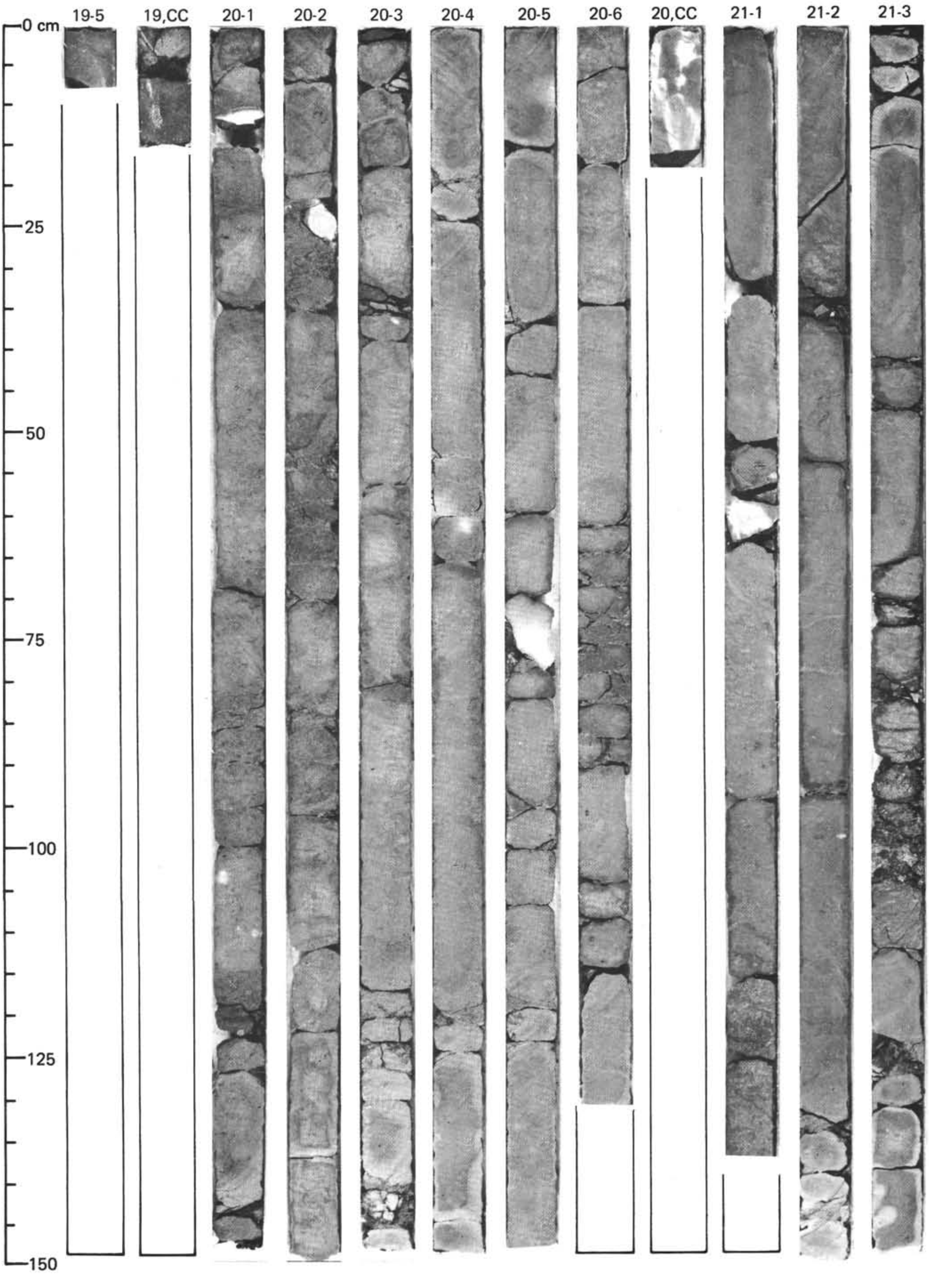
0 cm
25
50
75
100
125
150
19-5
19,CC
20-1
20-2
20-3
20-4
20-5
20-6
20,CC
21-1
21-2
21-3

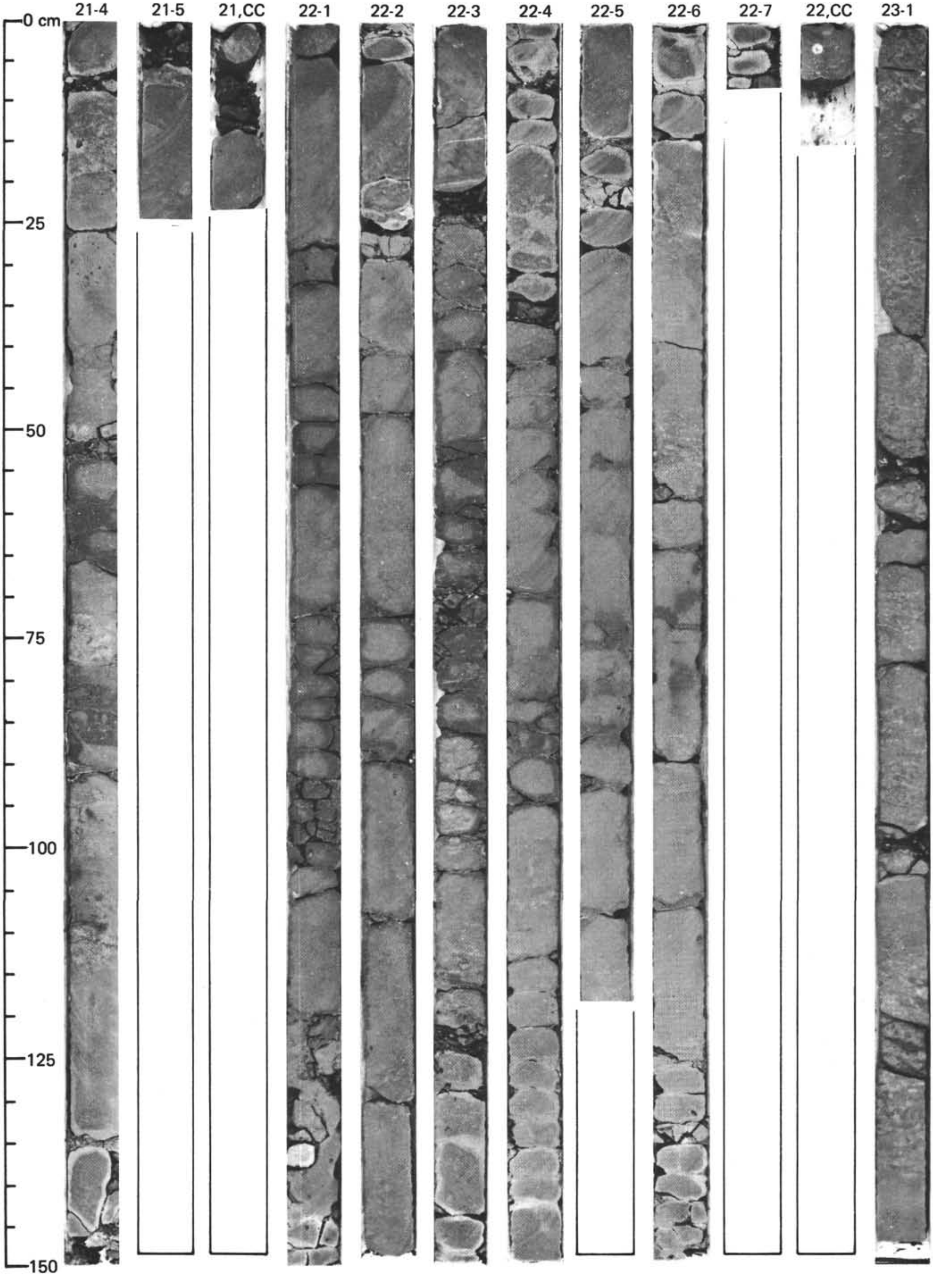
0 cm
25
50
75
100
125
150
21-4
21-5
21,CC
22-1
22-2
22-3
22-4
22-5
22-6
22-7
22,CC
23-1

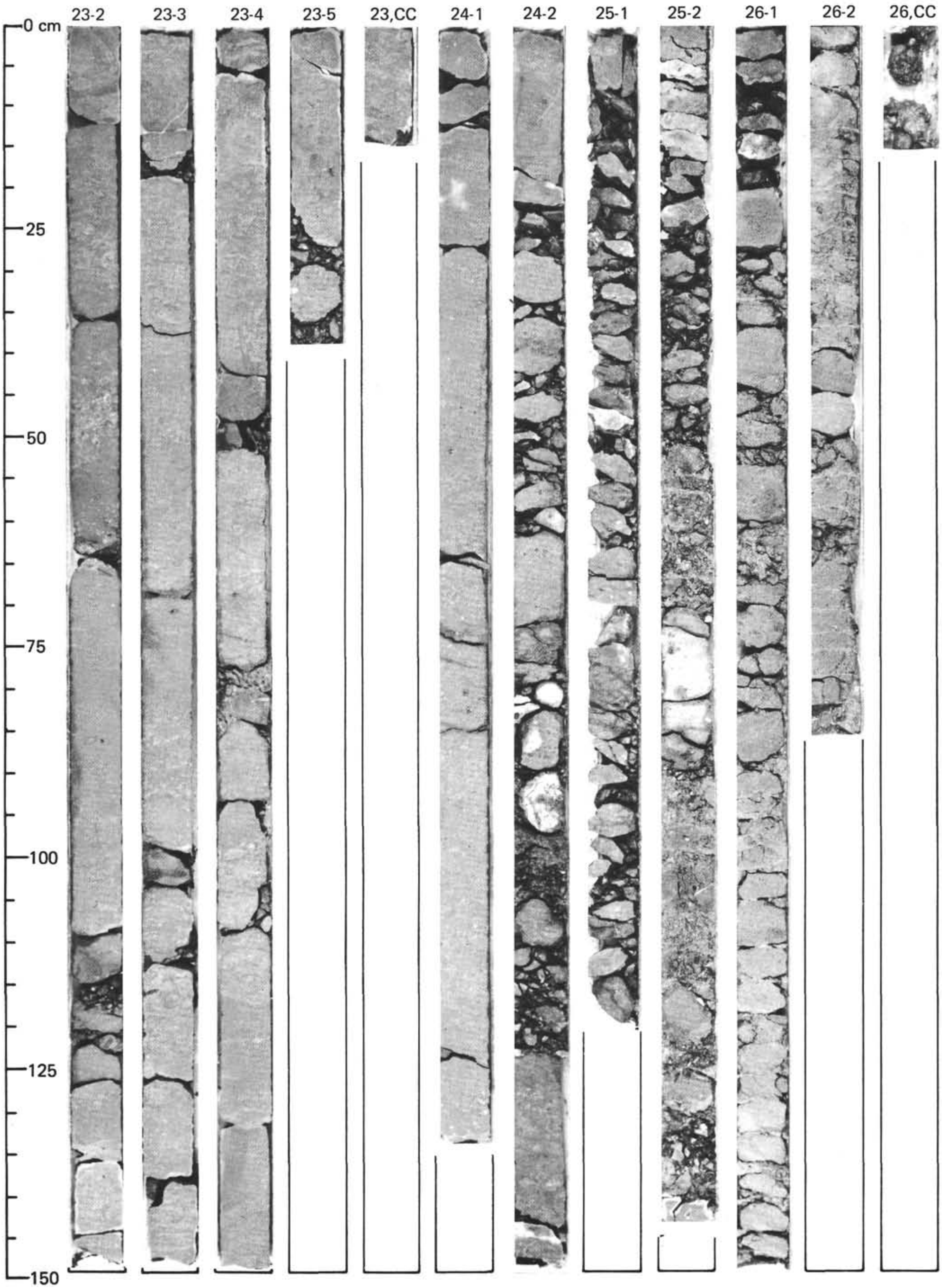
23-2
23-3
23-4
23-5
23,CC
24-1
24-2
25-1
25-2
26-1
26-2
26,CC
0 cm
25
50
75
100
125
150


0 cm
25
50
75
100
125
150
27-1
27-2
27-3
27-4
27-5
27-6
27,CC
28,CC
29,CC
31,CC
32,CC
33,CC
NO RECOVERY

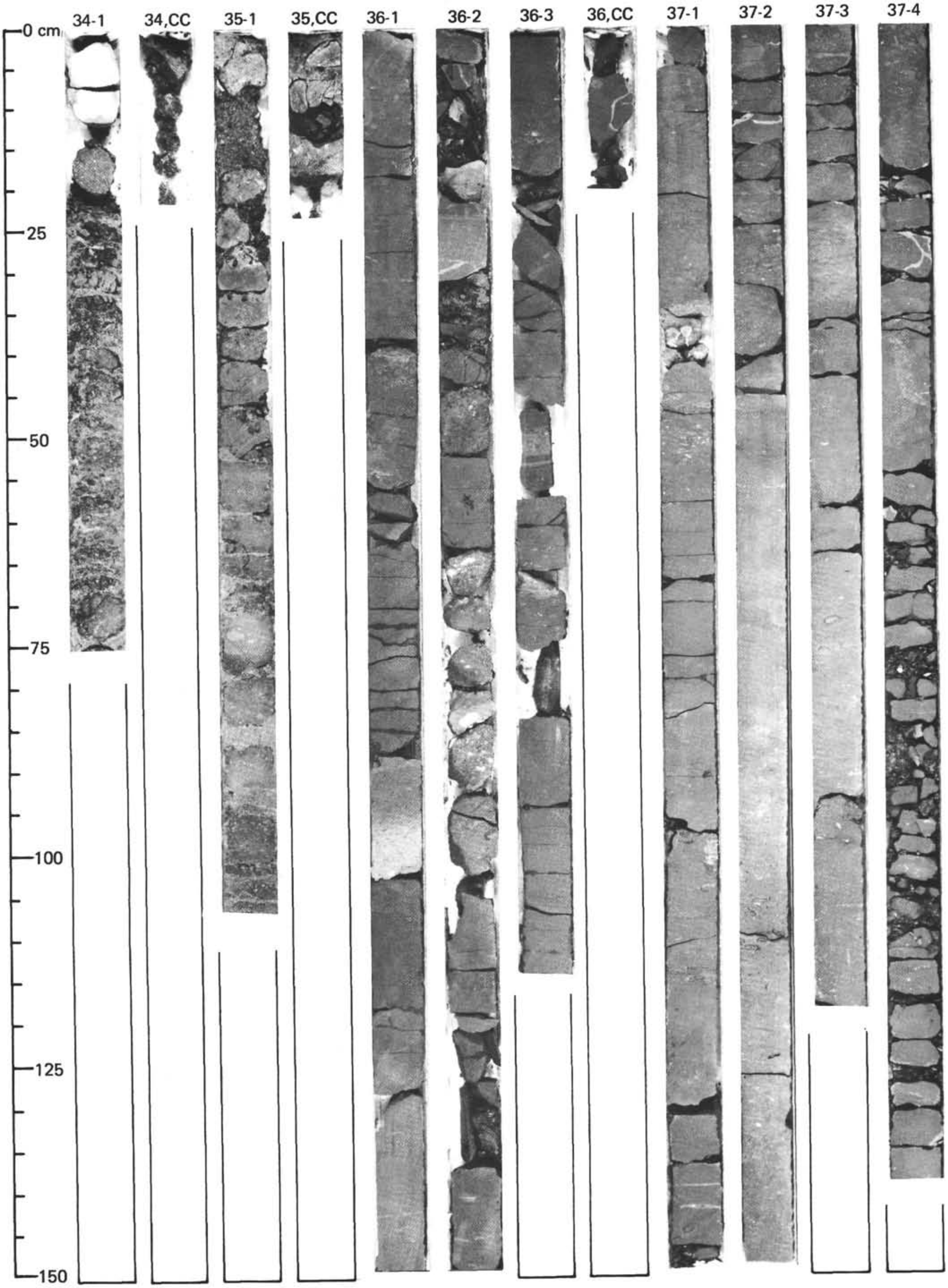
34-1
34,CC
35-1
35,CC
36-1
36-2
36-3
36,CC
37-1
37-2
37-3
37-4
0 cm
25
50
75
100
125
150

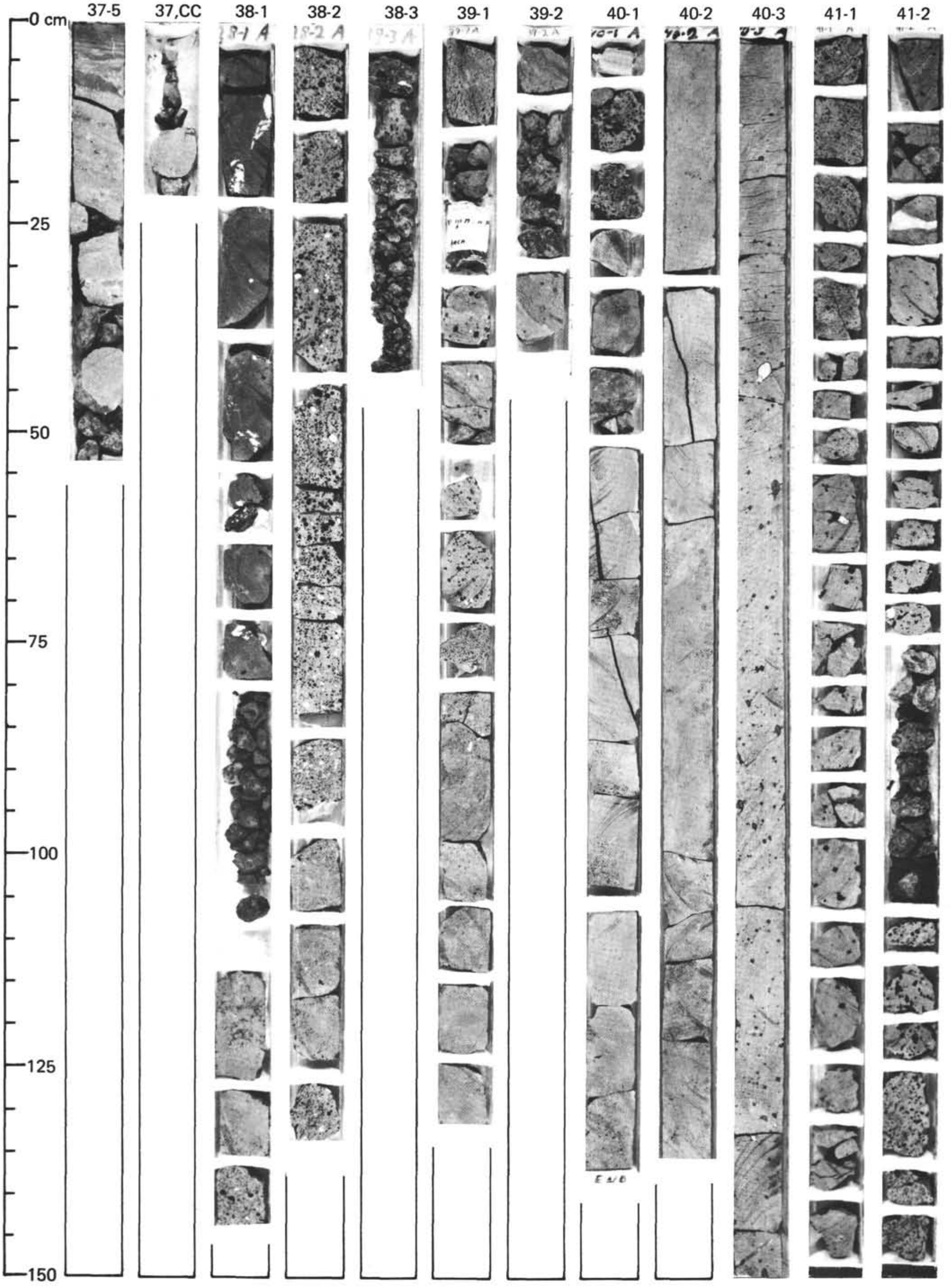
0 cm
25
50
75
100
125
150
37-5
37,CC
38-1
38-2
38-3
39-1
39-2
40-1
40-2
40-3
41-1
41-2

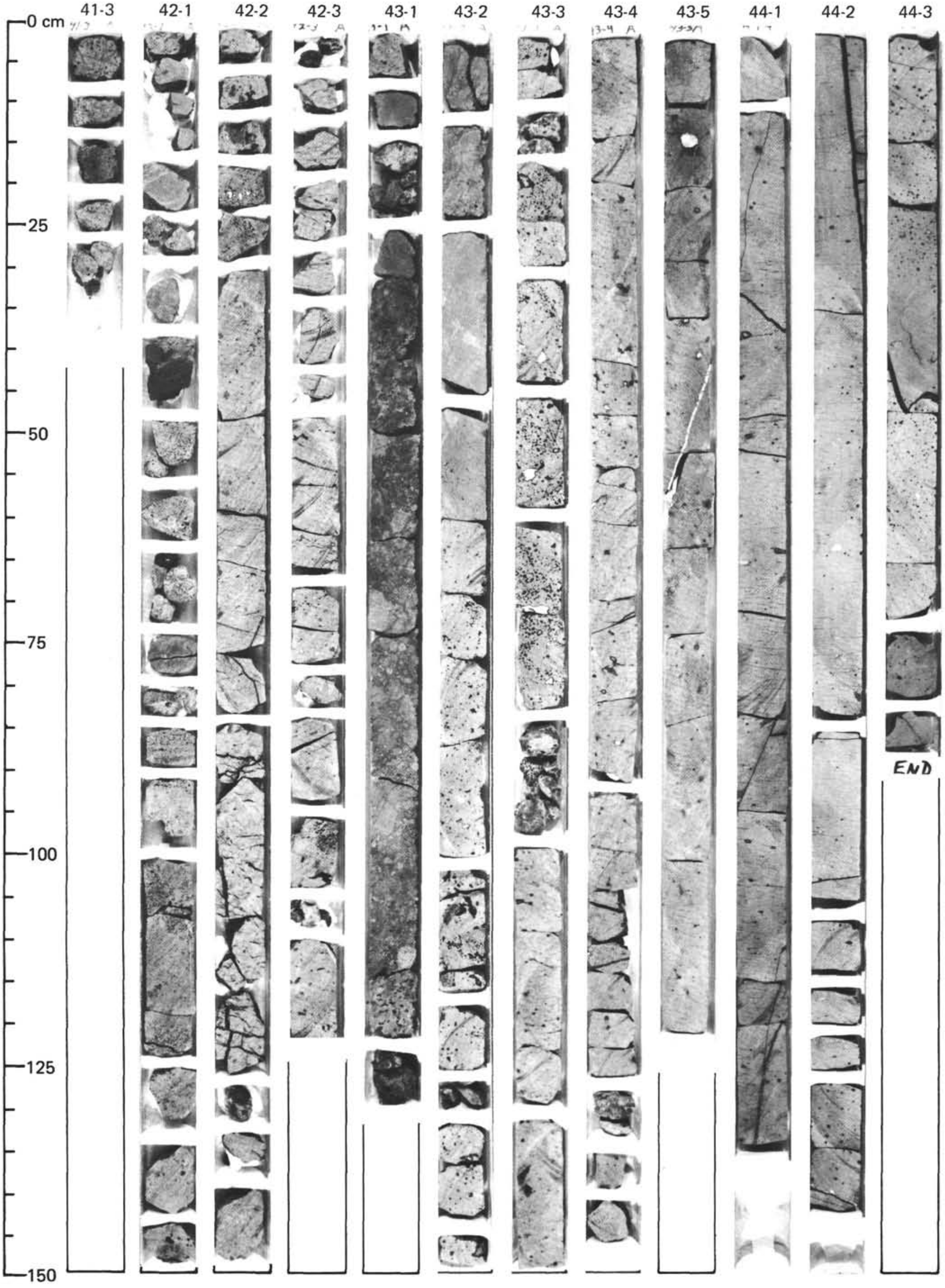
41-3
42-1
42-2
42-3
43-1
43-2
43-3
43-4
43-5
44-1
44-2
44-3
0 cm
25
50
75
100
125
150
END

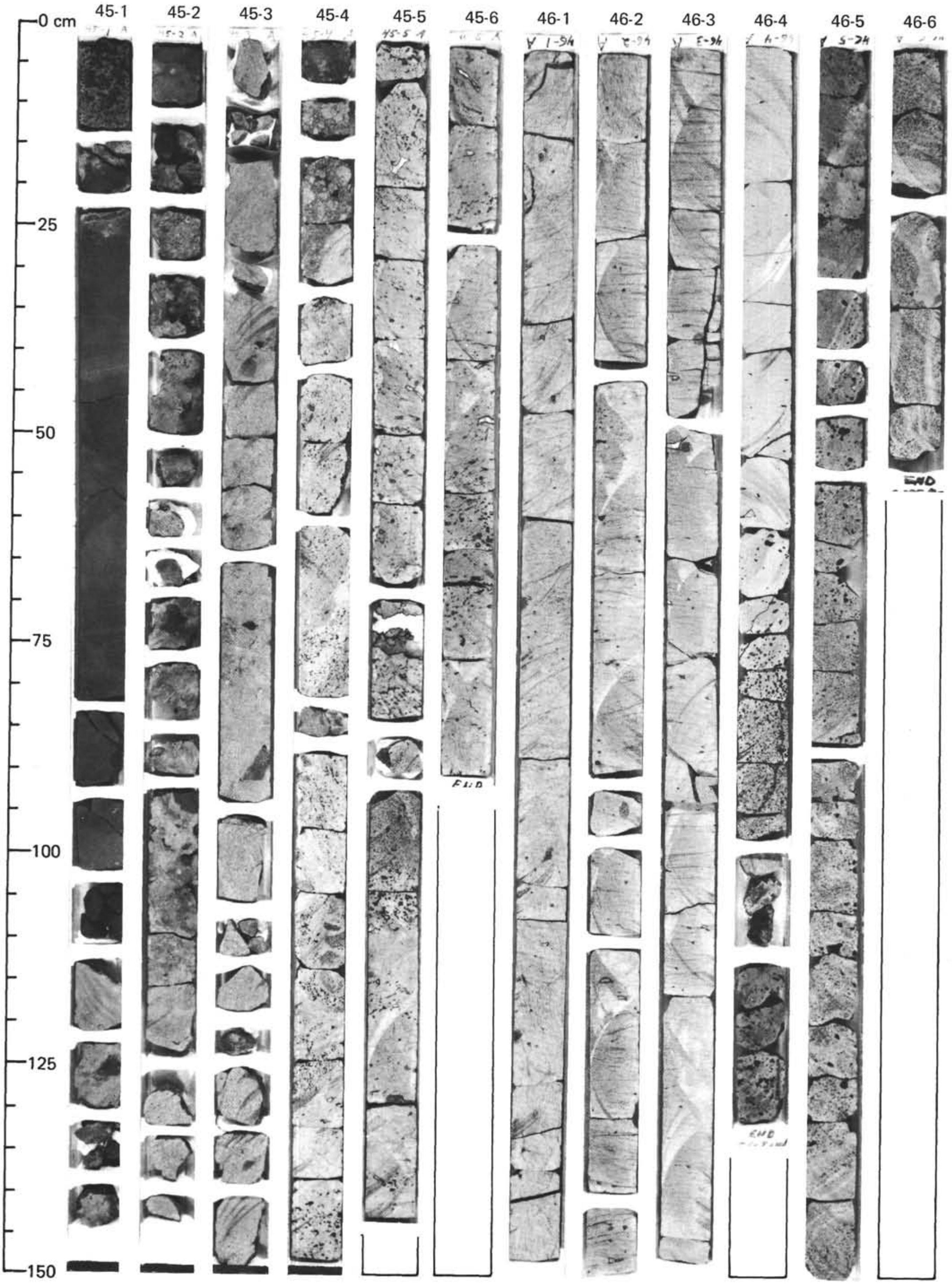
0 cm
25
50
75
100
125
150
45-1
45-2
45-3
45-4
45-5
45-6
46-1
46-2
46-3
46-4
46-5
46-6
END
END
END

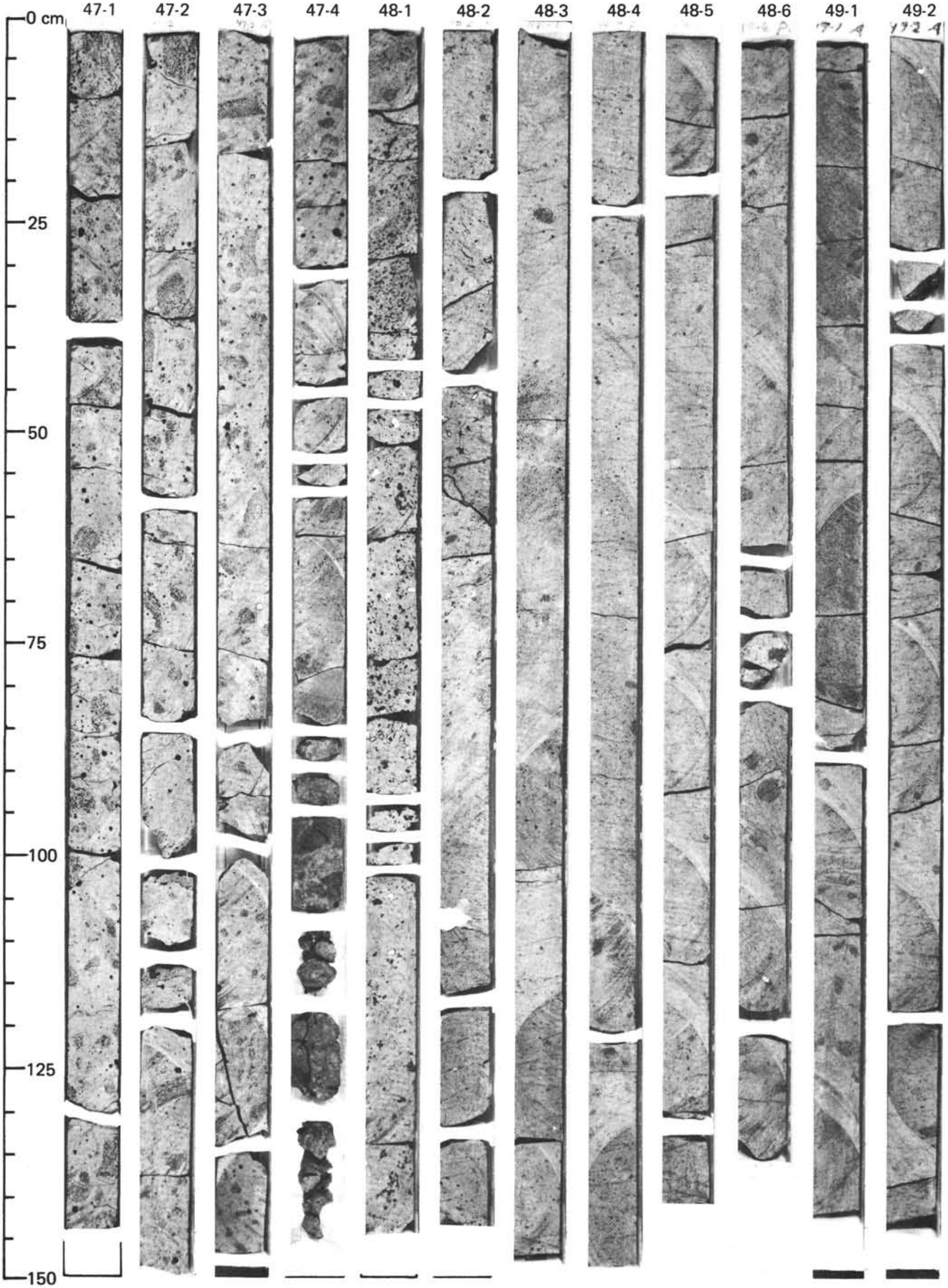
0 cm
25
50
75
100
125
150
47-1
47-2
47-3
47-4
48-1
48-2
48-3
48-4
48-5
48-6
49-1
49-2

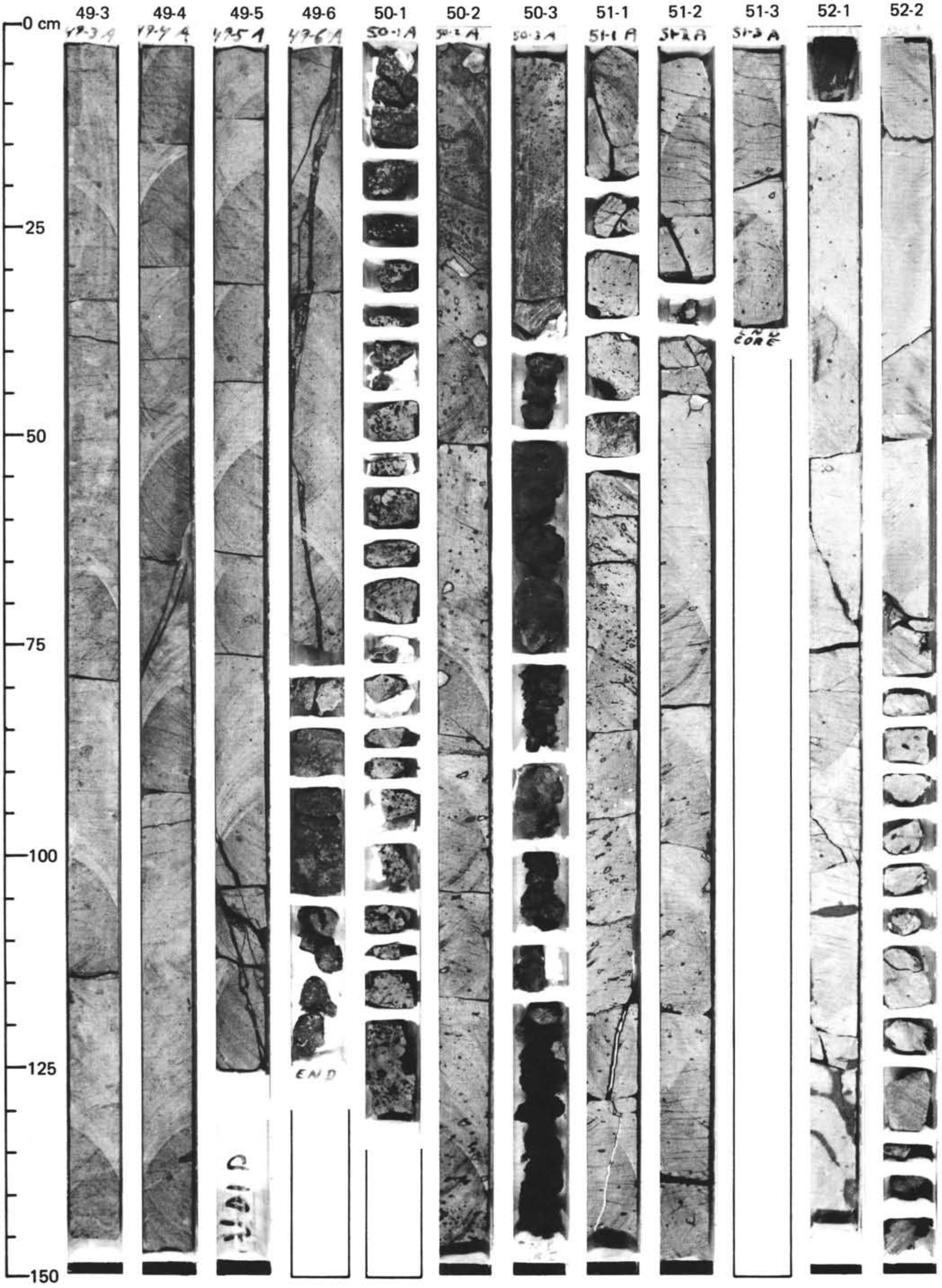
49-3
49-4
49-5
49-6
50-1
50-2
50-3
51-1
51-2
51-3
52-1
52-2
0 cm
25
50
75
100
125
150
END
END CORE

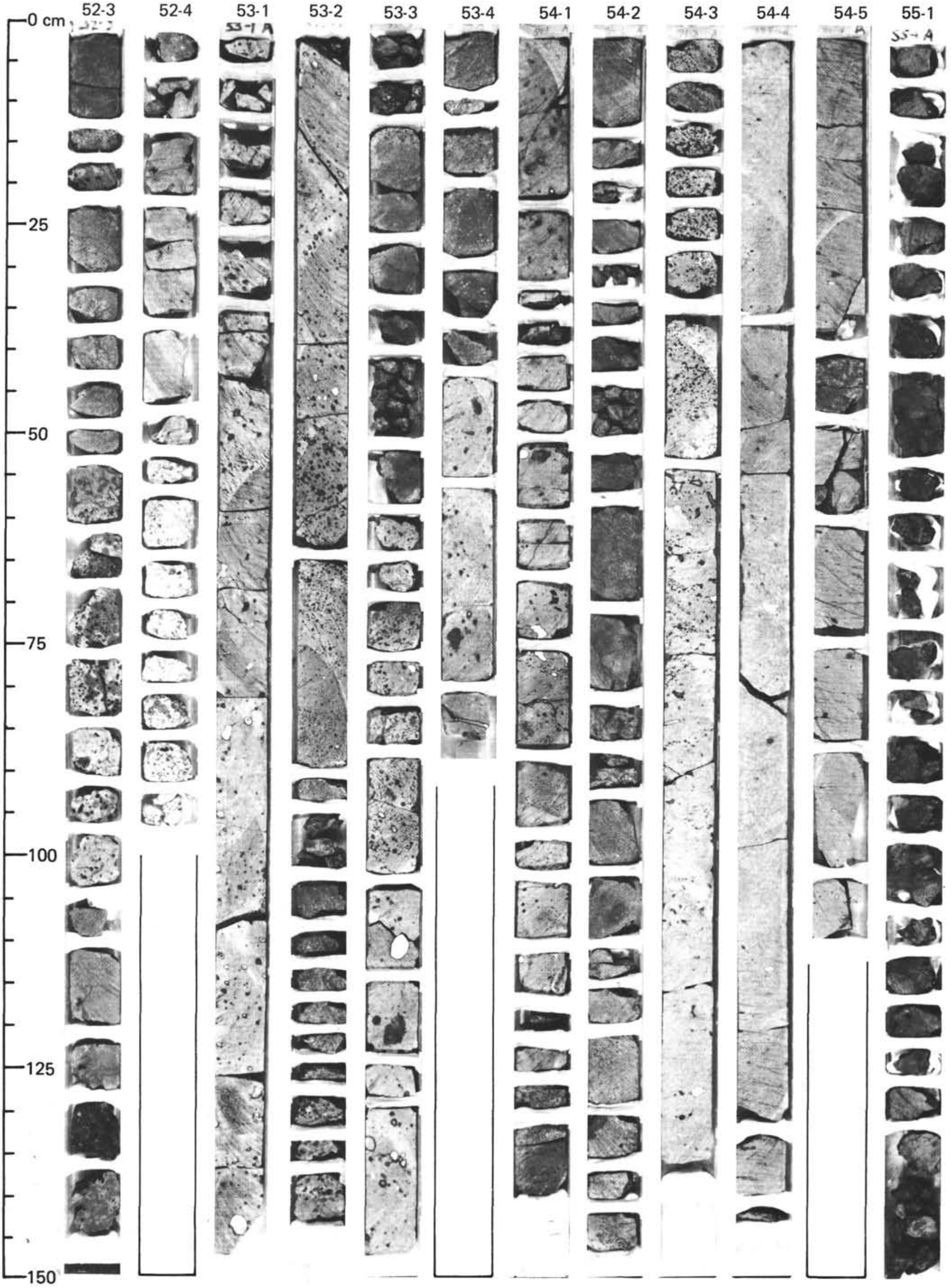
0 cm
25
50
75
100
125
150
52-3
52-4
53-1
53-2
53-3
53-4
54-1
54-2
54-3
54-4
54-5
55-1

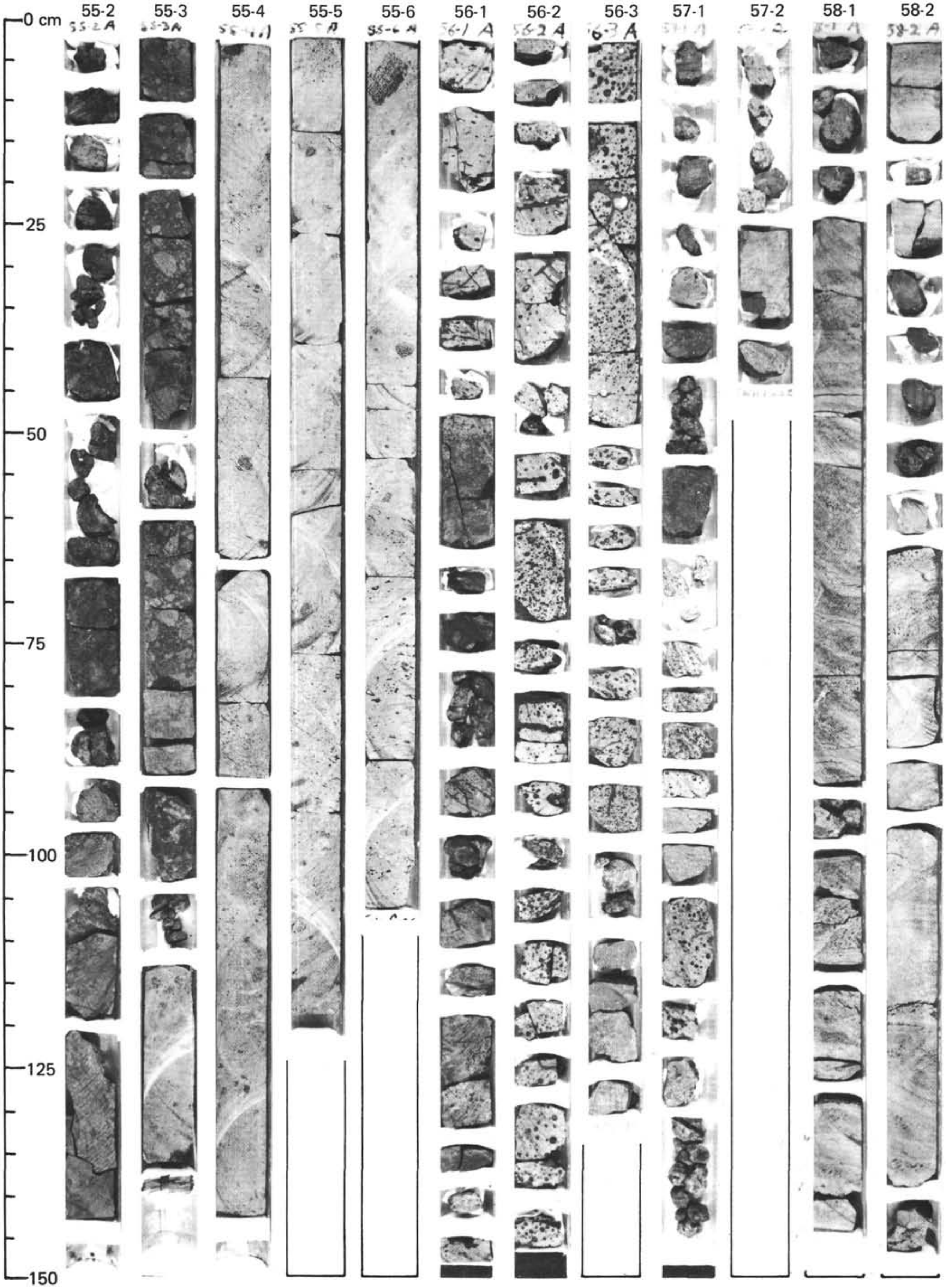
0 cm
25
50
75
100
125
150
55-2
55-3
55-4
55-5
55-6
56-1
56-2
56-3
57-1
57-2
58-1
58-2

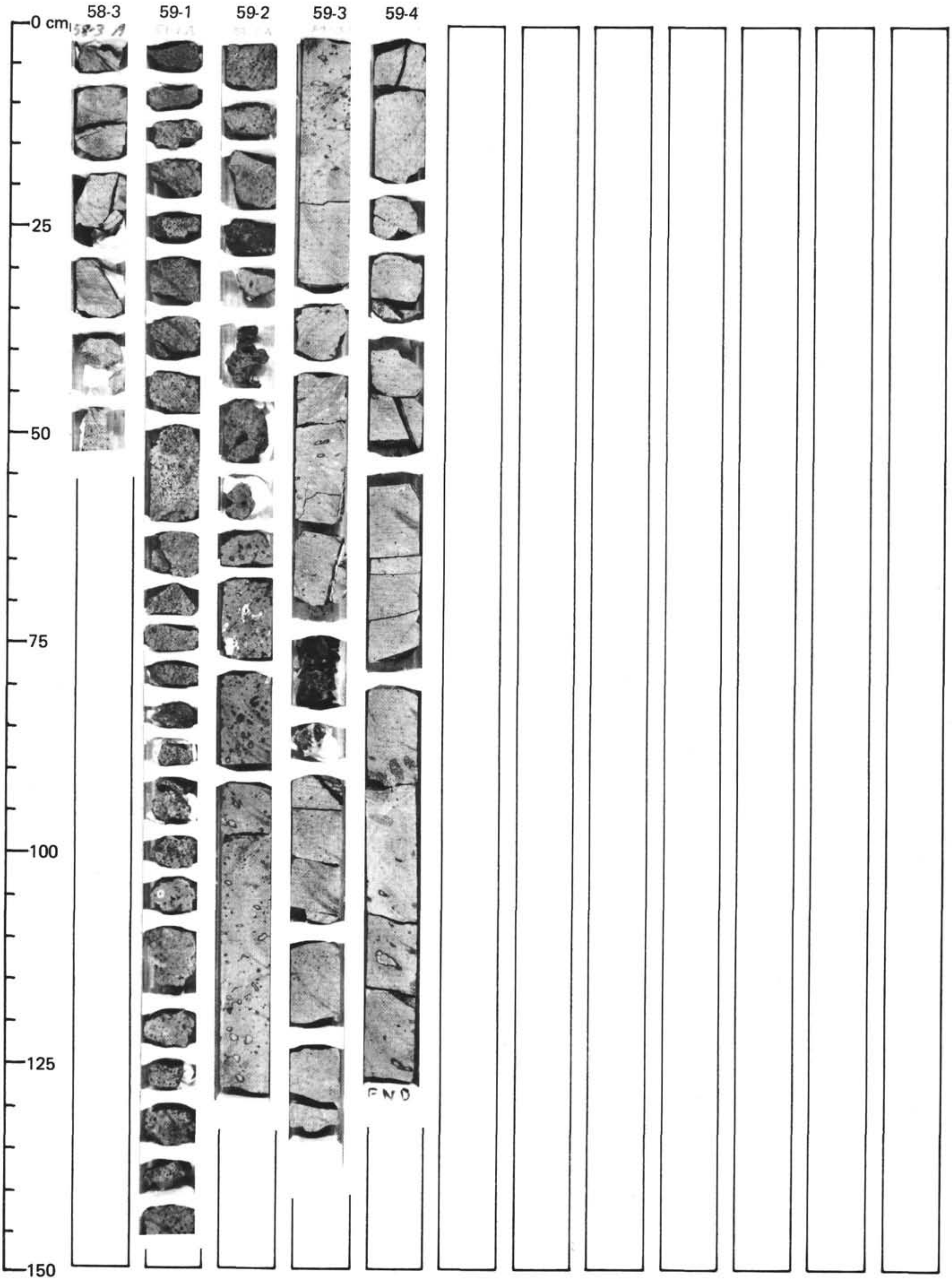
58-3
59-1
59-2
59-3
59-4
0 cm
25
50
75
100
125
150
END

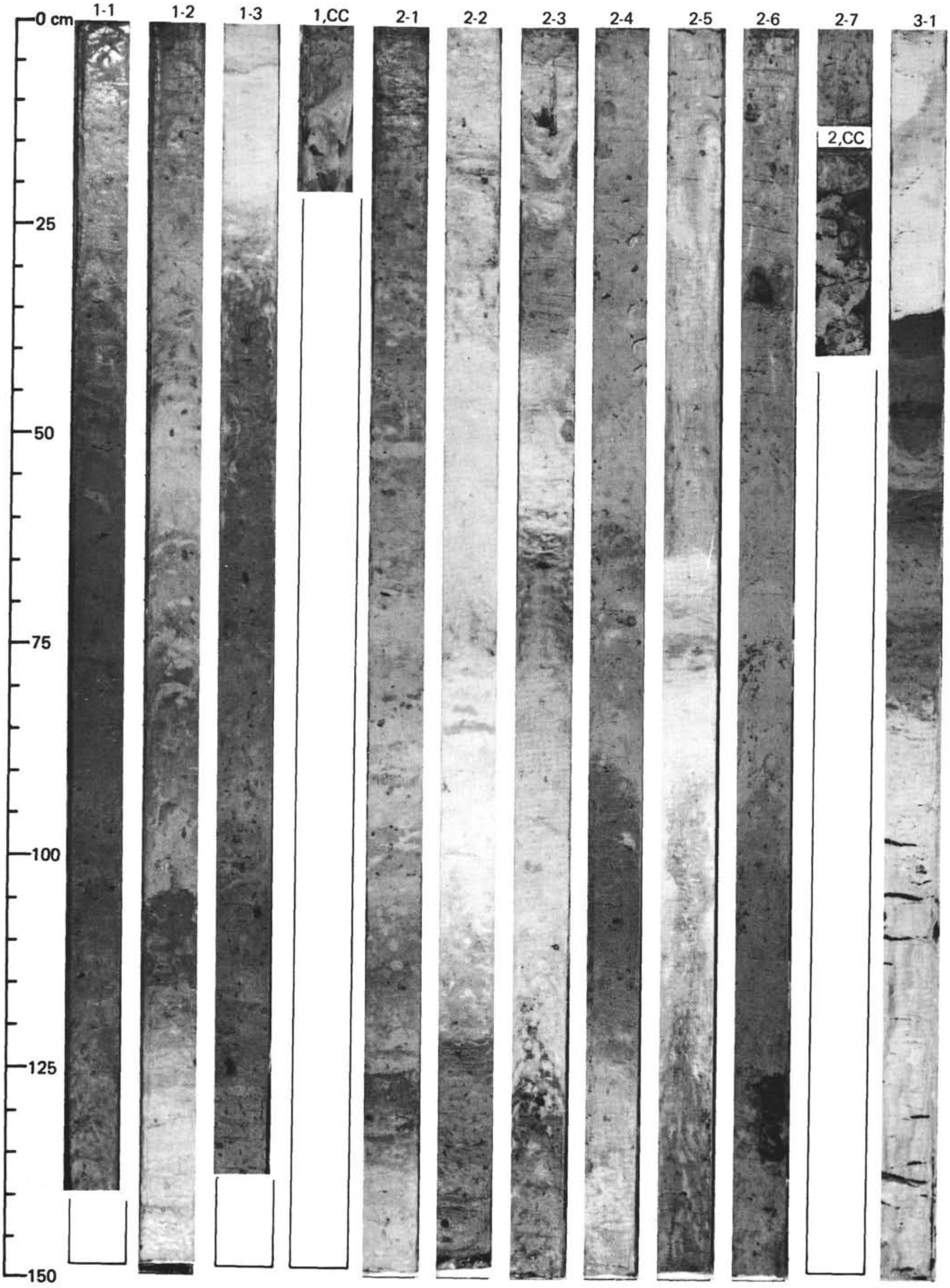
0 cm
25
50
75
100
125
150
1-1
1-2
1-3
1,CC
2-1
2-2
2-3
2-4
2-5
2-6
2-7
2,CC
3-1

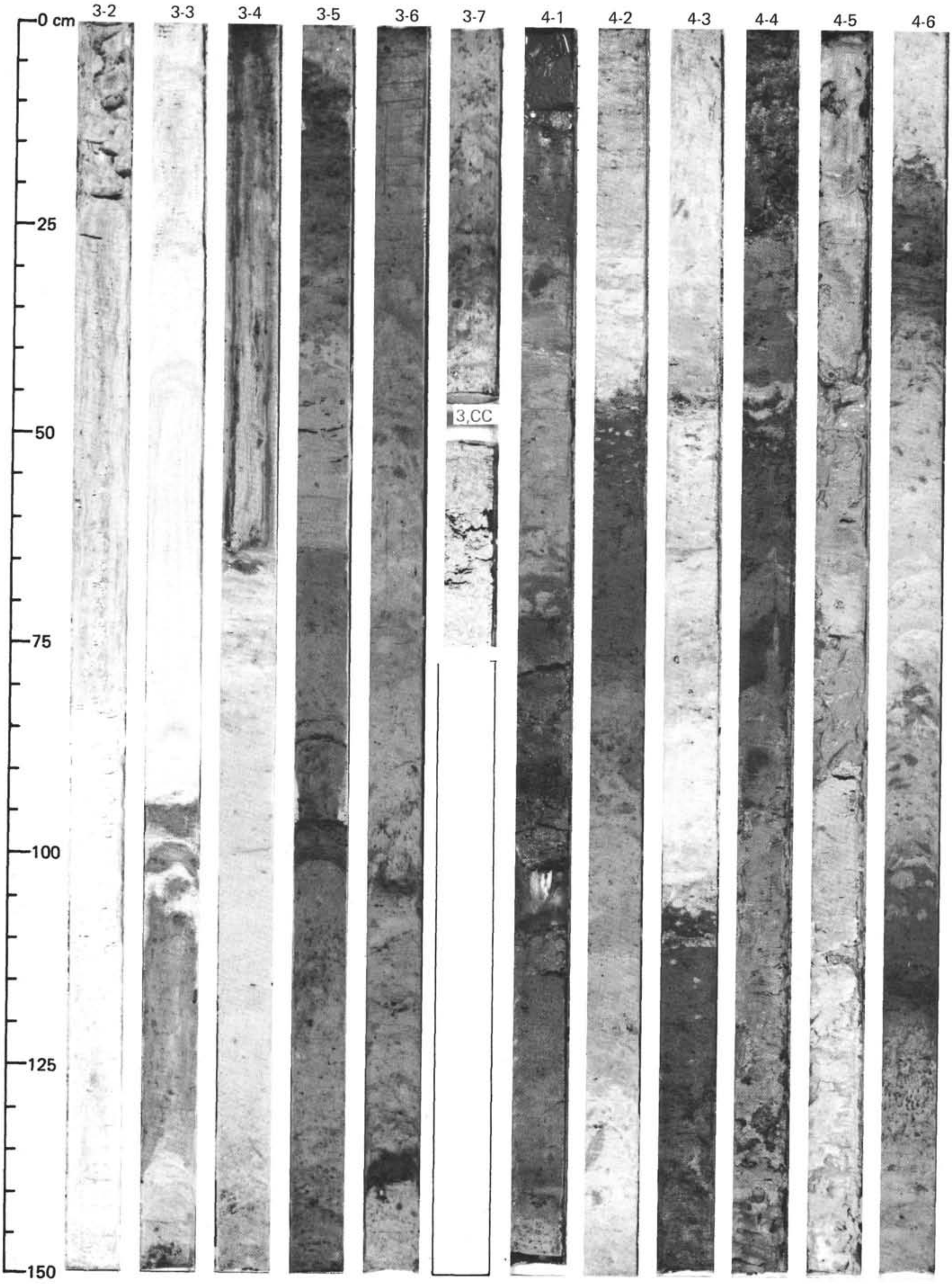
0 cm
25
50
75
100
125
150
3-2
3-3
3-4
3-5
3-6
3-7
3,CC
4-1
4-2
4-3
4-4
4-5
4-6

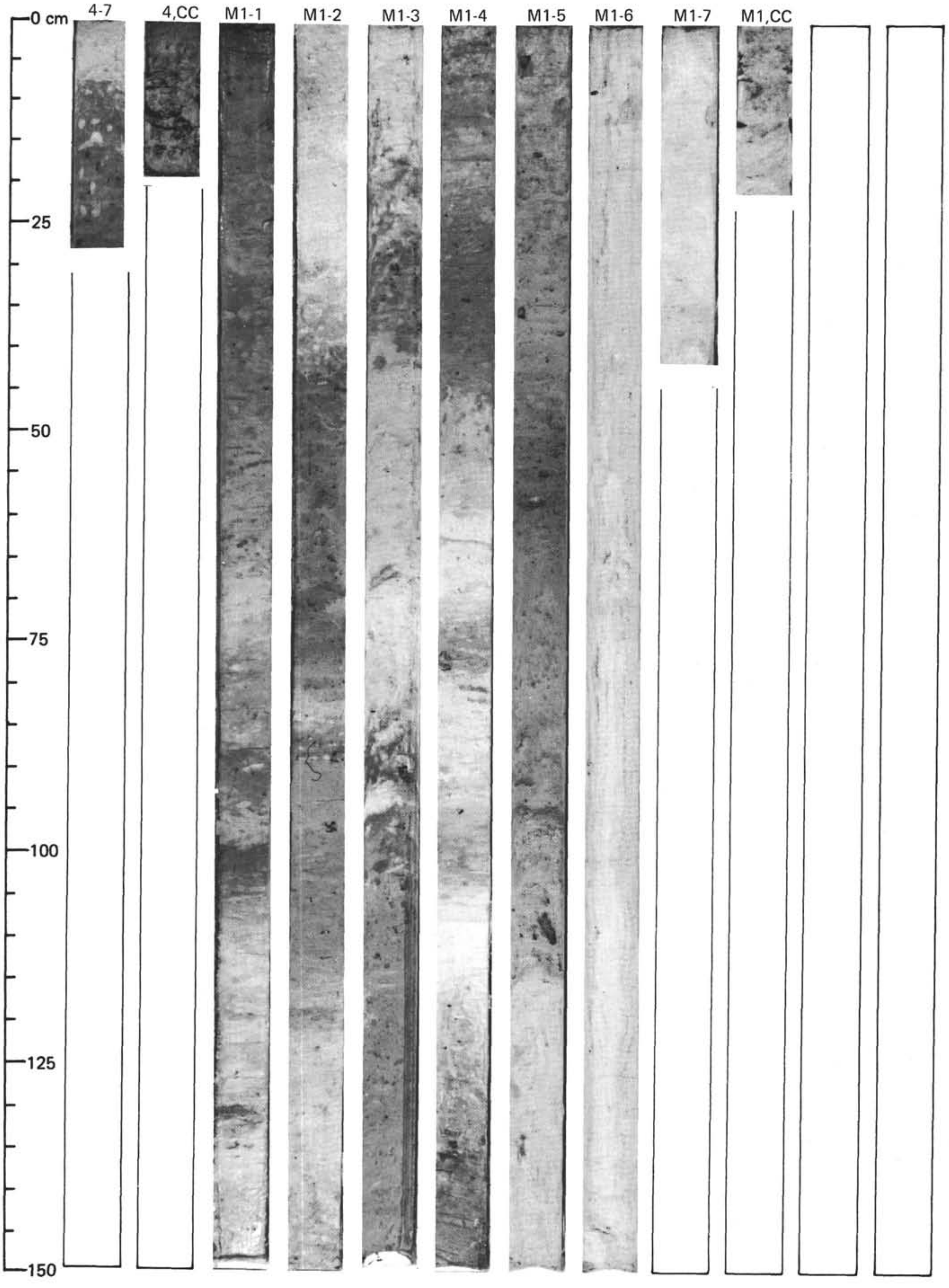
0 cm
25
50
75
100
125
150
4-7
4,CC
M1-1
M1-2
M1-3
M1-4
M1-5
M1-6
M1-7
M1,CC